British Journal of Pharmacology

July 1995

Volume 115 Number 5 pages 713–868

British Journal of Pharmacology (1995) 115, 713-715

SPECIAL REPORT

Regulation of muscle glycogen metabolism by CGRP and amylin: CGRP receptors not involved

[1]Kevin Beaumont, Richard A. Pittner, Candace X. Moore, Deborah Wolfe-Lopez, Kathryn S. Prickett, Andrew A. Young & Timothy J. Rink

Amylin Pharmaceuticals, Inc., 9373 Towne Centre Drive, San Diego, CA 92121, U.S.A.

The aim of the present study was to determine whether amylin and calcitonin gene-related peptide (CGRP) act through shared or distinct receptors to inhibit insulin-stimulated incorporation of [^{14}C]-glucose into glycogen. Rat amylin was 3 fold more potent than either rat αCGRP or rat βCGRP at reducing glycogen synthesis from [^{14}C]-glucose in insulin-treated rat soleus muscle. This action was blocked by peptide antagonists, with the rank order of potency being AC187 > salmon calcitonin$_{8-32}$ (sCT$_{8-32}$) > h-αCGRP$_{8-37}$ for antagonism of either amylin or CGRP. The antagonist potency order correlated with affinity for amylin receptors measured in rat nucleus accumbens but not CGRP receptors measured in rat L6 muscle cells. Inhibition of glucose incorporation into glycogen by amylin and CGRP appears to be mediated by shared receptors that have the pharmacological characteristics of amylin receptors, and are distinct from previously described CGRP receptors.

Keywords: Amylin; CGRP; diabetes; insulin resistance; glycogen; glucose metabolism; peptide receptors; calcitonin

Introduction Amylin is a 37 amino acid peptide that is released from pancreatic β-cells in response to feeding, and has been proposed as an endocrine partner to insulin in the regulation of carbohydrate disposal and storage (Pittner *et al.*, 1994). It shares 41-51% sequence identity with calcitonin gene-related peptide (CGRP), a neuropeptide that is widely distributed in peripheral motor and sensory nerves. Both human amylin and rat αCGRP potently inhibit insulin-stimulated glycogen synthesis in rat skeletal muscle (Leighton & Cooper, 1988). However, amylin is 100 fold less potent than CGRP in competing for [^{125}I]-CGRP binding sites in membranes from rat skeletal muscle (Chantry *et al.*, 1991) or rat L6 skeletal muscle cells (Poyner *et al.*, 1992).

We have identified amylin receptors in rat brain, concentrated in the nucleus accumbens, which have a binding profile that is quite distinct from CGRP receptors (Beaumont *et al.*, 1993). These amylin receptors have high affinity for AC187 (Acetyl-[Asn^{30},Tyr^{32}]-sCT$_{8-32}$), a potent and selective antagonist of amylin-induced hyperglycaemia and hyperlactaemia (Young *et al.*, 1994), and have moderate affinity for h-αCGRP$_{8-37}$, which antagonizes actions of both amylin and CGRP (Wang *et al.*, 1991).

In the studies described here, we addressed the question of whether amylin and CGRP act through common or distinct receptors to inhibit muscle glycogen synthesis.

Methods *Receptor binding* Binding of [^{125}I]-BH-rat amylin (Bolton-Hunter labelled at the N-terminal lysine) to membranes from the nucleus accumbens of male Harlan Sprague Dawley rats (180-250 g) was measured as previously described (Beaumont *et al.*, 1993), in a modified binding buffer consisting of 20 mM NaHEPES, pH 7.4, 1 mM $MgCl_2$, 1 mg ml^{-1} bacitracin, 1 mg ml^{-1} BSA, 1 μg ml^{-1} phosphoramidon, and 5 μg ml^{-1} bestatin. To measure CGRP receptor binding, rat L6 cell membranes were incubated with 28 pM [^{125}I]-h-αCGRP (^{125}I-labelled at his$_{10}$) and unlabelled peptides, with buffer and experimental methods as described for amylin receptor binding.

Radioiodinated peptides were from Amersham (Arlington Heights, IL, U.S.A.). Amylin, CGRP, and h-αCGRP$_{8-37}$ were from Bachem (Torrance, CA, U.S.A.). AC187 and sCT$_{8-32}$ were synthesized as described (Young *et al.*, 1994).

[^{14}C]-glucose incorporation into muscle glycogen Incorporation of [^{14}C]-glucose into glycogen in soleus muscle strips from fasted rats was measured essentially as previously described (Young *et al.*, 1992). A 4-parameter logistic function was fitted to the data by a curve-fitting programme (InPlot, GraphPad Software, San Diego, CA, U.S.A.) to derive IC$_{50}$s and 95% confidence intervals (CIs). Incubations were performed in quadruplicate with muscles randomly assigned from separate animals. Results are means ± s.e.mean of data from 4-36 muscle strips measured in the indicated number of experiments. Data were analyzed for statistical significance by analysis of variance (ANOVA) and post-hoc Bonferroni test.

Results *Amylin receptor binding* To determine amylin receptor affinity, we measured the ability of peptides to inhibit binding of [^{125}I]-BH-rat amylin to rat nucleus accumbens membranes. As reported previously (Beaumont *et al.*, 1993), rat amylin was more potent than rat αCGRP or rat βCGRP in competing for [^{125}I]-BH-rat amylin binding (Table 1). Among the antagonists, AC187 was the most potent inhibitor of [^{125}I]-BH-amylin binding, with an IC$_{50}$ = 0.48 nM (Table 1).

CGRP receptor binding To determine CGRP receptor affinity, we measured the ability of peptides to compete for [^{125}I]-h-αCGRP binding to rat L6 cell membranes (Poyner *et al.*, 1992). Rat amylin was considerably less potent than rat αCGRP or rat βCGRP in competing for [^{125}I]-h-αCGRP binding (Table 1). Of the antagonists, h-αCGRP$_{8-37}$ was by far the most potent inhibitor of CGRP receptor binding with an IC$_{50}$ = 1.1 nM. For all peptides, IC$_{50}$s for inhibition of [^{125}I]-h-αCGRP binding differed significantly from IC$_{50}$s for inhibition of [^{125}I]-BH-rat amylin binding ($P < 0.05$, Student's unpaired t test).

Functional responses to amylin and CGRP in soleus muscle Rat amylin (EC$_{50}$ = 5 nM, 95% CI = 2.2-11 nM, n = 9) was 3 fold more potent than rat αCGRP (EC$_{50}$ = 15 nM, 95%

[1]Author for correspondence.

Table 1 Inhibition by peptides and antagonists of [^{125}I]-BH-rat amylin binding to rat nucleus accumbens membranes and of [^{125}I]-hCGRP-α binding to L6 cell membranes

Compound	*[^{125}I]-BH-rat amylin rat n. accumbens* (IC_{50} nM)	*[^{125}I]-hCGRP-α rat L6 cells* (IC_{50} nM)
Agonists		
Rat amylin	0.054±0.021 (3)	4.2±0.5 (3)
Rat αCGRP	0.656±0.130 (3)	0.092±0.021 (3)
RatβCGRP	0.105±0.015 (3)	0.030±0.011 (3)
Antagonists		
AC187	0.48±0.16 (5)	73±20 (3)
sCT_{8-32}	1.9±0.37 (7)	2700±1400 (3)
h-$\alpha CGRP_{8-37}$	13±6.2 (4)	1.1±0.22 (3)

Results are means±s.e.mean for the indicated number of separate experiments.

CI=7–32 nM, $n=3$) or rat βCGRP (EC_{50}=14 nM, 95% CI=12–16 nM, $n=3$) at reducing the incorporation of [^{14}C]-glucose into glycogen in insulin-treated soleus muscles from fasted rats (Figure 1).

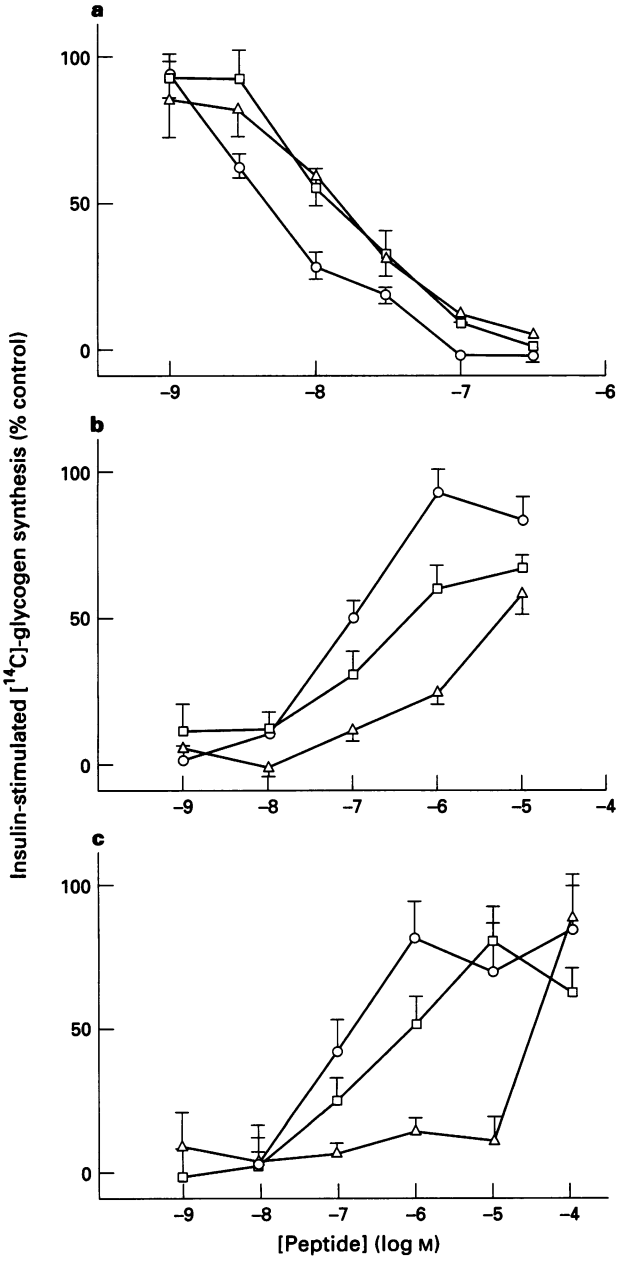

Insulin-treated soleus muscles were incubated with 100 nM rat amylin or 100 nM rat αCGRP in the presence of increasing concentrations of antagonists, resulting in reversal of the inhibition of [^{14}C]-glucose incorporation into glycogen (Figure 1). IC_{50}s (with 95% confidence intervals) for antagonizing rat amylin were AC187=0.10 μM (0.043–0.23 μM, $n=4$), sCT_{8-32}=0.78 μM (0.22–2.8 μM, $n=2$), and h-$\alpha CGRP_{8-37}$=5.7 μM (3.2–9.9 μM, $n=6$). IC_{50}s for antagonizing rat αCGRP were AC187=0.26 μM (0.030–2.3 μM, $n=2$), sCT_{8-32}=1.6 μM (0.23–12 μM, $n=2$) and h-$\alpha CGRP_{8-37}$ =30 μM (12–78 μM, $n=2$). The antagonists had similar rank order potencies (AC187>sCT_{8-32}>h-$\alpha CGRP_{8-37}$) in blocking either rat amylin or rat αCGRP. This rank order of potency corresponded to the rank order for inhibiting amylin binding sites in rat nucleus accumbens, and was quite distinct from the rank order for inhibiting CGRP receptor binding in rat L6 cells.

Discussion These results indicate that amylin and CGRP act through a common receptor population to alter glycogen metabolism in rat skeletal muscle. The evidence for this conclusion is pharmacological, based on the similar potencies of antagonists at inhibiting the actions of either rat amylin or rat αCGRP. The relative potency of antagonists strongly suggests that CGRP receptors do not mediate the effects of either CGRP or amylin on muscle glucose metabolism. Instead, the effects of both amylin and CGRP are mediated by receptors that have high affinity for AC187 and sCT_{8-32}, like the amylin receptors concentrated in the nucleus accumbens region.

Data available from functional studies are consistent with the idea that the effects of amylin on glycogen phosphorylase and glycogen synthase are produced through stimulation of an adenylyl cyclase-coupled receptor. Amylin stimulates increased cyclic AMP in intact rat soleus muscle with an EC_{50}=0.3 nM (Pittner *et al.*, 1994).

The pharmacological evidence described here indicates that CGRP receptors measured by [^{125}I]-CGRP binding to rat muscle membranes (Chantry *et al.*, 1991) do not regulate muscle glucose metabolism. One function that has been proposed for CGRP receptors in skeletal muscle is regulation of nicotinic cholinoceptor expression and sensitivity (New &

Figure 1 (a) Inhibition of insulin-stimulated [^{14}C]-glucose incorporation into glycogen in isolated soleus muscles by rat amylin (○), rat αCGRP (□), or rat βCGRP (△). Rat amylin differed significantly ($P<0.05$, ANOVA) from rat αCGRP at 3, 10, and 100 nM and from rat βCGRP at 10 and 100 nM. Inhibition of the effects of (b) 100 nM rat amylin or (c) 100 nM rat αCGRP on [^{14}C]-glucose incorporation into soleus muscle glycogen by AC187 (○), sCT_{8-32} (□), or h-$\alpha CGRP_{8-37}$ (△). AC187 differed significantly ($P<0.05$, ANOVA) from h-$\alpha CGRP_{8-37}$ at 0.1 and 1 μM. Means±s.e.mean of at least 4 soleus muscle strips.

Mudge, 1986). CGRP receptors may also be present in vascular elements in membranes prepared from skeletal muscles.

In conclusion, inhibition of muscle glycogen synthesis by amylin and CGRP appears to be mediated by shared receptors that have pharmacological characteristics of amylin receptors, not CGRP receptors.

References

BEAUMONT, K., KENNEY, M.A., YOUNG, A.A. & RINK, T.J. (1993). High affinity amylin binding sites in rat brain. *Mol. Pharmacol.*, **44,** 493–497.

CHANTRY, A., LEIGHTON, B. & DAY, A.J. (1991). Cross-reactivity of amylin with calcitonin-gene-related peptide binding sites in rat liver and skeletal muscle membranes. *Biochem. J.*, **277,** 139–43.

LEIGHTON, B. & COOPER, G.J. (1988). Pancreatic amylin and calcitonin gene-related peptide cause resistance to insulin in skeletal muscle in vitro. *Nature*, **335,** 632–635.

NEW, H.V. & MUDGE, A.W. (1986). Calcitonin gene-related peptide regulates muscle acetylcholine receptor synthesis. *Nature*, **323,** 809–811.

PITTNER, R.A., ALBRANDT, K., BEAUMONT, K., GAETA, L.S.L., KODA, J.E., MOORE, C.X., RITTENHOUSE, J. & RINK, T.J. (1994). Molecular physiology of amylin. *J. Cell. Biochem.*, **55S,** 19–28.

POYNER, D.R., ANDREW, D.P., BROWN, D., BOSE, C. & HANLEY, M.R. (1992). Pharmacological characterization of a receptor for calcitonin gene-related peptide on rat, L6 myocytes. *Br. J. Pharmacol.*, **105,** 441–447.

WANG, M.W., YOUNG, A.A., RINK, T.J. & COOPER, G.J. (1991). $^{8-37}$h-CGRP antagonizes actions of amylin on carbohydrate metabolism in vitro and in vivo. *Febs. Lett.*, **291,** 195–8.

YOUNG, A.A., GEDULIN, B., GAETA, L.S.L., PRICKETT, K.S., BEAUMONT, K., LARSON, E. & RINK, T.J. (1994). Selective amylin antagonist suppresses rise in plasma lactate after intravenous glucose in the rat. *FEBS Lett.*, **343,** 237–241.

YOUNG, A.A., GEDULIN, B., WOLFE-LOPEZ, D., GREENE, H., RINK, T.J. & COOPER, G.S. (1992). Amylin and insulin in rat soleus muscle: dose-responses for co-secreted non-competitive antagonists. *Am. J. Physiol.*, **263,** E274–E281.

(Received January 27, 1995
Accepted March 30, 1995)

British Journal of Pharmacology (1995) 115, 717-722

Release of endothelium-derived hyperpolarizing factor (EDHF) by M_3 receptor stimulation in guinea-pig coronary artery

Anna K.M. Hammarström, [1]Helena C. Parkington & Harold A. Coleman

Department of Physiology, Monash University, Clayton, Victoria, 3168, Australia

1 The muscarinic receptor subtype(s) involved in the release of endothelium-derived hyperpolarizing factor (EDHF) were studied in the guinea-pig coronary artery by recording the membrane potential in the smooth muscle cells with intracellular microelectrodes.

2 Acetylcholine (ACh, pD_2 6.68) was 10 times more potent than the M_2 agonist, oxotremorine (pD_2 5.65) and 500 fold more potent than the M_1 agonist, McN-A-343 (pD_2 3.95) in evoking the EDHF hyperpolarization.

3 The M_3 muscarinic antagonist, 4-diphenylacetoxy-N-methylpiperidine methiodide (4-DAMP) was the most potent (pA_2 9.5) in inhibiting the release of EDHF evoked by ACh, being more potent than pirenzepine (pA_2 6.7), and AFDX-116 (pA_2 6.1) which preferentially block M_1 and M_2 receptors, respectively.

4 These results suggest that EDHF is released from the endothelium of the guinea-pig coronary artery upon the activation of the muscarinic M_3 receptor subtype.

Keywords: Coronary artery; endothelium; hyperpolarization; EDHF; muscarinic receptors; M_3 receptors

Introduction

Stimulation of muscarinic receptors on the endothelium in most vascular beds produces muscle relaxation upon the release of up to three relaxing agents; endothelium-derived relaxing factor (EDRF), identified as nitric oxide (NO), prostacyclin (PGI_2) and endothelium-derived hyperpolarizing factor (EDHF), all of which are also capable of hyperpolarizing the underlying smooth muscle (Parkington *et al.*, 1993). Pharmacological and radioligand binding studies suggest that the muscarinic receptor involved in the release of both NO and PGI_2 is of the M_3 subtype (see review Eglen & Whiting, 1990, Jaiswal & Malik, 1990; Adeagbo & Triggle, 1993). The muscarinic receptor involved in the release of EDHF is still controversial. It has been proposed that EDHF is released upon M_1 receptor stimulation because atropine, a non-specific agonist, was as effective as pirenzepine at inhibiting the hyperpolarization induced by acetylcholine (ACh) but was 100 times more potent at inhibiting the ACh-induced relaxation in rabbit saphenous artery (Komori & Suzuki, 1987b). These same authors (Komori & Suzuki, 1987a) found that oxotremorine did not evoke membrane hyperpolarization in the rabbit saphenous artery, suggesting that M_2 receptors were not involved in initiating the endothelium-dependent hyperpolarization. In another study, atropine was found to be more potent than pirenzepine at inhibiting the ACh-evoked hyperpolarization in the guinea-pig circumflex coronary artery, suggesting that M_1 receptors were not involved in the endothelium-derived hyperpolarization in this artery (Keef & Bowen, 1989). In the perfused rat mesenteric arterial bed, *p*-F-HHSiD (a M_3 receptor antagonist) was more potent than pirenzepine at inhibting the EDHF-induced, L-NAME-and indomethacin-insensitive dilatation, suggesting that EDHF release occurs through M_3 receptor stimulation (Adeagbo & Triggle, 1993). However, it has been suggested that *p*-F-HHSiD may not be a suitable probe with which to distinguish between M_3 and M_1 receptors with any degree of confidence (Eglen *et al.*, 1990).

The aim of the present study was to clarify the nature of the muscarinic receptor(s) involved in the release of EDHF. The release of EDHF cannot be studied directly since its chemical identity remains elusive. The hyperpolarization it induces is particularly large in the guinea-pig coronary artery which makes this a suitable tissue in which to investigate this factor. The component of hyperpolarization evoked by EDHF is clearly distinguishable from the components induced by NO and PGI_2, whereas the relaxations merge into one (Parkington *et al.*, 1995). The relationship between the hyperpolarization and relaxation in guinea-pig coronary artery has been studied in detail (Parkington *et al.*, 1995). NO and PGI_2 can produce relaxation in the absence of hyperpolarization. In contrast, the relaxation evoked by EDHF appears to be elicited through hyperpolarization of the smooth muscle cells. Thus, the hyperpolarization response to EDHF was studied in preference to the relaxation because it was clearly separable and closely associated with relaxation.

The responses to three muscarinic agonists; ACh, (non-specific), McN-A-343, M_1 and oxotremorine, M_2 were studied. The effect of three antagonists; pirenzepine, M_1, AFDX-116, M_2 and 4-DAMP, M_3 on the hyperpolarizations induced by ACh were assessed in guinea-pig coronary artery. Some of these results have been presented in abstract form (Hammarström *et al.*, 1993).

Methods

Preparation

Guinea-pigs of either sex, 250-800 g, were killed by decapitation and their hearts removed. The left descending main coronary artery, from the coronary sinus to its entry into the cardiac muscle underneath the pulmonary artery, was dissected free. Ring segments of artery (1-2 mm in length) were threaded with a pair of wires (40 μm in diameter) and fixed in two supports in a myograph. One support was attached to a micrometer screw and the other to a force transducer (Mulvany & Halpern, 1977). Segments were continuously superfused with physiological saline solution (PSS) (mM): NaCl 120, KCl 5, $CaCl_2$ 2.5, $MgSO_4$ 1.2, KH_2PO_4 1, $NaHCO_3$ 25, glucose 11, bubbled with O_2 : CO_2, 95% : 5% and maintained at 35°C. The flow of PSS was at a rate of 3.6 ml min^{-1} in the bath the capacity of which was approximately 0.5 ml. The segments were stretched incremently until their tension was equivalent to a transmural pressure of 60 mmHg, the mean arterial pressure in guinea-pigs. Membrane potential recordings were made with

[1] Author for correspondence.

conventional glass intracellular microelectrodes filled with 1 M KCl and having resistances of 80–100 MΩ as described by Parkington *et al.* (1993).

Agonist potency (pD_2)

The peak amplitude (in mV) of the transient component of the hyperpolarization, attributable to EDHF, recorded in response to each agent was plotted against the concentrations of agonist. A sigmoid curve was fitted to the concentration-response curves by a least-squares method in the computer software package InPlot (GraphPad Software Inc.). The concentration of agonist which was effective in producing a response that was 50% of maximal hyperpolarization (EC_{50}) was determined from the curve. The EC_{50} and slope of the concentration-response curve (20–80%) obtained for each preparation were used to generate an averaged curve that was representative of all preparations in each group. pD_2 ($-\log EC_{50}$), has been used as a measure of agonist potency throughout this study. The maximum amplitude of the hyperpolarization for each agonist has been designated V_{max} according to convention.

Antagonist potency (pA_2)

The concentration-response curves to ACh were repeated in the presence of three concentrations of each antagonist. Only 1–2 concentrations of antagonist were tested in each preparation. When two concentrations were applied to the same preparation, the antagonist was washed out and a new control concentration-response curve was established before the second antagonist concentration was applied. Antagonists were allowed to equilibrate for 20 min before repeating the concentration-response curve to ACh. The method of Arunlakshana & Schild (1959) was used to determine pA_2 values. The highest concentration of AFDX-116 caused a depolarization of the smooth muscle (5 ± 1 mV, $n=8$). This made the hyperpolarizations appear larger than in the absence of AFDX-116 due to an increase in the driving force for potassium, to which the conductance increases during the hyperpolarization (Bolton *et al.*, 1984). The peak amplitudes of these hyperpolarizations in the presence of high concentrations of AFDX-116 were therefore corrected for these changes in driving force which involved scaling the data according to the Goldman-Hodgkin-Katz equation for a potassium current to give the value expected with an unchanging membrane potential. In these calculations an equilibrium potential for potassium of −90 mV was assumed (Hirst & Edwards, 1989). These calculations had no significant effect on the pD_2 values.

Statistical analysis of data

The mean ± standard error of the mean (s.e.mean) of responses are quoted throughout. The n values quoted represent the number of preparations studied. Unpaired t tests were used to test and a significance level of $P<0.05$ was used throughout.

Solutions

Acetylcholine, oxotremorine, McN-A-343, L-NAME, pirenzepine and 4-DAMP were all dissolved in distilled water, to a stock of 10^{-2} M, and diluted to final concentrations in PSS. Indomethacin (10^{-2} M) was dissolved in 0.1 M Na_2CO_3 and diluted in PSS. Preparations were allowed to equilibrate for at least 20 min with L-NAME before and during the time that any agonists were applied. AFDX-116 was dissolved in dimethyl sulphoxide (DMSO). DMSO, 3 : 1000 dilution, had no effect on either membrane potential or on the amplitude of the hyperpolarizations induced by ACh ($n=2$).

Drugs

The following were used: acetylcholine Cl (Merck) (ACh); oxotremorine sesquifumerate salt; 4-(N[3-chlorophenyl]-carbamoyloxy)-2-butynyltrimethylammonium chloride (McN-A-343); N^{ω}-nitro-L-arginine-methyl-ester (L-NAME); indomethacin and pirenzepine dihydrochloride (all from Sigma), 11-([2-{(diethylamino)methyl}-1-piperidinyl]acetyl)-5,11-dihydro-6H-pyrido[2,3-b][1,4]benzodizepine-6-one (AFDX-116, a gift from Boehringer Ingleheim), 4-diphenylacetoxy-N-methylpiperidine methiodide (4-DAMP, Research Biochemicals Inc.); sodium nitroprusside (Ajax Chemicals); 5-[(E)-(1S,5S,6R,7R)-7-hydroxy-6-[(E)-(3S,4RS)-3-hydroxy-4-methyl-1-octen-6-inyl]-bicyclo[3.3.0]-octan-3-ylidene]-pentanoic acid (iloprost, a gift from Schering, Germany). Drugs were applied using two methods: for prolonged exposure, drugs were added to the superfusate. For short exposures, ACh, oxotremorine and McN-A-343 were applied for 10 s by direct injection into the superfusion line with a 1 s delay between the point of injection and the preparation. The concentration of agonist reached a steady state within 3–4 s (see Parkington *et al.*, 1993). Drugs to be injected close to the preparation were dissolved in PSS. Agonists were injected in 5–50 μl into the perfusion line. The injection of up to 250 μl of PSS alone had no effect on membrane potential.

Results

One minute and 10 s application of acetylcholine

The resting membrane potential of intact coronary artery preparations, in the absence of NO and prostaglandin synthesis inhibitors, was −59 ± 1 mV ($n=21$). The hyperpolarizations evoked by including ACh in the superfusate for 0.5–1 min, were biphasic and very long in duration, up to 15–20 min in response to 10^{-5} M ACh. This duration was reduced to 1–2 min in the presence of both L-NAME (2×10^{-5} M) and indomethacin (10^{-6} M). The pD_2 for ACh-induced hyperpolarization in the presence of both blockers was 6.86 ± 0.08 ($n=12$) and the V_{max} was 21 ± 1 mV (Figure 1).

Injection of ACh for 10 s evoked a complex hyperpolarization consisting of a transient component followed by a slower, more prolonged component. The resting membrane potential was depolarized significantly to −46 ± 1 mV ($n=44$) in the presence of L-NAME (2×10^{-5} M) and the onset of the slow component of hyperpolarization was very much delayed (confirming Figure 4 of Parkington *et al.*, 1993). In the presence of both L-NAME and indomethacin (10^{-6} M) the resting membrane potential was −45 ± 1 mV $n=37$ and the slow component of the hyperpolarization was abolished. The amplitude of the transient component which remained, and at-

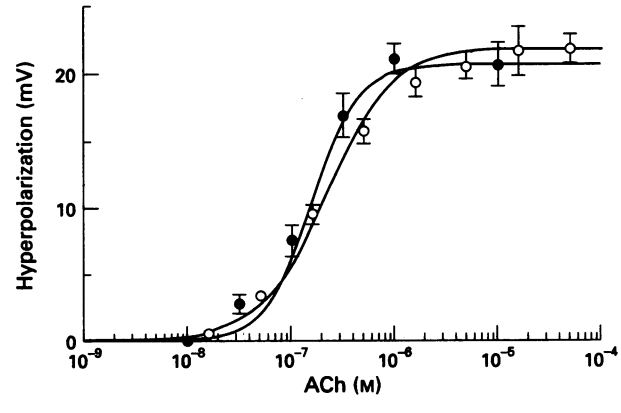

Figure 1 Neither the pD_2 nor the V_{max} were different when acetylcholine (ACh) was applied for 1 min (●, pD_2 6.86 ± 0.08, V_{max} 21 ± 1 mV, $n=12$) compared with 10 s (○, pD_2 6.68 ± 0.04, V_{max} 22 ± 1 mV, $n=38$). Thus, a 10 s injection was used for most experiments throughout this study.

tributable to EDHF, was larger due to the depolarization. At the level of the resting potential in control solution, i.e. after correcting for the change in driving force (see Methods), the peak amplitude of the response in L-NAME and indomethacin was not different from the peak amplitude of the transient component of the response in control solution, similar to previous results (Parkington *et al.*, 1993). The pD_2 (6.68 ± 0.08, $n = 38$) or the V_{max} (22 ± 1 mV) in response to 10 s exposure to ACh, in the presence of L-NAME alone, were not different when compared with 1 min application in the presence of both L-NAME and indomethacin (Figure 1).

Effect of other muscarinic agonists on membrane potential

The hyperpolarizations evoked by oxotremorine and McN-A-343 in control solution were similar in appearance and duration to those induced by ACh (Figure 2a). Due to the good separation between the transient component attributable to EDHF and the slow component in L-NAME alone, only this blocker was used when establishing full concentration-response curves to the agonists. ACh was 10 times more potent (pD_2 6.68) than oxotremorine (pD_2 5.65) and 500 times more potent than McN-A-343 (pD_2 3.95) (Figure 2b). The V_{max} evoked by ACh and oxotremorine were not significantly different. However, the maximum hyperpolarization attributable to EDHF evoked by McN-A-343, up to concentrations of 10^{-3} M, was only half the V_{max} elicited by ACh or oxotremorine (Figure 2b).

Effect of muscarinic antagonists on the EDHF evoked response

The effects of three muscarinic antagonists on the hyperpolarization in response to ACh-evoked release of EDHF from the endothelium were investigated. Three concentrations of each antagonist were applied; pirenzepine ($n = 12$, Figure 3a), AFDX-116 ($n = 11$, Figure 3b) and 4-DAMP ($n = 9$, Figure 3c) all caused concentration-dependent shifts of the hyperpolarization curve in response to ACh to the right. 4-DAMP proved to be the most potent antagonist, pA_2 9.5, being more potent than pirenzepine, pA_2 6.8 or AFDX-116, pA_2 6.1. The V_{max} was progressively reduced by increasing concentrations of pirenzepine (Figure 3a). A reduction of maximal responses by pirenzepine has been observed by others (Garcia-Villalon *et al.*, 1990).

The slope of the Schild plot for each of the antagonists was not different from unity, indicating that they were all acting in a competitive manner (Figure 4).

In addition, the effects of pirenzepine (10^{-6} M) and 4-DAMP (3×10^{-9} M) on the hyperpolarization evoked by longer exposures (0.5–1 min) to ACh were examined. The concentration-response curve in response to 0.5–1 min ex-

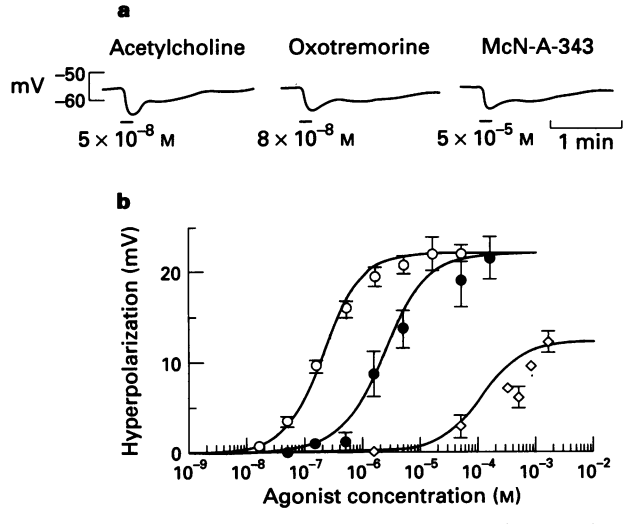

Figure 2 Acetylcholine (ACh) oxotremorine and McN-A-343 induced biphasic hyperpolarizations in control solution that were similar in appearance (a). [Responses obtained in separate preparations.] The transient component was isolated by including N^{ω}-nitro-L-arginine-methyl-ester (L-NAME) in the superfusate and full concentration-response curves were obtained for ACh (○) oxotremorine (●) and McN-A-343 (◇). pD_2 for ACh, 6.68 ± 0.04 ($n = 38$), oxotremorine, 5.65 ± 0.14 ($n = 5$) and McN-A-343, 3.95 ± 0.25 ($n = 5$). The V_{max} for ACh and oxotremorine were not different (22 ± 1 mV, $n = 38$ and 22 ± 2 mV, $n = 5$ respectively), while that of McN-A-343 was significantly less (12 ± 1 mV, $n = 2$).

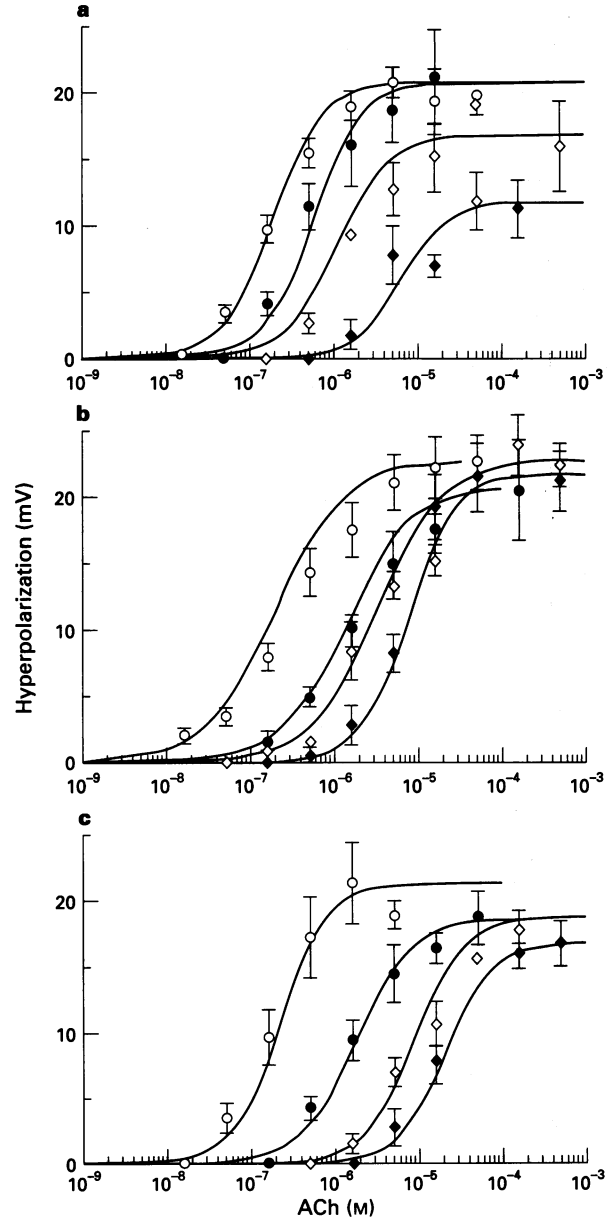

Figure 3 Full concentration-response curves to acetylcholine (ACh) were obtained in control (○) and in the presence of pirenzepine (3×10^{-7}●, 10^{-6}M ◇, and 3×10^{-6}M◆) (a); AFDX-116 (3×10^{-6}M●, 10^{-5}M◇, and 3×10^{-5}M◆) (b); 4-DAMP (3×10^{-9}M●, 10^{-8}M◇, and 3×10^{-8}M◆) (c). All antagonists shifted the concentration-response curve to the right in a concentration-dependent manner. Data in (b) have been corrected for non-linear summation (see Methods).

posure to ACh was shifted to the right by pirenzepine (Figure 5a(ii)) and 4-DAMP (Figure 5b(ii)) and the shift was not different compared with the shift in response to 10 s applications of ACh (Figure 5a(i),b(i)). The V_{max} in response to both 10 s and 1 min application of ACh were reduced by pirenzepine (Figure 5a), similar to that described above.

Direct effect of ACh on the smooth muscle

Earlier studies (Bolton *et al.*, 1984; Bény & Brunet, 1987) have shown that cholinoceptor agonists can have a direct effect on vascular smooth muscle, an action which might contaminate the endothelium-derived hyperpolarizing response observed in the present study. The direct effects of ACh on the smooth muscle were investigated in 12 preparations of coronary artery denuded of their endothelium. A 1 min application of ACh (10^{-6}–10^{-4} M) caused only a small depolarization of 3 ± 0.5 mV in 9 of the 12 preparations (data not shown). There was no change in membrane potential in response to ACh in the remaining 3 tissues. To ensure that the removal of the endothelium had not affected the ability of the smooth muscle to hyperpolarize, the smooth muscle was made to hyperpolarize with an endothelium-independent agonist, either sodium nitroprusside (a NO donor) or iloprost (a stable analogue of PGI_2). Thus, the direct effects of ACh on the smooth muscle of the guinea-pig coronary artery appear to be weak, as has been suggested (Parkington *et al.*, 1993), and hence are unlikely to be contaminating the endothelium-derived hyperpolarization described in this study.

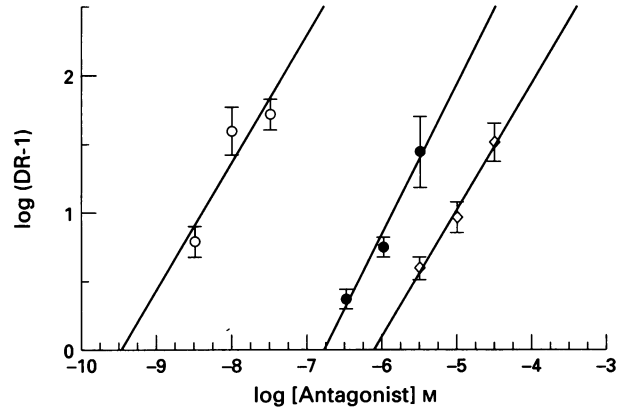

Figure 4 Log (dose-ratio −1) were plotted against the concentration of antagonist 4-DAMP (○), pirenzepine (●), and AFDX-116 (◇) (Arunlakshana & Schild, 1959). 4-DAMP was the most potent (pA_2 9.5) antagonist in inhibiting the release of EDHF while pirenzepine (pA_2 6.8) was slightly more potent than AFDX (pA_2 6.1). The slopes of the Schild plots were not different from unity, (pirenzepine 1.1 ± 0.2. AFDX-116 0.9 ± 0.1 and 4-DAMP 0.9 ± 0.4) indicating that the antagonism of all three antagonists was of a competitive nature.

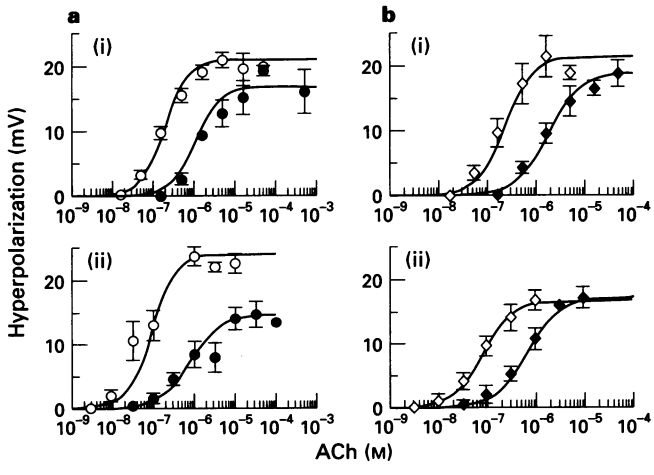

Figure 5 The effects of (a) 10^{-6} M pirenzepine (●) and (b) 3×10^{-9} M 4-DAMP (◆) on the hyperpolarizations evoked by 10 s applications (i) were compared with those in response to 0.5–1 min exposures (ii) (control ○ and ◇). The shift of the concentration-response curves caused by the antagonists was not different when longer exposure times were used (dose-ratio 6.8 ± 0.8 (n = 4) for 1 min compared to 9.0 ± 1.5 ($n = 4$) for 10 s and dose-ratio 10.4 ± 3.7 ($n = 5$) for 0.5 min compared to 8.4 ± 1.4 ($n = 6$) for 10 s).

Discussion

In this study we have shown that the muscarinic receptor subtype involved in the release of EDHF is likely to be of the M_3 subtype as demonstrated by the ranked potencies of the agonists ACh > oxotremorine > > McN-A-343 and the ranked affinities of the three antagonists, 4-DAMP > > pirenzepine > AFDX-116. These results differ from those reported for rabbit saphenous artery (Komori & Suzuki, 1987b), but are in agreement with observations in the rat mesenteric bed (Adeagbo & Triggle, 1993) and in the guinea-pig circumflex coronary artery (Keef & Bowen, 1989). However, only in the rat mesenteric vascular bed has an antagonist potency, pA_2, been determined. The M_3 antagonist, *p*-F-HHSiD, had a pA_2 8.47 in the rat perfused mesenteric arterial bed whereas pirenzepine in the same concentration-range had no effect. The pA_2 value observed for *p*-F-HHSiD is somewhat higher than that obtained by other workers for an M_3 receptor involvement (pA_2 7.7–7.9 in rat aorta, Eglen & Whiting, 1990; pA_2 7.18 in rabbit aorta, Jaiswal *et al.*, 1991).

The high pD_2 values for ACh obtained in the present study are very similar to the potency profile obtained by other workers for an M_3 receptor involvement in the endothelium-dependent relaxation evoked by ACh in rabbit aorta, bovine coronary artery and in the guinea-pig circumflex coronary artery (Choo *et al.*, 1986; Keef & Bowen, 1989; Brunner *et al.*, 1991). In contrast, McN-A-343, an M_1 agonist, had a low potency in the rat aorta (pD_2 4.2, Eglen & Whiting, 1990). Its potency was similarly low in the present study (pD_2 3.95), and it elicited a hyperpolarization the amplitude of which was only half of that evoked by ACh or oxotremorine. This may be explained by a partial agonists action of McN-A-343 in the guinea-pig coronary artery. Oxotremorine was 10 times less potent than ACh (present study) and has not been shown to evoke hyperpolarizations in rabbit saphenous artery (Komori & Suzuki, 1987a). Oxotremorine is more selective for M_2 receptors in the brain (Potter *et al.*, 1984).

According to receptor theory, the dissociation constant for a competitive antagonist acting on an identical drug receptor should be the same regardless of the agonist or preparation used (Kenakin, 1984). Pirenzepine distinguishes between M_1 (pA_2 8.1) and M_3 (pA_2 6.8) receptor subtypes (Hulme *et al.*, 1990). The low affinity for pirenzepine in our study (pD_2 6.8) indicates that the subtype involved in the release of EDHF is not M_1. The potency of AFDX-116 (present study) was also low and within the range of other results published for the endothelium-dependent relaxation (Duckles *et al.*, 1987). The high affinity for 4-DAMP and the low affinity for AFDX-116 are inconsistent with the characteristics of the M_2 receptor identified in other anatomical locations (Eglen & Whiting, 1990). Although there is some variability in the values determined for antagonists using different tissues and techniques, the pA_2 values observed here for pirenzepine, AFDX-116 and 4-DAMP are similar to those found in other arteries (Eglen & Whiting, 1985; Hynes *et al.*, 1986; Choo *et al.*, 1986; Duckles, 1988). In addition, since the Schild slopes for all three an-

tagonists did not differ from unity, it is possible to rule out the presence of a heterogeneous receptor population (Kenakin, 1987).

With the recent finding of another two muscarinic subtypes, M_4 and M_5, the possibility that one of these subtypes may be involved in the release of EDHF has to be considered. M_4 receptors in the rabbit lung and NG-108-15 cells (Lazareno *et al.*, 1990) as well as those found for cloned m4 and m5 receptors (Buckley *et al.*, 1989) are pharmacologically distinct from the M_3 receptor subtype. Pirenzepine has been shown to bind to M_4 receptors with relatively high affinity (Peralta *et al.*, 1987; Dörje *et al.*, 1991), and the affinity of AFDX-116 for M_4 receptors was found to be higher than the affinity for M_3 receptors (Dörje *et al.*, 1991). M_5 receptors have so far been identified only in neuronal tissue and their function has yet to be established.

The relationship between the hyperpolarization and relaxation in this tissue has been studied previously in our laboratory (Parkington *et al.*, 1995). The hyperpolarization and relaxation attributable to EDHF appeared to be closely linked. The hyperpolarization always preceded the relaxation. In addition, no relaxation was observed under conditions in which the hyperpolarization was abolished. In contrast, both endogenous and exogenous NO and PGI_2 could both hyperpolarize and relax arterial smooth muscle; however, the hyperpolarization was not essential for the relaxation in response to either of these two agents (Parkington *et al.*, 1995). Thus, EDRF/NO and PGI_2 induce relaxation via the second messengers cyclic GMP and cyclic AMP, respectively.

In conclusion, the possibility of independent mechanisms of release of EDHF versus NO and PGI_2 was exciting since it could provide a basis for preferential therapeutic control of endothelium-dependent relaxation. However, the present results demonstrate that the M_3 receptor mediates the release of EDHF. Thus, it is likely that all three endothelium-derived vasodilators are released through stimulation of the same muscarinic receptor subtype in most species and vessels studied to date.

The authors thank Professor M.E. Holman and Dr R.J. Lang for helpful discussion of the manuscript and Ms M. Mulholland for preparing the figures. The work was supported by the National Heart Foundation of Australia and the National Health and Medical Research Council of Australia. AFDX-116 was a gift from Boehringer Ingleheim and Iloprost was a gift from Schering (Germany).

References

ADEAGBO, A.S.O. & TRIGGLE, C.R. (1993). Varying extracellular [K^+]: A functional approach to separating EDHF- and EDNO-related mechanisms in perfused rat mesenteric arterial bed. *J. Cardiovasc. Pharmacol.*, **21**, 423–429.

ARUNLAKSHANA, O. & SCHILD, H.O. (1959). Some quantitative uses of drug antagonists. *Br. J. Pharmacol. Chemother.*, **14**, 48–58.

BÉNY, J.-L. & BRUNET, P.C. (1987). Electrophysiological and mechanical effects of substance P and acetylcholine on rabbit aorta. *J. Physiol.*, **398**, 277–289.

BOLTON, T.B., LANG, R.J. & TAKEWAKI, T. (1984). Mechanisms of action of noradrenaline and carbachol on smooth muscle of guinea-pig anterior mesenteric artery. *J. Physiol.*, **351**, 549–572.

BRUNNER, F., KÜHBERGER, E., GROSCHNER, K., PÖCH, G. & KUKOVETZ, W.R. (1991). Characterization of muscarinic receptors mediating endothelium-dependent relaxation of bovine coronary artery. *Eur. J. Pharmacol.*, **200**, 25–33.

BUCKLEY, N.J., BONNER, T.I., BUCKLEY, C.M. & BRANN, M.R. (1989). Antagonist binding properties of five cloned muscarinic receptors expressed in CHO-K1 cells. *Mol. Pharmacol.*, **35**, 469–476.

CHOO, L.K., MALTA, E. & MITCHELSON, F. (1986). The affinity of some selective muscarinic receptor antagonists for the muscarinic receptor mediating endothelial-dependent relaxation of the rabbit and rat thoracic aorta. *J. Pharm. Pharmacol.*, **38**, 843–845.

DÖRJE, F., WESS, J., LAMBRECHT, G., TACKE, G., MUTSCHLER, E. & BRANN, M.R. (1991). Antagonist binding profiles of five cloned human muscarinic receptor subtypes. *J. Pharmacol. Exp. Ther.*, **256**, 727–733.

DUCKLES, S.P. (1988). Vascular muscarinic receptors: Pharmacological characterization in the bovine coronary artery. *J. Pharmacol. Exp. Ther.*, **246**, 929–934.

DUCKLES, S.P., YAMAMURA, H.I. & LEE, V. (1987). AFDX-116 discriminates between muscarinic M_2 receptors of the heart and vasculature. *Life Sci.*, **40**, 1507–1511.

EGLEN, R.M., CORNETT, C.M. & WHITING, R.L. (1990). Interaction of p-F-HHSiD (p-Fluoro-hexahydrosila-difenidol) at muscarinic receptors in guinea-pig trachea. *Naunyn Schmied. Arch. Pharmacol.*, **342**, 394–399.

EGLEN, R.M. & WHITING, R.L. (1985). Determination of the muscarinic receptor subtype mediating vasodilatation. *Br. J. Pharmacol.*, **84**, 3–5.

EGLEN, R.M. & WHITING, R.L. (1990). Heterogeneity of vascular muscarinic receptors. *J. Auton. Pharmacol.*, **19**, 233–245.

GARCIA-VILLALON, A.L., EHLERT, F.J., KRAUSE, D.N. & DUCKLES, S.P. (1990). Muscarinic M_1 receptors stimulate phosphoinositide hydrolysis in bovine cerebral arteries. *Life Sci.*, **47**, 2163–2169.

HAMMARSTRÖM, A.K.M., PARKINGTON, H.C. & COLEMAN, H.A. (1993). M_3 receptor stimulation evokes EDHF release in the guinea-pig coronary artery. *Proc. Aust. Physiol. Pharmacol. Soc.*, **24**, 154P.

HIRST, G.D.S. & EDWARDS, F.R. (1989). Sympathetic neuroeffector transmission in arteries and arterioles. *Physiol. Rev.*, **69**, 546–604.

HULME, E.C., BIRDSALL, N.J.M. & BUCKLEY, N.J. (1990). Muscarinic receptor subtypes. *Annu. Rev. Pharmacol. Toxicol.*, **30**, 633–673.

HYNES, R.M., BANNER, W. Jr., YAMAMURA, H.I. & DUCKELS, S.P. (1986). Characterization of muscarinic receptors of the rabbit ear artery smooth muscle and endothelium. *J. Pharmacol. Exp. Ther.*, **238**, 100–105.

JAISWAL, N., LAMBRECHT, G., MUTSCHLER, E., TACKE, R. & MALIK, K.U. (1991). Pharmacological characterization of the vascular muscarinic receptors mediating relaxation and contraction in rabbit aorta. *J. Pharmacol. Exp. Ther.*, **258**, 842–850.

JAISWAL, N. & MALIK, K.U. (1990). Prostacyclin synthesis elicited by cholinergic agonists is linked to activation of M_2 alpha and M_2 beta receptors in rabbit aorta. *Prostaglandins*, **39**, 267–280.

KEEF, K.D. & BOWEN, S.M. (1989). Effect of ACh on electrical and mechanical activity in guinea-pig coronary arteries. *Am. J. Physiol.*, **257**, H1096–1103.

KENAKIN, T.P. (1984). The classification of drugs and drug receptors in isolated tissues. *Pharmacol. Rev.*, **36**, 165–222.

KENAKIN, T.P. (1987). *Pharmacologic Analysis of Drug-Receptor Interaction.* New York: Raven Press.

KOMORI, K. & SUZUKI, H. (1987a). Electrical responses of smooth muscle cells during cholinergic vasodilation in the rabbit saphenous artery. *Circ. Res.*, **61**, 586–593.

KOMORI, K. & SUZUKI, H. (1987b). Heterogeneous distribution of muscarinic receptors in the rabbit saphenous artery. *Br. J. Pharmacol.*, **92**, 657–664.

LAZARENO, S., BUCKELY, N.J. & ROBERTS, F.F. (1990). Characterization of muscarinic M_4 binding sites in rabbit lung, chicken heart, and NG108-15 cells. *Mol. Pharmacol.*, **38**, 805–815.

MULVANY, M.J. & HALPERN, W. (1977). Contractile properties of small arterial resistance vessels in spontaneously hypertensive and normotensive rats. *Circ. Res.*, **41**, 19–26.

PARKINGTON, H.C., TARE, M., TONTA, M.A. & COLEMAN, H.A. (1993). Stretch revealed three components in the hyperpolarization of guinea-pig coronary artery in response to acetylcholine. *J. Physiol.*, **465**, 459–476.

PARKINGTON, H.C., TONTA, M.A., COLEMAN, H.A. & TARE, M. (1995). Role of membrane potential in endothelium-dependent relaxation of guinea-pig coronary arterial smooth muscle. *J. Physiol.*, **484**, 469–480.

PERALTA, E.G., ASHKENAZI, A., WINSLOW, J.W., SMITH, D.H., RAMACHANDRAN, J. & CAPON, D.J. (1987). Distinct primary structures, ligand-binding properties and tissue specific expression of four human muscarinic acetylcholine receptors. *EMBO. J.*, **6**, 3923–3929.

POTTER, L.T., FLYNN, D.D., HANCHETT, H.E., KALINOSKI, D.L., LUBER-NAROD, J. & MASH, D.C. (1984). Independent M_1 and M_2 receptors: ligands, autoradiography and functions. *Trends. Pharmacol. Sci.*, **5 (Suppl)**, 22–31.

(Received January 19, 1995
Accepted March 2, 1995)

British Journal of Pharmacology (1995) 115, 723-732

Comparative effects of activation of soluble and particulate guanylyl cyclase on cyclic GMP elevation and relaxation of bovine tracheal smooth muscle

*Samuel C. Ijioma, *R.A. John Challiss & *†,[1]John P. Boyle

*Department of Cell Physiology & Pharmacology, and †MRC Centre for Mechanisms of Human Toxicity, University of Leicester, University Road, Leicester LE1 9HN

1 The effects of nitric oxide-donating compounds and atrial natriuretic peptide on cyclic GMP accumulation and mechanical tone were compared with the effects of isoprenaline in bovine tracheal smooth muscle.

2 Sodium nitroprusside, glyceryl trinitrate, S-nitroso-N-acetylpenicillamine (SNAP), atrial natriuretic peptide and isoprenaline each caused concentration-dependent inhibitions of histamine-maintained tone (EC_{50} values 320 ± 80, 150 ± 45, $14{,}000 \pm 4{,}000$, 2.8 ± 0.8 and 6.6 ± 4.3 nM respectively).

3 When compared with their effects on histamine-induced tone, sodium nitroprusside was equally potent and effective in causing relaxation of methacholine-supported tone (EC_{50} 290 ± 90 nM) while isoprenaline was as effective, but less potent (EC_{50} 30 ± 7 nM). SNAP was more potent and equi-effective as a relaxant of methacholine-supported tone (EC_{50} 340 ± 140 nM). At the maximum concentrations of glyceryl trinitrate and atrial natriuretic peptide tested against methacholine-supported tone, relaxations of 52% and 14% of the isoprenaline maximum were seen.

4 Sodium nitroprusside, glyceryl trinitrate and atrial natriuretic peptide each induced concentration-dependent increases in cyclic GMP accumulation. The time-courses of accumulation correlated closely with the relaxant actions of these compounds.

5 Pretreatment of tracheal smooth muscle with sodium nitroprusside or SNAP caused a rightward shift of the concentration-effect curve for histamine while reducing the maximum response.

6 LY 83583, a putative guanylyl cyclase inhibitor, caused a concentration-dependent reduction in basal cyclic GMP accumulation in tracheal smooth muscle and inhibited the effects of sodium nitroprusside on cyclic GMP accumulation.

7 LY 83583 also inhibited the relaxation of histamine-supported tone by glyceryl trinitrate, sodium nitroprusside, SNAP and atrial natriuretic peptide, and also sodium nitroprusside- and SNAP-induced relaxation of methacholine-supported tone. However, it had no significant effect on glyceryl trinitrate-induced relaxation of methacholine-supported tone.

8 It is concluded that the relaxant actions of sodium nitroprusside, glyceryl trinitrate, SNAP and atrial natriuretic peptide follow as a result of their ability to activate either soluble or particulate guanylyl cyclase leading to cyclic GMP accumulation. Although there does not seem to be any functional difference in the relaxant response to cyclic GMP generated by the particulate as opposed to soluble form(s) of guanylyl cyclase, atrial natriuretic peptide receptor/guanylyl cyclase activation was much less effective in causing relaxation of methacholine-supported tone when compared to activators of soluble guanylyl cyclase.

Keywords: Soluble guanylyl cyclase; sodium nitroprusside; atrial natriuretic peptide; cyclic GMP; tracheal smooth muscle relaxation

Introduction

Agents that cause an increase in intracellular guanosine 3':5'-cyclic monophosphate (cyclic GMP) accumulation, as well as those that increase cyclic AMP, have long been known to possess relaxant actions in airway smooth muscle of a number of species (Katsuki & Murad, 1977; Fiscus *et al.*, 1984; Francis *et al.*, 1988; Ishii & Murad, 1989; Chilvers *et al.*, 1991; Angus *et al.*, 1993). Evidence, obtained mainly from studies of vascular smooth muscle, strongly suggests that the majority of these compounds (e.g. sodium azide, glyceryl trinitrate, sodium nitroprusside, S-nitrosothiols) indirectly activate the soluble cytosolic form of guanylyl cyclase via the release of nitric oxide which then directly activates the enzyme (reviewed by Waldman & Murad, 1987). In contrast, atrial natriuretic peptide, which is also thought to induce relaxation through cyclic GMP accumulation, acts on a specific receptor which is a member of the membrane-spanning (particulate) family of guanylyl cyclase (Waldman & Murad, 1987; Chinkers & Garbers, 1991).

The presence of both of these structurally distinct types of guanylyl cyclase has been inferred in bovine (Katsuki & Murad, 1977; Ishii & Murad, 1989), guinea-pig (O'Donnell *et al.*, 1985; Jansen *et al.*, 1992) and human (Hulks *et al.*, 1990; Belvisi *et al.*, 1992; Angus *et al.*, 1993) tracheal smooth muscle from studies of the relaxant actions of NO-donating compounds and atrial natriuretic peptides. Activation of either form of guanylyl cyclase catalyses the formation of cyclic GMP from GTP which is then thought to exert its relaxant effects in smooth muscle by activating cyclic GMP-dependent protein kinase (Torphy *et al.*, 1982; Fiscus *et al.*, 1984).

Recent studies of non-adrenergic, non-cholinergic inhibitory neurotransmission in airway smooth muscle have demonstrated that inhibitors of nitric oxide synthase will, depending on species, either partially or completely inhibit the relaxant response to field stimulation of trachealis (Li & Rand, 1991; Belvisi *et al.*, 1992; Kannan & Johnson, 1992). These findings suggest that cyclic GMP plays a potentially significant role in the control of airways tone.

[1] Author for correspondence at Department of Cell Physiology and Pharmacology.

The present study was undertaken to examine, in bovine tracheal smooth muscle, the relaxant and cyclic GMP-elevating effects of agents known to activate soluble or particulate guanylyl cyclase and to examine the correlation between these events. In addition, the ability of these agents to relax tone supported by either histamine or methacholine has been compared to isoprenaline-induced relaxation under the same conditions and the anti-spasmogenic actions of certain activators of soluble guanylyl cyclase assessed. Results of some of these experiments have been communicated to the British Pharmacological Society (Ijioma *et al.*, 1993).

Methods

Tracheae from young bullocks were obtained immediately after slaughter from a local abattoir. The trachealis was dissected from the cartilage and then transported to the laboratory in cold HEPES-buffered Krebs-Henseleit solution (KHB, composition in mM: NaCl 118, KCl 4.7, $MgSO_4$ 1.2, $CaCl_2$ 1.8, KH_2PO_4 1.2, $NaHCO_3$ 25, HEPES 5, glucose 11). The tissue was then washed in fresh ice cold KHB and maintained in this solution while connective tissue and epithelium were carefully removed.

Tissue bath studies of mechanical activity

Small strips of trachealis (approximately 10 × 2 × 2 mm) were set up in a KHB solution without HEPES and bubbled with 95% O_2/5% CO_2 at 37°C for the isometric recording of tension changes. Strips were placed under an initial load of 0.5 g, left for 30 min and then the resting load readjusted to 0.5 g. Tone was then established in the tissue by the addition of either histamine (Hist) or methacholine (MCh) to a final concentration of 100 μM or 0.1 μM respectively. After stable tone had been achieved isoprenaline (Iso, 1 μM) was added in order to determine the recorder pen position at zero tone. The Iso was then washed from the tissue and tone re-established by the

Table 1 EC_{50} values for relaxation of bovine tracheal smooth muscle in which tone was induced by either 100 μM histamine of 100 nM methacholine

Spasmogen relaxant	*Histamine* (EC_{50})	*Methacholine* (EC_{50})
Sodium nitroprusside	$3.2 (\pm 0.8) \times 10^{-7}$	$2.9 (\pm 0.9) \times 10^{-7}$
Glyceryl trinitrate	$9.3 (\pm 0.5) \times 10^{-8}$	Not calculated
S-nitroso-N-acetylpenicillamine	$1.4 (\pm 0.4) \times 10^{-5}$	$3.4 (\pm 1.4) \times 10^{-7}$
Atrial natriuretic peptide	$2.8 (\pm 0.8) \times 10^{-9}$	Not calculated
Isoprenaline	$6.6 (\pm 4.3) \times 10^{-9}$	$3.0 (\pm 0.7) \times 10^{-8}$

In all cases the EC_{50} values were calculated from at least 6 tissues obtained from at least 3 tracheae.

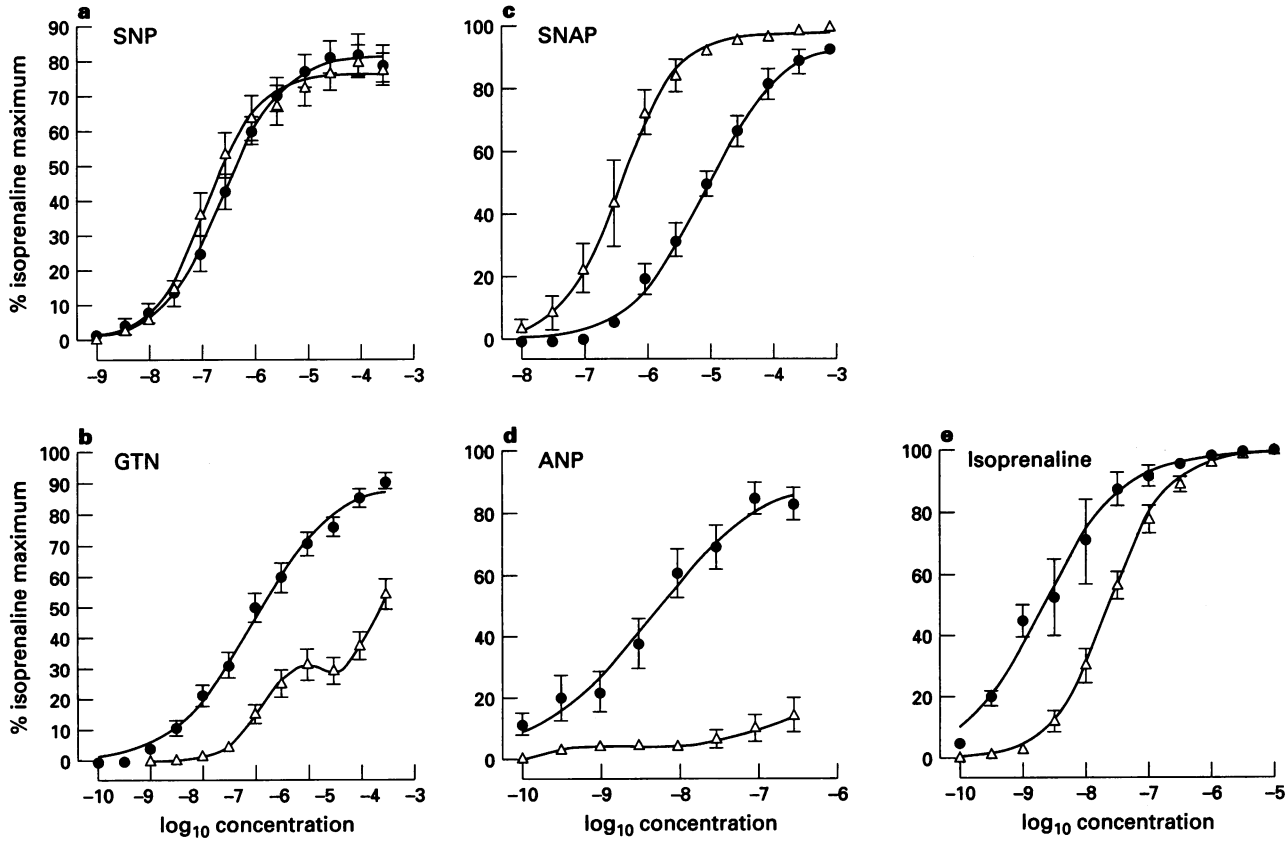

Figure 1 Concentration-effect curves to (a) SNP (b) GTN (c) SNAP (d) ANP and (e) isoprenaline on histamine (100 μM; ●) or methacholine (100 nM; △) supported tone in bovine tracheal smooth muscle strips. Relaxant responses are expressed as a percentage of the maximum response to isoprenaline in the same strip. Results expressed as mean ± s.e.mean. For abbreviations in all figure legends, see text.

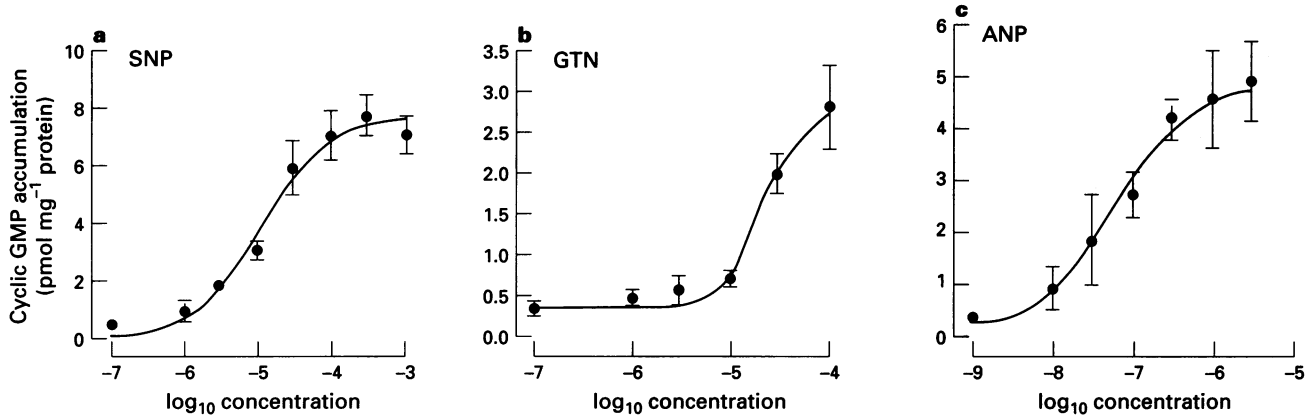

Figure 2 Concentration-dependent cyclic GMP accumulations induced by (a) SNP (b) GTN and (c) ANP in bovine tracheal smooth muscle slices. Cyclic GMP accumulations were assessed 5, 2 or 1 min after addition of SNP, GTN or ANP, respectively. Cyclic GMP concentrations are shown as pmol cyclic GMP mg^{-1} protein. Data are expressed as means ± s.e.mean of triplicate determinations from at least 4 tissues.

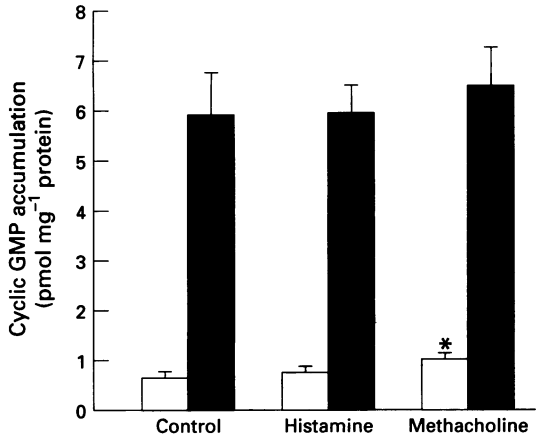

Figure 3 Effect of histamine (100 μM) or methacholine (MCh, 100 μM) on basal and SNP-stimulated rates of cyclic GMP accumulation in bovine tracheal smooth muscle. The basal value for cyclic GMP and the effects of histamine and MCh on cyclic GMP accumulation are shown (open columns). The effect of histamine or MCh on cyclic GMP accumulation stimulated by SNP (100 μM) are also shown (solid columns). Data are expressed as means ± s.e.mean of triplicate determinations from at least 4 tissues. $^{*}P<0.05$, compared to basal or stimulated control values.

addition of the relevant spasmogen. When the tone reached a stable maximum level, study of the relaxant drugs was started.

The relaxant action of Iso, sodium nitroprusside (SNP), S-nitroso-N-acetylpenicillamine (SNAP), glyceryl trinitrate (GTN) and atrial natriuretic peptide (ANP) were studied by the construction of cumulative concentration-effect curves, half log unit concentration increments being made at intervals of 4, 5, 5, 5 and 7 min respectively. After the maximum concentration of the test agent had been added each tissue was challenged with 1 μM Iso to re-establish the position of zero tone.

Although a clear maximum inhibitory effect was observed for each test relaxant when the tone was maintained with 100 μM Hist, the increase in tension induced by MCh was more difficult to suppress. It was not possible to obtain a maximum relaxant effect against MCh with GTN, since the source of this compound was 'Nitronal' (Lipha Pharmaceuticals Ltd.) a solution of GTN at 4.4 mM. This limited the maximum bath concentration that could be achieved to 10^{-5} M. Similarly, the maximal effect of ANP was not assessed due to the very low potency of this compound against MCh-supported tone. In a number of experiments, test tissues were pretreated with superoxide dismutase (50 u ml^{-1}) for 10 min prior to the addition of GTN.

In order to confirm that the relaxant effects of the various compounds tested were due to the measured increases in cellular cyclic GMP, relaxant curves were constructed as above and the tissues divided into test and control groups. Test tissues were then incubated in the presence of the putative soluble guanylyl cyclase inhibitor LY 83583 (10 μM) for 20 min prior to, and then throughout, the subsequent induction of tone and construction of relaxant curves. Control tissues were treated identically except that they were not exposed to LY 83583.

The time course of the relaxant effects of SNP, SNAP, GTN and ANP were studied by the addition of a maximally effective concentration of the test agent to tissues in which the tone had been induced by 100 μM Hist. Recording of the relaxation induced by the test drug was then continued for 40 min. Control tissues received only vehicle.

The anti-spasmogenic potencies of SNP and SNAP were compared to that of Iso by constructing cumulative log concentration-effect curves to Hist. A conditioning concentration-effect curve for Hist was constructed and, after establishing a clear maximum effect the tissue was extensively washed every 10 min, for a period of 30–40 min. A second Hist concentration-effect curve was then constructed for all tissues. This curve acted as the control curve and provided the 100% response against which the other curves was normalized. After washing as above, tissues were randomly allocated to test or control groups. Test tissues were pretreated with 1 μM SNP, 30 μM SNAP or 3 nM Iso for 5 min prior to construction of the Hist concentration-effect curves. Control tissues were treated in an identical manner, but did not receive the test agent. It was not possible to perform this type of experiment with ANP or GTN due to the short lifetime of their relaxant effect under these experimental conditions.

Measurement of cyclic nucleotide concentration

Bovine trachealis prepared as above was cross-chopped (300 μm × 300 μm) with a McIlwain tissue-chopper. The resulting slices were washed and incubated in 100 ml oxygenated KHB at 37°C for 60 min. At 15 min intervals, the slices were allowed to sediment and the buffer replaced by fresh medium. Gravity-packed slices were then either transferred into vials for immediate experimentation or were washed twice in sterile minimum essential medium (MEM), transferred to tissue culture flasks in fresh MEM and maintained overnight at 37°C in an incubator.

Gravity-packed slices (75 μl) in 400 μl KHB were placed in a shaking waterbath, at 37°C for 30 min. Test drugs were in-

troduced as 10 μl additions and the response terminated by the addition of 20 μl 10 M HCl and immersion in an icebath After 20 min the samples were neutralized to pH 6 with 200 μl NaOH (approximately 1 M), vortexed and then centrifuged for 20 min at 4000 r.p.m. The supernatant was carefully removed and the pellet resuspended in 1 ml of 2 M NaOH overnight for the estimation of protein concentration by the method of Lowry *et al.* (1951). Neutralized supernatant was diluted 1/20 with 100 mM sodium acetate and then acetylated prior to the estimation of cyclic GMP by radioimmunoassay as described by Chilvers *et al.* (1991). All results are expressed as pmol cyclic GMP mg^{-1} protein.

The effects of LY 83583 (100 μM) on cyclic GMP accumulation were tested by incubating the tissue slices in the presence of the inhibitor for 20 min prior to the addition of the test compound.

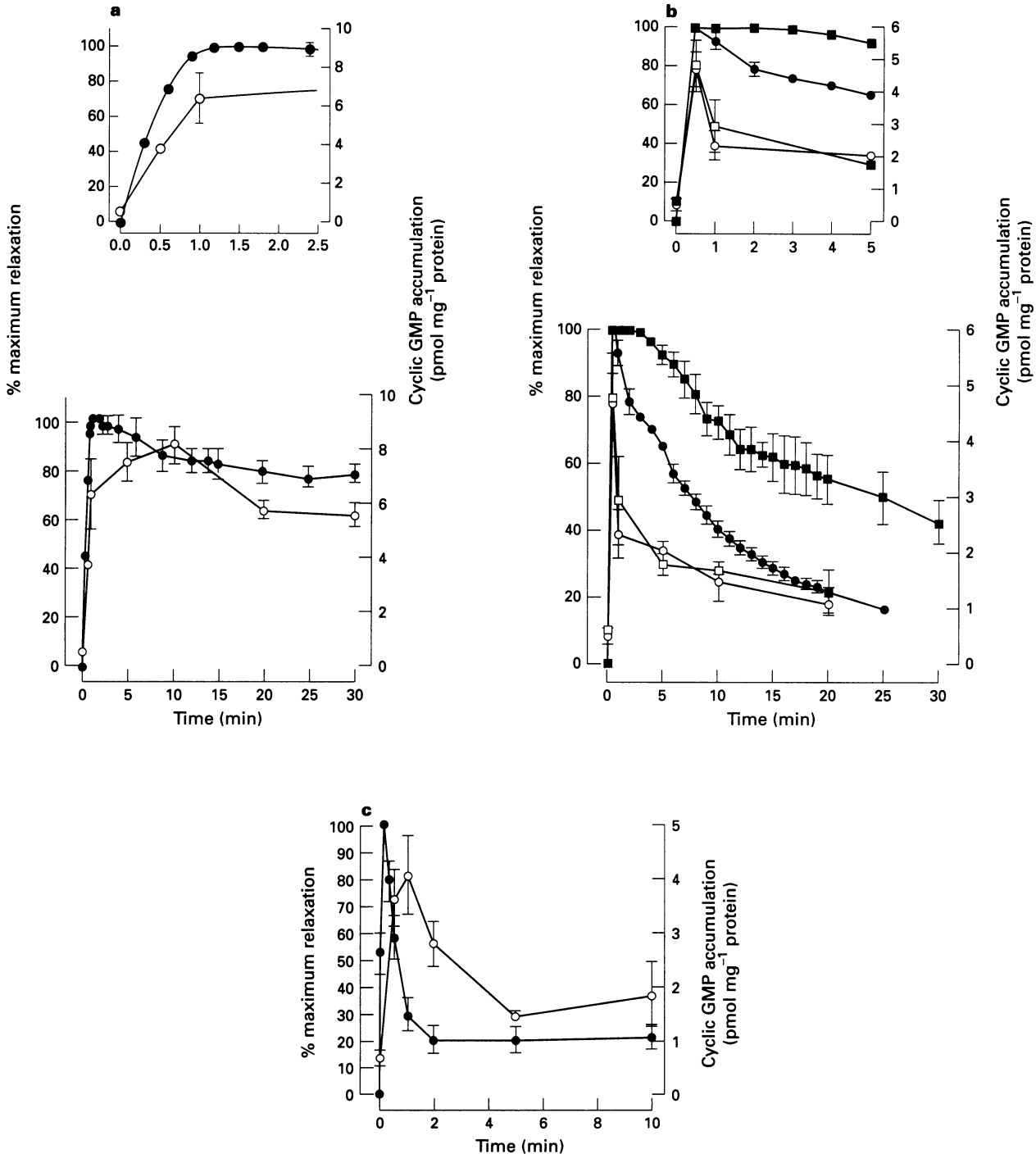

Figure 4 Comparative time-courses of cyclic GMP accumulation and relaxation of histamine-supported tone in bovine tracheal smooth muscle. At zero-time (a) SNP (100 μM), (b) GTN (20 μM), or (c) ANP (0.3 μM) were added. The ordinates on the left represent the relaxation (●) as a % of the maximum response to the test compound in same tissue strip, while the right ordinates represent the cyclic GMP concentration (○) in pmol mg^{-1} protein. The temporal correlation between cyclic GMP accumulation and relaxation at early time points is shown in the inserts where the same data are plotted on an expanded time scale in the main figure. In (b) relaxation (■) and cyclic GMP concentration (□) data obtained in the presence of superoxide dismutase (50 iu ml^{-1}) are also shown.

Muscarinic M_3 binding assay

The ability of sodium nitroprusside and SNAP to interact with muscarinic receptors was tested by competitive radioligand binding assays. Sodium nitroprusside and SNAP were assessed for the ability to displace specific N-[^{3}H]-methyl scopolamine ([^{3}H]-NMS) binding from membranes derived from Chinese hamster ovary cells expressing recombinant m3 muscarinic receptors (Tobin *et al.*, 1992). Atropine displacement of [^{3}H]-NMS was used as a positive control for the method.

Materials

Drug concentrations are expressed as the molar concentration of the active species. The following drugs were used: acetyl-β-methylcholine chloride (methacholine), histamine, sodium nitroprusside, isoprenaline and superoxide dismutase (Sigma), S-nitroso-N-acetylpenicillamine (Research Biochemicals Inc.), atrial natriuretic peptide (rat, 3-28) (Bachem UK Ltd) glyceryl trinitrate ("Nitronal", Lipha Pharmaceuticals, West Drayton, UK), LY 83583 (6-anilino-5,8-quinolinedione;. Eli Lilly, Indianapolis, U.S.A.), anti-cyclic GMP, [^{125}I]cyclic GMP and N-[^{3}H]-methyl scopolamine (Amersham International, UK).

Stock solutions of isoprenaline were prepared in 0.1 M HCl and atrial natriuretic peptide in 50 mM $NaHCO_3$, those of other agents in distilled water. Stocks of atrial natriuretic peptide were stored as aliquots at −80°C and thawed only when needed. Dilutions of isoprenaline were prepared in distilled water containing 500 μM ascorbic acid as an antioxidant.

Data analysis

Wherever possible the data have been fitted to the equation:

$$Fx = \frac{(X/E)^n}{1+(X/E)^n}$$

where X = concentration of the effector compound, E = 50% of the maximum response, and n = slope factor, using a commercial fitting programme. The solution to this equation was then used to produce a best fit curve to the data. Graphs and text display the data as the mean ± s.e.mean. The significance of differences between means was assessed using Student's unpaired *t* test.

Results

Effect of relaxants on histamine- and methacholine-induced tone

SNP, SNAP, GTN, ANP and Iso all produced concentration-dependent relaxations of bovine tracheal smooth muscle tone supported by either Hist (100 μM) or MCh (100 nM) (Figure 1). Concentrations of each relaxant which caused half-maximal relaxation of spasmogen-supported tone are summarized in Table 1.

SNP was equi-effective as a relaxant of both Hist- and MCh-supported tone causing a maximum relaxation of greater than 70% of the maximum response to Iso in the same tissue (Figure 1a). SNAP had a similar efficacy against both spasmogens causing greater than 90% of the maximum response to Iso, however S-nitrosothiol was a more potent relaxant against tone induced by MCh than against that induced by Hist (Figure 1c). For comparison, Figure 1e demonstrates that under these experimental conditions, Iso caused complete relaxation when tested against either spasmogen, but was approximately 15 fold less potent as a relaxant of MCh-induced tone.

When tested against Hist-maintained tone, ANP and GTN also induced maximum relaxant responses equivalent to 80–90% of the maximum relaxation induced by Iso (Figures 1b and 1d). However, when these agents were tested against MCh-supported tone it was not possible to produce a maximum relaxant response. Over the concentration-range tested, GTN clearly caused a biphasic effect on MCh-supported tone, with an apparent plateau phase occurring between 1 and 10 μM GTN (Figure1b). The presence of superoxide dismutase in some experiments had no effect on Hist-induced tone *per se*, and also had no effect on the concentration-effect curve for GTN against Hist-supported tone. The difference in the relaxant potencies of ANP towards MCh- and Hist-supported tone was dramatic. At a concentration of ANP which caused a maximal relaxation of Hist-supported tone, this agent was almost ineffective against tone supported by MCh (Figure 1d).

Measurement of cyclic GMP concentration

SNP, GTN and ANP each produced concentration-dependent increases in cyclic GMP accumulation (Figure 2). SNP caused a rapid increase in cyclic GMP accumulation with a half-maximal stimulation occurring at a concentration of 1.3 ($\pm$0.3) $\times 10^{-5}$ M. The maximum increase in cyclic GMP, measured in response to 300 μM SNP was 15–20 fold over basal levels. GTN caused a significant increase in cyclic GMP at 10 μM (approx. 2 fold), while at the highest concentration tested (100 μM) an increase of 7 fold was seen. ANP caused a concentration-dependent increase in cyclic GMP giving a 12 fold increase over basal values at the highest concentration tested (EC_{50}: 8.2 ($\pm$1.5) $\times 10^{-8}$ M). Iso (0.1–10 μM) failed to cause any increase in cyclic GMP accumulation (data not shown).

Hist (100 μM) did not cause an increase in cyclic GMP accumulation over control values measured in untreated tissue slices (Figure 3). In contrast, MCh (100 μM) caused a small, but significant increase in cyclic GMP accumulation. However, neither of these contractile agonists significantly modified the response to 100 μM SNP (Figure 3).

Time-course of induced relaxation and cyclic GMP accumulation

SNP and Iso both induced a rapid relaxation (>90% maximum response within 2 min) that was well-maintained for the duration of these experiments. In contrast, the relaxant responses to GTN and ANP, which were rapid in onset, were transient in nature. Thus, in the continued presence of GTN (20 μM), relaxation declined from a maximum level achieved within 30 s of addition, to 75%

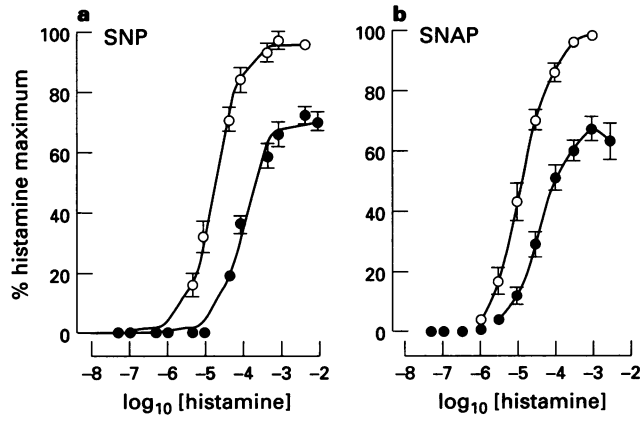

Figure 5 Concentration-effect curves to histamine in bovine tracheal smooth muscle strips pretreated with (a) SNP (1 μM) or (b) SNAP (30 μM). Spasmogenic responses are expressed as a percentage of the maximum response to histamine obtained from the first control curve obtained in the same strip. Time-matched control concentration-effect curves (○) and concentration-effect curves in the presence of SNAP or SNP (●) are shown. Data indicate the means ± s.e.mean of values from 6 tissues.

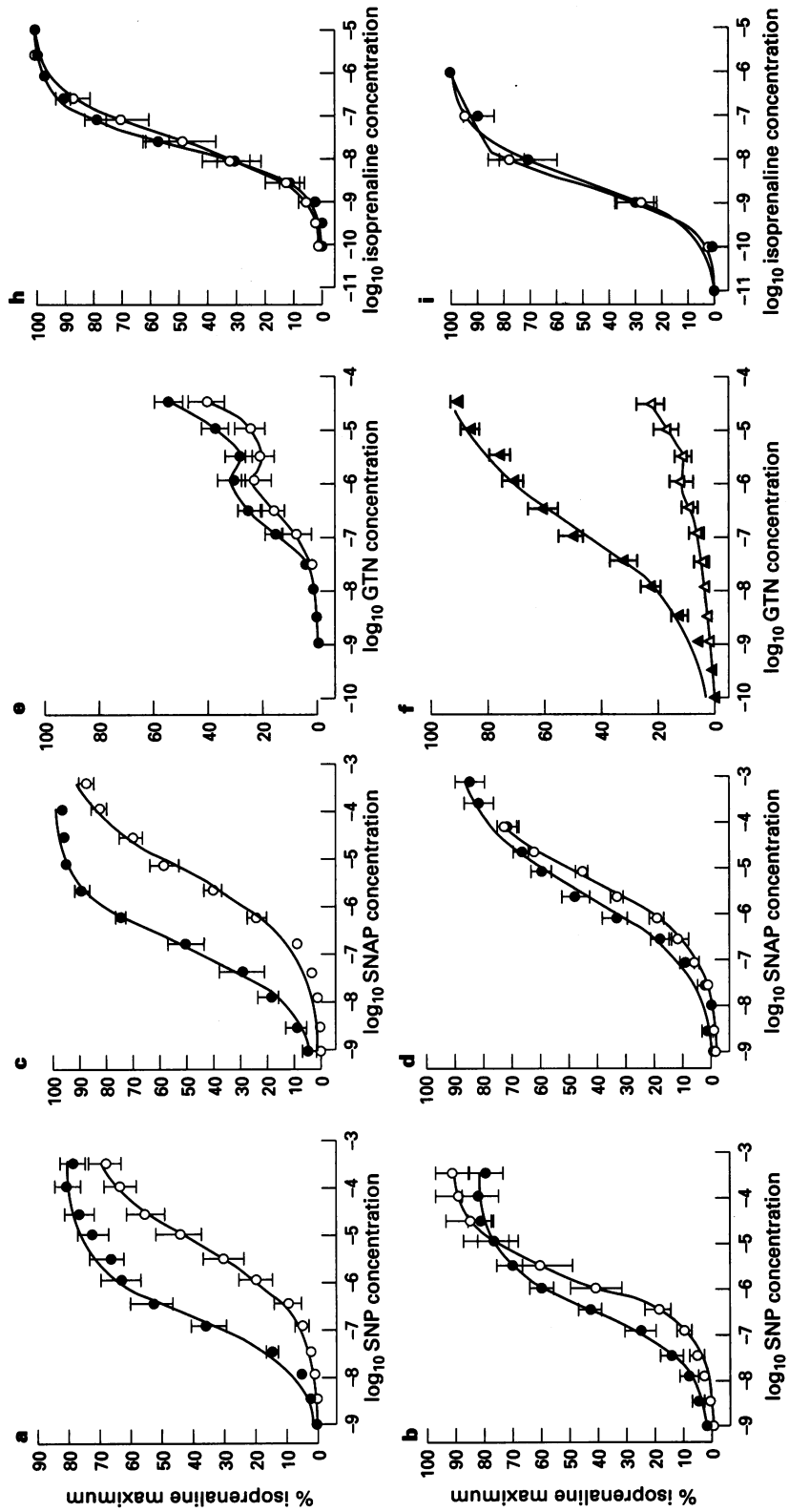

Figure 6 Concentration-effect curves in the presence (○) or absence (●) of LY 83583 (10 μM) for SNP (a, b), SNAP (c, d), GTN (e, f), ANP (g) and isoprenaline (h, i) against either methacholine- (a, c, e, h) or histamine- (b, d, f, g, i) supported tone in bovine tracheal smooth muscle. Relaxant responses are expressed as a percentage of the maximum response to isoprenaline in the same strip. Test concentration-effect curves were constructed in the continued presence of LY 83583 following 20 min pre-incubation. Data indicate the means ± s.e.mean of values from at least 5 tissues.

within 3 min; 50% within 7 min and 10–20% by 20 min of the peak response (Figure 4b). When GTN was added in the presence of superoxide dismutase (50 iu ml^{-1}) relaxation was better maintained, although the relaxation still declined by 50% over the 30 min exposure period (Figure 4b).

SNP, GTN and ANP each caused time-dependent increases in cyclic GMP accumulation in smooth muscle slices. SNP (100 μM) induced an elevation of cyclic GMP that reached a maximum within 5 min and which was well maintained (>70% of the maximum increase in cyclic GMP observed at 30 min) (Figure 4a). GTN (30 μM) induced its maximum increase in cyclic GMP within 30 s, but the concentration of this second messenger rapidly decreased to about 1.9 fold over basal values by 10 min. Repeating this experiment in the presence of superoxide dismutase had no significant effect on the size of the maximum response, or the rate of decrease of the cyclic GMP concentration (Figure 4b). ANP (0.3 μM) caused a rapid increase in cyclic GMP, reaching a maximum of 4.0 ($\pm$0.75) pmol ml^{-1} protein within 1 min. This increase in cyclic GMP was transient and had returned to near basal (1.6 x basal) 5 min after the addition of the agonist (Figure 4c).

Anti-spasmogenic actions of relaxants

Pretreatment of the tissue strips with SNP (1 μM) caused a suppression of the response to Hist at all concentrations tested and a reduction in the maximum spasmogenic response (EC_{50}s: control, 3.1 ($\pm$1.0) x 10^{-5}; +SNP, 8.8 ($\pm$1.5) x 10^{-5} M) (Figure 5a). Pretreatment of the strips with SNAP (30 μM) also caused a rightward-shift of the Hist concentration-effect curve and a reduction in the maximum response. (EC_{50}s: control, 1.4 ($\pm$0.4) x 10^{-5}; +SNAP, 4.3 ($\pm$1.0) x 10^{-5} M) (Figure 5b).

Effects of SNP and SNAP on agonist binding at M_3 receptors

One possible explanation for the apparent high potency of SNP and SNAP as relaxants of muscarinic tone was that these compounds were acting as antagonists at the muscarinic receptor. This hypothesis was tested. In experiments where atropine was demonstrated to cause 50% displacement of specific binding of [^{3}H]-NMS from membranes derived from Chinese hamster ovary cells expressing recombinant m3-muscarinic receptors at a concentration of 3.2 $\pm$ 0.1 x 10^{-9} M, neither sodium nitroprusside nor SNAP at 0.1–10 μM caused any displacement (data not shown).

Effects of LY 83583 on relaxation and cyclic GMP accumulation

Pretreatment of bovine tracheal smooth muscle BTSM strips with LY 83583 (10 μM) had no effect on the resting behaviour of the tissue.

The concentration-effect curve for the relaxation of MCh-supported tone by SNP was shifted approximately 25 fold to the right in the presence of LY83583 (10 μM) (EC_{50}s: control, 2.9 ($\pm$0.9) x 10^{-7}; +LY, 7.3 ($\pm$2.4) x 10^{-6} M, see Figure 6a). When tested against Hist-supported tone, the relaxant curve caused by SNP was shifted to the right (~9 fold) in the presence of 10 μM LY 83583 (EC_{50}s: control, 3.2 ($\pm$0.8) x 10^{-7}; +LY, 2.9 ($\pm$1.3) x 10^{-6} M, see Figure 6b). For both Hist- and MCh-supported tone, the maximum relaxation induced by SNP appeared to be unaffected by the presence of 10 μM LY 83583.

SNAP-induced relaxation of MCh-supported tone was inhibited by pretreatment of the tissue with 10 μM LY 83583 (EC_{50}s: control 2.1 ($\pm$0.2) x 10^{-7}; +LY, 3.3 ($\pm$1.2) x 10^{-6} M, see Figure 6c). This represents an approximately 16 fold shift to the right of the concentration-effect curve. When tested against Hist-supported tone, the relaxant curve for SNAP was shifted 2 fold to the right in the presence of 10 μM LY 83583 (EC_{50}s: control, 6.5 ($\pm$2.2) x 10^{-6}; +LY, 1.1 ($\pm$0.2) x 10^{-5} M, see Figure 6d). The maximum response to SNAP against both Hist and MCh-supported tone was unaffected by LY 83583.

LY 83583 (10 μM) had no significant effect on the concentration-effect curve for GTN when tone was induced by MCh (Figure 6e). However, after pretreatment with 10 μM LY 83583, the relaxation of tone supported by Hist was largely abolished (Figure 6f), with >20% relaxation at the highest concentration tested. Pretreatment with 10 μM LY 83583 also

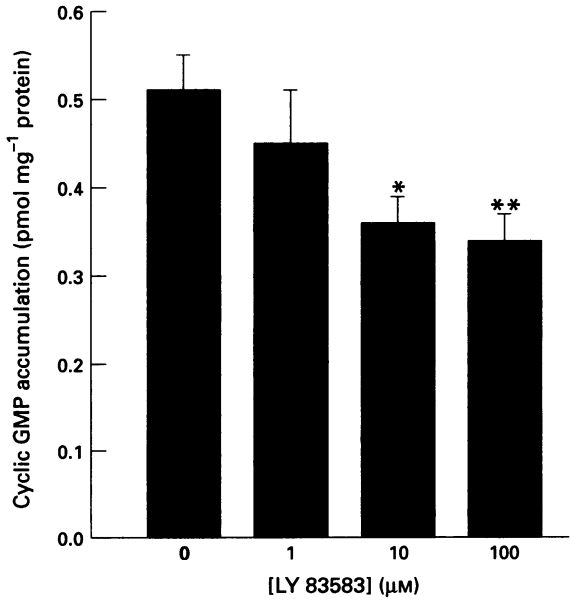

Figure 7 Effects of increasing concentrations of LY 83583 on basal rates of cyclic GMP accumulation in bovine tracheal smooth muscle slices. Cyclic GMP concentrations are shown as pmol cyclic GMP mg^{-1} protein. Data are expressed as means ± s.e.mean of triplicate determinations from at least 4 tissues. *P<0.05; **P<0.01 for comparisons of accumulations in the presence and absence of LY 83583.

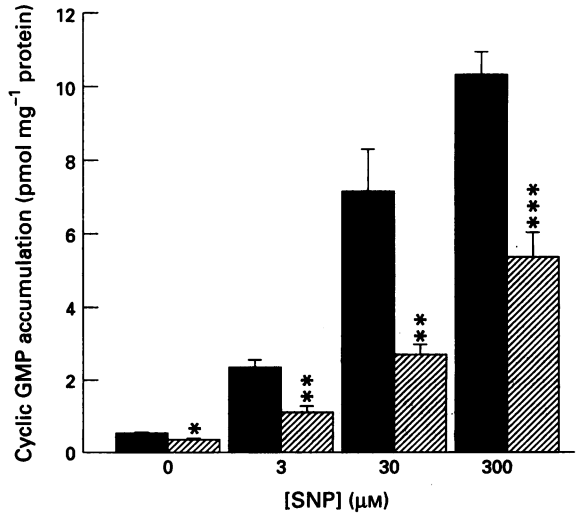

Figure 8 Effect of LY 83583 on concentration-dependent cyclic GMP accumulation induced by SNP in bovine tracheal smooth muscle. Bovine tracheal slices were incubated in the absence or presence of 10 μM LY 83583 for 20 min prior to the addition of SNP. Data are expressed as means ± s.e.mean of triplicate determinations from at least 4 tissues. *P<0.05; **P<0.01; ***P<0.001 for comparisons of cyclic GMP accumulations in the presence and absence of LY 83583.

inhibited the relaxation of Hist-supported tone induced by ANP (Figure 6g). It was not possible to quantify this inhibition, as a reliable maximum effect of ANP could not be measured after treatment with LY 83583.

Pretreatment of BTSM strips with LY 83583 (10 μM) had no effect on the relaxant potency or efficacy of Iso against either histamine- (EC_{50}s: control, $9.4 (\pm 2.7) \times 10^{-9}$; +LY, $1.3 (\pm 9.0) \times 10^{-8}$ M, see Figure 6i) or MCh-supported tone (EC_{50}s: control, $3.0 (\pm 0.7) \times 10^{-8}$; +LY, $8.0 (\pm 6.6) \times 10^{-8}$, see Figure 6h), but had complex effects on the relaxations induced by agents thought to act through increasing cyclic GMP accumulation.

Treatment with LY 83583 caused a concentration-dependent decrease in basal cyclic GMP levels in bovine tracheal smooth muscle (Figure 7) and at a concentration of 10 μM caused a significant decrease in cyclic GMP accumulation induced by SNP (3–300 μM) (Figure 8).

Discussion

The relaxation of airway smooth muscle by agents that increase cyclase GMP has been well documented (Katsuki & Murad, 1977; Fiscus *et al.*, 1984). However, such studies have often used a limited range of compounds and have dealt, in isolation, with either cyclic GMP accumulation or muscle relaxation. In the present study we were particularly interested in the correlation between cyclic GMP accumulation and relaxation and whether the response of bovine tracheal smooth muscle differed depending on whether cyclic GMP was elevated by soluble or particulate guanylyl cyclase activities.

Until recently, in spite of the finding that tracheal smooth muscle contained both soluble and particulate guanylyl cyclases, no endogenous mechanisms for the control of airway tone were known that used this second messenger pathway. However, intravenous infusion of ANP has been shown to produce significant bronchodilatation in both normal and asthmatic subjects (Hulks *et al.*, 1989; 1990) allowing speculation that endogenous circulating ANP may cause bronchodilatation and so play a role in the maintenance of airway diameter. Also, recent work on the identity of non-adrenergic, non-cholinergic inhibitory neurotransmitters has raised the possibility that nitric oxide, acting through soluble guanylyl cyclase, plays an important role in the neural control of airway diameter (Li & Rand, 1991; Kannan & Johnson, 1992).

Relaxation and cyclic GMP accumulation

The ability of SNP, SNAP, GTN and ANP to cause relaxation of tracheal smooth muscle seems to be closely related to their ability to cause the accumulation of cyclic GMP and presumably activation of either soluble or particulate guanylyl cyclase. However, the relationship between the magnitude of cyclic GMP accumulation and relaxation is not a simple one.

A concentration of SNP which causes a cyclic GMP accumulation which is 50% of maximal (13 μM) is sufficient to cause maximum relaxation against both histamine- and methacholine-supported tone. Furthermore 50% relaxation occurs at a concentration of SNP that does not cause a significant increase in cyclic GMP accumulation. A similar relationship is seen with GTN- and ANP-induced cyclic GMP accumulation and relaxation of histamine-supported tone suggesting that BTSM cells are very sensitive to small, perhaps localized, increases in cyclic GMP levels over basal. This high level of sensitivity probably also accounts for the biphasic relaxation curve caused by GTN against methacholine-supported tone. The relaxation caused by low ($\leqslant 1 \mu$M) concentrations of GTN is likely to be caused by small localized increases in cyclic GMP accumulation while the concentration-relaxation curve observed at higher GTN (>3 μM) concentrations is well-correlated with the rapid increase in cyclic GMP accumulation seen at higher concentrations of this agent.

The relationship between cyclic GMP accumulation and relaxation for ANP against methacholine-supported tone, appears to be more complicated. Even at concentrations of ANP that cause a maximum increase in cyclic GMP accumulation, which if generated by SNP would result in maximal relaxation, little relaxation was observed. Such a discrepancy raises at least two issues. Firstly, why is the tone induced by methacholine and histamine so differentially sensitive to inhibition by ANP? Secondly, why does elevation of intracellular cyclic GMP concentration ([cyclic GMP]$_i$) have such different consequences depending upon the route by which it was generated? The present study does not provide an answer to these questions, although it does suggest that further studies correlating [cyclic GMP]$_i$ with cyclic GMP-dependent protein kinase activation may be enlightening. The differential sensitivity to ANP resembles that observed when using agents that cause relaxation by increasing cyclic AMP accumulation and so may indicate that a similar inhibition to that thought to act on adenylyl cyclase (for review see Giembycz & Raeburn, 1991 or discussion below) may be active on the particulate form of guanylyl cyclase.

Atrial natriuretic peptide, at the highest concentration used, produced a 12 fold increase in cyclic GMP concentration, in good agreement with other published data (Ishii & Murad, 1989). The time course of ANP-stimulated cyclic GMP accumulation and relaxation were well-correlated and so resemble those evoked by agents which exert their activities via an activation of soluble guanylyl cyclases. ANP, as with the other agents tested, was required in higher concentrations to evoke measureable cyclic GMP accumulation than to cause relaxation. It seems likely that this result, which is similar to previous reports on cyclic nucleotide accumulation (Wong & Buckner, 1978; Zhou & Torphy, 1991), is due to the very high sensitivity of these cells to increases in cyclic GMP. It should be noted that specific phosphodiesterase inhibitors, such as zaprinast, that would have amplified any increase in cyclic GMP accumulation were not employed here.

The large increase in cyclic GMP (20 fold) observed in this study in response to sodium nitroprusside is in good agreement with the previous findings of Zhou & Torphy (1991) who reported a maximum 18 fold increase in cyclic GMP concentration produced by sodium nitroprusside in canine trachealis. They also reported a 2 fold increase in cyclic GMP in response to glyceryl trinitrate, a figure that is in fairly good agreement with the value of 5 fold reported here. Since both compounds are thought to act primarily by releasing nitric oxide to activate soluble guanylyl cyclase (Chung & Fung, 1990; Bates *et al.*, 1991; Kowaluk *et al.*, 1992; Harrison & Bates, 1993) an explanation should be sought for the difference in the magnitude of stimulation of soluble guanylyl cyclase. Evidence from vascular smooth muscle suggests that the answer may lie in the site at which cleavage of these compounds to release nitric oxide occurs. Sodium nitroprusside, which was originally thought to undergo spontaneous breakdown, has been shown to be exceptionally stable in the absence of light, and requires the presence of a membrane-bound reducing agent such as cysteine before nitric oxide release will take place (Bates *et al.*, 1991; Kowaluk *et al.*, 1992). The additional observation that this breakdown is enhanced by NADPH (Kowaluk *et al.*, 1992) and is resistant to inhibition by non-permeant haem proteins (Gruetter *et al.*, 1979) suggests that catalysis may occur on the cytoplasmic face of the membrane. If a similar mechanism pertains in airway smooth muscle, and the weak effect of haemoglobin on the potency of sodium nitroprusside as a relaxant of tracheal smooth muscle suggests that it might, then most of the nitric oxide released will be in close proximity to the cytosolic guanylyl cyclase and so available for activation. Glyceryl trinitrate is also a stable molecule that will not release nitric oxide until it interacts with the cell membrane, possibly being cleaved by an enzyme that has not yet been purified (Chung & Fung, 1990; Harrison & Bates, 1993; Seth & Fung, 1993). However, in contrast to nitroprusside, the nitric oxide generated from glyceryl trinitrate

seems to be vulnerable to non cell-permeant inhibitors, suggesting an extracellular release site. The nitric oxide generated at such an extracellular site may also be vulnerable to attack by superoxide ions reducing the efficiency of this molecule to act as a nitric oxide donor.

Evidence, consistent with this scheme, was obtained from the studies of the time-course of cyclic GMP accumulation and relaxation induced by nitroprusside or glyceryl trinitrate. In addition, the irreversible effects of high concentrations of SNP suggest a possible intracellular accumulation of SNP breakdown products which is likely to correspond to the reported *in vivo* cyanide toxicity following high doses of sodium nitroprusside (Harrison & Bates, 1993).

Relaxant responses against muscarinic agonist-supported tone

Unusually, sodium nitroprusside and SNAP, compounds that are thought to release nitric oxide at an intracellular site, appeared to be equipotent or, in the case of SNAP more potent, as relaxants of muscarinic- in comparison to histamine-supported tone. The more widely reported pattern of relaxant action in tracheal smooth muscle is that shown by the other agents tested i.e. relaxants are much less potent against methacholine-supported tone than tone maintained by histamine (Torphy *et al.*, 1985; Fedan *et al.*, 1990). Most of the work on mechanisms underlying the reduced potency of relaxants in the presence of muscarinic agonists has been performed on β-agonists and a variety of hypotheses have been put forward to explain this phenomenon (for review see Challiss & Boyle, 1994). The results obtained in this study with ANP suggests that this inhibitory action of muscarinic agonists may occur against cyclic GMP- as well as cyclic AMP-mediated relaxation. The fact that this inhibitory mechanism seems to act most potently on the membrane delimited form of guanylyl cyclase and the membrane bound adenylyl cyclase may indicate that part of this inhibition is also membrane delimited.

The fact that, in contrast to the result with glyceryl trinitrate, the potencies of sodium nitroprusside and SNAP are not reduced for relaxation of muscarinic-compared to histamine-maintained tone may point to sodium nitroprusside and SNAP causing, at least part of their relaxation by a mechanism other than activation of soluble guanylyl cyclase. A similar conclusion has been reached in a number of other studies on sodium nitroprusside (Diamond & Janis, 1978; Diamond, 1983; Zhou & Torphy, 1991). The possibility that SNAP and sodium nitroprusside exerted part of their relaxant effect against MCh-supported tone by acting as muscarinic antagonists was addressed by testing their ability to displace [^{3}H]-NMS from muscarinic M_3 receptors in a preparation of CHO-m3 cell membranes. The observation that neither sodium nitroprusside nor SNAP caused any displacement of specific [^{3}H]-NMS binding, strongly suggests that these compounds lack any activity as muscarinic antagonists. If these NO donor molecules are causing relaxation by mechanisms unrelated to guanylyl cyclase activation it must be through some other mechanism. Whether this is related to the site of cleavage of nitroprusside and SNAP or to a relaxant action of one of the by-products of nitric oxide release is unknown but recent observations that nitric oxide can directly activate the large-conductance, calcium-activated K^+ channel (K_{Ca}) in vascular smooth muscle (Bolotina *et al.*, 1994) suggests an alternative mechanism by which these compounds could cause relaxation in addition to their ability to increase cyclic GMP accumulation. Although not addressed in this study, the possible contribution of K_{Ca} activation to this response should be relatively easy to test.

The arguments listed above start from the assumption that the pattern of behaviour seen with agents that increase cyclic AMP will be repeated with agents that act through cyclic GMP. However, if increases in cyclic GMP cause inhibition of muscarinic-induced tone at least equally potently as inhibition of histamine-induced tone then an explanation would have to be sought for the pattern of behaviour of GTN rather than that of SNP and SNAP. Unlike sodium nitroprusside and SNAP, glyceryl trinitrate was more potent as a relaxant of histamine- as opposed to methacholine-supported tone. In addition, the latter response was clearly biphasic. This observation was interesting since similar observations on the biphasic nature of the relaxant response to glyceryl trinitrate have been made in vascular smooth muscle (Karaki *et al.*, 1984; Malta, 1989). Malta (1989) concluded that the biphasic curve was due to two separate mechanisms of action that both led to increased accumulation of cyclic GMP. One of the phases resembled the relaxation induced by endothelium-derived relaxant factor (EDRF), while the other was similar to that induced by sodium nitroprusside. If this is correct, then the observation of Bolotina *et al.* (1994) that K_{Ca} could be activated by endogenously-generated EDRF as well as exogenous nitric oxide might explain at least one phase of this relaxant response. The biphasic relaxant curve in the present study was only seen when tone was induced by methacholine, and whether this biphasic response would be seen using other spasmogens or is unique to muscarinic agonists was not examined. Also, no attempt was made to inhibit selectively one phase of this response as was done by Malta (1989). Therefore, the question of whether glyceryl trinitrate causes part of its relaxant action in tracheal smooth muscle by a mechanism that more closely resembles relaxation induced by EDRF (i.e. multiple effects of nitric oxide release) will require further study.

Cyclic GMP accumulation and LY 83583

The quinolinedione, LY 83583, has been reported to be a specific inhibitor of soluble guanylyl cyclase (Mülsch *et al.*, 1988; Malta, 1989) and as such has been used to distinguish between cyclic GMP accumulation induced by soluble and particulate guanylyl cyclases. We therefore planned to use this agent to confirm that the relaxation induced by sodium nitroprusside, SNAP and glyceryl trinitrate was dependent on their ability to increase cyclic GMP accumulation. In common with other studies we found that LY 83583 caused a concentration-dependent reduction in basal cyclic GMP levels. Additionally, as expected, we observed inhibition of cyclic GMP accumulation induced by sodium nitroprusside and relaxation induced by sodium nitroprusside, SNAP and glyceryl trinitrate. However, we also found that the relaxation of histamine-supported tone by ANP was sensitive to inhibition by this compound. This result is in agreement with the finding of O'Donnell & Owen (1986) that atrial natriuretic factor-induced stimulation of Na^+, K^+, Cl^- cotransport was inhibited by LY 83583 in vascular smooth muscle. One possible interpretation of this result is that ANP is working, at least in part, through soluble guanylyl cyclase; however, other mechanisms have been proposed to account for the reduction in cyclic GMP accumulation seen in the presence of LY 83583, including the generation of superoxide ions (Furchgott & Jothianandan, 1991). This mechanism alone would not explain our results as it is unlikely to account for the inhibition of sodium nitroprusside-induced relaxation and cyclic GMP accumulation and the reduction in basal cyclic GMP concentration. However, both inhibition of guanylyl cyclase and the production of superoxide ions together may explain our data. Whatever the mechanism involved, it is obvious that great care should be taken when interpreting results obtained from the use of LY 83583.

In summary, sodium nitroprusside, glyceryl trinitrate and atrial natriuretic peptide each caused concentration-dependent cyclic GMP accumulation and relaxation of bovine tracheal smooth muscle. Each of these agents and also SNAP caused a concentration-dependent relaxation of bovine tracheal smooth muscle where tone was supported by either histamine or methacholine. A good correlation existed between the time course of cyclic GMP accumulation and relaxation induced by these agents suggesting that their relaxant potency arises from their ability to stimulate either soluble or particulate guanylyl cyclase in this tissue.

This work was supported in part by a grant from The British Lung Foundation. S.C.I. was supported by the Leicestershire Health Authority and a Vacation Studentship from The Wellcome Trust.

References

ANGUS, R.M., MCCALLUM, J.A., HULKS, G. & THOMSON, N.C. (1993). Bronchodilator, cardiovascular, and cyclic guanylyl monophosphate response to high-dose infused atrial natriuretic peptide in asthma. *Am. Rev. Resp. Dis.*, **147,** 1122–1125.

BATES, J.N., BAKER, M.T., GUERRO, R.J.R. & HARRISON, D.G. (1991). Nitric oxide generation from nitroprusside by vascular tissue. Evidence that reduction of the nitroprusside anion and cyanide loss are required. *Biochem. Pharmacol.*, **42,** S157–S165.

BELVISI, M.G., STRETTON, D., YACOUB, M. & BARNES, P.J. (1992). Nitric oxide is the endogenous neurotransmitter of bronchodilator nerves in humans. *Eur. J. Pharmacol.*, **10,** 221–222.

BOLOTINA, V.M., NAJIBI, S., PALACINO, J.J., PAGANO, P.J. & COHEN, R.A. (1994). Nitric oxide directly activates calcium-dependent potassium channels in vascular smooth muscle. *Nature*, **368,** 850–853.

CHALLISS, R.A.J. & BOYLE, J.P. (1994). Modulation of agonist-stimulated phosphoinositide turnover in airways smooth muscle by cyclic nucleotide-dependent and independent mechanisms. In *Airways Smooth Muscle: Reference Source. Biochemical Control of Contraction and Relaxation.* ed. Raeburn, D. & Giembycz, M.A. pp. 309–327. Basel/Switzerland: Birkhäuser Verlag.

CHILVERS, E.R., GIEMBYCZ, M.A., CHALLISS, R.A.J., BARNES, P.J. & NAHORSKI, S.R. (1991). Lack of effect of zaprinast on methacholine-induced contraction and inositol 1,4,5-trisphosphate accumulation in bovine tracheal smooth muscle. *Br. J. Pharmacol.*, **103,** 1119–1125.

CHINKERS, M. & GARBERS, D.L. (1991). Signal transduction by guanylyl cyclases. *Annu. Rev. Biochem.*, **60,** 553–575.

CHUNG, S.H. & FUNG, H.L. (1990). Evidence of the subcellular site for nitroglycerin metabolism to nitric oxide in bovine coronary smooth muscle cells. *J. Pharmacol. Exp. Ther.*, **253,** 614–619.

DIAMOND, J. (1983). Lack of correlation between cyclic GMP elevation and relaxation of non-vascular smooth muscle by nitroglycerin, nitroprusside, hydroxylamine and sodium azide. *J. Pharmacol. Exp. Ther.*, **225,** 422–426.

DIAMOND, J. & JANIS, R.A. (1978). Increases in cyclic GMP levels may not mediate relaxant effects of SNP, verapamil and hydralazine in rat vas deferens. *Nature*, **271,** 472–473.

FEDAN, J.S., NUTT, M.E. & FRAZER, D.G. (1990). Reactivity of guinea-pig isolated trachea to methacholine, histamine and isoproterenol applied serosally versus mucosally. *Eur. J. Pharmacol.*, **190,** 337–345.

FISCUS, R.R., TORPHY, T.J. & MAYER, S.E. (1984). Cyclic GMP-dependent protein kinase activation in tracheal smooth muscle by methacholine and sodium nitroprusside. *Biochim. Biophys. Acta*, **805,** 382–392.

FRANCIS, S.H., NOBLETT, B.D., TODD, B.W., WELLS, J.N. & CORBIN, J.D. (1988). Relaxation of vascular and tracheal smooth muscle by cyclic nucleotide analogs that preferentially activate purified cGMP-dependent protein kinase. *Mol. Pharmacol.*, **34,** 506–517.

FURCHGOTT, R.F. & JOTHIANANDAN, D. (1991). Endothelium-dependent and -independent vasodilatation involving cyclic GMP: relaxation induced by nitric oxide, carbon monoxide and light. *Blood Vessels*, **28,** 52–62.

GIEMBYCZ, M.A. & RAEBURN, D. (1991). Putative substrates for cyclic nucleotide-dependent protein kinases and the control of airway smooth muscle tone. *J. Auton. Pharmacol.*, **11,** 365–368.

GRUETTER, C.A., BARRY, B.K., MCNAMARA, D.B., GRUETTER, D.Y., KADOWITZ, P.J. & IGNARRO, L.J. (1979). Relaxation of bovine coronary artery and activation of coronary arterial guanylate cyclase by nitric oxide, nitroprusside and a carcinogenic nitrosamine. *J. Cyclic Nucleotide Res.*, **5,** 211–224.

HARRISON, D.G. & BATES, J.N. (1993). The nitrovasodilators: new ideas about old drugs. *Circulation*, **87,** 1461–1467.

HULKS, G., JARDINE, A., CONNELL, J.M.C. & THOMSON, N.C. (1989). Bronchodilator effect of atrial natriuretic peptide in asthma. *Br. Med. J.*, **299,** 1081–1082.

HULKS, G., JARDINE, A., CONNELL, J.M.C. & THOMSON, N.C. (1990). Effect of atrial natriuretic peptide on bronchomotor tone in the normal human airway. *Clin. Sci.*, **79,** 51–55.

IJIOMA, S.C., CHALLISS, R.A.J. & BOYLE, J.P. (1993). Relaxant effects of cyclic GMP-elevating agents on spasmogen-supported tone in bovine tracheal smooth muscle. *Br. J. Pharmacol.*, **110,** 163P.

ISHII, K. & MURAD, F. (1989). ANP relaxes bovine tracheal smooth muscle and increases cGMP. *Am. J. Physiol.*, **256,** C495–C500.

JANSEN, A., DRAZEN, J., OSBORNE, J.A., BROWN, R., LOSCALZO, J. & STAMLER, J.S. (1992). The relaxant properties in guinea-pig airways of S-nitrosothiols. *J. Pharmacol. Exp. Ther.*, **261,** 154–160.

KANNAN, M.S. & JOHNSON, D.E. (1992). Nitric oxide mediates the neural nonadrenergic, noncholinergic relaxation of pig tracheal smooth muscle. *Am. J. Physiol.*, **262,** L511–L514.

KARAKI, H., MURAKAMI, K., NAKAGAWA, H. & URAKAWA, N. (1984). Nitroglycerine-induced biphasic relaxation in vascular smooth muscle of rat aorta. *Br. J. Pharmacol.*, **81,** 387–382.

KATSUKI, S. & MURAD, F. (1977). Regulation of cAMP and cGMP levels and contractility in bovine tracheal smooth muscle. *Mol. Pharmacol.*, **13,** 330–341.

KOWALUK, E.A., SETH, P. & FUNG, H.L. (1992). Metabolic activation of sodium nitroprusside to nitric oxide in vascular smooth muscle. *J. Pharmacol. Exp. Ther.*, **262,** 916–922.

LI, C.G. & RAND, M.J. (1991). Evidence that part of the NANC relaxant response of guinea-pig trachea to electrical field stimulation is mediated by nitric oxide. *Br. J. Pharmacol.*, **102,** 91–94.

LOWRY, O.H., ROSEBROUGH, N.J. FARR, A.L. & RANDALL, R.J. (1951). Protein measurement with the folin phenol reagent. *J. Biol. Chem.*, **193,** 265–275.

MALTA, E. (1989). Biphasic relaxant curves to glyceryl trinitrate in rat aortic rings: Evidence for two mechanisms of action. *Naunyn-Schmied. Arch. Pharmacol.*, **339,** 236–243.

MÜLSCH, A., BUSSE R., LIEBAU, S. & FÖRSTERMANN, U. (1988). LY 83583 interferes with the release of endothelium-derived relaxing factor and inhibits soluble guanylyl cyclase. *J. Pharmacol. Exp. Ther.*, **247,** 283–288.

O'DONNELL, M., GARIPPA, R. & WELTON, A.F. (1985). Relaxant activity of atriopeptins in isolated guinea-pig airway and vascular smooth muscle. *Peptides*, **6,** 597–601.

O'DONNELL, M. & OWEN, N.E. (1986). Role of cyclic GMP in atrial natriuretic factor stimulation of Na^+, K^+, Cl^- cotransport in vascular smooth muscle cells. *J. Biol. Chem.*, **261,** 15461–15466.

SETH, P. & FUNG, H.L. (1993). Biochemical characterization of a membrane-bound enzyme responsible for generating nitric oxide from nitroglycerin in vascular smooth muscle cells. *Biochem. Pharmacol.*, **46,** 1481–1486.

TOBIN, A.B., LAMBERT, D.G. & NAHORSKI, S.R. (1992). Rapid desensitization of muscarinic m3 receptor-stimulated polyphosphoinositide responses. *Mol. Pharmacol.*, **42,** 1042–1048.

TORPHY, T.J., FREESE, W.B., RINARD, G.A., BRUNTON, L.L. & MAYER, S.E. (1982). Cyclic nucleotide-dependent protein kinases in airway smooth muscle. *J. Biol. Chem.*, **257,** 11609–11616.

TORPHY, T.J., ZHENG, C., PETERSON, S.M., FISCUS, R.R., RINARD, G.A. & MAYER, S.E. (1985). Inhibitory effect of methacholine on drug-induced relaxation, cyclic AMP accumulation, and cyclic AMP-dependent protein kinase activity in canine tracheal smooth muscle. *J. Pharmacol. Exp. Ther.*, **233,** 409–417.

WALDMAN, S.A. & MURAD, F. (1987). Cyclic GMP synthesis and function. *Pharmacol. Rev.*, **39,** 163–196.

WONG, S.K. & BUCKNER, C.K. (1978). Studies on β-adrenoceptors mediating changes in mechanical events and adenosine 3′,5′-monophosphate levels in guinea-pig trachea. *Eur. J. Pharmacol.*, **47,** 273–280.

ZHOU, H.L. & TORPHY, T.J. (1991). Relationship between cyclic guanosine monophosphate accumulation and relaxation in canine trachealis induced by nitrovasodilators. *J. Pharmacol. Exp. Ther.*, **258,** 972–978.

(Received November 10, 1994
Revised March 1, 1995
Accepted March 8, 1995)

British Journal of Pharmacology (1995) 115, 733–738

Effect of frusemide, ethacrynic acid and indanyloxyacetic acid on spontaneous Ca-activated currents in rabbit portal vein smooth muscle cells

I.A. Greenwood, R.C. Hogg & [1]W.A. Large

Department of Pharmacology and Clinical Pharmacology, St. George's Hospital Medical School, Cranmer Terrace, London SW17 0RE

1 The effect of frusemide, ethacrynic acid and indanyloxyacetic acid was investigated on spontaneous calcium-activated chloride ($I_{Cl(Ca)}$) and potassium currents ($I_{K(Ca)}$) in rabbit portal vein cells with the perforated patch technique.

2 Frusemide ($0.3-1.0\times10^{-3}$ M) reduced the amplitude of spontaneous transient inward chloride currents (STICs) in a concentration-dependent manner. The degree of inhibition on STIC amplitude was similar between -50 and $+30$ mV and frusemide did not alter the STIC reversal potential (E_{rev}).

3 The voltage-dependent exponential decay of STICs, which is thought to represent closure of chloride channels, was not altered by frusemide.

4 The amplitude and frequency of spontaneous potassium outward currents (STOCs) were not altered by frusemide. Since both STICs and STOCs are activated by calcium released from intracellular stores these data indicate that frusemide may block directly $I_{Cl(Ca)}$.

5 Ethacrynic acid ($2-5\times10^{-4}$ M) decreased the amplitude of STICs in a concentration-dependent manner by a similar amount at potentials of -50 to $+30$ mV but did not alter the STIC E_{rev}. However, these concentrations of ethacrynic acid also reduced STOC amplitude and 5×10^{-4} M ethacrynic acid evoked a sustained outward current in most cells at 0 mV; thus ethacrynic acid has a more complex action than simple block of $I_{Cl(Ca)}$.

6 Indanyloxyacetic acid reduced both STIC amplitude and decay time without affecting STOCs and thus also seems to inhibit directly $I_{Cl(Ca)}$. It is discussed whether block of $I_{Cl(Ca)}$ mediates the vasodilator effect of these agents.

Keywords: Loop diuretics; calcium-activated currents; vascular smooth muscle; frusemide; ethacrynic acid, indanyloxyacetic acid

Introduction

Loop diuretics are used clinically in the treatment of congestive heart failure and essential hypertension. Whereas there is little doubt that much of their beneficial effect is due to their diuretic action there is also evidence to suggest that these agents may also relax vascular smooth muscle to produce vasodilatation. Thus, frusemide administered intravenously to patients with congestive heart failure increased venous capacitance prior to diuresis (Dikshit *et al.*, 1973) and reduced blood pressure in hypertensive patients by an action not directly correlated with a decrease in plasma volume (Gerkens, 1987). Furthermore, *in vitro* experiments have demonstrated that frusemide inhibited both the spontaneous and the evoked contractions to noradrenaline and angiotensin II in the rat isolated portal vein (Blair-West *et al.*, 1972). Some evidence has been put forward to suggest that the effect of frusemide on the vasculature is mediated by prostaglandin production (see Gerber, 1983; Gerkens, 1987). However, recent experiments have shown that frusemide relaxed vascular smooth muscle when cyclo-oxygenase was inhibited which indicates that at least part of the inhibitory effect is independent of prostaglandin release (Stevens *et al.*, 1992; Barthelmebs *et al.*, 1994). Moreover, since the vasorelaxant effect of frusemide was not altered by removal of the endothelium it seems likely that frusemide directly reduces smooth muscle contractility (Stevens *et al.*, 1992; Greenberg *et al.*, 1994).

It has been shown that noradrenaline stimulates a calcium-activated chloride current ($I_{Cl(Ca)}$) in rabbit portal vein (Byrne & Large, 1988) and it was suggested that this conductance, in addition to a non-selective cation current, may mediate the noradrenaline-induced depolarization and at least part of the subsequent contraction in vascular smooth muscle (Amédée & Large, 1989). Later it was shown that frusemide inhibited the noradrenaline-induced $I_{Cl(Ca)}$ in rabbit ear artery cells (Amédée *et al.*, 1990) which indicates that this action may contribute to the vasodilator effect of frusemide. However, in this latter paper the mechanism by which frusemide inhibits $I_{Cl(Ca)}$ was not studied. For example, it is possible that frusemide inhibited $I_{Cl(Ca)}$ by inhibiting the release of calcium from the sarcoplasmic reticulum which is responsible for the noradenaline-induced $I_{Cl(Ca)}$ (Amédée *et al.*, 1990) or even by blocking the α-adrenoceptor which mediates the noradrenaline-evoked current. In the present work we have re-investigated the action of frusemide on spontaneous calcium-activated chloride and potassium currents which are both activated by pulses of calcium released from the sarcoplasmic reticulum and these spontaneous currents occur independently of α-adrenoceptor activation (Wang *et al.*, 1992). Recently, it has been suggested that the decay of spontaneous transient inward currents ($I_{Cl(Ca)}$, STICs) in rabbit portal vein represents the closure of chloride channels (Hogg *et al.*, 1993a, b) and consequently agents that block open chloride channels may produce a characteristic change in the decay rate of STICs. Indeed, some established chloride channel blocking compounds have been shown to shorten or lengthen the decay rate of STICs (Hogg *et al.*, 1993b; 1994a) and niflumic acid converts the normal exponential decay into a bi-exponential form at some membrane potentials (Hogg *et al.*, 1994b). These data suggest that these agents interact with the chloride channels after they have

[1] Author for correspondence.

opened and the quantitative results provide some information on the rate with which the blockers interact with the channel (Hogg *et al.*, 1994b). Thus it would seem that the STIC may represent a good model to investigate the mechanisms by which drugs inhibit $I_{Cl(Ca)}$ in smooth muscle. In this paper we describe the effects of frusemide and another loop diuretic, ethacrynic acid, on STICs and compare the results on spontaneous transient outward currents (STOCs, calcium-activated potassium currents). In addition, we have studied the action of indanyloxyacetic acid (IAA-94) which has also been shown to possess vasodilator activity. IAA-94 has been demonstrated to be a potent inhibitor of endothelin-induced depolarization and contraction in renal blood vessels and mesangial cells and rat aorta which are considered to involve the opening of $I_{Cl(Ca)}$ (Ijima *et al.*, 1991; Takenaka *et al.*, 1992).

Methods

Experiments were carried out on smooth muscle cells freshly dispersed from rabbit portal vein. Female New Zealand White rabbits were killed by i.v. injection of sodium pentobarbitone and single cells obtained by enzymatic dissociation. After removal of adipose and connective tissue, strips of portal vein were incubated in nominally Ca-free physiological salt solution (PSS) for 10 min at 37°C. Strips were then exposed to Ca-free PSS containing protease (Sigma type I crude; 0.2–0.3 mg ml^{-1}) for 5 min followed by collagenase (Sigma type XI; 0.5–1 mg ml^{-1}) for 10 min. Cells were dissociated by gently passing the muscle strips through the mouth of a wide-bore glass pipette and were then stored on cover slips in PSS containing 0.75 mM Ca^{2+} at 4°C and used within 8 h of dispersion. Whole cell currents were measured from cells with the perforated patch method using a patch clamp amplifier (List EPC 7; List-Electronic; Darmstadt, Germany). To obtain a perforated patch the antibiotic nystatin (ICN; 200 μg ml^{-1}) was dissolved in dimethylsulphoxide (DMSO) and included in the pipette solution which was prepared every 3 h. Cells were constantly superfused at a rate of 2–3 ml min^{-1} with an external PSS containing (mM): NaCl 126, KCl 6, $MgCl_2$ 1.2, $CaCl_2$ 1.5, HEPES 10 and glucose 11 which was adjusted to pH 7.2 with NaOH. The pipette solution contained (mM): KCl 126, $MgCl_2$ 1.2, HEPES 10, glucose 11, EGTA 0.2 and the pH was adjusted to 7.2 with KOH. In K-free experiments, 126 mM KCl was replaced by an equimolar amount of NaCl in the pipette solution and was omitted from the external solution.

All currents were recorded on magnetic video tape and played back onto a Gould brush recorder to allow amplitudes to be calculated. Analysis of the time course of the spontaneous currents was performed using the SIGAVG signal-averaging programme via a CED 1401 interface (both systems Cambridge Electronic Design, Science Park, Cambridge). Signals were low-pass filtered at 1 kHz prior to digitization and sampled at 2.5 kHz by the software. Ten to twenty individual STICs were used to produce an averaged current and decay time constants were obtained by fitting an exponential with a least squares fitting routine. In the text, n, represents the number of cells required to obtain the mean value which is presented ± s.e.mean. All drugs were dissolved in the PSS perfusing the cells from stock solutions and introduced to the recording chamber downstream of the main PSS reservoir. All drugs were applied for between 2–4 min at which times the inhibitory effects of the drugs appeared to have reached equilibrium. Ethacrynic acid (Sigma, Poole, Dorset) and indanyloxyacetic acid (IAA-94; Research Biochemicals Incorporated, Natick, U.S.A.) were prepared as stock solutions in DMSO. The final concentration of DMSO did not exceed 0.1% in the bathing solution and this concentration had no effect on any of the electrical signals studied. Frusemide was obtained as a pre-injection format dissolved in water (Antigen Pharmaceuticals, Roscrea, Ireland). Statistical significance was assessed by Student's t test.

Results

Effect of frusemide and ethacrynic acid on the amplitude of spontaneous calcium-activated chloride currents

The effect of loop diuretics on STICs was investigated in rabbit portal vein cells initially with potassium-containing pipette and bathing solutions which approximate to physiological conditions. Figure 1a is a control record of STICs from a cell continuously superfused with PSS and shows that the amplitude and frequency of STICs remained stable over the period during which the inhibitors were studied. Figure 1b and c illustrate the effect of frusemide and ethacrynic acid (both at 5×10^{-4} M) on STICs in two different cells at a holding potential (V_h) of −77 mV. This potential was selected because it is the theoretical value of the potassium equilibrium potential so that the chloride currents could be studied without contamination from STOCs. The amplitude of STICs was rapidly attenuated by the addition of 5×10^{-4} M frusemide to the bathing solution (Figure 1b) and the mean reduction in STIC amplitude after 3 min exposure to 5×10^{-4} M frusemide was 50 ± 6% (n=7 cells). Frusemide, 10^{-3} M, inhibited STIC amplitude by 60 ± 5% (n=4). The threshold concentration of frusemide for decreasing STIC amplitude in the time course of the present experiments (about 3 min) was between $1-3 \times 10^{-4}$ M. In 4 cells the mean reduction in STIC amplitude by 3×10^{-4} M frusemide was 27 ± 4% whereas 10^{-4} M frusemide was without effect. Frusemide did not alter the holding current in any concentration used. In 7 cells the effect of frusemide was reversible while in 8 cells even prolonged washing produced only partial recovery of STIC amplitude (to 0.5–0.8 of the control amplitude). In Figure 1b it seems that

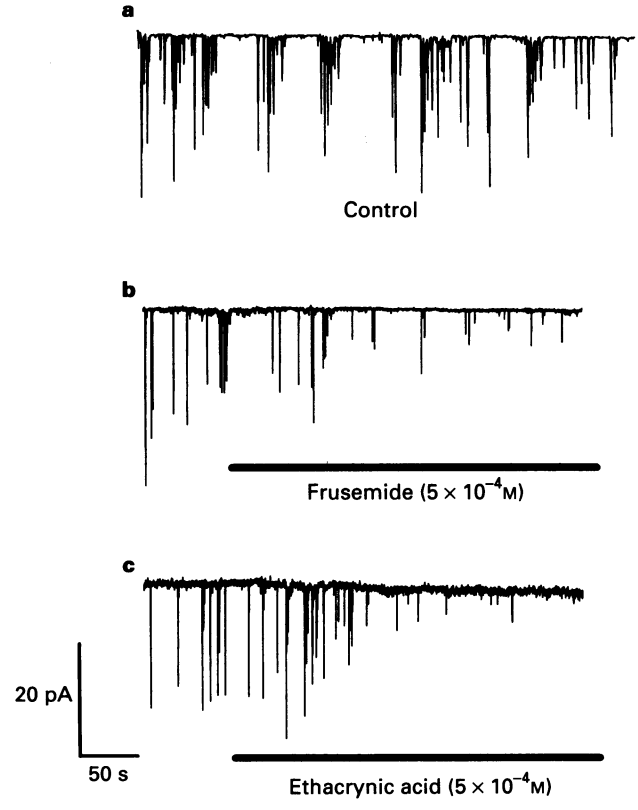

Figure 1 The effect of frusemide and ethacrynic acid on STICs. The holding potential, V_h, was −77 mV in potassium-containing solutions. (a) Shows control STICs and in (b) and (c) the drugs were added to the bathing solution as indicated by the horizontal bars.

frusemide may have inhibited STIC frequency but this apparent effect is likely to be due to the fact that some of the smaller STICs had been reduced to below the noise level.

Previously, we have demonstrated that some chloride channel blockers are more potent as the membrane is depolarized (Hogg *et al.*, 1993b; 1994a, b). In order to test the voltage-dependence of these agents it is necessary to carry out the experiments in potassium-free pipette and external solutions to remove spontaneous transient outward potassium currents (STOCs) which become prominent as the membrane potential is depolarized. Figure 2a illustrates the influence of membrane potential on STIC amplitude in the absence or presence of 5×10^{-4} M frusemide. It can be seen that the reversal potential (E_{rev}) was not changed by the inhibitor. Thus in 9 cells the control E_{rev} was -3 ± 2 mV and in 5×10^{-4} M frusemide E_{rev} was -2 ± 4 mV ($n=3$). Figure 2b demonstrates that the inhibitory effect of frusemide was similar at holding potentials of -50 to $+30$ mV and therefore is voltage-independent.

The addition of ethacrynic acid (5×10^{-4} M) to the bathing solution also produced a rapid decrease in STIC amplitude (Figure 1c) without changing the holding current. At -77 mV in K-containing solutions, 2×10^{-4} M and 5×10^{-4} M ethacrynic acid reduced STIC amplitude by $56 \pm 6\%$ ($n=4$) and $71 \pm 6\%$ ($n=8$), respectively. The effect of ethacrynic acid was also poorly reversible. Further experiments were carried out with ethacrynic acid in K-free conditions at -50 mV where the degree of inhibition was $45 \pm 8\%$ ($n=4$) and $76 \pm 9\%$ ($n=3$) for 2×10^{-4} M and 5×10^{-4} M ethacrynic acid, respectively. Also E_{rev} measured in K-free conditions was not altered by 2×10^{-4} M ethacrynic acid ($E_{rev}=2 \pm 3$ mV, $n=3$) compared to control ($E_{rev}=-3 \pm 2$ mV). Figure 2b demonstrates that the degree of inhibition by 2×10^{-4} M ethacrynic acid was similar at membrane potentials of -50 to $+30$ mV and therefore its effects are not voltage-dependent.

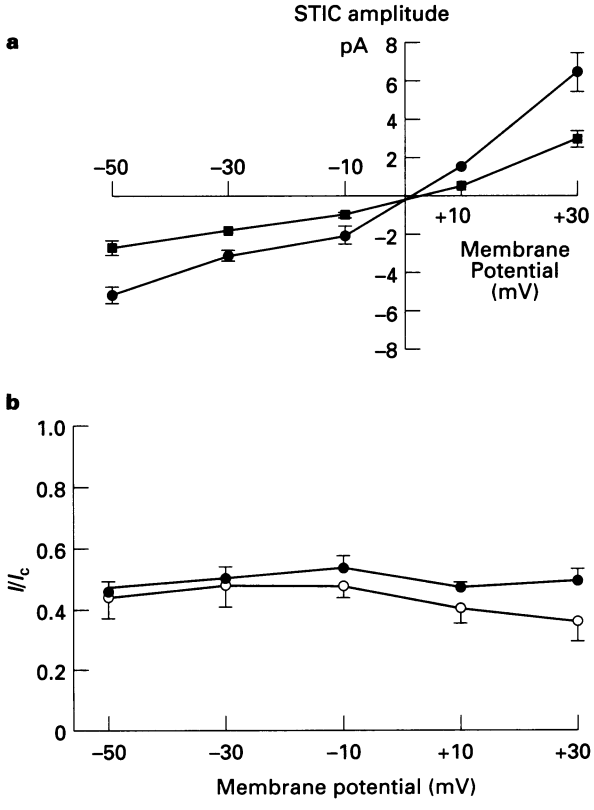

Figure 2 Effect of membrane potential on the inhibitory effect of frusemide and ethacrynic acid on STIC amplitude. (a) Shows the influence of membrane potential on STIC amplitude in the absence (●) or presence of 5×10^{-4}M frusemide (■); (b) illustrates the inhibitory effect of frusemide (●, 5×10^{-4}M) and ethacrynic acid (○, 2×10^{-4}M) at different holding potentials. I and I_C are the current amplitudes in the presence and absence of the inhibitors.

Effect of frusemide and ethacrynic acid on the decay of STICs

Earlier studies have shown that the STIC decays exponentially (Hogg *et al.*, 1993a,b) and that some chloride channel blockers produce a marked alteration in the time constant of the STIC decay (Hogg *et al.*, 1993b; 1994a,b). Figure 3a illustrates the effect of 5×10^{-4} M frusemide on the STIC time course at -50 mV in K-free conditions. In the presence of frusemide the decay remained exponential but the reduction in amplitude was not accompanied by a change in decay time constant (τ, 111 ms in frusemide compared to a control value of 106 ms). In 7 cells with 5×10^{-4} M frusemide the τ value was 101 ± 11 ms compared to the control τ value of 93 ± 7 ms. Frusemide, 10^{-3} M, also did not affect τ at -50 mV (in frusemide, $\tau=98 \pm 5$ ms compared to a control value of 101 ± 5 ms, $n=4$). It has been shown that some chloride channel antagonists produce a voltage-dependent effect on τ (Hogg *et al.*, 1993b; 1994a,b) but this did not occur with frusemide as is shown in Figure 3b. The control time constant at $+50$ mV, which was prolonged compared to the value at -50 mV (see Hogg *et al.*, 1993b), was not different from the value in the presence of frusemide 251 ms vs 231 ms, respectively. In 7 cells at $+50$ mV, the τ values in the absence and presence of 5×10^{-4} M frusemide were 195 ± 19 ms and 177 ± 22 ms, respectively. In 10^{-3} M frusemide at $+50$ mV, τ was 207 ± 16 ms compared to a control τ of 212 ± 10 ms ($n=7$).

The reduction in STIC amplitude by ethacrynic acid, also, was not accompanied by a change in the decay time at either -50 mV or $+50$ mV (Figure 4). The control τ values at -50 mV and $+50$ mV were 87 ± 6 ms and 265 ± 17 ms and in 5×10^{-4} M ethacrynic acid τ was 93 ± 6 ms and 278 ± 17 ms ($n=4$). The STIC decay time constants at -50 mV and $+50$ mV also were not altered by 2×10^{-4} M ethacrynic acid ($n=4$).

Effect of frusemide and ethacrynic acid on spontaneous potassium currents

We have shown that STICs and STOCs often occur as biphasic events (Wang *et al.*, 1992; Hogg *et al.*, 1993a) and that both currents are blocked by agents (e.g. caffeine) that deplete calcium from the sarcoplasmic reticulum. Consequently it seemed that both STICs and STOCs are triggered by the same pulses of calcium released randomly from the sarcoplasmic reticulum (Wang *et al.*, 1992; Hogg *et al.*, 1993a). It is possible that agents that decrease STIC

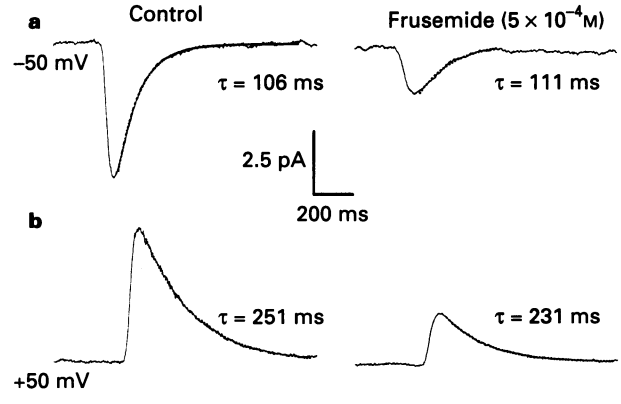

Figure 3 The effect of frusemide on the time course of STICs at different membrane potentials. The holding potential was -50 mV in (a) and $+50$ mV in (b). The time constant (τ) was estimated from an averaged current derived from 10–20 individual currents. K-free bathing and pipette solutions were used. The dotted curves show the exponential fits.

amplitude may produce this effect by depleting or inhibiting the release of calcium from the intracellular store. This possibility was examined by studying the effect of the loop diuretics on STOCs in K-containing solutions at 0 mV, i.e. close to the chloride equilibrium potential. Figure 5a shows that frusemide (10^{-3} M) has no inhibitory effect on the frequency and amplitude of STOCs and this result was found in 6 cells. Exposure of cells to 2×10^{-4} M ethacrynic acid (Figure 5b) had no effect on STOC frequency (0.4 ± 0.08 Hz compared to a control value of 0.5 ± 0.05 Hz) but resulted in a small but significant reduction ($P < 0.05$) in STOC amplitude (204 ± 17 pA compared to a control mean of 262 ± 44 pA, $n = 4$). Addition of 5×10^{-4} M ethacrynic acid produced a pronounced reduction of STOC amplitude (Figure 5c) and evoked an outward current in 6 out of 10 cells tested. The mean outward current was 59 ± 13 pA at 0 mV which peaked after 4–5 min and reversed after washout of ethacrynic acid. In the four other cells, ethacrynic acid (5×10^{-4} M) did not produce any change in holding current. In the presence of 5×10^{-4} M ethacrynic acid the STOC amplitude decreased by $69 \pm 9\%$ ($n = 10$). Consequently the inhibitory effect of frusemide on STIC amplitude does not appear to be mediated by an effect on the intracellular calcium store but in contrast, it seems that ethacrynic acid has an action on the intracellular store.

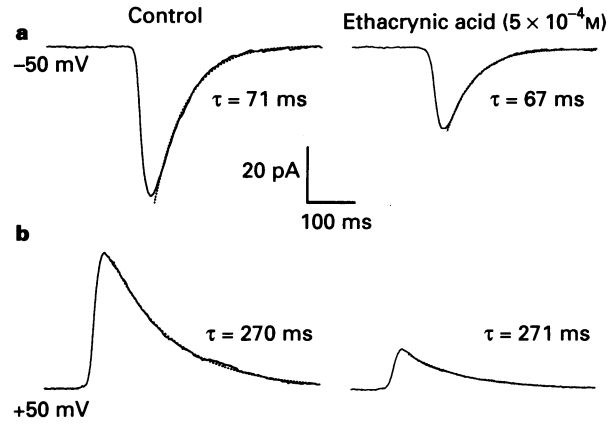

Figure 4 The effect of ethacrynic acid on the time course of STICs. The holding potential was −50 mV in (a) and +50 mV in (b). K-free conditions were used. The dotted curves show the exponential fits.

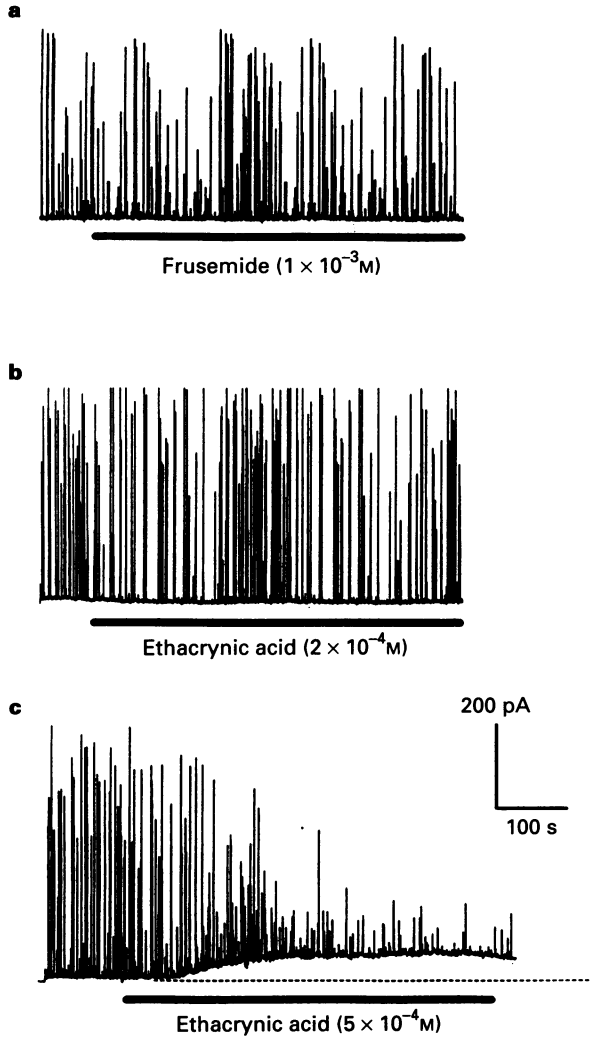

Figure 5 The effect of frusemide and ethacrynic acid on STOCs. The holding potential was 0 mV with K-containing solutions. In (c) the horizontal dashed line indicates the control holding current value.

Effect of IAA-94 on STICs and STOCs

Figure 6a shows that addition of 10^{-4} M IAA-94 to the bathing solution produced a pronounced reduction in STIC amplitude without altering the holding current In 4 cells, 10^{-4} M IAA-94 reduced STIC amplitude by $75 \pm 7\%$ and STICs were blocked totally by 5×10^{-4} M IAA-94 ($n = 3$). In contrast to the loop diuretics, the decrease in STIC amplitude caused by IAA-94 was accompanied by an increase in the STIC decay rate. Figure 6b illustrates that the STIC decay remained exponential in the

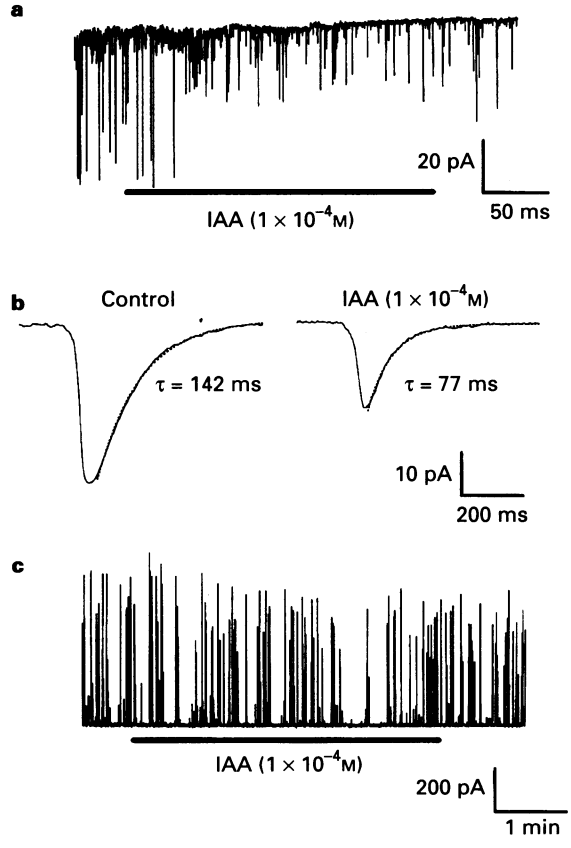

Figure 6 The effect of indanyloxyacetic acid (IAA-94) on STICs and STOCs. K-containing solutions were used and the holding potential in (a) and (b) was −77 mV and in (c) was 0 mV. (a) Illustrates an experimental trace while in (b) the effect of IAA-94 on averaged STICs from (a) is shown. The dotted curves show the exponential fits.

presence of 10^{-4} M IAA-94 but τ was reduced from a control value of 142 ms to 77 ms. In 4 cells the mean control τ was 106 ± 10 ms and in 10^{-4} M IAA-94 τ was 72 ± 2 ms ($P < 0.05$).

In contrast, IAA-94 had no effect on either the amplitude or the frequency of STOCs (Figure 6c). Thus, in 3 cells the ratio of STOC amplitude in the presence of IAA-94 compared to control values was 1.03 ± 0.09 and the ratio of STOC frequency was 1.0 ± 0.13. Therefore it seems unlikely that the reduction in STIC amplitude by IAA-94 was due to an effect on the intracellular calcium store but rather was due to direct inhibition of the chloride conductance.

Discussion

The data from this study indicate that all three compounds, frusemide, ethacrynic acid and IAA-94 inhibited $I_{Cl(Ca)}$ in rabbit portal vein cells but with different characteristics. Since frusemide and IAA-94 did not decrease STOC amplitude it seems unlikely that the reduction in STIC amplitude produced by these agents was due to inhibition of the calcium release mechanism of the sarcoplasmic reticulum which is the source of the calcium signal that triggers both STOCs and STICs. Rather, it is possible that frusemide and IAA-94 block directly the calcium-activated chloride conductance (see below). In contrast concentrations of ethacrynic acid that reduced STIC amplitude also decreased STOC amplitude. This could be due to an effect on the intracellular calcium store or block of the Ca-activated potassium channels that underlie STOCs. The present experiments do not differentiate between these two explanations but the ability of 5×10^{-4} M ethacrynic acid to evoke an outward current (potassium) in some cells at 0 mV indicates that ethacrynic acid can activate a potassium current rather than block potassium channels. Consequently the reduction in STOC amplitude may indicate a depletion of intracellular calcium stores which would also lead to a reduction in STIC amplitude. However it should be noted that 2×10^{-4} M ethacrynic acid produced a greater decrease in STIC amplitude than in STOC amplitude and therefore it is possible that this loop diuretic also inhibits $I_{Cl(Ca)}$ directly in vascular smooth muscle. This would be in agreement with the finding that ethacrynic acid inhibits both chloride transport and tritiated IAA-94 binding in epithelial cells (Landry *et al.*, 1987). Nevertheless ethacrynic acid has apparently complex effects on rabbit portal vein cells and is not simply a direct inhibitor of $I_{Cl(Ca)}$.

The present results with spontaneous chloride currents in portal vein cells confirm the blocking effect of frusemide on $I_{Cl(Ca)}$ reported for noradrenaline-evoked currents in rabbit ear artery cells (Amédée *et al.*, 1990). The latter study did not present any information on the mechanism of action of frusemide which was one of the major aims of the present work but it seems likely that reduction of the noradrenaline-evoked $I_{Cl(Ca)}$ by frusemide is not due to an inhibitory action on the intracellular calcium store (see above). Also since spontaneous chloride currents were inhibited by frusemide in the present study, reduction of noradrenaline-evoked $I_{Cl(Ca)}$ probably occurs as a direct block of the chloride conductance rather than the α-adrenoceptor. Marty and his coworkers (Evans *et al.*, 1986) observed a similar degree of inhibition of $I_{Cl(Ca)}$ by frusemide in the same concentration-range in rat lacrimal gland cells. In their experiments, frusemide displayed a weak degree of voltage-dependence and also appeared to be more effective against large rather than small currents. It was concluded therefore that frusemide bound to the open state of the channel (Evans *et al.*, 1986). In portal vein cells the reduction of STIC amplitude by frusemide was similar at potentials between -50 and $+30$ mV and consequently there appears to be no voltage-dependence in smooth muscle. Also it appears that frusemide did not affect the STIC τ value, which represents the mean channel open time if the STIC decay represents channel closure (Hogg *et al.*, 1993a,b). In the light of these comments it has been shown that the inhibitory action of anthracene-9-carboxylic acid (A-9-C) and niflumic acid on STIC amplitude is increased by depolarization (Hogg *et al.*, 1993b; 1994a,b) which would be expected if the negatively charged form of the molecule blocks the channel. Moreover the reduction in STIC amplitude by both these compounds was accompanied by a concentration-dependent alteration in the STIC decay time, consistent with rapid block of the open channel (for fuller explanation see Hogg *et al.*, 1993b; 1994a,b). By analogy the present data show that frusemide does not alter the STIC decay time constant which suggests that either the chloride conductance is inhibited before channel opening or that $I_{Cl(Ca)}$ is inhibited by a 'slow' channel blocking mechanism in which the apparent mean open time is little affected. In contrast, the reduction of STIC amplitude by IAA-94 was associated with a significant decrease in the STIC decay τ value which suggests that this compound may interact with the open calcium-activated chloride channel and dissociate slowly relative to the mean channel open time. Also IAA-94 was more potent than frusemide and did not affect intracellular calcium stores and therefore might serve as a useful probe to investigate the role of $I_{Cl(Ca)}$ in smooth muscle. However, it should be pointed out that IAA-94 is considerably less potent than niflumic acid which inhibits STICs in the micromolar concentration range and appears to be selective against $I_{Cl(Ca)}$ (Hogg *et al.*, 1994b). However, the observation that IAA-94 inhibited $I_{Cl(Ca)}$ in rabbit portal vein cells supports the previous hypothesis that the attenuation of the endothelin-induced depolarization and vasoconstriction by IAA-94 in the renal microcirculation was due to block of chloride channels (Ijima *et al.*, 1991; Takenaka *et al.*, 1992).

Finally it is worth considering whether inhibition of $I_{Cl(Ca)}$ might contribute to the vasodilator action of frusemide which has been observed in many studies (see Introduction). Chloride ions are transported into smooth muscle cells primarily by the Cl^-/HCO_3^- exchanger with possible involvement of the Na^+, K^+, $2Cl^-$ cotransporter with the result that the chloride equilibrium potential is normally considered to be between -20 mV and -30 mV (Aickin, 1990). The resting chloride conductance is low in smooth muscle but any stimulus (e.g. a pharmacological agent) that increases intracellular calcium might activate $I_{Cl(Ca)}$ and thereby produce membrane depolarization and contraction. There is evidence that frusemide inhibits the cotransporter in some tissues in concentrations greater than 10^{-4} M (Aickin & Brading, 1990; Cabantchik & Greger, 1992) which may convey a vasorelaxant effect (see O'Donnell & Owen, 1994). The concentrations of frusemide required to inhibit $I_{Cl(Ca)}$ in our experiments were rather high ($\geqslant 10^{-4}$ M) but this is the case also in some functional studies. Indeed there was a good degree of similarity in the quantitative data in our electrophysiological study and some contraction experiments. For example, in rat portal vein about 3×10^{-4} M frusemide inhibited spontaneous contraction by approximately 40% after 10 min exposure and inhibited maximum noradrenaline and angiotensin-induced contractions by respectively 25% and 52% (Blair-West *et al.*, 1972). In guinea-pig pulmonary artery, 3×10^{-4} M frusemide (10 min contact time) decreased the noradrenaline-evoked contraction by 40% (Stevens *et al.*, 1992). Also several types of canine veins pre-contracted with noradrenaline or a stable thromboxane-mimetic were relaxed by 30–70% with 3×10^{-4} M frusemide (Greenberg *et al.*, 1994). In our study 3×10^{-4} M frusemide reduced $I_{Cl(Ca)}$ by 27% after a 3 min exposure. Consequently it is possible that blockade of $I_{Cl(Ca)}$ may contribute to the vasodilator action of frusemide when used in relatively high concentrations.

This work was supported by The Wellcome Trust.

References

AICKIN, C.C. (1990). Chloride transport across the sarcolemma of vertebrate smooth and skeletal muscle. In *Chloride Channels and Carriers in Nerve, Muscle and Clial cells*. ed. Alvarez-Leefmans F.J. & Russell, J.M. New York: Plenum Press.

AICKIN, C.C. & BRADING, A.F. (1990). The effect of loop diuretics on Cl^- transport in smooth muscle of the guinea-pig vas deferens and taenia from the caecum. *J. Physiol.*, **421**, 33–53.

AMÉDÉE, T. & LARGE, W.A. (1989). Microelectrode study on the ionic mechanisms which contribute to the noradrenaline-induced depolarization in isolated cells of the rabbit portal vein. *Br. J. Pharmacol.*, **97**, 1331–1337.

AMÉDÉE, T., LARGE, W.A., & WANG, Q. (1990). Characteristics of chloride currents activated by noradrenaline in rabbit ear artery cells. *J. Physiol.*, **428**, 501–516.

BARTHELMEBS, D., STEPHAN, D., FONTAINE, C., GRIMA, M. & IMBS, J.-L. (1994). Vascular effects of loop diuretics: an *in vivo* and *in vitro* study in the rat. *Naunyn-Schmied. Arch. Pharmacol.*, **349**, 209–216.

BLAIR-WEST, J.R., MCKINLEY, M.J. & MCKENZIE, J.S. (1972). Effect of frusemide on the reactivity of rat portal vein. *J. Pharmac. Pharmacol.*, **24**, 442–446.

BYRNE, N.G. & LARGE, W.A. (1988). Membrane ionic mechanisms activated by noradrenaline in cells isolated from the rabbit portal vein. *J. Physiol.*, **404**, 557–573.

CABANTCHIK, Z.I. & GREGER, R. (1992). Chemical probes for anion transporters of mammalian cell membranes. *Am. J. Physiol.*, **262**, C803–C827.

DIKSHIT, K., VYDEN, J.B., FORRESTER, J.S., CHATTERJEE, K., PRAKESH, R. & SWAN, H.J.C. (1973). Renal and extrarenal hemodynamic effects of furosemide in congestive heart failure after acute myocardial infarction. *N. Engl. J. Med.*, **228**, 1087–1090.

EVANS, M.G., MARTY, A., TAN, Y.P. & TRAUTMANN, A. (1986). Blockage of Ca-activated Cl conductance by furosemide in rat lacrimal glands. *Pflügers Arch.*, **406**, 65–68.

GERBER, J.G. (1983). Role of prostaglandins in the hemodynamic and tubular effects of furosemide. *Fed. Proc.*, **42**, 1707–1711.

GERKENS, J.F. (1987). Does furosemide have vasodilator activity? *Trends Pharmacol. Sci.*, **8**, 254–257.

GREENBERG, S., MCGOWAN, C., XIE, J. & SUMMER, W.R. (1994). Selective pulmonary and venous smooth muscle relaxation by furosemide: a comparison with morphine. *J. Pharmacol. Exp. Ther.*, **270**, 1077–1085.

HOGG, R.C., WANG, Q., HELLIWELL, R.M. & LARGE, W.A. (1993a). Properties of spontaneous inward currents in rabbit pulmonary artery smooth muscle cells. *Pflügers Arch.*, **425**, 233–240.

HOGG, R.C., WANG, Q. & LARGE, W.A. (1993b). Time course of spontaneous calcium-activated chloride currents in smooth muscle cells from the rabbit portal vein. *J. Physiol.*, **464**, 15–31.

HOGG, R.C., WANG, Q. & LARGE, W.A. (1994a). Effects of Cl channel blockers on Ca-activated chloride and potassium currents in smooth muscle cells from rabbit portal vein. *Br. J. Pharmacol.*, **111**, 1333–1341.

HOGG, R.C., WANG, Q. & LARGE, W.A. (1994b). Action of niflumic acid on evoked and spontaneous calcium-activated chloride and potassium currents in smooth muscle cells from rabbit portal vein. *Br. J. Pharmacol.*, **112**, 977–984.

IJIMA, K., LIN, L., NASJLETTI, A. & GOLIGORSKY, M.S. (1991). Intracellular ramification of endothelin signal. *Am. J. Physiol.*, **260**, C982–C992.

LANDRY, D.W., REITMAN, M., GRAGOE, E.J. (Jnr) & AL-AWQATI, Q. (1987). Epithelial chloride channel - Development of inhibitory ligands. *J. Gen. Physiol.*, **90**, 779–798.

O'DONNELL, M.E. & OWEN, N.E. (1994). Regulation of ion pumps and carriers in vascular smooth muscle. *Physiol. Rev.*, **74**, 683–721.

STEVENS, E.L., UYEHARA, C.F.T., SOUTHGATE, M.W. & NAKAMURA, K.T. (1992). Furosemide differentially relaxes airway and vascular smooth muscle in fetal, newborn and adult guinea-pigs. *Am. Rev. Respir. Dis.*, **146**, 1192–1197.

TAKENAKA, T., EPSTEIN, M., FORSTER, H., LANDRY, D.W., IJIMA, K. & GOLIGORSKY, M.S. (1992). Attenuation of endothelin effects by a chloride channel inhibitor, indanyloxyacetic acid. *Am. J. Physiol.*, **262**, F779–F806.

WANG, Q., HOGG, R.C. & LARGE, W.A. (1992). Properties of spontaneous inward currents in smooth muscle cells isolated from the rabbit portal vein. *J. Physiol.*, **451**, 525–537.

(Received January 13, 1995
Revised March 3, 1995
Accepted March 14, 1995).

British Journal of Pharmacology (1995) 115, 739-744

Functional characterization of the adenosine receptor mediating inhibition of peristalsis in the rat jejunum

Debra L. Hancock & [1]Ian M. Coupar

Department of Pharmaceutical Biology and Pharmacology, Victorian College of Pharmacy, Monash University, 381, Royal Parade, Parkville, Victoria, 3052, Australia

1 The non-selective adenosine agonist, 5'-N-ethylcarboxamidoadenosine (NECA), is a potent inhibitor of morphine withdrawal diarrhoea in rats. More recently we found that NECA exerts its antidiarrhoeal effect by inhibiting secretion in both the jejunum and ileum and also by inhibiting peristalsis in the ileum. The specific aim of this study was to characterize the receptor in the rat jejunum mediating inhibition of peristalsis via functional studies using a range of metabolically stable adenosine analogues based on the pharmacological criteria of relative agonist and antagonist potencies.

2 Peristalsis in the rat isolated jejunum was achieved by raising the pressure to between 7–11 cmH_2O for 3 min followed by a 3 min rest period (pressure at zero). The mean rate of peristalsis during inflation was 7.3 ± 0.1 peristaltic waves per 3 min and this rate remained consistent for up to 30 min, in 5 separate tissues. The inhibitory effects of the adenosine analogues were quantified by expressing their effects as a % reduction in the mean number of peristaltic contractions derived from the control tissues.

3 The rank order of agonist potency to reduce the rate of peristalsis was: N^6-cyclopentyladenosine (CPA) > NECA > **R**(–)-N^6-(2-phenylisopropyl)adenosine (**R**-PIA) > chloroadenosine (2-CADO) > **S**-PIA > 2-phenylaminoadenosine (CV-1808). This order complies well with the rank order of agonist potency that represents the activation of the A_1 receptor subtype (CPA > **R**-PIA = CHA = > NECA > 2-CADO > **S**-PIA > CV-1808).

4 The selective A_1 adenosine antagonist 1,3-dipropyl-8-cyclopentylxanthine (DPCPX) and the non-selective adenosine antagonist 8-phenyltheophylline (8-PT) at their respective concentrations of 10 nM and 2 μM caused parallel rightward shifts in the concentration-response curve to the non-selective A_1/A_2 agonist NECA. DPCPX was significantly more potent at inhibiting NECA than 8-PT as revealed by their apparent pA_2 values; DPCPX (9.5) and 8-PT (7.26). The high affinity of DPCPX relative to that of 8-PT suggests the presence of an A_1 and not an A_{2B} receptor. In addition, the high affinity of DPCPX (pA_2:9.37) against the selective A_1 agonist CPA, further confirms the presence of the A_1 receptor subtype.

5 In this study we found that the A_1 adenosine receptor is involved in regulating *in vitro* peristalsis which is different from the adenosine receptor regulating inhibition of secretion (A_{2B}) in the same region of intestine of the same species. We propose that A_{2B} adenosine agonists could be of clinical value in the management of diarrhoea that is due to microbiological organisms where antimotility effects are not desired.

Keywords: Adenosine receptors; rat intestine; peristalsis; antidiarrhoeal; A_1 receptor; NECA; *in vitro* technique

Introduction

It is now well established that adenosine has pharmacological actions on a variety of smooth muscle preparations and these effects are mediated via receptors which have been classified as P_1-purinoceptors (Burnstock, 1990; Kennedy, 1990). These receptors have been further subdivided into A_1, A_2 and A_3 receptors based on the orders of both agonist potency and antagonist affinity, G-protein coupling mechanisms, cellular responses and receptor cloning studies (Fredholm *et al.*, 1994). The A_1 receptor is differentiated from the A_2 receptor by the selective A_1 agonist, N^6-cyclopentyladenosine (CPA) which has a 2,500 fold A_1 selectivity vs A_2 in radioligand binding studies (Lohse *et al.*, 1988) and the selective A_1 antagonist 1,3-dipropyl-8-cyclopentylxanthine (DPCPX) which has a dissociation constant in the nanomolar range at A_1 and in the micromolar range at A_2 receptors (Bruns *et al.*, 1987a). The A_{2A} receptor is differentiated from the A_{2B} receptor by the selective A_{2A} agonist, CGS-21680 (Jarvis *et al.*, 1989) and the selective A_{2A} antagonist, PD-115199 (Bruns *et al.*, 1987b). At present there are no ligands available that are specific for the A_{2B} receptor. Consequently, the A_{2B} receptor is identified by the low affinity of A_{2A} selective ligands as highlighted in the agonist potency order and antagonist affinity order used to characterize adenosine receptor subtypes (Collis & Hourani, 1993). The recently described A_3 receptor can be identified by the selective agonist, N^6-benzyl-NECA which shows a 14 fold selectivity for A_3 receptors vs A_1 and A_{2A} (Van Galen *et al.*, 1994). This receptor is also insensitive to block by methylxanthines unlike the other adenosine receptor subtypes (Fredholm *et al.*, 1994) but is antagonized by 8-phenyl-substituted xanthines, such as BWA522, which is a potent antagonist in the nanomolar range (Fozard & Hannon, 1994).

It has been known for some time that adenosine and synthetic analogues have effects on the gut muscle of a variety of mammals, birds and amphibians and in particular the guinea-pig ileum (Drury & Szent-Gyorgi, 1929; Barsoum & Gaddum, 1935; Hayashi *et al.*, 1978; Collier & Tucker, 1983). The recent availability of adenosine analogues of known selectivities has facilitated the functional characterization of adenosine receptors. Some progress has been made in characterizing the adenosine receptors in the rat intestine. For example, it has been shown that the distal colon contains A_1 excitatory receptors in the muscularis mucosa (Bailey *et al.*, 1992) and A_2 inhibitory receptors in the longitudinal muscle (Bailey & Hourani, 1992) while the longitudinal muscle of the duodenum contains A_1 and A_{2B} receptor subtypes, both of which subserve relaxation (Nicholls *et al.*, 1992a). However, other regions of the small intestine, such as the jejunum and ileum have been

[1] Author for correspondence.

relatively neglected except for our recent study which showed that the non-selective adenosine agonist, NECA, inhibits secretion and peristalsis in the rat ileum (Coupar & Hancock, 1994) and also inhibits secretion in the rat jejunum; this particular effect has been shown to be mediated via the A_{2B} receptor (Hancock & Coupar, 1995).

The specific aim of this study was to characterize the receptor mediating inhibition of peristalsis by use of a range of metabolically stable adenosine analogues based on the pharmacological criteria of relative agonist and antagonist potencies.

Methods

Male Hooded Wistar rats (250–350 g body weight) were stunned by a blow to the head and killed by exsanguination. A segment of proximal jejunum was excised close to the Ligament of Trietz and flushed of luminal contents with Krebs-Henseleit solution (composition mM: NaCl 118, KCl 4.7, $NaHCO_3$ 25, KH_2PO_4 1.2, $CaCl_2$ 2.5, $MgSO_4$ 1.2, D-(+)-glucose 11; bubbled with 95% O_2 and 5% CO_2). The segments were cut to approximately 7–10 cm lengths and were mounted vertically in a 30 ml organ bath containing Krebs-Henseleit solution maintained at 37°C and gassed with 95% O_2 and 5% CO_2. The open aboral end of each segment was secured over a glass tube connected to a reservoir containing Krebs-Henseleit solution. The reservoir contained a float which was linked to an isotonic transducer to measure luminal volume displacement as an index of circular muscle contraction. The oral end of each segment was closed off and connected to an isotonic transducer for recording longitudinal contractions under a load of 1 g. An intraluminal water pressure of 7–11 cm was required to elicit peristaltic activity. The tissues were allowed to equilibrate for 45 min during which time the Krebs-Henseleit solution was replaced every 15 min. Preliminary experiments showed that inflating the segments for 3 min followed by a 3 min rest period (water pressure at zero) produced regular peristaltic activity during the periods of inflation compared to a sustained elevated intraluminal pressure which produced variable and short lasting bursts of peristaltic activity. Consequently, the segments were inflated for 3 min followed by a 3 min rest period in all further experiments. The mean rate of peristalsis during this period was 7.3 ± 0.1 peristaltic waves per 3 min up to 30 min in 5 separate tissues. In these control tissues the rate of peristalsis in the first period of peristalsis was not significantly different from the final burst of peristalsis (Student's paired t test, $P < 0.05$).

Experimental design and analysis of results

In separate tissues, the inhibitory effects of the adenosine analogues were quantified by expressing their effects as a % reduction in the mean number of peristaltic contractions derived from the experiments described above. The presence of peristalsis was confirmed in each of the 3 min periods by allowing two peristaltic contractions to occur before adding the test drug. The number of contractions was then recorded in the presence of the drug in the remainder of the 3 min period. This number was then expressed as a % of the possible 5 contractions (mean number of peristaltic contractions being 7 in 3 min. Refer to Figure 1 for further details). This method of analysis was chosen because the number of peristaltic waves in consecutive inflations was too variable to measure a before and after agonist effect in one tissue. The tissues were washed after each concentration of agonist. A higher concentration of the same agonist was tested when 2 peristaltic contractions were achieved in the subsequent 3 min period of elevated pressure. Each tissue was only functionally viable for up to 30 min which limited the number of concentrations of each agonist to four. The potency of each agonist (EC_{50} value) was calculated by linear regression analysis with 95% confidence intervals of the estimates.

The non-selective adenosine agonist, NECA and the A_1-selective agonist, CPA, were employed in the experiments designed to measure the affinity of the antagonists. In these experiments the antagonists were added 30 min prior to adding the first concentration of NECA or CPA to the bath and their affinities were estimated by measuring their apparent pA_2 values. The resultant dose ratios (DR) with associated CI were used to calculate the apparent pA_2 values from the K_B values derived from the equation-:

$$K_B = B/DR\text{-}1$$

where B is the concentration of the antagonist and the apparent pA_2 value is equal to -log K_B. Student's unpaired t test was used to compare single treatment means with their respective controls. The criterion for statistical significance was set at $P < 0.05$. Each rat is represented by $n = 1$.

Drugs

Agonists: chloroadenosine (2-CADO), N^6-cyclopentyladenosine (CPA),2-phenylaminoadenosine (CV-1808),5'-N-ethylcarboxamidoadenosine (NECA), **R**-(-)-N^6-(2-phenylisopropyl) adenosine (**R**(-)-PIA) and (**S**(+)-PIA). All were obtained from RBI, Natick, U.S.A. The agonists were dissolved in 0.9% w/v saline except CV-1808 and CPA which were dissolved in 6% and 1% ethanol in saline respectively and then diluted with saline to give the required concentration. The vehicle had no effect on the responses of the tissues.

Antagonists: atropine sulphate (Sigma, Castle Hill, Australia), 1,3-dipropyl-8-cyclopentylxanthine (DPCPX, RBI, Natick, USA) and 8-phenyltheophylline (8-PT, RBI, Natick, U.S.A.) were dissolved in 1% v/v dimethylsulphoxide (DMSO), 0.75% v/v 1 M NaOH in saline and further diluted with saline to give the required concentration. This vehicle had no significant effect on the peristaltic activity of the jejunum ($P > 0.05$, Student's unpaired t test).

Results

Atropine (100 nM, 10 min incubation) abolished peristaltic activity in the jejunum ($n = 4$). Each of the adenosine agonists caused a concentration-related reduction in the number of peristaltic waves occurring within 3 min with the following order of potency: CPA > NECA > **R**-PIA > 2-CADO > **S**-PIA > CV-1808 (Table 1, Figure 2). The inhibition elicited by each adenosine agonist was very rapid in onset, reaching its maximum within 30s and was readily reversible on washing (Figure 1).

The adenosine antagonists DPCPX and 8-PT at their respective concentrations of 10 nM and 2 μM caused parallel rightward shifts in the concentration-response curve to NECA. The respective dose-ratios were 30.46 ($n = 17$) and 37.46 ($n = 12$), corresponding to apparent pA_2 values of 9.47 (95% CI 9.41–9.54) for DPCPX and 7.26 (95% CI 7.20–7.33) for 8-PT using NECA as the agonist (Figure 3a and b). In addition,

Table 1 Potencies of adenosine agonists at reducing the number of peristaltic waves within 3 min

Adenosine agonist	EC_{50} (nM)	(n)	*95% CI*
CPA	2.3	(12)	2.9
NECA	25.4	(7)	3.8
R-PIA	41.2	(6)	3.7
2-CADO	150.9	(10)	2.8
S-PIA	239	(7)	1
CV-1808	7700	(7)	1500

For abbreviations, see text.

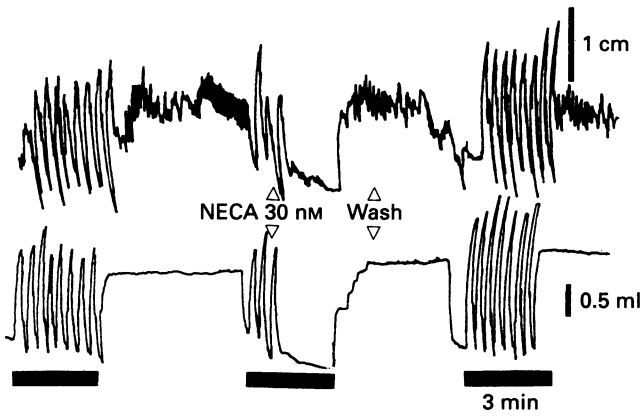

Figure 1 The inhibitory effect of 5'-N-ethylcarboxamidoadenosine (NECA) on peristalsis in a segment (10 cm in length) of rat jejunum. The top trace represents the contraction of the longitudinal muscle and the bottom trace shows the associated volume expulsion as a result of circular muscle contraction in response to increasing the intraluminal pressure to 10 cmH_2O. The 3 min periods of elevated intraluminal pressure are represented by the thick black bars. In the second period of peristaltic activity, NECA (30 nM) was administered after the second peristaltic contraction which produced an 80% reduction in the rate of peristalsis (i.e. one contraction out of a possible 5 contractions). The inhibition was very rapid in onset and was readily reversible on washing.

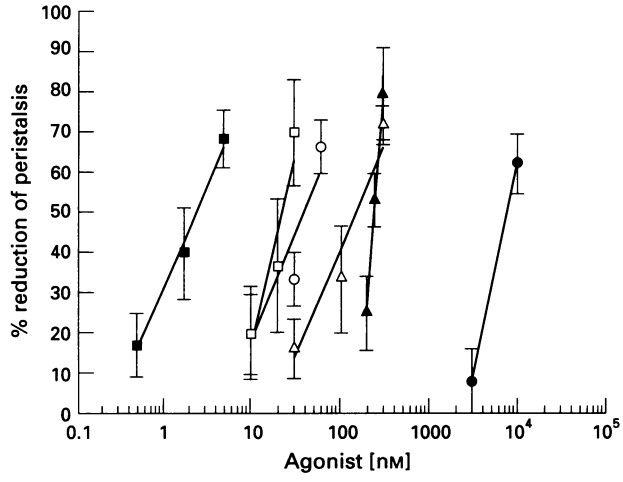

Figure 2 The concentration-effect relationships for a range of adenosine agonists at inhibiting peristalsis in the rat jejunum. The decreasing order of potency is as follows:- CPA (■), NECA (□), R-PIA (○), 2-CADO (△), S-PIA (▲), CV-1808 (●). Values are means ± s.e. means. For abbreviations, see text.

DPCPX (10 nM) also produced a parallel rightward shift in the concentration-response relationship to CPA. The dose-ratio for DPCPX was 24.24 ($n=19$) using CPA as the agonist giving an apparent pA_2 value of 9.37 (95% CI 9.01–9.73) (Figure 3c). Neither antagonist altered the number of peristaltic contractions within 3 min that occurred during the first burst of peristalsis (control: 8.6 ± 1.2, $n=5$; DPCPX: 9.67 ± 0.94, $n=9$; 8-PT: 8.83 ± 0.98, $n=6$, Student's unpaired t test, $P>0.05$).

Discussion

The rank order of adenosine agonist potencies and antagonist affinities obtained in this study suggest that the A_1 adenosine receptor is involved in mediating inhibition of peristaltic activity in the rat jejunum based on the classification table described by Collis & Hourani (1993). These results, in conjunction with our previous findings on the rat jejunum

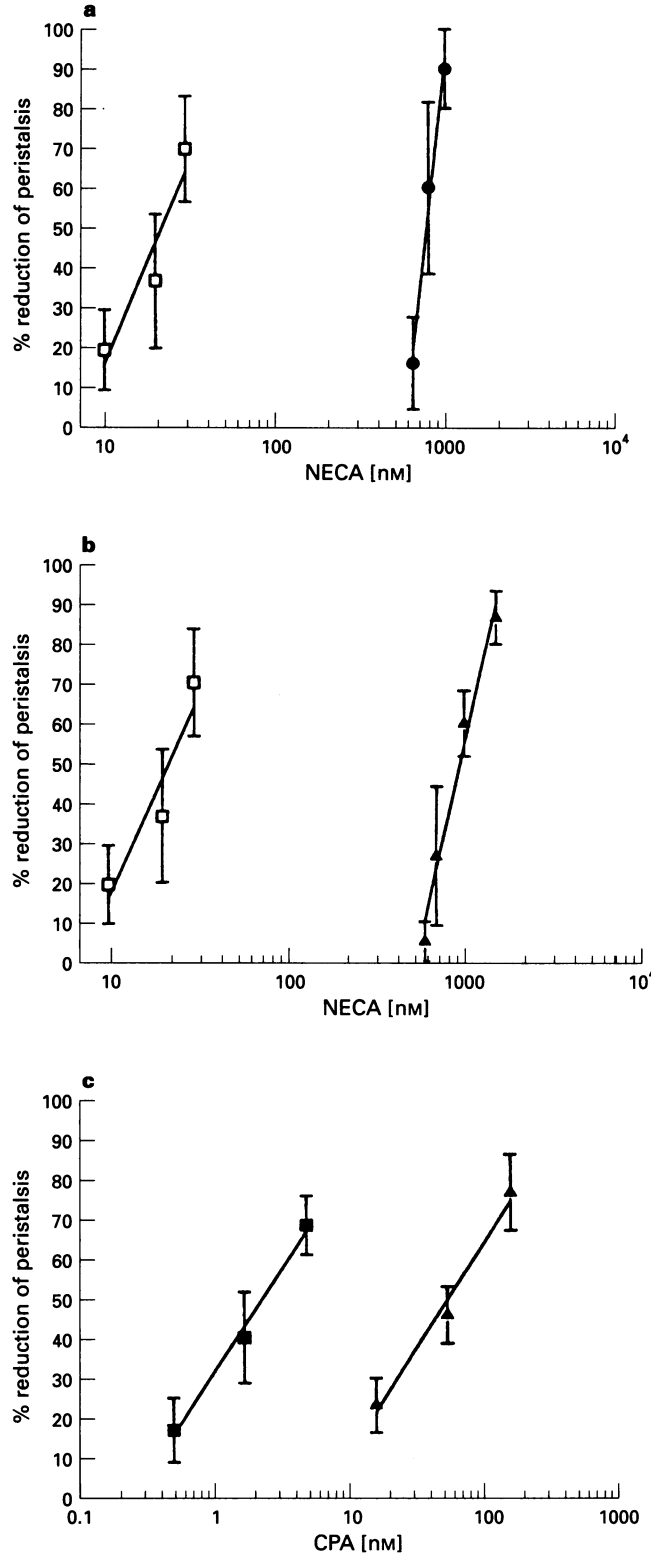

Figure 3 (a) Concentration-effect relationship of the non-selective adenosine agonist, NECA at inhibiting peristalsis in the rat jejunum in the absence (□) and in the presence (●) of the antagonist, DPCPX (10 nM). (b) NECA in the absence (□) and in the presence (▲) of the antagonist, 8-PT (2 μM). (c) The A_1 selective agonist, CPA at inhibiting peristalsis in the rat jejunum in the absence (■) and in the presence (▲) of the A_1 selective antagonist, DPCPX (10 nM). Values are means ± s.e. means. For abbreviations, see text.

(Hancock & Coupar, 1995), show that adenosine agonists exert their antidiarrhoeal action in rats (Dionyssopoulos *et al.*, 1992) by inhibiting both intestinal secretion via the A_{2B} ade-

nosine receptor (Hancock & Coupar, 1995) and intestinal motility or peristalsis via the A_1 adenosine receptor.

The agonists used in this study inhibited intestinal peristaltic activity in the order of CPA > NECA > **R**-PIA > 2-CADO > S-PIA > CV-1808 which almost coincides with the rank order of agonist potency that represents activation of the A_1 receptor: CPA > **R**-PIA = CHA = > NECA > 2-CADO > S-PIA > CV-1808 (Collis & Hourani, 1993). The only discrepancy in the order of agonist potencies is that NECA is more potent than **R**-PIA in this study, whereas **R**-PIA is equipotent or more potent than NECA in the A_1 receptor classification. However, this difference in potency between the two agonists is relatively small. The order of agonist potency in this study is also similar to the A_{2B} receptor classification where the order of agonist potency is: NECA > 2-CADO > **R**-PIA = CHA > S-PIA > = CV-1808 > = CGS-21680 (Collis & Hourani, 1993). The only contrast is that **R**-PIA is more potent than 2-CADO in this study which is the reverse of that found in the A_{2B} classification. Unfortunately the A_{2B} receptor classification does not include our most potent agonist CPA but there is no evidence in the literature to indicate that CPA is without activity at the A_{2B} receptor. However, CPA is structurally and pharmacologically similar to CHA, so it is reasonable to assume that it will also be less potent than NECA at A_{2B} receptors.

The order of agonist potencies in this study to inhibit peristalsis is almost the opposite of the order that represents activation of the A_{2A} adenosine receptor where CGS-21680 = NECA > CV-1808 > = 2-CADO > **R**-PIA = CHA = CPA > S-PIA (Collis & Hourani, 1993). For instance, CV-1808 is the least potent agonist to inhibit peristalsis but is a potent agonist in the A_{2A} order and CPA the most potent agonist in this study is almost without activity in the A_{2A} receptor classification. The single exception is that NECA is a potent agonist in both this study and the A_{2A} receptor classification. CGS-21680, the selective A_{2A} agonist was not tested in this study since the agonists tested indicated the activation of an A_{2B} or A_1 receptor where CGS-21680 is the least potent in both classifications. Similarly the A_3 receptor was excluded because NECA was significantly more potent than **R**-PIA at inhibiting peristalsis in the rat jejunum unlike the equipotent activity of these agonists found in the A_3 classification (Collis & Hourani, 1993). In addition, xanthine antagonists, such as DPCPX and 8-PT as used in this study have low affinity at the A_3 receptor.

The rank order of agonist potencies together with antagonist affinity orders are used to characterize functional adenosine receptors as outlined by Collis & Hourani (1993). The antagonists, DPCPX and 8-PT were investigated specifically to differentiate between A_1 and A_2 receptors since the order of agonist potencies suggests the presence of either an A_1 or an A_{2B} adenosine receptor that is responsible for mediating inhibition of peristaltic activity in the rat jejunum. The differences between the affinities of the two antagonists is evident in isolated tissues where 8-PT is non-selective for A_1 and A_2 receptors, whilst DPCPX has a 30–50 fold greater affinity for A_1 but is equi-effective with 8-PT at A_2 receptors (Collis *et al.*, 1989). In this study, DPCPX is significantly more potent at inhibiting NECA-evoked responses than 8-PT, as revealed by their apparent pA_2 values; DPCPX (9.47) and 8-PT (7.26). In addition, the apparent pA_2 value for DPCPX against the selective A_1 agonist, CPA was 9.53 which further confirms the presence of an A_1 receptor. These pA_2 values for both antagonists in the rat jejunum are in line with the pA_2 values reported in the rat and guinea-pig atria (Collis *et al.*, 1988) which are thought to possess the A_1 receptor (Collis, 1983; Haleen *et al.*, 1987). The apparent pA_2 for 8-PT against NECA in the rat jejunum (95% CI 7.20–7.33) is similar to the pA_2 value for 8-PT reported in the rat (95% CI 6.54–7.95) and guinea-pig atria (95% CI 5.89–7.23). In addition, the apparent pA_2 values for DPCPX in the rat jejunum against NECA (95% CI 9.41–9.54) and CPA (95% CI 9.01–9.73) are the same as the value for DPCPX in the rat atria (95% CI 7.33–9.42). However, the affinity values for DPCPX in the rat jejunum are significantly higher than that found in the guinea-pig atria (95% CI 7.67–8.65). One possible reason for the low affinity of DPCPX in the guinea-pig atria compared to that of the rat jejunum could be due to a species difference. For instance, Ukena *et al.* (1986) reported that the affinity of xanthine derivatives at A_1 binding sites in the brain are significantly higher in the rat than the guinea-pig. The high affinity values of DPCPX against NECA and CPA compared to the relatively low affinity of 8-PT against NECA found in this study discounts the possibility that adenosine agonists are inhibiting peristalsis in the rat jejunum via the A_2 adenosine receptor. This high antagonist potency of DPCPX along with the order of agonist potency indicates the presence of an A_1 adenosine receptor in the rat jejunum.

In the absence of exogenous adenosine agonists, neither DPCPX nor 8-PT altered the rate of peristalsis at the concentrations employed. Similarly, in a previous study these antagonists were free of intrinsic pro-secretory activity in the rat jejunum (Hancock & Coupar, 1995). It appears that under the conditions of both experiments, endogenous adenosine is not released in the rat jejunum to inhibit either peristalsis or fluid secretion. This situation is unlike that found in the guinea-pig atria, where both antagonists in the absence of exogenous adenosine increased the rate of beating of the isolated atria which was due to antagonism of the negative chronotropic action of endogenous adenosine (Collis *et al.*, 1989). The antagonist concentrations employed in the guinea-pig atria were considerably higher than those used in the rat jejunum which could explain the detection of endogenous adenosine activity in the atria.

In this study the intestine was radially distended with fluid which is thought to be detected by mechanoreceptors in the muscularis externa (Yokoyama & North, 1983; Smith *et al.*, 1990) to initiate peristalsis. The present study has not precisely determined the tissue location of the adenosine receptor involved in controlling peristalsis. However, our previous studies do suggest that the receptor is not located on intestinal smooth muscle or cholinergic neurones since high concentrations of NECA failed to affect transmurally stimulated cholinergic contractions of the rat jejunum (Coupar & Hancock, 1994). From these results, together with our more recent finding that atropine inhibits peristalsis in the jejunum it could be postulated that adenosine analogues act proximal to the final cholinergic neurone in the peristaltic reflex arc.

There is evidence from other functional studies that adenosine receptors do exist in the rat intestine. For instance, CPA and NECA have been shown to relax the duodenum by activating A_1 and A_{2B} receptors respectively (Nicholls *et al.*, 1992a). Additionally, A_1 agonists caused contraction of the muscularis mucosa (Bailey *et al.*, 1992) and A_2 agonists cause relaxation of the longitudinal muscle of the distal colon (Bailey & Hourani, 1992). There is also evidence from molecular biology that adenosine receptors (A_1, A_2, A_{2B}) are expressed in numerous rat tissues such as the brain, spinal cord, heart, lung, urinary bladder and in particular the large intestine (A_{2B}) but not in the small intestine (Stehle *et al.*, 1992). A recent binding study has established the existence of A_1 binding sites using the A_1-selective ligand, DPCPX in the duodenum and colon (Peachey *et al.*, 1994). In another binding study the non-selective ligand, NECA, was shown to bind to both A_1 and A_2 receptors in the rat brain, but did not exhibit any specific binding in the small intestine (Bruns *et al.*, 1986). This emphasizes the importance of functional studies to reveal and characterize receptor subtypes. From the above studies, it is apparent that the duodenum is the only section of the small intestine previously shown to contain adenosine receptors.

The guinea-pig has been the only species used to date to investigate the effect of adenosine or its analogues on intestinal peristalsis (Okwuasaba & Hamilton, 1975; Van Nueten *et al.*, 1976). This seems surprising since it is well accepted that the effects and mechanisms of drug action, particularly of opiates, is species-dependent. This situation is highlighted by our finding that the adenosine agonist, NECA inhibits transmu-

rally stimulated contractions of the guinea-pig ileum but not of the rat ileum or jejunum (Coupar & Hancock, 1994). In this recent study we also tested the effect of NECA on the peristaltic reflex in the rat ileum to find that NECA at 10 nM slowed the reflex while 30 nM virtually abolished it (Coupar & Hancock, 1994). The potency of NECA in the ileum is in line with the potency of NECA (EC_{50} = 25.4 nM) found in the rat jejunum in the present study, despite the finding that the rate of peristalsis is faster in the jejunum (1 contraction per 25.7 s) than that previously found in the rat ileum (1 contraction per min). In the guinea-pig, peristalsis was also found to be faster in the upper than the lower portion of the small intestine (Kromer *et al.*, 1981). It has been suggested that regional differences in the amounts of inhibitory neuromodulators released, such as endogenous opioids, are responsible for regulating the decrease in rate of peristaltic activity observed aborally in the guinea-pig small intestine (Kromer *et al.*, 1981). The endogenous inhibitory neuromodulator could also be adenosine formed from ATP. It has been known for some time that ATP is taken up and can be released in response to stimulation of non-adrenergic inhibitory fibres that innervate the gut (Burnstock *et al.*, 1970; Satchell & Burnstock, 1971; Su *et al.*, 1971). In the rat duodenum it has been shown that ATP is rapidly metabolized to ADP, AMP and inosine, a metabolite of adenosine which is inactive at purinoceptors (Nicholls *et al.*, 1992b). Adenosine itself is rapidly inactivated in this tissue by adenosine deaminase (Franco *et al.*, 1988). In addition, studies by Reiter *et al.* (1989) detected adenosine deaminase in the human intestinal mucosa. However, in this study we were unable to reveal the presence of endogenous adenosine as indicated by a lack of enhancement of the peristaltic reflex at the antagonist concentrations employed.

It must be emphasized that the results of this study are only an approximation of the inhibitory effect of adenosine analogues on intestinal motility because of the *in vitro* technique employed. *In vivo* studies in this area need to be performed to confirm that inhibition of peristalsis seen *in vitro* leads to decreased transit in the whole animal. However, in this study we have found that the adenosine receptor involved in regulating *in vitro* peristalsis in the rat jejunum (A_1) is different from that regulating secretion (A_{2B}) (Hancock & Coupar, 1995) in the same region of intestine of the same species. Our recent characterization of adenosine receptors in the rat jejunum provides the opportunity to inhibit motility selectively without affecting secretion and *vice versa* by the use of selective adenosine agonists in the management of diarrhoea. On this basis we postulate that A_{2B} adenosine agonists could be of clinical value in the management of diarrhoea that is due to microbiological organisms where antimotility effects are not desired.

References

BAILEY, S.J., HICKMAN, D. & HOURANI, S.M.O. (1992). Characterisation of the P_1-purinoceptors mediating contraction of the rat colon muscularis mucosae. *Br. J. Pharmacol.*, **105**, 400–404.

BAILEY, S.J. & HOURANI, S.M.O. (1992). Effects of purines on the longitudinal muscle of the rat colon. *Br. J. Pharmacol.*, **105**, 885–892.

BARSOUM, G.S. & GADDUM, J.H. (1935). The pharmacological estimation of adenosine and histamine in blood. *J. Physiol.*, **85**, 1–14.

BRUNS, R.F., FERGUS, J.H., BADGER, E.W., BRISTOL, J.A., SANTAY, L.A., HARTMAN, J.D., HAYS, S.J. & HUANG, C.C. (1987a). Binding of the A_1-selective adenosine antagonist 8-cyclopentyl-1,3-dipropylxanthine to rat brain membranes. *Naunyn Schmied. Arch. Pharmacol.*, **334**, 59–63.

BRUNS, R.F., FERGUS, J.H., BADGER, E.W., BRISTOL, J.A., SANTAY, L.A. & HAYS, S.J. (1987b). PD115,199: an antagonist ligand for adenosine A_2-receptors. *Naunyn Schmied Arch. Pharmacol.*, **335**, 64–69.

BRUNS, R.F., LU, G.H. & PUGSLEY, T.A. (1986). Characterisation of the A_2-adenosine receptor labelled by [^{3}H]-NECA in rat striatal membranes. *Mol. Pharmacol.*, **29**, 331–346.

BURNSTOCK, G. (1990). Purinergic mechanisms. *Ann. N.Y. Acad. Sci.*, **603**, 1–17.

BURNSTOCK, G., CAMPBELL, G., SATCHELL, D.G. & SMYTHE, A. (1970). Evidence that adenosine triphosphate or a related nucleotide is the transmitter substance released by non-adrenergic nerves in the gut. *Br. J. Pharmacol.*, **40**, 668–688.

COLLIER, H.O.J. & TUCKER, J.F. (1983). Novel form of drug-dependence on adenosine in guinea pig ileum. *Nature*, **302**, 618–621.

COLLIS, M.G. (1983). Evidence for an A_1 adenosine receptor in the guinea-pig atrium. *Br. J. Pharmacol.*, **78**, 207–212.

COLLIS, M.G., CULVER, J.C. & HOLMES, S. (1988). Comparison of the affinity of 8-substituted xanthines for adenosine receptors in atria from rats and guinea-pigs. *Br. J. Pharmacol.*, **94**, 423P.

COLLIS, M.G. & HOURANI, M.O. (1993). Adenosine receptor subtypes. *Trends Pharmacol. Sci.*, **14**, 360–366.

COLLIS, M.G., STOGGALL, S.M. & MARTIN, S.M. (1989). Apparent affinity of 1,3-dipropyl-8-cyclopentylxanthine for adenosine A_1 and A_2 receptors in isolated tissues from guinea-pigs. *Br. J. Pharmacol.*, **97**, 1274–1278.

COUPAR, I.M. & HANCOCK, D.L. (1994). The adenosine agonist NECA inhibits intestinal secretion and peristalsis. *J. Pharm. Pharmacol.*, **46**, 801–804.

DIONYSSOPOULOS, A., HOPE, W. & COUPAR, I.M. (1992). Effect of adenosine analogues on the expression of opiate withdrawal in rats. *Pharmacol. Biochem. Behav.*, **42**, 201–206.

DRURY, A.N. & SZENT-GYORGI, A. (1929). The physiological activity of adenine compounds with especial reference to their action upon the mammalian heart. *J. Physiol.*, **68**, 213–237.

FOZARD, J.R. & HANNON, J.P. (1994). BW - A 522 blocks adenosine A_3 receptor-mediated hypotensive responses in the rat. *Eur. J. Pharmacol.*, **252**, R5–6.

FRANCO, R., HOYLE, C.H.V., CENTELLES, J.J. & BURNSTOCK, G. (1988). Degradation of adenosine by extracellular adenosine deaminase in the rat duodenum. *Gen. Pharmacol.*, **19**, 679–681.

FREDHOLM, B.B., ABBRACCHIO, M.P., BURNSTOCK, G., DALY, J.W., HARDEN, T.K., JACOBSON, K.A., LEFF, P. & WILLIAMS, P. (1994). Nomenclature and classification of purinoceptors. *Pharmacol. Rev.*, **46**, 143–156.

HALEEN, S.J., STEFFEN, R.P. & HAMILTON, H.W. (1987). PD116,948, a highly selective A_1 adenosine receptor antagonist. *Life Sci.*, **40**, 555–561.

HANCOCK, D.L. & COUPAR, I.M. (1995). Functional characterisation of the adenosine receptor mediating inhibition of intestinal secretion. *Br. J. Pharmacol.*, **114**, 152–156.

HAYASHI, E., MORI, M., YAMADA, S. & KUNITOMO, M. (1978). Effects of purine compounds on cholinergic nerves. Specificity of adenosine and related compounds on acetylcholine release in electrically stimulated guinea pig ileum. *Eur. J. Pharmacol.*, **48**, 297–307.

JARVIS, M.F., SCHULZ, R., HUTCHINSON, A.J., DO, U.H., SILLS, M.A. & WILLIAMS, M. (1989). [^{3}H]-CGS-21690, a selective A_2-adenosine receptor agonist directly labels A_2-receptors in rat brain. *J. Pharmacol. Exp. Ther.*, **251**, 888–893.

KENNEDY, C. (1990). P_1- and P_2-purinoceptor subtypes - an update. *Arch. Int. Pharmacodyn.*, **303**, 30–50.

KROMER, W., PRETZLAFF, W. & WOINOFF, R. (1981). Regional distribution of an opioid mechanism in the guinea-pig isolated intestine. *J. Pharm. Pharmacol.*, **33**, 98–101.

LOHSE, M.J., KLOTZ, K.N., SCHWABE, U., CRISTALLI, G., VITTORI, S. & GRIFANTINI, M. (1988). 2-Chloro-N^6-cyclopentyladenosine: A highly selective agonist at A_1 adenosine receptors. *Naunyn-Schmied. Arch. Pharmacol.*, **337**, 687.

NICHOLLS, J., HOURANI, S.M.O. & KITCHEN, I. (1992a). Characterisation of P_1-purinoceptors on rat duodenum and urinary bladder. *Br. J. Pharmacol.*, **105**, 639–642.

NICHOLLS, J., HOURANI, S.M.O. & KITCHEN, I. (1992b). Degradation of extracellular adenosine and ATP by adult and neonatal rat duodenum and urinary bladder. *Pharmacol. Commun.*, **2**, 203–210.

OKWUASABA, F.K. & HAMILTON, J.T. (1975). The effect of metoclopramide on inhibition induced by purine nucleotides, noradrenaline, and theophylline ethlenediamine on intestinal muscle and on peristalsis *in vitro*. *Can. J. Physiol. Pharmacol.*, **53,** 972–977.

PEACHEY, J.A., HOURANI, S.M.O. & KITCHEN, I. (1994). The binding of 1,3-[^{3}H]-dipropyl-8-cyclopentylxanthine to adenosine. A_1 receptors in rat smooth muscle preparations. *Br. J. Pharmacol.*, **113,** 1249–1256.

REITER, S., LOFFLER, W. & ZOLLNER, N. (1989). Intraluminal deamination of adenosine in the human duodenum. *Ann. Nutr. Metab.*, **33,** 200–201.

SATCHELL, D.G. & BURNSTOCK, G. (1971). Quantitative studies of the release of purine compounds following stimulation of non-adrenergic inhibitory nerves in the stomach. *Biochem. Pharmacol.*, **29,** 1694–1697.

SMITH, T.K., BORNSTEIN, J.C. & FURNESS, J.B. (1990). Distension-evoked ascending and descending reflexes in the circular muscle of the guinea-pig ileum: an intracellular study. *J. Auton. Nerv. System.*, **29,** 203–218.

STEHLE, J.H., RIVKEES, S.A., LEE, J.J.., WEAVER, D.R., DEEDS, J.D. & REPPERT, S.M. (1992). Molecular cloning and expression of the cDNA for a novel A_2-adenosine receptor subtype. *Mol. Endocrinol.*, **6,** 384–393.

SU, C., BEVAN, J. & BURNSTOCK, G. (1971). [^{3}H]Adenosine: release during stimulation of enteric nerves. *Science*, **173,** 337–339.

UKENA, D., JACOBSON, K.A., PADGETT, W.L., AYALA, C., SHAMIN, M.T., KIRK, K.L., OLSSON, R.A. & DALY, J.W. (1986). Species differences in structure activity relationships of adenosine agonists and xanthine antagonists at brain A_1 adenosine receptors. *Fedn. Eur. Biochem. Soc. Lett.*, **209,** 122–128.

VAN GALEN, P.J.M., VAN BERGEN, A.H., GALLO-RODRIGUEZ, C., MELMAN, N., OLAH, M., IJZERMAN, A.P., STILES, G.L. & JACOBSON, K.A. (1994). A binding site model and structure activity relationships for the rat A_3 adenosine receptor. *Mol. Pharmacol.*, **45,** 1101–1111.

VAN NUETEN, J.M., JANSEEN, P.A.J. & FONTAINE, J. (1976). Unexpected reversal effects of naloxone on the guinea-pig ileum. *Life Sci.*, **18,** 803–810.

YOKOYAMA, S. & NORTH, R.A. (1983). Electrical activity of longitudinal and circular muscle during peristalsis. *Am. J. Physiol.*, **244** (Gastrointest. Liver Physiol., **7,**) G83–G88.

(Received November 24, 1994
Revised March 7, 1995
Accepted March 15, 1995)

British Journal of Pharmacology (1995) 115, 745-752

Extended concentration-response curves used to reflect full agonist efficacies and receptor occupancy-response coupling ranges

Michael J. Lew

Department of Pharmacology, The University of Melbourne, Parkville, 3052, Victoria, Australia

1 An approach is described for generating extended agonist concentration-response curves where the responses are unconstrained by the normal tissue maximum response. Functional antagonism is employed to hold the tissue state in the range where any change in stimulus can be translated into a measurable response.

2 The maximum response of these extended concentration-response curves provides an index of intrinsic activity reflecting the agonist efficacy and the receptor occupancy-response coupling range.

3 The use of this approach is illustrated with extended concentration-response curves for noradrenaline (NA), vasopressin, acetylcholine (ACh), and 5-methylfurmethide in the small mesenteric and tail arteries of the rat. Both NA and vasopressin can maximally activate the arteries, but the new protocol shows that NA can produce more cellular activation than vasopressin in the tail artery. Both ACh and 5-methylfurmethide are full agonists but ACh has a higher intrinsic activity than 5-methylfurmethide. The ACh muscarinic receptors in the mesenteric artery have a larger occupancy-response range than the ACh muscarinic-receptors in the tail artery, and the α-adrenoceptors in the tail artery appear to have a larger occupancy-response coupling range than those in the mesenteric artery.

4 This approach extends our ability to compare the efficacies of full agonists, and to compare the occupancy-response coupling ranges of receptors that can normally maximally activate the assay tissue. This is achieved without the use of an irreversible antagonist and should be applicable to many receptors and pharmacological assay systems where responses are stable and functional antagonists are available.

Keywords: Agonism; efficacy; intrinsic activity; receptor reserve; stimulus-response coupling; functional antagonism

Introduction

Concentration-response curves provide two useful measures of agonist activity. The location of the curve (e.g. the pEC_{50}) provides a measure of the agonist potency and the sensitivity of the assay system to an agonist (two different expressions of the same property). The maximum response provides an index of the agonist efficacy using Ariëns' scale of intrinsic activity (Ariëns, 1954). Because the maximum effect of the agonist can be constrained by the assay tissue, the intrinsic activity scale does not allow discrimination between full agonists, which are all assigned an intrinsic activity of 1. When an irreversible antagonist is available it is possible to expose any efficacy differences between full agonists by reducing receptor numbers until the agonists become effectively partial. However, such antagonists are not available for many receptor types.

An alternative approach exploits functional antagonism between agonists with opposite effects in the assay (Buckner & Saini, 1974; Broadley & Nicholson, 1979). These methods were primarily intended to provide affinity estimates for the agonists rather than efficacies, indeed the method of Broadley & Nicholson (1979) requires that the agonist affinity be calculated before the efficacy can be estimated. There are many levels at which functional interactions between agonists occur, and the patterns of concentration-response curves obtained are dependent on the nature of the interaction. Thus, there are theoretical considerations that limit the reliability of the affinity estimates obtained using functional antagonism (Mackay, 1981; Leff *et al.*, 1985) which makes the method of Broadley & Nicholson (1979) potentially unreliable. However, because efficacy estimates are useful on a relative rather than absolute scale, these considerations do not invalidate the use of functional antagonism for comparisons of efficacy between full agonists by the method of Buckner & Saini (1974). They compared the effects of isoprenaline and soterenol on carbachol concentration-response curves in guinea-pig trachea and found that isoprenaline caused a greater rightward shift than soterenol, indicating that isoprenaline has the higher efficacy. Because the comparison is between agonists acting at the same receptor in the same tissue with the same functional interaction, uncertainties about the form of the interaction could not result in the more efficacious agonist erroneously appearing less efficacious. At worst the difference in efficacy would not be discernible. Few studies have used functional antagonism to compare full agonist efficacies, despite the importance of agonist relative efficacies and the fact that functional antagonists are probably available for far more systems than irreversible antagonists. This may be the result of concerns about the theoretical limitations of functional antagonism in characterization of agonist properties, or the indirect nature of the efficacy index obtained from such studies.

The approach described in this paper uses functional antagonism in a different manner from that normally employed. A functional antagonist is applied as needed to keep the assay responses to the agonist of interest below the maximum level that can be expressed in the assay. This generates extended agonist concentration-response curves that are not bounded by the normal tissue maximum response. The protocol, called 'up/down', thus exploits functional antagonism between excitatory agonists ('up' agonists) and inhibitory agonists ('down' agonists) to hold the level of the assay response within the range where a change in the level of stimulus can be translated into a measurable response. The range of the extended concentration-response curves generated by this protocol is readily interpreted as an extension of Ariëns' scale of intrinsic activity (Ariëns, 1954). The functional antagonism interactions in the up/down protocol are the same as in other functional antagonism protocols, so the theoretical limitations of the values obtained are the same. However the up/down protocol produces a more

[1] Author for correspondence.

straightforward display of the agonist efficacy, and smaller efficacy differences may be discerned than with the standard functional antagonism experiments.

Because intrinsic activity is dependent on both agonist and tissue properties, the up/down protocol can be used for at least three types of comparisons: (i) discrimination between high efficacy agonists acting at the same receptor; (ii) comparison of the stimulus-response coupling range of different receptors in the same tissue; (iii) comparison of the occupancy-response coupling efficiency of a single receptor type in different tissues. The experiments described in this paper illustrate the use of the up/down protocol in making each of these types of comparisons by (i) comparing ACh and 5-methylfurmethide as high efficacy ACh muscarinic (M)-receptor agonists, (ii) comparing vasopressin receptor-mediated responses with α-adrenoceptor-mediated responses within tissues, and (iii) comparing responses mediated by ACh M-receptors, vasopressin receptors and α-adrenoceptors between the rat small mesenteric and tail arteries.

Methods

General

Male Wistar Kyoto or Sprague Dawley rats aged between 15 and 20 weeks were anaesthetized with carbon dioxide (80% CO_2, 20% O_2) and killed by exsanguination. A portion of intestine and mesentery was removed and place in cool Krebs solution (composition in mM: Na^+ 144, K^+ 5.9, Mg^{2+} 1.2, Ca^{2+} 2.5, HPO_4^- 1.2, Cl^-129, SO_4^-1.2, HCO_3^- 25, glucose 11) bubbled with 5% CO_2:95% O_2. Under a dissecting microscope, a mesenteric artery (three branch orders proximal to the arteries that enter the intestine) was carefully dissected free of the fat and connective tissue around it, and a 2 mm long segment was mounted on 40 μm wires in a Mulvany-Halpern style myograph (JP Trading, Aarhus, Denmark) and warmed to 37°C. In other experiments the tail of the rat was removed and the main caudal artery was dissected free under a microscope and segments mounted in a myograph as for the mesenteric arteries. The artery was incrementally stretched radially with about four steps, and the force measured and the arterial circumference calculated at each step. A diameter-force curve was thereby generated where the diameter is that of a circle with the same circumference as the vessel at each level of stretch. The diameter of the artery was then set to be 90% of the diameter predicted for distending pressure of 100 mmHg using standard calculations (Mulvany & Halpern, 1977). The rat mesenteric and tail arteries set up under these conditions do not develop any spontaneous active contractile force. Each artery was fully activated twice by either potassium depolarizing solution (KPSS, K^+ 120 mM substituted for Na^+) or NA (10 μM). The response to the second activation was always larger than the first and was used as an estimate of tissue maximum response, and used in normalising subsequent responses. This normalising response underestimates the true tissue maximum response pertaining to the subsequent concentration-response curves because the tissue maximum response of these arteries mounted in this fashion commonly increase with successive activations. This is evident in the fact that both NA and vasopressin (AVP) normal concentration-response curves have normalised maxima larger than one. In all experiments where NA was applied, desipramine (0.1 μM) was added to the Krebs solution to inhibit neuronal uptake. The mesenteric arteries had diameters of 317 μm ± 10 (mean ± s.d.) and the tail arteries 703 μm ± 68.

Concentration-response curves

Only one concentration-response curve (either normal or up/down) was constructed in each tissue. All drug additions were made in a cumulative fashion with 3.2 fold concentration increments. Normal concentration-response curves were constructed in the standard fashion. Extended concentration-response curves for vasoconstrictor and vasodilator agonists were constructed simultaneously to hold the active force close to 50% of tissue maximum response: the curve for the vasoconstrictor was started first, and when force exceeded 50%, the curve for the vasodilator was started. When the force declined below 50%, the next concentration of vasoconstrictor was applied and so on, until the full range of agonist concentrations was applied. Responses to each increment of agonist concentration were cumulated and a concentration-cumulated response curve generated. This protocol for drug application frequently resulted in a simple alternation between vasoconstrictor application and vasodilator application after the first few concentrations of each agonist. At very high concentrations of agonist no increase in response was found with increased agonist concentration, indicating that the maximum effect of the agonist had been obtained. When this occurred for the vasoconstrictor agonist before the vasodilator agonist, a second (or third) vasoconstrictor agonist was added. Similarly when the vasodilator agonist reached a maximum before the vasoconstrictor, a second vasodilator was added. Responses were calculated as the simple summation of the change in force elicited by each concentration increment. These cumulated responses were expressed as a fraction of the second KPSS or NA 10 μM response.

Protocols

Mesenteric arteries Normal concentration-response curves for NA, AVP and ACh were constructed for comparison with the up/down curves. For these normal ACh curves, the arteries were precontracted to 50–80% of tissue maximum response by AVP.

Up/down concentration-response curves for NA were constructed with ACh used as the down agonist. In these experiments the NA responses were exhausted before the ACh concentration-response curve was complete, so AVP and then endothelin-1 were added to allow completion of the ACh curve. This protocol yielded two sets of data, extended concentration-response curves for NA and for ACh.

Extended concentration-response curves for AVP were constructed with ACh used as the down agonist. The ACh concentration-response curve was not completed after the AVP responses were exhausted, so only the AVP extended concentration-response curve resulted from these experiments.

Tail artery Extended concentration-response curves for NA were constructed with either ACh or sodium nitroprusside as the first down agonist. When the responses to the first down agonist were exhausted, the other was added to extend the NA curve, and when both were exhausted, calcitonin gene-related peptide (CGRP) was added if needed. Three concentration-response curves were obtained from each of these experiments: NA; the first down agonist; and the second down agonist.

Extended AVP concentration-response curves were obtained as in the mesenteric arteries.

Extended NA concentration-response curves in the absence and presence (for at least 30 min) of various concentrations of prazosin (3, 30 and 300 nM) or yohimbine (100 and 1000 nM) were constructed with 5-methylfurmethide as the first down agonist. When the responses to 5-methylfurmethide were exhausted, sodium nitroprusside, and on one occasion, CGRP were added to allow completion of the extended NA curve. Each of these experiments yielded three concentration-response curves, one for NA, one for 5-methylfurmethide, and one for sodium nitroprusside as the second down agonist.

Analysis

Concentration-response curves were analysed by fitting a four parameter logistic equation to the data to obtain location and slope parameters. The equation is

$$y = a + \frac{b}{1 + e^{-d(c + \log[A])}}$$

where A is the agonist concentration, a is the basal value, b is the vertical range, c is the pEC_{50}, d is the mid-point slope, and e is the base of the natural logarithm. Where the concentration-response curves started at zero, the basal value parameter, a, was deleted to give a three parameter logistic. When needed, any pEC_x was calculated from the logistic equation. Agonist potencies were compared as pEC_x values using an unpaired t test (2 tailed). Experimentally observed maximum responses were also compared by the unpaired t test (2 tailed). Data are shown in the figures as the mean ± s.e.mean.

Drugs

Acetylcholine bromide, desmethylimipramine hydrochloride, noradrenaline bitartrate, prazosin hydrochloride and yohimbine hydrochloride were purchased from Sigma Chemical Company (St Louis, MO, U.S.A.) and sodium nitroprusside from David Bull Laboratories (Mulgrave, Victoria, Australia). Arginine vasopressin, calcitonin gene-related peptide (human) were obtained from Auspep, (Parkville, Victoria, Australia) and endothelin-1 from Peninsula Laboratories (Belmont, CA, U.S.A). 5-Methylfurmethide iodide was a gift from Wellcome Research Laboratories (Beckenham, U.K.). All drugs were dissolved and diluted in water. Prazosin, yohimbine, 5-methylfurmethide and DMI were kept as 1 or 10 mM stock solutions at 5°C, and all other drugs were dissolved on the day of use.

Results

An example of the results from an up/down protocol obtained on the rat tail artery are shown in Figure 1. The active force was held in the range where changes in NA or ACh concentration always had the potential to elicit responses by incrementing the concentration of vasoconstrictor when the force was less than 50% of the tissue maximum response, and incrementing the vasodilator when the force was more than 50%. Figure 1b shows the data expressed as active force displayed as a family of NA concentration-response curves in the presence of various concentrations of ACh, and as a family of ACh concentration-response curves with various concentrations of NA. Figure 1c shows the data for the agonists cumulated to produce a single extended concentration-response curve for each. These graphs show the relationship between the up/down data and the data that would be obtained from a normal procotol using functional antagonism.

NA and AVP in mesenteric arteries

NA and AVP produce steep concentration-response curves in the rat mesenteric artery with the active force changing from about 10% to 90% over an agonist concentration-range of only ten fold. The time-courses of the responses were dissimilar, with the response to NA reaching a steady level in only 1–2 min and the responses to low concentrations of AVP taking more than twice as long. The maxima of normal concentration-response curves to NA and AVP in the mesenteric arteries were similar (20.0 ± 0.06 and 17.6 ± 1.9 mN respectively, $P = 0.30$, unpaired t test), and were approximately 10% larger than the responses to KPSS (Figure 2a), probably reflecting a time-related increase of the maximum response. Larger responses to other vasoconstrictor agonists have not been observed, so these maxima probably represent the maximum force that the mesenteric arteries can produce. The pEC_{50} values from these concentration-response curves were 6.07 ± 0.09 for NA and 9.01 ± 0.10 for AVP.

Responses to the vasoconstrictor agonists were measured over an extended concentration-range with ACh used as a functional antagonist with the up/down protocol. The cumulated response maxima for AVP and NA in the mesenteric artery were 2.01 ± 0.20 and 2.34 ± 0.35 times the force elicited by KPSS respectively (Figure 2b). The location of the up/down curves were measured as the $pEC_{0.55}$ (corresponding to the half-maximal response to NA and AVP applied in the normal manner) and these were found to be similar to the pEC_{50} values obtained from the normal concentration-response curves (6.25 ± 0.10, $P = 0.20$ and 9.23 ± 0.12, $P = 0.23$).

NA and AVP in tail arteries

The tail artery was more sensitive to NA than the mesenteric artery, with a threshold concentration of about 1 nM. Up/down concentration-response curves were constructed with either ACh or sodium nitroprusside as the vasodilator. Each of these vasodilators was exhausted well before the full range of NA concentrations was applied and thus both ACh and sodium nitroprusside were applied sequentially to each tissue to extend the NA concentration-response curve over a large range. In most of these experiments CGRP was also added after both of the other vasodilators to further extend the up/down protocol. Responses to NA were not noticeably affected by the sequence of vasodilator additions, but the responses to the vasodilators were affected by the prior application of the other vasodilators (see below). The cumulated response to NA was almost 4 times the response to KPSS (Figure 2c). In contrast to NA, the up/down concentration-response curve for AVP was completed with only a single vasodilator (ACh) and the maximum cumulated response was only 1.69 ± 0.23 times the response to KPSS (Figure 2c).

NA up/down concentration-response curves were constructed in the tail artery in the absence and presence of prazosin and yohimbine. The down agonists were 5-methylfurmethide, an ACh M-receptor agonist, followed by sodium nitroprusside. Prazosin caused a parallel rightward shift of the NA extended concentration-response curve (Figure 3a). When the data were analysed by the method of Stone & Angus (1978), it was found that the spacing of the curves was appropriate for a simple competitive interaction with a pK_B for prazosin of 9.14 ± 0.13. Yohimbine also caused a rightward shift of the NA concentration-response curve, but the spacing of the curves was inconsistent with simple competitive interaction (Figure 3b).

Vasodilators

ACh fully relaxed mesenteric arteries precontracted by NA, with a maximum response at 1 μM ACh, and a pEC_{50} of 7.6 ± 0.1 (Figure 4). When the up/down protocol was used, the cumulated maximum response to ACh was a relaxation of over four times the force elicited by KPSS, and relaxation responses were observed with ACh concentrations of up to 30 μM and the $pEC_{-0.5}$ was 7.8 ± 0.2 (Figure 4). ACh was less potent in the rat tail artery than in the mesenteric artery, and the maximum cumulated response was smaller, about 2.6 ± 0.1 times the force elicited by KPSS (Figure 5a). In the tail artery experiments where ACh was tested after sodium nitroprusside, the responses to ACh were greatly attenuated (Figure 5b). Similarly, the cumulated responses to sodium nitroprusside were much larger when it was applied before ACh rather than after, with cumulated responses of −3.1 ± 0.3 and −0.42 ± 0.07, respectively at 100 μM, the maximum concentration applied (Figures 5a and b). 5-Methylfurmethide caused a smaller maximal cumulated response in the tail artery than ACh (−1.85 ± 0.09, $P < 0.001$, Figure 5c). There was no effect of prazosin or yohimbine on the responses to 5-methylfurmethide. Pre-application of 5-methylfurmethide greatly reduced the effect of sodium nitroprusside (−0.77 ± 0.05 at 100 μM), but this response was significantly larger than the equivalent response in the presence of ACh ($P < 0.001$).

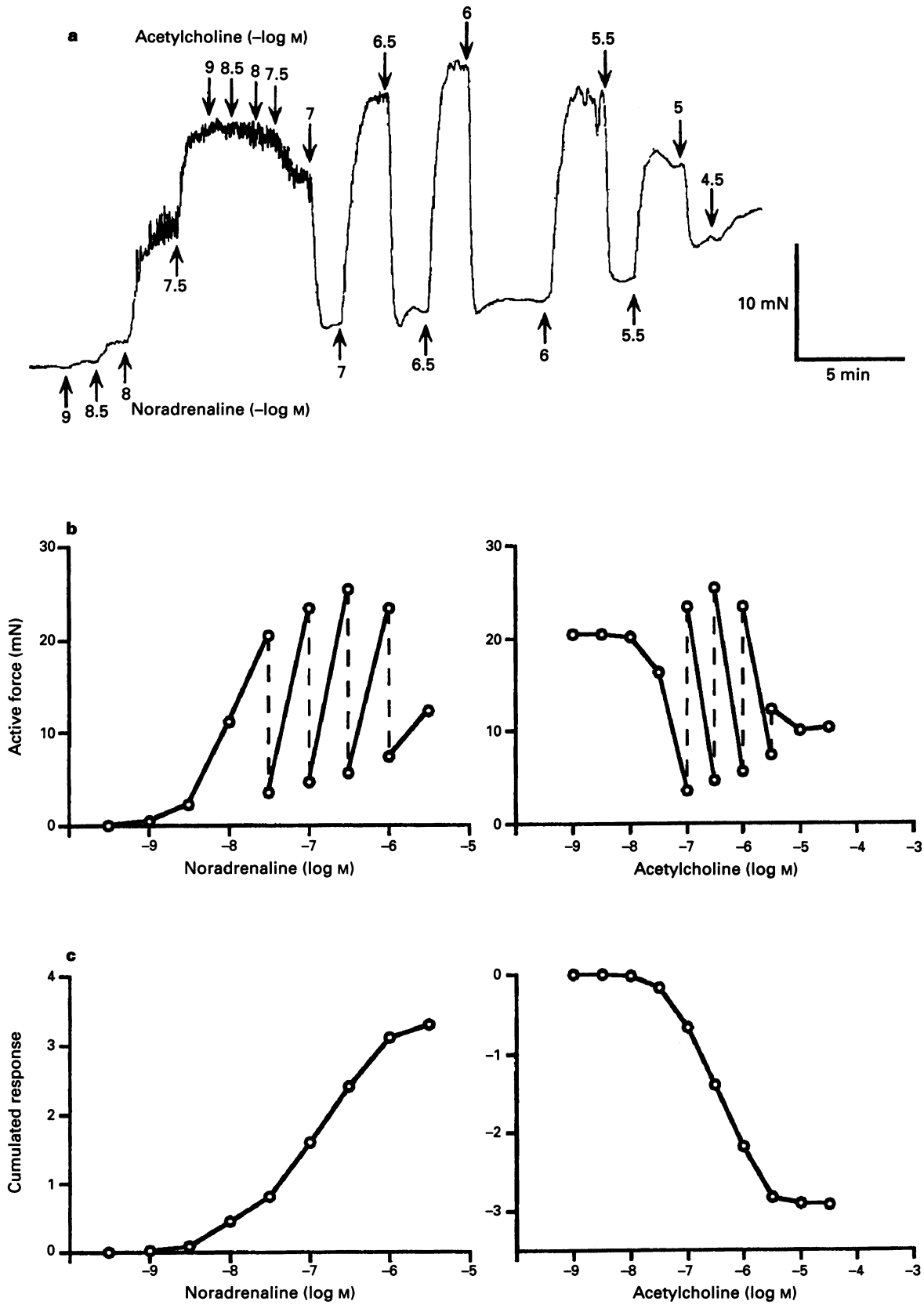

Figure 1 An example of an up/down experiment. (a) Chart record showing the active force produced by a rat tail artery in response to noradrenaline (NA) and relaxation produced by acetylcholine (ACh). (b) Data plotted to show the relationship between up/down data and data from 'normal' functional antagonism protocols. NA concentration-response curves in the presence of different concentrations of ACh (left) and ACh concentration-response curves in the presence of different concentrations of NA (right). (c) Data plotted using cumulated responses to produce extended concentration-response curves for NA (left) and ACh (right).

Discussion

Maximum response as a constraint

The maximal effect measured for an agonist may, in general, be limited by three kinds of constraint. First, the maximum might reflect the response resulting from complete occupation of the receptors by the agonist. This case occurs when the agonist is partial, and the maximum is a useful index of the agonist efficacy. Second, the maximum may reflect the maximum level of the measured parameter that the assay system can express: the 'tissue maximum response'. An example of this type is where a vasodilator agonist is able to relax completely an arterial assay. No further response can be measured in response to increased agonist concentration, even though more receptors can be occupied and additional intracellular stimulus produced. Third, the maximum may be constrained by the attainment of a maximal possible, or maximally effective, level of an intermediate stimulus between the receptor and the measured response: the 'receptor transduction maximum'. This maximum can be less than the maximum produced in the same assay by activation of another receptor type. An example of this type of constraint is provided by α_2-adrenoceptor activation in canine saphenous veins, where B-HT 933 has a receptor reserve, and so is a full agonist, but does not cause as large a response as the α_1-adrenoceptor agonist, cirazoline (Ruffolo & Zeid, 1985).

The agonists used in this study can be shown to be full agonists in normal concentration-response curves. NA and AVP were able to activate maximally the mesenteric artery (Figure 2), ACh was able to relax AVP-induced precontraction completely (Figure 4) as was 5-methylfurmethide (data not shown). For each of these agonists, the assay maximum was therefore equal to the tissue maximum response. The receptor transduction maximum and agonist effiacy can be described only as greater than that needed to elicit the tissue maximum response. Data from normal concentration-response curves such as these do not allow useful comparisons between full agonists, between the receptor transduction maximum of different receptors, or between the receptor transduction maxima in different tissues.

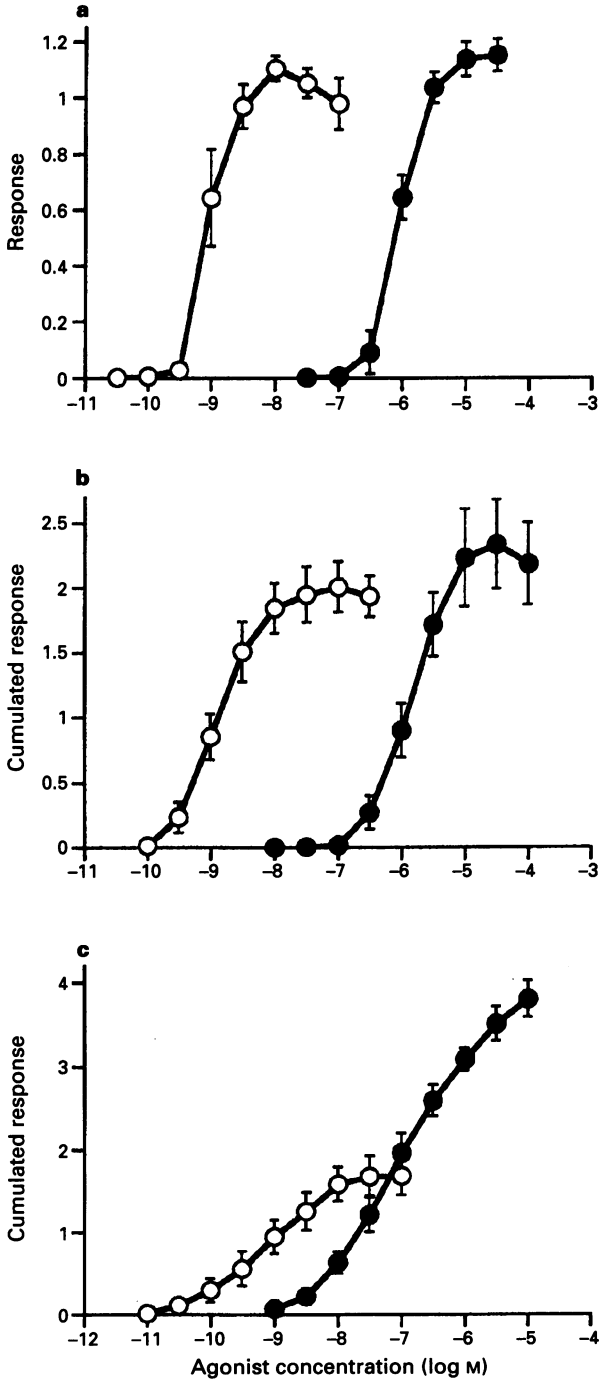

Figure 2 Concentration-response curves for vasopressin (AVP, ○) and noradrenaline (●). (a) Normal concentration-response curves in the rat mesenteric artery. (b) Up/down concentration-response curves in the rat mesenteric artery. (c) Up/down concentration-response curves in the rat tail artery. Responses are expressed as a fraction of the response to potassium depolarizing solution (KPSS). Values are mean ± s.e.mean ($n = 3$ to 7).

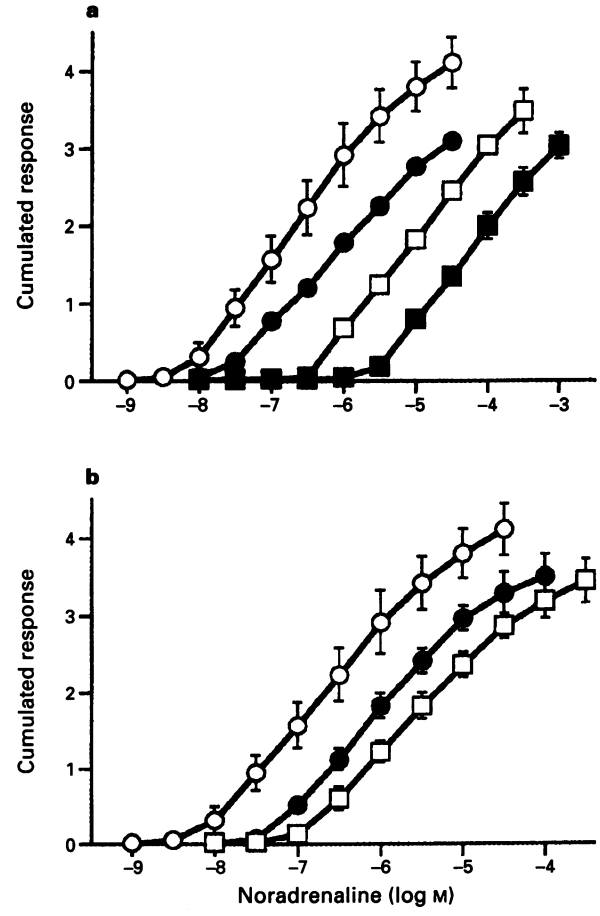

Figure 3 Up/down extended concentration-response curves in the rat tail artery for noradrenaline in the presence of (a) prazosin 0 (○), 3 (●), 30 (□) and 300 nM (■), or (b) yohimbine 0 (○), 0.1 (●) and 1 μM (□). Values are mean ± s.e.mean ($n = 3$, 2, 4 and 4 respectively for prazosin, and $n = 3$, 4 and 4 for yohimbine).

A different 'response'

In normal concentration-response curves the absolute level of the measured parameter (force or active force in the present experiments) or the change of the measured parameter from its initial value are used as the 'response'. However, to generate an up/down concentration-response curve the 'response' to each agonist concentration increment is the change of the measured parameter from its value immediately prior to the concentration increment. Cumulation of these responses allows the data to be expressed as a single concentration-response curve rather than a family of partial curves (Figure 1).

The resulting range of the up/down concentration-response curve will reflect the agonist efficacy or receptor transduction maximum, whichever is less. In the latter case two agonists of different efficacies at the same receptor would elicit the same maximum cumulated response, a situation directly analogous to full agonism in normal concentration-response curves. Nonetheless, for two drugs acting at the same receptor (in the absence of extraneous complications such as secondary drug actions), a larger range can result only from a higher efficacy. Thus the range of the up/down concentration-response curve is an open-ended extension of the intrinsic activity scale (Ariëns, 1954), increasing discrimination between high efficacy agonists in a straightforward manner. The up/down data show that ACh has a higher intrinsic activity than 5-methylfurmethide (Figure 5), and if they act at the same muscarinic receptors, then ACh has a higher efficacy than 5-methylfurmethide.

The up/down protocol also extends the range of comparisons between tissues and between receptors. The muscarinic receptors on the endothelium of the mesenteric artery can produce a larger response (scaled to the force elicited by KPSS) than the same system in the tail artery. In these arteries the maximum possible effect of muscarinic receptor stimulation in normal concentration-response curves is always 100% relaxation of the precontraction, so comparisons of response ranges from normal concentration-response curves between the tissues are meaningless. NA caused larger cumulated responses in the tail artery than in the mesenteric artery, and in the tail artery NA was able to elicit larger responses than AVP. 'It only makes sense to relate in one scale the intrinsic activities for compounds that interact with the same receptors' (Ariëns *et al.*, 1960), so it should be concluded that the α-adrenoceptors have a larger transduction maximum than the AVP receptors, rather than NA having a higher intrinsic activity than AVP. It is likely that the NA responses in the tail artery were large because of the presence of both α_1- and α_2-adrenoceptors (Medgett & Langer, 1984). The expriements with prazosin and yohimbine were intended to test this possibility, but were not really conclusive. Prazosin behaved competitively with a pA_2 appropriate for α_1-adrenoceptors (Flavahan & Vanhoutte, 1986). Yohimbine did not behave in a simple competitive fashion, but the antagonism by yohimbine at the lower concentration (0.1 μM) was consistent with a pA_2 of about 7.7, close to what would be expected for α_2-adrenoceptors. As it is often difficult to obtain clear evidence for the coexistence of two different receptor subtypes in experiments such as these using a non-selective agonist (Kenakin, 1992), these experiments do not rule out the presence of both receptors in the tail artery. Indeed, if 'responses mediated via postjunctional α_2-adrenoceptors in [vascular smooth muscle] are dependent upon a degree of vascular smooth muscle stimulation by some other receptor system' (Dunn *et al.*, 1991), then it is easy to see how

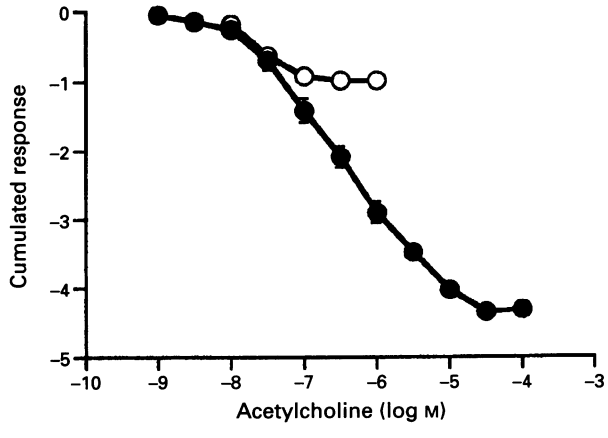

Figure 4 Normal concentration-response curve (○) and extended up/down concentration-response curve (●) for acetylcholine in the rat mesenteric artery. Values are mean ± s.e.mean ($n = 6$ and 4).

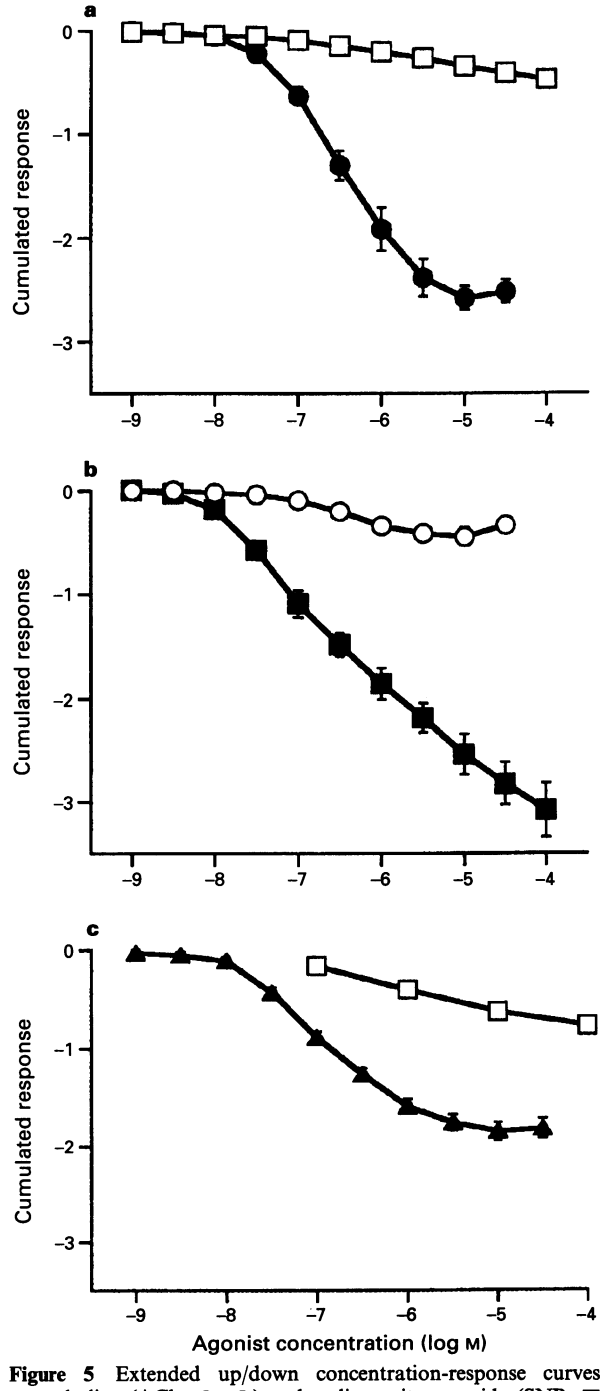

Figure 5 Extended up/down concentration-response curves for acetycholine (ACh, ○, ●) and sodium nitroprusside (SNP, □, ■) and 5-methylfurmethide (▲) in the rat tail artery. In each experiment both drugs were applied sequentially. (a) ACh followed by SNP ($n = 4$); (b) SNP followed by ACh ($n = 4$); (c) 5-methylfurmethide followed by SNP ($n = 12$). Values are means ± s.e.mean.

prazosin might appear competitive over the whole concentration-range even where both α_1- and α_2-adrenoceptors are involved in the response.

The possibility of NA acting through more than one receptor highlights a potential complication in using the up/down protocol. Agonists concentrations in an up/down concentration-response curve cover a larger range than in a normal concentration-response curve. This leads inevitably to the possibility of secondary actions of the agonists influencing the results. This problem can exist for any concentration-response curve, but is more likely during the up/down protocol. Where an agonist is acting at more than one type of receptor, the resulting up/down curve more properly reflects the overall tissue stimulus-response coupling than the agonist efficacy.

Spare receptors

The concept of spare receptors or receptor reserve results directly from the existence of a ceiling to the range of a concentration-response curve. This means that the up/down protocol will reduce or eliminate spare receptors. This can be seen by comparison of normal and up/down concentration-response curves for ACh. In the normal curve, ACh elicits a maximum response at 1 μM, but in the up/down curve it continues to elicit responses at concentrations up to 30 μM. If removal of the constraint of tissue maximum response leads to the occupancy-response curve becoming unconstrained overall, then there can be no receptor reserve in an up/down curve. However, while the up/down protocol removes the constraint of tissue maximum response, it does not necessarily remove all constraints. As assay where agonist responses are normally constrained by the tissue maximum may be constrained by the receptor transduction maximum in an up/down protocol. The up/down curve of ACh in the tail artery probably almost saturates the cyclic GMP system in the smooth muscle cells, on the evidence that sodium nitroprusside is nearly ineffectual after ACh. 5-Methylfurmethide does not reduce the effectiveness of sodium nitroprusside quite as much, as would be expected from its lower efficacy. These data probably indicate that there is a maximally effective, or maximal achievable, concentration of cyclic GMP, with neither ACh nor 5-methylfurmethide being sufficiently powerful to produce that concentration of cyclic GMP without further stimulation by sodium nitroprusside. It is possible that in another tissue the cyclic GMP system would be saturated by both ACh and 5-methylfurmethide, and thus their efficacy difference would not be exposed by the up/down protocol, and both agonists would have spare receptors.

Functional antagonism

Agonst dissociation constants (K_As) have been assessed using functional antagonism with limited success (Buckner & Saini, 1974; Broadley & Nicholson, 1979; Broadley & McNeill, 1983). It has been demonstrated that valid estimates of pK_As can be obtained from functional antagonism experiments with only some forms of functional interaction (Mackay, 1981; Leff *et al.*, 1985). However, even with those forms of functional interaction agonist affinity cannot be estimated directly from the pEC_{50} of an up/down concentration-response curve for two reasons. First, where the range of the curve is constrained by the receptor transduction maximum, then there can be a receptor reserve, and pEC_{50} of the resulting concentration-response curve will not approximate to the pK_A. Second, even where the responses are not constrained by the receptor transduction maximum, the slope of the occupancy-response relationship probably will not be constant over the whole range of agonist concentrations. Thus the response level that corresponds to agonist occupancy of half of the receptors will not be half of the maximum. Changes in the shape of the occupancy-response relationship during the protocol can be expected as a result of non-linear interactions of second messenger systems, so the form of the functional interaction will, in part, determine the slope of the occupancy-response relationship. This means that the location of the extended concentration-response curve can be dependent on the choice of functional antagonist. The pEC_{50} of an up/down curve cannot be relied upon to correspond to the pK_A of the agonist.

Agonist efficacies have also been estimated from functional antagonism experiments in the past (Buckner & Saini, 1974; Broadley & Nicholson, 1979; Emmerson & Mackay, 1981; Broadley & McNeill, 1983). The method used by Broadley involved calculation of K_A from functional antagonism data, and calculating relative efficacies using these values and the method of Besse & Furchgott (1976). The problems with K_A estimations from functional antagonism data probably make this strategy unreliable. In principle, the relative efficacy of an agonist used as a functional antagonist can be estimated, at least qualitatively (Mackay, 1981) from the amount that it can shift the concentration-response curve of another agonist (Van der Brink, 1973). Thus, the efficacy of a test drug of interest would be estimated from the potency ratio of a standard agonist in the absence and presence of a maximally effective concentration of the test drug. In practice, useful data can only result where the test drug has a low enough efficacy that it does not obliterate the responses to the standard drug. Furthermore, the confidence band for the potency ratio can be rather wide because its variability is the product of the variability of efficacy of both the test drug and the standard drug. Estimations of relative intrinsic activities using the up/down protocol are not subject to either of these limitations. If the test drug has enough efficacy to obliterate the responses to the standard drug, then another agonist acting in the same direction as the standard agonist can be added. The variability of efficacy of the standard agonist in the up/down protocol should have a negligible effect on the estimate of intrinsic activity for the test drug because the standard agonist is titrated to effect, and the concentration needed for that effect is not important.

Comparisons between assays (scaling)

For comparisons between agonists or receptors within a single assay tissue, no normalisation of the data is necessary, and absolute units should be used. When comparing between tissues, however, some sort of normalisation of the data is necessary to control for between tissue differences that are irrelevant to the comparison being made. The difference in tissue maximum active force between the mesenteric artery and the tail artery is an irrelevant difference. Two possible normalisation methods are applicable to the between artery comparisons: calculation of 'equivalent distending pressure' from the force and arterial dimensions (Mulvany & Halpern, 1977; Lew & Angus, 1992), and simple expression of the force as a fraction of the tissue maximum response. The latter method was chosen because it would be applicable to all types of assay (not only to vascular tissues), and because the resulting intrinsic activities for the agonists are effectively part of the same scale as that for which the concept of intrinsic activity was originally defined (Ariëns, 1954). The use of this normalisation will not have affected data comparisons within tissue (other than possibly decreasing variance), as essentially the same concentration-response curves would be seen with the data expressed as cumulated active force.

Conclusions

The up/down protocol described in this paper circumvents the tissue maximum response as a constraint on the maximum effect of an agonist. This extends the scale of intrinsic activity to allow discrimination between high efficacy agonists and should be a useful approach in comparisons of agonist efficacies, in comparisons of tissue stimulus-response coupling efficiencies between tissues, and within tissues between disease states. Interpretation of any experiment involving functional interactions between agonists is more complex than interpretation of normal concentration-response curves, but the

information available froma normal concentration-response curve is also available from an up/down concentration-response curve. The first few concentrations of each agonist in the up/down protocol are applied exactly as they would be in a conventional concentration-response curve, so the threshold concentration of an agonist determined from an up/down curve is identical to that obtained in the conventional curve. Further, because the concentration of each agonist is increased until the force of contraction crosses the 50% of tissue maximum response, the pEC_{50} that would be obtained from the normal concentration-response curve can be obtained from the up/down concentration-response curve. Thus, the up/down concentration-response curves for NA, AVP and ACh contain all of the information that can be obtained from the normal concentration-response curves for these agonists. The range of the up/down concentration-response curve is additional information. This method does not require the use of an irreversible antagonist, so it is applicable to most receptor types. The protocol is demonstrated in this paper using small vascular tissues, but it has been used successfully in other small and large arteries measuring either isobaric diameter or isometric force, and in cardiac tissues measuring either atrial rate or driven force. As long as responses of the assay do not fade excessively during the protocol and a functional antagonist is available, this approach may increase the information gained from agonist concentration-response curves.

The author would like to thank Prof J.A. Angus for support and many helpful discussions, and Mr M. Ross-Smith and Ms T. Fredrickson for technical assistance. This work was supported by Glaxo Australia Pty Ltd.

References

ARIËNS, E.J. (1954). Affinity and intrinsic activity in the theory of competitive inhibition. *Arch. Int. Pharmacodyn. Ther.*, **99**, 32–49.

ARIËNS, E.J., VAN ROSSUM, J.M. & KOOPMAN, P.C. (1960). Receptor reserve and threshold phenomena I. Theory and experiments with autonomic drugs tested on isolated organs. *Arch. Int. Pharmacodyn.*, **127**, 459–478.

BESSE, J.C. & FURCHGOTT, R.F. (1976). Dissociation constants and relative efficacies of agonists acting on alpha adrenergic receptors in the rabbit aorta. *J. Pharmacol. Exp. Ther.*, **197**, 66–78.

BROADLEY, K.J. & MCNEILL, J.H. (1983). Dissociation constants (K_A) and relative efficacies of sympathomimetic amines in isolated atria during hypothermia-induced supersensitivity. *Can. J. Physiol. Pharmacol.*, **61**, 572–580.

BROADLEY, K.J. & NICHOLSON, C.D. (1979). Functional antagonism as a means of determining dissociation constants and relative efficacies of sympathomimetic amines in guinea-pig isolated atria. *Br. J. Pharmacol.*, **66**, 397–404.

BUCKNER, C.K. & SAINI, R.K. (1974). On the use of functional antagonism to estimate dissociation constants for *beta* adrenergic receptor agonists in isolated guinea-pig trachea. *J. Pharmacol. Exp. Ther.*, **194**, 565–574.

DUNN, W.R., MCGRATH, J.C. & WILSON, V.G. (1991). Postjunctional α-adrenoceptors in the rabbit isolated distal saphenous artery: indirect sensitivity to prazosin of responses to noradrenaline mediated via postjunctional α_2-adrenoceptors. *Br. J. Pharmacol.*, **103**, 1484–1492.

EMMERSON, J. & MACKAY, D. (1981). A test of the null equation for functional antagonism. *Br. J. Pharmacol.*, **73**, 135–141.

FLAVAHAN, N.A. & VANHOUTTE, P.M. (1986). α-Adrenoceptor subclassification in vascular smooth muscle. *Trends Pharmacol. Sci.*, **7**, 347–349.

KENAKIN, T.P. (1992). Tissue response as a functional discriminator of receptor heterogeneity: effects of mixed receptor populations on Schild regressions. *Mol. Pharmacol.*, **41**, 699–707.

LEFF, P., MARTIN, G.R. & MORSE, J.M. (1985). Application of the operational model of agonism to establish conditions when functional antagonism may be used to estimate agonist dissociation constants. *Br. J. Pharmacol.*, **85**, 655–663.

LEW, M.J. & ANGUS, J.A. (1992). Wall thickness to lumen diameter ratios of arteries from SHR and WKY: comparison of pressurised and wire-mounted preparations. *J. Vasc. Res.*, **29**, 435–442.

MACKAY, D. (1981). An analysis of functional antagonism and synergy. *Br. J. Pharmacol.*, **73**, 127–134.

MEDGETT, I.C. & LANGER, S.Z. (1984). Heterogeneity of smooth muscle *alpha* adrenoceptors in rat tail artery *in vitro*. *J. Pharmacol. Exp. Ther.*, **229**, 823–830.

MULVANY, M.J. & HALPERN, W. (1977). Contractile properties of small arterial resistance vessels in spontaneously hypertensive and normotensive rats. *Circ. Res.*, **41**, 19–26.

RUFFOLO, R.R. & ZEID, R.L. (1985). Relationship between *alpa* adrenoceptor occupancy and response for the *alpha*-1 adrenoceptor agonist, cirazoline, and the *alpha*-2 adrenoceptor agonist, B-HT 933, in canine saphenous vein. *J. Pharmacol. Exp. Ther.*, **235**, 636–643.

STONE, M. & ANGUS, J.A. (1978). Developments of computer-based estimation of pA_2 values and associated analysis. *J. Pharmacol. Exp. Ther.*, **207**, 705–718.

VAN DEN BRINK, F.G. (1973). The model of functional interaction. I. Development and first check of a new model of functional synergism and antagonism. *Eur. J. Pharmacol.*, **22**, 270–278.

(Received October 31, 1984
Revised January 23, 1995
Accepted March 15, 1995)

British Journal of Pharmacology (1995) 115, 753-760

A role for endothelin in bicuculline-induced neurogenic pulmonary oedema in rats

C. Herbst, B. Tippler, *H. Shams & [1]Th. Simmet

Department of Pharmacology & Toxicology and *Department of Physiology, Ruhr University, D-44780 Bochum, Germany

1 The possible contribution of endogenous endothelin (ET) to the pathogenesis of seizure-associated pulmonary oedema was examined in mechanically ventilated rats after intravenous bolus injection of the γ-aminobutyric acid (GABA) antagonist, bicuculline (1.2 mg kg^{-1}).

2 Recurrent seizure activity elicited by bicuculline injection led to rapidly developing pulmonary oedema. Within 4 min after bicuculline application (1.2 mg kg^{-1}), arterial O_2 partial pressure (P_aO_2) significantly dropped from 17.49 ± 1.20 kPa to 7.51 ± 2.21 kPa ($P < 0.01$) and arterial CO_2 partial pressure (P_aCO_2) significantly increased from 4.64 ± 0.56 kPa to 8.15 ± 0.99 kPa ($P < 0.01$). Gradually a progressive acidosis developed. Moreover, mean arterial blood pressure (MABP) and end-inspiratory airway pressure (P_{aw}) rapidly increased.

3 Concomitantly there was a time-dependent increase of big ET-1 and ET-1 levels in bronchoalveolar lavage (BAL) as determined by combined reverse phase high performance liquid chromatography (h.p.l.c.) and radioimmunoassay. BAL levels of both peptides increased up to 8 min after bicuculline injection and slowly decreased subsequently. In contrast, BAL from animals injected with vehicle did not contain detectable amounts of ET.

4 Pretreatment with the endothelin-converting enzyme inhibitor, phosphoramidon (5.4 mg kg^{-1}, i.v.) for 5 min significantly ($P < 0.001$) reduced peak ET-1 levels in BAL fluid by 65.4 ± 9.9% at 8 min after bicuculline injection. Simultaneously it afforded protection from hypoxia. P_aCO_2 did not increase and P_aO_2 decreased only slightly from 14.63 ± 1.00 kPa to 12.97 ± 0.61 kPa ($P > 0.05$) after phosphoramidon pretreatment. In contrast, vehicle-treated animals that received bicuculline showed both significant hypercapnia as well as profound hypoxia. Phosphoramidon significantly diminished the maximum increase in P_{aw} by 76.7 ± 12.4% ($P < 0.005$), but only slightly affected the MABP. Phosphoramidon pretreatment had no effect on the acidosis.

5 Pretreatment with the ET_A receptor antagonist, BQ-123 (1 mg kg^{-1}, i.v.), for 5 min did not affect the levels of ET-1 in the BAL fluid at 8 min after bicuculline injection but did ameliorate the development of hypoxia. No hypercapnia developed and P_aO_2 decreased only moderately from 16.65 ± 0.25 kPa to 14.19 ± 2.15 kPa ($P > 0.05$) in BQ-123-treated animals. In contrast, vehicle-treated animals that received bicuculline exhibited significant hypercapnia as well as profound hypoxia. BQ-123 significantly reduced the increase in P_{aw} by 51.3 ± 12.8% ($P < 0.01$). It affected MABP only slightly and had no effect on the acidosis.

6 These results suggest that ET peptides play a significant role in this model of neurogenic pulmonary oedema and may act as mediators of respiratory distress. The deleterious effects of endogenous ET in this model are primarily mediated via the ET_A receptor, for they were inhibited by the ET_A receptor antagonist, BQ-123. ET_A receptor antagonists may therefore be of potential therapeutic value in respiratory distress.

Keywords: Endothelin-1; big endothelin-1; endothelin-converting enzyme; phosphoramidon; BQ-123; pulmonary oedema; respiratory distress

Introduction

Since the isolation and purification of endothelin (ET)-1 from the culture medium of porcine aortic endothelial cells, numerous studies have emphasized the role of ET isopeptides in the vascular system, both under physiological and pathophysiological conditions (Haynes & Webb, 1993). Due to their vasoactive properties, ET isopeptides have been implicated in the pathophysiology of hypertension, coronary and digital vasospasm, myocardial infarction and renal failure (Haynes & Webb, 1993). However, ET also appear to play an important role in the respiratory system (Filep, 1993; Hay *et al.*, 1993). Thus, ET may be generated locally in lung respiratory epithelium, bronchioles and blood vessels of all sizes in close vicinity to ET receptors which also appear to be located on pulmonary nerve trunks (Filep, 1993; Hay *et al.*, 1993).

In the pulmonary circulation a complex pattern of responses to ET has emerged, which may depend on both species and ET doses used (Filep, 1993). ET may elicit pulmonary vasoconstriction (Horgan *et al.*, 1991; Raffestin *et al.*, 1991), induce bronchoconstriction (Matsuse *et al.*, 1990) and release 15*S*-hydroxyeicosatetraenoic acid (Nagase *et al.*, 1990), another vasoconstrictor able to trigger pulmonary oedema (Burhop *et al.*, 1988).

We have previously demonstrated that ET isopeptides are released in oleic acid-induced respiratory distress syndrome in rats (Simmet *et al.*, 1992). Interestingly, in this model, where respiratory distress develops over a time interval of several hours in conscious rats, peak levels of immunoreactive ET in the bronchoalveolar lavage (BAL) fluid preceded the maximum hypoxia. This suggests that ET generation could be related to the pathophysiological changes observed (Simmet *et al.*, 1992). However, the limited availability of pharmacokinetic data on ET receptor antagonists or endothelin-converting enzyme inhibitors makes it difficult to judge the effects of such compounds in this model. Hence, no further insight into the role of ET could be obtained in the oleic acid-induced respiratory distress syndrome.

[1] Author for correspondence.

Thus we sought a model of rapidly developing respiratory distress. Pulmonary oedema often develops in human subjects after various cerebral insults, such as head injury, subarachnoid haemorrhage, intracranial hypertension and epileptic seizures. This type of oedema, known as neurogenic pulmonary oedema, is rapid in onset, is associated with a massive response of the autonomic nervous system, and is rich in protein content (Colice *et al.*, 1984; Malik, 1985). Because of its pathophysiological relevance and its rapid development we chose as a model the seizure-associated neurogenic, pulmonary oedema elicited in rats by i.v. injection of bicuculline (Kreisman *et al.*, 1987). In this model we have investigated the release of ET-1 and big ET-1 into BAL fluid as well as the effects of the endothelin-converting enzyme inhibitor, phosphoramidon, and the ET_A receptor antagonist, BQ-123.

Methods

Experimental protocol

Male Wistar rats, weighing 290–340 g, were tracheotomized during diethylether anaesthesia and paralysed with (+)-tubocurarine (0.2 mg kg^{-1}, i.v.). Anaesthesia was maintained by positive pressure ventilation with a mixture of 70% N_2O:30% O_2. Respiratory rate was kept constant at 55 strokes min^{-1} with a tidal volume of 2.1–2.4 ml. Catheters made of PE-50 tubing were inserted into the right femoral artery for blood pressure measurement (via Statham P23Db transducers) and withdrawal of blood samples for blood gas analysis, and into the right femoral vein for injection of drugs. Body temperature was monitored with a rectal thermometer and maintained at 37°C with a thermostatically controlled heating pad. Arterial O_2 (P_aO_2) and CO_2 (P_aCO_2) partial pressures as well as pH were determined at 37°C using an ABL-2 blood gas analyzer (Radiometer, Copenhagen, DK). Seizure activity was recorded with bitemporal electrodes.

After about 40 min adaptation to mechanical ventilation, recurrent seizures were elicited by single i.v. bolus injections of 1.2 mg kg^{-1} bicuculline dissolved in 0.1 M HCl, adjusted to pH 4–5 with 0.1 M NaOH and diluted with saline. Pilot studies had shown that doses of bicuculline below 1.2 mg kg^{-1} (e.g. 0.9 mg kg^{-1}) elicited seizures accompanied by pulmonary oedema in a fraction of the animals only, while higher doses (e.g. 1.5 mg kg^{-1}) led to a high mortality rate within a few minutes. Injection of vehicle alone had no significant effects on the various parameters determined. Thirty seconds before bicuculline injection, 3.5 ml of arterial blood was withdrawn. Blood gases were always analysed twice in each animal: once before bicuculline and at the end point of the experiments which was 2, 4, 8, 12 or 16 min later. In some experiments rats were pretreated for 5 min with either phosphoramidon, dissolved in saline (5.4 mg mg^{-1}, i.v., injection volume 100 μl), or BQ-123 [cylo-(D-Asp-Pro-D-Val-Leu-D-Trp)], dissolved in saline containing 10 mM $NaHCO_3$ (1 mg kg^{-1}, i.v., injection volume 100 μl). Doses used were selected on the basis of pilot studies. Vehicle injections had no effect either on the course of the seizures or on the development of pulmonary oedema. Controls received the appropriate vehicle.

Analytical procedures

At the end of the experiments lungs were macroscopically inspected and bronchoalveolar lavage (BAL) was performed by flushing the lungs with 5 × 10 ml 150 mM NaCl containing aprotinin (500 u ml^{-1}) and Na_2 EDTA (2.0 mM) as previously described (Simmet *et al.*, 1992). BAL samples were further processed as described by Simmet *et al.* (1992). Briefly, BAL fluid was immediately centrifuged (525 *g*, 20 min, 4°C) and mixed with Triton X 305 (0.01%) and acetic acid (100 mM) (all final concentrations). Protein was pelleted by centrifugation at 3200 *g* at 4°C for 10 min. The supernatants were extracted on C_{18} SEP-PAK cartridges conditioned with 10 ml acetonitrile, 10 ml methanol and 10 ml H_2O, all containing trifluoroacetic acid (TFA) 0.1%. The sample was then applied and the cartridge was washed with 1.6 ml H_2O/TFA 0.1% and 1.6 ml 40% methanol/TFA 0.1%. ET were eluted with 3.2 ml 75% methanol/TFA 0.1% containing Triton X 305 0.01%. After evaporation the samples were analysed for ET-1 and big ET-1 by combined reverse phase high performance liquid chromatography (h.p.l.c.) and radioimmunoassay (Simmet *et al.*, 1992; Tippler *et al.*, 1994). The material was loaded onto a C_{18} Nucleosil column (250 × 4 mm, particle size 5 μm) protected by a precolumn of the same material. Flow rate was 1.0 ml min^{-1} and absorption was monitored at 210 nm. A gradient from 30 to 40% acetonitrile in H_2O (containing TFA 0.1% final conc.) was applied from 0 to 30 min and was then increased from 40 to 60% acetonitrile from 30 to 60 min. Eluate fractions comigrating with the retention times of synthetic ET-1 and rat big ET-1 were collected, evaporated and, after reconstitution in assay buffer, were analysed radioimmunologically (Simmet *et al.*, 1992; Tippler *et al.*, 1994). The anti-plasma used recognizes mainly ET-1 and has a relative cross-reaction of 21.5% and 1.7% with rat big ET-1 and ET-2, respectively; cross-reactivity with ET-3 is < 0.005%. The detection limit of the assays was 5.1 fmol/tube and 11.2 fmol/tube for ET-1 and rat big ET-1, respectively.

Materials

ET-1, rat big ET-1 and phosphoramidon were from Peninsula, Merseyside, UK and [^{125}I]-Tyr^{13} ET-1 (sp. act. 74 TBq $mmol^{-1}$) was from Amersham, Braunschweig, Germany. BQ-123 [cyclo(D-Asp-Pro-D-Val-Leu-D-Trp)] was from Bachem, Heidelberg, Germany and bicuculline was purchased from Sigma, St Louis, MO, U.S.A. Other chemicals were of analytical grade and solvents were of h.p.l.c. grade.

Statistical analysis

Data are expressed as means ± s.e.mean. The results were statistically evaluated by means of Student's *t* test for paired or unpaired values as applicable. Differences were considered significant at $P < 0.05$.

Results

Effects of bicuculline injection

Figure 1 shows a typical tracing of electrocorticogram (ECoG), arterial blood pressure, and airway pressure before and after intravenous injection of bicuculline 1.2 mg kg^{-1}. Bicuculline induced epileptiform activity, as shown in Figure 1, accompanied by an immediate rise in mean arterial blood pressure (MABP) from 133.3 ± 8.9 mmHg to a maximum of 196.8 ± 9.5 mmHg ($P < 0.001$) at 2 min, followed by a decrease to 150.7 ± 8.6 mmHg at 16 min after bicuculline injection ($n = 4$). In addition, the end-inspiratory airway pressure (P_{aw}) rapidly increased from 1.18 ± 0.08 kPa at time 0 to a maximum of 2.34 ± 0.08 pKa ($P < 0.001$) at 3 min after bicuculline injection ($n = 4$). It decreased only slightly to 2.13 ± 0.09 kPa ($n = 4$) at 16 min. More detailed data on these parameters are given in the context of the various treatment regimens described below.

Bicuculline injection triggered a progressive acidosis as shown in Figure 2. Significant hypercapnia ($P < 0.01$) with an arterial CO_2 partial pressure (P_aCO_2) of 8.15 ± 0.99 kPa ($n = 4$) was detectable as early as 4 min after bicuculline injection and remained elevated at 8 min. Values at 12 and 16 min were not significantly different from that before bicuculline. Severe hypoxia similarly developed within 2 min of bicuculline injection as shown by a significant ($P < 0.01$) drop of arterial O_2 partial pressure (P_aO_2) from 17.05 ± 0.5 kPa to 9.47 ± 2.4 kPa ($n = 4$). The maximum depression of P_aO_2 was observed between 4–

8 min after bicuculline injection. Later a slight but consistent increase in P_aO_2 values up to 16 min after bicuculline injection was observed (Figure 2).

When BAL fluid from control animals, injected with vehicle instead of bicuculline, was analysed by combined reverse phase h.p.l.c. and radioimmunoassay for big ET-1 or ET-1 levels, both peptides were below the detection limit of the analytical method employed (data not shown). However, after bicuculline injection (1.2 mg kg^{-1}) the peptides became clearly detectable within 2 min (Figure 3). Both big ET-1 and ET-1 reached peak levels in BAL fluid at 8 min after bicuculline injection with 6.32 ± 0.82 ng/BAL and 1.54 ± 0.15 ng/BAL, respectively ($n = 7$ each). BAL fluid levels of both peptides steadily decreased during the following 8 min. Concentrations of big ET-1 in BAL fluid were generally about 4 fold higher than those of ET-1 (Figure 3).

Effects of phosphoramidon pretreatment

In order to investigate further the putative role of ET in this experimental model of neurogenic pulmonary oedema, additional experiments were carried out with the endothelin-converting enzyme inhibitor, phosphoramidon. When rats received phosphoramidon, 5.4 mg kg^{-1}, i.v., 5 min before bicuculline injection, the ECoG was basically unchanged as compared to vehicle-treated animals (data not shown). However, by contrast there was a slight decrease in the MABP during the first few min after bicuculline injection (Figure 4). A significant fall in blood pressure ($P < 0.05$) was seen at 2 and 3 min after bicuculline in the phosphoramidon-treated rats as compared to vehicle-treated animals (Figure 4). Pretreatment with phosphoramidon (5.4 mg kg^{-1}) profoundly reduced the increase in P_{aw} induced by i.v. bicuculline. This effect became

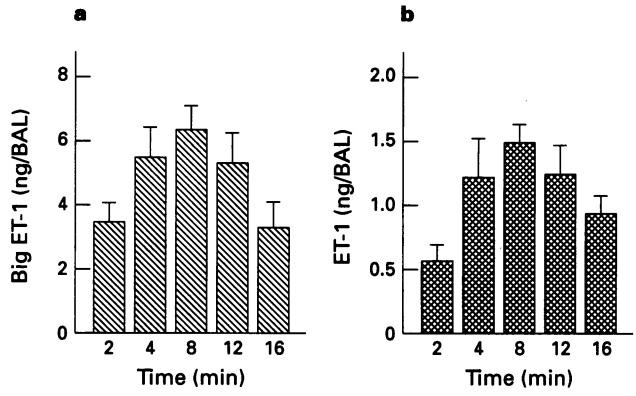

Figure 3 Time-dependent levels of (a) rat big endothelin-1 (big ET-1) and (b) endothelin-1 (ET-1) in the bronchoalveolar lavage (BAL) from rats injected with bicuculline (1.2 mg kg^{-1}, i.v.). Each column represents the mean ± s.e.mean of 4 to 7 experiments.

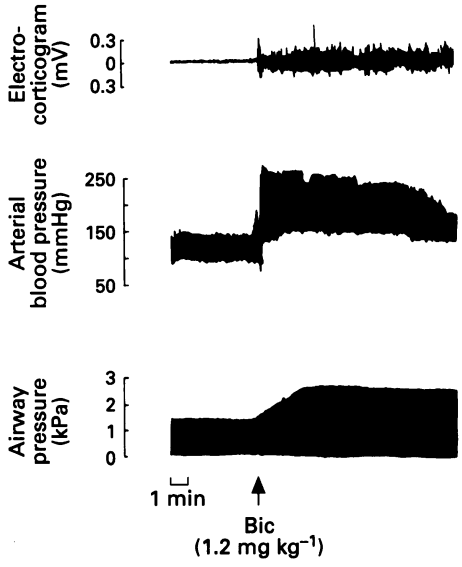

Figure 1 Typical tracings of electrocorticogram (ECoG), arterial blood pressure and airway pressure from a rat injected with bicuculline (Bic, 1.2 mg kg^{-1}, i.v.).

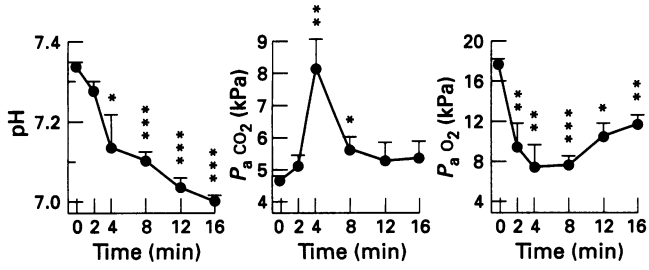

Figure 2 Blood gas parameters before and after intravenous injection of bicuculline (1.2 mg kg^{-1}) in rats. The values shown are means ± s.e.mean of 4 to 7 experiments except for time 0 which includes the basal values of all animals ($n = 25$). (*$P < 0.05$, **$P < 0.01$ and ***$P < 0.001$ versus paired values at 0 min).

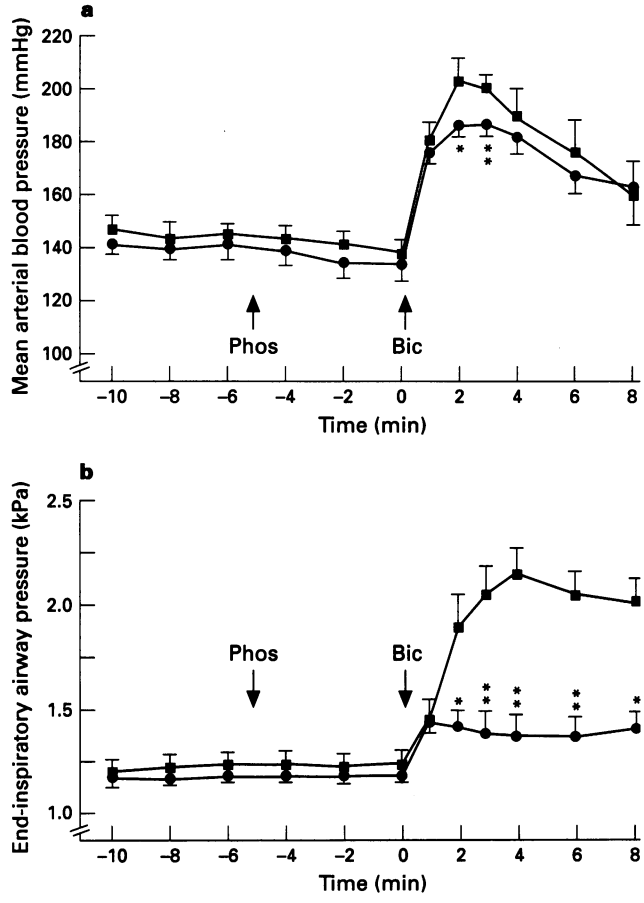

Figure 4 Effects of pretreatment with phosphoramidon (5.4 mg kg^{-1}) (●) on (a) mean arterial blood pressure (MABP) and (b) end-inspiratory airway pressure (P_{aw}) as compared to vehicle-treated rats (■). Phosphoramidon (5.4 mg kg^{-1}) was injected intravenously 5 min before injection of bicuculline (1.2 mg kg^{-1}, Bic). The values are means ± s.e.mean of 7 experiments. (*$P < 0.05$ and **$P < 0.02$ versus vehicle-treated control animals).

significant ($P<0.05$) as early as 2 min after bicuculline (1.2 mg kg^{-1}) injection and lasted throughout the observation period of 8 min (Figure 4). Phosphoramidon pretreatment reduced the maximum increase in P_{aw} significantly ($P<0.02$) to $23.3\pm12.4\%$ ($n=7$) of that in vehicle-treated control animals ($n=7$).

Phosphoramidon (5.4 mg kg^{-1}) treatment had no effect on the development of acidosis (Figure 5). However, it prevented the increase of P_aCO_2 in rats killed 8 min after bicuculline injection (Figure 5). In addition, the drop in P_aO_2 which amounted to 6.64 ± 0.72 kPa in vehicle-treated controls ($n=7$) was significantly ($P<0.001$) ameliorated to 1.66 ± 0.61 kPa ($n=7$) indicating that phosphoramidon afforded protection from the development of hypoxia (Figure 5).

Analysis of BAL fluid obtained 8 min after bicuculline injection revealed that phosphoramidon pretreatment (5.4 mg kg^{-1}, i.v.) did not significantly affect the levels of big ET-1 ($n=7$). In contrast, however, the level of ET-1 was significantly reduced ($P<0.05$) by $65.4\pm9.9\%$ ($n=7$) (Figure 6) in phosphoramidon-treated animals.

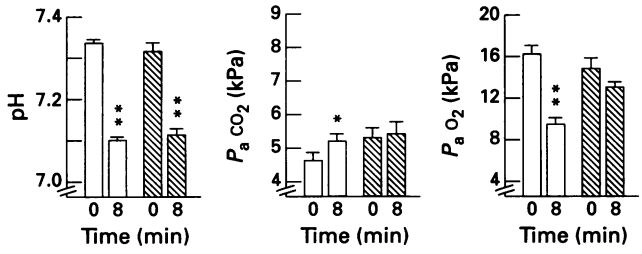

Figure 5 Blood gas parameters before and 8 min after i.v. injection of bicuculline (1.2 mg kg^{-1}) in rats pretreated either with vehicle (open columns) or phosphoramidon (5.4 mg kg^{-1}, hatched columns) for 5 min before injection of bicuculline. Each column represents the mean±s.e.mean of 7 experiments. (*$P<0.05$ and **$P<0.001$ versus values at 0 min).

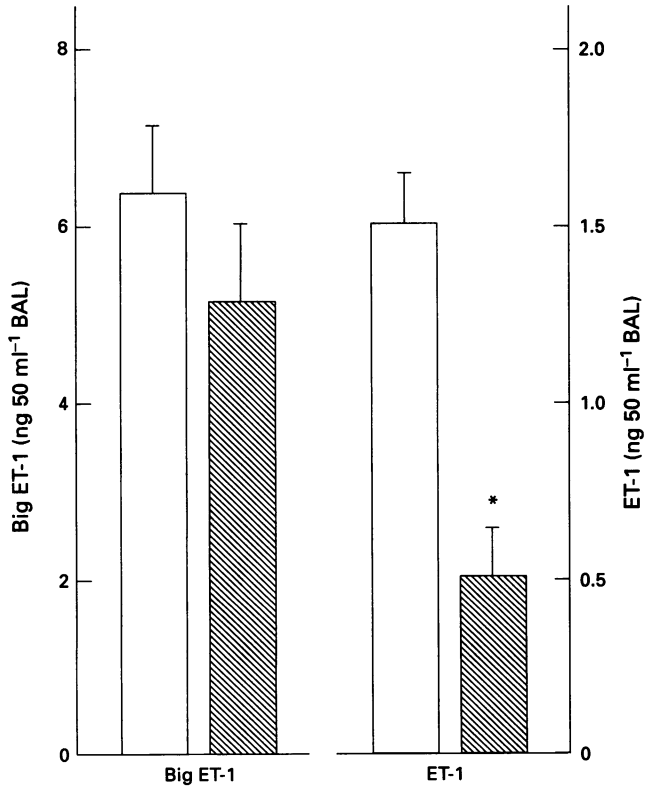

Figure 6 Effects of pretreatment with phosphoramidon (5.4 mg kg^{-1}, i.v.) for 5 min on the levels of big ET-1 and ET-1 in the bronchoalveolar lavage (BAL) at 8 min after intravenous injection of bicuculline (1.2 mg kg^{-1}, hatched columns) as compared to rats pretreated with vehicle (open columns). Each column represents the mean±s.e.mean of 7 experiments. (*$P<0.05$ versus vehicle-treated animals).

Effects of BQ-123 pretreatment

In order to gain some evidence for the type of ET receptor that might be involved in the development of the neurogenic pulmonary oedema in this model, we performed further experi-

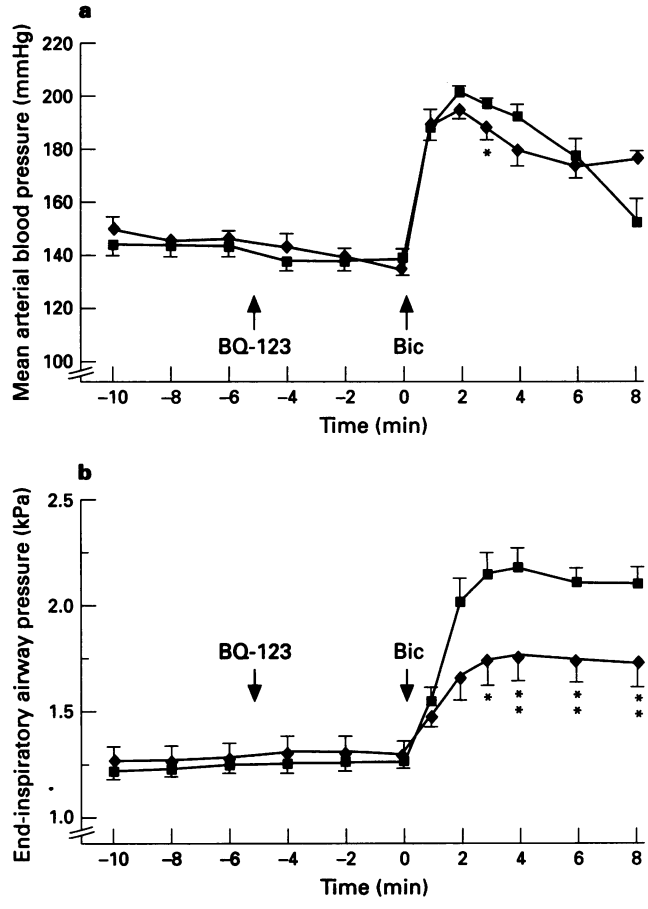

Figure 7 Effects of pretreatment with the endothelin ET_A receptor antagonist, BQ-123 (1 mg kg^{-1}, ◆), on (a) mean arterial blood pressure (MABP) and (b) end-inspiratory airway pressure (P_{aw}) as compared to vehicle-treated rats (■). BQ-123 (1 mg kg^{-1}) was injected intravenously 5 min before injection of bicuculline (1.2 mg kg^{-1}). The values are means±s.e.mean of 6 to 11 experiments. (*$P<0.05$ and **$P<0.02$ versus vehicle-treated control animals).

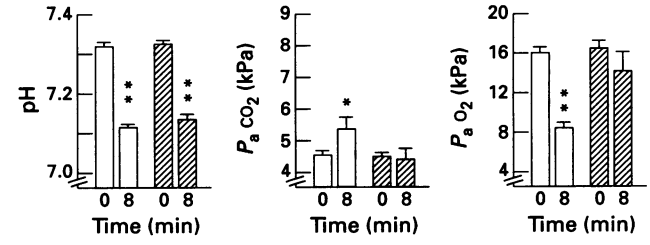

Figure 8 Blood gas parameters before and 8 min after intravenous injection of bicuculline (1.2 mg kg^{-1}) in rats pretreated either with vehicle (open columns) or BQ-123 (1 mg kg^{-1}, i.v., hatched columns) for 5 min before bicuculline injection. Each column represents the mean±s.e.mean of 6 to 11 experiments. (*$P<0.05$ and **$P<0.001$ versus values at 0 min).

ments with the ET_A receptor antagonist, BQ-123. Pretreatment with BQ-123 at 1 mg kg^{-1}, i.v. had no significant effect on the ECoG (data not shown). However, during the first few min after bicuculline injection, pretreatment with BQ-123 (1 mg kg^{-1}) appeared to lower MABP. This effect became significant ($P<0.05$) at 3 min after bicuculline injection (Figure 7). Pretreatment with BQ-123 significantly ($P<0.05$) decreased the rise in P_{aw} starting from 3 min after bicuculline injection when compared to untreated rats. This inhibitory effect lasted throughout the observation period of 8 min. The maximum increase of P_{aw} was lowered to 48.7 ± 12.8% ($n=6$, $P<0.02$) of that seen in vehicle-treated control animals ($n=11$) (Figure 7).

As with phosphoramidon pretreatment, injection of BQ-123 (1 mg kg^{-1}, i.v.) 5 min before bicuculline completely prevented the hypercapnia ($n=6$) observed at 8 min in control animals ($n=11$) (Figure 8). In addition, the significant decline ($P<0.001$) in P_aO_2 which amounted to 7.43 ± 0.65 kPa ($n=11$) in vehicle-treated control rats was significantly ($P<0.02$) ameliorated to 2.45 ± 2.15 kPa ($n=6$) after BQ-123 pretreatment, indicating that BQ-123 provided protection from the development of hypoxia (Figure 8).

When BAL fluid from rats pretreated with BQ-123 (1 mg kg^{-1}) was analysed for ET, the amounts of both big ET-1 and ET-1 were similar to those detected in vehicle-treated control animals (Figure 9).

Discussion

We have previously observed that development of the oleic acid-induced respiratory distress syndrome in conscious rats was accompanied by generation of ET. Immunoreactive ET could be recovered from both plasma as well as BAL fluid of rats injected with oleic acid (Simmet *et al.*, 1992). It was particularly intriguing that the maximum changes in P_aO_2 and P_aCO_2, as indicators of the pulmonary oedema, was apparently preceded by a maximum release of immunoreactive ET into the BAL fluid (Simmet *et al.*, 1992). In light of these findings and the well-known biological effects of ET (Filep, 1993; Haynes & Webb, 1993) it seemed conceivable that ET might contribute to the pathophysiological changes during pulmonary oedema. However, the long latency phase of 2–3 h for full expression of pulmonary oedema, severely hampered the use of ET receptor antagonists or endothelin-converting enzyme inhibitors in investigations with this model. We now took advantage of the bicuculline-induced neurogenic pulmonary oedema in rats (Kreisman *et al.*, 1987), because its rapid development permits pharmacological modulation and analysis of ET generation.

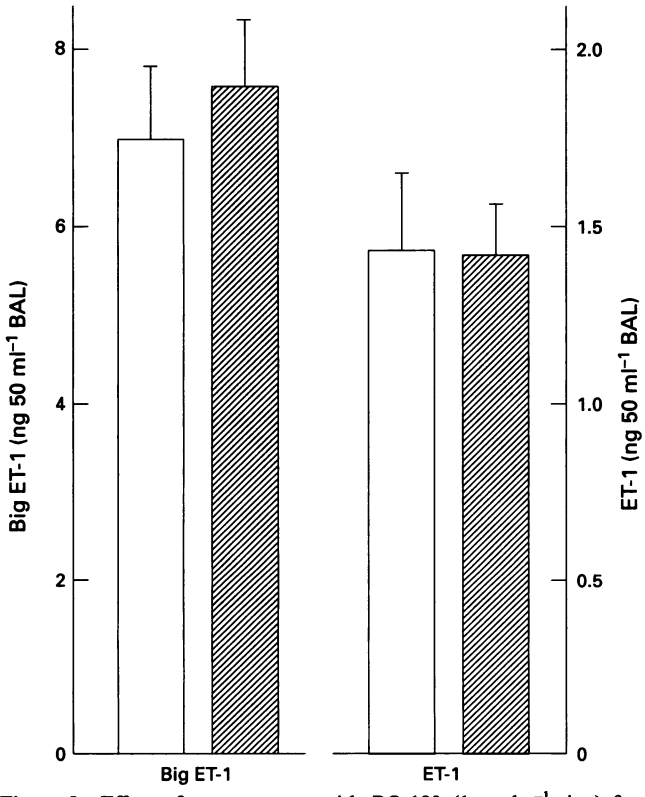

Figure 9 Effect of pretreatment with BQ-123 (1 mg kg^{-1}, i.v.) for 5 min on the levels of rat big endothelin-1 (big ET-1) and endothelin-1 (ET-1) in the bronchoalveolar lavage (BAL) at 8 min after intravenous injection of bicuculline (1.2 mg kg^{-1}, hatched columns) as compared to rats pretreated with vehicle (open columns). Each column represents the mean ± s.e.mean of 6 to 11 experiments.

Our data show that in this type of experimental pulmonary oedema, there is also release of ET-1 and big ET-1 into BAL fluid similar to that in the oleic acid model (Simmet *et al.*, 1992). That ETs are being released in two different experimental models of pulmonary oedema further supports the notion that these peptides might play a pathophysiological role in pulmonary oedemas. Indeed, it has recently been reported that patients with early acute lung injury and adult respiratory distress (ARDS) have increases in circulating ET-1 plasma levels (Druml *et al.*, 1993; Langleben *et al.*, 1993). These increases are in the low pg ml^{-1} plasma range and are apparently due to both pulmonary release of ET-1 and an abnormally decreased pulmonary ET-1 metabolism (Druml *et al.*, 1993; Langleben *et al.*, 1993). Similar to ET generation associated with the pulmonary oedema in rats, in patients the endothelin plasma levels are apparently unrelated to the specific cause of respiratory distress (Langleben *et al.*, 1993).

Based on our previous observation of elevated plasma levels of immunoreactive ET in oleic acid-injected rats, we also intended to determine the plasma levels of ET isopeptides in our model of neurogenic pulmonary oedema. However, in rats with neurogenic pulmonary oedema we could not detect any consistent elevation of ET plasma levels (data not shown). The different time course of oedema development might account for this discrepancy. Although ET mRNA has been identified in various compartments of the rat lung (MacCumber *et al.*, 1989), so far we do not know the cellular origin of ET generated in connection with oedema development. Considering the large amounts of ET in the BAL fluid from oleic acid-injected rats compared to those in plasma, one could speculate that the rapid onset of the neurogenic pulmonary oedema might not leave enough time for ET to reach the systemic circulation in detectable quantities. On the other hand, in the oleic acid model, ET levels peaked in BAL fluid at 2 h. This roughly coincided with the development of pulmonary oedema, as judged from the concurrent blood gas changes (Simmet *et al.*, 1992). By contrast, peak plasma levels of ET were observed rather early, at 45 min (Simmet *et al.*, 1992). ET plasma levels could therefore represent an endothelial response to injury upon intravenous oleic acid injection (Derks & Jacobovitz-Derks, 1977).

Increases in ET plasma levels in ARDS patients have been associated with a worsening of the clinical condition and similarly a decrease was associated with an improvement (Langleben *et al.*, 1993). This does not exclude a response to injury reaction and no causal relationship between ET generation and the pathophysiological changes in ARDS has so far been established. Indeed, the decreased metabolic clearing function of the lung for ET in ARDS patients (Druml *et al.*, 1993; Langleben *et al.*, 1993) is rather supportive of the response to injury hypothesis. Obviously, it is of utmost importance to answer the key question, whether ET are markers or mediators of respiratory distress. Our experiments for the first time provide conclusive eivdence that, at least in our model of neurogenic pulmonary oedema, ET actively participate in the pathophysiological changes related to pulmonary oedema as reflected by the blood gas changes.

First, we used phosphoramidon, a metalloprotease in-

hibitor, known to inhibit the neutral endopeptidase-like, endothelin-converting enzyme in a dose which causes substantial inhibition of the pressor effects of big ET-1 in rats (Fukuroda *et al.*, 1990; Matsumura *et al.*, 1990; Gardiner *et al.*, 1991; Pollock & Opgenorth, 1991). Although rat lung may contain an aspartic protease-like endothelin-converting enzyme (Wu-Wong *et al.*, 1990) as well, it was shown to contain a phosphoramidon-sensitive endothelin-converting enzyme (Takaoka *et al.*, 1991; Gui *et al.*, 1993; Télémaque *et al.*, 1993; Hisaki *et al.*, 1994). This enzyme has recently been purified to homogeneity (Takahashi *et al.*, 1993). Consistent with these reports, we observed a 65% reduction of ET-1 in BAL fluid after phosphoramidon pretreatment. Phosphoramidon is also an inhibitor of neutral endopeptidase 24.11 (Hudgin *et al.*, 1981; Mumford *et al.*, 1981), which may contribute to the degradation of ET (Vijayaraghavan *et al.*, 1990; Abassi *et al.*, 1992). Therefore, the possibility cannot be excluded that in our experiments phosphoramidon pretreatment had a dual effect, inhibiting generation as well as degradation of ET at the same time. Nevertheless, the net effect of this compound was a reduction of ET-1 in BAL fluid which was accompanied by a complete blockade of hypercapnia. Moreover, the severe hypoxia observed in controls was not detected after phosphoramidon pretreatment. These improvements of blood gas parameters reflect a significant reduction of the pulmonary oedema, which in untreated animals severely hampered pulmonary gas exchange.

Since by inhibition of neutral endopeptidase, phosphoramidon may have effects other than inhibition of the transformation of big ET-1 or degradation of ET-1, in our second approach we used the ET_A receptor antagonist, BQ-123, in a dose which effectively inhibits ET_A receptor-mediated responses in rats *in vivo* (Ihara *et al.*, 1992; Bigaud & Pelton, 1992; Douglas *et al.*, 1992; Filep *et al.*, 1992; Bonvallet *et al.*, 1993; McMurdo *et al.*, 1993). Rat lung has been shown to possess mRNA for both ET_A and ET_B receptors, throughout the lung parenchyma (Filep, 1993; Hay *et al.*, 1993). Porcine bronchi and pulmonary blood vessels are rich in ET_A receptors, but lung parenchyma is rich in ET_B receptors (Nakamichi *et al.*, 1992). In rat lungs, ET_B receptors, similarly located in lung parenchyma (Durham *et al.*, 1993), are apparently involved in the clearance of circulating ET-1 (Fukuroda *et al.*, 1994a). In contrast, ET_A receptors seem to mediate the ET-1-induced vasoconstriction in the rat pulmonary circulation, but also prostacyclin biosynthesis (D'Orléans-Juste *et al.*, 1992; Bonvallet *et al.*, 1993). In addition, ET_A receptors appear to play a role in the development of hypoxic pulmonary hypertension in rats (Bonvallet *et al.*, 1994). Thus, this type of ET receptor is seemingly connected to pathophysiologically relevant pulmonary reactions. This concept is further supported by our findings that the ET_A receptor antagonist, BQ-123, brings about the same beneficial effects as phosphoramidon, namely blockade of hypercapnia combined with a significant inhibition of hypoxia. The effects of BQ-123 provide an important piece of evidence for the pathophysiological relevance of ET in our model. Thus, we can demonstrate that two chemically distinct compounds, with different mechanisms of action, produce the same net result in this model, i.e. the reduction of the pulmonary oedema, as shown by the blood gas data. We therefore conclude that in this model, ET are actively involved in the genesis of pulmonary oedema.

Both treatment regimens had effects apart from the apparent normalization of blood gas values. They affected only slightly the mean arterial blood pressure after the onset of seizures, but greatly reduced the end-inspiratory airway pressure, indicating that the increase in airway resistance was directly or indirectly due to liberation of endogenous ET. ET-1 is a potent bronchoconstrictor, which even upon intravenous application triggers a long lasting increase in airway resistance in rats (Matsuse *et al.*, 1990). The increases in airway pressure in our experiments could functionally be related to bronchoconstriction and/or oedema formation, which cannot be differentiated from our results. However, in light of the anti-oedemogenic effects of both phosphoramidon as well as BQ-123, the significant decrease in end-inspiratory airway pressure might be largely due to oedema reduction. Phosphoramidon had a greater efficacy regarding the end-inspiratory airway pressure than BQ-123 which could be related to effects other than inhibition of the endothelin-converting enzyme. Alternatively, ET may act on both ET_A as well as ET_B receptors which at least in the rabbit pulmonary artery have been shown to act synergistically (Fukuroda *et al.*, 1994b). Further studies with selective ET_B receptor antagonists will have to clarify the role of these receptors in this model.

The complexity of the neurogenic pulmonary oedema is not yet fully understood (Colice *et al.*, 1984; Malik, 1985). At present one can only speculate on the precise role of ET in this model. Intravenously applied ET-1 may increase vascular permeability in various organs of the rat, including pulmonary tissues (Filep *et al.*, 1991; Zimmerman *et al.*, 1992). At least with respect to pulmonary parenchyma, this effect seems to depend critically on the dose of ET used (Filep *et al.*, 1991; Zimmerman *et al.*, 1992). It is therefore not clear, to what extent such results might be relevant to our experiments with endogenous ET formation, as different local concentrations of ET might be achieved. Future studies will also have to take into account the complex pre- and postjunctional interactions of ET with the autonomic neurotransmission (Wiklund *et al.*, 1991; Warner *et al.*, 1993), particularly since the autonomic nervous system is known to play a key role in the pathogenesis of neurogenic pulmonary oedema (Colice *et al.*, 1984; Malik, 1985). We assume that the increased metabolic rate due to sympathetic stimulation (Lang *et al.*, 1989), is the reason for the progressive metabolic acidosis observed after bicuculline injection, irrespective of oedema development. Such pronounced acidotic changes have also been described in another experimental model of neurogenic pulmonary oedema (Maron, 1985).

From our experiments we cannot conclude at which stage in the cascade of pathophysiological events, ET exert their deleterious effects. However, the fact that phosphoramidon, an inhibitor of the endothelin-converting-enzyme, as well as the ET_A receptor antagonist, BQ-123, inhibit the detrimental development of neurogenic pulmonary oedema indicates that ET act as mediators in this model of respiratory distress. Therefore, appropriate pharmacological intervention, e.g. with ET_A receptor antagonists, may prove to be of potential therapeutic value in respiratory distress.

This project was supported by the Deutsche Forschungsgemeinschaft.

References

ABASSI, Z.A., TATE, J.E., GOLOMB, E. & KEISER, H.R. (1992). Role of neutral endopeptidase in the metabolism of endothelin. *Hypertension*, **20**, 89–95.

BIGAUD, M. & PELTON, J.T. (1992). Discrimination between ET_A- and ET_B-receptor-mediated effects of endothelin-1 and [$Ala^{1,3,11,15}$]endothelin-1 by BQ-123 in the anaesthetized rat. *Br. J. Pharmacol.*, **107**, 912–918.

BONVALLET, S.T., OKA, M., YANO, M., ZAMORA, M.R., MCMURTY, I.F. & STELZNER, T.J. (1993). BQ123, an ET_A receptor antagonist, attenuates endothelin-1-induced vasoconstriction in rat pulmonary circulation. *J. Cardiovasc. Pharmacol.*, **22**, 39–43.

BONVALLET, S.T., ZAMORA, M.Z., HASUNUMA, K., SATO, K., HANASATO, N., ANDERSON, D., SATO, K. & STELZNER, T.J. (1994). BQ123, an ET_A-receptor antagonist, attenuates hypoxic pulmonary hypertension in rats. *Am. J. Physiol.*, **266**, H1327–H1331.

BURHOP, K.E., SELIG, W.M. & MALIK, A.B. (1988). Monohydroxyeicosatetraenoic acids (5-HETE and 15-HETE) induce pulmonary vasoconstriction and edema. *Circ. Res.*, **62**, 687–698.

COLICE, G.L., MATTHAY, M.A., BASS, E. & MATTHAY, R.A. (1984). Neurogenic pulmonary edema. *Am. Rev. Respir. Dis.*, **130**, 941–948.

DERKS, C.M. & JACOBOVITZ-DERKS, D. (1977). Embolic pneumopathy induced by oleic acid. A systematic morphologic study. *Am. J. Pathol.*, **87**, 143–158.

D'ORLÉANS-JUSTE, P., TÉLÉMAQUE, S., CLAING, A., IHARA, M. & YANO, M. (1992). Human big-endothelin-1 and endothelin-1 release prostacyclin via activation of ET_1 receptors in the rat perfused lung. *Br. J. Pharmacol.*, **105**, 773–775.

DOUGLAS, S.A., ELLIOTT, J.D. & OHLSTEIN, E.H. (1992). Regional vasodilation to endothelin-1 is mediated by a non-ETA receptor subtype in the anaesthetized rat: effect of BQ-123 on systemic haemodynamic responses. *Eur. J. Pharmacol.*, **221**, 315–324.

DRUML, W., STELTZER, H., WALDHÄUSL, W., LENZ, K, HAMMERLE, A., VIERHAPPER, H., GASIC, S. & WAGNER, O. (1993). Endothelin-1 in adult respiratory distress syndrome. *Am. Rev. Respir. Dis.*, **148**, 1169–1173.

DURHAM, S.K., GOLLER, N.L., LYNCH, J.S., FISHER, S.M. & ROSE, P.M. (1993). Endothelin receptor B expression in the rat and rabbit lung as determined by in situ hybridization using nonisotopic probes. *J. Cardiovasc. Pharmacol.*, **22** (Suppl. 8), S1–S3.

FILEP, J.G. (1993). Endothelin peptides: biological actions and pathophysiological significance in the lung. *Life Sci.*, **52**, 119–133.

FILEP, J.G., FÖLDES-FILEP, E., ROUSSEAU, A., FOURNIER, A., SIROIS, P. & YANO, M. (1992). Endothelin-1 enhances vascular permeability in the rat heart through the ET_A receptor. *Eur. J. Pharmacol.*, **219**, 343–344.

FILEP, J.G., SIROIS, M.G., ROUSSEAU, A., FOURNIER, A. & SIROIS, P. (1991). Effects of endothelin-1 on vascular permeability in the conscious rat: interactions with platelet-activating factor. *Br. J. Pharmacol.*, **104**, 797–804.

FUKURODA, T., FUJIKAWA, T., OZAKI, S., ISHIKAWA, K., YANO, M. & NISHIKIBE, M. (1994a). Clearance of circulating endothelin-1 by ET_B receptors in rats. *Biochem. Biophys. Res. Commun.*, **199**, 1461–1465.

FUKURODA, T., NOGUCHI, K., TSUCHIDA, S., NISHIKIBE, M., IKEMOTO, F., OKADA, K. & YANO, M. (1990). Inhibition of biological actions of big endothelin-1 by phosphoramidon. *Biochem. Biophys. Res. Commun.*, **172**, 390–395.

FUKURODA, T., OZAKI, S., IHARA, M., ISHIKAWA, K., YANO, M. & NISHIKIBE, M. (1994b). Synergistic inhibition by BQ-123 and BQ-788 of endothelin-1-related contractions of the rabbit pulmonary artery. *Br. J. Pharmacol.*, **113**, 336–338.

GARDINER, S.M., COMPTON, A.M., KEMP, P.A. & BENNETT, T. (1991). The effects of phosphoramidon on the regional haemodynamic responses to human proendothelin [1–38] in conscious rats. *Br. J. Pharmacol.*, **103**, 2009–2015.

GUI, G., XU, D., EMOTO, N. & YANAGISAWA, M. (1993). Intracellular localization of membrane-bound endothelin-converting enzyme from rat lung. *J. Cardiovasc. Pharmacol.*, **22** (Suppl. 8), S53–S56.

HAY, D.W.P., HENRY, P.J. & GOLDIE, R.G. (1993). Endothelin and the respiratory system. *Trends Pharmacol. Sci.*, **14**, 29–32.

HAYNES, W.G. & WEBB, D.J. (1993). The endothelin family of peptides: local hormones with diverse roles in health and disease? *Clin. Sci.*, **84**, 485–500.

HISAKI, K., MATSUMURA, Y., MAEKAWA, H., FUJITA, K., TAKAOKA, M. & MORIMOTO, S. (1994). Conversion of big ET-1 in the rat lung: role of phosphoramidon-sensitive endothelin-1-converting enzyme. *Am. J. Physiol.*, **266**, H422–H428.

HORGAN, M.J., PINHEIRO, J.M.B. & MALIK, A.B. (1991). Mechanism of endothelin-1-induced pulmonary vasoconstriction. *Circ. Res.*, **69**, 157–164.

HUDGIN, R.L., CHARLESON, S.E., ZIMMERMAN, M., MUMFORD, R. & WOOD, P.L. (1981). Enkephalinase: Selective peptide inhibitors. *Life Sci.*, **29**, 2593–2601.

IHARA, M., NOGUCHI, K., SAEKI, T., FUKURODA, T., TSUCHIDA, S., KIMURA, S., FUKAMI, T., ISHIKAWA, K., NISHIKIBE, M. & YANO, M. (1992). Biological profiles of highly potent novel endothelin antagonists selective for the ET_A receptor. *Life Sci.*, **50**, 247–255.

KREISMAN, N.R., HODIN, R.A., BRIZZEE, B.L., ROSENTHAL, M., SICK, T.J., BUSTO, R. & GINSBERG, M.D. (1987). Seizure-associated pulmonary edema and cerebral oxygenation in the rat. *J. Appl. Physiol.*, **62**, 658–667.

LANG, S.A., MARON, M.B. & SIGNS, S.A. (1989). Oxygen consumption after massive sympathetic nervous system discharge. *Am. J. Physiol.*, **256**, E345–E351.

LANGLEBEN, D., DEMARCHIE, M., LAPORTA, D., SPANIER, A.H., SCHLESINGER, R.D. & STEWART, D.J. (1993). Endothelin-1 in acute lung injury and the adult respiratory distress syndrome. *Am. Rev. Respir. Dis.*, **148**, 1545–1650.

MACCUMBER, M.W., ROSS, C.A., GLASER, B.M. & SNYDER, S.H. (1989). Endothelin: Visualization of mRNAs by in situ hybridization provides evidence for local action. *Proc. Natl. Acad. Sci. U.S.A.*, **86**, 7285–7289.

MALIK, A.B. (1985). Mechanisms of neurogenic pulmonary edema. *Circ. Res.*, **57**, 1–18.

MARON, M.B. (1985). A canine model of neurogenic pulmonary edema. *J. Appl. Physiol.*, **59**, 1019–1025.

MATSUMURA, Y., HISAKI, K., TAKAOKA, M. & MORIMOTO, S. (1990). Phosphoramidon, a metalloproteinase inhibitor, suppresses the hypertensive effect of big endothelin-1. *Eur. J. Pharmacol.*, **185**, 103–106.

MATSUSE, T., FUKUCHI, Y., SURUDA, T., NAGASE, T., OUCHI, Y. & ORIMO, H. (1990). Effect of endothelin-1 on pulmonary resistance in rats. *J. Appl. Physiol.*, **68**, 2391–2393.

MCMURDO, L., CORDER, R., THIEMERMANN, C. & VANE, J.R. (1993). Incomplete inhibition of the pressor effects of endothelin-1 and related peptides in the anaesthetized rat with BQ-123 provides evidence for more than one vasoconstrictor receptor. *Br. J. Pharmacol.*, **108**, 557–561.

MUMFORD, R.A., PIERZCHALA, P.A., STRAUSS, A.W. & ZIMMERMAN, M. (1981). Purification of a membrane-bound metalloendopeptidase from porcine kidney that degrades peptide hormones. *Proc. Natl. Acad. Sci. U.S.A.*, **78**, 6623–6627.

NAGASE, T., FUKUCHI, Y., JO, C., TERAMOTO, S., UEJIMA, Y., ISHIDA, K., SHIMIZU, T. & ORIMO, H. (1990). Endothelin-1 stimulates arachidonate 15-lipoxygenase activity and oxygen radical formation in the rat distal lung. *Biochem. Biophys. Res. Commun.*, **168**, 485–489.

NAKAMICHI, K., IHARA, M., KOBAYASHI, M., SAEKI, T., ISHIKAWA, K. & YANO, M. (1992). Different distribution of endothelin receptor subtypes in pulmonary tissues revealed by the novel selective ligands BQ-123 and $[Ala^{1,3,11,15}]$ET-1. *Biochem. Biophys. Res. Commun.*, **182**, 144–150.

POLLOCK, D.M. & OPGENORTH, T.J. (1991). Evidence for metalloprotease involvement in the in vivo effects of big endothelin 1. *Am. J. Physiol.*, **261**, R257–R263.

RAFFESTIN, B., ADNOT, S., EDDAHIBI, S., MACQUIN-MAVIER, I., BRAQUET, P. & CHABRIER, P.E. (1991). Pulmonary vascular response to endothelin in rats. *J. Appl. Physiol.*, **70**, 567–574.

SIMMET, TH., PRITZE, S., THELEN, K.I. & PESKAR, B.A. (1992). Release of endothelin in the oleic acid-induced respiratory distress syndrome in rats. *Eur. J. Pharmacol.*, **211**, 319–322.

TAKAHASHI, M., MATSUSHITA, Y., IIJIMA, Y. & TANZAWA, K. (1993). Purification and characterization of endothelin-converting enzyme from rat lung. *J. Biol. Chem.*, **268**, 21394–21398.

TAKAOKA, M., SHIRAGAMI, K., FUJINO, K., MIKI, K., MIYAKE, Y., YASUDA, M., WANG, G.F., HISAKI, K., MATSUMURA, Y. & MORIMOTO, S. (1991). Phosphoramidon-sensitive endothelin converting enzyme in rat lung. *Biochem. Int.*, **25**, 697–704.

TÉLÉMAQUE, S., GRATTON, J.P., CLAING, A. & D'ORLÉANS-JUSTE, P. (1993). Pharmacologic evidence for the specificity of the phosphoramidon-sensitive endothelin-converting enzyme for big endothelin-1. *J. Cardiovasc. Pharmacol.*, **22** (Suppl. 8), S85–S89.

TIPPLER, B., HERBST, C. & SIMMET, TH. (1994). Evidence for the formation of endothelin by lysed red blood cells from endogenous precursor. *Eur. J. Pharmacol.*, **271**, 131–139.

VIJAYARAGHAVAN, J., SCICLI, A.G., CARRETERO, O.A., SLAUGHTER, C., MOOMAW, C. & HERSH, L.B. (1990). The hydrolysis of endothelins by neutral endopeptidase 24.11 (enkephalinase). *J. Biol. Chem.*, **265**, 14150–14155.

WARNER, T.D., ALLCOCK, G.H., MICKLEY, E.J. & VANE, J.R. (1993). Characterization of endothelin receptors mediating the effects of the endothelin/sarafotoxin peptides on autonomic neurotransmission in the rat vas deferens and guinea pig ileum. *Br. J. Pharmacol.*, **110**, 783–789.

WIKLUND, N.P., WIKLUND, C.U., CEDERQVIST, B., ÖHLÉN, A., HEDQVIST, P. & GUSTAFSSON, L.E. (1991). Endothelin modulation of neuroeffector transmission in smooth muscle. *J. Cardiovasc. Pharmacol.*, **17** (Suppl. 7), S335–S339.

WU-WONG, J.R., BUDZIK, G.P., DEVINE, E.M. & OPGENORTH, T.J. (1990). Characterization of endothelin converting enzyme in rat lung. *Biochem. Biophys. Res. Commun.*, **171**, 1291–1296.

ZIMMERMAN, R.S., MARTINEZ, A.J., MAYMIND, M. & BARBEE, R.W. (1992). Effect of endothelin on plasma volume and albumin escape. *Circ. Res.*, **70**, 1027–1034.

(Received October 17, 1994
Revised February 23, 1995
Accepted March 16, 1995)

British Journal of Pharmacology (1995) 115, 761-766

D-Cycloserine transport in human intestinal epithelial (Caco-2) cells: mediation by a H^+-coupled amino acid transporter

David T. Thwaites, Gillian Armstrong, Barry H. Hirst & [1]Nicholas L. Simmons

Gastrointestinal Drug Delivery Research Centre, Department of Physiological Sciences, University of Newcastle upon Tyne, Medical School, Newcastle upon Tyne, NE2 4HH

1 The ability of D-cycloserine to act as a substrate for H^+/amino acid symport has been tested in epithelial layers of Caco-2 human intestinal cells.

2 In Na^+-free media with the apical bathing media held at pH 6.0, D-cycloserine (20 mM) is an effective inhibitor of net transepithelial transport (J_{net}) of L-alanine (100 μM) and its accumulation (across the apical membrane) in a similar manner to amino acid substrates (L-alanine, β-alanine, L-proline and glycine). In contrast L-valine was ineffective as an inhibitor for H^+/amino acid symport. Both inhibition of L-alanine J_{net} and its accumulation by D-cycloserine were dose-dependent, maximal inhibition being achieved by 5-10 mM.

3 Both D-cycloserine and known substrates for H^+/amino acid symport stimulated an inward short circuit current (I_{sc}) when voltage-clamped monolayers of Caco-2 epithelia, mounted in Ussing chambers, were exposed to apical substrate in Na^+-free media, with apical pH held at 6.0. The D-cycloserine dependent increase in I_{sc} was dose-dependent with an apparent $K_m = 15.8 \pm 2.0$ (mean $\pm$ s.e.mean) mM, and $V_{max} = 373 \pm 21$ nmol cm^{-2} h^{-1}.

4 D-Cycloserine (20 mM) induced a prompt acidification of Caco-2 cell cytosol when superfused at the apical surface in both Na^+ and Na^+-free conditions. Cytosolic acidification in response to D-cycloserine was dependent upon superfusate pH, being attenuated at pH 8 and enhanced in acidic media.

5 The increment in I_{sc} with 20 mM D-cycloserine was non-additive with other amino acid substrates for H^+/amino acid symport.

Keywords: Proton-coupled transport; amino acid; D-cycloserine; intracellular pH; intestine; epithelium; Caco-2 cells

Introduction

D-Cycloserine is an oral antibiotic used in combination therapy against *mycobacterium tuberculosis* resistant to isoniazid/rifampicin (Weltman & Rose, 1994). Since D-cycloserine may also enhance activation of the N-methyl-D-aspartate-coupled glycine receptor there is considerable interest in D-cycloserine as a potential therapeutic agent in age-associated memory impairment and Alzheimer's disease (Lanthorn, 1994; Quartermain *et al.*, 1994). Recently, Ranaldi *et al.* (1994) have shown that D-cycloserine is subject to net absorptive transport across monolayers of the human intestinal epithelial cell line Caco-2. Net transport in the apical to basal direction was saturable with a K_m of 4.2 mM, and subject to competitive inhibition by a variety of amino acids including L-alanine, D-alanine, β-alanine, and α-aminoisobutyric acid. Absorptive transport was also stimulated by acidic apical media and was largely independent of bathing medium Na^+.

Recently we have characterized a H^+/amino acid symport in Caco-2 cells (Thwaites *et al.*, 1993b,c; 1994b). Proton coupling was directly established by measuring pH-dependent acceleration of net transport and acidification of the cytosol during superfusion of the apical medium with amino acids in Na^+-free media. Additionally, since amino acids such as β-alanine are predominantly zwitterionic at the pH of the superfusion media used, we predicted that H^+/substrate co-transport should be associated with an inward short-circuit current in voltage-clamped monolayers of Caco-2 cells (Thwaites *et al.*, 1993b,c; 1994b). Indeed those amino acids subject to H^+ symport did generate an inward I_{sc} which was stoichiometrically related to substrate transport (Thwaites *et al.*, 1994b).

The possibility that the oral bioavailability of D-cycloserine resulted from interaction with an endogenous transport pathway for amino acids linked to the transmembrane proton gradient has been investigated in the present paper by measurement of inhibition of proton-simulated L-alanine transport (Thwaites *et al.*, 1994b), by intracellular acidification after superfusion of the apical surface with D-cycloserine-containing media and by the rheogenic nature of this transport in Na^+-free media with the apical media held at acidic pH to optimize H^+/symport activity (Thwaites *et al.*, 1994b). We conclude that D-cycloserine is indeed a substrate for the H^+-coupled amino acid transporter expressed in the apical membrane of Caco-2 human intestinal cells.

Methods

Cell culture

Caco-2 cells (passage number 95-114) were cultured in DMEM (with 4.5 g l^{-1} glucose), with 1% non-essential amino acids, 2 mM L-glutamine, 10% (v/v) foetal calf serum and gentamicin (60 μg ml^{-1}). Cell monolayers were prepared by seeding at high density ($4.4-5.0 \times 10^5$ cells cm^{-2}) onto tissue culture inserts [Transwell polycarbonate filters (Costar)]. Cell monolayers were maintained at 37°C in a humidified atmosphere of 5% CO_2 in air. Cell confluence was estimated by microscopy and determination of transepithelial electrical resistance (R_T), measured at 37°C.

Transport experiments

Transport experiments were performed at least 16 days after seeding and 18-24 h after feeding. Transepithelial flux measurements were performed as described previously (Thwaites *et al.*, 1993a; 1994a). Briefly, the cell monolayers (24.5 mm in diameter) were washed by sequential transfer through 4

[1] Author for correspondence.

beakers containing 500 ml of modified Na^+-free Krebs buffer (all mM): choline Cl 137, KCl 5.4, $CaCl_2$ 2.8, $MgSO_4$ 1.0, KH_2PO_4 0.3, glucose 10, HEPES/Tris 10 (pH 7.4, 37°C) and placed in 6-well plates, each well containing 2 ml of modified Krebs buffer. Na^+-free Krebs buffer (pH 7.4) (2 ml) was placed in the upper filter cup (apical solution) and the filters were incubated for 10 min at 37°C. The apical/basal solutions were then changed for experimental solutions containing radioisotope. The apical solution was held at pH 6.0 (prepared by replacement of 10 mM HEPES with 10 mM MES and adjustment to the required pH using Tris base). Radiolabelled [^{3}H]-or [^{14}C]-L-alanine (0.5 μCi ml^{-1}; total concentration 100 μM) containing solutions were added to the apical and basal chamber, respectively. In experiments involving high (20 mM) concentrations of substrates, iso-molarity was maintained by addition of mannitol to control samples. Fluxes in the absorptive (apical-to-basal, J_{a-b}) and secretory (basal-to-apical, J_{ba}) directions were determined for 1 h and are expressed as pmol cm^{-2} h^{-1}. Net flux $J_{aet} = J_{a-b} - J_{ba}$. At the end of the incubation period cell monolayers were washed by sequential transfer through 4 beakers containing 500 ml volumes of Na^+-free Krebs buffer (pH 7.4) at 4°C to remove any loosely-associated radiolabel, and removed from the insert. Cell monolayer-associated radiolabel was determined by scintillation counting. Cellular accumulation of L-alanine is expressed as μM or as a cell to medium ratio (C/M). Cell height was determined by confocal microscopy and this value was used in the determination of intracellular volume.

Electrophysiological determinations

Measurements of short-circuit current (I_{sc}) were made essentially as described previously (Thwaites *et al.*, 1993b,d). Cultured epithelial layers [on 12 mm diameter Snapwell (Costar) polycarbonate filters] were mounted in Ussing type chambers (Precision Instrument Design) maintained at 37°C, connected to an automatic voltage current clamp (WPI DVC 1000) via KCl/agar salt-bridges and reversible electrodes (Ag/AgCl for current passage, calomel for voltage sensing). Measurements of open-circuit electrical p.d., transepithelial resistance and short-circuit current (I_{sc}) were made in modified and Na^+-free Krebs solutions (see above). The chemical flux equivalent of the I_{sc} ($I_{sc} = JzF$, where J is the chemical flux, z the valence and F the Faraday constant) is 1 μA cm^{-2} = 36 nmol cm^{-2} h^{-1} for a monovalent ion.

Intracellular pH measurements

For intracellular pH (pH_i) measurements (Thwaites *et al.*, 1993a,b), Caco-2 cells grown to confluence (15 days after seeding) on 12 mm diameter Transwell polycarbonate filters (Costar) were loaded by incubation with BCECF-AM (5 μM), in both apical and basal chambers, for 40 min at 37°C. After loading, the inserts were placed in a 24 mm diameter perfusion chamber mounted on the stage of an inverted fluorescence microscope (Nikon Diaphot). Perfusion of the apical and basolateral chambers was accomplished by a compressed air-driven system (flow rate 5 ml min^{-1}, at 37°C). Media were either Na^+-containing Krebs (choline Cl replaced by NaCl see above) or Na^+-free where stated. Medium was pH 8.0 or 7.4 (TRIS/HEPES), or pH 7.0 to pH 5.0 (MES 10 mM adjusted with Tris). Intracellular H^+ concentration was quantified by fluorescence (excitation at 440/490 nm and emission at 520 nm) from a small group of cells (5–10) using a photon counting system (Newcastle Photometric Systems). Intracellular BCECF fluorescence was converted to pH_i by comparison with values from an intracellular calibration curve using nigericin (10 μM) and high K^+ solutions (Thwaites *et al.*, 1994a). The initial rate of change (0–30 s) of pH_i (ΔpH_i min^{-1}) following exposure to D-cycloserine was calculated by linear regression using Photon Counter System 4.7 (Newcastle Photometric Systems).

Materials

Cell culture media, supplements and plastic were supplied by Life Technologies. All other chemicals were from Sigma or Merck.

Statistics

Results are expressed as mean ± s.e.mean (n). Statistical analyses was performed by one-way analysis of variance (ANOVA) using Dunnett's multiple comparison test to compare mean values. Constants for Michaelis-Menten kinetics were calculated by non-linear regression with the method of least-squares (FIG-P, Biosoft).

Results

L-Alanine transport in Na^+-free media can be energized via a proton gradient across the apical membrane of intact Caco-2 intestinal epithelial layers (Thwaites *et al.*, 1994b). With the apical medium held at pH 6.0, apical to basal (J_{a-b}) L-alanine transport (8.2 ± 0.6 (mean ± s.e.mean) nmol cm^{-2} h^{-1}, n = 6)

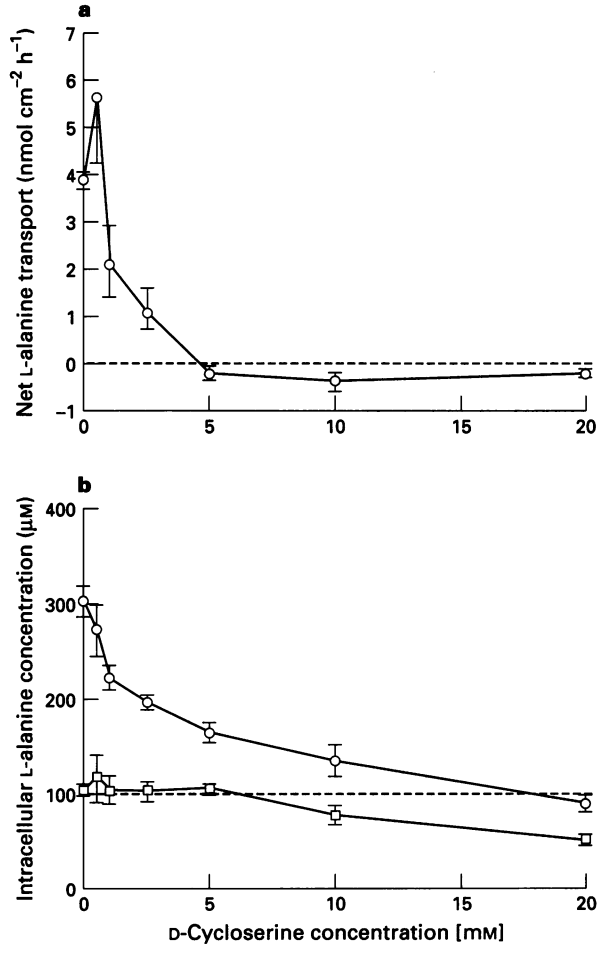

Figure 1 Concentration-dependence of inhibition of net L-alanine transport (J_{net}) and cellular accumulation of L-alanine by D-cycloserine in Caco-2 intestinal epithelial layers. L-Alanine transport and accumulation was determined using [^{14}C]-L-alanine and [^{3}H]-L-alanine as described in Methods. Caco-2 epithelia were incubated in Na^+-free media in which the apical solution was held at pH 6.0 and the basal bathing medium pH 7.4. D-Cycloserine was present in both bathing media at the concentrations indicated. L-Alanine was present in both bathing media at 100 μM. (a) Inhibition of J_{net}; (b) inhibition of L-alanine accumulation across apical (○) or basal (□) cell borders. Data are expressed as the mean ± s.e.mean of 3/4 separate layers.

exceeds basal to apical (J_{b-a}) L-alanine transport (4.1 ± 0.6 nmol cm^{-2} h^{-1}, $n=6$) and a significant net absorption ($J_{net} = J_{a-b} - J_{b-a} = 3.9 \pm 0.2$ nmol cm^{-2} h^{-1}, $n=6$, paired determinations) is observed (Figure 1a, see also Table 1). In addition L-alanine accumulates across the apical membrane above medium values, a cell/medium ratio of 3.0 ± 0.1 ($n=6$) being observed (Figure 1b). No such L-alanine accumulation is detected at the basal membrane (C/M ratio $= 1.1 \pm 0.1$, $n=6$, Figure 1b). Table 1 shows that a number of amino acids (all present at 20 mM in both apical and basal bathing media) will inhibit the proton-driven net L-alanine transport (J_{net}) and cellular accumulation at the apical membrane; L-alanine, β-alanine, L-proline and glycine are all effective. In contrast L-valine is ineffective (Table 1). This is in agreement with the partial specificity of this transporter as described previously (Thwaites *et al.*, 1993b,c; 1994b). D-Cycloserine (20 mM) is an effective inhibitor both of L-alanine net transport (J_{net}) and cellular accumulation (Table 1, Figure 1), consistent with its transport by the H^+/coupled amino acid transporter. In addition to inhibition of apical L-alanine accumulation, 20 mM D-cycloserine also inhibits equilibration of L-alanine at the basal membrane (from a C/M ratio of 1.04 ± 0.01 ($n=6$) to 0.51 ± 0.03 ($n=6$), $P<0.05$). At 20 mM, D-serine is a more effective inhibitor of L-alanine net transport and apical accumulation than is L-serine (Table 1). Inhibition of basal accumulation of L-alanine by 20 mM D-serine and L-serine was not significantly reduced (C/M ratio 0.74 ± 0.06 ($n=4$) and 0.75 ± 0.08 ($n=8$), respectively).

The inhibition of L-alanine J_{net} and accumulation across the apical membrane by D-cycloserine is dose-dependent (Figure 1). Half maximal inhibition of net alanine transport was observed at 1.2 ± 0.45 mM D-cycloserine, whilst half-maximal inhibition of apical accumulation of L-alanine was observed at 2.5 ± 1.0 mM D-cycloserine. This value compares to half-maximal saturation of D-cycloserine transport in Caco-2 epithelia of 4.2 mM observed by Ranaldi *et al.* (1994).

Substrate-induced H^+-flow may be monitored by substrate-induced cytosolic acidification (Thwaites *et al.*, 1993b,c; 1994b). Figures 2–4 demonstrate that apical superfusion of D-cycloserine causes marked intracellular acidification which is reversed upon removal of the substrate. The effect of D-cycloserine (5 mM) at the basolateral surface is not as marked as at the apical surface (Figure 2). The initial rate (30 s) of intracellular acidification with D-cycloserine (20 mM) at pH 6.0 was 0.48 ± 0.08 pH units min^{-1} ($n=4$). The response to D-cycloserine (20 mM) is unaffected by Na^+ removal (Figure 3). In Na^+-free media the initial rate of cytosolic acidification with apical D-cycloserine at pH 6.0 was 0.59 ± 0.10 pH units min^{-1} ($n=8$). Figure 4 shows that intracellular acidification upon D-cycloserine superfusion is dependent upon medium pH, the extent of intracellular acidification being more marked as apical media are made progressively more acidic. A similar pattern of response is observed for L-proline (Figure 4b). These observations of D-cycloserine-induced acidification are consistent with H^+/D-cycloserine cotransport. Recovery of intracellular pH after an acid load (Figure 3) is dependent upon Na^+ in the apical medium.

Substrate-induced H^+-flow may also be monitored by substrate induced I_{sc} in Na^+-free media (Thwaites *et al.*, 1993d; 1994b), where the apical pH is held at pH 6.0. Table 1 shows that those amino acids capable of H^+/symport induce an inward I_{sc} under these conditions (L-alanine, β-alanine, L-proline and glycine are all effective in stimulating an inward I_{sc}). In contrast L-valine is ineffective. There is thus concordance between the ability to inhibit L-alanine J_{net}, apical accumulation and stimulate inward I_{sc}. This correlation extends to D-cycloserine and D-serine. L-Serine is a relatively poor substrate (see above). Figure 5 shows that the ability of D-cycloserine to stimulate inward I_{sc} is dose-dependent; half-maximal saturation of the increase in I_{sc} is observed at 15.8 ± 2.0 mM. The maximal transport rate from the increment in I_{sc} is 373.7 ± 20.8 nmol cm^{-2} h^{-1}; this compares to 21 nmol mg^{-1} protein reported by Ranaldi *et al.* (1994) and to a maximal rate of β-alanine transport (from measurements of I_{sc}) of

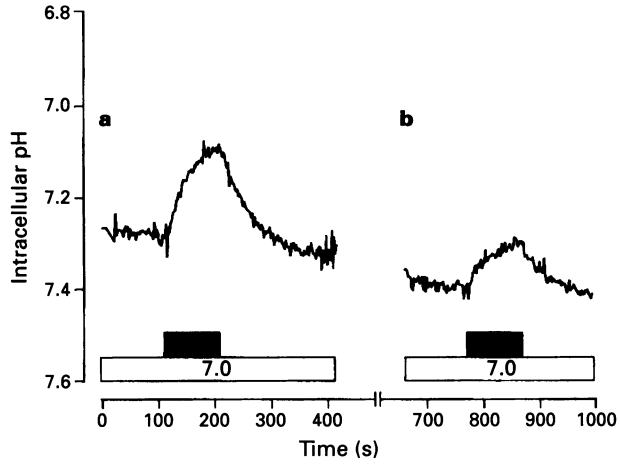

Figure 2 Intracellular pH measured in BCECF-loaded Caco-2 cell monolayers. The effect on intracellular pH of exposure to D-cycloserine (5 mM) (solid bars) at the apical surface (a) (superfused with Na^+-containing Krebs at pH 7.0) and the basolateral surface (b) (superfused with Na^+-containing Krebs at pH 7.0).

Table 1 Inhibition of L-alanine net transport, cellular accumulation (across the apical membrane) and stimulation of rheogenic I_{sc} by amino acids and by D-cycloserine (all 20 mM)

	J_{net} (nmol cm^{-2} h^{-1})	*Apical accumulation* (μM)	I_{sc} (μA cm^{-2})
Control	4.1 ± 0.5 (10)	335 ± 9 (10)	–
L-Alanine	0.8 ± 0.2 (4)*	208 ± 4 (4)*	4.0 ± 0.5 (3)
D-Serine	0.4 ± 0.4 (4)*	150 ± 8 (4)*	4.3 ± 0.5 (10)
L-Serine	2.1 ± 0.2 (8)*	324 ± 7 (8)^{NS}	0.9 ± 0.2 (10)
D-Cycloserine	-0.2 ± 0.1 (4)*	90 ± 8 (4)*	10.6 ± 1.5 (6)
β-Alanine	1.0 ± 0.2 (4)*	237 ± 15 (4)*	10.1 ± 1.1 (7)
L-Proline	0.8 ± 0.2 (4)*	191 ± 6 (4)*	5.2 ± 1.5 (4)
AIB	1.5 ± 0.3 (3)*	249 ± 15 (3)*	1.9 ± 0.1 (5)
Glycine	0.9 ± 0.2 (3)*	258 ± 4 (3)*	4.8 ± 1.0 (6)
L-Valine	3.1 ± 0.2 (4)^{NS}	406 ± 12 (4)*	0.1 ± 0.1 (5)^{NS}

Caco-2 epithelia were bathed in Na^+-free choline media with the apical medium pH held at pH 6.0 and basal bathing medium held at pH 7.4. For determination of net flux (J_{net}), and cellular accumulation from the apical medium, L-alanine was at 100 μM. Numbers of separate determinations on individual epithelial layers are shown in parentheses. Data are the mean ± s.e.mean. AIB = α-aminoisobutyric acid.

NS: not significantly different from control data or zero (I_{sc}). *$P<0.01$ versus control data.

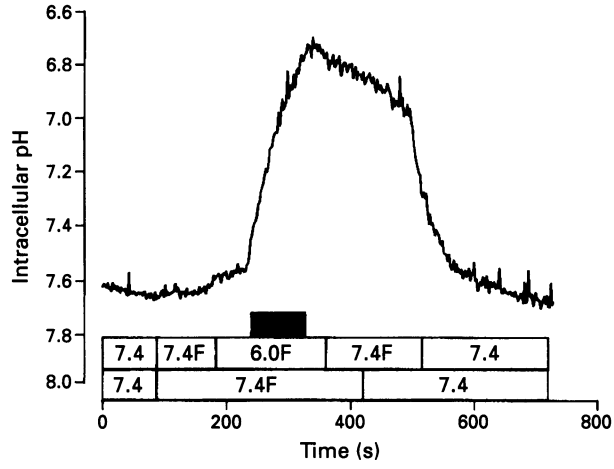

Figure 3 D-Cycloserine (20 mM) causes intracellular acidification in the absence of extraceullar Na^+. The Caco-2 cell monolayer was initially superfused with Na^+-containing solutions (pH 7.4) across both apical (upper open bar) and basolateral (lower open bar) surfaces. Both epithelial surfaces were then superfused with a Na^+-free Krebs (pH 7.4). The pH of the apical superfusate was then reduced to pH 6.0 (Na^+-free) and D-cycloserine (solid bar) added. After removal of D-cycloserine, recovery of intracellular pH was relatively slow on reintroduction of Na^+ to the basal superfusate (lower open bar) but was more rapid after reintroduction of Na^+ at the apical surface (upper open bar).

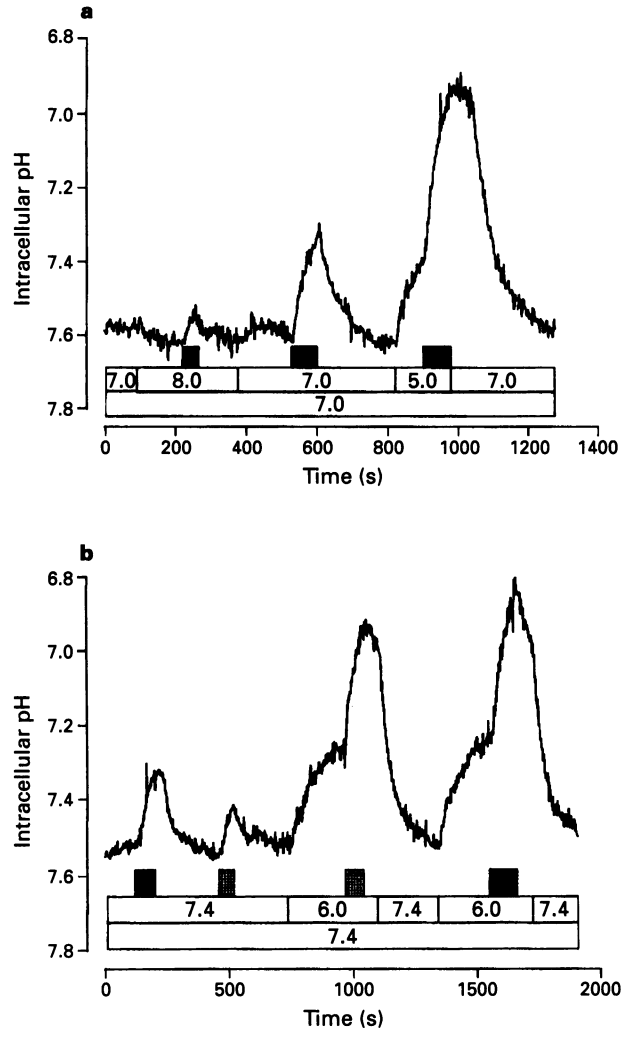

Figure 4 Dependence of D-cycloserine-stimulated cytosolic acidification upon medium pH. (a) D-Cycloserine (20 mM) (solid bars) was superfused at the apical surface (upper open bar) in Na^+-Krebs at pH 8.0, 7.0 and 5.0. (b) Comparison of D-cycloserine (20 mM)-dependent acidification (solid bars) with that caused by L-proline (20 mM) (stippled bars) in Na^+-Krebs at pH 7.4 and 6.0 (upper open bar). Basolateral perfusate composition is indicated in the lower open bar.

215 nmol cm^{-2} h^{-1} (Thwaites *et al.*, 1993b) and for L-alanine of 270 nmol cm^{-2} h^{-1} (Thwaites *et al.*, 1994b). If D-cycloserine transport is via the H^+/amino acid symport alone then sequential addition of substrate amino acids and D-cycloserine should give rise to non-additive actions on inwards I_{sc}. Figure 6 compares the response of I_{sc} to 20 mM β-alanine superfusion at the apical membrane followed by 20 mM D-cycloserine together with further additions of β-alanine and glycine. It is apparent that the response to β-alanine (and glycine) in the presence of D-cycloserine is markedly reduced or abolished. Thus D-cycloserine must share the H^+/amino acid transporter at the apical membrane of Caco-2 epithelia.

Discussion

The gastrointestinal epithelium presents the major rate-limiting factor in the absorption of many hydrophilic compounds of pharmaceutical interest. Surprisingly high levels of oral bioavailability are observed with peptide-like drugs (Humphrey, 1986; Humphrey & Ringrose, 1986). Some β-lactam antibiotics (cefadroxil and cephalexin) and angiotensin converting enzyme (ACE) inhibitors (enalapril maleate and captropril) are now known to be effective substrates for the H^+/di-tripeptide transporter present in the apical membrane of intestinal enterocytes (Fei *et al.*, 1994; Boll *et al.*, 1994; Thwaites *et al.*, 1994a). Conversely, cefazolin and lisinopril, which are poor substrates, have poor oral bioavailability (Boll *et al.*, 1994; Thwaites *et al.*, 1994a; 1995a). The H^+/di-tripeptide transporter (PepT1) has recently been cloned and sequenced (Fei *et al.*, 1994; Boll *et al.*, 1994). The specificity of PepT1 expressed in *Xenopus laevis* oocytes is essentially identical to that observed for human intestinal Caco-2 epithelial cells (Thwaites *et al.*, 1994a). Thus there is precedent for endogenous transporters (whose physiological function is substrate absorption from the gastrointestinal tract) acting as specific portals for drug entry from oral dosage forms.

This work has tested the hypothesis that D-cycloserine is a substrate for the previously described H^+/amino acid symport present in the apical membranes of Caco-2 epithelial cells. Measurements of acid-stimulated amino acid flux in Na^+-free choline media, amino acid inhibition of substrate flux, amino

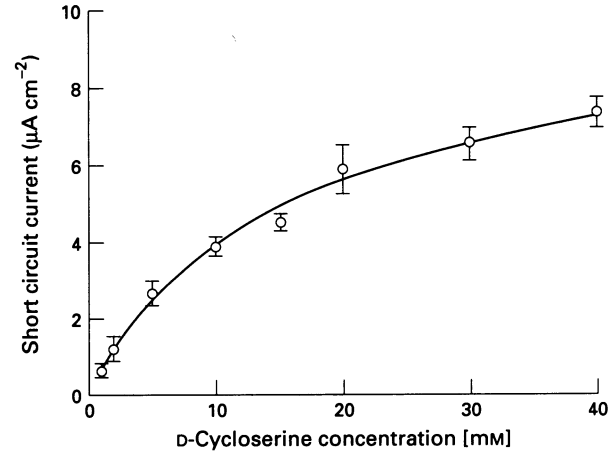

Figure 5 Concentration-dependence of D-cycloserine stimulation of inward short-circuit current (I_{sc}) in voltage-clamped Caco-2 epithelial layers mounted in Ussing chambers. Incubations were in Na^+-free media in which the apical pH was held at pH 6.0 and the basal bathing medium pH 7.4. Data are the mean ± s.e. of 3–5 separate layers. Solid line is the Michaelis-Menten fit of the data, $K_m = 15.8 \pm 2.0$ (s.e.mean) mM, $V_{max} = 373 \pm 21$ nmol cm^{-2} h^{-1}.

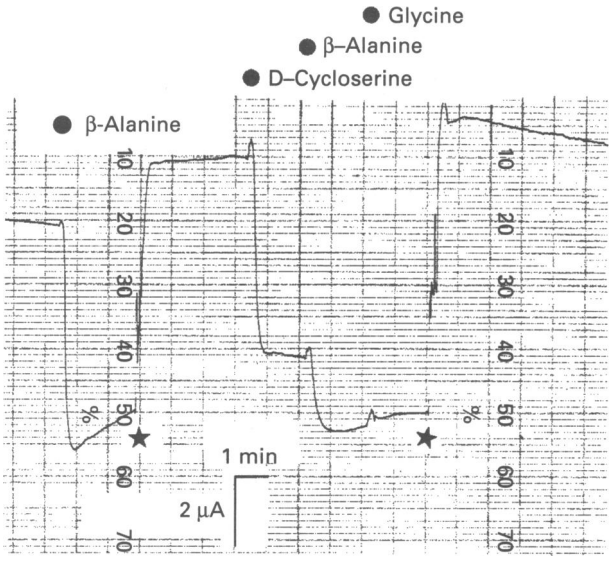

Figure 6 Comparison of response of inward I_{sc} to amino acids (20 mM) and to D-cycloserine (20 mM). Note that β-alanine and glycine do not give additive responses after D-cycloserine. Stars denote washout of added substrates. Representative trace.

acid-dependent intracellular acidification and measurement of amino acid increments in inward I_{sc} have indicated that glycine, proline, hydroxyproline, sarcosine, betaine, taurine, β-alanine, α-aminoisobutyric acid (AIB), α-methylaminoisobutyric acid (MeAIB), γ-amino-n-butyric acid (GABA) and L-alanine are all substrates for pH-dependent transport in the brush-border of Caco-2 cells (Thwaites *et al.*, 1993b,c; 1994b; 1995b; unpublished observations). Both D-serine and D-alanine were also substrates (unpublished observations). In contrast leucine, isoleucine, valine, phenylalanine, methionine, threonine, cysteine, asparagine, glutamine, histidine, arginine, lysine, glutamate and D-aspartate were not effective substrates (Thwaites *et al.*, 1993b,c; 1994b; 1995; unpublished observations). Many of the amino acid substrates (including proline, β-alanine, taurine, sarcosine and GABA) accessing the H^+-coupled carrier in this human intestinal epithelium are also transported via the Na^+-dependent (Cl^--independent) Imino carrier characterized in rat small intestine (Munck *et al.*, 1994). Also the rat Imino carrier and the Caco-2 H^+-coupled transporter both show preference for the D- rather than L-form of serine. The main difference in transport via these two transporters is that L-alanine is transported in Caco-2 cells (Thwaites *et al.*, 1994b) but is not transported by the rat Imino carrier (Munck *et al.*, 1994).

The present data have used inhibition of acid-stimulated L-alanine transport and accumulation in Na^+-free media, together with acidification of intracellular pH and stimulation of inward I_{sc} as measures of H^+/amino acid symport. The stoichiometry of the cotransport was 1:1 for H^+/L-alanine cotransport (Thwaites *et al.*, 1994b). The rheogenic nature of the H^+-coupled dipeptide transport has been established in intestine (Ganapathy & Leibach, 1985), in oocytes where the cloned transporter (PepT1) has been expressed (Fei *et al.*, 1994), and in Caco-2 epithelia (Thwaites *et al.*, 1993d). For H^+/amino acid cotransport an analogous situation exists and amino acid substrates stimulate an inward I_{sc} whose magnitude is entirely consistent with a 1:1 stoichiometry for H^+/amino acid cotransport. This suggests that measurements of substrate-stimulated I_{sc} can be used to characterize a candidate substrate. The present data show that D-cycloserine is capable of strong inhibition of both L-alanine transport and accumulation in Na^+-free media and of stimulation of an inward I_{sc} similar to that observed with other amino acid substrates and derivatives. That D-cycloserine is a zwitterion at the pH values used in this study (Ranaldi *et al.*, 1994) indicates that the most likely explanation of the rheogenicity of D-cycloserine transport is proton/D-cycloserine symport. This is confirmed by the marked intracellular acidification observed with D-cycloserine upon superfusion of the apical surface. The Na^+-independence of the intracellular acidification with D-cycloserine substantiates the finding of Ranaldi *et al.* (1994) that D-cycloserine net transport is only slightly reduced in Na^+-free media. That β-alanine and glycine give non-additive responses to inward I_{sc} when added in conjunction is compelling evidence that these amino acids share a common H^+/amino acid transporter.

Competition studies of D-cycloserine absorption in Caco-2 epithelia (Ranaldi *et al.*, 1994) are in broad agreement with the present data; those amino acids capable of competitive inhibition include L-alanine, β-alanine, D-alanine, L-proline, hydroxy-L-proline and α-aminoisobutyric acid. Those amino acids not capable of inhibition of D-cycloserine absorption included leucine, isoleucine, valine, phenylalanine, methionine, asparagine, glutamine, histidine, arginine, lysine, glutamate and D-aspartate. Those amino acids where there is inhibition of D-cycloserine absorption but which are not substrates for H^+/amino acid symport are threonine and cysteine (Ranaldi *et al.*, 1994). Thus in broad terms there is good agreement that D-cycloserine absorption is mediated via the H^+/amino acid transporter expressed in the apical membrane of intestinal Caco-2 cells.

In order to achieve transepithelial absorption, D-cycloserine must exit across the basolateral membrane into the basal medium. In intestinal enterocytes exit of amino acids across the basolateral membrane may occur by simple diffusion. In addition the Na^+-dependent systems A and ASC and the Na^+-independent systems L and asc contribute to amino acid transport across the basolateral membrane (Barker & Ellory, 1990; Lash & Jones, 1984; Stevens *et al.*, 1984). In Caco-2 epithelia equilibration of glycine across the basolateral membrane in Na^+-free conditions is inhibited by glycine L-alanine, proline, AIB, leucine, valine, serine, phenylalanine, methionine, threonine, isoleucine, cysteine, glutamine, asparagine and histidine (D.T. Thwaites, unpublished). These are all substrates for the Na^+-independent systems L and/or asc (Shotwell *et al.*, 1981; Lash & Jones, 1984; Barker & Ellory, 1990) so that this suggests that systems L and asc co-exist at the basolateral membrane of Caco-2 cells. The inhibition of accumulation of L-alanine by D-cycloserine in Na^+-free media suggests that D-cycloserine exit is mediated in part by systems L and/or asc. In contrast to amino acids D-cycloserine causes a small intracellular acidification at the basal-lateral surface. This is similar to that seen with cephalexin at the basolateral surface (Thwaites *et al.*, 1993a) suggesting alternate pathways for D-cycloserine transport at the basolateral membrane. It is possible that inhibitory effects of amino acids on D-cycloserine absorption may be due to inhibition at the basolateral membrane, thus explaining the differences observed between the specificity of H^+/amino acid transport and inhibition of D-cycloserine transport.

Under physiological conditions the existence of an acidic microclimate adjacent to the absorptive epithelium will be important for H^+-coupled solute absorption (Lucas *et al.*, 1975; McEwan *et al.*, 1988). Whether pathophysiological change in microclimate acidity alters nutrient absorptive capacity remains to be determined. D-Cycloserine absorption is thus an additional example of oral bioavailability being dependent upon intrinsic transport mechanisms enabling transepithelial transport. Attention should be paid at an early stage to the structure-activity requirements for absorptive transport versus the structure-activity of the pharmaceutical site of action to determine common or contradictory requirements.

Charlotte Ward provided excellent technical assistance. This work was supported by the Wellcome Trust (to DTT). G.A. is a BBSRC CASE student with Pfizer Central Research (UK).

References

BARKER, G.A. & ELLORY, J.C. (1990). The identification of neutral amino acid transport systems. *Exp. Physiol.*, **75**, 3–26.

BOLL, M., MARKOVICH, D., WEBER, W.-M., KORTE, H., DANIEL, H. & MURER, H. (1994). Expression cloning of a cDNA from rabbit small intestine related to proton-coupled transport of peptides, β-lactam antibiotics and ACE inhibitors. *Pflügers Arch.*, **429**, 146–149.

FEI, Y.J., KANAI, Y., NUSSBERGER, S., GANAPATHY, V., LEIBACH, F.H., ROMERO, M.F., SINGH, S.K., BORON, W.F. & HEDIGER, M.A. (1994). Expression cloning of a mammalian proton-coupled oligopeptide transporter. *Nature*, **368**, 563–566.

GANAPATHY, V. & LEIBACH, F.H. (1985). Is intestinal peptide transport energized by a proton gradient? *Am. J. Physiol.*, **249**, G153–G160.

HUMPHREY, M.J. (1986). The oral bioavailability of peptides and related drugs. In *Delivery Systems for Peptide Drugs*, ed. Davis, S.S., Ilum, L. & Tomlinson, E. NATO ASI Series 125, pp. 139–151. New York: Plenum.

HUMPHREY, M.J. & RINGROSE, P.S. (1986). Peptides and related drugs: a review of their absorption, metabolism, and excretion. *Drug Metab. Rev.*, **17**, 283–310.

LANTHORN, T.H. (1994). D-Cycloserine, agonist turned antagonist. *Amino Acids*, **6**, 247–260.

LASH, L.H. & JONES, D.P. (1984). Characterisation of cysteine uptake in intestinal basolateral membrane vesicles. *Am. J. Physiol.*, **247**, G394–G401.

LUCAS, M.L., SCHNEIDER, W., HABERICH, F.J. & BLAIR, J.A. (1975). Direct measurement by pH-microelectrode of the pH-microclimate in rat proximal jejunum. *Proc. R. Soc. B*, **192**, 39–48.

MCEWAN, G.T.A., DANIEL, H., FETT, C., BURGESS, M.N. & LUCAS, M.L. (1988). The effect of *Escherichia coli* STa enterotoxin and other secretagogues on mucosal surface pH of rat small intestine *in vivo*. *Proc. R. Soc. B*, **234**, 219–237.

MUNCK, B.G., MUNCK, L.K., RASMUSSEN, S.N. & POLACHE, A. (1994). Specificity of the imino acid carrier in rat small intestine. *Am. J. Physiol.*, **266**, R1154–R1161.

QUARTERMAIN, D., MOWER, J., RAFFERTY, M.F., HERTING, R.L. & LANTHORN, T.H. (1994). Acute but not chronic activation of the NMDA-coupled glycine receptor with D-cycloserine facilitates learning and retention. *Eur. J. Pharmacol.*, **257**, 7–12.

RANALDI, G., ISLAM, K. & SAMBUY, Y. (1994). D-Cycloserine uses an active transport mechanism in the human intestinal cell-line Caco-2. *Antimicrobial Agents Chemother.*, **38**, 1239–1245.

SHOTWELL, M.A., JAYME, D.W., KILBERG, M.S. & OXENDER, D.L. (1981). Neutral amino acid transport systems in Chinese hamster ovary cells. *J. Biol. Chem.*, **256**, 5422–5427.

STEVENS, B.R., KAUNITZ, J.D. & WRIGHT, E.M. (1984). Intestinal transport of amino acids and sugars. Advances using membrane vesicles. *Annu. Rev. Physiol.*, **46**, 417–433.

THWAITES, D.T., BROWN, C.D.A., HIRST, B.H. & SIMMONS, N.L. (1993a). H^+-coupled dipeptide (glycylsarcosine) transport across apical and basal borders of human intestinal Caco-2 cell monolayers display distinctive characteristics. *Biochim. Biophys. Acta*, **1151**, 237–245.

THWAITES, D.T., CAVET, M., HIRST, B.H. & SIMMONS, N.L. (1995a). Angiotensin-converting enzyme (ACE) inhibitor transport in human intestinal epithelial (CaCo-2) cells. *Br. J. Pharmacol.*, **114**, 981–986.

THWAITES, D.T., HIRST, B.H. & SIMMONS, N.L. (1994a). Substrate specificity of the di/tripeptide transporter in human intestinal epithelia (Caco-2): identification of substrates that undergo H^+-coupled absorption. *Br. J. Pharmacol.*, **113**, 1050–1056.

THWAITES, D.T., MCEWAN, G.T.A., BROWN, C.D.A., HIRST, B.H. & SIMMONS, N.L. (1993b). Na^+-independent, H^+-coupled transepithelial β-alanine absorption by human intestinal Caco-2 cell monolayers. *J. Biol. Chem.*, **268**, 7640–7642.

THWAITES, D.T., MCEWAN, G.T.A., BROWN, C.D.A., HIRST, B.H. & SIMMONS, N.L. (1994b). L-Alanine absorption in human intestinal Caco-2 cells driven by the proton electrochemical gradient. *J. Membr. Biol.*, **140**, 143–151.

THWAITES, D.T., MCEWAN, G.T.A., COOK, M.J., HIRST, B.H. & SIMMONS, N.L. (1993c). H^+-coupled (Na-independent) proline transport in human intestinal (Caco-2) epithelial cell monolayers. *FEBS Lett.*, **333**, 78–82.

THWAITES, D.T., MCEWAN, G.T.A., HIRST, B.H. & SIMMONS, N.L. (1993d). Transepithelial dipeptide (glycylsarcosine) transport across epithelial monolayers of human Caco-2 cells is rheogenic. *Pflügers Arch.*, **425**, 179–180.

THWAITES, D.T., MCEWAN, G.T.A., HIRST, B.H. & SIMMONS, N.L. (1995b). H^+-coupled α-methylaminoisobutyric acid transport in human intestinal Caco-2 cells. *Biochim. Biphys. Acta*, **1234**, 111–118.

WELTMAN, A.C. & ROSE, D.N. (1994). Tuberculosis susceptibility patterns, predictors of multi-drug resistance and implications for initial therapeutic regimens at a New York City Hospital. *Arch. Int. Med.*, **154**, 2161–2167.

(Received February 8, 1995
Revised March 13, 1995
Accepted March 16, 1995)

British Journal of Pharmacology (1995) 115, 767-774

Evidence that [^{3}H]-α,β-methylene ATP may label an endothelial-derived cell line 5'-nucleotidase with high affinity

[1]A.D. Michel, N.-M. Chau, T.-P.D. Fan, E.E. Frost & P.P.A. Humphrey

Glaxo Institute of Applied Pharmacology and Department of Pharmacology, University of Cambridge, Tennis Court Road, Cambridge CB2 1QJ

1 In membranes prepared from a permanent cell line of endothelial origin (WEC cells), [^{3}H]-α,β-methylene ATP ([^{3}H]-α,β-meATP) labelled high ($pK_d = 9.5$; $B_{max} = 3.75$ pmol mg^{-1} protein) and low ($pK_d = 7.2$; $B_{max} = 23.3$ pmol mg^{-1} protein) affinity binding sites. The high affinity [^{3}H]-α,β-meATP binding sites in the WEC cell membranes could be selectively labelled with a low concentration of the radioligand (1 nM). In competition studies performed at a radioligand concentration of 1 nM, 88.6% of the sites possessed high affinity ($pIC_{50} = 8.26$) for α,β-meATP.

2 The high affinity [^{3}H]-α,β-meATP binding sites appeared heterogeneous since in competition studies a number of nucleotide analogues (α,β-meADP, ATP, ADP, AMP, GTP, GppNHp, GMP) and adenosine identified two populations of the sites labelled by 1 nM [^{3}H]-α,β-meATP. The proportion of sites with high affinity for these compounds was found to vary between 42 and 69%.

3 Approximately 60–69% of the binding sites labelled with 1 nM [^{3}H]-α,β-meATP possessed high affinity for α,β-meADP ($pIC_{50} = 8.87$), AMP ($pIC_{50} = 7.12$), GMP ($pIC_{50} = 7.34$), UTP ($pIC_{50} = 6.12$), GTP ($pIC_{50} = 7.59$), GppNHp ($pIC_{50} = 7.35$) and adenosine ($pIC_{50} = 5.45$). The sites at which these compounds possessed high affinity were probably the same, since, in the presence of GMP at a concentration (10 μM) sufficient to inhibit selectively the binding of [^{3}H]-α,β-meATP, the [^{3}H]-α,β-meATP binding sites with high affinity for AMP, UTP, α,β-meADP, GTP, GppNHp and adenosine were also occluded.

4 WEC cell membranes were able to metabolize a trace concentration (6 nM) of [^{3}H]-AMP to [^{3}H]-adenosine under the conditions of the binding assay. The pIC_{50} values of adenosine (5.99), GMP (7.55) and the substrate AMP (7.19) for inhibiting this [^{3}H]-AMPase activity were almost identical to their high affinity pIC_{50} estimates obtained in the binding assay. Although α,β-meADP, α,β-meATP, β,γ-meATP, ATP, ADP and GppNHp identified heterogeneity in the [^{3}H]-AMPase activity of the WEC cells, their pIC_{50} values for inhibiting the major portion of the [^{3}H]-AMPase activity were similar to their respective high affinity pIC_{50} values in the binding assay. It thus seems likely that WEC cells express a form of 5'-nucleotidase that possesses high affinity for both α,β-meADP and α,β-meATP and that this enzyme can be labelled by [^{3}H]-α,β-meATP.

5 In the presence of 10 μM GMP, the affinity estimates for α,β-meADP, AMP, GMP, GTP, GppNHp, ADP and adenosine at the high affinity [^{3}H]-α,β-meATP binding sites that remained available, were low and similar to their affinity estimates at the high affinity [^{3}H]-α,β-meATP binding sites of rat vas deferens. Since the high affinity [^{3}H]-α,β-meATP binding sites in rat vas deferens are thought to be P_{2x} purinoceptors it is possible that the high affinity [^{3}H]-α,β-meATP binding sites in the WEC which possess low affinity for α,β-meADP are also P_{2x} purinoceptors.

Keywords: [^{3}H]-α,β-methylene ATP; α,β-methylene ADP; endothelial cell; 5'-nucleotidase

Introduction

The ATP analogue α,β-methylene ATP (α,β-meATP) has been described as a selective P_{2x} purinoceptor agonist (Burnstock & Kennedy, 1985). Recently, this agonist has become available in a tritiated form and has been shown to label high affinity binding sites in rat vas deferens and rat bladder (Bo & Burnstock, 1990; Bo *et al.*, 1992). Since the rank order of agonist affinities in competing for the high affinity [^{3}H]-α,β-meATP binding sites in the rat vas deferens is similar to that obtained in functional studies on the P_{2x} purinoceptor it has been suggested that the high affinity binding sites for [^{3}H]-α,β-meATP are P_{2x} purinoceptors (Bo *et al.*, 1992; Michel & Humphrey, 1993). The demonstration that a number of P_{2x} purinoceptor antagonists, including pyridoxalphosphate-6-azophenyl-2',5'-disulphonic acid (iso-PPADS), suramin and cibacron blue, can compete for the high affinity [^{3}H]-α,β-meATP binding sites over the same concentration-range that they inhibit P_{2x} purinoceptor-mediated responses in functional studies, has provided further, corroborative, evidence that the high affinity [^{3}H]-α,β-meATP binding sites in the rat vas deferens are P_{2x} purinoceptors (Michel & Humphrey, 1993; Khakh *et al.*, 1994).

The availability of [^{3}H]-α,β-meATP as a radioligand for studying the P_{2x} purinoceptor could be of considerable value in determining the distribution of these receptors both in the periphery and particularly in the CNS where a role for P_{2x} purinoceptors in neurotransmission has recently been demonstrated (Edwards *et al.*, 1992). Indeed, preliminary studies with this radioligand have shown that high affinity binding sites for [^{3}H]-α,β-meATP are to be found in rat heart, spleen, liver and brain (Michel & Humphrey, 1993). At these sites the rank order of agonist affinities is similar to that obtained in the rat vas deferens and since binding of the radioligand can be inhibited by the P_{2x} purinoceptor antagonists, suramin and cibacron blue (Michel & Humphrey, 1993), it would appear that these sites represent P_{2x} purinoceptors.

As part of a study to screen cell lines for the presence of [^{3}H]-α,β-meATP binding sites, WEC cells, a rat endothelial cell line (Cole *et al.*, 1986), were found to contain very high levels of [^{3}H]-α,β-meATP binding. This observation was unexpected since endothelial cells are not thought to contain P_{2x} purinoceptors (Boeynaems & Pearson, 1990). Here we describe the

[1] Author for correspondence.

characterization of the [³H]-α,β-meATP binding sites in the WEC cells and report that the majority of these sites do not appear to be P_{2x} purinoceptors; rather they appear to represent labelling of a 5'-nucleotidase enzyme. These observations emphasize the need for caution when using [³H]-α,β-meATP as a radioligand for studying P_{2x} purinoceptors. A preliminary account of some of these results has been presented to the British Pharmacological Society (Michel *et al.*, 1994).

Methods

Cell culture

WEC cells (passages 16 to 25), originally isolated from Wistar rat aortic endothelium (Cole *et al.*, 1986), were grown as a monolayer culture in Dulbecco's modified Eagle's medium containing 10% foetal bovine serum in an humidified atmosphere of 5% CO_2 and 95% air at 37°C. For receptor binding assays the WEC cells were grown to 80–90% confluence and then harvested with a cell scraper. We used pre-confluent cells in these studies because we have found that the density of [³H]-α,β-meATP binding sites in the WEC cells progressively increased until the cells became confluent but thereafter decreased dramatically (unpublished observations).

Membrane preparation

WEC cells from twelve to fourteen 165 cm^2 flasks were homogenized in 60 ml of ice-cold assay buffer (50 mM Tris, 1 mM EDTA, 4 mM $CaCl_2$; pH 7.4 at 4°C) with a Polytron P10 tissue disrupter (2 × 10 s bursts on full setting). The cell homogenate was centrifuged at 48,000 *g* for 20 min and the crude membrane pellet resuspended in assay buffer and stored at −80°C until required. Rat vas deferens membranes were prepared as described previously by Michel & Humphrey (1993).

Receptor binding studies

Binding assays were conducted in a final volume of 250 µl of assay buffer (50 mM Tris buffer, 1 mM EDTA, 4 mM $CaCl_2$, pH 7.4 at 4°C). Non-specific binding (NSB) of the radioligand was defined by use of 30 µM α,β-meATP. Incubations were initiated by addition of membranes (approximately 10 µg protein) and maintained for 40 min at 4°C before terminating by vacuum filtration over wet GF/B glass fibre filters, pretreated with ice cold 20 mM $Na_4P_2O_7$, using a Brandel cell harvester. The filters were washed for 10 s with 10 mM KH_2PO_4/K_2HPO_4 buffer (pH 7.4 at 22°C), placed in scintillation vials and, after addition of 4 ml of Emulsifier Safe scintillant, were shaken for 1 h and left to stand for at least 1 h at 22°C before determination of bound radioligand by liquid scintillation spectrophotometry. In competition studies, the ability of a series of nucleotide analogues to compete for the binding sites labelled by 1 nM [³H]-α,β-meATP was determined over a range of concentrations spanning at least 5 log units. All determinations in the presence of competing compound were made in duplicate at each concentration, and for each compound under test, independent determinations of total binding and NSB were also made in duplicate. In saturation studies, binding of the radioligand was measured at ten different concentrations over the concentration range of 0.1 to 65 nM. In these studies total binding was measured in triplicate and NSB in duplicate at each radioligand concentration. Protein was determined by the dye binding method (Biorad).

Assay of 5'-nucleotidase

The 5'-nucleotidase activity of the WEC cell membranes was determined by measuring the production of [³H]-adenosine from [³H]-AMP (Sun *et al.*, 1982). In these studies WEC cell membranes (10 µg protein) were incubated in the presence of 6 nM [³H]-AMP and competing compounds in 250 µl of assay buffer (50 mM Tris, 1 mM EDTA, 4 mM $CaCl_2$, pH 7.4 at 4°C) for 20 min at 4°C. Reactions were terminated by addition of 250 µl of 0.3 M $ZnSO_4$ and 250 µl of 0.3 M $Ba(OH)_2$ in order to precipitate [³H]-AMP and retain the [³H]-adenosine formed during the reaction in solution. After centrifugation at 1500 *g* a 200 µl aliquot of the supernatant was removed from each sample, added to 2 ml Ultima Gold XR scintillant and the radioactivity present in the sample, presumed to be [³H]-adenosine (Sun *et al.*, 1982), was determined by liquid scintillation spectrophotometry.

Data analysis

Saturation binding data were analysed using LIGAND (Munson & Rodbard, 1980). The specific binding data were analysed by assuming that the radioligand was binding to either one or more populations of non-interacting binding sites. Estimates of the dissociation equilibrium constant (K_d) are expressed as the negative base 10 logarithm (pK_d). An *F*-test was used to compare between the various models (Munson & Rodbard, 1980) with the more complex model only being accepted if a significant ($P < 0.05$) reduction in the sum of the squares could be achieved by using this model.

Competition binding data were analysed by iterative curve-fitting techniques (Michel & Whiting, 1984). Using this approach the specific binding data were initially analysed to determine the IC_{50} and Hill slope (n_H) for the competition curve. When the Hill slope of the competition curve was less than unity the data were futher analysed to determine if they could be better described by assuming the compounds to be com-

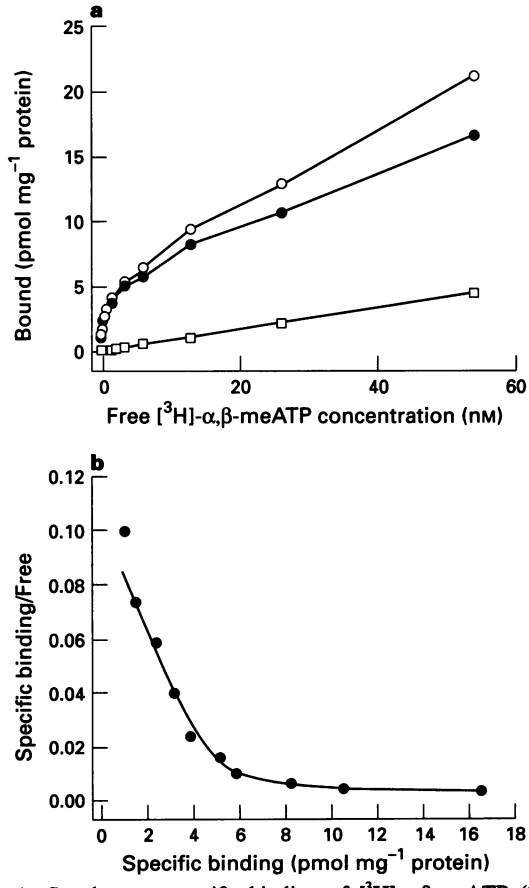

Figure 1 Steady state specific binding of [³H]-α,β-meATP (0.1 to 56 nM) to WEC cell membranes. (a) Total (○), specific (●) and non-specific (□) binding of [³H]-α,β-meATP (pmol mg^{-1} protein) are plotted against the free concentration of radioligand (nM). (b) The specific binding data from (a) are presented as a Scatchard plot. In both (a) and (b) the lines were drawn by hand.

peting with two or more populations of specific binding sites. For this analysis, an iterative curve-fitting programme was used that determined the IC_{50} for each site and the proportion of specific binding that each site comprised (Michel & Whiting, 1984). Comparisons between various binding models were made using a modified *F*-test (Munson & Rodbard, 1980) and significance was assessed at the 0.05 probability level. The enzyme inhibition data were analysed in the same manner as the competition binding data.

The IC_{50} values that were determined in the binding studies were not adjusted to take account of the presence of radioligand since, given the heterogeneity of the [³H]-α,β-meATP binding sites (see results), it was not possible to definitively determine a radioligand K_d for use in the Cheng & Prusoff (1973) approximation. All IC_{50} values are presented as the negative logarithm of the IC_{50} (pIC_{50}).

Unless otherwise stated the data presented are the mean ± s.e. mean of between 3 and 5 separate experiments.

Materials

The tetrasodium salt of 2-methyl-thio-ATP (2-me-S-ATP) was obtained from Semat (St Albans, UK). All other compounds were obtained from Sigma. With the exception of ouabain, cyclopropyladenosine, adenosine, guanosine, inosine and S-(*p*-nitrobenzyl)-6-thio-inosine (NBTI), the compounds were dis-

Table 1 Competition binding studies at WEC cell membrane [³H]-α,β-meATP (1nM) binding sites in the presence and absence of 10 μM GMP

	WEC cells		*WEC cells in the presence of 10 μM GMP*	
Compound	*pIC_{50}*	*Hill slope*	*pIC_{50}*	*Hill slope*
α,β-meATP	8.12 ± 0.03	0.83 ± 0.03	8.11 ± 0.13	0.88 ± 0.06
β,γ-meATP	7.63 ± 0.15	0.56 ± 0.06	ND	ND
2-me-S-ATP	5.98 ± 0.07	0.74 ± 0.05	ND	ND
ATP	6.89 ± 0.13	0.58 ± 0.03	6.82 ± 0.11	0.64 ± 0.10
ADP	6.80 ± 0.11	0.53 ± 0.04	6.07 ± 0.12*	0.85 ± 0.06*
Adenosine	4.64 ± 0.13	0.53 ± 0.04	2.91 ± 0.31*	2.30 ± 0.27*
Suramin	4.87 ± 0.03	0.76 ± 0.04	4.91 ± 0.04	0.92 ± 0.04*
UTP	5.64 ± 0.03	0.76 ± 0.10	4.85 ± 0.03*	1.02 ± 0.04
GMP	6.52 ± 0.03	0.36 ± 0.04	< 4*	NA
GppNHp	6.66 ± 0.08	0.52 ± 0.03	4.31 ± 0.14*	0.82 ± 0.09*
GTP	7.01 ± 0.09	0.50 ± 0.04	5.20 ± 0.03*	0.82 ± 0.07*
AMP	6.18 ± 0.12	0.45 ± 0.04	3.90 ± 0.21*	1.07 ± 0.05*
α,β-meADP	8.25 ± 0.24	0.29 ± 0.02	4.50 ± 0.31*	0.40 ± 0.10

Competition binding studies on the sites labelled by 1 nM [³H]-α,β-meATP in WEC cell membranes were performed either in the absence or presence of 10 μM GMP. The data are the mean ± s.e.mean of $n = 3-5$ determinations. NA = not applicable; ND = not determined.

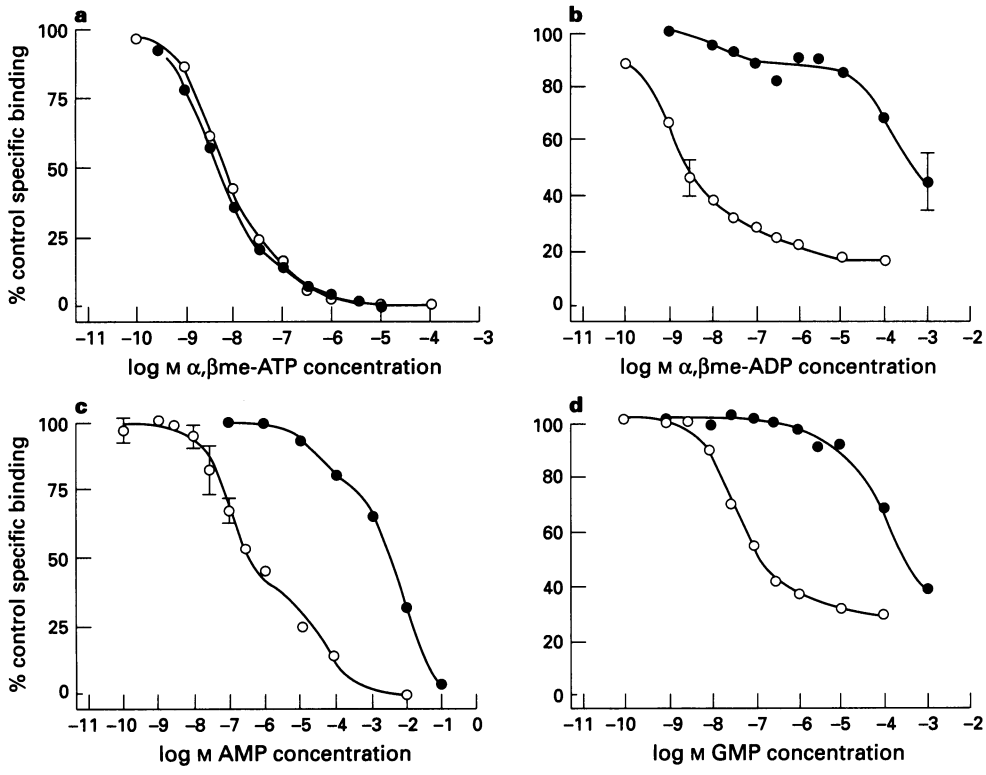

Figure 2 Competition curves for (a) α,β-meATP, (b) α,β-meADP, (c) AMP and (d) GMP in either WEC cell membranes (○) or rat vas deferens membranes (●). The results are presented as a percentage of the control specific binding levels. Each point represents the mean ± s.e.mean ($n = 3-5$). In the vas deferens, the pIC_{50} values for α,β-meADP and AMP were 3.17 ± 0.26 and 2.66 ± 0.13, respectively, while their n_H values were 0.30 ± 0.07 and 0.41 ± 0.04, respectively; the pIC_{50} for GMP was < 4. All lines were drawn through the data points and do not necessarily represent lines of best fit.

solved in assay buffer before addition to the assay. Ouabain and NBTI were dissolved in dimethylsulphoxide (DMSO), whereas cyclopropyladenosine (CPA), adenosine, 5'-(N-ethyl-carboxamido)-adenosine (NECA), inosine and guanosine were dissolved in 1M HCl, before dilution into assay buffer. In separate studies it was shown that these vehicles did not affect specific binding of the radioligand at their final assay concentrations. [³H]-α,β-meATP (specific activity 28 Ci mmol^{-1}) and [³H]-AMP (specific activity 23 Ci mmol^{-1}) were obtained from Amersham International Plc., UK.

Results

Saturation binding studies

In saturation studies, there were high levels of total [³H]-α,β-meATP binding in WEC cell membranes. Non specific binding represented between 10 and 20% of total binding (Figure 1a). Specific binding of the radioligand did not appear to saturate readily and when the specific binding data were presented as a Scatchard plot the resultant graph showed marked signs of

Table 2 Multi-site analysis of [³H]-α,β-meATP binding data obtained from competition studies performed on WEC cell membranes

	Site 1		*Site 2*	
Compound	*pIC$_{50}$*	*% sites*	*pIC$_{50}$*	*% sites*
α,β-meATP	8.26±0.08	88.6±1.6	6.50±0.18	11.4±1.6
β,γ-meATP	7.95±0.13	82.2±3.3	3.96±0.11	17.8±3.3
2-me-S-ATP	5.87±0.03	100	NA	NA
ATP	7.79±0.11	42.4±1.8	6.09±0.05	57.6±1.8
ADP	7.57±0.20	49.3±3.9	5.61±0.13	50.7±3.9
Adenosine	5.45±0.06	63.2±1.9	2.77±0.04	36.8±1.9
Suramin	4.87±0.03	100	NA	NA
UTP	6.12±0.22	67.0±12.7	4.63±0.23	33.0±12.7
GMP	7.34±0.03	69.0±2.0	<4	31.0±2.0
GppNHp	7.35±0.02	68.8±3.6	4.60±0.28	31.2±3.6
GTP	7.59±0.08	68.1±1.6	5.40±0.03	31.9±1.6
AMP	7.12±0.30	60.9±4.3	3.71±0.09	39.1±4.3
α,β-meADP*	8.87±0.15	68.5±3.8	6.13±0.04	13.9±2.5

The competition curves for each compound were analysed assuming that the compounds were identifying either one or more populations of the 1nM [³H]-α,β-meATP binding sites in the WEC cells. For those compounds that identified heterogeneity of the [³H]-α,β-meATP binding sites, the site at which the compounds possessed highest affinity was designated as site 1. The data are the mean±s.e.mean (n=3–5) for the pIC$_{50}$ at either site 1 or 2 and the % of specific binding that each site comprised. * For α,β-meADP the data were best described by assuming that this compound identified three populations of sites. Affinity estimates at two of these sites are presented in the table. At the third site (17.5±2.2% of sites) a pIC$_{50}$ <4 was assumed. NA=not applicable, data could only be fitted to a 1 site model.

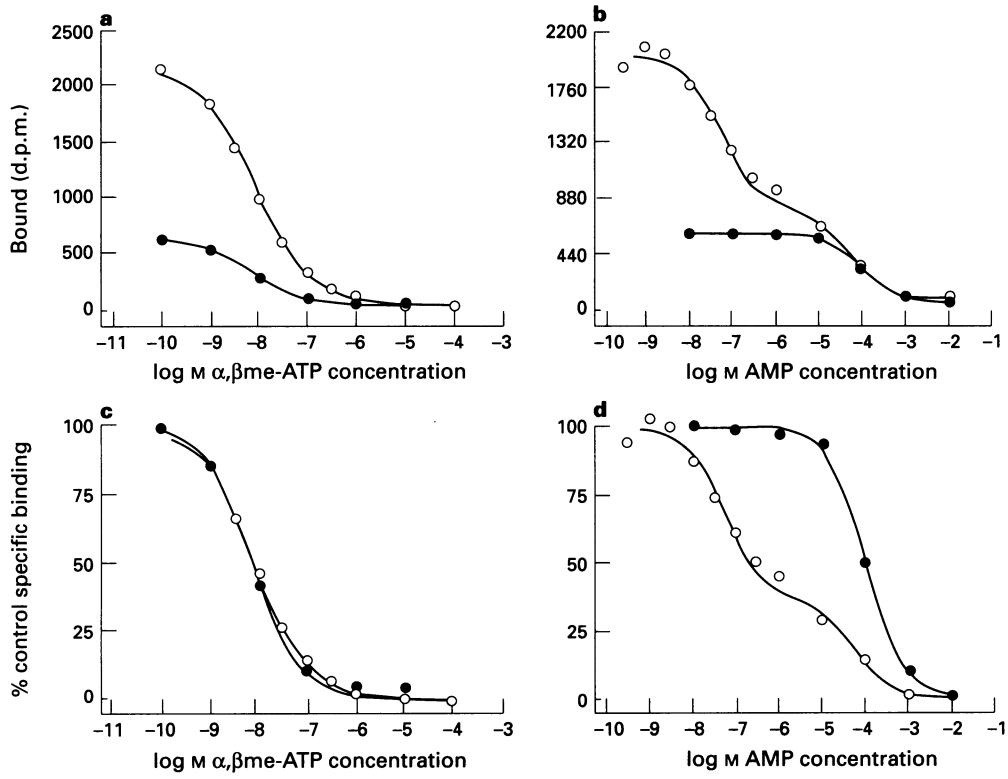

Figure 3 Competition curves for α,β-meATP (a and c) or AMP (b and d) obtained in the absence (○) or presence (●) of 10μM GMP. In (a) and (b) the raw binding data (d.p.m. bound) are presented while in (c) and (d) the data have been normalised and are presented as a percentage of the control specific binding measured either in the absence or presence of 10μM GMP. The data are from a single representative experiment repeated 3–5 times with similar results.

Table 3 Effect of nucleotides on the metabolism of [³H]-AMP (6 nM) by WEC cell membranes

	Hill model		*Two component model*			
			Component 1		*Component 2*	
Compound	pIC_{50}	n_H	pIC_{50}	*% total activity*	pIC_{50}	*% total activity*
α,β-meATP	7.68±0.10	0.29±0.10	9.21±0.07	60.1±2.6	6.08±0.17	39.9±2.6
β,γ-meATP	7.98±0.01	0.39±0.01	8.89±0.17	62.1±2.4	6.31±0.16	37.9±2.4
2-me-S-ATP	5.68±0.06	0.67±0.09	5.75±0.08	100	NA	NA
ATP	7.38±0.03	0.51±0.04	7.93±0.01	72.2±1.7	5.52±0.07	27.8±1.7
ADP	7.06±0.07	0.75±0.08	7.40±0.17	80.0±6.4	6.00±0.05	20.0±6.4
Adenosine	5.59±0.04	0.73±0.02	5.58±0.02	100	NA	NA
GMP	7.55±0.08	0.73±0.07	7.44±0.09	100	NA	NA
GppNHp	7.03±0.11	0.50±0.03	7.52±0.07	71.1±1.3	5.16±0.19	28.9±1.3
AMP	7.19±0.01	0.73±0.02	7.23±0.02	100	NA	NA
α,β-meADP	7.47±0.22	0.29±0.01	8.87±0.17	54.4±2.7	5.02±0.11	45.6±2.7

The data for each compound were first analysed to determine the pIC_{50} and Hill slope (n_H) of the competition curve (Hill model) and then to determine if the data were better described by assuming two components of [³H]-AMP metabolism. For those compounds for which a two component model was significantly better than a one component model the affinity estimates for each component and the proportion of total activity that each component comprised, are presented. The component for which the compounds possessed highest affinity has been designated as component 1. The data are the mean±s.e.mean ($n=3-6$). NA = not applicable, data could only be fitted to a 1 component model.

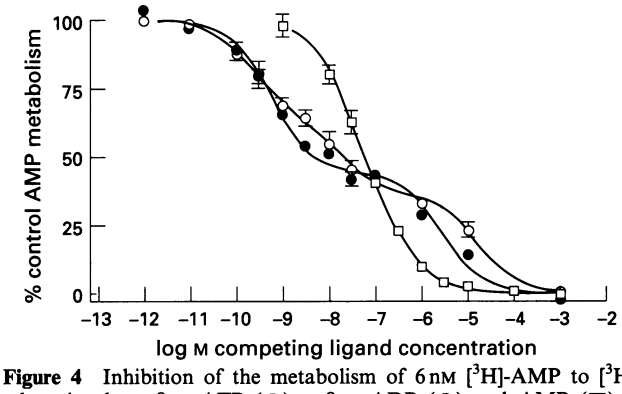

Figure 4 Inhibition of the metabolism of 6 nM [³H]-AMP to [³H]-adenosine by α,β-meATP (●), α,β-meADP (○) and AMP (□) in WEC cell membranes at 4°C during a 20 min incubation. The data are the mean±s.e.mean of 3–4 determinations. Control basal conversion of [³H]-AMP to [³H]-adenosine by the WEC cell membranes was 5944±375 d.p.m. while the blank value in the absence of membranes was 1071±60 d.p.m. All lines were drawn through the data points and do not necessarily represent lines of best fit.

curvature (Figure 1b). The specific binding data could be best described by assuming that [³H]-α,β-meATP was labelling two populations of specific binding site in the WEC cell membranes. One of these sites possessed high affinity for [³H]-α,β-meATP ($pK_d=9.5\pm0.1$) and a relatively low capacity ($B_{max}=3.75\pm0.4$ pmol mg^{-1} protein). The second site was of lower affinity and higher capacity ($pK_d=7.20\pm0.1$; $B_{max}=23.3\pm6.2$ pmol mg^{-1} protein).

Competition binding studies

The high affinity [³H]-α,β-meATP sites in the WEC cell membranes were selectively labelled with a low concentration of radioligand (1 nM). Under these conditions, competition curves for α,β-meATP were relatively steep ($n_H=0.83$; Table 1) and a two site analysis of the data indicated that α,β-meATP possessed high affinity for 88.6% of the sites (Table 2). The competition curve for α,β-meATP was almost identical to that obtained in rat vas deferens (Figure 2a).

In competition studies a number of purinoceptor agonists competed for the [³H]-α,β-meATP (1 nM) binding sites in the WEC cell membranes (Table 1). The rank order of agonist affinities in competing for the [³H]-α,β-meATP binding sites was: α,β-meATP > β,γ-meATP > ATP = ADP > 2-me-S-ATP ⩾ UTP > adenosine. This rank order of affinities was similar, although not identical, to the rank order of affinity obtained in the rat vas deferens (Michel & Humphrey, 1993): α,β-meATP > β,γ-meATP > 2-me-S-ATP > ATP ⩾ ADP > UTP > adenosine.

Suramin, possessed similar affinity in rat vas deferens and WEC cells (cf. Table 1 and Michel & Humphrey, 1993). The absolute affinities of the purinoceptor agonists in competing for the sites in WEC cells differed from the affinity estimates obtained in rat vas deferens. In particular, UTP and adenosine were 32 and 118 fold more potent, respectively, at competing for the [³H]-α,β-meATP binding sites labelled in the WEC cells than in rat vas deferens (cf. Table 1 and Michel & Humphrey, 1993). When additional nucleotide analogues were examined, even greater differences between affinity estimates in the WEC cells and the rat vas deferens were apparent. Thus, the adenine nucleotides, α,β-meADP (Figure 2b) and AMP (Figure 2c) had more than 1000 fold, and the guanine nucleotide GMP (Figure 2d) had at least 300 fold higher affinity in the WEC cells than in the vas deferens. Binding of the radioligand to the WEC cell membranes was inhibited with very low affinity ($pIC_{50}<4$) by NBTI, ouabain, CPA, NECA, inosine and guanosine (data not shown).

Detailed analysis of competition binding curves in WEC cells

In the WEC cells the slope of the competition curve for many of the compounds was low ($n_H<0.6$; Table 1) and several compounds (α,β-meADP and GMP) did not compete for all of the sites labelled by 1 nM [³H]-α,β-meATP (Figure 2b and d). These data were therefore further analysed assuming that the compounds were competing for more than one population of [³H]-α,β-meATP binding site. For most compounds studied the specific binding data could be fitted to a model assuming that they were competing for two populations of [³H]-α,β-meATP binding site (Table 2). The only exceptions were 2-me-S-ATP and suramin, for which the data were best described by assuming that they identified a single population of sites, and α,β-meADP for which a 3 site model best described the data (Table 2). Note that since GMP did not compete for all the [³H]-α,β-meATP binding sites the multi-site analysis for the compound excluded the NSB determination made using 30 μM α,β-meATP. Instead the total binding data were analysed and it was found that GMP identified a single population of [³H]-α,β-meATP binding sites with high affinity. This population corresponded to 69% of the specific [³H]-α,β-meATP binding sites, as defined by 30 μM α,β-meATP.

For the compounds that identified two populations of [³H]-α,β-meATP binding sites, the relative proportions of the two

sites differed. However, it appeared that the compounds could be separated into three main groups on the basis of the proportion of high affinity sites that they identified (Table 2). Thus, the methylene bridged ATP analogues, α,β-meATP and β,γ-meATP identified between 82.2% and 88.6% of the sites with high affinity. The majority of the compounds, including AMP, GMP, GppNHp, GTP, adenosine and UTP appeared to identify between 60.9% and 69% of the sites with high affinity. Finally, ATP and ADP identified between 42.4% and 49.3% of the total number of sites with relatively high affinity.

The competition curve for α,β-meADP was complex and since the compound did not compete for all of the [^{3}H]-α,β-meATP binding sites, the data analysis for the compound was similar to that described for GMP. Using this approach it was found that α,β-meADP was identifying three populations of the specific [^{3}H]-α,β-meATP binding sites (Table 2). The proportion of sites (68.5%) which possessed highest affinity ($pIC_{50}=8.87$) for α,β-meADP was similar to the proportion of high affinity sites identified by GMP, UTP and GTP (approximately 60–69%). The other two sites for α,β-meADP possessed either intermediate affinity ($pIC_{50}=6.13$; 13.9%) or very low affinity ($pIC_{50}<4$; 17.5%).

Characterization of the binding sites with low affinity for GMP and α,β-meADP

In the competition studies, GMP maximally inhibited the binding of 1 nM [^{3}H]-α,β-meATP by 69.0%. In separate competition studies performed in the presence of 10 μM GMP the binding of [^{3}H]-α,β-meATP was inhibited by 74.6±3.1% compared to binding measured in its absence, and under these conditions the affinity of α,β-meATP for the sites that remained was not changed ($pIC_{50}=8.11$; Table 1; Figure 3a and c). In the presence of 10 μM GMP the Hill slopes for most compounds were steeper and closer to unity (Table 1). Furthermore affinity estimates for AMP (Figure 3b and d), ADP, GTP, GppNHp, UTP and adenosine decreased in the presence of 10 μM GMP and were similar to the affinity estimates at the low affinity site identified in the absence of 10 μM GMP (cf. Tables 1 and 2).

The affinity estimate for ATP was not affected by 10 μM GMP whereas that of α,β-meADP was considerably reduced. For both compounds the Hill slope of the competition curve was still less than unity (Table 1).

Studies on the 5'-nucleotidase activity of WEC cell membranes at 4°C

Conversion of [^{3}H]-AMP to [^{3}H]-adenosine by WEC cell membranes was evident at 4°C. The apparent K_m for AMP calculated from the competition data in Table 3 was 54.5 nM. This [^{3}H]-AMPase activity was inhibited by a number of nucleotides and nucleotide analogues (Figure 4 and Table 3). Hill slopes of the competition curves for most compounds were less than unity and it was evident that there were two components of [^{3}H]-AMPase activity (Figure 4 and Table 3). The high affinity pIC_{50} values of the compounds for inhibiting [^{3}H]-AMPase activity were almost identical to their respective pIC_{50} values at inhibiting [^{3}H]-α,β-meATP binding to the high affinity α,β-meADP binding sites (cf. Tables 2 and 3: correlation coefficient = 0.946).

Discussion

The WEC cells used in this study are a permanent cell line derived from Wistar rat aortic endothelium (Cole *et al.*, 1986). These cells display many of the characteristics of endothelial cells, including the ability to take up acetylated LDL (T.-P.D. Fan, unpublished observation). Since endothelial cells have not been previously shown to express P_{2x} purinoceptors (Boeynaems & Pearson, 1990) it was therefore surprising in our preliminary studies to find high levels of [^{3}H]-α,β-meATP binding in this cell line. Given this unexpected observation, the main purpose of this study was to characterize these sites in detail and to compare them with the [^{3}H]-α,β-meATP binding sites previously identified in rat vas deferens, which are thought to be P_{2x} purinoceptors (Bo *et al.*, 1992; Michel & Humphrey, 1993). We found that a large proportion of the binding sites labelled by [^{3}H]-α,β-meATP in these cells did not appear to reflect labelling of a P_{2x} purinoceptor, but more plausibly represented labelling of a 5'-nucleotidase enzyme.

In saturation studies, the binding characteristics of the radioligand to WEC cell membranes were very similar to those in rat vas deferens which have already been described in detail (Bo *et al.*, 1992; Michel & Humphrey, 1993). Thus, there were high levels of specific binding of [^{3}H]-α,β-meATP in WEC cell membranes and only low levels of non-specific binding. In the WEC cell membranes the radioligand identified two populations of binding sites and the estimated pK_d values for the equilibrium dissociation constant of the radioligand for these two sites (9.50 and 7.20, respectively) were very similar to the pK_d values at the high (9.14) and low (7.15) affinity sites, respectively, identified in rat vas deferens (Michel & Humphrey, 1993). The high affinity sites in WEC cells could be selectively labelled with a low concentration of [^{3}H]-α,β-meATP (1 nM) and under these conditions 88.6% of the sites possessed high affinity for the radioligand.

In competition studies the rank order of affinities for a limited series of P_2 purinoceptor agonists in competing for the high affinity binding sites labelled by 1 nM [^{3}H]-α,β-meATP was similar to that obtained in rat vas deferens. Furthermore, affinity estimates for suramin in the WEC cells and rat vas deferens were not different. These initial findings suggested that the high affinity [^{3}H]-α,β-meATP binding sites in the WEC cells were similar to those in rat vas deferens (Bo *et al.*, 1992; Michel & Humphrey, 1993). However, several compounds possessed higher affinity in the WEC cells than in rat vas deferens, and, when a larger number of compounds was examined, considerable differences between the high affinity [^{3}H]-α,β-meATP binding sites in the WEC cells and the vas deferens became apparent. In particular, several guanine nucleotides, as well as AMP and α,β-meADP, were found to be very potent competing ligands in the WEC cells but to possess much lower affinity in the vas deferens.

These latter observations suggest that the high [^{3}H]-α,β-meATP binding sites in vas deferens and WEC cells are different. While the sites in the vas deferens appear to be P_{2x} receptors (Bo *et al.*, 1992; Michel & Humphrey, 1993), the identity of the high affinity [^{3}H]-α,β-meATP binding sites in the WEC cell membranes was not immediately apparent. Furthermore, characterization of the high affinity [^{3}H]-α,β-meATP binding sites in the WEC cell membranes was complicated by the demonstration that these sites were heterogeneous. Thus, even under conditions where the majority (>88%) of the sites displayed high affinity for α,β-meATP, several compounds produced biphasic competition curves and the data could be best described by assuming that these compounds possessed high affinity for between 40 and 70% of the sites.

Several compounds competed for a similar proportion (60.9–69%) of the sites with relatively high affinity. These included α,β-meADP, AMP, GTP, UTP, GMP, GppNHp and adenosine. The sites at which these compounds possessed highest affinity were probably the same, since in the presence of a concentration of GMP that was sufficient to inhibit selectively the binding of [^{3}H]-α,β-meATP to those sites with highest affinity for GMP, the [^{3}H]-α,β-meATP binding sites with highest affinity for AMP, ADP, UTP, α,β-meADP, GTP, GppNHp, adenosine and AMP were also occluded. As α,β-meADP was the most potent ligand at competing for these sites ($pIC_{50}=8.87$), being even more potent than α,β-meATP ($pIC_{50}=8.26$), it would seem more appropriate that these sites be referred to as high affinity α,β-meADP binding sites. Since, α,β-meADP, ADP, adenosine, AMP and GMP do not possess any appreciable activity as P_{2x} purinoceptor agonists in guinea-

pig vas deferens (Fedan *et al.*, 1982; 1986), it is most unlikely that the high affinity α,β-meADP binding sites in the WEC cells are P_{2x} purinoceptors.

The relatively high affinity of adenosine for the [^{3}H]-α,β-meATP binding sites with high affinity for α,β-meADP was of interest and might suggest that these sites are adenosine receptors or uptake sites. However, this is not the case since the adenosine receptor agonists, NECA and CPA, and the adenosine transport inhibitor, NBTI, possessed low affinity in competing for [^{3}H]-α,β-meATP binding sites in WEC cells. Alternatively, the relatively high affinity of the guanine nucleotides, GTP and GppNHp, might suggest that the high affinity α,β-meADP binding sites represent labelling of a G-protein coupled receptor, since their affinity in competing for the high affinity α,β-meADP binding sites was similar to their affinity for G-protein coupled P_{2y} purinoceptors in turkey erythrocyte membranes (Cooper *et al.*, 1989). However the high affinity of GMP, relative to GTP, for these sites rules this out, as would the high affinity exhibited by α,β-meATP, ADP, AMP and adenosine.

α,β-meADP is a potent 5'-nucleotidase inhibitor (Burger & Lowenstein, 1970) and its affinity at inhibiting membrane bound 5'-nucleotidases in brain ($K_i = 0.6$ nM; Mallol & Bozal, 1983), intestinal smooth muscle ($K_i = 2$ nM; Burger & Lowenstein, 1970) and heart ($K_i = 5$ nM; Naito & Lowenstein, 1985) is similar to its affinity at competing for the [^{3}H]-α,β-meATP binding sites in this study ($IC_{50} = 1.3-5.6$ nM). Consequently, the population of [^{3}H]-α,β-meATP binding sites in the WEC cell membranes that possess high affinity for α,β-meADP may represent labelling of a 5'-nucleotidase. Certainly, 5'-nucleotidase can be a membrane-bound enzyme (Zimmermann, 1992) and has been identified in endothelial cells (Gordon *et al.*, 1986). Furthermore, in rat heart membranes α,β-meATP has been shown to possess relatively high affinity at inhibiting 5'-nucleotidase ($K_i = 66$ nM; Naito & Lowenstein, 1985). Consistent with the suggestion that the high affinity α,β-meADP binding sites are 5'-nucleotidase was the demonstration that AMP and GMP, which are substrates of the enzyme (Burger & Lowenstein, 1970), were also potent at competing for the binding sites. Similarly, ATP, ADP and other nucleotide di- and triphosphates are potent inhibitors of 5'-nucleotidase from various tissues (Burger & Lowenstein, 1970) and all of these compounds were potent competing ligands at the high affinity α,β-meADP binding sites. In particular the IC_{50} value for ADP at the high affinity α,β-meADP binding sites (27 nM) was similar to the K_i values reported for inhibition of 5'-nucleotidase activity in bovine brain and rat heart (i.e. $K_i = 22$ nM, Burger & Lowenstein, 1975; $K_i = 9$ nM, Mallol & Bozal, 1983). Of particular importance was our demonstration that WEC cell membranes could metabolize AMP to adenosine under the conditions of the binding studies, and that a significant proportion of this enzymatic activity could be inhibited by α,β-meADP, α,β-meATP, β,γ-meATP, ATP, ADP, AMP, GMP, GppNHp, 2-me-S-ATP and adenosine with similar affinity to that displayed at those [^{3}H]-α,β-meATP binding sites with high affinity for α,β-meADP.

While these data are consistent with the high affinity α,β-meADP sites representing labelling of 5'-nucleotidase, there are some features of the observed enzyme profile that are at variance with previous studies. Notably both the K_m value for AMP in these cells of approximately 54 nM, and the affinity estimates of GMP and AMP at the high affinity α,β-meADP binding sites of 45.7 and 75 nM, respectively, differed considerably from the respective K_m values for AMP and GMP of 3–20 μM determined in functional studies on 5'-nucleotidase in other tissues (Burger & Lowenstein, 1975; Naito & Lowenstein, 1981). In addition, α,β-meATP possessed a high affinity ($IC_{50} \approx 0.3-3$ nM) in both the binding and functional studies in the WEC cells whereas in rat heart its K_i for inhibition of 5'-nucleotidase activity is 66 nM (Naito & Lowenstein, 1985).

It is not known at present whether these discrepancies indicate that the high affinity α,β-meADP binding sites are not a 5'-nucleotidase or are due to some other reason such as different experimental conditions or enzyme heterogeneity. With respect to experimental conditions, our binding and enzyme assays were both performed at 4°C whereas the previous enzyme studies were conduced at 25–37°C and further study would be required to address this issue. Alternatively, the discrepancies between the affinity estimates may reflect the presence of a different form of 5'-nucleotidase in the WEC cells. Certainly, several isoforms of 5'-nucleotidase have been described (Zimmermann, 1992) which differ in their preference for AMP and IMP and also their cellular location since the enzyme can be either membrane-bound or soluble. Furthermore the membrane-bound liver form of 5'-nucleotidase has been reported to possess a very low affinity ($K_i = 60$ μM) for α,β-meADP (Evans & Gurd, 1973).

While it seems likely that the high affinity α,β-meADP binding sites in the WEC cells are 5'-nucleotidase, the nature of the remaining 30% of the [^{3}H]-α,β-meATP binding sites which were not inhibited with high affinity by α,β-meADP is not certain. However, in the presence of GMP the binding characteristics of these sites were similar to those determined in the vas deferens. In particular these sites possessed high affinity for [^{3}H]-α,β-meATP but low affinity for adenosine, α,β-meADP and AMP. This suggests that these sites may be P_{2x} purinoceptors and additional functional studies would be required to confirm or refute this suggestion.

In conclusion the present study has identified high and low affinity [^{3}H]-α,β-meATP binding sites in a cell line derived from rat aortic endothelial cells. The high affinity [^{3}H]-α,β-meATP binding sites were characterized and found to be heterogeneous with at least two populations of the high affinity [^{3}H]-α,β-meATP binding site being identified. One of these sites, which possessed high affinity for α,β-meADP, showed marked differences from the high affinity [^{3}H]-α,β-meATP binding site present in rat vas deferens and may represent labelling of a form of 5'-nucleotidase. The other site possessed low affinity for α,β-meADP and may represent labelling of a site that is similar to the high affinity [^{3}H]-α,β-meATP binding sites previously identified in rat vas deferens, and so may represent labelling of P_{2x} purinoceptors. These results therefore indicate that considerable caution should be exerted in interpreting data obtained with [^{3}H]-α,β-meATP and emphasize the importance of rigorously characterizing the binding sites for this radioligand before concluding that they represent P_{2x} purinoceptors. While this may be possible in studies using membrane preparations, a similar approach is not always possible in autoradiographical studies and so this will limit the use of the radioligand in such studies.

Finally, if the high affinity α,β-meADP binding sites do represent a 5'-nucleotidase, then it is clear that α,β-meATP has high affinity for this enzyme, comparable to that of α,β-meADP, at least in WEC cells. Consequently, α,β-meATP, like α,β-meADP, could inhibit the breakdown of AMP to adenosine. This property could complicate interpretation of data obtained with α,β-meATP and raises the issue of the specificity of α,β-meATP which is widely employed as a selective P_{2x} purinoceptor agonist.

T.-P.D.F. thanks the Wellcome trust for financial support.

References

BO, X.N. & BURNSTOCK, G. (1990). High- and low-affinity binding sites for [^{3}H]-α,β-methylene ATP in rat urinary bladder membranes. *Br. J. Pharmacol.*, **101**, 291–296.

BO, X.N., SIMON, J., BURNSTOCK, G. & BARNARD, E.A. (1992). Solubilization and molecular size determination of the P_{2x} purinoceptor from rat vas deferens. *J. Biol. Chem.*, **267**, 17581–17587.

BOEYNAEMS, J.M. & PEARSON, J.D. (1990). P_2 purinoceptors on vascular endothelial cells: physiological significance and transduction mechanisms. *Trends Pharmacol. Sci.*, **11**, 34–37.

BURGER, R.M. & LOWENSTEIN, J.M. (1970). Preparation and properties of 5′-nucleotidase from smooth muscle of small intestine. *J. Biol. Chem.*, **245**, 6274–6280.

BURGER, R.M. & LOWENSTEIN, J.M. (1975). 5′-Nucleotidase from smooth muscle of small intestine and from brain. Inhibition by nucleotides. *Biochemistry*, **14**, 2362–2366.

BURNSTOCK, G. & KENNEDY, C. (1985). Is there a basis for distinguishing two types of P_2-purinoceptor? *Gen. Pharmacol.*, **16**, 433–440.

CHENG, Y. & PRUSOFF, W.H. (1973). Relationship between the inhibition constant (K_i) and the concentration of inhibitor which causes 50 per cent inhibition (I_{50}) of an enzymatic reaction. *Biochem. Pharmacol.*, **22**, 3099–3108.

COLE, O.F., FAN, T.-P.D. & LEWIS, G.P. (1986). Isolation, characterization, growth and culture of endothelial cells from the rat aorta. *Cell Biol. Int. Rep.*, **10**, 399–405.

COOPER, C.L., MORRIS, A.J. & HARDEN, T.K. (1989). Guanine nucleotide-sensitive interaction of a radiolabeled agonist with a phospholipase C-linked P_{2y}-purinergic receptor. *J. Biol. Chem.*, **264**, 6202–6206.

EDWARDS, F.A., GIBB, A.J. & COLQUHOUN, D. (1992). ATP receptor-mediated synaptic currents in the central nervous system. *Nature*, **359**, 144–147.

EVANS, W.H. & GURD, J.W. (1973). Properties of a 5′nucleotidase purified from mouse liver plasma membranes. *Biochem. J.*, **133**, 189–199.

FEDAN, J.S., HOGABOOM, G.K. & O'DONNELL, J.P. (1986). Further comparison of contractions of the smooth muscle of the guinea-pig isolated vas deferens induced by ATP and related analogs. *Eur. J. Pharmacol.*, **129**, 279–291.

FEDAN, J.S., HOGABOOM, G.K., WESTFALL, D.P. & O'DONNELL, J.P. (1982). Comparison of contractions of the smooth muscle of the guinea-pig vas deferens induced by ATP and related nucleotides. *Eur. J. Pharmacol.*, **81**, 193–204.

GORDON, J.L., PEARSON, J.D. & SLAKEY, L.L. (1986). The hydrolysis of extracellular adenine nucleotides by cultured endothelial cells from pig aorta. Feed-forward inhibition of adenosine production at the cell surface. *J. Biol. Chem.*, **261**, 15496–15507.

KHAKH, B.S., MICHEL, A.D. & HUMPHREY, P.P.A. (1994). Estimates of antagonist affinities at P_{2x} purinoceptors in rat vas deferens. *Eur. J. Pharmacol.*, **263**, 301–309.

MALLOL, J. & BOZAL, J. (1983). Modification of 5′-nucleotidase activity by divalent cations and nucleotides. *J. Neurochem.*, **40**, 1205–1211.

MICHEL, A.D., CHAU, N.-M., FAN, T.-P.D., FROST, E.E. & HUMPHREY, P.P.A. (1994). Differences between the high affinity [^{3}H]αβmeATP binding sites in rat vas deferens and in a rat aortic endothelial-derived cell line. *Br. J. Pharmacol.*, **113**, 116P.

MICHEL, A.D. & HUMPHREY, P.P.A. (1993). Distribution and characterization of [^{3}H]αβ-methylene ATP binding sites in the rat. *Naunyn Schmied. Arch. Pharmacol.*, **348**, 608–617.

MICHEL, A.D. & WHITING, R.L. (1984). Analysis of ligand binding data using a microcomputer. *Br. J. Pharmacol.*, **108**, 144P.

MUNSON, P.J. & RODBARD, D. (1980). Ligand: a versatile computerized approach for characterization of ligand-binding systems. *Anal. Biochem.*, **107**, 220–239.

NAITO, Y. & LOWENSTEIN, J.M. (1981). 5′-Nucleotidase from rat heart. *Biochemistry*, **20**, 5188–5194.

NAITO, Y. & LOWENSTEIN, J.M. (1985). 5′-Nucleotidase from rat heart membranes. Inhibition by adenine nucleotides and related compounds. *Biochem. J.*, **226**, 645–651.

SUN, A.S., HOLLAND, J.F., OHNUMA, T. & SLANKARD-CHAHINIAN, M. (1982). 5′-Nucleotidase activity in permanent human lymphoid cell lines. Implication for cell proliferation and aging in vitro. *Biochim. Biophys. Acta*, **714**, 530–535.

ZIMMERMANN, H. (1992). 5′-Nucleotidase: molecular structure and functional aspects. *Biochem. J.*, **285**, 345–365.

(Received December 13, 1994
Revised February 28, 1995
Accepted March 16, 1995)

British Journal of Pharmacology (1995) 115, 775-780

The enantiomers of zacopride: an intra-species comparison of their potencies in functional and anxiolytic models

David J. Bill, *James Coleman, Ian Hallett, Vicki C. Middlefell, *Keith F. Rhodes & [1]Allan Fletcher

Departments of Neuropharmacology and *Molecular Pharmacology, Wyeth Research (U.K.) Ltd, Huntercombe Lane South, Taplow, Maidenhead, Berkshire SL6 0PH

1 The 5-HT_3 receptor antagonist, zacopride, and its enantiomers, R(+)-zacopride and S(−)-zacopride, were examined in three pharmacological models: (i) 5-HT-induced depolarizarion of the mouse isolated vagus nerve preparation, (ii) the 5-HT-evoked von Bezold-Jarisch reflex in the mouse, and (iii) the mouse light:dark box model of anxiety. Other standard 5-HT_3 receptor antagonists were also included for comparison in these studies.

2 Racemic zacopride, and both of the enantiomers, displayed potent 5-HT_3 receptor antagonist activity in the isolated vagus nerve and in the von Bezold-Jarisch model. No 5-HT_3 receptor agonist or partial agonist effects of these compounds were detected.

3 In the isolated vagus nerve, **R**(+)-zacopride and ondansetron were surmountable 5-HT_3 receptor antagonists (pA_2 values of 9.3 and 8.3, respectively), whereas racemic zacopride, **S**(−)-zacopride and tropisetron were insurmountable antagonists, markedly suppressing the maximum response to 5-HT.

4 *In vivo*, racemic zacopride, **R**(+)-zacopride, **S**(−)-zacopride and WAY100289 were potent antagonists of the 5-HT-evoked von Bezold-Jarisch reflex, with minimum effective doses (lowest dose required to reduce the reflex by $\geqslant 85\%$; MED_{85}) of 1.0, 3.0, 0.3 and 3.0 $\mu g\ kg^{-1}$, s.c., respectively.

5 Racemic zacopride, **R**(+)-zacopride and **S**(−)-zacopride were active in the mouse light:dark box model of anxiety, with similar potencies (minimum effective dose 1 $\mu g\ kg^{-1}$, s.c.) and similar active dose-ranges (1-1000 $\mu g\ kg^{-1}$, s.c.).

6 The doses of racemic zacopride, **R**(+)-zacopride and S(-)-zacopride required to block 5-HT_3 receptors *in vivo* correlated reasonably well with their potencies in an anxiety model within the same species. In these studies, there was no evidence of a marked difference between the anxiolytic potencies of **R**(+)-zacopride and **S**(−)-zacopride.

Keywords: Zacopride enantiomers; mouse; anxiety; von Bezold-Jarisch reflex; isolated vagus nerve; light:dark box

Introduction

A range of highly potent and selective 5-HT_3 receptor antagonists have become available (Kilpatrick *et al.*, 1990) since the development of the first of these agents, MDL72222 (Fozard, 1984) and tropisetron (ICS-205,930; Richardson *et al.*, 1985). In addition to possessing anti-emetic properties (Andrews *et al.*, 1988; Barnes *et al.*, 1991), there is some evidence from animal behavioural experiments that 5-HT_3 receptor antagonists may be useful as anxiolytics, antipsychotics, cognition-enhancers and as anti-addictive agents (Costall *et al.*, 1988b; 1990). One compound which has aroused particular interest, with regard to its functional and behavioural properties, is the substituted benzamide, zacopride, which was initially described as a selective 5-HT_3 receptor antagonist (Smith *et al.*, 1988). The zacopride molecule possesses an asymmetric centre and, therefore, exists as two distinct **R**(+)-and **S**(−)-conformational enantiomers. The first reports describing the binding and functional properties of these enantiomers indicated that, compared to **R**(+)-zacopride, the **S**(−)-form has a higher binding affinity for central (Waeber *et al.*, 1990; Pinkus *et al.*, 1990) and peripheral (Pinkus *et al.*, 1990) 5-HT_3 receptor sites in several species, and is a more potent 5-HT_3 receptor antagonist in the rat (Middlefell *et al.*, 1990; Coleman *et al.*, 1991). This difference in potency/binding affinity varied according to species and functional model, but was within the range of a 10-40 fold greater potency of the **S**(−)-, relative to the **R**(+)-enantiomer. Therefore, it was an unexpected finding that the activities of the two enantiomers differed remarkably in several behavioural models where **R**(+)-zacopride was reported to be at least 10,000 times more potent than **S**(−)-zacopride in an anxiety model, whereas the **S**(−)-enantiomer was more potent in an animal model of psychosis (Barnes *et al.*, 1990). Since these behavioural studies were performed in several species, and in view of the fact that a species variation is known to exist in the functional properties of zacopride (Middlefell *et al.*, 1990), we have compared the effects of racemic zacopride, and its two enantiomers, in models of 5-HT_3 receptor function and in an anxiety model, within the same species (the mouse). Reports of some of these data have appeared in preliminary form (Bill *et al.*, 1991; Coleman & Rhodes, 1992).

[1] Author for correspondence.

Methods

Isolated vagus nerve preparation

A grease-gap extracellular recording technique (Ireland & Tyers, 1987) was used to detect 5-HT (10 nM-1 mM)-evoked depolarizations of the mouse (male Tuck, T/O strain, 20-50 g) cervical vagus nerve. The nerve was placed in a two chamber tissue bath, one chamber being perfused (3 ml min^{-1}) with Krebs solution (2.5 mM $CaCl_2$, at 27°C, gassed with 5% CO_2 in O_2) to which drugs were added. Agonist contact time was 3 min (15 min washout) and antagonists were equilibrated for 50 min. Depolarizations were expressed as a percentage of an initial response to 5-HT (10 μM), as described previously (Rhodes *et al.*, 1992) obtained 50 min before a 5-HT concentration-response curve (CRC). One CRC only was obtained in each tissue.

Von Bezold-Jarisch reflex

Female albino Tuck T/O mice weighing 25–38 g were used throughout. Urethane anaesthetized mice (1.5–2.5 g kg^{-1}, i.p.) were cannulated in the left or right jugular vein with a luer mount Portex cannula (o.d. = 0.63 mm), and the tip advanced so that it lay in, or near the atrium. Heart rate was monitored continuously with ECG leads attached to steel needles through the fore- and hindlegs and connected to a Grass polygraph.

Bolus doses of 5-HT were injected via the jugular vein cannula at 10 min intervals to induce a reproducible bradycardia, or von Bezold-Jarisch (B-J) reflex. 5-HT was initially given in increasing doses from 30–60 $\mu g\ kg^{-1}$ in order to establish the minimum dose to give a reproducible response. The 5-HT-induced bradycardia (B-J reflex) was measured as an increase in heart period, i.e. the R-R interval measured from the ECG trace, induced by 5-HT, and expressed in ms. The increase in heart period was calculated by averaging 10 consecutive R-R intervals prior to rapid 5-HT injection, and by averaging 4 consecutive R-R intervals starting immediately following the rapid injection of a bolus dose of 50 μl of 5-HT; the increase in heart period was the difference between these two averages. The effect of the test compound on this 5-HT-induced bradycardia was measured for 1 h at 10 min intervals following subcutaneous injection of 0.1 ml of saline or test compound. Throughout the experiment, the temperature of the mice was maintained with a thermostatically-heated blanket at 37°C.

Once the dose of 5-HT required to give a reproducible B-J reflex had been established, saline or the test compound was administered subcutaneously in 0.1 ml of saline. The effect of the test compound on the B-J reflex was measured for 1 h at 10 min intervals. Results were expressed as the percentage inhibition of the B-J reflex produced by the test compound or saline. As an i.v. injection of saline accounts for a 15% increase in heart-period, the minimum effective dose was taken as the dose causing >85% inhibition of the increase in heart period (MED_{85}). Results were analysed by 2-way analysis of variance by comparing the mean response of two consecutive doses of 5-HT in the absence of the antagonist, with the response in the presence of the antagonist, for each mouse.

Light:dark box anxiety model

Female Tuck T/O mice (22–30 g; Tuck) were transferred to the laboratory at 09 h 00 min on the day of an experiment, where they were weighed and allocated to groups of nine. The laboratory was dimly illuminated (50 lux); the only illumination being that of the lighting associated with the light:dark box apparatus. Each experiment was performed between 11 h 00 min and 17 h 00 min.

The design of the two-compartment open field (light:dark box) was based on that of Crawley (1981). The apparatus comprised a rectangular open-topped box (81 × 36 × 27 cm high) divided into a smaller (27 cm long) and larger (54 cm long) compartment by a partition. The smaller compartment was painted black and illuminated by a dim red light, whereas the larger compartment was painted white and brightly illuminated by a 60 W spotlight located approximately 40 cm above the floor of the box (800 lux illumination). Free access between the two compartments was allowed by an opening

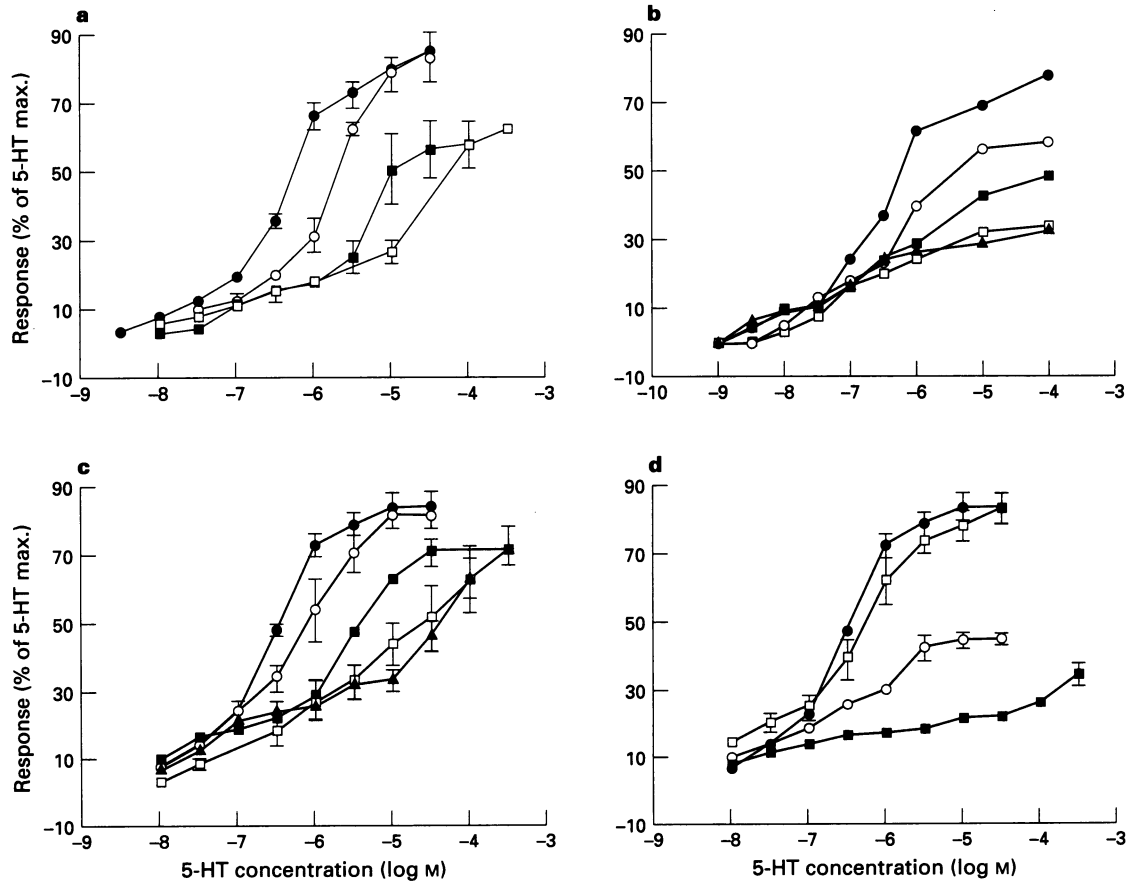

Figure 1 Effects of 5-HT_3 receptor antagonists on 5-HT-induced depolarization of the mouse isolated vagus nerve. The effects of (a) ondansetron (● control; ○ 10 nM; ■ 30 nM; □ 100 nM); (b) racemic zacopride (● control; ○ 0.3 nM; ■ 1 nM; □ 3 nM; ▲ 10 nM); (c) **R**(+)-zacopride (● control; ○ 1 nM; ■ 3 nM; □ 10 nM; ▲ 30 nM); and (d) **S**(−)-zacopride (● control; □ 0.03 nM; ○ 0.3 nM; ■ 3 nM) on the concentration-response curve (CRC) for 5-HT-induced depolarization are shown. Ondansetron and **R**(+)-zacopride caused a rightward shift of the 5-HT CRC, consistent with competitive 5-HT_3 receptor antagonism. Racemic zacopride and **S**(−)-zacopride dose-dependently depressed the maximum response to 5-HT, indicating non-competitive 5-HT_3 receptor antagonism.

(7.5 × 7.5 cm) in the centre of the partition at floor level. The following behavioural measures were monitored: (a) the number of transitions between compartments, (b) the horizontal motor activity of the mouse in the light or dark compartments (measured as crossings of a grid of lines drawn on the floor of the apparatus forming 9 cm squares), (c) the number of rearing episodes occurring in both compartments, and (d) the time spent in either compartment. A rear was defined as the raising of both forepaws clear of the floor, either unsupported or supported by a side-wall. Observations were made either live or from video-tape recordings. Thirty minutes following s.c. administration of drug or vehicle, animals were placed individually in the centre of the light compartment (facing away from the partition opening) and allowed to explore the apparatus, undisturbed, for a period of 5 min.

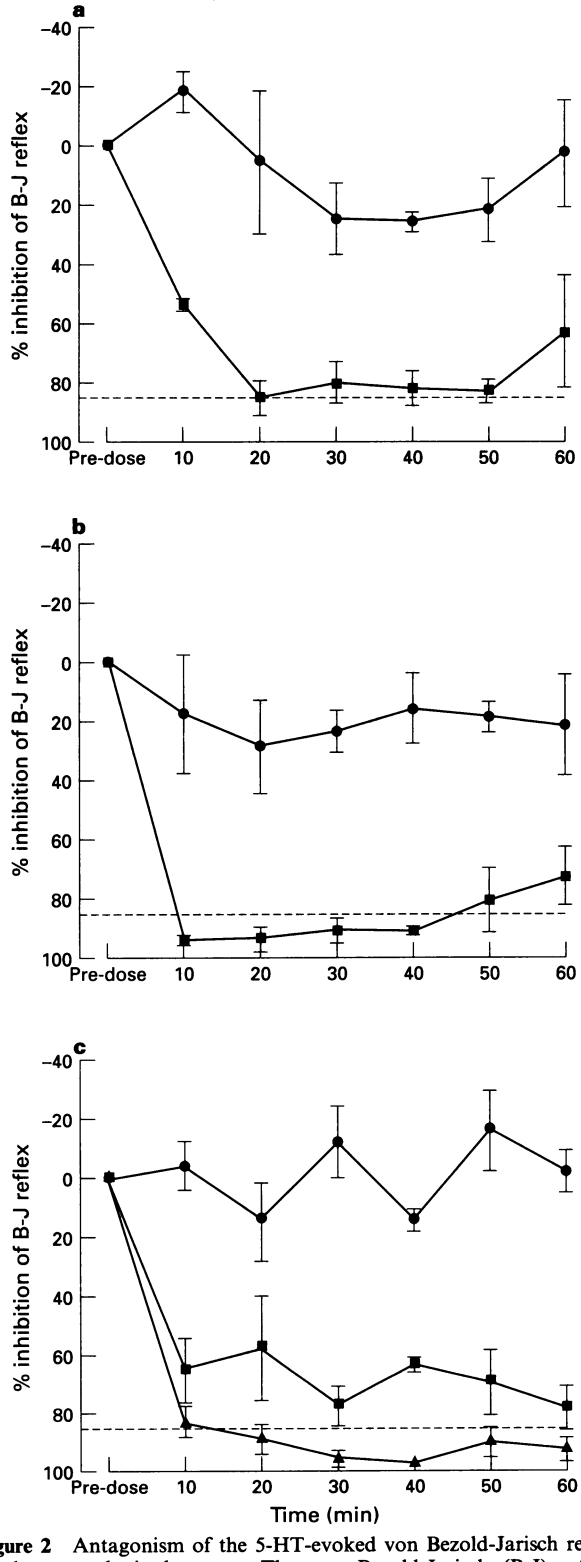

Figure 2 Antagonism of the 5-HT-evoked von Bezold-Jarisch reflex in the anaesthetized mouse. The von Bezold-Jarisch (B-J) reflex, induced by the intravenous administration of a bolus dose of 5-HT, was dose-dependently antagonized by (a) racemic zacopride (● 0.1 $\mu g\,kg^{-1}$; ■ 0.3 $\mu g\,kg^{-1}$), (b) **R**(+)-zacopride (● 1.0 $\mu g\,kg^{-1}$; ■ 3.0 $\mu g\,kg^{-1}$); or (c) S(−)-zacopride (● 0.03 $\mu g\,kg^{-1}$; ■ 0.1 $\mu g\,kg^{-1}$; ▲ 0.3 $\mu g\,kg^{-1}$) with MED_{85} values of 1.0, 3.0 or 0.3 $\mu g\,kg^{-1}$, s.c., respectively. Data are presented as mean ± s.e. mean percentage inhibition of the B-J reflex.

In all experiments the observers rating animal behaviour were unaware of the treatment each animal had received. Treatments were allocated randomly following the weighing and numbering of the animals, and experiments were balanced such that equal numbers from each treatment group were included in each experimental session. The effects of zacopride and its enantiomers were examined in a single large experiment over a period of three consecutive days using a total vehicle-treated control group size of 18 animals (i.e. 6 vehicle-treated control animals were tested on each day) in order to balance the experiment and to test for possible between-days variation in the data. It is also statistically valid to increase the size of the control group in any experiment in which a large number of different treatment groups are examined simultaneously. In addition to a vehicle-control group, a positive control group (receiving the standard anxiolytic, chlordiazepoxide; 2 $mg\,kg^{-1}$) was included in these experiments. Data were analysed by one-way ANOVA followed by Dunnett's test for comparing drug-treated groups with controls.

Drugs

Zacopride racemate and the enantiomers were prepared as hydrochloride salts in the Department of Medicinal Chemistry, Wyeth Research (U.K.) Ltd. The optical purity of the enantiomers was determined by h.p.l.c. using a chiral cellulose-carbamate column (Chiralcell OD). This method was sufficiently sensitive to detect 0.1% of one enantiomer as an impurity in the other. The (**R**)- and (**S**)-enantiomers were 98% and 97% pure, respectively. WAY 100289 (endo-N-[(8-methyl-8-azabicyclo [3.2.1] octan-3-yl) aminocarbonyl] -2- cyclopropyl-methoxybenzamide]maleate was synthesized at Wyeth Research (U.K.) Ltd.

Results

Isolated vagus nerve preparation

In control tissues a mean maximum depolarization of 0.27 (0.24–0.30) mV, ($n = 16$) was evoked by 5-HT. The CRC was monophasic with an EC_{50} of 0.39 (0.21–0.57) μM. In the presence of either ondansetron (10 nM–0.1 μM) or **R**(+)-zacopride (1–30 nM), 5-HT CRCs were displaced to the right and appeared biphasic with 5-HT (10 nM–1 μM) evoking a depolarization (first phase) of 10–20% of the 5-HT maximum response which was not displaced by increasing concentrations of antagonists. This first phase was not observed in preparations equilibrated (50 min) with 5-methoxytryptamine (10 μM) which itself evoked a mean maximum depolarization of 84.4 μV ($n = 3$) in this preparation. A second phase of the CRC to 5-HT was displaced to the right in the presence of either ondansetron or **R**(+)-zacopride (Figure 1a and c) with pA_2 values for the antagonists of 8.3 (8.0–8.9; $n = 11$) and 9.3 (9.1–9.6; $n = 16$) and Schild plot slopes of 1.1 and 1.0 respectively, consistent with a $5\text{-}HT_3$ mechanism. The S(−)-enantiomer of zacopride (0.3 and 3 nM; pIC_{50} 9.4) and racemic zacopride (0.3 nM–10 nM; pIC_{50} 9.1) markedly depressed the maximum response to 5-HT with little evidence of a rightward shift in CRC's (Figure 1b and d).

Von Bezold-Jarisch reflex

Because different injection doses of 5-HT were needed to induce a B-J reflex in different mice, the size of this reflex prior to

administration of the test compounds or saline, was variable. The mean ± s.e. mean change in heart period induced by 5-HT was 535 ± 34 ms, and ranged from 180–1761 ms ($n=76$). Following the administration of saline vehicle, a significant 5-HT-induced B-J reflex was observed at 10 min after dosing ($P<0.05$; $n=4$).

WAY100289 (3 $\mu g\ kg^{-1}$, s.c.) completely blocked the 5-HT-induced B-J reflex for at least 60 min following administration ($P<0.001$; $n=3$), whereas at a lower dose of 1.0 $\mu g\ kg^{-1}$, there was a maximum of 32% inhibition which was significant at 10, 20 and 40 min ($P<0.05$; $n=4$).

Zacopride racemate (1.0 $\mu g\ kg^{-1}$, s.c.) completely blocked the 5-HT-induced B-J reflex for at least 60 min ($P<0.001$; $n=4$; Figure 2a), whereas a dose of 0.1 $\mu g\ kg^{-1}$ showed no inhibition ($P>0.05$; $n=4$). At an intermediate dose of 0.3 $\mu g\ kg^{-1}$, although inhibition of the B-J reflex was significant for 60 min ($P<0.001$; $n=4$), the maximum inhibition was 78%. **R**(+)-zacopride blocked the 5-HT-induced B-J reflex at a dose of 3.0 $\mu g\ kg^{-1}$ ($P<0.001$; $n=4$; Figure 2b) for at least 60 min, though complete inhibition only occurred for <50 min. A lower dose of 1.0 $\mu g\ kg^{-1}$ showed only partial inhibition of 34% at 20 min after dosing ($P<0.05$; $n=4$). **S**(−)-zacopride blocked the 5-HT-induced B-J reflex at a dose of 0.3 $\mu g\ kg^{-1}$, s.c. ($P<0.001$; $n=4$; Figure 2c), whereas 0.03 $\mu g\ kg^{-1}$, s.c. showed no inhibition ($P>0.05$: $n=4$). An intermediate dose of 0.1 $\mu g\ kg^{-1}$, s.c. caused a maximum inhibition of 80% ($P<0.001$; $n=4$).

Light:dark box

Since the activity of zacopride and its enantiomers was examined in a single large experiment spread over three days, an equal number of animals from each treatment group were tested on each of the three days. Analysis of data by ANOVA revealed that there were no significant differences in behavioural measures between days for the control animals or other treatment groups (e.g. $F(2,159)=0.413$ for light compartment motor activity, and $F(2,159)=0.265$ for light compartment rears; $P>0.05$). Following subcutaneous administration, zacopride racemate, and both enantiomers, significantly increased the exploratory behaviour of mice in the light compartment (Table 1). All three compounds had similar minimum effective doses, i.e. the minimum dose which induced a significant ($P<0.05$) increase in light compartment rearing was 0.001 mg kg^{-1}, s.c. Both enantiomers also significantly ($P<0.05$) increased light compartment motor activity with a minimum effective dose of 0.001 mg kg^{-1}, s.c. Although ANOVA revealed no significant effect of treatment on time spent in the light compartment ($F(16,145)=1.40$), doses of zacopride and the enantiomers which induced significant increases in light compartment exploration also appeared to increase time spent in the light compartment. The effects of the positive control (chlordiazepoxide, 2 mg kg^{-1}, s.c.) were similar to those of zacopride and its enantiomers.

Discussion

To our knowledge, the data from our mouse isolated vagus nerve and von Bezold-Jarisch studies provide the first published information (Bill *et al.*, 1991) on the functional activity of zacopride and its enantiomers in this species. A previous study (Newberry *et al.*, 1991) compared the pharmacological properties of the 5-HT_3 receptor in isolated superior cervical ganglia from the mouse, rat and guinea-pig. The latter study, and our own data (Coleman *et al.*, 1991; Coleman & Rhodes, 1992), indicate that the pharmacological properties of the mouse and rat 5-HT_3 receptors are similar, but differ markedly from the receptors in other species, such as the guinea-pig (Lattimer *et al.*, 1989). The activity of zacopride and its enantiomers in the mouse isolated vagus nerve preparation was very similar to that demonstrated in the corresponding rat preparation (Coleman *et al.*, 1991), i.e. **R**(+)-zacopride was a potent and surmountable 5-HT_3 receptor antagonist, whereas the racemate and **S**(−)-zacopride were more potent, but insurmountable, antagonists. These *in vitro* functional data were reflected in the results of the mouse B-J reflex studies, in which the racemate and the **R**(+)- and **S**(−)-enantiomers displayed 5-HT_3 receptor antagonist actions, with potencies (MED_{85} values) of 1.0, 3.0 and 0.3 $\mu g\ kg^{-1}$, s.c., respectively. In terms of measuring 5-HT_3 receptor antagonist potency, therefore, the results of these functional studies are unremarkable, in that the zacopride molecule displays a stereoselective interaction with the 5-HT_3 receptor; the **R**(+)-enantiomer being less potent than the **S**(−)-enantiomer. These results are consistent with published data showing that the **S**(−)-enantiomer binds with

Table 1 Effects of zacopride racemate and enantiomers on mouse light:dark box activity

	Exploratory activity						
	Light section			*Dark section*			
Treatment (mg kg^{-1} s.c)	*Activity*	*Rears*	*Time (s)*	*Activity*	*Rears*	*Times (s)*	*Transitions*
Vehicle (saline)	68 ± 5	15 ± 2	133 ± 6	109 ± 8	36 ± 2	167 ± 6	18 ± 1
S-zacopride (0.0001)	71 ± 7	16 ± 3	136 ± 10	101 ± 10	35 ± 3	164 ± 10	18 ± 1
S-zacopride (0.001)	109 ± 11*	24 ± 2*	158 ± 9	89 ± 5	27 ± 3	142 ± 9	19 ± 2
S-zacopride (0.01)	105 ± 13*	25 ± 4*	154 ± 7	90 ± 7	30 ± 3	146 ± 7	23 ± 3
S-zacopride (0.1)	94 ± 19	23 ± 6	151 ± 8	97 ± 5	29 ± 2	149 ± 8	17 ± 3
S-zacopride (1.0)	94 ± 10	20 ± 3	144 ± 9	92 ± 7	28 ± 2	156 ± 9	20 ± 2
R-zacopride (0.0001)	69 ± 6	14 ± 2	134 ± 5	101 ± 5	30 ± 2	166 ± 5	18 ± 1
R-zacopride (0.001)	102 ± 7*	27 ± 3*	157 ± 6	89 ± 6	32 ± 3	143 ± 6	18 ± 2
R-zacopride (0.01)	116 ± 13*	29 ± 4*	152 ± 9	102 ± 6	32 ± 4	148 ± 9	25 ± 3*
R-zacopride (0.1)	108 ± 12*	25 ± 4*	159 ± 6	95 ± 6	31 ± 4	141 ± 6	21 ± 1
R-zacopride (1.0)	87 ± 9	19 ± 4	154 ± 11	83 ± 7	29 ± 3	146 ± 11	17 ± 1
Zacopride (0.0001)	63 ± 10	15 ± 4	133 ± 7	92 ± 7	32 ± 4	167 ± 7	14 ± 2
Zacopride (0.001)	96 ± 9	25 ± 4*	159 ± 8	91 ± 6	29 ± 2	141 ± 8	21 ± 1
Zacopride (0.01)	104 ± 10*	29 ± 3*	151 ± 9	98 ± 7	32 ± 4	149 ± 9	22 ± 2
Zacopride (0.1)	108 ± 15*	20 ± 4	149 ± 9	106 ± 8	36 ± 4	151 ± 9	24 ± 3
Zacopride (1.0)	103 ± 9*	25 ± 3*	153 ± 11	100 ± 7	34 ± 4	147 ± 11	21 ± 2
Chlordiazepoxide (2.0)	103 ± 6*	28 ± 2*	145 ± 8	96 ± 7	31 ± 3	155 ± 8	21 ± 2
ANOVA values $F(16,145)=$	2.75	2.28	1.40	1.02	0.82	1.40	2.14
	$P=0.001$	$P=0.005$	$P=0.15$	$P=0.44$	$P=0.66$	$P=0.15$	$P=0.009$

All values are means ± s.e.mean ($n=9$, except for the vehicle controls where $n=18$) and represent total values recorded over a 5 min test session. Activity refers to horizontal motor activity measured as the number of line crossings.
*$P<0.05$ (one-way ANOVA followed by Dunnett's test for comparing all drug-treated groups with the vehicle-treated control).

higher affinity to the 5-HT_3 receptor, than the **R**(+)-enantiomer (Pinkus *et al.*, 1990; Waeber *et al.*, 1990). Although both enantiomers are 5-HT_3 receptor antagonists in the mouse, there is clearly a species variation in their functional activity, i.e. in the ferret the **R**(+)-enantiomer is a 5-HT_3 antagonist but the S(−)-enantiomer is a 5-HT_3 receptor agonist or partial agonist (Middlefell & Price, 1991). It is not known whether this latter property of S(−)-zacopride is related to its non-competitive interaction with the mouse 5-HT_3 receptor.

The results of our functional studies would predict, assuming that there are no significant differences between central and peripheral 5-HT_3 receptors in the mouse, that racemic zacopride and both of the enantiomers should be active in the mouse light:dark box behavioural model. In our hands this prediction was generally confirmed, i.e. the subcutaneous administration of racemic zacopride, the **R**(+)-enantiomer or the S(−)-enantiomer, induced significant increases in the light compartment exploratory behaviour, with similar potencies and active dose-ranges. Allowing for the 10 fold dose-step used in these latter studies (necessary to encompass a wide dose-range) and for the inherently less quantitative nature of the behavioural model, the potencies of the racemate and enantiomers in the anxiety paradigm were consistent with their potencies in the mouse B-J reflex model (and were in the same rank order as determined in the mouse vagus nerve assay). The potencies of another selective 5-HT_3 receptor antagonist, WAY100289 (Bradley *et al.*, 1992; Rhodes *et al.*, 1993), in the functional and behavioural models also correspond closely (MED_{85} in the mouse B-J reflex = 3 $\mu g\ kg^{-1}$, s.c.; MED in the mouse light:dark box (Bill *et al.*, 1992) = 10 $\mu g\ kg^{-1}$, s.c.). Therefore, it appears reasonable to conclude that the activity of 5-HT_3 receptor antagonists in the mouse light:dark box anxiety model is a result of central 5-HT_3 receptor blockade; a conclusion that is further supported by the observation that the quaternary ammonium analogue of ICS-205,930, which enters the brain less readily than the parent compound, is not active in the light:dark box (Bill *et al.*, 1992) despite being a potent 5-HT_3 receptor antagonist (Watling *et al.*, 1988).

The results of our behavioural studies on the enantiomers of zacopride differ markedly from those published previously (Barnes *et al.*, 1990; Young & Johnson, 1991) in which the **R**(+)-enantiomer was remarkably potent in anxiety models. In these studies **R**(+)-zacopride was active at doses of 0.00001 mg kg^{-1}, i.p., or greater, in the mouse light:dark box, and the minimum effective dose of zacopride racemate was 0.0001 mg kg^{-1}, i.p. (Costall *et al.*, 1988a), whereas the S(−)-enantiomer was inactive up to a dose of 100 mg kg^{-1}, i.p. (Barnes *et al.*, 1990). It has been suggested (Barnes *et al.*, 1992) that the use of different strains of mouse in the light:dark box may be one reason for such inter-laboratory differences in data obtained from this anxiety model. However, this may not be a viable explanation, since we have found that the potencies of several 5-HT_3 receptor antagonists (Bill *et al.*, 1992) and 5-HT_{1A} ligands (Bill *et al.*, 1989) are similar to those reported previously (Costall *et al.*, 1990). There is a tendency for the latter data to report slightly higher drug potencies than measured in our hands but this would not explain why such a small difference in the sensitivity of the methods used would have opposing effects on the potencies of the two enantiomers of zacopride, i.e. we find the (**R**)-enantiomer to be less potent and the (**S**)-enantiomer to be more potent than in the previous studies of Barnes *et al.* (1990) and Young & Johnson (1991).

There does not appear to be an obvious explanation for the reported marked differences in the CNS actions of the two enantiomers of zacopride. However, the results of our studies indicate that the anxiolytic potencies, at least, of the racemate and enantiomers do not differ widely and appear to fall within the range of the potency differences determined using an *in vivo* model of 5-HT_3 receptor function in the same species. It has also been reported (File & Andrews, 1993) that both enantiomers of zacopride had similar potencies for reversal of the anxiogenic effect of diazepam withdrawal in the rat elevated plus maze. The close correlation between functional and anxiolytic potencies of 5-HT_3 receptor antagonists in the present paper may indicate that any anxiolytic (or other behavioural) effects of very low doses of **R**(+)-zacopride obtained in some previous studies may not be a consquence of 5-HT_3 receptor antagonism.

References

ANDREWS, P.L.R., RAPEPORT, W.G. & SANGER, G.J. (1988). Neuropharmacology of emesis induced by anti-cancer therapy. *Trends Pharmacol. Sci.*, **9**, 334–341.

BARNES, J.M., BARNES, N.M., COSTALL, B., DOMENEY, A.M., JOHNSON, D.N., KELLY, M.E., MUNSON, H.R., NAYLOR, R.J. & YOUNG, R. (1990). The differential activities of R(+)- and S(−)-zacopride as 5-HT_3 receptor antagonists. *Pharmacol. Biochem. Behav.*, **37**, 717–727.

BARNES, J.M., BARNES, N.M., COSTALL, B. & NAYLOR, R.J. (1991). Development of 5-HT_3 receptor antagonists as anti-emetics. *Pharmac. J.*, **246**, 112–114.

BARNES, N.M., COSTALL, B., GE, J., KELLY, M.E. & NAYLOR, R.J. (1992). The interaction of R(+)- and S(−)-zacopride with PCPA to modify rodent aversive behaviour. *Eur. J. Pharmacol.*, **218**, 15–25.

BILL, D.J., FLETCHER, A., GLENN, B.D. & KNIGHT, M. (1992). Behavioural studies on WAY100289, a novel 5-HT_3 receptor antagonist, in two animal models of anxiety. *Eur. J. Pharmacol.*, **218**, 327–334.

BILL, D.J., FLETCHER, A., HALLETT, I. & MIDDLEFELL, V.C. (1991). The enantiomers of zacopride: correlation of anxiolytic activity with *in vivo* functional 5-HT_3 antagonism in the mouse. *Br. J. Pharmacol.*, **104**, 250P.

BILL, D.J., FLETCHER, A. & KNIGHT, M. (1989). Actions of 5-HT_{1A} ligands and standard anxiolytics on mouse exploratory behaviour in a two-compartment light:dark arena. *Br. J. Pharmacol.*, **98**, 679P.

BRADLEY, G., WARD, T.J., WHITE, J.C., COLEMAN, J., TAYLOR, A. & RHODES, K.F. (1992). Novel antagonists of the 5-HT_3 receptor. Synthesis and structure-activity relationships of (2-alkoxybenzoyl) ureas. *J. Med. Chem.*, **35**, 1515–1520.

COLEMAN, J., LATTIMER, N., RHODES, K.F. & SAVILLE, L. (1991). 5-HT_3- and 5-HT_4-like actions of the enantiomers of zacopride in some *in vitro* functional assays. *Br. J. Pharmacol.*, **104**, 249P.

COLEMAN, J. & RHODES, K.F. (1992). The 5-HT_3 receptor antagonist actions of the enantiomers of zacopride and some other antagonists in the mouse isolated vagus nerve. *Br. J. Pharmacol.*, **107**, 451P.

COSTALL, B., DOMENEY, A.M., GERRARD, P.A., KELLY, M.E. & NAYLOR, R.J. (1988a). Zacopride: anxiolytic profile in rodent and primate models of anxiety. *J. Pharm. Pharmacol.*, **40**, 302–305.

COSTALL, B., NAYLOR, R.J. & TYERS, M.B. (1988b). Recent advances in the neuropharmacology of 5-HT_3 agonists and antagonists. *Rev. Neurosci.*, **2**, 41–65.

COSTALL, B., NAYLOR, R.J. & TYERS, M.B. (1990). The psychopharmacology of 5-HT_3 receptors. *Pharmacol. Ther.*, **47**, 181–202.

CRAWLEY, J.N. (1981). Neuropharmacological specificity of a simple animal model for the behavioural actions of benzodiazepines. *Pharmac. Biochem. Behav.*, **15**, 695–699.

FILE, S.E. & ANDREWS, N. (1993). Enhanced anxiolytic effect of zacopride enantiomers in diazepam-withdrawn rats. *Eur. J. Pharmacol.*, **237**, 127–130.

FOZARD, J.R. (1984). MDL72222: a potent and highly selective antagonist at neuronal 5-hydroxytryptamine receptors. *Naunyn-Schmied. Arch. Pharmacol.*, **326**, 36–44.

IRELAND, S.J. & TYERS, M.B. (1987). Pharmacological characterisation of 5-hydroxytryptamine-induced depolarisation of the rat isolated vagus nerve. *Br. J. Pharmacol.*, **90**, 229–238.

KILPATRICK, G.J., BUNCE, K.T. & TYERS, M.B. (1990). 5-HT_3 receptors. *Med. Res. Rev.*, **10**, 441–475.

LATTIMER, N., RHODES, K.F. & SAVILLE, V.L. (1989). Possible differences in 5-HT_3-like receptors in the rat and the guinea-pig. *Br. J. Pharmacol.*, **96,** 270P.

MIDDLEFELL, V.C., PRICE, T.L. & THOMSON, I.A. (1990). 5-HT_3 agonist effects of zacopride in the ferret. *Br. J. Pharmacol.*, **101,** 560P.

MIDDLEFELL, V.C. & PRICE, T.L. (1991). 5-HT_3 receptor agonism may be responsible for the emetic effects of zacopride in the ferret. *Br. J. Pharmacol.*, **103,** 1011–1012.

NEWBERRY, N.R., CHESHIRE, S.H. & GILBERT, M.J. (1991). Evidence that the 5-HT_3 receptors of the rat, mouse and guinea-pig superior cervical ganglion may be different. *Br. J. Pharmacol.*, **102,** 615–620.

PINKUS, L.M., SARBIN, N.S., GORDON, J.C. & MUNSON, H.R. (1990). Antagonism of [^{3}H]zacopride binding to 5-HT_3 recognition sites by its (R) and (S) enantiomers. *Eur. J. Pharmacol.*, **179,** 231–235.

RHODES, K.F., COLEMAN, J. & LATTIMER, N. (1992). A component of 5-HT-evoked depolarization of the rat isolated vagus nerve is mediated by a putative 5-HT_4 receptor. *Naunyn Schmied. Arch. Pharmacol.*, **346,** 496–503.

RHODES, K.F., MIDDLEFELL, V.C., LATTIMER, N., BRAMMER, N.T., COLEMAN, J., TAYLOR, A.P., SAVILLE, V.L. & WARD, T.J. (1993). WAY100289: Pharmacological profile of a novel 5-HT_3 receptor antagonist. *Drug Dev. Res.*, **28,** 128–140.

RICHARDSON, B.P., ENGEL, G., DONATSCH, P. & STADLER, P.A. (1985). Identification of serotonin M-receptor subtypes and their specific blockade by a new class of drugs. *Nature*, **316,** 126–131.

SMITH, W.L., SANCILIO, L.F., OWERA-ATEPO, J.B., NAYLOR, R.J. & LAMBERT, L. (1988). Zacopride, a potent 5-HT_3 antagonist. *J. Pharm. Pharmacol.*, **40,** 301–302.

WAEBER, C., PINKUS, L.M. & PALACIOS, J.M. (1990). The (S)-isomer of [^{3}H]zacopride labels 5-HT_3 receptors with high affinity in rat brain. *Eur. J. Pharmacol.*, **181,** 283–287.

WATLING, K.J., ASPLEY, S., SWAIN, C.J. & SAUNDERS, J. (1988). [^{3}H]-Quarternised ICS 205,930 labels 5-HT_3 receptor binding sites in rat brain. *Eur. J. Pharmacol.*, **149,** 397–398.

YOUNG, R. & JOHNSON, D.N. (1991). Anxiolytic-like activity of R(+)-and S(−)-zacopride in mice. *Eur. J. Pharmacol.*, **201,** 151–155.

(Received February 15, 1995
Revised March 16, 1995
Accepted March 20, 1995)

British Journal of Pharmacology (1995) 115, 781-786

Noradrenaline contractions of human prostate mediated by α_{1A}-(α_{1c}-) adrenoceptor subtype

[1]Ian Marshall, Richard P. Burt & *Christopher R. Chapple

Department of Pharmacology, University College London, Gower Street, London WC1E 6BT and *Department of Urology, The Royal Hallamshire Hospital, Glossop Road, Sheffield S10 2JF

1 The subtype of α_1-adrenoceptor mediating contractions of human prostate to noradrenaline was characterized by use of a range of competitive and non-competitive antagonists.

2 Contractions of the prostate to either noradrenaline (pD_2 5.5), phenylephrine (pD_2 5.1) or methoxamine (pD_2 4.4) were unaltered by the presence of neuronal and extraneuronal uptake blockers. Noradrenaline was about 3 and 10 times more potent than phenylephrine and methoxamine respectively. Phenylephrine and methoxamine were partial agonists.

3 Pretreatment with the alkylating agent, chlorethylclonidine (10^{-4} M) shifted the noradrenaline concentration-contraction curve about 3 fold to the right and depressed the maximum response by 31%. This shift is 100 fold less than that previously shown to be produced by chlorethylclonidine under the same conditions on α_{1B}-adrenoceptor-mediated contractions.

4 Cumulative concentration-contraction curves for noradrenaline were competitively antagonized by WB 4101 (pA_2 9.0), 5-methyl-urapidil (pA_2 8.6), phentolamine (pA_2 7.6), benoxathian (pA_2 8.5), spiperone (pA_2 7.3), indoramin (pA_2 8.2) and BMY 7378 (pA_2 6.6). These values correlated best with published pK_i values for their displacement of [^{3}H]-prazosin binding on membranes expressing cloned α_{1c}-adrenoceptors and poorly with values from cloned α_{1b}- and α_{1d}-adrenoceptors.

5 The good correlation between the functional data on the prostate and the binding data on the expressed α_{1c}-subtype clone for the affinities of the competitive antagonists suggests that they are the same subtype. As the expressed α_{1c}-adrenoceptor clone corresponds to the α_{1A}-adrenoceptor expressed in tissues, contraction of the human prostate to noradrenaline is therefore mediated by an α_{1A}-adrenoceptor.

Keywords: α_1-Adrenoceptor subtypes; human prostate; chlorethylclonidine; WB 4101; 5-methyl-urapidil; phentolamine; benoxathian; spiperone; indoramin; BMY 7378

Introduction

Benign prostatic hyperplasia is frequent in elderly males with a prevalence of 43% in those over 65 displaying some symptoms (Garraway *et al.*, 1991). Bladder outlet obstruction caused by this condition has two components: static, related to cellular mass and dynamic, related to prostatic smooth muscle tone. One pharmacological approach in treatment is to relax prostatic smooth muscle by antagonizing α_1-adrenoceptors.

It has been known for many years that stimulation of the pre-sacral sympathetic nerves in man causes the prostate to contract (Learmonth, 1931). Subsequent work has shown that α-adrenoceptors mediate contraction of the prostate (Caine *et al.*, 1975) and ligand binding experiments revealed both α_1- and α_2-adrenoceptors, the former predominating in the stroma (Chapple *et al.*, 1989; James *et al.*, 1989). Experiments on isolated prostatic tissue showed that it was only the α_1-adrenoceptors which mediated contraction of the tissue (Hieble *et al.*, 1985; Chapple *et al.*, 1989). These studies provided a scientific basis for the use of selective α_1-adrenoceptor antagonists e.g. prazosin, in the treatment of benign prostatic hyperplasia (e.g. Chapple *et al.*, 1990) after initial trials with phenoxybenzamine (Caine *et al.*, 1978). While prazosin may provide symptomatic relief including improved urinary flow rate, there is a therapeutic ceiling to the dose that can be employed due to side effects e.g. hypotension, which also arise from α_1-adrenoceptor antagonism.

Recent research has demonstrated heterogeneity of α_1-adrenoceptors using both pharmacological analysis and receptor cloning. Thus α_{1A}- and α_{1B}-adrenoceptors can be distinguished in functional and ligand binding experiments by their sensitivity to the alkylating agent, chlorethylclonidine and by their affinities for a number of competitive antagonists such as WB 4101 and 5-methyl urapidil (Morrow & Creese, 1986; Gross *et al.*, 1988; Han *et al.*, 1987a,b). The α_{1A} subtype is relatively insensitive to chlorethylclonidine and has a high affinity for WB 4101 and 5-methyl urapidil while the opposite is true for the α_{1B} subtype. On the basis of these selectivities the α_1-adrenoceptor mediating contraction of smooth muscle in several tissues has been characterized. For example, in the rat epididymal vas deferens, contractions are mediated via α_{1A}-adrenoceptors while in the spleen they are mediated via α_{1B}-adrenoceptors (Aboud *et al.*, 1993; Burt *et al.*, 1995).

Molecular cloning studies have identified three subtypes of the α_1-adrenoceptor, α_{1b}, α_{1c} and α_{1d} (upper case letters refer to pharmacologically defined subtypes and lower case letters to those defined by molecular biology; Bylund *et al.*, 1994). All three subtypes have been cloned from both rat and human cDNA libraries (Lomasney *et al.*, 1991; Bruno *et al.*, 1991; Ramarao *et al.*, 1992; Laz *et al.*, 1993; Hirasawa *et al.*, 1993) and are expressed tissue-dependently in both species (Rokosh *et al.*, 1994; Price *et al.*, 1994). The α_{1b} clone when expressed in cell lines that have been transfected with the cDNA for this subtype and the tissue α_{1B} adrenoceptor have very similar pharmacological profiles (Lomasney *et al.*, 1991). The α_{1d} subtype clone when expressed in cells was originally thought to correspond to the classical α_{1A} subtype and was therefore called the α_{1a} clone (Lomasney *et al.*, 1991). However, a near identical clone was isolated which had a different pharmacology from the α_{1A} or α_{1B} subtypes and was therefore called the α_{1d} clone (Perez *et al.*, 1991). Schwinn & Lomasney (1992) then agreed that their clone was the same subtype as that cloned by

[1] Author for correspondence.

Perez *et al.* (1991), and also had a different pharmacology from the α_{1A} subtype. There is currently little evidence for functional α_{1D}-adrenoceptors although they may be present in the rat vasculature (Saussy *et al.*, 1994). The α_{1c} clone is now considered to represent the classical α_{1A} subtype found in tissues (Laz *et al.*, 1993; Perez *et al.*, 1994; Burt *et al.*, 1995). The α_{1c} clone was originally isolated from a bovine brain cDNA library and although it had a very similar pharmacology to the α_{1A}-adrenoceptor, it was thought to represent a new subtype as it was also chlorethylclonidine-sensitive (Schwinn *et al.*, 1990). However, the degree to which it is sensitive to chlorethylclonidine has been questioned recently and it may only be partially sensitive, at least in the rat (Forray *et al.*, 1994a).

All three α_1-adrenoceptor clones have been found to be expressed in the human prostate by RNAse protection assay and quantitative solution hybridization assays showed that the predominant subtype expressed was the α_{1c}-adrenoceptor. The mRNA for this subtype was also found to be predominantly expressed in the stromal (fibromuscular) compartment by *in situ* hybridization (Price *et al.*, 1993).

These findings raise the possibility that the α_1-adrenoceptor subtype in the prostate might differ from that in the vasculature. Therefore the aim of the present experiments was to use drugs with known subtype selectivity to characterize pharmacologically the α_1-adrenoceptor in the prostate as a step in the development of prostate-selective α_1-adrenoceptor antagonists for treatment of benign prostatic hyperplasia. A preliminary account of some of these results has been published (Marshall *et al.*, 1992).

Methods

Prostatic chips taken from patients undergoing transurethral resection for benign prostatic hyperplasia (age 60–85 years, $n=12$) were collected in Tyrode solution and stored overnight at 4°C for experimental use the next day. Prostatic chips (about 20 mm × 4 mm × 2 mm) were selected which contained the most smooth muscle. They were suspended in Tyrode solution (composition mM: Na^+ 149, Cl^- 141, HCO_3^- 12, D-glucose 5.6, HPO_4^{2-} 0.3, K^+ 2.7, Mg^{2+} 0.5 and Ca^{2+} 1.8) at 37°C in 5 ml tissue baths and bubbled with 95%O_2/5%CO_2. The strips were placed under 1 g resting tension, and equilibrated for 1 h. Changes in isometric tension were measured with Grass FT.03 transducers and recorded by Biopac Systems Inc. MP100WS for Windows.

Cumulative additions of noradrenaline were added to each tissue to produce concentration-response curves as the response to noradrenaline was maintained and the maximum response was not much different to a single dose of noradrenaline producing a maximal response. After 1 h the curve was then either repeated, or repeated in the presence of cocaine and β-oestradiol (both 10^{-5} M), or in the presence of an antagonist (equilibrated with the tissue for 30 min). In some tissues a concentration-effect curve to another agonist was measured. The alkylating agent chlorethylclonidine was incubated with the tissue for 30 min and then washed out for 30 min. The effect of the highest concentration of dimethylsulphoxide DMSO (0.01%) resulting in the tissue bath due to the stock solution of some compounds being dissolved in it, was also measured on the noradrenaline repeat curve.

Data analysis

All the responses were calculated as percentage maximum response to noradrenaline in the initial curve and plotted as the mean ± s.e.mean of 3 or 4 separate experiments. For the competitive antagonists, WB 4101, 5-methyl urapidil, phentolamine, benoxathian, spiperone, indoramin and BMY 7378, Schild plots were constructed from the dose-ratios obtained to calculate their pA_2 values (Arunlakshana & Schild, 1959). Curve fitting for the calculation of EC_{50} values by non linear regression and linear regression for the calculation of pA_2 values was performed using InPlot (GraphPAD Software, San Diego, Calif., U.S.A.). Dose-ratios were calculated using the second concentration-response curve in the absence and presence of the antagonists.

Drugs and solutions

WB 4101 (2(2,6-dimethoxyphenoxyethyl)amino-methyl-1,4-benzodioxane hydrochloride) and chlorethylclonidine were donated by Pfizer Central Research, Kent. Noradrenaline bitartrate, phenylephrine hydrochloride, methoxamine hydrochloride, cocaine hydrochloride, β-oestradiol and phentolamine were obtained from Sigma and 5-methyl-urapidil, benoxathian hydrochloride, spiperone hydrochloride and BMY

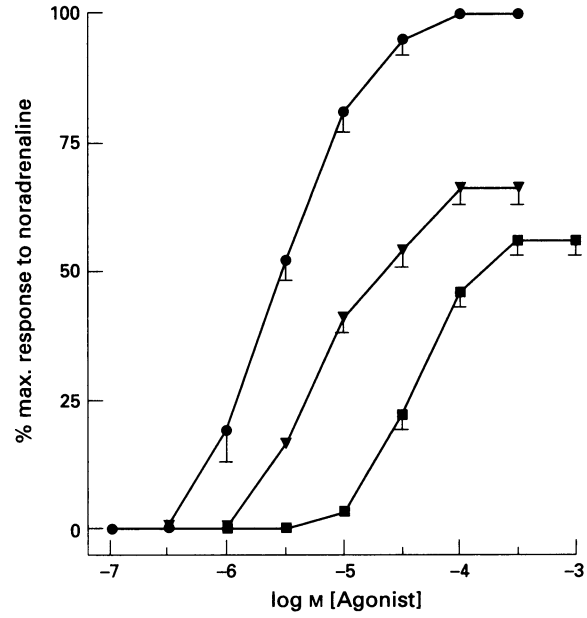

Figure 1 Cumulative concentration-effect curves for noradrenaline (●), phenylephrine (▼), and methoxamine (■), in human prostate. Each plot represents the mean with s.e.mean of at least 4 separate experiments.

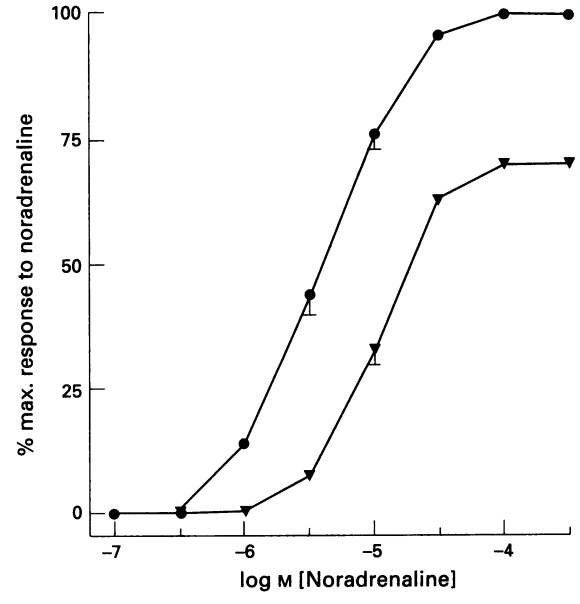

Figure 2 The effect of chlorethylclonidine on contractions to noradrenaline in human prostate. Control (●); plus chlorethylclonidine 10^{-4} M (▼). Each plot represents the mean with s.e.mean of at least 4 separate experiments.

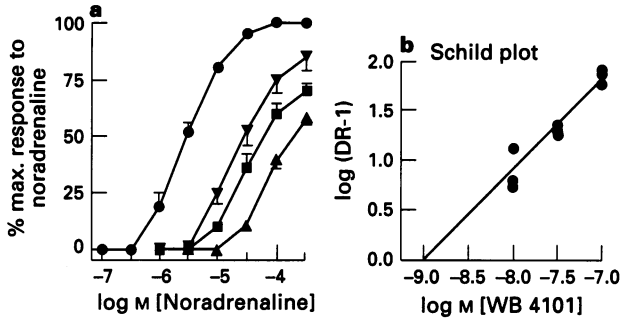

Figure 3 Antagonism of contractions to noradrenaline in human prostate by WB 4101. (a) Control (●); plus WB 4101 1×10^{-8} M (▼), 3×10^{-8} M (■), 1×10^{-7} M (▲). Each plot represents the mean with s.e.mean of at least 4 separate experiments. (b) Schild plot using dose ratios from (a).

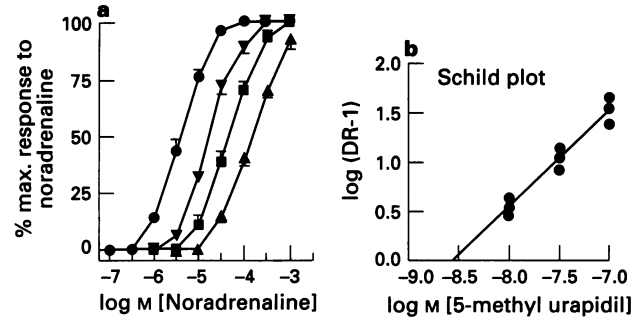

Figure 4 Antagonism of contractions to noradrenaline in human prostate by 5-methyl urapidil. (a) Control (●); plus 5-methyl urapidil 1×10^{-8} M (▼), 3×10^{-8} M (■), 1×10^{-7} M (▲). Each plot represents the mean with s.e.mean of at least 3 separate experiments. (b) Schild plot using dose ratios from (a).

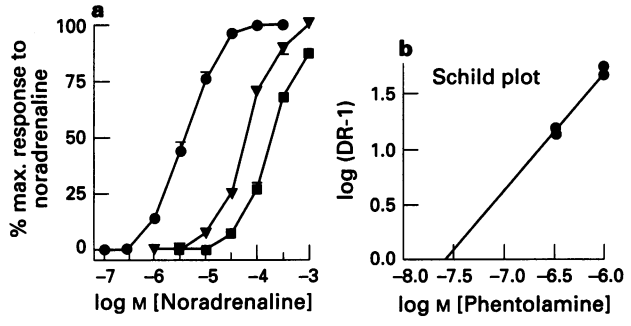

Figure 5 Antagonism of contractions to noradrenaline in human prostate by phentolamine. (a) Control (●); plus phentolamine 3×10^{-7} M (▼), 1×10^{-6} M (■). Each plot represents the mean with s.e.mean of at least 3 separate experiments. (b) Schild plot using dose ratios from (a).

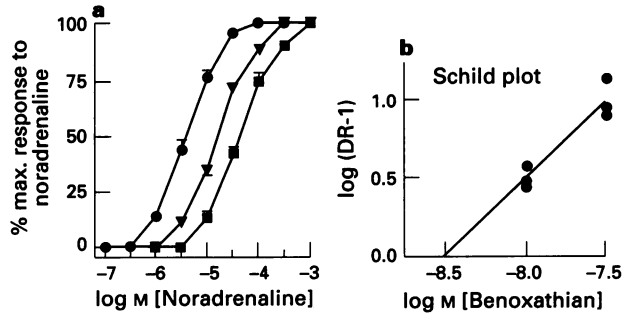

Figure 6 Antagonism of contractions to noradrenaline in human prostate by benoxathian. (a) Control (●); plus benoxathian 1×10^{-8} M (▼), 3×10^{-8} M (■). Each plot represents the mean with s.e.mean of at least 3 separate experiments. (b) Schild plot using dose ratios from (a).

7378 dihydrochloride (8[2-[4-(2-methoxyphenyl)-1-piperazinyl]ethyl]-8-azaspiro[4,5]decane-7,9-dione dihydrochloride) were obtained from RBI. All stock solutions were made in distilled water and diluted to working concentrations in Krebs solution except for spiperone and β-oestradiol which were dissolved in DMSO first, then diluted in Krebs solution. Stock solutions of antagonists were stored frozen while agonists were prepared fresh each day.

Results

Noradrenaline produced a dose-dependent contraction of the human prostate and the repeat concentration-effect curve was not significantly different from the initial curve (pD_2 5.5 ± 0.1, maximum response 0.66 ± 0.07 g, Figure 1). The responses to noradrenaline were not affected by the highest concentration

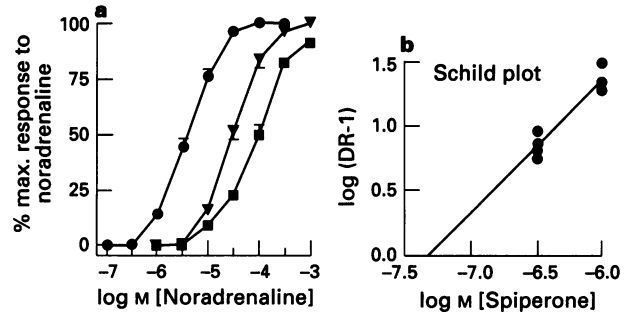

Figure 7 Antagonism of contractions to noradrenaline in human prostate by spiperone. (a) Control (●); plus spiperone 3×10^{-7} M (▼), 1×10^{-6} M (■). Each plot represents the mean with s.e.mean of at least 3 separate experiments. (b) Schild plot using dose ratios from (a).

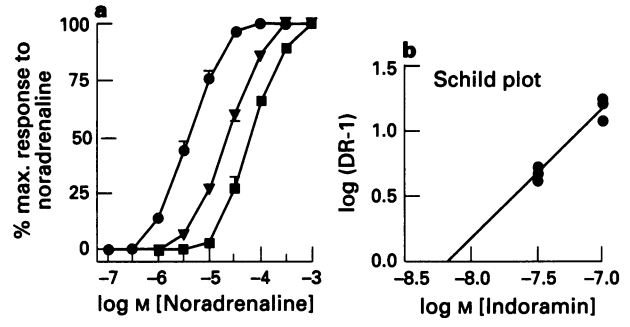

Figure 8 Antagonism of contractions to noradrenaline in human prostate by indoramin. (a) Control (●); plus indoramin 3×10^{-8} M (▼), 1×10^{-7} M (■). Each plot represents the mean with s.e.mean of at least 3 separate experiments. (b) Schild plot using dose ratios from (a).

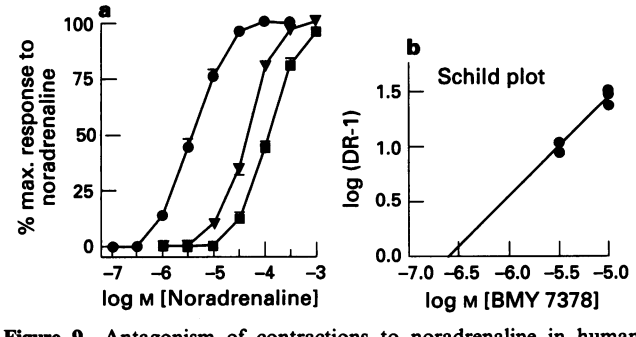

Figure 9 Antagonism of contractions to noradrenaline in human prostate by BMY 7378. (a) Control (●); plus BMY 7378, 3×10^{-6} M (▼), 1×10^{-5} M (■). Each plot represents the mean with s.e.mean of at least 3 separate experiments. (b) Schild plot using dose ratios from (a).

Table 1 Comparison of pA_2 values for the antagonists with their published pK_i on cloned subtypes

Antagonist	pK_i on cloned α_1-adrenoceptors expressed in cells* α_{1b}	α_{1c}	α_{1d}	pA_2 human prostate
Prazosin	9.6±0.2	9.2±0.2	9.4±0.2	8.5[1]
WB4101	8.2±0.1	9.5±0.3	9.2±0.1	9.0
5-methyl urapidil	6.8±0.3	8.8±0.1	7.3±0.3	8.6
Phentolamine	7.3±0.2	8.1±0.3	7.6±0.2	7.6
Benoxathian	7.8	9.0	8.7	8.5
Spiperone	8.3±0.2	7.9±0.3	7.9±0.2	7.3
Indoramin	7.3±0.1	8.2±0.3	6.8±0.2	8.2
BMY 7378	7.2	6.6	9.4	6.6

*Data are mean±s.e.mean for values from Faure *et al.*, 1994; Forray *et al.*, 1994b; Kenny *et al.*, 1994a,b; Testa *et al.*, 1994; Goetz *et al.*, 1995 (no s.e.mean for compounds with only one or two values). In each study the hamster α_{1b}, bovine α_{1c} and rat α_{1d} clones were used except for Goetz *et al.* (1995) and Forray *et al.* (1994b) where the three human α_1-subtype clones were used.
[1]Data from Marshall *et al.* (1992).

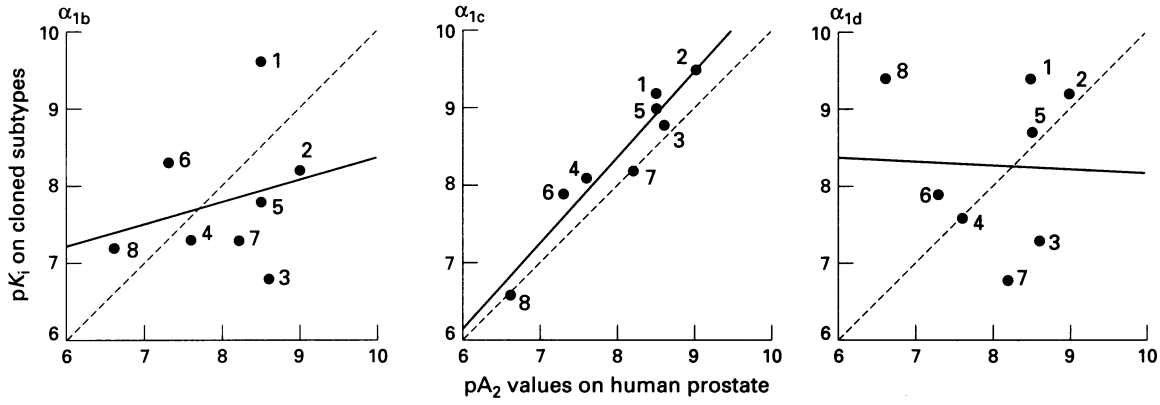

Figure 10 Correlation of average pK_i values for the displacement of [^{3}H]-prazosin on cloned α_1-adrenoceptor subtypes (Table 1) from Faure *et al.*, 1994; Forray *et al.*, 1994b; Kenny *et al.*, 1994a,b; Testa *et al.*, 1994; Goetz *et al.*, 1995, with pA_2 values for the antagonists prazosin (1), WB 4101 (2), 5-methyl urapidil (3), phentolamine (4), benoxathian (5), spiperone (6), indoramin (7) and BMY 7378 (8) against human prostate noradrenaline contractions. The solid line is a linear regression fit through all the points and the dashed line has a slope equal to unity, passing through the origin.

Table 2 Correlation values and slopes of the correlations for the pA_2 values with their pK_i values shown in Table 1

α_1-Subtype	Correlation (r)	Slope
α_{1b}	0.26	0.29±0.44
α_{1c}	0.96	1.11±0.13
α_{1d}	−0.04	−0.05±0.52

of DMSO (0.01%) in the tissue bath. When neuronal and extraneuronal uptake was blocked by cocaine and β-oestradiol (both 10^{-5} M) the concentration-effect curve to noradrenaline was not altered. Phenylephrine and methoxamine also dose-dependently contracted the prostate (pD_2 5.1±0.1 and 4.4±0.1 respectively, Figure 1) but appeared to be partial agonists in this tissue (maximum response compared to noradrenaline 66±1% for phenylephrine and 56±1% for methoxamine). The responses to phenylephrine and methoxamine were not altered in the presence of cocaine and β-oestradiol (both 10^{-5} M).

Chlorethylclonidine (1×10^{-4} M, 30 min), produced about a 3 fold rightward shift in the concentration-effect curve and a 31±1% decrease in the maximum (Figure 2). WB 4101 was a competitive antagonist producing dose-dependent rightward shifts in the concentration-effect curves (pA_2 9.0, slope 0.91±0.11, Figure 3). The same was also true for 5-methyl urapidil (pA_2 8.6, slope 0.99±0.09, Figure 4), phentolamine (pA_2 7.6, slope 1.06±0.06, Figure 5), benoxathian (pA_2 8.5, slope 0.99±0.16, Figure 6), spiperone (pA_2 7.3, slope 1.04±0.12, Figure 7), indoramin (pA_2 8.2, slope 1.01±0.12, Figure 8) and BMY 7378, (pA_2 6.6, slope 0.91±0.11, Figure 9).

Discussion

The human prostate was shown to contract to noradrenaline, with its potency and maximal response being unaffected by neuronal and extraneuronal uptake blockade by cocaine and β-oestradiol, which were therefore not included in further experiments. The α_1-adrenoceptor agonists, phenylephrine and methoxamine, also contracted the prostate, indicating that α_1-adrenoceptors mediate at least part of the response to noradrenaline. The most potent of the three agonists was noradrenaline with phenylephrine and methoxamine being about 3 and 10 fold less potent respectively. Phenylephrine and methoxamine also appeared to be partial agonists with respect to the maximum response to noradrenaline. Although they are usually considered to be full agonists, it may be that they have a slightly lower efficacy compared to noradrenaline and this is not noticeable in other tissues where there is a larger receptor reserve.

Another possible reason for the maximum response to noradrenaline being greater than that of the other agonists in this tissue is that it may also be mediated by α_2-adrenoceptors. However the full α_2-adrenoceptor agonist, UK-14,304, did not have any contractile effect in preliminary experiments, in agreement with Chapple *et al.* (1989) and prazosin has a pA_2 against the noradrenaline contraction consistent for an α_1-

adrenoceptor (Marshall *et al.*, 1992). Therefore the response to noradrenaline is mediated by α_1-adrenoceptors, in agreement with Chapple *et al.* (1989) and was therefore a suitable agonist to study the α_1-adrenoceptor subtype(s) in this tissue. Human hyperplastic prostatic tissue shows no relaxation to isoprenaline in *in vitro* function studies (Caine *et al.*, 1975; Kitada, 1983). Therefore it was considered unnecessary to include a β-adrenoceptor antagonist in these experiments.

Chlorethylclonidine selectively alkylates tissue α_{1B}-adrenoceptors (e.g. in rat spleen, Burt *et al.*, 1995) and the expressed α_{1b}-adrenoceptor clone (Perez *et al.*, 1991) rather than tissue α_{1A}-adrenoceptors (e.g. lack of effect in rat vas deferens, Burt *et al.*, 1995) or the expressed α_{1c}- and α_{1d}-adrenoceptor clones (Forray *et al.*, 1994a; Perez *et al.*, 1991). The degree of sensitivity to chlorethylclonidine of the α_{1c} clone may however be species-dependent to some extent (Forray *et al.*, 1994a). The response to noradrenaline in the prostate was antagonized by chlorethylclonidine under the same conditions that were used for the rat spleen and vas (Burt *et al.*, 1995). However, its effect was not as great as that observed on the rat spleen where it caused about a 300 fold shift of the phenylephrine curve compared to about a 3 fold shift of the noradrenaline curve in the prostate. Hence, contraction of the prostate is unlikely to be mediated solely by α_{1B}-adrenoceptors but could be mediated by α_{1A}- or α_{1D}-adrenoceptors, as the corresponding expressed clones for these two subtypes (α_{1c} and α_{1d}), have both been shown to be partially chlorethylclonidine-sensitive.

However, chlorethylclonidine did have a greater effect in the prostate than in the rat vas deferens where it had no effect. One problem with the interpretation of the effects of chlorethylclonidine is that the degree to which it affects a functional response depends to some extent on the receptor reserve of the tissue. If a tissue has a large receptor reserve then a reduction in receptor density may result in a rightward shift in the concentration-response curve without a reduction in the maximum response. On the other hand, if a tissue has a small receptor reserve then an equivalent reduction in receptor density may result in a rightward shift of the concentration-response curve and also a decrease in the maximum response. The fact that a decrease in maximum response was observed in the prostate after chlorethylclonidine treatment with a relatively small rightward shift is consistent with a small receptor reserve in this tissue. The rat vas deferens does have a large α_1-adrenoceptor reserve (Diaz-Toledo & Marti, 1988) so a small shift in the noradrenaline curve in this tissue would probably not be accompanied by a reduction in maximum response. The reduced maximum response in the prostate would then only represent a difference in receptor reserve between the prostate and the vas deferens. Therefore it could be argued that the 3 fold shift for the noradrenaline curve in the prostate shows relatively little difference in the effects of chlorethylclonidine between the two tissues. The classical α_{1A}-subtype such as that found in the rat vas deferens corresponds to the cloned α_{1c}-adrenoceptor (Laz *et al.*, 1993; Perez *et al.*, 1994; Burt *et al.*, 1995) and this clone also shows some species differences in chlorethylclonidine-sensitivity. Therefore the subtypes in the rat vas deferens and the human prostate could both be the α_{1A}-subtype and the difference in chlorethylclonidine sensitivity may reflect a species difference. Alternatively the subtype in the prostate could be an α_{1D}-adrenoceptor. However, there are currently no functional data for chlorethylclonidine on a known α_{1D}-mediated response with which to compare its effect in the prostate. In comparison the α_1-adrenoceptors in the rat spleen were much more sensitive to chlorethylclonidine than those in the rat vas deferens (Burt *et al.*, 1995) and human prostate, as a 300 fold shift in the concentration-response curve could not be explained away in terms of receptor reserve and experimental variability.

Due to the problems of interpreting the effects of chlorethylclonidine in some cases (particularly in distinguishing between the α_{1c}- and α_{1d}-subtypes), affinities of subtype-selective competitive antagonists may give more reliable information. The affinity of a range of competitive antagonists has now been measured on membranes from cells transfected with the cDNA for each of the three cloned α_1 subtypes in several studies. While prazosin has been found to be non-selective, others have shown some degree of selectivity between the subtypes (Faure *et al.*, 1994; Forray *et al.*, 1994b; Kenny *et al.*, 1994a,b; Testa *et al.*, 1994; Goetz *et al.*, 1995). The affinity of the same antagonists has been measured here in functional studies for the α_1 subtype mediating contraction of the prostate by calculation of pA_2 values. Table 1 compares the pA_2 values obtained for these antagonists with their average published pK_i values on the expressed cloned subtypes (Faure *et al.*, 1994; Forray *et al.*, 1994b; Kenny *et al.*, 1994a,b; Testa *et al.*, 1994; Goetz *et al.*, 1995). The pA_2 values have been plotted against their average pK_i values for each of the cloned subtypes in order to see with which one the functional α_1-adrenoceptor mediating contraction in the human prostate most closely correlates (Figure 10). The correlation values (r) and slopes of the correlations are shown in Table 2. They show that the subtype in the prostate is unlike either the α_{1b} or α_{1d}-subtypes but correlates very well with the α_{1c}-subtype ($r = 0.96$).

In conclusion, the α_1-adrenoceptor mediating contractions to noradrenaline in the human prostate was only partially sensitive to chlorethylclonidine and the affinities of subtype-selective antagonists for this functional receptor correlated very well with the expressed α_{1c}-subtype clone. On this evidence the α_1-adrenoceptor mediating the contraction is the same as the expressed α_{1c} subtype clone, which corresponds well with this subtype having the highest expression in the prostatic stroma (Price *et al.*, 1993). As the expressed α_{1c} subtype clone corresponds to the tissue α_{1A}-adrenoceptor (Laz *et al.*, 1993; Perez *et al.*, 1994; Burt *et al.*, 1995), the subtype mediating contraction of the human prostate is the α_{1A}-adrenoceptor. This conclusion is therefore consistent with the findings that α_1-adrenoceptors in human prostate were similar to tissue α_{1A}-adrenoceptors in binding studies (Testa *et al.*, 1993) and similar to the expressed bovine α_{1c} clone in functional studies (Lepor *et al.*, 1993). An antagonist selective for the α_{1A}-subtype may therefore be of benefit in the treatment of benign prostatic hyperplasia.

We thank Pfizer Central Research, Kent, for supporting this work.

References

ABOUD, R., SHAFI, M. & DOCHERTY, J.R. (1993). Investigation of the subtypes of α_1-adrenoceptor mediating contractions of rat aorta, vas deferens and spleen. *Br. J. Pharmacol.*, **109**, 80–87.

ARUNLAKSHANA, O. & SCHILD, H.O. (1959). Some quantitative uses of drug antagonists. *Br. J. Pharmacol. Chemother.*, **14**, 48–52.

BRUNO, J.F., WHITTAKER, J., SONG, J. & BERELOWITZ, M. (1991). Molecular cloning and sequencing of a cDNA encoding a human α_{1A} adrenergic receptor. *Biochem. Biophys. Res. Commun.*, **179**, 1485–1490.

BURT, R.P., CHAPPLE, C.R. & MARSHALL, I. (1995). Evidence for a functional α_{1A}- (α_{1C}-) adrenoceptor mediating contraction of the rat epididymal vas deferens and an α_{1B}-adrenoceptor mediating contraction of the rat spleen. *Br. J. Pharmacol.*, (in press).

BYLUND, D.B., EIKENBERG, D.C., HIEBLE, J.P., LANGER, S.Z., LEFKOWITZ, R.J., MINNEMAN, K.P., MOLINOFF, P.B., RUFFOLO, R.R. & TRENDELENBURG, U. (1994). IV. International Union of Pharmacology nomenclature of adrenoceptors. *Pharmacol. Rev.*, **46**, 121–136.

CAINE, M., PERLBERG, S. & MERETYK, S. (1978). A placebo-controlled double blind study of the effect of phenoxybenzamine in benign prostatic obstruction. *Br. J. Urol.*, **50**, 551–554.

CAINE, M., RAZ, S. & ZIEGLER, M. (1975). Adrenergic and cholinergic receptors in the human prostate, prostatic capsule and bladder neck. *Br. J. Urol.*, **47**, 193–202.

CHAPPLE, C.R., AUBRY, M.L., JAMES, S., GREENGRASS, P.M., BURNSTOCK, G., TURNER-WARWICK, R.T., MILROY, E.J.G. & DAVEY, M.J. (1989). Characterization of human prostatic adrenoceptors using pharmacology receptor binding and localisation. *Br. J. Urol.*, **63**, 487–496.

CHAPPLE, C.R., CHRISTMAS, T.J. & MILROY. (1990). A twelve-week placebo-controlled study of prazosin in the treatment of prostatic obstruction. *Urol. Int.*, **45**, (suppl. 1): 47–55.

DIAZ-TOLEDO, A. & MARTI, M.C. (1988). Relationship between α-adrenoceptor occupancy and contractile response in rat vas deferens. Experimental and theoretical analysis. *Eur. J. Pharmacol.*, **156**, 315–324.

FAURE, C., PIMOULE, C., ARBILLA, S., LANGER, S. & GRAHAM, D. (1994). Expression of α_1-adrenoceptor subtypes in rat tissues: implications for α_1-adrenoceptor classification. *Eur. J. Pharmacol.* (Mol. Pharmacol. Section), **268**, 141–149.

FORRAY, C., BARD, J.A., LAZ, T.M., SMITH, K.E., VAYSSE, P.J.-J., WEINSHANK, R.L., GLUCHOWSKI, C. & BRANCHEK, T.A. (1994a). Comparison of the pharmacological properties of the cloned bovine, human and rat α_{1c}-adrenergic receptors. *FASEB*, **8**, A253.

FORRAY, C., BARD, J.A., WETZEL, J.M., CHIU, G., SHAPIRO, E., TANG, R., LEPOR, H., HARTIG, P.R., WEINSHANK, R.L., BRANCHEK, T.A. & GLUCHOWSKI, C. (1994b). The α_1-adrenergic receptor that mediates smooth muscle contraction in human prostate has the pharmacological properties of the cloned human α_{1c} subtype. *Mol. Pharmacol.*, **45**, 703–708.

GARRAWAY, W.M., COLLINS, G.N. & LEE, R.J. (1991). High prevalence of benign prostatic hypertrophy in the community. *Lancet.*, **338**, 469–471.

GOETZ, A.S., KING, H.K., WARD, S.D.C., TRUE, T.A., RIMELE, T.J. & SAUSSY, D.L. (1995). BMY 7378 is a selective antagonist of the D subtype of α_1-adrenoceptors. *Eur. J. Pharmacol.*, **272**, R5–R6.

GROSS, G., HANFT, G. & RUGEVICS, C. (1988). 5-methyl urapidil discriminates between subtypes of the α_1-adrenoceptor. *Eur. J. Pharmacol.*, **151**, 333–335.

HAN, C., ABEL, P.W. & MINNEMAN, K.P. (1987a). Heterogeneity of α_1-adrenergic receptors revealed by chlorethylclonidine. *Mol. Pharmacol.*, **32**, 505–510.

HAN, C., ABEL, P.W. & MINNEMAN, K.P. (1987b). α_1-Adrenoceptor subtypes linked to different mechanisms for increasing intracellular Ca^{2+} in smooth muscle. *Nature*, **329**, 333–335.

HIEBLE, J.P., CAINE, M. & ZALAZNIK, E. (1985). *In vitro* characterization of the α-adrenoceptors in human prostate. *Eur. J. Pharmacol.*, **107**, 111–117.

HIRASAWA, A., HORIE, K., TANAKA, T., TAKAGAKI, K., MURAI, M., YANO, J. & TSUJIMOTO, G. (1993). Cloning, functional expression and tissue distribution of human cDNA for the α_{1C} adrenergic receptor. *Biochem. Biophys. Res. Commun.*, **195**, 902–909.

JAMES, S., CHAPPLE, C.R., PHILIPS, M.I., GREENGRASS, P.M., DAVEY, M.J., TURNER-WARWICK, R.T., MILROY, E.J.G. & BURNSTOCK, G. (1989). Autoradiographic analysis of alpha-adrenoceptors and muscarinic cholinergic receptors in the hyperplastic human prostate. *J. Urol.*, **142**, 438–444.

KENNY, B.A., NAYLOR, A.M., GREENGRASS, P.M., RUSSELL, M.J., FRIEND, S.J., READ, A.M. & WYLLIE, M.G. (1994a). Pharmacological properties of the cloned $\alpha_{1A/D}$-adrenoceptor subtype are consistent with the α_{1A}-adrenoceptor characterized in rat cerebral cortex and vas deferens. *Br. J. Pharmacol.*, **111**, 1003–1008.

KENNY, B.A., PHILPOTT, P.C., NAYLOR, A.M. & WYLLIE, M.G. (1994b). Comparative properties of cloned mammalian and human $\alpha_{1A/D}$ and α_{1C} adrenoceptors. *Br. J. Pharmacol.*, **113**, 98P.

KITADA, S. (1983). Pharmacological characteristics of smooth muscle in prostatic hyperplastic nodule and significance of clinical aspects. *Jpn. J. Urol.*, **74**, 2054–2069.

LAZ, T.M., FORRAY, C., SMITH, K.E., VACSSE, P.J.J., HARTIG, P.R., GLUCHOWSKI, C., BRANCHEK, T.A. & WEINSHANK, R.L. (1993). Cloned rat homolog of the bovine α_{1c}-adrenergic receptor exhibits an α_{1A}-like receptor pharmacology. *Soc. Neurosci. Abstracts*, **19**, 1788.

LEARMONTH, J.R. (1931). A contribution to the neurophysiology of the urinary bladder in man. *Brain*, **54**, 147–176.

LEPOR, H., TANG, R. & SHAPIRO, E. (1993). The alpha-adrenoceptor subtype mediating the tension of human prostatic smooth muscle. *Prostate*, **22**, 301–307.

LOMASNEY, J.W., COTECCHIA, S., LORENZ, W., LEUNG, W.Y., SCHWINN, D.A., YANG-FENG, T.L., BROWNSTEIN, M., LEFKOWITZ, R.J. & CARON, M.G. (1991). Molecular cloning and expression of the cDNA for the α_{1A}-adrenergic receptor. *J. Biol. Chem.*, **266**, 6365–6369.

MARSHALL, I., BURT, R.P., ANDERSSON, P.O., CHAPPLE, C.R., GREENGRASS, P.M., JOHNSON, G.I. & WYLLIE, M.G. (1992). Human α_{1C}-adrenoceptor: functional characterization in prostate. *Br. J. Pharmacol.*, **112**, 59P

MORROW, A.L. & CREESE, I. (1986). Characterization of α_1-adrenergic receptor subtypes in rat brain: a reevaluation of [^{3}H]WB4101 and [^{3}H]prazosin binding. *Mol. Pharmacol.*, **29**, 321–330.

PEREZ, D.M., CHEN, J.-L., MALIK, N. & GRAHAM, R.M. (1994). Is the α_{1C}-adrenergic receptor the α_{1A} subtype. *FASEB*, **8**, A353.

PEREZ, D.M., PIASCIK, M.T. & GRAHAM, R.M. (1991). Solution phase library screening for the identification of rare clones: isolation of an α_{1D} adrenergic receptor cDNA. *Mol. Pharmacol.*, **40**, 876–883.

PRICE, D.T., LEFKOWITZ, J., CARON, M.G., BERKOWITZ, D. & SCHWINN, D.A. (1994). Localization of mRNA for three distinct α_1-adrenergic receptor subtypes in human tissues: implications for human α-adrenergic physiology. *Mol. Pharmacol.*, **45**, 171–175.

PRICE, D.T., SCHWINN, D.A., LOMASNEY, J.W., ALLEN, L.F., CARON, M.G. & LEFKOWITZ, R.J. (1993). Identification, quantification and localization of mRNA for three distinct alpha$_1$ adrenergic receptor subtypes in human prostate. *J. Urol.*, **150**, 546–551.

RAMARAO, C.S., KINKADE DENKER, J.M., PEREZ, D.M., GAIVIN, R.J., REIK, R.P. & GRAHAM, R.M. (1992). Genomic organization and expression of the human α_{1B}-adrenergic receptor. *J. Biol. Chem.*, **267**, 21936–21945.

ROKOSH, D.G., BAILEY, B.A., STEWART, A.F.R., KARNS, L.R., LONG, C.S. & SIMPSON, P.C. (1994). Distribution of α_{1c}-adrenergic receptor mRNA in adult rat tissues by RNAse protection assay and comparison with α_{1b} and α_{1d}. *Biochem. Biophys. Res. Commun.*, **200**, 1177–1184.

SAUSSY, D.L., GOETZ, A.S., KING, H.K. & TRUE, T. (1994). BMY 7378 is a selective antagonist of α_{1d}-adrenoceptors (AR): further evidence that vascular α_{1d}-AR are of the α_{1d} subtype. *Can. J. Physiol. Pharmacol.*, **72**, (Suppl. 1), P13.1.008.

SCHWINN, D.A. & LOMASNEY, J.W. (1992). Pharmacological characterization of cloned α_1-adrenoceptor subtypes: selective antagonists suggest the existence of a fourth subtype. *Eur. J. Pharmacol.*, **227**, 433–436.

SCHWINN, D.A., LOMASNEY, J.W., LORENZ, W., SZKLUT, P.J., FREMEAU, Jr, R.T., YANG-FENG, T.L., CARON, M.G., LEFKOWITZ, R.J. & COTECCHIA, S. (1990). Molecular cloning and expression of the cDNA for a novel α_1-adrenergic receptor subtype. *J. Biol. Chem.*, **265**, 8183–8189.

TESTA, R., GUARNERI, L., IBBA, M., STRADA, G., POGGESI, E., TADDEI, C., SIMONAZZI, I. & LEONARDI, A. (1993). Characterization of α_1-adrenoceptor subtypes in prostate and prostatic urethra of rat, rabbit, dog and man. *Eur. J. Pharmacol.*, **249**, 307–315.

TESTA, R., POGGESI, E., TADDEI, C., GUARNERI, L., IBBA, M. & LEONARDI, A. (1994). REC 15/2739, a new α_1-antagonist selective for the lower urinary tract: *in vitro* studies. *Neurourol. Urodynam.*, **13**, 84B.

(Received December 7, 1994
Revised February 17, 1995
Accepted March 23, 1995)

British Journal of Pharmacology (1995) 115, 787-794

Effects of the two enantiomers, S-16257-2 and S-16260-2, of a new bradycardic agent on guinea-pig isolated cardiac preparations

[1]Onésima Pérez, Pilar Gay, Laura Franqueza, *Rosalía Carrón, Carmen Valenzuela, Eva Delpón & Juan Tamargo

Department of Pharmacology, School of Medicine, Universidad Complutense, 28040 Madrid, Spain and *Department of Physiology and Pharmacology, School of Pharmacy, Universidad of Salamanca, 37007 Salamanca, Spain

1 The electromechanical effects of two enantiomers, S-16257-2 (S57) and S-16260-2 (R60), were studied and compared in guinea-pig isolated atria and ventricular papillary muscles. The possible stereoselectivity of the interaction on the cardiac Na^+ channel was analysed by comparing the effects of the two enantiomers on the onset and recovery kinetics of the frequency-dependent V_{max} block.

2 In spontaneously beating right atria, S57 and R60 (10^{-8} M - 10^{-4} M) exerted a negative chronotropic effect ($pIC_{50} = 5.07 \pm 0.19$ and 4.76 ± 0.18, respectively) and prolonged the sinus node recovery time, this effect being more marked with S57. In electrically driven left atria, S57 decreased ($P < 0.05$) contractile force only at 10^{-4} M and R60 at concentrations $\geq 5 \times 10^{-5}$ M, whereas in papillary muscles the negative inotropic effect appeared at concentrations $> 10^{-5}$ M.

3 In papillary muscles driven at 1 Hz, S57 and R60 at concentrations higher than 5×10^{-6} M produced a concentration-dependent decrease in the maximum upstroke velocity (V_{max}) and amplitude of the cardiac action potential without altering the resting membrane potential or the action potential duration. S57 and R60 had no effect on the characteristics of the slow action potentials elicited by isoprenaline in ventricular muscle fibres depolarized in high K^+ (27 mM) solution.

4 At 5×10^{-5} M, S57 and R60 produced a small tonic V_{max} block. However, in muscles driven at rates between 0.5 and 3 Hz both enantiomers produced an exponential decline in V_{max} (frequency-dependent V_{max} block) which augmented at higher rates of stimulation. The onset and offset rates of the frequency-dependent V_{max} block were similar for both drugs. Both S57 and R60 prolonged the recovery time constant from the frequency-dependent block from 20.1 ± 2.9 ms to 2-3 s.

5 At 5×10^{-5} M, S57 and R60 shifted the membrane responsiveness curve in a hyperpolarizing direction.

6 It can be concluded that S57 and R60, the two enantiomers of the new bradycardic agent, produced a similar frequency-dependent V_{max} block which indicated that the interaction with the Na^+ channel was not stereospecific. The analysis of the onset and offset kinetics of the frequency-dependent V_{max} block suggested that both enantiomers can be considered as Na^+ channel blockers with intermediate kinetics, e.g., class IA antiarrhythmic drugs.

Keywords: S 16257; contractile force; action potential; frequency-dependent V_{max} block; bradycardic agents

Introduction

Sinus tachycardia is a common physiological response that may help to maintain homeostasis by increasing cardiac output but also increases myocardial oxygen demands and decreases time for myocardial relaxation and diastolic ventricular filling (Sonnenblick *et al.*, 1968). In the presence of a flow-limiting coronary artery stenosis a decrease in diastolic perfusion time, secondary to exercise-induced tachycardia, may be especially deleterious by further reducing subendocardial myocardial perfusion (Boudoulas *et al.*, 1979; Hoffman, 1984). Under these circumstances, a reduction of heart rate prolongs the diastolic perfusion time and reduces myocardial oxygen demands, thus leading to an improvement in ischaemic zone perfusion and function. Bradycardic agents, i.e. β-adrenoceptor blocking agents and calcium channel blockers are frequently used in the treatment of effort-induced angina pectoris (Cruickshank & Prichard, 1987; Opie, 1989). However, these drugs also exhibit negative inotropic and hypotensive effects which may antagonize the beneficial effects of the bradycardia on myocardial blood flow by unmasking α-adrenoceptor vasoconstrictor mechanisms or increasing the extracellular component of coronary resistance (via an increase in left ventricular end-diastolic pressure) and reducing coronary artery perfusion pressure, respectively.

Specific bradycardic agents represent a new approach in the management of angina pectoris with depressed left ventricular function (Kobinger & Lillie, 1987; Guth, 1991). They block sinus tachycardia and markedly attenuate exercise-induced increases in heart rate at concentrations at which they have no direct effects on the inotropic state or vascular tone (Kobinger & Lillie, 1987; Guth, 1991; O'Brien *et al.*, 1992). The precise mechanism of action of these agents is still uncertain even when in rabbit sinoatrial node cells the bradycardic effect of zatebradine has been attributed to a frequency-dependent inhibition of the hyperpolarizing-activated current (I_f) (Goethals *et al.*, 1993).

S-16257-2 (7,8-dimethoxy 3-{3{[1S)-(4,5-dimethoxybenzocyclobutan-1-yl) methyl] methylamino}propyl} 1,3,4,5-tetrahydro-2H-benzazepine 2-one) is a new bradycardic agent that slows the spontaneous rate in rabbit isolated sino-atrial node and sheep Purkinje fibres and prolongs the action potential duration (APD), this effect being quite marked in Purkinje fibres, but very weak in guinea-pig ventricular papillary muscles (Thollon *et al.*, 1994). However, the effects of the drug on phase 0 characteristics of the cardiac action potential have not yet been reported. Furthermore, S-16257-2 is the (S)-enantiomer of a chiral molecule (Figure 1) and the (R)-enantiomer, S-16260-2, has been recently synthesized. Thus, the present work was undertaken to compare the effects of S-16257-2 (S57) and S-16260-2 (R60) on: (1) rate and contractile

[1] Author for correspondence.

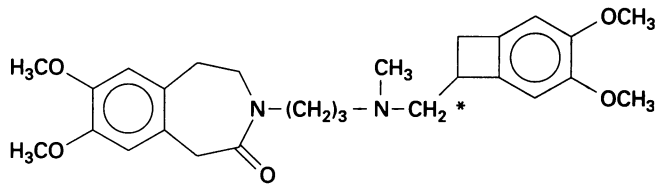

Figure 1 Chemical structure of 7,8-dimethoxy 3-{3-{[(4,5-dimethoxy benzocyclobutan-1-yl)methyl]methylamino}propyl}1,3,4,5-tetrahydro-2H-benzazepine 2-one. The asterisk shows the asymmetric carbon that differentiates S-16257-2 (S57) from S-16260-2 (R60).

force in guinea-pig isolated atria and papillary muscles, and (2) ventricular action potential characteristics. Moreover, (3) the possible stereoselectivity of the interaction on the cardiac Na^+ channel was analysed by comparing the effects of the two enantiomers on the onset and recovery kinetics of the frequency-dependent V_{max} block.

Methods

General procedure

Guinea-pigs of either sex weighing 350–450 g were killed by cervical dislocation and their hearts were rapidly removed. Right and left atria and left ventricular papillary muscles were dissected and mounted vertically in 10 ml organ baths containing Tyrode solution of the following composition (mM): NaCl 125, KCl 5.4, $CaCl_2$ 1.8, $MgCl_2$ 1.05, $NaHCO_3$ 24, NaH_2PO_4 0.42 and glucose 11. The solution was bubbled with 95% O_2: 5% CO_2 and maintained at 34°C. Under these conditions right atria beat spontaneously, while left atria and papillary muscles were electrically driven at a basal rate of 1 Hz through bipolar platinum electrodes with rectangular pulses (1 ms duration, twice threshold strength) delivered from a multipurpose programmable stimulator (Cibertec CS 220, Madrid, Spain). Rate and amplitude of contractions were measured isometrically by a force-displacement transducer and recorded on a Letica 2000 (Cibertec S.A., Madrid, Spain) polygraph. Resting tension was adjusted to 1 g (left atria) and 0.5 g (papillary muscles) and a 30 min equilibration period was allowed to elapse before control measurements were taken. The sinus node recovery time was determined as described elsewhere (Tamargo, 1980). After control values for each parameter were obtained, incremental concentrations of each drug were added every 30 min to the bath to obtain a complete concentration-response curve. The values for the different parameters obtained in the absence of each drug were used as controls and compared with those obtained after each increment in drug concentration. Only one drug was tested in each experiment.

Electrophysiological studies

Guinea-pigs of either sex (250–350 g) were killed by cervical dislocation and hearts were rapidly removed and brought into a dissection chamber where papillary muscles of 2–3 mm in length and less than 1 mm in diameter were excised from the right ventricle. The muscles were pinned to the bottom of a Lucite chamber and superfused continuously at a constant rate of 7 ml min^{-1} with Tyrode solution bubbled with 95% O_2 and 5% CO_2 and maintained at 34 ± 0.5°C (pH = 7.4). The preparations were initially driven at 1 Hz and a period of 1 h was allowed for equilibration during which a stable impalement was obtained. Driving stimuli were rectangular pulses (1 ms duration, twice threshold strength) delivered to the preparation from a multipurpose programmable stimulator (Cibertec CS-220). Electrical stimulation was applied to the surface of the preparation through Teflon-coated bipolar electrodes of silver wire.

Transmembrane action potentials were conventionally recorded through glass microelectrodes filled with 3 M KCl (tip resistance of 8–15 MΩ). The microelectrode was connected via Ag-AgCl wire to high impedance, capacity neutralizing amplifiers (WPI model 701, New Haven, CT, U.S.A.). The maximal rate of depolarization (V_{max}) of the action potential was obtained by electronic differentiation (Valenzuela *et al.*, 1988). The amplifier output was linear between 10–1000 V s^{-1} and had variable input filters (3 Hz-260 KHz, E. Ehler, Homburg/Saar, Germany). A suitable frequency filter for minimizing noise without reducing the V_{max} was selected for each individual experiment. In order to avoid latency-induced alterations of V_{max}, stimulus intensity and duration were adjusted throughout each experiment to maintain a constant latency (1–2 ms) between stimulus and upstroke of the action potential (Valenzuela *et al.*, 1988). Both action potential and V_{max} were displayed on a storage oscilloscope (model 4104N, Tektronix Inc., Beaverton, OR, U.S.A.) and the oscilloscope traces were photographed with a kymographic camera (Grass C4, Grass Instrument Co., Quincy, MA, U.S.A.). The following action potential characteristics were determined from

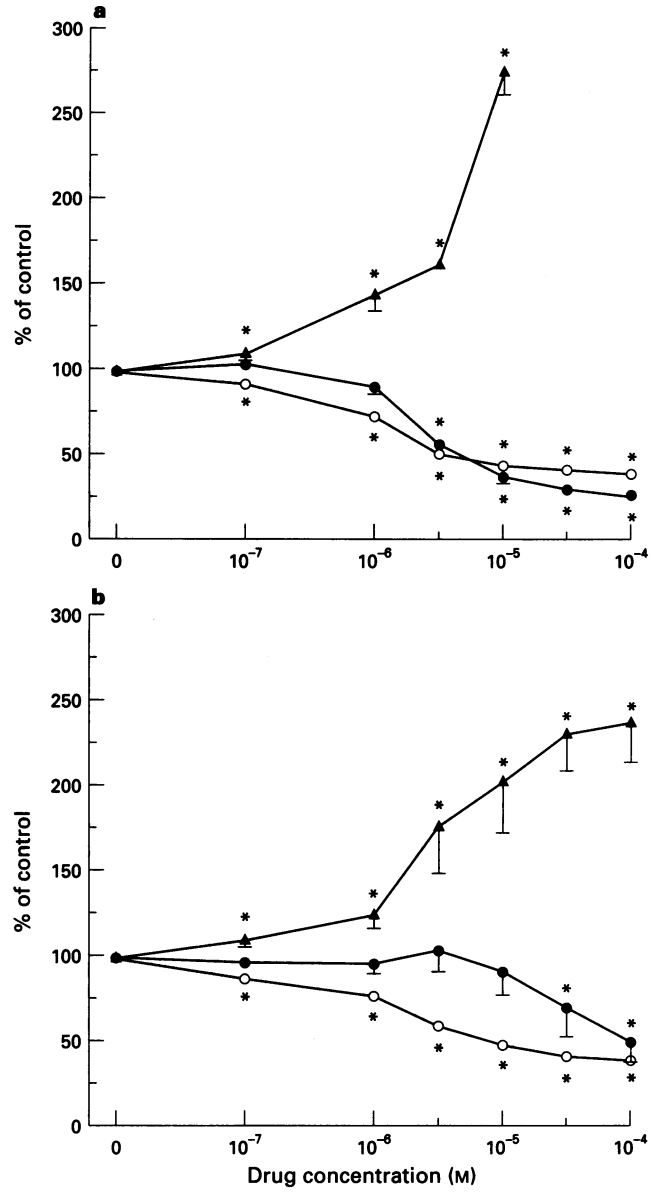

Figure 2 Concentration-response effects of (a) S57 and (b) R60 on (○) sinus rate, (●) peak contractile force and (▲) sinus node recovery time in spontaneously beating guinea-pig isolated right atria. Ordinate scale: % of control values. Abscissa scale: drug concentration (M). Each point represents the mean ± s.e.mean of at least 6 experiments. $^*P < 0.05$ vs control.

recordings: resting membrane potential, amplitude, V_{max} and action potential duration at the 50% (APD_{50}) and 90% (APD_{90}) level of repolarization. All experimental results were obtained from a single continuous impalement throughout the whole experiment.

To study rate-dependent effects on V_{max} block produced by S57 and R60, muscles were initially driven at a basal rate of 0.02 Hz. Following the equilibration period, the preparations were driven by trains of stimuli at varying rates for 40 s (0.5, 1 and 2 Hz) and 16 s (3 Hz). Rest periods of 5 min, which were sufficient to ensure full recovery from frequency-dependent decreases in V_{max}, were interpolated between the trains of stimuli (Valenzuela *et al.*, 1988; Delpón *et al.*, 1990). A similar experimental protocol was followed after exposure to S57 and R60. Under these circumstances two types of V_{max} inhibition were detected, i.e. Tonic and frequency (use)-dependent V_{max} block. Tonic blockade is the decrease of V_{max} of the first action potential preceded by a rest period, whereas frequency-dependent blockade was defined by the decrease of V_{max} during a train from the value of the first action potential to a new steady-state. Recovery from frequency-dependent V_{max} block was studied by applying a single test stimulus at various coupling intervals after a stimulation train for 8 s at 3 Hz. The strength of the test stimuli was adjusted so that the latency of the conditioning and the test stimuli were identical and constant (1–2 ms). For each drug, the onset of and recovery from frequency-dependent V_{max} block were fitted by exponential functions for calculations of the respective rate constants.

The effective refractory period (ERP), defined as the period in which no propagated action potentials can be obtained, was measured by introducing premature test-stimuli (S_2) of twice threshold strength at different intervals from the preceding basic action potential. S_2 was delivered every eighth basic stimulus. Premature test-stimuli were initially introduced late in the diastole and then progressively earlier in the cycle. The relationship between V_{max} and the resting membrane potential, i.e. membrane responsiveness, was studied in papillary muscles driven at 0.1 Hz and the resting membrane potential was de-

Table 1 Electrophysiological effects of S57 on transmembrane action potentials in guinea-pig papillary muscles driven at 1.0 Hz

Concentration (M)	*RMP* (mV)	*APA* (mV)	V_{max} (Vs^{-1})	APD_{50} (ms)	APD_{90} (ms)	ERP/APD_{90}
Control	−84.1 ± 0.8	122.8 ± 1.0	206.4 ± 9.1	179.3 ± 9.4	208.2 ± 8.9	1.03 ± 0.01
10^{-7}	−84.0 ± 0.9	123.1 ± 0.9	206.5 ± 10.3	178.2 ± 7.8	208.6 ± 7.6	1.03 ± 0.01
10^{-6}	−83.1 ± 1.0	122.7 ± 0.7	207.1 ± 11.6	184.3 ± 8.2	211.4 ± 8.9	1.03 ± 0.01
5×10^{-6}	−83.4 ± 1.4	123.4 ± 0.9	193.1 ± 16.2	181.0 ± 12.8	213.0 ± 11.5	1.02 ± 0.01
10^{-5}	−82.0 ± 1.4	122.7 ± 0.8	185.4 ± 12.3*	188.2 ± 9.1	219.6 ± 10.0	1.03 ± 0.01
5×10^{-5}	−82.7 ± 2.2	120.5 ± 1.8*	141.2 ± 16.1**	154.4 ± 3.6	194.4 ± 5.2	1.04 ± 0.01

Mean ± s.e.mean, $n = 7$. RMP, resting membrane potential; APA, amplitude of the action potential; V_{max}, maximal upstroke of the action potential; APD_{50} and APD_{90}, action potential duration at the 50% and 90% level of repolarization; ERP, effective refractory period. *$P < 0.05$; **$P < 0.01$.

Table 2 Electrophysiological effects of R60 on transmembrane action potentials in guinea-pig papillary muscles driven at 1.0 Hz

Concentration (M)	*RMP* (mV)	*APA* (mV)	V_{max} (Vs^{-1})	APD_{50} (ms)	APD_{90} (ms)	ERP/APD_{90}
Control	−86.2 ± 1.3	120.0 ± 0.8	211.9 ± 13.6	171.0 ± 10.3	201.5 ± 9.7	1.04 ± 0.00
10^{-7}	−86.0 ± 1.4	121.2 ± 0.8	213.0 ± 13.3	174.5 ± 9.2	206.0 ± 8.0	1.03 ± 0.00
10^{-6}	−85.6 ± 1.5	121.4 ± 0.9	207.5 ± 11.7	177.0 ± 10.4	210.5 ± 9.8	1.03 ± 0.00
5×10^{-6}	−85.5 ± 1.8	121.0 ± 0.7	201.4 ± 12.5	182.5 ± 9.5	218.7 ± 8.1	1.02 ± 0.01
10^{-5}	−85.5 ± 1.8	119.8 ± 0.5	191.0 ± 7.1*	173.5 ± 6.3	212.5 ± 7.0	1.02 ± 0.00
5×10^{-5}	−85.2 ± 1.7	117.0 ± 1.1*	152.0 ± 8.6*	154.4 ± 8.4	198.1 ± 10.1	1.03 ± 0.00

Mean ± s.e.mean, $n = 7$. *$P < 0.05$; **$P < 0.01$. For abbreviations, see Table 1.

Table 3 Effects of S57 (A) and R60 (B) on slow action potentials elicited by 10^{-6} M isoprenaline in guinea-pig papillary muscles depolarized with KCl (27 mM) driven at a basal rate of 0.1 Hz

Concentration (M)	*RMP* (mV)	*APA* (ms)	V_{max} (Vs^{-1})	APD_{50} (ms)	APD_{50} (ms)
A					
Control	−46.3 ± 2.3	84.0 ± 1.9	18.4 ± 1.9	219.0 ± 13.7	234.5 ± 15.4
10^{-7}	−46.5 ± 2.3	83.8 ± 1.3	20.1 ± 1.6	228.5 ± 14.6	243.7 ± 13.4
10^{-6}	−46.5 ± 2.3	85.0 ± 1.6	19.8 ± 1.7	223.0 ± 12.9	238.5 ± 12.1
10^{-5}	−46.5 ± 2.3	82.8 ± 1.5	19.2 ± 1.8	224.0 ± 10.8	240.5 ± 10.8
10^{-4}	−45.5 ± 1.8	81.0 ± 2.1	16.1 ± 1.6	232.0 ± 12.8	256.0 ± 12.5
B					
Control	−43.4 ± 0.9	83.6 ± 1.0	16.9 ± 1.1	272.5 ± 19.3	291.0 ± 20.7
10^{-7}	−43.4 ± 0.9	83.6 ± 1.1	18.5 ± 1.3	263.5 ± 15.0	288.0 ± 16.6
10^{-6}	−43.8 ± 1.1	83.0 ± 1.2	18.6 ± 2.0	247.5 ± 14.4	271.5 ± 16.3
10^{-5}	−43.6 ± 1.3	82.6 ± 0.7	18.2 ± 1.9	264.0 ± 18.5	289.5 ± 21.1
10^{-4}	−43.2 ± 1.1	82.0 ± 1.1	15.5 ± 1.8	240.0 ± 20.1	273.5 ± 21.4

Mean ± s.e.mean, $n = 6$. *$P < 0.05$; **$P < 0.01$. For abbreviations, see Table 1.

Table 4 Frequency-dependent V_{max} block induced by S57 and R60 in guinea-pig papillary muscles

	Frequency-dependent V_{max} *block (%)*			
	0.5 Hz	*1 Hz*	*2 Hz*	*3 Hz*
Control	2.2±0.3	4.2±0.5	8.4±1.0	10.1±1.3
S57 (5×10^{-5} M)	16.4±0.8**	30.5±1.3***	46.2±1.9***	56.1±1.7***
Control	1.6±0.7	3.4±0.5	7.2±1.1	10.8±1.9
R60 (5×10^{-5} M)	11.8±0.4**	22.5±0.8***	37.7±1.2***	49.3±1.8***

Mean ± s.e.mean, $n=7$; **$P<0.01$; ***$P<0.001$.

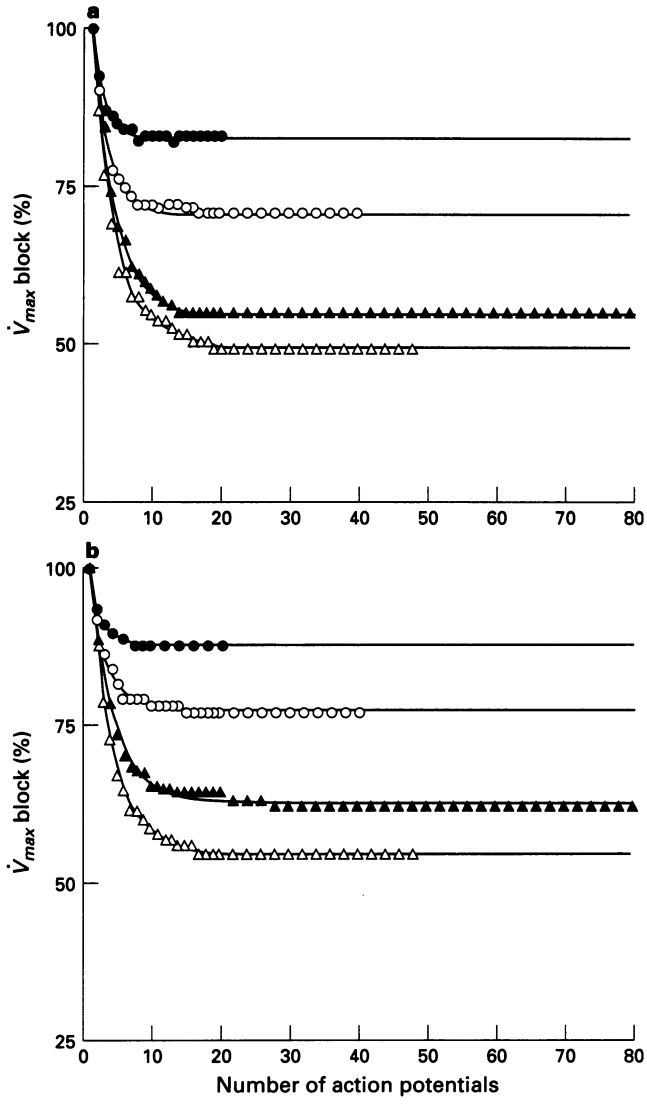

Figure 3 Onset of frequency-dependent depression of V_{max} induced by (a) S57 and (b) R60, 5×10^{-5} M, in guinea-pig papillary muscles driven by trains of stimuli at various rates (0.5–3 Hz). Ordinate scale: percentage of V_{max} block. Frequency-dependent V_{max} block (%) results from [1-V_{max}(ss,drug)/V_{max}(first beat, drug)], where V_{max}(ss) is the steady-state value attained during continuous stimulation and V_{max}(first beat) the value of the first beat of each train of stimuli. Abscissa scale: number of action potentials. (●) 0.5 Hz, (○) 1 Hz, (▲) 2 Hz and (△) 3 Hz.

polarized by increasing the extracellular K^+ concentration, $[K^+]_o$, from 2 to 16 mM (Delpón *et al.*, 1990). The V_{max} was measured each time after an equilibration period of 8 min. Curves were obtained in the absence and after 30 min exposure to the desired concentration of S57 and R60.

Slow action potentials were elicited in papillary muscles rendered unexcitable by depolarizing with 27 mM K^+ Tyrode solution. Under these conditions, the fast inward Na^+ current was voltage-inactivated and excitability, i.e. slow action potentials, was restored in depolarized muscles driven at 0.1 Hz by adding isoprenaline (10^{-6} M) to the perfusate (Delpón *et al.*, 1989).

Table 5 Rate constant of development of frequency-dependent V_{max} block [$K(AP^{-1})$] in the presence of S57 or R60 (5×10^{-5} M)

Frequency of stimulation (Hz)	*S57*	*R60*
0.5	0.70±0.04	0.59±0.07
1.0	0.38±0.02	0.41±0.04
2.0	0.28±0.02	0.30±0.04
3.0	0.27±0.02	0.28±0.03

Mean ± s.e.mean, $n=6$.

After control values for each parameter were obtained, incremental concentrations of each drug were added to the bath to obtain a complete concentration-response curve. The interval between concentrations of each drug was 30 min, since preliminary time-response studies indicated that their effects had stabilized within 30 min. The values for the different parameters obtained in the absence of each drug were used as a control and compared with those obtained after each increment in drug concentration. Only one drug was tested in each experiment.

Drugs used

S57 and R60 were synthesized and kindly provided by Servier (IRIS, Courbevoie, France). Drugs, as a powder, were initially dissolved in distilled deionized water as a 10^{-2} M stock solution. Further dilutions were carried out in Tyrode solution. Ascorbic acid (10^{-4} M) was added to prevent oxidation of isoprenaline. Throughout the paper data are given as the means ± s.e. mean and Student's paired t test was used to estimate the significance of differences from control values. The negative logarithm of the concentration of S57 or R60 producing 50% inhibition of the maximal inotropic or chronotropic response (pIC_{50}) was calculated as the mean ± s.e. mean of the individual pIC_{50}s using non-linear regression analysis. For statistical comparison of more than two groups, a one-way analysis of variance was performed. A P value of less than 0.05 was considered as significant. More details on each procedure are given under Results.

Results

Effects on atrial rate and cardiac contractility

The effects of S57 and R60, 10^{-8} M–10^{-4} M, were compared on rate and amplitude of spontaneous contractions in 12 right atria. Control values of both parameters were 158±5 beats min^{-1} and 321±24 mg, respectively. Figure 2 shows that both

drugs produced a concentration-dependent decrease in both rate and amplitude of spontaneous contractions. For S57 and R60 the negative chronotropic effect reached significant values at all concentrations tested (pIC_{50} values being 5.07 ± 0.19 and 4.76 ± 0.18, respectively), while the negative inotropic effect reached significant values at concentrations higher than 10^{-6} M for S57 ($pIC_{50} = 5.15 \pm 0.22$) and higher than 10^{-4} M for R60 ($pIC_{50} = 4.13 \pm 0.07$. $P < 0.05$). The negative inotropic effect was reversed by increasing the Ca^{2+} concentration in the bathing media from 1.8 to 6 mM or by adding 10^{-6} M isoprenaline. In contrast, the negative chronotropic effect was only slightly reversed by adding 10^{-6} M isoprenaline to the bathing media. The control values for the sinus node recovery time averaged 380 ± 27 ms ($n = 12$). S57 and R60 produced a concentration-dependent prolongation of the sinus node recovery time ($P < 0.05$), but at concentrations higher than 5×10^{-6} M this effect was more marked for S57 than for R60 ($P < 0.05$). At these high concentrations the sinus node recovery time could not be measured in 2 out of 8 experiments exposed to S57 because atria recovered their spontaneous activity 10 s after being electrically paced. This is the reason why these data were not included in Figure 2.

In isolated left atria and papillary muscles driven at a basal rate of 1 Hz the control values for contractile force were 560 ± 30 mg ($n = 19$) and 75 ± 14 mg ($n = 12$) respectively. At concentrations up to 10^{-5} M, S57 and R60 had no significant effects on atrial contractile force, but at higher concentrations R60 produced a significant ($P < 0.05$) negative inotropic effect which was also observed in the presence of 10^{-4} M S57. At concentrations $> 10^{-5}$ M, S57 and R60 also produced a significant ($P < 0.05$) negative inotropic effect in papillary muscles. Thus, at 10^{-4} M, S57 decreased atrial and ventricular contractile force by $13 \pm 6\%$ and $60 \pm 7\%$ and R60 by $33 \pm 7\%$ and $37 \pm 5\%$, respectively.

Effects of S57 and R60 on transmembrane action potentials

The electrophysiological effects of S57 and R60 (10^{-7} M to 5×10^{-5} M) on the action potential characteristics were studied in guinea-pig papillary muscles driven at the basal rate of 1 Hz. Results obtained under control conditions and 30 min after

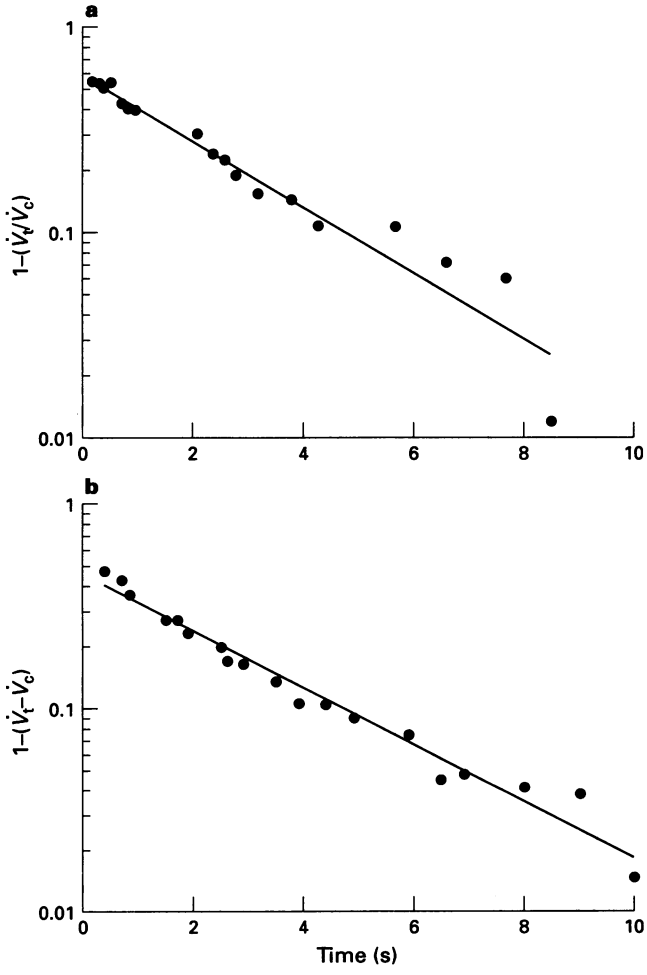

Figure 4 Effects of (a) S57 and (b) R60 on the recovery process of V_{max} block. Ordinate scale: normalized V_{max} values (V_t/V_c), where V_t is the V_{max} of the test action potential and V_c is the V_{max} of the first action potential of the train. Abscissa scale: test interval defined as the interval between the V_{max} of the last action potential of the train and the V_{max} of the test action potential.

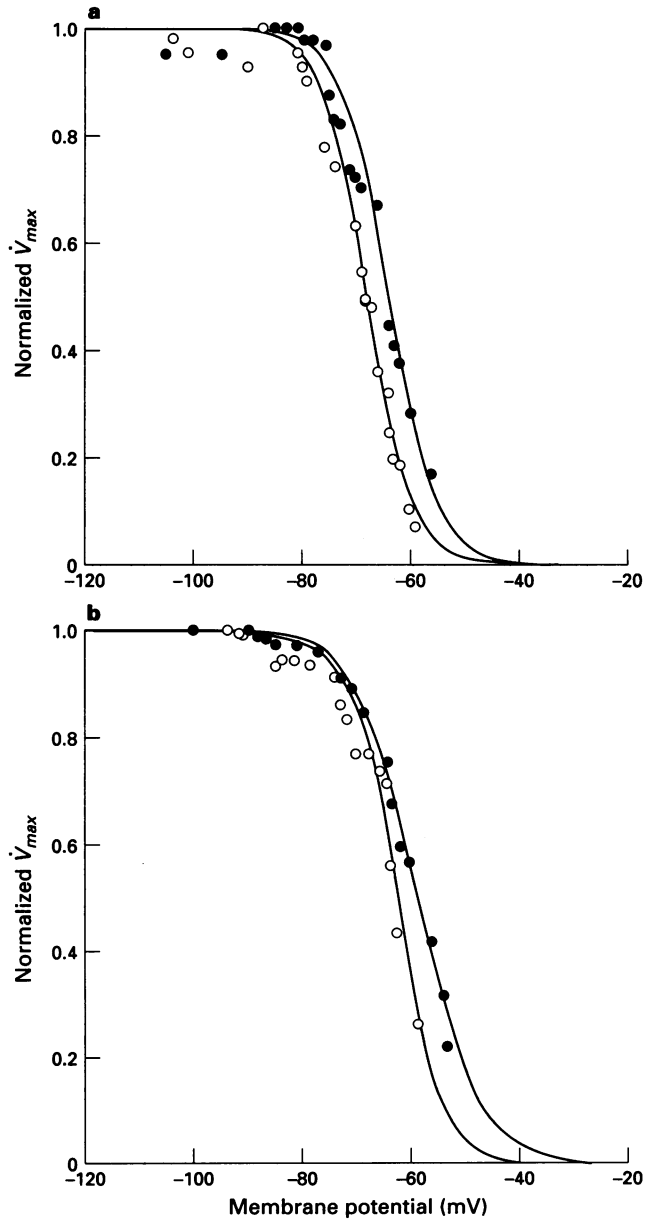

Figure 5 Effects of (a) S57 and (b) R60 on the relationship between V_{max} and the resting membrane potential from which the action potential arises. Ordinate scale: normalized V_{max} values. Abscissa scale: membrane potential. (●) Controls; (○) S57 and R60, 5×10^{-5} M.

each increment in drug concentration are shown in Tables 1 and 2. At concentrations between 10^{-7} and 5×10^{-6} M, S57 and R60 had no effect on transmembrane action potential characteristics. At higher concentrations and even when they had no effect on resting membrane potential or APD_{50} and APD_{90} values, both enantiomers significantly ($P<0.05$) decreased the amplitude and V_{max} of the action potential. S57 and R60 did not modify the ERP and thus, the ERP/APD_{90} ratio remained unaltered.

The effects of S57 and R60 were also studied on the slow, Ca^{2+}-dependent, action potentials elicited by isoprenaline, 10^{-6} M, in ventricular muscles depolarized in high K^+ (27 mM) Tyrode solution and driven at 0.1 Hz. Results obtained in 12 papillary muscles following perfusion with increasing drug concentrations, between 10^{-7} M and 10^{-4} M, are summarized in Table 3. It can be observed that neither S57 nor R60 produced changes in the characteristics of the slow action potentials and, therefore, did not exhibit Ca^{2+} channel blocking properties.

Frequency-dependent effects of S57 and R60

The influence of stimulation frequency on the inhibitory effect of S57 and R60 on V_{max} was studied in papillary muscles by applying trains of pulses at different rates (0.5–3 Hz), separated from one another by a rest period of 5 min. Following the perfusion with 5×10^{-5} M S57 and R60, the V_{max} of the first action potential in each train preceded by a rest period was reduced (e.g. tonic block) by $8.8 \pm 0.4\%$ ($n=7$) and $6.2 \pm 1.1\%$ ($n=7$), respectively. These data indicated that even at this high concentration these drugs exhibited a low affinity for the resting state of the Na^+ channels. When applying a train of pulses in the presence of S57 and R60 there was a gradual decrease of V_{max} from beat to beat to a new steady-state, which depended on the stimulation frequency. Table 4 summarizes the percentage decrease in V_{max} from the first action potential of the train to a new steady-state level in the absence and in the presence of 5×10^{-5} M S57 and R60 in muscles driven at 0.5–3 Hz. Under control conditions an increase in driving rate progressively decreased V_{max} by approximately 10%. In the presence of S57 and R60, the degree of frequency-dependent V_{max} block significantly increased with the driving rate ($P<0.01$), this increase being more marked at fast (2 and 3 Hz, $P<0.001$) than at slow (0.5 and 1 Hz, $P<0.01$) stimulation frequencies. However, the maximum frequency-dependent V_{max} block produced at 3 Hz was similar for both enantiomers. The frequency-dependent V_{max} block produced by 5×10^{-5}M S57 and R60 in two different papillary muscles driven at 0.5–3 Hz is shown in Figure 3.

Onset kinetics of frequency-dependent V_{max} block can be defined in terms of a rate-dependent process. In muscles driven at 0.5–3 Hz, the onset kinetics of S57 and R60 were best fitted by a single exponential curve, from which the onset rate constant per action potential [K, (AP^{-1})] was calculated. The value of K depends on stimulation frequency, decreasing to a similar extent at faster driving rates in the presence of S57 and R60 (Table 5).

Recovery kinetics of frequency-dependent V_{max} *block*

To study the effects of S57 and R60 on the recovery kinetics of frequency-dependent V_{max} block, papillary muscles were driven every 5 min by a train of stimuli at a frequency of 3 Hz for 8 s and a test-stimulus was applied at variable coupling intervals from 250 ms to 10 s. Under control conditions, the recovery from inactivation occurred as a monoexponential process with a time constant (τ_{re}) which averaged 21.7 ± 2.9 ms ($n=12$). In the presence of S57 and R60, 5×10^{-5} M, the recovery from V_{max} block was also fitted by a monoexponential function and the values of the τ_{re} averaged 2.3 ± 0.4 s ($n=6$) and 2.9 ± 0.2 s ($n=6$) (Figure 4), respectively. The y-intercept of the exponential fit can be taken as the fraction of Na^+ channels blocked, which rose to values of $56.1 \pm 2.2\%$ and $52.6 \pm 2.8\%$ for S57 and R60, respectively ($P>0.05$). These data suggested that the block of Na^+ channels induced by both enantiomers was not stereoselective.

Effect on membrane responsiveness

The relationship between V_{max} and the membrane resting potential from which the action potential arises, i.e. membrane responsiveness, was analysed in 8 papillary muscles driven at a basal rate of 0.1 Hz. The resting membrane potential was depolarized stepwise by increasing the $[K^+]_o$ in the bathing media from 2 to 16 mM and the V_{max} values were measured when the resting membrane potential reached steady-state at each $[K^+]_o$. Figure 5 shows that at 5×10^{-5} M, S57 and R60 shifted the membrane responsiveness curve in a hyperpolarizing direction, so that the membrane potential at which V_{max} was reduced to half of its maximum value was shifted by 3.2 ± 0.5 mV ($n=4$) and 4.3 ± 0.4 mV ($n=4$). These results indicated that depressant effects on V_{max} were slightly more pronounced at depolarized than at normal membrane potentials.

Discussion

This study compared the electromechanical properties of two enantiomers, S57 and R60, in guinea-pig isolated atrial and ventricular muscle fibres. The present results indicated that S57 and R60: (a) reduced atrial rate and prolonged the sinus node recovery time at concentrations which induced no negative inotropic effects; (b) produced a similar voltage- and frequency-dependent V_{max} block of the ventricular action potential, which suggested that their interaction with the Na^+ channel was not stereospecific; and (c) the onset and recovery kinetics of frequency-dependent V_{max} block are compatible with those of intermediate kinetics Na^+ channel blockers, e.g., class IA antiarrhythmic drugs. Both S57 and R60 produced a similar decrease in atrial rate and prolonged the sinus node recovery time, a more sensitive test for sinus function, but this prolongation was more marked with S57. Since the negative chronotropic effect was observed at concentrations ($<5 \times 10^{-6}$ M) at which both drugs had no effect on action potential characteristics, it is unlikely that it may be associated with an inhibition of the I_{Na} or with changes in action potential duration. However, at higher concentrations the bradycardic effect produced by both enantiomers can be related, at least partly, to their inhibitory effect on the I_{Na}. Both enantiomers also decreased contractile force in spontaneous right atria, S57 being more potent than R60. Because in guinea-pig atria a decrease in rate may produce parallel changes in contractile force (Koch-Weser & Blinks, 1963), their inotropic effects were also studied in electrically driven left atria and papillary muscles. Under these conditions, S57 and R60 decreased contractile force only at the highest concentrations tested ($>10^{-5}$ M). Therefore, S57 and R60 depress sinoatrial function at concentrations two to three orders of magnitude lower than those that decrease cardiac contractile force and suggested that the negative inotropic effects observed in right atria may be related to their negative chronotropic effect.

Na^+ channel blockers are characterized by their ability to depress the V_{max} of the cardiac action potentials (Hondeghem & Katzung, 1984; Tamargo *et al.*, 1992). In this study, V_{max} values were used as an indirect index of the magnitude of the I_{Na}. The V_{max} is a monotonic but non-linear index of peak I_{Na}, but there is little doubt that V_{max} is mainly generated by this current (Hondeghem, 1978; Sheets *et al.*, 1988). Whether or not possible non-linearities between V_{max} and Na^+ conductance affect the present results remains to be seen in reliable patch-clamp experiments performed under physiological conditions of both temperature and external Na^+ concentration.

S57 and R60 inhibited the V_{max} of the ventricular action potentials without altering the resting membrane potential and

thus, they exhibied Na^+ channel blocking (class I antiarrhythmic) actions. According to the modulated receptor hypothesis (Hondeghem & Katzung, 1984), Na^+ channel blockers bind to a specific binding site located within or functionally associated with the Na^+ channel and its affinity increases with the transition from the rested to the activated/inactivated state of the channel. Like other Na^+ channel blockers (Campbell, 1983a,b; Hondeghem & Katzung, 1984; Tamargo *et al.*, 1992), high concentrations of S57 and R60 caused little tonic V_{max} block in normally polarized ventricular fibres, which indicated that they exhibit little affinity for the resting state of the channel. Frequency-dependent V_{max} block can be explained by a preferential binding of the drugs to the activated and/or inactivated state of the Na^+ channel during a train of action potentials when the diastolic interval between pulses is too short to allow complete recovery of Na^+ availability (Hondeghem & Katzung, 1984; Tamargo *et al.*, 1992). In the presence of S57 and R60, the onset rate of frequency-dependent V_{max} block was faster at higher drug concentrations and at the lower stimulation frequencies. At 3 Hz the K values (0.27 ± 0.02 AP^{-1} and 0.28 ± 0.03 AP^{-1}, respectively) were quite similar to those reported for tocainide, a fast kinetics Na^+ channel blocker (Campbell, 1983a,b). The rate of onset of frequency-dependent V_{max} block, however, is affected by changes in drug concentration and stimulation rate (Hondeghem & Katzung, 1984; Grant *et al.*, 1984; Tamargo *et al.*, 1992). The τ_{re}, which represents the rate of unbinding of the drugs from the inactivated Na^+ channels, is independent of changes in drug concentration or the stimulation rate and, therefore, is considered one of the most reliable parameters to subdivide Na^+ channel blockers (Campbell, 1983a,b; Hondeghem & Katzung, 1984; Tamargo *et al.*, 1992). S57 and R60 prolonged the τ_{re} to 2.3–2.9 s. These values are similar to those previously described for procainamide (2.3 s, Courtney, 1980), imipramine (2.5 s, Delpón *et al.*, 1993) and quinidine (3.7, Sánchez-Chapula, 1985), e.g. intermediate kinetics Na^+ channel blockers (class IA antiarrhythmic drugs). The similar prolongation of the τ_{re} explains why the diastolic interval during the trains was short enough to avoid a complete recovery of V_{max} and thus, S57 and R60 produced a similar frequency-dependent V_{max} block at all driving rates. Therefore, since no differences in the onset and offset kinetics of the V_{max} block were observed in the presence of S57 and R60, their interaction with the Na^+ channel was not stereospecific. Furthermore, in muscles driven at a basic rate much greater than the τ_{re}, S57 and R60 shifted the relationship between V_{max} and resting membrane potential in the hyperpolarizing direction, causing a greater depression of V_{max} at less negative membrane potentials. This result suggested that both enantiomers exhibited a somewhat enhanced affinity for the inactivated state of the Na^+ channel. However, our experiments do not allow us to estimate the relative contribution of activated vs. inactivated block of Na^+ channels that causes the voltage- and frequency-dependent V_{max} block.

The repolarization of the cardiac action potential is the result of a delicate balance between inward (Na^+ and Ca^{2+}) and outward K^+ currents. S57 and R60 did not modify the V_{max} of the slow action potentials, a fairly good approximation of the slow inward Ca^{2+} current (I_{Ca}) (Malecot & Trautwein, 1987), so that it is unlikely that they had an inhibitory effect on this ionic current. Because S57 and R60 inhibited the I_{Na}, an acceleration of the repolarization and a shortening of the ventricular APD would be expected, particularly at high drug concentrations. In fact, a blockade of the Na^+ 'window' current has been suggested to operate for lignocaine and quinidine (Carmeliet & Saikawa, 1982). However, this APD shortening might be counteracted if S57 and R60 inhibited outward K^+ currents. Very recently, we have demonstrated that S57 and R60 inhibited the human cloned K^+ channel (hKv1.5) expressed in a stable mouse cell line (Delpón *et al.*, 1994).

The clinical relevance of the use-dependent V_{max} block produced by S57 and R60 is at present unknown. Since both enantiomers reduce heart rate and may suppress sinus tachycardia, it would be expected that the frequency-dependent decrease in intracardiac conduction velocity secondary to I_{Na} inhibition might be progressively relieved as the driving rate was slowed. The frequency-dependent V_{max} block, however, may be an interesting property that can lead to the suppression of cardiac arrhythmias in an ischaemic cardiac substrate. In addition, the I_{Na} plays a role in the final phase of diastolic depolarization. Whether the inhibition of I_{Na} could contribute, at least partly, to their bradycardic effect must be clarified in further patch-clamp studies.

We thank Dr Y. Joulin (IRIS, Courbevoie, France) for valuable suggestions. This work was supported by a CICYT Grant (SAF92-0157).

References

BOUDOULAS, H., RITTGERS, S.E., LEWIS, R.P., LEIER, C.V. & WEISSLER, A.M. (1979). Changes in diastolic time with various pharmacologic agents: implications for myocardial perfusion. *Circulation*, **60**, 164–169.

CAMPBELL, T. (1983a). Importance of physico-chemical properties in determining the kinetics of the effects of Class I antiarrhythmic drugs on maximum rate of depolarization in guinea-pig ventricle. *Br. J. Pharmacol.*, **80**, 33–40.

CAMPBELL, T. (1983b). Kinetics of onset of rate-dependent effects of Class I antiarrhythmic drugs are important in determining their effects on refractoriness in guinea-pig ventricle and provide a theoretical basis for their subclassification. *Cardiovasc. Res.*, **17**, 344–352.

CARMELIET, E. & SAIKAWA, T. (1982). Shortening of the action potential and reduction of pacemaker activity by lidocaine, quinidine, and procainamide in sheep cardiac Purkinje fibers: an effect on Na or K currents? *Circ. Res.*, **50**, 257–272.

COURTNEY, K. (1980). Interval-dependent effects of small antiarrhythmic drugs on excitability of guinea-pig myocardium. *J. Mol. Cell. Cardiol.*, **12**, 1273–1286.

CRUICKSHANK, J.M. & PRICHARD, B.N.C. (1987). Angina pectoris. In *Beta-Blockers in Clinical Practice*. ed. Cruickshank, J.M. & Prichard, B.N.C. pp. 505–576. London: Churchill Livingstone.

DELPON, E., VALENZUELA, C. & TAMARGO, J. (1989). Electrophysiological effects of E-3753, a new antiarrhythmic drug, in guinea-pig ventricular muscles. *Br. J. Pharmacol.*, **96**, 970–976.

DELPON, E., VALENZUELA, C. & TAMARGO, J. (1990). Tonic and use-dependent V_{max} block induced by imipramine in guinea-pig ventricular muscle fibres. *J. Cardiovasc. Pharmacol.*, **15**, 414–420.

DELPON, E., VALENZUELA, C., PEREZ, O. & TAMARGO, J. (1993). Electrophysiological effects of the combination of imipramine and desipramine in guinea pig papillary muscles. *J. Cardiovasc. Pharmacol.*, **21**, 13–20.

DELPON, E., VALENZUELA, C., PEREZ, O., SNYDERS, D.J. & TAMARGO, J. (1994). Effects of the enantiomers of a new bradycardic agent on hKv1.5 channels. *Biophys. J.*, **66**, A206.

GOETHALS, M., RAES, A. & VAN BOGAERT, P-P. (1993). Use-dependent block of the pacemaker current I_f in rabbit sinoatrial node cells by zatabredine (UL-FS 49). On the mode of action of sinus node inhibitors. *Circulation*, **88**, 2398–2401.

GRANT, A., STARMER, C. & STRAUSS, H. (1984). Antiarrhythmic drug action. Blockade of the inward sodium current. *Circ. Res.*, **55**, 427–439.

GUTH, B.D. (1991). Sinus node inhibitors for reducing exercise-induced myocardial ischemia: Evidence from experimental studies. In *Sinus Node Inhibitors*. ed. Hjalmarson, A & Remme, W.J. pp. 21–36. Darmstadt: Steinkopff Verlag.

HOFFMAN, J.I.E. (1984). Maximal coronary flow and the concept of coronary vascular reserve. *Circulation*, **70,** 153–159.

HONDEGHEM, L. (1978). Validity of V_{max} as a measure of the sodium current in cardiac and nervous tissues. *Biophys. J.*, **23,** 147–152.

HONDEGHEM, L. & KATZUNG, B. (1984). Antiarrhythmic agents: The modulated receptor mechanism of action of sodium and calcium channel-blocking drugs. *Annu. Rev. Pharmacol. Toxicol.*, **24,** 387–423.

KOBINGER, W. & LILLIE, C. (1987). Specific bradycardic agents- a novel pharmacologic class. *Eur. Heart J.*, **8** (suppl. L), 7–15.

KOCH-WESER, J. & BLINKS, J.R. (1963). The influence of the interval between beats on myocardial contractility. *Pharmacol. Rev.*, **15,** 601–652.

MALECOT, C. & TRAUTWEIN, W. (1987). On the relationship between V_{max} of the slow responses and Ca-current availability in whole-cell clamped guinea-pig heart. *Pflügers Arch.*, **410,** 15–22.

O'BRIEN, P., DRAGE, D., SAEIAN, K., BROOKS, H. & WARLTIER, D. (1992). Regional distribution of myocardial perfusion by UL-FS 49, a selective bradycardic agent. *Am. Heart J.*, **123,** 566–574.

OPIE, L.H. (1989). Pharmacology of acute effort angina. *Cardiovasc. Drugs Ther.*, **3,** 257–270.

SANCHEZ-CHAPULA, J. (1985). Electrophysiological interactions between quinidine-lidocaine and quinidine-phenytoin in guinea-pig papillary muscle. *Naunyn-Schmied. Arch. Pharmacol.*, **331,** 369–375.

SHEETS, M., HANCK, D. & FOZZARD, H. (1988). Nonlinear relation between V_{max} and I_{Na} in cardiac Purkinje fibres. *Circ. Res.*, **63,** 386–398.

SONNENBLICK, E.H., ROSS, J. JR. & BRAUNWALD, E. (1968). Oxygen consumption of the heart. Newer concepts of its multifactorial determination. *Am. J. Cardiol.*, **22,** 328–336.

TAMARGO, J. (1980). Electrophysiological effects of bunaphtine on isolated rat atria. *Eur. J. Pharmacol.*, **62,** 81–88.

TAMARGO, J., VALENZUELA, C. & DELPON, E. (1992). New insights into the pharmacology of sodium channel blockers. *Eur. Heart J.*, **13,** (suppl F), 2–12.

THOLLON, C., CAMBA..RAT, C., VIAN, J., PROST, J-F., PEGLION, J.L. & VILAINE, J.P. (1994). Electrophysiological effects of S 16257, a novel sino-atrial node modulator, on rabbit and guinea-pig preparations: comparisons with UL-FS 49. *Br. J. Pharmacol.*, **112,** 37–42.

VALENZUELA, C., DELPON, E. & TAMARGO, J. (1988). Tonic and phasic V_{max} block induced by 5-hydroxypropafenone in guinea-pig ventricular muscles. *J. Cardiovasc. Pharmacol.*, **12,** 423–431.

(Received July 11, 1994
Revised January 18, 1995
Accepted March 23, 1995)

British Journal of Pharmacology (1995) 115, 795-800

Mechanisms of angiotensin II chronotropic effect in anaesthetized dogs

C. Lambert

Faculty of Medicine, Department of Pharmacology, Université de Montréal, C.P. 6128, Succursale Centre-Ville, Montréal, Québec, Canada H3C 3J7

1 The chronotropic effect of angiotensin II (5 μg in 1 ml of Tyrode solution), injected directly into the sinus node artery of 24 anaesthestized and vagotomized dogs pretreated with a β-adrenoceptor antagonist, was evaluated before and after the administration of: (a) an angiotensin II AT_1 receptor antagonist (losartan, 50 $\mu g\ kg^{-1}\ min^{-1}$ infused i.v. for 120 min), (b) an α-adrenoceptor antagonist (prazosin, 1 mg kg^{-1} i.v. bolus injected), (c) a Ca^{2+} channel blocker (nifedipine 50, 100 and 200 $\mu g\ kg^{-1}$ i.v. bolus injected) and (d) a protein kinase inhibitor (staurosporine, 800 nM infused via the sinus node artery at 0.6 ml min^{-1} for 15 min).

2 Losartan and staurosporine by themselves had no effect on basal systemic arterial pressure and heart rate, whereas prazosin and nifedipine caused significant diminutions of both parameters.

3 Angiotensin II induced significant increases in heart rate, the mean augmentations being 29 ± 2 beats min^{-1}. Losartan, nifedipine and staurosporine significantly decreased the chronotropic effect of angiotensin II, the mean respective diminutions being 65 ± 8, 40 ± 9 and $64 \pm 10\%$, whereas prazosin had no effect.

4 This work has demonstrated that angiotensin II exerts *in vivo* a significant positive chronotropic effect that is mediated via AT_1 receptors located in the region of the sinoatrial node. This effect is independent of the adrenergic system. It is decreased by the inhibition of the production of protein kinases, most probably of protein kinase C, and by the blockade of the voltage-sensitive L-type Ca^{2+} channels. Other studies are obviously needed to ascertain the role of angiotensin II in the control of heart rate and/or the genesis of arrhythmias.

Keywords: Angiotensin II; chronotropic effect; AT_1 receptors; losartan; α-adrenoceptors; prazosin; Ca^{2+} channels; nifedipine; protein kinase C; staurosporine

Introduction

Recent biochemical and functional evidence strongly suggests the presence of a renin-angiotensin system, as well as, the synthesis of angiotensin II in the heart (Lindpainter & Ganten, 1988). It has been suggested that angiotensin II may, in the normal heart, modulate coronary blood flow, inotropy, and chronotropy, whereas under pathological conditions, the cardiac renin-angiotensin system may influence or contribute to ventricular growth, postinfarction ventricular remodelling and myocardial metabolism. It may also generate ventricular arrhythmias during ischaemia and reperfusion-induced myocardial injury (Dostal & Baker, 1993).

It has been shown by this laboratory that angiotensin II has a significant positive chronotropic effect, when injected into the sinus node artery of dogs (Lambert *et al.*, 1991). It has also been reported that the stimulatory effects of angiotensin II on the contractile frequency of spontaneously beating cardiomyocytes of neonatal rats are blocked by specific angiotensin II receptor antagonists (Rogers *et al.*, 1986). These results indicate that angiotensin II can increase heart rate. Furthermore, they are in agreement with the findings that high-affinity angiotensin II binding sites are present in heart membrane preparations, as well as, in the specialized conduction system of the rat heart, where the highest concentrations were found in the sinoatrial but mainly in the atrioventricular nodes (Saito *et al.*, 1987; Sechi *et al.*, 1992).

It has been demonstrated that the binding of angiotensin II to its specific G-protein-coupled AT_1 receptors can stimulate phospholipase C in the majority of its target tissues. In turn, this results in the hydrolysis of phosphoinositides and the production of two intracellular second messengers, inositoltriphosphate and diacylglycerol. Inositoltriphosphate releases Ca^{2+} from intracellular stores and diacylglycerol increases the affinity of protein kinase C for Ca^{2+}. It has also been shown that the activation of angiotensin II receptors promotes Ca^{2+} influx either by increasing the activity of receptor-operated channels or by modulating the activity of voltage-sensitive Ca^{2+} channels (Catt *et al.*, 1993; Edwards & Ruffolo, 1994). The mechanisms implicated in the angiotensin II chronotropic effect are still unknown. The aim of the present study was to evaluate the roles of angiotensin II AT_1 receptors, of extracellular Ca^{2+} influx and of protein kinase C, in this effect. To do so, the chronotropic effect of angiotensin, injected directly into the canine sinus node artery, was evaluated before and after the administration of a specific angiotensin II AT_1 receptor antagonist (losartan), of a Ca^{2+} channel blocker (nifedipine) and of a protein kinase inhibitor (staurosporine). Since it is well recognized that an interaction exists between the renin-angiotensin system and the sympathetic nervous system, the influence of α-adrenoceptors on the angiotensin II chronotropic effect was investigated by studying the chronotropic effect of angiotensin II before and after the administration of a specific α-adrenoceptor antagonist (prazosin).

Methods

Animal preparation

Adult mongrel dogs ($n = 24$) of either sex, weighing 20 to 30 kg, were anaesthetized with sodium thiopentone (25 mg kg^{-1}, i.v.) and α-chloralose (80 mg kg^{-1} followed by 300 mg i.v. hourly) and heparinized (200 iu kg^{-1}, i.v.). Artificial respiration was maintained with room air through an endotracheal tube by means of a Harvard pump (model 607). A right thoracotomy was performed at the level of the fourth intercostal space, the pericardium was incised and the heart was suspended in a pericardial cradle. The main sinus node artery was cannulated with a polyethylene catheter connected

to a 3-way stopcock. The sinus node arterial flow, evaluated retrogradely in all the preparations, ranged from 0.35 to 1.00 ml min^{-1}. The sinus node artery was perfused with fresh blood, withdrawn from the femoral vein, at an individualized constant flow (mean value of 0.55 ± 0.05 ml min^{-1}) using a Harvard pump (model 22) until the end of the experiment. This technical procedure has no effect on sinus node function because of extensive arterial anastomoses in the region of the canine sinus node (Nadeau & James, 1966). The left femoral artery and vein were cannulated for pressure measurements and drug injections, respectively. The animals were submitted to a bilateral cervical vagotomy and administered propranolol (1 mg kg^{-1}, i.v.). The blockade of β-adrenoceptors was ascertained in 4 dogs by the pre- and post-propranolol administration of isoprenaline (0.01 μg kg^{-1}, i.v.). Isoprenaline produced mean increases of 40 ± 22 beats min^{-1} before propranolol, whereas it had no effect (0 ± 0 beats min^{-1}) after administration of propranolol.

Experimental protocol

After the completion of all the surgical preparations and a 30 min period of stabilization, Tyrode solution (2×1 ml) was bolus injected (1 min) into the sinus node artery with an intervening 30 min interval. These control injections were followed by 2 injections of angiotensin II (5 μg in 1 ml of Tyrode solution) also at 30 min intervals. Systolic and diastolic blood pressures and heart rate were determined.

Following these 4 baseline determinations, the animals were separated into 4 groups ($n = 6$ per group) and received either: (1) losartan (DuP 753) 50 μg kg^{-1} min^{-1} infused for 120 min via the femoral vein at 0.4 ml min^{-1} (Timmermans *et al.*, 1993); (2) prazosin 1 mg kg^{-1} bolus injected via the femoral vein (Stanaszek *et al.*, 1983); (3) nifedipine 50, 100 and 200 μg kg^{-1} bolus injected via the femoral vein at 30-min intervals (Talajic & Nattel, 1986); or (4) staurosporine 800 nM infused for 15 min via the sinus node artery at 0.6 ml min^{-1} (Matsui *et al.*, 1991).

The blockade of α-adrenoceptors was ascertained in 6 dogs by the pre- and post-prazosin administration of phenylephrine (1.0 μg kg^{-1}, i.v.). Phenylephrine produced significant mean increases in blood pressure of 21 ± 3 mmHg before prazosin, whereas it had only a slight effect (3 ± 2 mmHg) after administration of prazosin. The doses of nifedipine were based on the results of Talajic & Nattel (1986) who demonstrated that these dosages produce blood concentrations that significantly decrease arterial blood pressure and significantly increase AV conduction time, effective refractory period and Wenckebach cycle length in anaesthetized dogs. The concentration of staurosporine was based on a previous report by Tamaoki *et al.* (1986) who demonstrated *in vitro* that nanomolar concentrations of staurosporine significantly inhibit protein kinase C extracted from rat brain. However, as suggested by Matsui *et al.* (1991), in our study the concentration of staurosporine was increased to counteract the poor intracellular penetration of the drug when administered *in vivo*. Direct sinus node artery injections of angiotensin II were repeated: (1) 60 and 120 min following the beginning of losartan infusion; (2) 15 and 45 min following the bolus injection of prazosin; (3) 15 min after each bolus injection of nifedipine; and (4) immediately and 30 min after the end of staurosporine infusion. Systolic and diastolic arterial blood pressures and heart rate derived from an electrocardiogram (lead II) were recorded on a polygraph system (Ealing Scientific Ltd., model 50-9927).

Angiotensin II was injected into the sinus node artery at 30 min intervals to avoid tachyphylaxis. A previous study in this laboratory, using the same experimental model, demonstrated that under these conditions, the chronotropic effect of angiotensin I or II, is maintained for at least 150 min (Lambert *et al.*, 1991). Since the present protocols never exceeded 150 min, it was assumed that the responses to angiotensin II remained constant with the different time cycles that were used.

All the procedures for animal experimentation were done in accordance with the guidelines of the Canadian Council for Animal Care and monitored by an institutional animal care committee.

Drugs

Angiotensin II acetate salt (Sigma Chemical Co., St-Louis, Mo, U.S.A.) was dissolved in Tyrode solution. The solutions of angiotensin II were kept on ice to assure stability and warmed to 37°C immediately prior to injection. Losartan (DuP 753) potassium salt (Du Pont Medical Products, Billerica, Ma., U.S.A.) was dissolved in NaCl 0.9%. Prazosin hydrochloride (Sigma Chemical Co., St-Louis, Mo., U.S.A.) was dissolved in dimethylsulphoxide (DMSO):NaCl 0.9% (5:35 ml) immediately before use. Nifedipine (Sigma Chemical Co., St-Louis, Mo., U.S.A.) was dissolved in 2 ml of ethanol 90%. Staurosporine (Boehringer Mannheim Biochemica, Laval, Canada) was dissolved in DMSO:Tyrode solution (10 μl:25 ml). (±)-Propranolol hydrochloride, (±)-isoprenaline hydrochloride and (−)-phenylephrine hydrochloride (Sigma Chemical Co., St-Louis, Mo, U.S.A.) were dissolved in NaCl 0.9%. DMSO and all the components of the Tyrode solution were purchased from Fischer Scientific (Montréal, Canada).

Statistics

Data are presented as the mean ± s.e.mean. Results were evaluated by Student's paired t tests or one-way repeated measures analysis of variance (ANOVA) and Bonferroni t tests. The critical level of significance was set at $P \leqslant 0.05$.

Results

Effects of bilateral vagotomy and blockade of β-adrenoceptors

Bilateral vagotomy and blockade of β-adrenoceptors caused a significant decrease ($7 \pm 3\%$) in basal heart rate, which remained relatively constant throughout the control period, the mean value being 115 ± 4 beats min^{-1}. Basal mean systemic arterial pressure was not affected by these manipulations, the mean value being 104 ± 4 mmHg.

Effects of Tyrode solution and angiotensin II

The injection of Tyrode solution (1 ml) into the sinus node artery of the 24 dogs caused a slight increase in heart rate with a mean augmentation of 6 ± 1 beats min^{-1}, whereas it had no effect on mean systemic arterial pressure.

The injection of angiotensin II (5 μg in 1 ml of Tyrode solution) into the sinus node artery of the 24 dogs caused significant increases in heart rate and mean systemic arterial pressure with mean augmentations of 29 ± 2 beats min^{-1} and 44 ± 2 mmHg, respectively.

Effects of angiotensin II AT_1 receptor antagonist, losartan

Lambert *et al.* (1994) reported, using the same experimental model in 2 dogs, that a slight increase (3 and 5%) in heart rate and a decrease (26 and 8%) in mean systemic arterial pressure were noted following an infusion of NaCl 0.9% at 2 ml min^{-1} for 180 min. In the present study, losartan was dissolved in NaCl 0.9% and infused i.v. at 0.4 ml min^{-1} for 120 min. Losartan had no significant chronotropic or pressor effects, the mean values being 117 ± 7, 109 ± 7 and 104 ± 7 beats min^{-1} and, 85 ± 9, 64 ± 12 and 65 ± 6 mmHg at baseline as well as after 60 and 120 min of infusion. However, the chronotropic effect of angiotensin II was diminished ($37 \pm 16\%$) and significantly reduced ($65 \pm 8\%$) following the 60 and 120 min

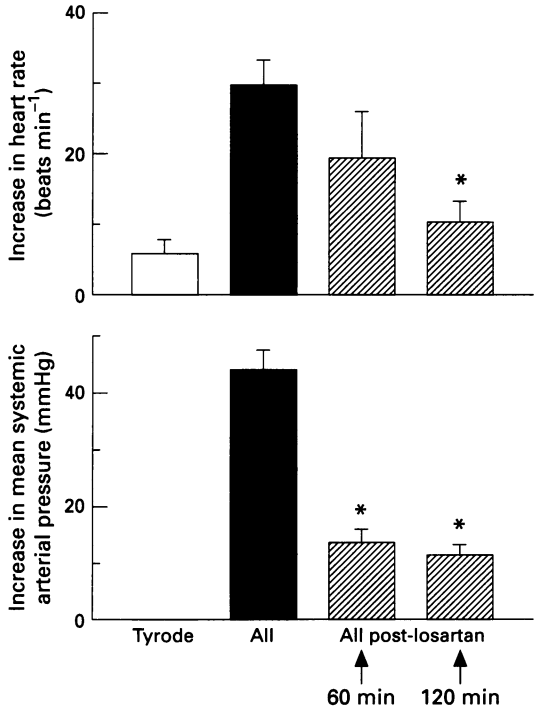

Figure 1 Effects on heart rate and mean systemic arterial pressure of Tyrode solution (1 ml) and angiotensin II (AII) (5 μg in 1 ml of Tyrode solution) bolus injected directly into the sinus node artery of anaesthetized and vagotomized dogs pretreated with a β-adrenoceptor antagonist, before as well as after the i.v. infusion of losartan (50 μg kg^{-1} min^{-1} for 120 min). Data are shown as mean ± s.e.mean (n = 6). Results were evaluated by one-way repeated measures analysis of variance (ANOVA) and Bonferroni t tests. Asterisks (*) indicate significant differences from the baseline response to AII.

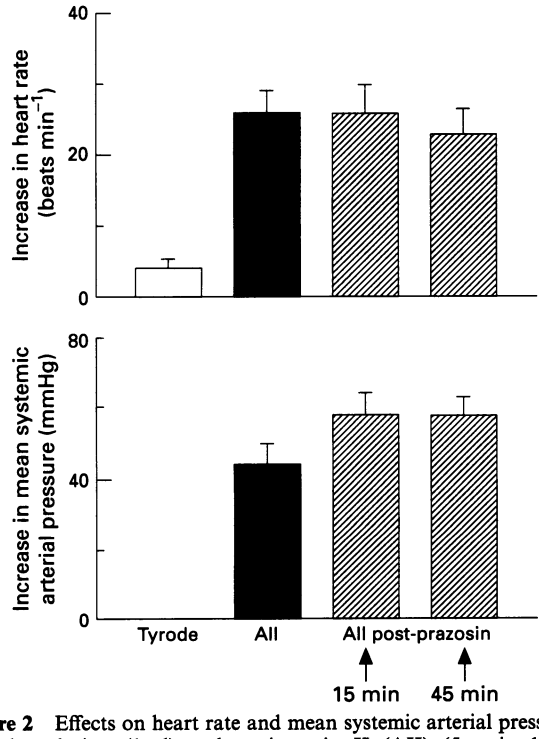

Figure 2 Effects on heart rate and mean systemic arterial pressure of Tyrode solution (1 ml) and angiotensin II (AII) (5 μg in 1 ml of Tyrode solution) bolus injected directly into the sinus node artery of anaesthetized and vagotomized dogs pretreated with a β-adrenoceptor antagonist, before as well as 15 and 45 min after a bolus i.v. injection of prazosin (1 mg kg^{-1}). Data are shown as mean ± s.e.mean (n = 6). Results were evaluated by one-way repeated measures analysis of variance (ANOVA) and Bonferroni t tests.

infusion of losartan. The systemic arterial pressor effect of angiotensin II was also affected with significant decreases of 70 ± 4 and 74 ± 4% after 60 and 120 min of losartan, respectively (Figure 1).

Effects of α-adrenoceptor antagonist, prazosin

Prazosin was dissolved in DMSO: NaCl 0.9% (5:35 ml). Preliminary studies in 4 dogs have determined that the injection of the vehicle alone had no chronotropic (131 ± 13 vs 131 ± 14 beats min^{-1}) or pressor (116 ± 4 vs 112 ± 5 mmHg) effect in our experimental model. Nor did it have any effect on the chronotropic (↑30 ± 3 vs ↑28 ± 4 beats min^{-1}) or pressor (↑35 ± 1 vs ↑34 ± 2 mmHg) effect of angiotensin II. Prazosin caused significant decreases in heart rate and mean systemic arterial pressure with mean values of 108 ± 8 and 102 ± 6 beats min^{-1} and, 104 ± 8 and 90 ± 4 mmHg before and after the bolus injection, respectively. However, as depicted in Figure 2, the α-blockade had no influence on the chronotropic or pressor effect of angiotensin II.

Effects of Ca^{2+} channel blocker, nifedipine

Nifedipine was dissolved in ethanol 90% (2 ml). Preliminary studies in 4 dogs have determined that the injection of the vehicle alone had no chronotropic (114 ± 12 vs 114 ± 12 beats min^{-1}) or pressor (78 ± 18 vs 74 ± 19 mmHg) effect in our experimental model. Nor did it have any effect on the chronotropic (↑36 ± 10 vs↑36 ± 10 beats min^{-1}) or pressor (↑55 ± 9 vs↑46 ± 5 mmHg) effect of angiotensin II. The bolus injections of nifedipine caused significant dose-dependent decreases in heart rate and systemic arterial pressure, the mean maximal reductions being 27 ± 11 and 30 ± 7%, respectively (Table 1). As depicted in Figure 3, the Ca^{2+} channel blockade significantly reduced the chronotropic and pressor effect of angiotensin II, the mean maximal reductions being 40 ± 9 and 68 ± 5%, respectively. These decreases were both dose-related.

Effects of protein kinase inhibition by staurosporine

Staurosporine was dissolved in DMSO: Tyrode solution (10 μl:25 ml). Preliminary studies have determined that the injection of the vehicle alone, directly into the sinus node artery for 15 min at 0.6 ml min^{-1}, had no chronotropic or pressor effect, nor any effect on the chronotropic or pressor effect of angiotensin II in our experimental model. Staurosporine caused no significant effect in heart rate and mean systemic arterial pressure with mean values of 114 ± 10 and 115 ± 12 beats min^{-1} and, 111 ± 14 and 116 ± 12 mmHg before and after the 15 min infusion. The chronotropic effect of angiotensin II was significantly reduced (64 ± 10%) immediately

Table 1 Effects on heart rate and mean systemic arterial pressure of i.v. injections of nifedipine at 30 min intervals, to anaesthetized and vagotomized dogs pretreated with a β-adrenoceptor antagonist

		Nifedipine (μg kg^{-1})		
	Baseline	*50*	*100*	*200*
Heart rate (beats min^{-1})	125 ± 11	119 ± 11	108 ± 12	87 ± 11*
Mean arterial systemic pressure (mmHg)	93 ± 11	70 ± 12*	61 ± 9*	63 ± 9*

Data are shown as mean ± s.e.mean (n = 6). Results were evaluated by one-way repeated measures analysis of variance (ANOVA) and Bonferroni t tests. Asterisks (*) indicate significant differences from the baseline values.

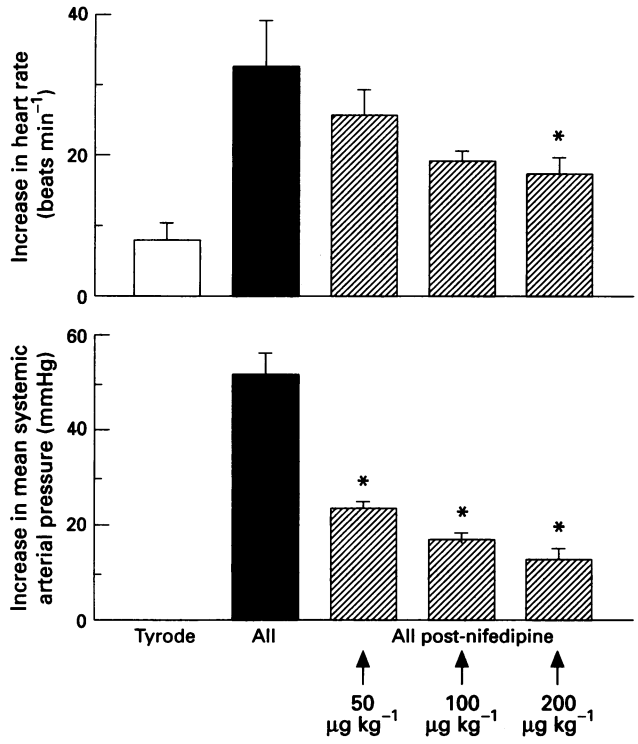

Figure 3 Effects on heart rate and mean systemic arterial pressure of Tyrode solution (1 ml) and angiotensin II (AII) (5 μg in 1 ml of Tyrode solution) bolus injected directly into the sinus node artery of anaesthetized and vagotomized dogs pretreated with a β-adrenoceptor antagonist, before as well as 15 min after bolus i.v. injections of nifedipine (50, 100 and 200 μg kg^{-1}) at 30 min intervals. Data are shown as mean ± s.e.mean ($n=6$). Results were evaluated by one-way repeated measures analysis of variance (ANOVA) and Bonferroni t tests. Asterisks (*) indicate significant differences from the baseline response to AII.

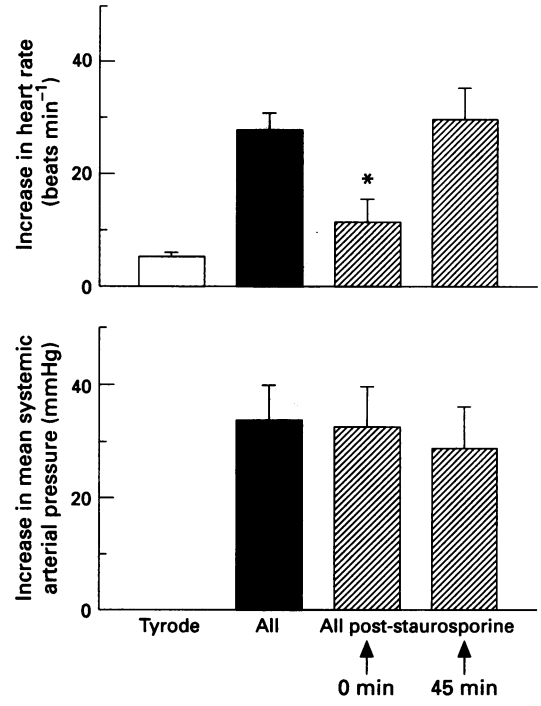

Figure 4 Effects on heart rate and mean systemic arterial pressure of Tyrode solution (1 ml) and angiotensin II (AII) (5 μg in 1 ml of Tyrode solution) bolus injected directly into the sinus node artery of anaesthetized and vagotomized dogs pretreated with a β-adrenoceptor antagonist, before as well as immediately and 30 min after the direct infusion into the sinus node artery of staurosporine (800 nM at 0.6 ml min^{-1} for 15 min). Data are shown as mean ± s.e.mean ($n=6$). Results were evaluated by one-way repeated measures analysis of variance (ANOVA) and Bonferroni t tests. Asterisk (*) indicates significant differences from the baseline response to AII.

after the infusion of staurosporine, but it had returned to baseline values 30 min later. The pressor effect of angiotensin II was not affected by the infusion of staurosporine (Figure 4).

Discussion

The dose of angiotensin II injected in our model (5 μg) was selected to produce a significant and reproducible positive chronotropic effect. It is similar to the doses used by other investigators in the dog (Doursout *et al.*, 1988), rat (Knape & van Zwieten, 1988), and sheep (Lee *et al.*, 1980). The cardiac concentrations obtained after the injection of this dose of angiotensin II into the sinus node artery, are certainly many times higher than the normal endogenous plasma concentrations. Nevertheless, we believe that our findings are compatible with physiopathological roles of angiotensin II since following the discovery of local renin-angiotensin systems, it has been suggested by Dzau (1987) that tissue angiotensin concentrations might exceed those of circulating plasma and by Dostal & Baker (1993) that in the presence of the appropriate stimuli, high concentrations of angiotensin II might be achieved in the heart, which could influence cardiac function. In agreement with these propositions, Lambert *et al.* (1991) have previously reported that the injection of 5 μg of angiotensin I into the canine sinus node artery produced an increase in heart rate similar to the augmentation related to the same dose of angiotensin II. This effect of angiotensin I was almost completely blocked by the administration of captopril, an angiotensin converting enzyme inhibitor, suggesting the presence of a converting enzyme system in the region of the sinus node and moreover, that the tissue concentrations of angiotensin I obtained were in a physiopathological range.

Losartan is a potent, non-agonistic, orally active, selective and competitive angiotensin receptor antagonist with a long duration of action (Timmermans *et al.*, 1991). It shows a very high selectivity for the AT_1 receptor subtype (30,000 more than for AT_2) (Chiu *et al.*, 1990). Its effects have been studied in numerous conscious and anaesthetized, as well as, normotensive and hypertensive experimental dog models. It has been demonstrated that an i.v. infusion of 5 μg kg^{-1} min^{-1} of losartan does not lower blood pressure in anaesthetized dogs, but that it does block the pressor response to an i.v. bolus of angiotensin II (Chan *et al.*, 1991; Timmermans *et al.*, 1993). Our results are in agreement with these findings since, in our model, the 120 min i.v. infusion of losartan had no effect on basal heart rate, caused only a non-significant diminution in basal mean systemic arterial pressure and, significantly decreased the chronotropic and pressor effects induced by angiotensin II injected directly into the sinus node artery. In our study, the pressor effect induced by angiotensin II was affected first by losartan before the chronotropic effect. As already discussed, when angiotensin II is injected locally, its concentrations in the area of the sinus node are certainly many times higher than its systemic and vascular concentrations. Losartan is a competitive antagonist of angiotensin II receptors. Our results suggest that a significant degree of cardiac accumulation of losartan was required before it could inhibit the chronotropic effect related to the high cardiac concentrations of angiotensin II that were obtained. Our findings also strongly suggest that the activity of angiotensin II on heart rate is mediated through the AT_1 receptors. A recent report by Saavedra *et al.* (1993) supports this concept. Using quantitative autoradiography in rat heart sections, they demonstrated that binding could be totally displaced by losartan in both the sinoatrial and atrioventricular nodes, whereas it was in-

sensitive to a specific AT_2 receptor antagonist (PD 123177), again suggesting that angiotensin II receptors in the conduction system belong to the AT_1 subtype.

It is well established that the sympathetic nervous system has an important role in the control of myocardial function. For many years, β-adrenoceptors have been considered to be the exclusive adrenoceptor population through which catecholamines exert their actions on cardiac muscle. In our experiment, blockade of the β-adrenoceptors was accomplished with propranolol so that these receptors could not be implicated as mediators of any of the effects that we observed on heart rate. On the other hand, during the last 20 years, α_1-adrenoceptors have also been identified in myocardial extracts. Furthermore, it is now recognised that these receptors could participate in the regulation of the cardiac rhythm, conduction and force of contraction by affecting different electromechanical processes under either physiological or pathological conditions (Terzic *et al.*, 1993). Even if usually, in normal adult hearts, α_1-adrenoceptor agonists induce no effect on sinus node automaticity (Hewett & Rosen, 1985), since the α-adrenoceptors were not blocked in our study, the possibility that a direct or reflex mediated stimulation of these receptors might have contributed to or modulated the angiotensin II-induced chronotropic effect was not totally precluded.

To examine this possibility, the chronotropic effect of angiotensin II was evaluated before and after the acute i.v. administration of prazosin, a potent competitive postsynaptic α_1-adrenoceptor antagonist (Stanaszek *et al.*, 1983). In this study, prazosin significantly decreased both basal mean systemic arterial pressure and heart rate. This is in agreement with the observation of other investigators who have reported that the arteriolar and venous vasodilatation produced by prazosin is not consistently associated with reflex tachycardia (Brogden *et al.*, 1977) and that prazosin exerts a direct negative chronotropic effect on the canine sinus node (Schwartz *et al.*, 1982). In the present experimental model, the blockade of the α_1-adrenoceptors had no influence on angiotensin II-induced increase in heart rate, suggesting that these receptors do not directly or indirectly participate or contribute to the chronotropic effect of angiotensin II.

The chronotropic effect of angiotensin II was evaluated before and after the administration of increasing doses of nifedipine. As expected, nifedipine by itself caused dose-related significant decreases in basal mean systemic arterial pressure and heart rate. It also significantly reduced both the chronotropic and pressor effect induced by angiotensin II. It is obvious that the interaction between angiotensin II and nifedipine might be an entirely non-specific relation between a positive and a negative chronotropic agent. In the case of specific interaction, our results suggest that angiotensin II produces its effect on heart rate, at least in part, through the activation of voltage-sensitive Ca^{2+} channels of the L-type. Other studies are obviously needed to investigate the possibility that angiotensin II modulates cardiac voltage-sensitive Ca^{2+} channels of the T-type and that this modulation participates in its chronotropic effect.

The chronotropic effect of angiotensin II was also evaluated before and after the administration of staurosporine a highly potent, nonselective, inhibitor of several kinases (Xu *et al.*, 1993). Staurosporine was selected because it is the most potent inhibitor of protein kinase C available to date (Takenaka *et al.*, 1993). It was injected directly into the sinus node artery to assure that maximal concentrations were obtained at this site of action. Staurosporine had no significant effect on basal mean systemic arterial pressure and heart rate nor did it have any influence on the pressor effect induced by angiotensin II. The lack of effect of staurosporine on angiotensin II induced-increase in blood pressure was certainly related to low systemic concentrations of staurosporine due to its general blood and tissue distribution, generating non-effective or non-significant inhibitory concentrations in the vascular cells, the site of action of angiotensin II pressor effect. On the other hand, staurosporine significantly decreased the chronotropic effect generated by angiotensin II. The inhibitory effect of staurosporine was totally reversible, since the angiotensin II effect on heart rate was fully restored 30 min following the end of the administration of staurosporine. The results suggest that protein kinase C participated in the activation of Ca^{2+} channels stimulated by angiotensin II and that this second messenger had a crucial role in the mediation of its chronotropic effect. This observation is in agreement with the results of Xu *et al.* (1993) who, using neonatal rat cardiomyocytes, demonstrated a diminution in cytoplasmic Ca^{2+} concentration in response to angiotensin II in cells pretreated with protein kinase C inhibitors (staurosporine and NPC 15437). This is also consistent with the report of Chardonnens *et al.* (1990) who found that tumour promoting phorbol ester, a potent stimulator of protein kinase C, was able to modulate the cellular action of several vasoactive hormones, including angiotensin II. Nevertheless, since it is well established that staurosporine has only a limited selectivity for protein kinase C and that it strongly inhibits other protein kinases such as protein kinase A and $p60^{v\text{-}src}$ tyrosine kinase (Tamaoki, 1991; Matsui *et al.*, 1991), other studies are obviously needed to confirm the specific and exclusive participation of protein kinase C in the chronotropic effect of angiotensin II.

In summary, it has been demonstrated that angiotensin II exerts *in vivo* a significant positive chronotropic effect that is mediated via AT_1 receptors located in the region of the sinoatrial node. This effect is independent of the adrenergic system. It is decreased by the inhibition of the production of protein kinases, most probably of protein kinase C, and by the blockade of the voltage-sensitive L-type Ca^{2+} channels. It is beyond the scope of this study to extrapolate the physiological and/or pathological roles of the chronotropic effect induced by angiotensin II. Further studies are obviously needed to ascertain this. However, as in many other investigations, it is very tempting to postulate that the renin-angiotensin system, via angiotensin II, is implicated in the control of heart rate and/or the genesis of arrhythmias.

The losartan (Dup 753) was kindly supplied by Dr Ronald D. Smith from Du Pont Merck Pharmaceutical Company. The author wishes to thank Mrs Marie-France Legault and Claudette Lamoureux for their excellent technical assistance and Mrs Elisabeth Pérès for the art work. C.L. is a Canadian Heart and Stroke Foundation scholar. This work was supported by a grant from the Medical Research Council of Canada (MA-11527).

References

BROGDEN, R.N., HEEL, R.C., SPEIGHT, T.M. & AVERY, G.S. (1977). Prazosin: A review of its pharmacological properties and therapeutic efficacy in hypertension. *Drugs*, **14**, 163–197.

CATT, K.J., SANDBERG, K. & BALLA, T. (1993). Angiotensin II receptors and signal transduction mechanisms. In *Cellular and Molecular Biology of the Renin-Angiotensin System*. ed. Raizada, M.K., Phillips, M.I. & Summers, C. pp. 307–356. Boca Raton: CRC Press.

CHAN, D.P., AARHUS, L.L., HEUBLEIN, D.M. & BURNETT, J.R. (1991). The role of angiotensin II in the regulation of basal renal and cardiovascular function. *Circulation*, **84** (Suppl. II), II-107.

CHARDONNENS, D., LANG, U., ROSSIER, M.F., CAPPONI, A.M. & VALLOTTON, M.B. (1990). Inhibitory and stimulatory effects of phorbol esters on vasopressin induced cellular responses in cultures rat aortic smooth muscle cells. *J. Biol. Chem.*, **265**, 10451–10457.

CHIU, A.T., MCCALL, D.E., ARDECKY, R.J., DUNCIA, J.V., NGUYEN, T.T. & TIMMERMANS, P.B.M.W.M. (1990). Angiotensin II receptor subtypes and their selective nonpeptide ligands. *Receptor*, **1**, 33–40.

DOSTAL, D.E. & BAKER, K.M. (1993). Evidence for a role of an intracardiac renin-angiotensin system in normal and failing hearts. *Trends Cardiovasc. Med.*, **3**, 67–74.

DOURSOUT, M.F., CHELLY, J.E., HARTLEY, C.J., SZILAGYI, J., MONTASTRUC, J.L. & BUCKLEY, J.P. (1988). Regional blood flow and cardiac function changes induced by angiotensin II in conscious dogs. *J. Pharmacol. Exp. Ther.*, **246**, 591–596.

DZAU, V.J. (1987). Implications of local angiotensin production in cardiovascular physiology and pharmacology. *Am. J. Cardiol.*, **59**, 59A–65A.

EDWARDS, R.M. & RUFFOLO, R.R. (1994). Angiotensin II receptor signal transduction mechanisms. In *Angiotensin II Receptors*. ed. Ruffolo, R.R. pp. 53–70. Boca Raton: CRC Press.

HEWETT, K.W. & ROSEN, M.R. (1985). Developmental changes in the rabbit sinus node action potential and its response to adrenergic agonists. *J. Pharmacol. Exp. Ther.*, **235**, 308–312.

KNAPE, J.T.A. & VAN ZWIETEN, P.A. (1988). Positive chronotropic activity of angiotensin II in the pithed normotensive rat is primarily due to activation of cardiac β_1-adrenoreceptors. *Naunyn-Schmied. Arch. Pharmacol.*, **338**, 185–190.

LAMBERT, C., GODIN, D., FORTIER, P. & NADEAU, R. (1991). Direct effects in vivo of angiotensins I and II on the canine sinus node. *Can. J. Physiol. Pharmacol.*, **69**, 389–392.

LAMBERT, C., RIBUOT, C., ROBICHAUD, A. & CUSSON, J. (1994). Negative chronotropic effect of the atrial natriuretic peptide in an anaesthetized dog model. *Eur. J. Pharmacol.*, **252**, 245–252.

LEE, W.B., ISMAY, M.J. & LUMBERS, E.R. (1980). Mechanisms by which angiotensin II affects the heart rate of the conscious sheep. *Circ. Res.*, **47**, 286–292.

LINDPAINTER, K. & GANTEN, D. (1988). The cardiac renin-angiotensin system: an appraisal of present experimental and clinical evidence. *Circ. Res.*, **68**, 905–921.

MATSUI, T., TAKUWA, Y., JOHSHITA, H., YAMASHITA, K. & ASANO, T. (1991). Possible role of protein kinase C-dependent smooth muscle contraction in the pathogenesis of chronic cerebral vasospasm. *J. Cereb. Flow Metab.*, **11**, 143–149.

NADEAU, R. & JAMES, T.N. (1966). The behaviour of atrioventricular nodal rhythm following direct perfusion of the sinus node. *Can. J. Physiol. Pharmacol.*, **44**, 317–324.

ROGERS, T.B., GAA, S.T. & ALLEN, I.S. (1986). Identification and characterization of functional angiotensin II receptors on cultured heart myocytes. *J. Pharmacol. Exp. Ther.*, **236**, 438–444.

SAAVEDRA, J.M., VISWANATHAN, M. & SHIGEMATSU, K. (1993). Localization of angiotensin AT_1 receptors in the rat heart conduction system. *Eur. J. Pharmacol.*, **235**, 301–303.

SAITO, K., GUTKIND, J.S. & SAAVEDRA, J.M. (1987). Angiotensin II binding sites in the conduction system of rat hearts. *Am. J. Physiol.*, **253**, H1618–H1622.

SCHWARTZ, K.M., URTHALER, F. & JAMES, T.N. (1982). The direct negative chronotropic action of prazosin on the canine sinus node. *J. Pharmacol. Exp. Ther.*, **221**, 801–805.

SECHI, L.A., GRIFFIN, C.A., GRADY, E.F., KALINYAK, J.E. & SCHAMBELAN, M. (1992). Characterization of angiotensin II receptor subtypes in rat heart. *Circ. Res.*, **71**, 1482–1489.

STANASZEK, W.F., KELLERMAN, D., BROGDEN, R.N. & ROMANKIEWICZ, J.A. (1983). Prazosin update: A review of its pharmacological properties and therapeutic use in hypertension and heart failure. *Drugs*, **25**, 339–384.

TAKENAKA, T., FORSTER, H. & EPSTEIN, M. (1993). Protein kinase C and calcium channel activation as determinants of renal vasoconstriction by angiotensin II and endothelin. *Circ. Res.*, **73**, 743–750.

TALAJIC, M. & NATTEL, S. (1986). Frequency-dependent effects of calcium antagonists on atrioventricular conduction and refractoriness: demonstration and characterization in anesthetized dogs. *Circulation*, **74**, 1156–1167.

TAMAOKI, T. (1991). Use and specificity of staurosporine, UCN-01, and calphostin C as protein kinase inhibitors. *Methods Enzymol.*, **201**, 340–347.

TAMAOKI, T., NOMOTO, H., TAKAHASHI, I., KATO, Y., MORIMOTO, M. & TOMITA, F. (1986). Staurosporine,a potent inhibitor of phospholipid/Ca^{++} dependent protein kinase. *Biochem. Biophys. Res. Commun.*, **135**, 397–402.

TERZIC, A., PUCEAT, M., VASSORT, G. & VOGEL, S.M. (1993). Cardiac α_1-adrenoceptors: an overview. *Pharmacol. Rev.*, **45**, 147–175.

TIMMERMANS, P.B.M.W.M., WONG, P.C., CHIU, A.T. & HERBLIN, W.F. (1991). Nonpeptide angiotensin II receptor antagonists. *Trends Pharmacol. Sci.*, **12**, 55–61.

TIMMERMANS, P.B.M.W.M., WONG, P.C., CHIU, A.T., HERBLIN, W.F., BENFIELD, P., CARINI, D.J., LEE, R.J., WEXLER, R.R., SAYE, J.A.M. & SMITH, R.D. (1993). Angiotensin II receptors and angiotensin II receptor antagonists. *Pharmacol. Rev.*, **45**, 205–251.

XU, Y., SANDIRASEGARANE, L. & GOPALAKRIHNAN, V. (1993). Protein kinase C inhibitors enhance endothelin-1 and attenuate vasopressin and angiotensin II evoked $[Ca^{2+}]_i$ elevation in the rat cardiomyocyte. *Br. J. Pharmacol.*, **108**, 6–8.

(Received July 14, 1994
Revised January 23, 1995
Accepted March 23, 1995)

British Journal of Pharmacology (1995) 115, 801-810

Adenosine A_1 receptor-mediated changes in basal and histamine-stimulated levels of intracellular calcium in primary rat astrocytes

[1]Marie-Claire Peakman & [2]Stephen J. Hill

Department of Physiology & Pharmacology, Medical School, Queen's Medical Centre, Nottingham NG7 2UH

1 The effects of adenosine A_1 receptor stimulation on basal and histamine-stimulated levels of intracellular free calcium ion concentration ($[Ca^{2+}]_i$) have been investigated in primary astrocyte cultures derived from neonatal rat forebrains.

2 Histamine (0.1 μM - 1 mM) caused rapid, concentration-dependent increases in $[Ca^{2+}]_i$ over basal levels in single type-2 astrocytes in the presence of extracellular calcium. A maximum mean increase of 1,468 ± 94 nM over basal levels was recorded in 90% of type-2 cells treated with 1 mM histamine ($n = 49$). The percentage of type-2 cells exhibiting calcium increases in response to histamine appeared to vary in a concentration-dependent manner. However, the application of 1 mM histamine to type-1 astrocytes had less effect, eliciting a mean increase in $[Ca^{2+}]_i$ of 805 ± 197 nM over basal levels in only 30% of the cells observed ($n = 24$).

3 In the presence of extracellular calcium, the A_1 receptor-selective agonist, N^6-cyclopentyladenosine (CPA, 10 μM), caused a maximum mean increase in $[Ca^{2+}]_i$ of 1,110 ± 181 nM over basal levels in 30% of type-2 astrocytes observed ($n = 53$). The size of this response was concentration-dependent; however, the percentage of type-2 cells exhibiting calcium increases in response to CPA did not appear to vary in a concentration-dependent manner. A mean calcium increase of 605 ± 89 nM over basal levels was also recorded in 23% of type-1 astrocytes treated with 10 μM CPA ($n = 30$).

4 In the absence of extracellular calcium, in medium containing 0.1 mM EGTA, a mean increase in $[Ca^{2+}]_i$ of 504 ± 67 nM over basal levels was recorded in 41% of type-2 astrocytes observed ($n = 41$) after stimulation with 1 μM CPA. However, in the presence of extracellular calcium, pretreatment with the A_1 receptor-selective antagonist, 8-cyclopentyl-1,3-dipropylxanthine, for 5 - 10 min before stimulation with 1 μM CPA, completely antagonized the response in 100% of the cells observed.

5 In type-2 astrocytes, prestimulation with 10 nM CPA significantly increased the size of the calcium response produced by 0.1 μM histamine and the percentage of responding cells. Treatment with 0.1 μM histamine alone caused a mean calcium increase of 268 ± 34 nM in 41% of the cells observed ($n = 34$). After treatment with 10 nM CPA, mean calcium increase of 543 ± 97 nM was recorded in 100% of the cells observed ($n = 33$).

6 These data indicate that adenosine A_1 receptors couple to intracellular calcium mobilization and extracellular calcium influx in type-1 and type-2 astrocytes in primary culture. In addition, the simultaneous activation of adenosine A_1 receptors on type-2 astrocytes results in an augmentation of the calcium response to histamine H_1 receptor stimulation.

Keywords: Rat astrocytes; intracellular calcium; adenosine A_1 receptors; histamine H_1 receptors

Introduction

In 1979, Van Calker *et al.* proposed the existence of adenosine A_1 and A_2 receptors which were respectively negatively and positively coupled to adenylyl cyclase via G_i- and G_s-proteins. The A_2 receptor subtype has since been further subdivided into A_{2a} and A_{2b} populations on the basis of the selective actions of the agonist, CGS 21680 (Jarvis *et al.*, 1989) and the antagonist, PD115,199 (Bruns *et al.*, 1987) at A_2 receptors in rat striatal membranes (Daly *et al.*, 1983). Support for this classification has been obtained from the molecular cloning and expression of proteins which appear to correspond to the rat (Mahan *et al.*, 1991), dog (Libert *et al.*, 1991), human (Libert *et al.*, 1992) and bovine (Olah *et al.*, 1992) A_1 receptors, the dog (Maenhaut *et al.*, 1990) and human (Furlong *et al.*, 1992) A_{2a} receptors and the rat (Rivkees & Reppert, 1992; Yakel *et al.*, 1993) and human (Pierce *et al.*, 1992) A_{2b} receptors. Recently novel proteins from rat (Zhou *et al.*, 1992), sheep (Linden *et al.*, 1993) and human (Salvatore *et al.*, 1993) brain have been cloned and expressed and are thought to represent a putative A_3 adenosine receptor binding site.

The presence of A_1 receptors with the ability to inhibit adenosine 3':5'-cyclic monophosphate (cyclic AMP) production via G_i-proteins has been demonstrated in various brain regions such as rat cerebral cortex, cerebellum, hippocampus and striatum (Ebersolt *et al.*, 1983). However, it is now clear that A_1 receptors can also couple to a variety of effector systems other than adenylyl cyclase. In peripheral tissues such as guinea-pig myometrium (Schiemann *et al.*, 1991), a rabbit cortical collecting tubule cell line (Arend *et al.*, 1989), the hamster vas deferens smooth muscle cell line, DDT_1MF-2 (White *et al.*, 1992) and in CHO-K1 cells expressing the human A_1 receptor transfect (Megson *et al.*, 1995), A_1 receptor stimulation causes the production of inositol phosphates. Furthermore, A_1 receptor-mediated increases in intracellular free calcium ion concentration have been reported in a renal epithelial cell line (Weinberg *et al.*, 1989), cultured mesangial cells (Olivera *et al.*, 1992), cortical collecting tubule cells (Arend *et al.*, 1988), tracheal epithelial cells (Galietta *et al.*, 1992) and in both CHO-K1 cells expressing the transfected human A_1 receptor (Iredale *et al.*, 1994) and DDT_1MF-2 cells (Dickenson & Hill, 1993a), in which the effects were sensitive to pertussis toxin treatment. The precise mechanism for this response has not yet been determined; however, it may involve either a di-

[1] Present address: Department of Molecular Biophysics and Biochemistry, Yale Medical School, New Haven. CT. 06510, U.S.A.
[2] Author for correspondence.

rect coupling of A_1 receptors to phospholipase C via a G_i-protein or the activation of phospholipase C by G_i-derived $\beta\gamma$ subunits (Dickenson & Hill, 1994).

Kriegler & Chiu (1993) have previously described transient elevations of $[Ca^{2+}]_i$ mediated by adenosine in glial cells of intact neonatal rat optic nerves injected with a fluorescent calcium indicator. However the receptor subtype involved in this response, was not characterized. In the present paper we have used subtype selective compounds combined with dynamic imaging techinques to investigate the coupling of adenosine A_1 receptors to the elevation of $[Ca^{2+}]_i$ in primary mixed astrocyte cultures. Furthermore, in type-2 astrocytes we have also studied the effects of A_1 receptor activation on the histamine H_1 receptor-mediated increases in intracellular calcium.

Methods

Cell culture

Primary cultures of mixed astrocytes were prepared by mechanical dissociation of tissue from 2 day old rat forebrains as previously reported (Peakman & Hill, 1994). Cells in 75 cm^2 flasks were maintained in Dulbecco's modified Eagle's medium (DMEM) supplemented with 2 mM L-glutamine and 10% foetal calf serum (FCS) at 37°C in a water saturated atmosphere of 10% CO_2 in air. Penicillin 100 u ml^{-1} and streptomycin 100 μg ml^{-1} were also present during the first 24 h of culture. The medium was changed after 1 and 3 days *in vitro* and thereafter every 5 days.

Image analysis

After 13–17 days *in vitro*, cells were removed with trypsin-EDTA solution and reseeded, using a 1:2 or 1:3 split ratio, onto glass coverslips. Two days later, cells had become attached to the coverslips and had differentiated into the classic polygonal, type-1 and stellate, type-2 morphologies. The cells were washed 3 times with 2 ml physiological saline (PSS, composition, mM: NaCl 145, KCl 5.0, $CaCl_2$ 2.0, $MgSO_4$ 1.0 HEPES 10.0, glucose 10.0, adjusted to pH 7.4) and incubated at 37°C with 200 μl PSS containing 10% foetal calf serum and 5 μM fura-2 acetoxymethylester. After 1 h, excess dye was removed by a further 2 washes with 2 ml PSS. The coverslips were maintained in 2 ml PSS at 37°C in the dark and used within 2 h of loading.

Coverslips were mounted so that they formed the base of an open, cylidrical coverslip holder which was maintained at 37°C. The cells were bathed in 900 μl PSS or calcium-free PSS containing 0.1 mM EGTA. Where appropriate, the antagonist 8-cyclopentyl-1,3-dipropyladenosine (DPCPX, 0.1 μM) was included in this solution and incubated with the cells for 5–10 min before image capture. Dynamic video imaging was performed with MagiCal hardware and TARDIS software supplied by Applied Imaging International Ltd. (Hylton Park, Sunderland, Tyne and Wear) as previously described (Marsh & Hill, 1993; see also Neylon *et al.*, 1990 for detail). Two images, I (340 nm) and J (380 nm) were captured from an area of the coverslip which was devoid of cells in order to record the background fluorescence. An appropriate field of view containing type-1 and/or type-2 cells was then selected on the basis of cell morphology as observed through the eyepiece of the microscope. A sequence of 118 frames (each 256 × 256 pixels) was captured at alternating 340 nm (A frames) and 380 nm (B frames) wavelengths with a 1.5 s delay between each image pair. A 200 ms switch time between the two wave lengths was imposed by the hardware averaging of 8 consecutive images to produce each frame. Agonists were added in 100 μl PSS after approximately 14 A and B frames had been captured to provide basal measurements. When the effects of two agonists were investigated in the same capture sequence, the first agonist was added in 90 μl of PSS to a coverslip bathed in 810 μl PSS. The second agonist was then added in 100 μl PSS as usual. At the end of sequence capture, frame I was subtracted from all A images and frame J from all B images. The corrected A and B frames were ratioed to produce R frames. Single cells in the R frames were defined by using a light pen and the average fluorescence intensity of all pixels in the defined region was calculated by TARDIS for each time point in the experiment. The average fluorescence intensities of pixels were correlated with calcium ion concentration using the Grynkiewicz *et al.* (1985) equation:

$$[Ca^{2+}] = K_d\beta\ [R\text{-}R_{min}/R_{max}\text{-}R]$$

where K_d = the dissociation constant (224 nM) for fura-2 and calcium at 37°C; R = the measured fluorescence ratio (intensity at 340 nm/intensity at 380 nm); R_{max} = the measured fluorescence ratio of Ca^{2+}-saturated fura-2; R_{min} = the measured fluorescence ratio in the absence of Ca^{2+} ions; β = (the fluorescence intensity at 380 nm in the absence of Ca^{2+} ions)/(the fluorescence intensity at 380 nm of Ca^{2+}-saturated fura-2)

Values for R_{max} and R_{min} were calculated by the addition of 100 μl PSS containing either 20 mM $CaCl_2$ and 40 μM ionomycin (for R_{max}) or 15 mM EGTA, 40 μM ionomycin and 0.1 M NaOH (for R_{min}). The two types of astrocytes in primary cultures were initially calibrated separately. The average values obtained for type-1 astrocytes were $R_{max} = 1.6 \pm 0.2$ ($n = 20$ cells, 10 separate coverslips), $R_{min} = 0.5 \pm 0.1$ ($n = 16$ cells, 8 separate coverslips) and $\beta = 4.4 \pm 1.7$. The average values obtained for type-2 astrocytes were $R_{max} = 1.6 \pm 0.1$ ($n = 41$ cells, 12 separate coverslips), $R_{min} = 0.5 \pm 0.05$ ($n = 34$ cells, 9 separate coverslips) and $\beta = 6.7 \pm 1.0$. Since the calibration values were so similar for each cell type, they were combined to produce values of $R_{max} = 1.6 \pm 0.1$ ($n = 61$ cells), $R_{min} = 0.5 \pm 0.05$ ($n = 50$ cells) and $\beta = 5.9 \pm 0.8$. Plots of calcium ion concentration against time were generated by TARDIS for each individual cell within the R frames.

Data analysis

Agonist concentration-response data were combined so that each data point represented the mean ± s.e.mean of the increase in $[Ca^{2+}]_i$ over basal levels from n cells on at least 3 separate coverslips derived from different preparations. These values were calculated using two different values for n so that the results were expressed either as a mean ± s.e.mean of all cells observed (regardless of whether they responded or not) or as a mean ± s.e.mean of only those cells which exhibited increases in $[Ca^{2+}]_i$. Agonist concentration-response curves were fitted to a logistic equation using the non-linear regression program, GraphPAD (ISI). The equation fitted was:

$$\text{Response} = \frac{E_{max} \times A^n}{(EC_{50})^n + A^n}$$

where E_{max} is the maximal response, A is the agonist concentration, EC_{50} is the concentration of agonist producing half maximal stimulation, and n is the Hill coefficient.

Statistical analysis was performed within single experiments by using Student's unpaired *t* test or one way analysis of variance (ANOVA) with *post-hoc* Newman-Keuls. Statistical analysis was performed between multiple experiments by using Student's paired *t* test or two way analysis of variance (ANOVA) with *post-hoc* Newman-Keuls.

Materials

Wistar rats were obtained from the Medical School Animal Unit, University of Nottingham. DMEM was obtained from Biological Industries (Cumbernauld, U.K.) and foetal calf serum was purchased from Advanced Protein Products (Brierley Hill, U.K.). Fura-2 acetoxymethylester was purchased from Calbiochem Novabiochem Corpn., Beeston, Nottingham. N^6-cyclopentyladenosine and histamine were supplied by Sigma Chemical Co. (Poole U.K.). 8-Cyclopentyl-1,3-dipropylxanthine (DPCPX) was supplied by Research Biochemicals Inc. Semat (St. Albans, U.K.).

Results

Imaging experiments were performed using coverslips containing populations of both type-1 and type-2 astrocytes as described in the Methods. The calcium responses of each cell type were then analysed separately by use of a light pen to outline single cells within each field of view. In this section, the results obtained for each astrocyte subtype have been considered individually.

Type-2 astrocytes

Type-2 astrocytes in cultures containing a mixture of type-1 and type-2 populations had a mean basal $[Ca^{2+}]_i$ of 192 ± 5 nM ($n = 697$ cells). In the presence of extracellular calcium, the application of high concentrations of histamine caused a large elevation in this level. Figure 1a and 1b shows examples of traces obtained from single cells stimulated with either 1 mM or 10 μM histamine respectively. The peak $[Ca^{2+}]_i$ attained in each type-2 cell was recorded and the size of this response was found to be concentration-dependent (Figure 2). In Figure 2a the effects of increasing concentrations of histamine are expressed as the mean increases in $[Ca^{2+}]_i$ over basal levels in all type-2 astrocytes which were visible in the captured frames. However, a number of cells did not respond to histamine with an increase in $[Ca^{2+}]_i$ and therefore, Figure 2b shows the mean values calculated from responding cells only. An apparently maximal response was achieved with histamine at concentrations between 1 μM and 1 mM (1 mM histamine, mean $[Ca^{2+}]_i$ increase in responding cells = 1,468 ± 94 nM over basal levels, $n = 44$). A much lower response, however, was obtained with 0.1 μM histamine (mean $[Ca^{2+}]_i$ increase in responding cells = 337 ± 34 nM over basal levels, $n = 26$). The percentage of

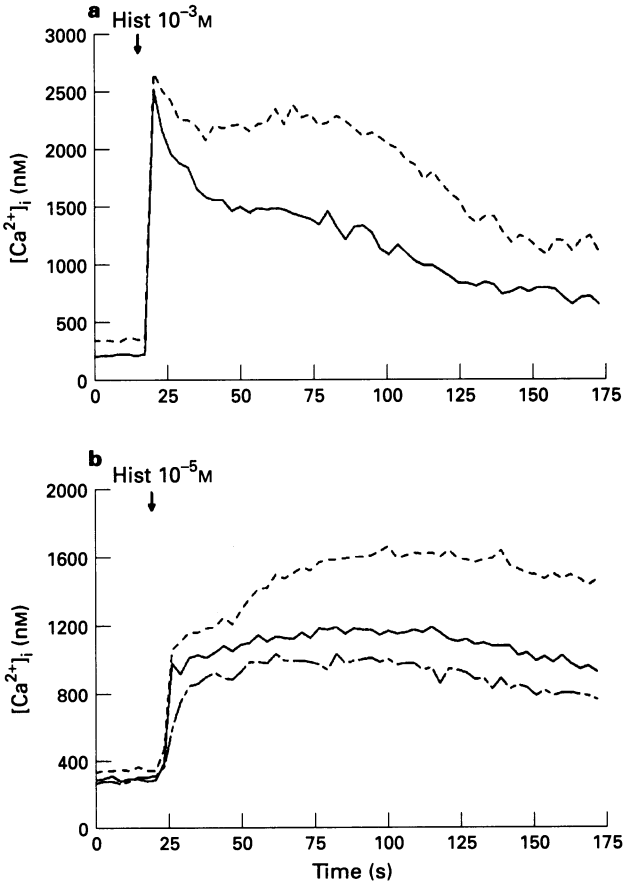

Figure 1 Effect of histamine (Hist) on the intracellular calcium ion concentration in single type-2 astrocytes shown in real time. (a) Traces represent the changes in $[Ca^{2+}]_i$ in 2 single cells in the same field of view, in response to treatment with 1 mM histamine added at the arrow. (b) Traces represent the changes in $[Ca^{2+}]_i$ in 3 single cells in the same field of view, in response to treatment with 10 μM histamine added at the arrow.

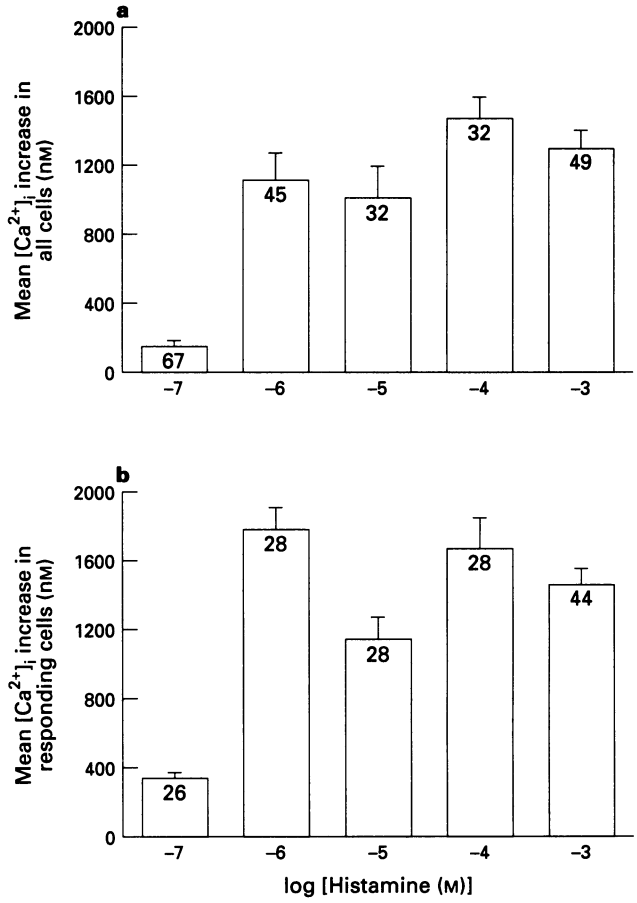

Figure 2 Mean effects of histamine on the elevation of intracellular calcium ion concentration in single type-2 astrocytes. Numbers inside the columns indicate the number of cells analysed, from at least 3 separate animal preparations, in order to generate the value at that agonist concentration. (a) Values represent the means ± s.e.means of the maximal increases in $[Ca^{2+}]_i$ over basal in all visible type-2 astrocytes. (b) Values represent the means ± s.e.means of the maximal increases in $[Ca^{2+}]_i$ over basal in responding type-2 astrocytes only.

Table 1 Frequency of the intracellular calcium responses to histamine and N^6-cyclopentyladenosine in single type-2 astrocytes

Agonist (M)	*Frequency of response (%)*	
	Histamine	*N^6-cyclopentyladenosine*
10^{-3}	90 (44/49)	NR
10^{-4}	88 (28/32)	NR
10^{-5}	88 (28/32)	30 (16/53)
10^{-6}	62 (28/45)	31 (32/104)
10^{-7}	39 (26/67)	11 (4/36)
10^{-8}	NR	17 (14/82)
10^{-9}	NR	22 (4/18)

The frequency of response was obtained from cells on at least 3 separate coverslips derived from different primary mixed astrocyte preparations and was calculated by expressing the number of responding type-2 astrocytes as a percentage of the total number of type-2 astrocytes observed. The numbers in parentheses indicate the number of responding type-2 cells/the total number of type-2 cells observed. NR, not recorded.

responding cells at each agonist concentration is shown in Table 1. Calcium elevations were recorded in approximately 90% of cells after stimulation with 10 μM histamine or above, however, only 39% of the 67 cells treated with 0.1 μM histamine responded with increases in $[Ca^{2+}]_i$. Typical traces from 3 type-2 cells which did not respond to stimulation with 0.1 μM histamine are shown in Figure 8a. The traces in Figure 1 indicate that the temporal pattern of the response to histamine was not the same in all cells. Figure 3 shows example traces from individual cells which illustrate the types of response observed. The most frequent response, recorded in 68% of the 154 cells responding to histamine, was a dramatic, transient peak in $[Ca^{2+}]_i$ which declined to basal (Figure 3a) or to some

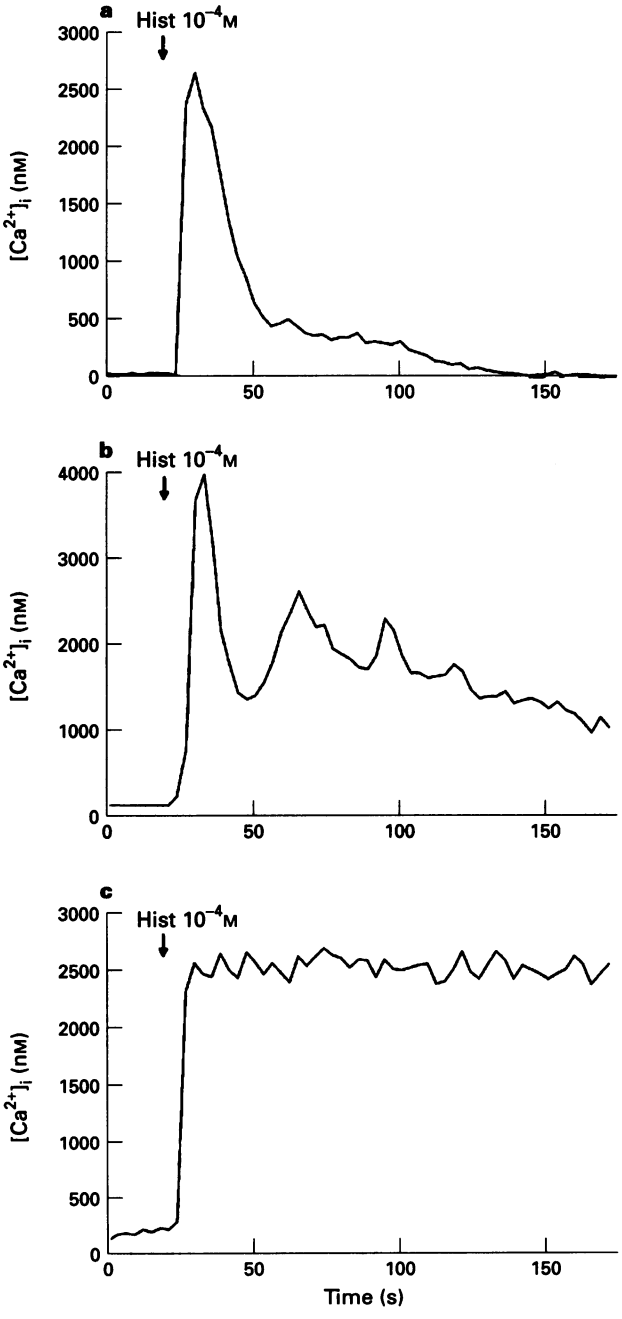

Figure 3 Typical examples of the alterations in intracellular calcium ion concentration observed in type-2 astrocytes after treatment with 0.1 mM histamine (Hist). The most frequent response was a dramatic elevation in $[Ca^{2+}]_i$ which was either transient, declining quickly to basal values (a) or biphasic, declining to some persistently elevated level (b). On a number of occasions the elevation of $[Ca^{2+}]_i$ was sustained for the remainder of the experiment (c).

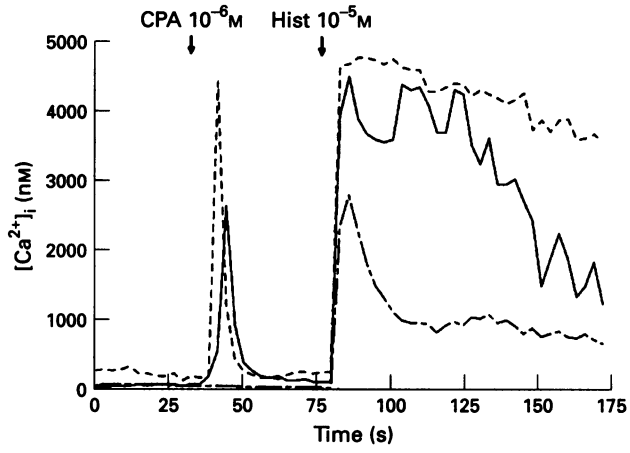

Figure 4 Effect of N^6-cyclopentyladenosine on the intracellular calcium ion concentration in single type-2 astrocytes shown in real time. Traces represent the changes in $[Ca^{2+}]_i$ in 3 single cells in the same field of view, in response to the addition of 1 μM N^6-cyclopentyladenosine (CPA) at the first arrow followed by the further addition of 10 μM histamine (Hist) at the second arrow. Two cells responded to both CPA and histamine. One cell did not exhibit an increase in $[Ca^{2+}]_i$ in response to CPA but did subsequently respond to histamine.

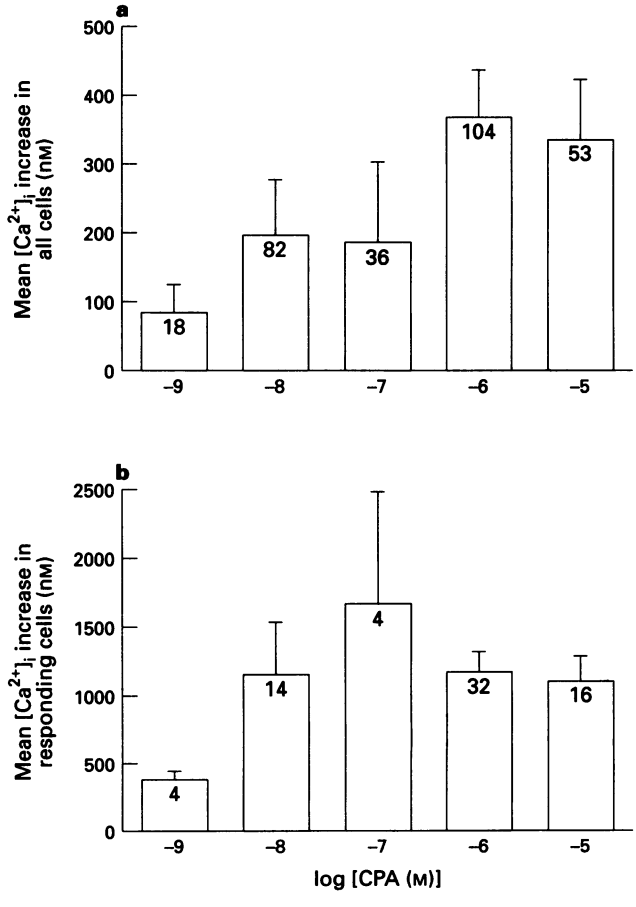

Figure 5 Mean effects of N^6-cyclopentyladenosine on the intracellular calcium ion concentration in single type-2 astrocytes. Numbers inside the columns indicate that the number of cells analysed, from at least 3 separate animal preparations, in order to generate the value at the agonist concentration. (a) Values represent the means ± s.e.means of the maximal increases in $[Ca^{2+}]_i$ over basal in all visible type-2 astrocytes. (b) Values represent the means ± s.e.means of the maximal increases in $[Ca^{2+}]_i$ over basal in responding type-2 astrocytes only.

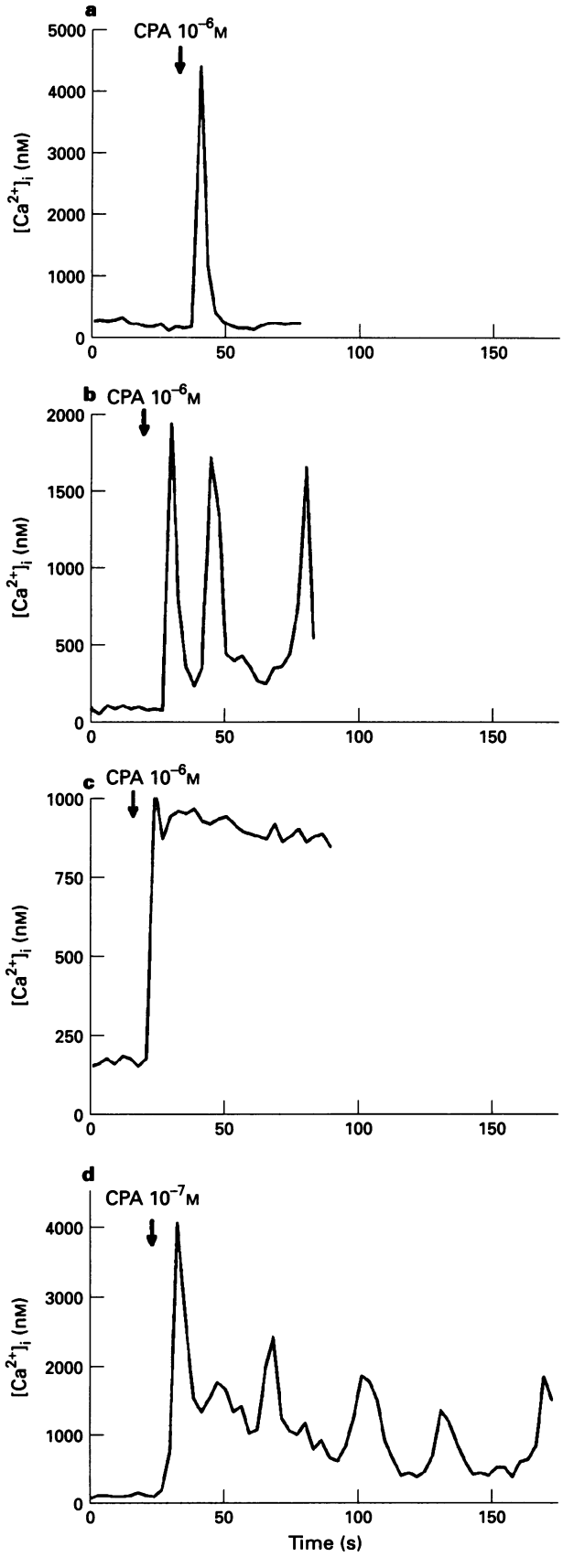

Figure 6 Typical examples of the alterations in intracellular calcium ion concentration observed in type-2 astrocytes after treatment with various concentrations of N^6-cyclopentyladenosine. Responses were generally spiky and predominantly transient (a) or oscillatory (b). Sustained (c) and biphasic (d) responses were also observed.

lower but persistently elevated level (Figure 3b). A sustained increase in $[Ca^{2+}]_i$ was observed in 21% of responding cells (Figure 3c). The shape of the calcium response observed did not appear to correlate with agonist concentration.

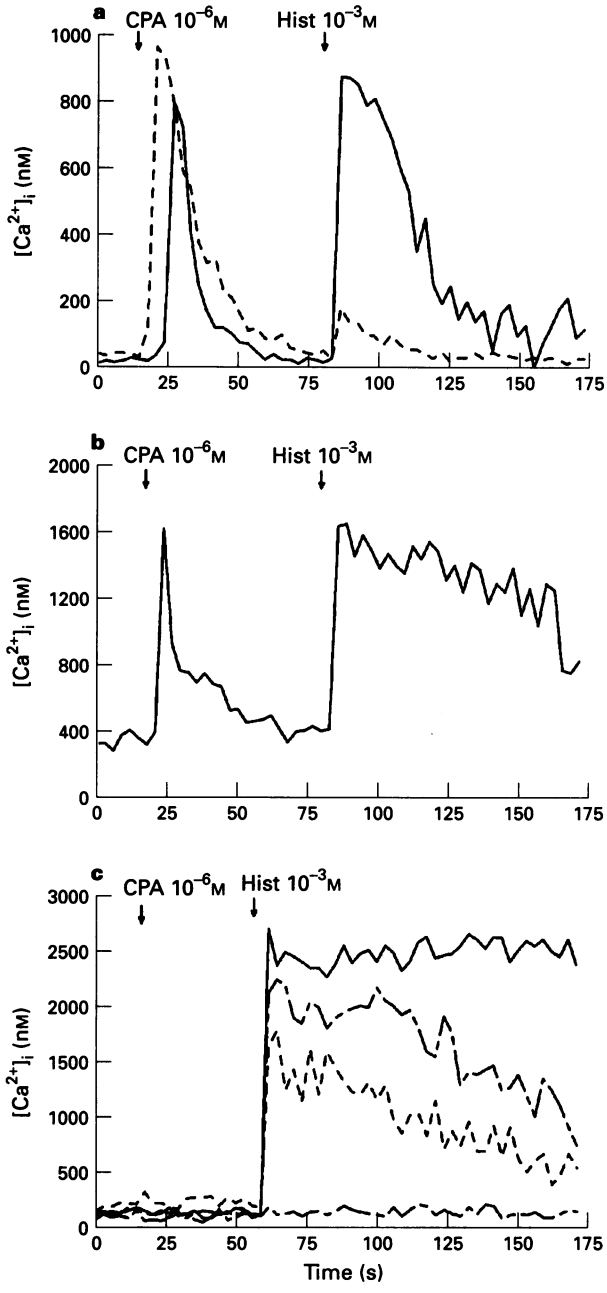

Figure 7 Effect of 8-cyclopentyl-1,3-dipropylxanthine or the absence of extracellular calcium on the N^6-cyclopentyladenosine-mediated increases in intracellular calcium ion concentration in single type-2 astrocytes shown in real time. Traces represent the changes in $[Ca^{2+}]_i$ in single type-2 astrocytes on separate coverslips derived from the same animal preparation and analysed on the same day, in response to the addition of 1 μM N^6-cyclopentyladenosine (CPA) at the first arrow followed by the further addition of 1 mM histamine (Hist) at the second arrow. (a) Traces show that in the absence of extracellular calcium (EGTA 0.1 mM) elevations in $[Ca^{2+}]_i$ were still generated by both CPA and histamine. (b) The control trace for a single type-2 astrocyte in the presence of extracellular calcium and the absence of 8-cyclopentyl-1,3-dipropylxanthine (DPCPX) reveals responses to both agonists. (c) Traces show that in the presence of extracellular calcium and after 10 min pretreatment with 0.1 μM DPCPX, three cells did not respond to 1 μM CPA with an increase in $[Ca^{2+}]_i$ but subsequently responded to 1 mM histamine. In addition, one cell did not respond to either CPA or histamine.

Table 2 Characteristics of the intracellular calcium responses to a combination of histamine (0.1 μM) and N^6-cyclopentyladenosine (10 nM) in type-2 astrocytes

Agonist	*Mean $[Ca^{2+}]_i$ increase* (nM) *All cells*	*Responding cells*	*Frequency of response (%)*
Histamine (0.1 μM)	108 ± 25	268 ± 34	41 (14/34)
CPA (10 nM) + histamine	543 ± 97	543 ± 97	100 (33/33)

The mean increase in intracellular calcium ion concentration was calculated both for all type-2 astrocytes observed in each field (*All cells*) of view and for just those cells which responded to histamine or a combination of N^6-cyclopentyladenosine (CPA) and histamine (*Responding cells*). The frequency of response was obtained from cells on 5 separate coverslips derived from 3 different animal preparations and was calculated by expressing the number of responding type-2 astrocytes as a percentage of the total number of type-2 astrocytes observed. The numbers in parentheses indicate the number of responding type-2 cells/total number of type-2 astrocytes observed. Where appropriate CPA was applied prior to addition of histamine (see Figure 8). No change in $[Ca^{2+}]_i$ was observed in response to the application of CPA in 32 of the 33 cells observed. In one cell, CPA produced a calcium elevation of 611 nM.

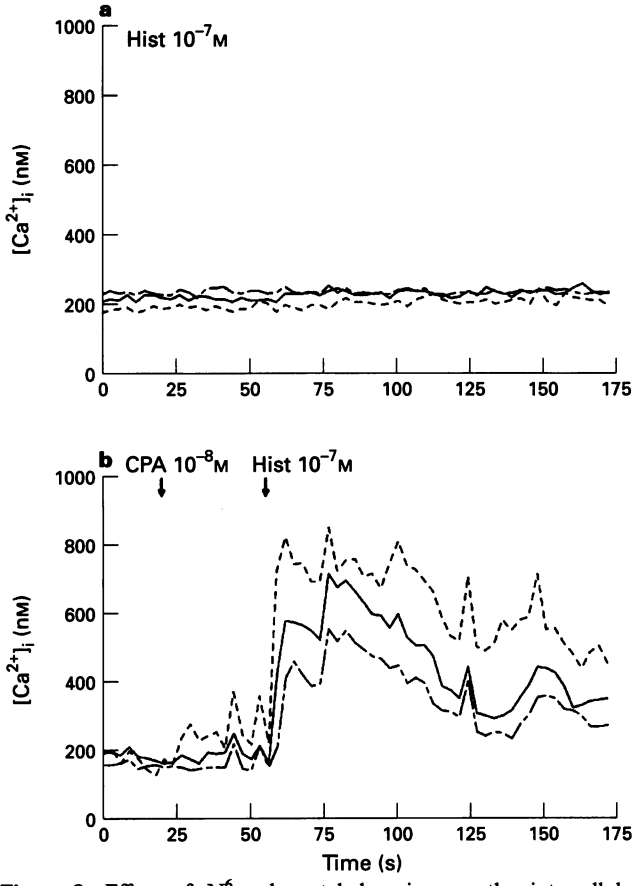

Figure 8 Effect of N^6-cyclopentyladenosine on the intracellular calcium ion concentration in histamine-treated single type-2 astrocytes shown in real time. (a) Traces represent the effect of 0.1 μM histamine (Hist, added at the arrow) on 3 single type-2 astrocytes. No responses were visible. (b) A second coverslip derived from the same animal preparation and analysed on the same day as the coverslip in (a) was used to investigate the effects of N^6-cyclopentyladenosine (CPA) pretreatment. Traces represent the changes in $[Ca^{2+}]_i$ in 3 single type-2 astrocytes in response to the addition of 10 nM CPA at the first arrow followed by the further addition of 0.1 μM histamine at the second arrow. The addition of 10 nM CPA had little or no direct effect on $[Ca^{2+}]_i$, however, a significant augmentation of the effects of 0.1 μM histamine was seen in all cells.

In further studies, in the presence of extracellular calcium, the adenosine A_1 receptor-selective agonist, N^6-cyclopentyladenosine (CPA) also caused an elevation of $[Ca^{2+}]_i$ in some type-2 astrocytes. In 16 cells (30%) out of a total of 53 which were observed, 10 μM CPA increased $[Ca^{2+}]_i$ by a mean value of 1,110 ± 181 nM over basal levels. Examples of the profiles obtained from 3 single type-2 cells after stimulation with 1 μM CPA are shown in Figure 4. Rapid spikes in $[Ca^{2+}]_i$ were generated by two cells whereas a third cell did not appear to exhibit a calcium response. Since the frequency of response was much lower than had previously been observed for histamine, a relatively high concentration of histamine was added to the cells towards the end of each experiment in order to provide some indication of their viability. In Figure 5a the effects of a range of concentrations of CPA are expressed as the mean increases in $[Ca^{2+}]_i$ in all type-2 astrocytes which were visible in the captured frames. These results are expressed in Figure 5b as the mean increases in $[Ca^{2+}]_i$ in only those type-2 cells which responded to CPA. The elevations in $[Ca^{2+}]_i$ were apparently concentration-dependent and the frequency of responding cells at each agonist concentration is shown in Table 1. A maximal responding frequency of approximately 30% was recorded after stimulation with 1 μM ($n = 104$ cells in total) or 10 μM ($n = 53$ cells in total) CPA; however, there did not appear to be a concentration-dependent increase in the frequency of the response up to this level. The profiles in Figure 6 provide typical examples of the responses to CPA observed in individual cells. Approximately 65% of the 70 CPA-mediated calcium responses observed were rapid and spiky in appearance, the majority of these being transient in nature (Figure 6a). In approximately 21% of the responding cells, oscillatory responses with a mean frequency of 3.3 ± 0.4 min^{-1} ($n = 15$ cells) were recorded (Figure 6b). Sustained elevations of $[Ca^{2+}]_i$ were observed in approximately 16% of responding cells (Figure 6c) and the remaining responses tended to be biphasic with a rapid elevation of $[Ca^{2+}]_i$ followed by a slower decline to basal levels (Figure 6d). No apparent relationship was evident between the agonist concentration and the shape of the resulting response.

The CPA-mediated response in type-2 astrocytes was further investigated either in the presence of A_1 receptor-selective antagonist, DPCPX, or in the absence of extracellular calcium. A protocol was adopted using 3 consecutive coverslips of cells derived from the same animal preparation so that, as far as was possible, direct comparisons could be made between coverslips. The first coverslip (in the absence of DPCPX) was stimulated with 1 μM CPA in calcium-free PSS (containing 0.1 mM EGTA). The second coverslip was stimulated with 1 μM CPA in the absence of DPCPX and in calcium-containing PSS. The third coverslip (in calcium-containing PSS) was stimulated with 1 μM CPA in the presence of 0.1 μM DPCPX. This design enabled the second coverslip, to be considered as a control for both the first and the third coverslips. In 5 separate control coverslips derived from 3 different animal preparations, 1 μM CPA, produced a mean increase in $[Ca^{2+}]_i$ of 975 ± 189 nM over basal levels in 31% (10) of 32 cells observed. Figure 7b shows responses to 1 μM CPA and 1 mM histamine obtained from a single type-2 cell on a typical control coverslip.

In the presence of extracellular calcium, the CPA-mediated elevation of $[Ca^{2+}]_i$ in type-2 astrocytes was antagonized by the A_1 receptor-selective antagonist, DPCPX. In 28 type-2 cells on 5 coverslips pretreated with 0.1 μM DPCPX for 5–10 min, no

Table 3 Characteristics of the intracellular calcium responses to histamine and N^6-cyclopentyladenosine (CPA) in single type-1 astrocytes

Agonist	(M)	*Mean $[Ca^{2+}]_i$ increase* (nM) *All cells*	*Responding cells*	*Frequency of response* (%)
Histamine	10^{-3}	268 ± 99	805 ± 197	33 (8/24)
	10^{-4}	337 ± 127	1123 ± 300	30 (9/30)
CPA	10^{-5}	141 ± 50	605 ± 89	23 (7/30)
	10^{-6}	0	0	0 (0/33)

The mean increase in intracellular calcium ion concentration was calculated both for all type-1 astrocytes observed in each field (*All cells*) of view and for just those cells which responded to the agonist (*Responding cells*). The frequency of response was obtained from cells on at least 3 separate coverslips derived from different primary mixed astrocyte preparations and was calculated by expressing the number of responding type-1 astrocytes as a percentage of the total number of type-1 astrocytes observed. The numbers in parentheses indicate the number of responding type-1 cells/the total number of type-1 cells observed.

increases in $[Ca^{2+}]_i$ were recorded in response to 1 μM CPA. The traces in Figure 7c were obtained from 4 cells on a separate coverslip which were derived from the same animal preparation as the cell in Figure 7b and analysed immediately after it. The cells were pretreated with DPCPX for 10 min and then stimulated with 1 μM CPA followed by 1 mM histamine. Three of the cells did not exhibit calcium responses to CPA but did subsequently respond to histamine. One cell did not respond to either CPA or histamine (Figure 7b). The mean increase in $[Ca^{2+}]_i$ obtained in response to histamine (1 mM) following DPCPX (0.1 μM) treatment in responding cells (1907 ± 119 nM; $n = 11$), and the frequency of responding cells (85%; 11/13), were similar to the values obtained in the absence of DPCPX (Table 1, Figure 2b).

In the absence of extracellular calcium ions there was a significant drop ($P < 0.001$, Student's unpaired t test) in the mean basal level of $[Ca^{2+}]_i$ in type-2 astrocytes from 192 ± 5 nM ($n = 607$ cells), calculated in the presence of extracellular calcium, to 141 ± 7 nM ($n = 103$ cells). Under these conditions, however, CPA was still able to elicit increases in $[Ca^{2+}]_i$ in type-2 astrocytes. On 5 separate coverslips stimulated with 1 μM CPA in the absence of extracellular calcium and in the presence of 0.1 mM EGTA, a mean elevation in $[Ca^{2+}]_i$ of 504 ± 67 nM over basal levels was observed in 41% (17) of 41 cells analysed. Figure 7a shows profiles obtained from two individual cells which were derived from the same animal preparation as the cell in Figure 7b. The cells were bathed in calcium-free medium and then stimulated wth 1 μM CPA followed by 1 mM histamine. One cell produced large responses to both CPA and histamine. The second cell gave a large response to CPA but subsequently only a small response to histamine.

The effect of CPA on the response to a low histamine concentration was studied. Coverslips of cells derived from the same animal preparation were alternatively stimulated with either 0.1 μM histamine alone or with 10 nM CPA followed by 0.1 μM histamine. In 5 separate control coverslips from 3 different animal preparations, treatment with 0.1 μM histamine alone caused a mean increase in $[Ca^{2+}]_i$ of 268 ± 34 nM over basal levels in 41% (14) of 34 type-2 cells analysed (Table 2). In 5 corresponding coverslips pretreated with 10 nM CPA, all of the 33 cells observed, responded to 0.1 μM histamine with a mean increase in $[Ca^{2+}]_i$ of 543 ± 97 nM over basal levels (Table 2). In these experiments, however, a calcium elevation of 611 nM over basal levels was only recorded in a single cell in response to treatment with 10 nM CPA. The other cells were insensitive to the first application of CPA. This was notably lower than the 17% responding frequency (see Table 1) previously observed at this concentration of CPA. Figure 8 shows examples of responses observed in corresponding coverslips from the same animal preparation. In Figure 8a traces from 3 cells show no elevations of $[Ca^{2+}]_i$ in response to 0.1 μM histamine alone. In Figure 8b the addition of 10 nM CPA to a separate coverslip appeared to cause a small increase in $[Ca^{2+}]_i$ in one cell but to have no effect on 2 other cells. Subsequent treatment with 0.1 μM histamine resulted in a much augmented effect and elevations of $[Ca^{2+}]_i$ were recorded in all 3 cells.

Type-1 astrocytes

In cultures containing mixed type-1 and type-2 astrocyte populations a mean basal $[Ca^{2+}]_i$ of 207 ± 8 nM ($n = 254$ cells) was calculated for type-1 cells. At high concentrations, histamine caused elevations of $[Ca^{2+}]_i$ in approximately 30% of the type-1 astrocytes observed. The data obtained are summarized in Table 3. The application of 1 mM histamine elicited a mean $[Ca^{2+}]_i$ elevation of 805 ± 197 nM over basal levels in 8 of 24 type-1 cells observed on 6 separate coverslips derived from 5 different animal preparations. A mean $[Ca^{2+}]_i$ increase of 605 ± 89 nM over basal levels was also recorded in 23% of type-1 astrocytes on 7 separate coverslips derived from 5 different animal preparations which were stimulated with 10 μM CPA ($n = 30$). When 1 μM CPA was used, no calcium responses were observed. Table 3 summarises the data which were obtained.

Discussion

Previous investigations in our laboratory have shown that in the hamster-derived DDT_1MF-2 cell line and in CHO-K1 cells expressing the human A_1 receptor transfect, A_1 receptor activation causes the stimulation of phospholipase C resulting in an elevation of inositol phosphate accumulation and a subsequent increase in $[Ca^{2+}]_i$ (White *et al.*, 1992; 1993; Dickenson & Hill, 1993a; Iredale *et al.*, 1994). Furthermore, in the smooth muscle cell line, A_1 receptor-mediated potentiations of the calcium responses elicited by low concentrations of histamine have also been reported (Dickenson & Hill, 1993b). In slices of guinea-pig cerebral cortex, A_1-like receptor activation appears to potentiate histamine H_1 receptor-mediated phosphoinositide turnover (Hollingsworth *et al.*, 1986); however, the cell type involved in this interaction remains to be defined. In the present studies we have therefore investigated the effect of A_1 receptor activation on $[Ca^{2+}]_i$ in rat-derived type-1 and type-2 astrocytes in culture.

Previous studies investigating calcium responses in type-1 astrocytes have reported that in 3–9% of cells, spontaneous oscillations in basal $[Ca^{2+}]_i$ with a frequency of 1.2–1.8 min^{-1} were observed (Nilsson *et al.*, 1991a,b; Helen *et al.*, 1992). In these experiments the authors noted that agonist addition often caused an increase in the frequency and magnitude of these fluctuations. One out of 23 type-2 astrocytes examined by Dave *et al.* (1991) exhibited similar spontaneous oscillations although the frequency of these was not reported. In the present studies, spontaneous oscillations were observed in a total of 5 type-2 astrocytes ($n = 697$) but in no type-1 cells ($n = 254$). Unfortunately, the frequency of these fluctuations

could not be measured as only one spike in $[Ca^{2+}]_i$ was observed prior to agonist addition (at approximately 20 s) in each case. Four of the oscillating cells were treated with CPA (1 μM or 10 μM) and of these, three responded with an increase in the frequency of oscillations and one produced a sustained $[Ca^{2+}]_i$ increase.

Histamine at concentrations of 0.1 μM and above caused elevations of $[Ca^{2+}]_i$ in some type-2 astrocytes. Previously, these effects have been shown to be the result of intracellular calcium mobilisation and extracellular calcium influx mediated via the stimulation of H_1 receptors coupled in a pertussis toxin-insensitive manner to phospholipase C and inositol phosphate production (Fukui *et al.*, 1991; Inagaki *et al.*, 1991b). However, even after the application of 1 mM histamine, a proportion of type-2 astrocytes did not appear to respond in this manner. The frequency of responding cells at each agonist concentration was in close agreement with the values of 62% at 1 μM and 73% at 10 μM reported by Inagaki *et al.* (1991b). A constant maximum responding frequency of approximately 90% was recorded over the concentration range of 10 μM to 1 mM which suggests that about 10% of type-2 astrocytes in the neonatal rat forebrain do not express functional histamine H_1 receptors coupled to phospholipase C. These observations support earlier works which have described a heterogeneous expression of neurotransmiiter receptors in populations of the two astrocyte subtypes (Lerea & McCarthy, 1989; Dave *et al.*, 1991; Inagaki *et al.*, 1991a,b; Jensen & Chiu, 1991; McCarthy & Salm, 1991; Nilsson *et al.*, 1991a,b). When the sizes of the elevations in $[Ca^{2+}]_i$ were combined to produce mean responses for all the cells observed at a specific histamine concentration, they were found to increase in a concentration-dependent manner. The EC_{50} value for histamine appeared to be between 0.1 – 1 μM which was somewhat lower than the value of approximately 10 μM which has previously been observed for this effect (Fukui *et al.*, 1991; Inagaki *et al.*, 1991b). The contribution of non-responding cells to the relationship was indicated by combining the data from responding cells only. The increasing recruitment of responsive cells with increasing histamine concentration may indicate that different cells express receptors which possess variable agonist sensitivities. The temporal patterns of histamine-mediated calcium responses were similar in nature to those previously described by Fukui *et al.* (1991) who classified them into transient, oscillatory, sustained and biphasic (transient peak declining to a persistently elevated level) patterns of response. This group suggested that oscillatory and transient responses were predominantly mediated by intracellular calcium release whereas extracellular calcium influx had greater importance in biphasic and sustained responses. At all concentrations of histamine investigated in the studies described here, the predominant responses were sustained or biphasic and no purely oscillatory responses were observed.

Histamine-stimulated $[Ca^{2+}]_i$ elevations were only apparent in 30% of type-1 astrocytes treated with 0.1 mM agonist indicating that histamine H_1 receptors functionally coupled to phospholipase C are predominantly expressed by type-2 astrocytes. These data concur with earlier studies which have recorded calcium elevations in only 25% (McCathy & Salm, 1991) and 17% (Fukui *et al.*, 1991) of cortical type-1 astrocytes stimulated with 0.1 mM histamine and have shown no effect of histamine on inositol phospholipid hydrolysis (Fukui *et al.*, 1991; Kondou *et al.*, 1991).

In type-2 astrocytes concentration-dependent elevations of $[Ca^{2+}]_i$ were recorded after treatment with CPA at concentrations of 1 nM or above. The percentage of cells responding with calcium increases was lower than previously seen with histamine, reaching a maximum of approximately 30% at 1 μM CPA, and did not appear to be dependent on agonist concentration. The temporal changes in $[Ca^{2+}]_i$ produced by CPA in type-2 astrocytes tended to be more spiky than those produced by histamine and transient or oscillatory profiles were notably more frequent. These effects appeared to be mediated via the stimulation of adenosine A_1 receptors since they were completely abolished by pretreatment of the cells with 0.1 μM DPCPX, an A_1 receptor-selective antagonist. In the absence of extracellular calcium the response to 1 μM CPA was still observed. However, under these conditions, the mean increase in $[Ca^{2+}]_i$ calculated from 17 responding cells was significantly reduced to 51.7% ($P<0.01$ Student's unpaired t test) of the mean increase calculated from 10 responding cells on matched coverslips in calcium containing buffer. Similar effects on the histamine-induced elevation of $[Ca^{2+}]_i$ in DDT_1MF-2 cells have been reported (Dickenson & Hill, 1991; 1992) although, in contrast, the CPA-mediated increases of $[Ca^{2+}]_i$ in this cell line were unaffected by removal of extracellular calcium (White *et al.*, 1992). The data imply that the CPA response in type-2 astrocytes has two components: (1) the release of calcium from intracellular stores and (2) influx of extracellular calcium through calcium channels in the plasma membrane. Numerous reports are now appearing which describe A_1 receptor coupling to phosphoinositide turnover (Arend *et al.*, 1988; Schiemann *et al.*, 1991) or the elevation of $[Ca^{2+}]_i$ (Arend *et al.*, 1988; Weinberg *et al.*, 1989; Galietta *et al.*, 1992; Olivera *et al.*, 1992) in peripheral cell lines and tissues. Adenosine has also been observed to cause transient calcium elevations in glial cells of rat intact neonatal optic nerves (Kriegler & Chiu, 1993). These experiments, provide the first description of A_1 receptor-mediated calcium responses in primary cultures of astrocytes derived from the CNS.

CPA induced elevations of $[Ca^{2+}]_i$ in only a small proportion (23%) of type-1 astrocytes even when used at a concentration of 10 μM. These data suggest that in rat forebrain cultures, adenosine A_1 receptors are predominantly located on type-2 and not type-1 astrocytes. In previous experiments we have shown a lack of A_1 receptor-mediated inhibition of elevated [^{3}H]-cyclic AMP levels in forebrain-derived type-1 astrocytes (unpublished observations) providing further support for this proposal. A recent study by Ogata *et al.* (1994) which reported the presence of adenosine A_1 receptors on type-1 astrocytes derived from embryonic rat hippocampi may therefore indicate that glial A_1 receptor expression varies with brain region.

The calcium response induced in type-2 astrocytes by low concentrations of histamine (0.1 μM) was significantly potentiated by prior treatment with a low (10 nM) concentration of CPA. Two separate effects were apparent. The frequency of responding cells on matched coverslips increased from 41% ($n=34$) responding to 0.1 μM histamine alone, to 100% ($n=33$) after pretreatment with 10 nM CPA. In addition, the mean increase in $[Ca^{2+}]_i$ calculated for the 33 cells pretreated with CPA, was double that calculated for the 14 cells responding to 0.1 M histamine alone. A similar augmentation of calcium responses to submaximal concentrations of histamine has been described in DDT_1MF-2 cells after prior treatment with maximal or submaximal concentrations of CPA (Dickenson & Hill, 1993b). Similar effects were reported in slices of guinea-pig cerebral cortex where adenosine analogues which had no effect on phosphoinositide turnover (Brown *et al.*, 1984) potentiated the histamine H_1 receptor-mediated response (Hollingsworth *et al.*, 1986). More recently, Alexander *et al.* (1994) have demonstrated that activation of metabotropic glutamate receptors can likewise augment histamine-induced inositol phosphate accumulation in the guinea-pig brain.

The effects of CPA on the calcium response to histamine were not examined in type-1 astrocytes because of the low responding frequencies observed after stimulation with each agonist alone. It is therefore interesting that in hippocampal astrocytes which had the morphology of type-1 cells, the elevation of $[Ca^{2+}]_i$ caused by metabotropic glutamate receptor activation was recently augmented by the stimulation of receptors which were apparently of the A_1 subtype (Ogata *et al.*, 1994).

The mechanism(s) for the potentiations which have been reported has not yet been fully elucidated but it appears to require the presence of receptor systems coupled to different G-proteins. Hence in DDT_1MF-2 cells the pertussis toxin-sensi-

tive A_1 receptor-mediated effect has additionally been shown to augment responses to ATP (Gerwins & Fredholm, 1992a) and bradykinin (Gerwins & Fredholm, 1992b) which, like histamine (Dickenson & Hill, 1993a,b) mediate their effects through receptors coupled to phospholipase C via pertussis toxin-insensitive G-proteins. In addition, in mouse striatal astrocytes, somatostatin and A_1 receptors which couple to pertussis toxin-sensitive G-proteins, both interact synergistically with the pertussis toxin-insensitive, α_1-adrenoceptor-mediated increase in inositol phosphate accumulation (El-Etr *et al.*, 1992a,b; Marin *et al.*, 1993). Since the H_1 receptor-mediated response in type-2 astrocytes has previously been shown to be pertussis toxin-insensitive (Fukui *et al.*, 1991), it appears likely that the CPA response in these cells is effected via a pertussis toxin-sensitive G-protein but this remains to be established. In DDT_1MF-2 cells, these interactions have been suggested to involve extracellular and intracellular calcium, protein kinases A and C, and the products of arachidonic acid metabolism (Gerwins & Fredholm, 1992a,b). The cross-talk between A_1 receptors and α_1-adrenoceptors in mouse astrocytes appears to be mediated via the inhibition of glutamate reuptake into astrocytes by arachidonic acid and a similar mechanism may mediate the effects of adenosine on glutamate receptor-mediated calcium responses in hippocampal astrocytes (Ogata *et al.*, 1994), although the latter effect, unlike the former is independent of extracellular calcium. The activity of G_i-derived $\beta\gamma$ subunits which can stimulate some isoforms (mainly β_2 and β_3) of phospholipase C (see Clapham & Neer, 1993) has also been proposed but has yet to be fully investigated (Dickenson & Hill, 1994b).

In conclusion, the results of this study support earlier indications that adenosine A_1 receptors in glial cultures are primarily located on type-2 astrocytes and demonstrate that in these cells, A_1 receptor activation can cause intracellular calcium mobilisation and extracellular calcium influx. In addition, the data provided evidence that adenosine A_1 and histamine H_1 receptors on astrocytes interact synergistically to raise levels of $[Ca^{2+}]_i$ and therefore indicate that glial cells may be responsible, at least in part, for interactions which have previously been reported in brain slices.

We would like to thank The Wellcome Trust for providing a Prize Studentship to support this work.

References

ALEXANDER, S.P.H., HILL, S.J. & KENDALL, D.A (1994). Synergistic interaction betwen glutamate analogues and histamine receptor-stimulated phosphoinositide turnover. *Can. J. Physiol. Pharmacol.*, **72**, p18.7.20.

AREND, L.J., BURNATOWSKA-HLEDIN, M.A. & SPIELMAN, W.S. (1988). Adenosine receptor-mediated calcium mobilisation in cortical collecting tubule cells. *Am. J. Physiol.*, **255**, C581–C588.

AREND, L.J., HANDLER, J.S., RHIM, J.S., GUSOVSKY, F. & SPIELMAN, W.S. (1989). Adenosine-sensitive phosphoinositide turnover in a newly established renal cell line. *Am. J. Physiol.*, **256**, F1067–F1074.

BROWN, E., KENDALL, D.A. & NAHORSKI, S.R. (1984). Inositol phospholipid hydrolysis in rat cerebral cortical slices. I. Receptor characterisation. *J. Neurochem.*, **42**, 1379–1387.

BRUNS, R.F., FERGUS, J.H., BADGER, E.W., BRISTOL, J.A., SANTAY, L.A. & HAYS, S.J. (1987). PD115,199: an antagonist ligand for adenosine A_2-receptors. *Naunyn-Schmied. Arch. Pharmacol.*, **335**, 64–69.

CLAPHAM, D.E. & NEER, E.J. (1993). New roles for G-protein $\beta\gamma$-dimers in transmembrane signalling. *Nature*, **365**, 403–406.

DALY, J.W., BUTTS-LAMB, P. & PADGETT, W. (1983). Subclasses of adenosine receptors in the central nervous system: interaction with caffeine and related methylxanthines. *Cell. Mol. Neurobiol.*, **3**, 69–80.

DAVE, V., GORDON, G.W. & MCCARTHY, K.D. (1991). Cerebral type-2 astroglia are heterogeneous with respect to their ability to respond to neuroligands linked to calcium mobilization. *Glia*, **4**, 440–447.

DICKENSON, J.M. & HILL, S.J. (1991). Histamine-stimulated increases in intracellular calcium in the smooth muscle cell line, DDT_1MF-2. *Biochem. Pharmacol.*, **42**, 1545–1550.

DICKENSON, J.M. & HILL, S.J. (1992). Histamine H_1-receptor-mediated calcium influx in DDT_1MF-2 cells. *Biochem. J.*, **284**, 425–431.

DICKENSON, J.M. & HILL, S.J. (1993a). Adenosine A_1-receptor stimulated increases in intracellular calcium in the smooth muscle cells line, DDT_1MF-2. *Br. J. Pharmacol.*, **108**, 85–92.

DICKENSON, J.M. & HILL, S.J. (1993b). Intracellular cross-talk between receptors coupled to phospholipase C via pertussis toxin-sensitive and insensitive G-proteins in DDT_1MF-2 cells. *Br. J. Pharmacol.*, **109**, 719–724.

DICKENSON, J.M. & HILL, S.J. (1994). Interactions between adenosine A_1- and histamine H_1-receptors. *Int. J. Biochem.*, **26**, 959–969.

EBERSOLT, C., PREMONT, J., PROCHIANTZ, A., PEREZ, M. & BOCKAERT, J. (1983). Inhibition of brain adenylate cyclase by A_1 adenosine receptors: Pharmacological characteristics and locations. *Brain Res.*, **267**, 123–129.

EL-ETR, M., LOMBES, M., BAULIEU, E.E. & ERLANGER, B.F. (1992a). A monoclonal anti-idiotypic 'internal image' antibody that recognizes the A_1 adenosine receptor potentiates the α_1-adrenergic activation of phospholipase C in primary cultures of mouse striatal astrocytes. *Neurosci. Lett.*, **145**, 15–18.

EL-ETR, M., MARIN, P., TENCE, M., DELUMEAU, J.C., CORDIER, J., GLOWINSKI, J. & PREMONT, J. (1992b). 2-Chloroadenosine potentiates the α_1-adrenergic activation of phospholipase C through a mechanism involving arachidonic acid and glutamate in striatal astrocytes. *J. Neurosci.*, **12**, 1363–1369.

FUKUI, H., INAGAKI, N., ITO, S., KUBO, H., KONDOU, H., YAMATODANI, A. & WADA, H. (1991). Histamine H_1-receptors on astrocytes in primary cultures: A possible target for histaminergic neurones. In *New Perspectives in Histamine Research*. ed. Timmerman, H. & van der Goot, H. pp. 161–180. Basel: Birkhauser Verlag.

FURLONG, T.J., PIERCE, K.D., SELBIE, L.A. & SHINE, J. (1992). Molecular characterization of a human brain adenosine A_2 receptor. *Mol. Brain Res.*, **15**, 62–66.

GALIETTA, L.J.V., RASOLA, A., RUGOLO, M., ZOTTINI, M., MASTROCOLA, T., GRUENERT, D. & ROMEO, G. (1992). Extracellular 2-chloroadenosine and ATP stimulate volume-sensitive Cl^- current and calcium mobilisation in human tracheal 9HTEo- cells. *FEBS Lett.*, **304**, 61–65.

GERWINS, P. & FREDHOLM, P.P. (1992a). ATP and its metabolite adenosine act synergistically to mobilise intracellular calcium via the formation of inositol 1,4,5-trisphosphate in a smooth muscle cell line. *J. Biol. Chem.*, **267**, 16081–16087.

GERWINS, P. & FREDHOLM, P.P. (1992b). Stimulation of adenosine A_1-receptors and bradykinin receptors, which act via different G-proteins, synergistically raised inositol 1,4,5-trisphosphate and intracellular calcium in DDT_1MF-2 smooth muscle cells. *Proc. Natl. Acad. Sci. U.S.A.*, **89**, 7330–7334.

GRYNKIEWICZ, G., POENIE, M. & RINK, T.J. (1985). A new generation of Ca^{2+} indicators with greatly improved fluorescence properties. *J. Biochem. Sci.*, **260**, 3440–3450.

HELEN, C., KASTRITSIS, C., SALM, A.K. & MCCARTHY, K. (1992). Stimulation of the P_{2Y} purinergic receptor on type-1 astroglia results in inositol phosphate formation and calcium mobilization. *J. Neurochem.*, **58**, 1277–1284.

HOLLINGSWORTH, E.B., DE LA CRUZ, R.A. & DALY, J.W. (1986). Accumulations of inositol phosphates and cyclic AMP in brain slices: Synergistic interactions of histamine and 2-chloroadenosine. *Eur. J. Pharmacol.*, **122**, 45–50.

INAGAKI, N., FUKUI, H., ITO, S. & WADA, H. (1991a). Type-2 astrocytes show intracellular Ca^{2+} elevation in response to various neuroactive substances. *Neurosci. Lett.*, **128**, 257–260.

INAGAKI, N., FUKUI, H., ITO, S., YAMATODANI, A. & WADA, H. (1991b). Single type-2 astrocytes show multiple independent sites of Ca^{2+} signaling in response to histamine. *Proc. Natl. Acad. Sci. U.S.A.*, **88,** 4215–4219.

IREDALE, P.A., ALEXANDER, S.P.H. & HILL, S.J. (1994). Coupling of a transfected human brain A1 adenosine receptor in CHO-K1 cells to calcium mobilisation via a pertussis toxin-sensitive mechanism. *Br. J. Pharmacol.*, **111,** 1252–1256.

JARVIS, M.F., SCHULTZ, R., HUTCHINSON, A.J., DO, U.H., SILLS, M.A. & WILLIAMS, M. (1989). [^{3}H]CGS 21680, a selective A_2-adenosine receptor agonist directly labels A_2 receptors in rat brain. *J. Pharmacol. Exp. Ther.*, **251,** 888–893.

JENSEN, A.M. & CHIU, S.Y. (1991). Differential intracellular calcium responses to glutamate in type-1 and type-2 cultures brain astrocytes. *J. Neurosci.*, **11,** 1674–1684.

KONDOU, H., INAGAKI, N., FUKUI, H., KOYAMA, Y., KANAMURA, A. & WADA, H. (1991). Histamine-induced inositol phosphate accumulation in type-2 astrocytes. *Biochem. Biophys. Res. Commun.*, **177,** 734–738.

KRIEGLER, S. & CHIU, S.Y. (1993). Calcium signaling of glial cells along mammalian axons. *J. Neurosci.*, **13,** 4229–4245.

LEREA, L.S. & MCCARTHY, K.D. (1989). Astroglial cells *in vitro* are heterogeneous with respect to expression of the α_1-adrenergic receptor. *Glia*, **2,** 135–147.

LIBERT, F., SCHIFFMANN, S.N. LEFORT, A., PARMENTIER, M., GERARD, C., DUMONT, J.E., VANDERHAEGHEN, J.-J. & VASSART, G. (1991). The orphan receptor cDNA RDC7 encodes an A_1 adenosine receptor. *EMBO J.*, **10,** 1677–1682.

LIBERT, F., VAN SANDE, J., LEFORT, A., CZERNILOFSKY, A., DUMONT, J.E., VASSART, G. ENSINGER, H.A. & MENDLA, K.D. (1992). Cloning and functional characterization of a human A_1 adenosine receptor. *Biochem. Biophys. Res. Commun.*, **187,** 919–926.

LINDEN, J., TAYLOR, H.E., ROBEVA, A.S., TUCKER, A.L., STEHLE, J.H., RIVKEES, S.A., FINK, J.S. & REPPERT, S.M. (1993). Molecular cloning and functional expression of a sheep A_3 adenosine receptor with widespread tissue distribution. *Mol. Pharmacol.*, **44,** 524–532.

MAENHAUT, C., VAN SANDE, J., LIBERT, F., ABRAMOWICZ, M., PARMENTIER, M., VANDERHAEGEN, J.-J., DUMONT, J.E., VASSART, G. & SHIFFMANN, S. (1990). RDC8 codes for an adenosine A_2 receptor with physiological constitutive activity. *Biochem. Biophys. Res. Commun.*, **173,** 1169–1178.

MAHAN, L.C., MCVITTIE, L.D., SMYK-RANDALL, E.M. NAKATA, H., MONSMA, Jr, F.J., GERFEN, C.R. & SIBLEY, D.R. (1991). Cloning and expression of an A_1 adenosine receptor from rat brain. *Mol. Pharmacol.*, **40,** 1–7.

MARIN, P., TENCE, M., DELUMEAU, J.-C., GLOWINSKI, J. & PREMONT, J. (1993). Adenosine and somatostatin potentiate the a1-adrenergic activation of phospholipase C in striatal astrocytes through a mechanism involving arachidonic acid and glutamate. *Biochem. Soc. Trans.*, **21,** 1114–1119.

MARSH, K.A., & HILL, S.J. (1993). Characteristics of the bradykinin-induced changes in intracellular calcium ion concentration of single bovine tracheal smooth muscle cells. *Br. J. Pharmacol.*, **110,** 29–35.

MCCARTHY, K.D. & SALM, A.K. (1991). Pharmacologically-distinct subsets of astroglia can be identified by their calcium response to neuroligands. *Neuroscience*, **41,** 325–333.

MEGSON, A.C., DICKENSON, J.M., TOWNSEND-NICHOLSON, A. & HILL, S.J. (1995). Synergy between inositol phosphate responses to transfected human adenosine A_1-receptors and constitutive P_2-purinoceptors in CHO-K1 cells. *Br. J. Pharmacol.*, (in press).

NEYLON, C.B., HOYLAND, J., MASON, W.T. & IRVINE, R.F. (1990). Spatial dynamics of intracellular calcium in agonist-stimulated smooth muscle cells. *Am. J. Physiol.*, **259,** C675–C686.

NILSSON, M., HANSSON, E. & RONNBACK, L. (1991a). Adrenergic and 5-HT_2 receptors on the same astroglial cell. A microspectrofluorimetric study on cytosolic Ca^{2+} responses in single cells in primary culture. *Dev. Brain Res.*, **63,** 33–41.

NILSSON, M., HANSSON, E. & RONNBACK, L. (1991b). Heterogeneity among astroglial cells with respect to 5HT-evoked cytosolic Ca^{2+} responses. A microspectrofluorimetric study on single cells in primary culture. *Life Sci.*, **49,** 1339–1350.

OGATA, T., NAKAMURA, Y., TSUJI, K., SHIBATA, T., KATAOKA, K. & SCHUBERT, P. (1994). Adenosine enhances intracellular Ca^{2+} mobilization in conjunction with metabotropic glutamate receptor activation by *t*-ACPD in cultured hippocampal astrocytes. *Neurosci. Lett.*, **170,** 5–8.

OLAH, M.E., REN, H., OSTROWSKI, J., JACOBSON, K.A. & STILES, G.L. (1992). Cloning, expression and characterization of the unique bovine A_1 adenosine receptor. *J. Biol. Chem.*, **267,** 10764–10770.

OLIVERA, A., LOPEZ-RIVAS, A. & LOPEZ-NOVOA, J.M. (1992). Adenosine stimulates Ca^{2+} fluxes and increases cytosolic free Ca^{2+} in cultured rat mesangial cels. *Biochem. J.*, **282,** 871–876.

PEAKMAN, M.-C. & HILL, S.J. (1994). Adenosine A_{2B}-receptor-mediated cyclic AMP accumulation in primary rat astrocytes. *Br. J. Pharmacol.*, **111,** 191–198.

PIERCE, K.D., FURLONG, T.J., SELBIE, L.A. & SHINE, J. (1992). Molecular cloning and expression of an adenosine A_{2B} receptor from human brain. *Biochem. Biophys. Res. Commun.*, **187,** 86–93.

RIVKEES, S.A. & REPPERT, S.M. (1992). RFL9 encodes an A_{2B} adenosine receptor. *Mol. Endocrinol.*, **6,** 1598–1604.

SALVATORE, C.A., JACOBSON, M.A., TAYLOR, H.E., LINDEN, J. & JOHNSON, R.G. (1993). Molecular cloning and characterization of the human A_3 adenosine receptor. *Proc. Natl. Acad. Sci. U.S.A.*, **90,** 10365–10369.

SCHIEMANN, W.P., DOGGWILER, K.O. & BUXTON, I.L.O. (1991). Action of adenosine in estrogen-primed nonpregnant guinea-pig myometrium: characterisation of the smooth muscle receptor and coupling to phosphoinositide metabolism. *J. Pharmacol. Exp. Ther.*, **258,** 429–437.

VAN CALKER, D., MULLER, M. & HAMPRECHT, B. (1979). Adenosine regulates via two different types of receptors, the accumulation of cyclic AMP in cultured brain cells. *J. Neurochem.*, **33,** 999–1005.

WEINBERG, J.M., DAVIS, J.A., SHAYMAN, J.A. & KNIGHT, P.R. (1989). Alterations of cytosolic calcium in LL-PK_1 cells induced by vasopressin and exogenous purines. *Am. J. Physiol.*, **256,** C967–C976.

WHITE, T.E., DICKENSON, J.M., ALEXANDER, S.P.H. & HILL, S.J. (1992). Adenosine A_1-receptor stimulation of inositol phospholipid hydrolysis and calcium mobilisation in DDT_1MF-2. *Br. J. Pharmacol.*, **106,** 215–221.

WHITE, T.E., DICKENSON, J.M. & HILL, S.J. (1993). Histamine H_1-receptor-mediated inositol phospholipid hydroylsis in DDT_1MF-2 cells: agonist and antagonist properties. *Br. J. Pharmacol.*, **108,** 196–203.

YAKEL, J.L., WARREN, R.A., REPPERT, S.M. & NORTH, R.A. (1993). Functional expression of adenosine A_{2b} receptor in *Xenopus* oocytes. *Mol. Pharmacol.*, **43,** 277–280.

ZHOU, Q.-Y., LI, C., OLAH, M.E., JOHNSON, R.A., STILES, G.L. & CIVELLI, O. (1992). Molecular cloning and characterization of an adenosine receptor: The A_3 adenosine receptor. *Proc. Natl. Acad. Sci. U.S.A.*, **89,** 7432–7436.

(Received January 25, 1995
Revised March 20, 1995
Accepted March 27, 1995)

British Journal of Pharmacology (1995) 115, 811-821

Regenerative caffeine-induced responses in native rabbit aortic endothelial cells

[1]J. Rusko, X. Wang & C. van Breemen

Department of Pharmacology & Therapeutics, Faculty of Medicine, The University of British Columbia, 2176 Health Sciences Mall, Vancouver, B.C. V6T 1Z3, Canada

1 Single native aortic endothelial cells obtained by enzymatic dispersion of the rabbit aortic endothelium were held under voltage clamp using patch pipette and whole-cell membrane currents were measured. In parallel experiments performed on cells from the same batches, the free internal calcium concentration, $[Ca^{2+}]_i$, in the cell was estimated by use of the Ca^{2+}-sensitive fluorescent dye, fura-2.

2 Caffeine (20 mM) applied to the cell evoked an outward current and an initial peak in $[Ca^{2+}]_i$ followed by a lower sustained rise (plateau). Ca^{2+}-free, EGTA-containing solution applied outside the cells did not reduce these responses.

3 Following caffeine stimulation there was a biphasic rising phase of outward current both in the presence and absence of extracellular Ca^{2+}.

4 Application of graded doses of caffeine revealed all-or-none type responses of both the outward current and the rise in $[Ca^{2+}]_i$.

5 Preincubation with lower doses of caffeine reduced the magnitude of both the outward current and the $[Ca^{2+}]_i$ transient evoked by 20 mM caffeine.

6 Tetraethylammonium (3 mM) applied to the bathing solution blocked unitary and spontaneous transient outward currents (STOCs) stimulated by Ca^{2+}-free solution, but only reduced the outward current evoked by caffeine (20 mM).

7 In conclusion, our results reveal the all-or-none nature of Ca^{2+} release from the endoplasmic reticulum (ER) in native aortic endothelial cells. Lower concentrations of caffeine (0.4-0.5 mM) may deplete intracellular Ca^{2+} stores. Extracellular Ca^{2+} is not necessary for maintaining the activity of spontaneous and caffeine-induced outward currents in native aortic endothelial cells. Spontaneous outward currents are believed to represent the sporadic release of calcium from store sites independent of both extracellular Ca^{2+} and the caffeine-sensitive Ca^{2+} stores which stimulate the outward current.

Keywords: Aortic endothelial cells; caffeine; Ca^{2+}-induced Ca^{2+} release; all-or-none response

Introduction

It is widely recognized that most cells employ both intracellular and extracellular sources of Ca^{2+} in cellular signaling. In native rabbit aortic endothelial cells, the dependence of both unitary and spontaneous transient outward currents (STOCs, characterized by a large amplitude $\leqslant 50$ pA) on the internal concentration of Ca^{2+} and EGTA shows that internal Ca^{2+} concentration is important for regulating this activity (Rusko *et al.*, 1992). The currents probably represent the release of stored calcium close to the internal surface of the plasma membrane, causing a temporary and localized rise in $[Ca^{2+}]_i$ which activates potassium channels similar to those described in smooth muscle cells (Benham & Bolton, 1986; Ohya *et al.*, 1987).

The studies of endothelial cells that employed fluorescent Ca^{2+} indicators revealed that endothelium-dependent vasodilators (e.g. bradykinin) activate the cells by eliciting a large transient increase in cytosolic calcium derived from intracellular stores, followed by a smaller sustained increment caused by influx of Ca^{2+} (Johns *et al.*, 1987; Schilling, 1989; Sage *et al.*, 1989; Luckhoff & Busse, 1990; Laskey *et al.*, 1990; Campbell *et al.*, 1991; Buchan & Martin, 1991). This process is probably responsible for subsequent opening of Ca^{2+}-activated K^+ channels stimulated by bradykinin and other agonists (e.g. ATP, acetylcholine) in native aortic endothelial cells (Rusko *et al.*, 1992).

It has been established that the release of Ca^{2+} from internal stores is related to an increase in inositol-1,4,5-trisphosphate (Freay *et al.*, 1989; Schilling & Elliott, 1992). The contribution of the second known Ca^{2+} release mechanism; namely, Ca^{2+}-induced Ca^{2+} release (CICR) in endothelial cells is controversial. While in the presence of extracellular Ca^{2+}, caffeine (5 mM) induced a small elevation of $[Ca^{2+}]_i$ (Buchan & Martin, 1991) this increase in $[Ca^{2+}]_i$was not observed in another study using a higher concentration of caffeine (10 mM) (Schilling & Elliott, 1992). It was suggested that Ca^{2+}-induced Ca^{2+} release either does not contribute to agonist-induced changes in $[Ca^{2+}]_i$ in endothelial cells or has a different pharmacological sensitivity compared with that in skeletal or cardiac muscle.

However, recently it has been shown that human aortic endothelial cell lines responded to caffeine (10 mM) by elevation of $[Ca^{2+}]_i$, but only when placed in low $[Mg^{2+}]_o$ (0.3 mM) (Zhang *et al.*, 1993). These results indicate the need for studying the effect of caffeine in the regulation of $[Ca^{2+}]_i$ to elucidate the mechanism(s) of intracellular Ca^{2+} release and subsequent activation of potassium channels in native aortic endothelial cells.

Recent studies have demonstrated that the membrane hyperpolarization of coronary endothelial cells induced by caffeine is concentration-dependent and is sensitive to the removal of Ca^{2+} from the perfusing solution (Chen & Cheung, 1992). Although the physiological function of the Ca^{2+}-dependent K^+ channels is unknown, channel activation may hyperpolarize the endothelial cell and increase the

[1] Author for correspondence.

driving force for Ca^{2+} entry during stimulation by agonists (Busse *et al.*, 1988; Schilling, 1989; Luckhoff & Busse, 1990).

The purpose of the present study was to describe evidence for the relationship between intracellular stores and the plasmalemma in native aortic endothelial cells. We have examined the effects of the Ca^{2+}-release activator, caffeine, on correlation between membrane currents and $[Ca^{2+}]_i$ in the presence and absence of extracellular Ca^{2+} using whole-cell membrane current recordings under voltage clamp and parallel cytosolic $[Ca^{2+}]_i$ measurements using imaging fluorescence microscopy.

Methods

Preparation of cells

Rabbits of either sex weighing (1.5–2.2 kg) were anaesthetized and killed by carbon dioxide. Freshly dissociated endothelial cells were obtained from the aorta by procedures previously described (Rusko *et al.*, 1992). Briefly, several pieces of endothelium were incubated at 37°C for 35 min in dispersal solution containing 0.9 mg ml^{-1} papain and 0.8 mg ml^{-1} dithiothreitol. After the enzyme digestions, tissue fragments were washed with enzyme-free, Dulbecco's phosphate-buffered

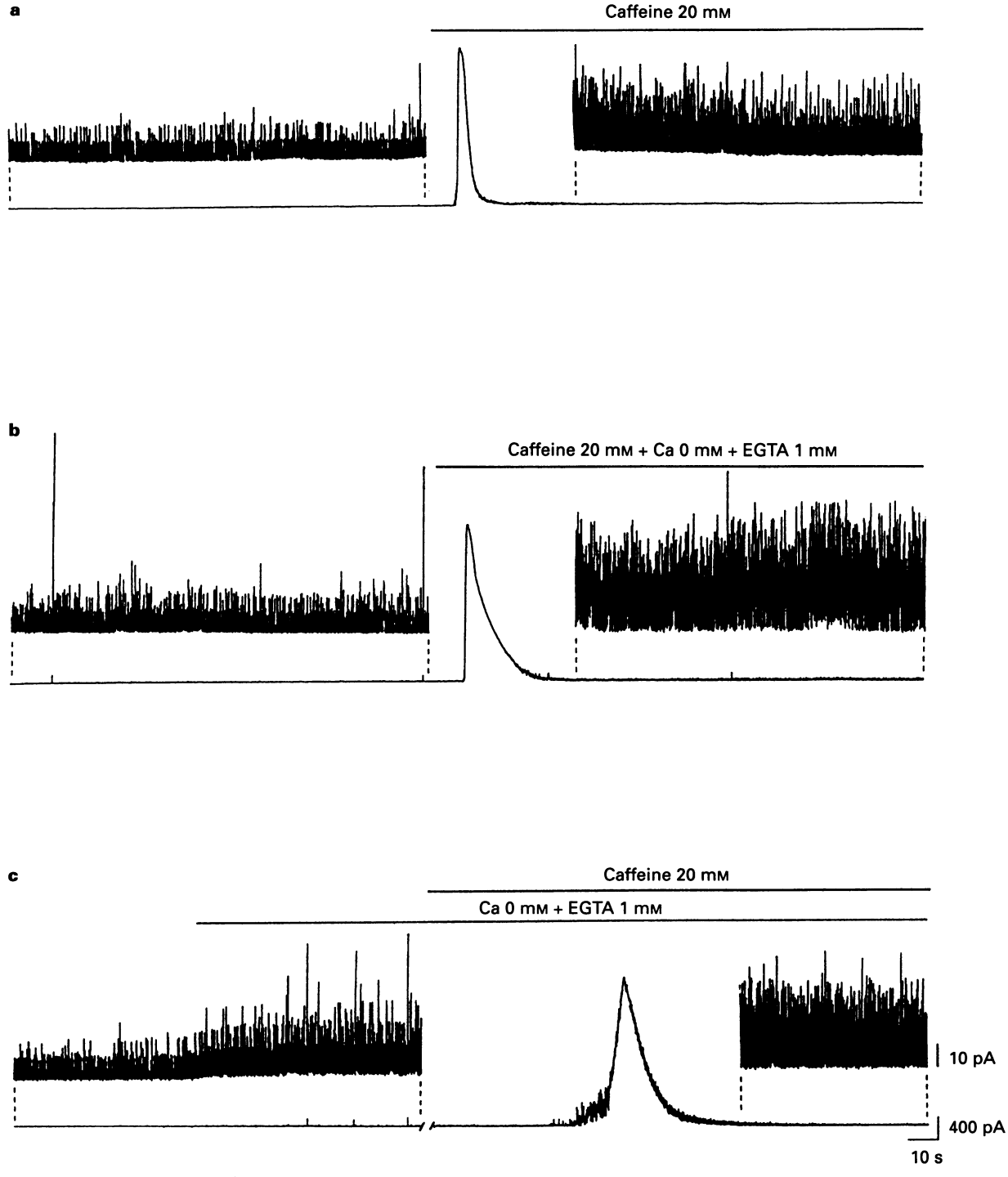

Figure 1 Responses of endothelial cells to caffeine application. Continuous records of whole cell currents in the presence (a) and in absence of extracellular Ca^{2+} (c). (b) Extracellular Ca^{2+} was omitted at the same time as caffeine was applied. The upper traces of each pair show current activity on expanded current scale. Horizontal bars indicate period during which cells were bathed in extracellular solution containing caffeine (20 mM) and no added Ca^{2+}; (a) and (b), the same scale as (c). Outward currents are upward in these and in subsequent records. Holding potential +20 mV.

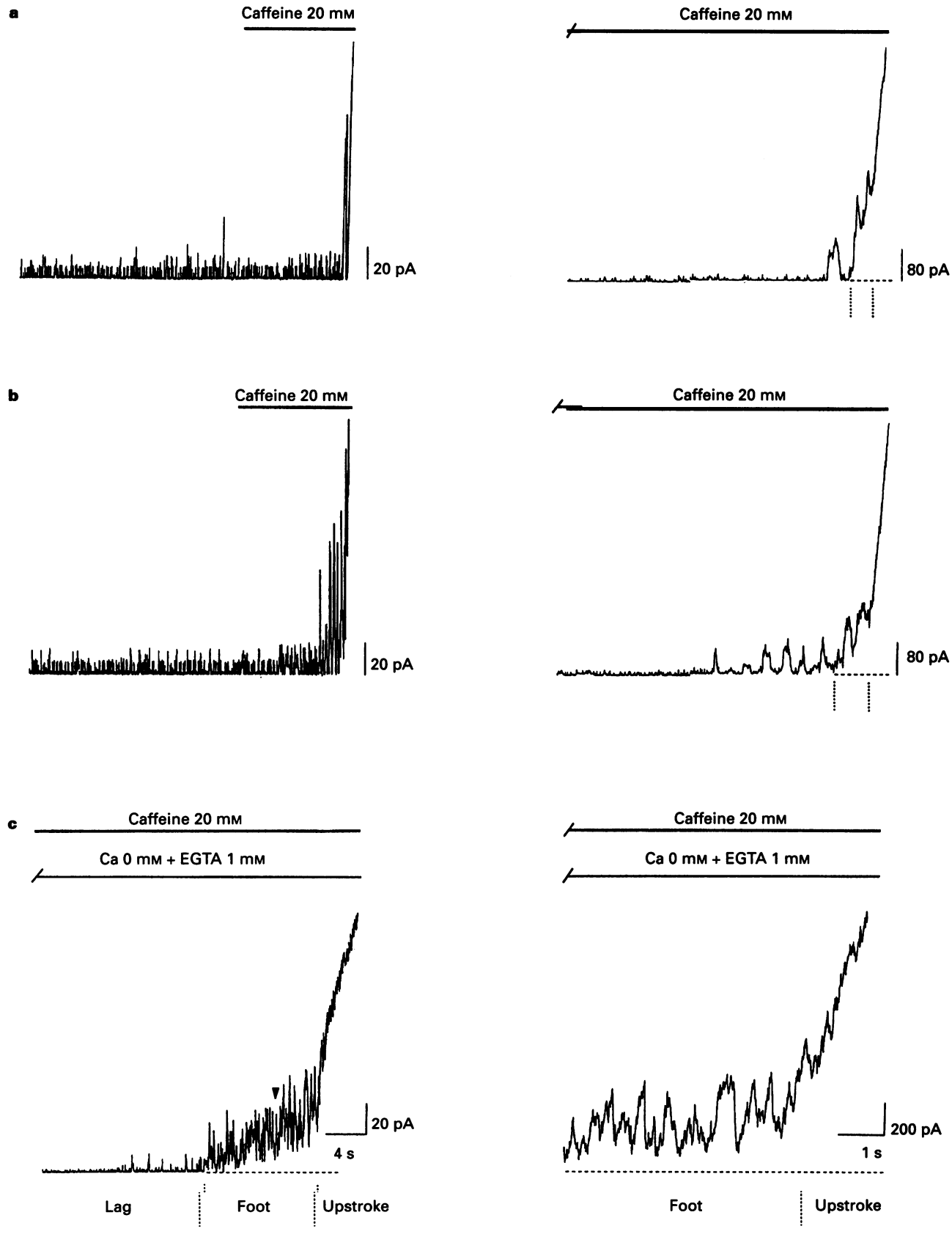

Figure 2 Sections of the rising portions of outward current responses to 20 mM caffeine. (a,b) In the presence of extracellular Ca; (c) response of the cell after 6 min bathing in a solution with no added Ca. Exposure times to caffeine and Ca^{2+}-free, EGTA containing solution are indicated by the horizontal bars. Note the different current scale for the recordings in (a) and (b) compared to (c). The time scales apply to all records in the same column. Right hand records in (a), (b) and (c) are shown at expanded time scale. The transitions to foot and upstroke phases are indicated by the dotted lines. In (c), (▼) at left side indicates the time from which the record at the expanded time scale was made (c, right side). Cells held at +20 mV.

saline, then filtrated and centrifuged. Supernatant containing the cells were resuspended in 0.8 mM-Ca^{2+} containing solution and placed on glass cover-slips. The cells were kept at 4°C until use on the same day.

Electrophysiological recording

Voltage clamp recordings were made from single endothelial cells using standard patch-clamp techniques (Hamill *et al.*, 1981). Whole-cell membrane currents were recorded with borosilicate patch pipettes of 2–5 Mohms. The currents were recorded with a List LM/EPC-7 patch-clamp amplifier (List Electronics), filtered at 2.5 kHz (–3 dB, 4-pole Bessel filter; Ithaco 4302) and stored for later analysis on videotape using a digital VCR recorder adaptor (PCM-1; Medical systems Corp., NY, U.S.A.). Membrane currents were continuously monitored and the amplitude was analyzed by direct measurement on a digital oscilloscope (Tektronix 5223). The currents were displayed on a chart recorder (Gould 220) and their outward records are shown in the upward direction.

Fura-2 digital fluorescence imagine microscopy

The endothelial cells on the coverslip were loaded with 0.75 μM fura-2/AM (acetoxymethylester) in normal PSS (1 mM stock in dimethylsulphoxide (DMSO)) for 30 min at room temperature. The coverslip chamber was mounted on an inverted microscope (Nikon, Diaphot). A Nikon 20 × phase/fluor objective was used to visualize the cells. A glass tube was used to infuse (by gravity) the chamber with fresh experimental solution (total volume of the chamber is 0.5 ml which is continually maintained using vacuum suction at the surface of the fluid). A total of 3 ml solution was used to change the solution. The endothelial cells were exposed to alternating 340 and 380 nm (bandwidth 10 nm) wavelengths of u.v. light and emission light was passed through a 510 nm (bandwidth 40 nm) filter prior to acquisition by an ICCD camera (Intensified Charge-Coupled Device; Cohu, 4810 Series). A Sun Sparc workstation and the Inovision Image Software (Inovision Corp. Research Triangle Park, NC, U.S.A.) were used to record and analyze the fluorescence ratio (340/380). Before measurement, background fluorescence at 340 nm and 380 nm was measured by bringing the cells out of the focus. Ratio images were collected every 10 s. All results given are reported as changes in the 340/380 signal ratio. Averaged numerical data obtained from dose responses of caffeine by both electrophysiological and fura-2 fluorescence methods are represented as the mean ± one standard error of the mean (s.e.mean).

Solutions

The physiological salt solution (PSS) used in the experiments had the following ionic composition (in mM): NaCl 125.4, KCl 5.9, $CaCl_2$ 1.5, $MgCl_2$ 1.2, glucose 11.5, N-2-hydroxyethylpiperazine-N'-2-ethanesulphonic acid (HEPES) 10, adjusted to pH 7.35 with NaOH. The pipette (intracellular solution) contained (in mM): NaCl 5, KCl 126, $MgCl_2$ 1.2, glucose 11, EGTA 0.8, HEPES 10, adjusted to pH 7.2 with KOH. The osmotic activity (280–290 mmol kg^{-1}) of the solution was monitored with a vapor pressure osmometer (Wescor 5500). Experiments were carried out at a bath temperature of 28 ± 2°C.

Drugs and chemicals

The following drugs and chemicals were used: papain, DL-dithiothreitol, caffeine all of which were purchased from Sigma Chemicals Co., St Louis, MO, U.S.A., tetraethylammonium chloride (TEA) (Eastman Kodak Co., Rochester, NY, U.S.A.), ethylene *bis* (oxyethylenenitrilo) tetra acetic acid (EGTA) (Fisher Scientific, Fair Lawn, NJ, U.S.A.). The fluoresence indicator fura-2/AM was purchased from molecular Probes, Inc. (Eugene, OR, U.S.A.).

Results

Caffeine

The activator of calcium release from agonist-releasable stores, caffeine, was applied to the bathing solution in the presence and absence of Ca^{2+} in the extracellular solution. In the cells which were voltage clamped at potential +20 mV and bathed in PSS, 20 mM caffeine elicited an outward current up to 2400 pA (1771 ± 205 pA, $n = 7$) (Figure 1a) after an initial burst of unitary currents and STOCs (Figure 2a,b). The increased spontaneous current activity started after ≈5 s pre-

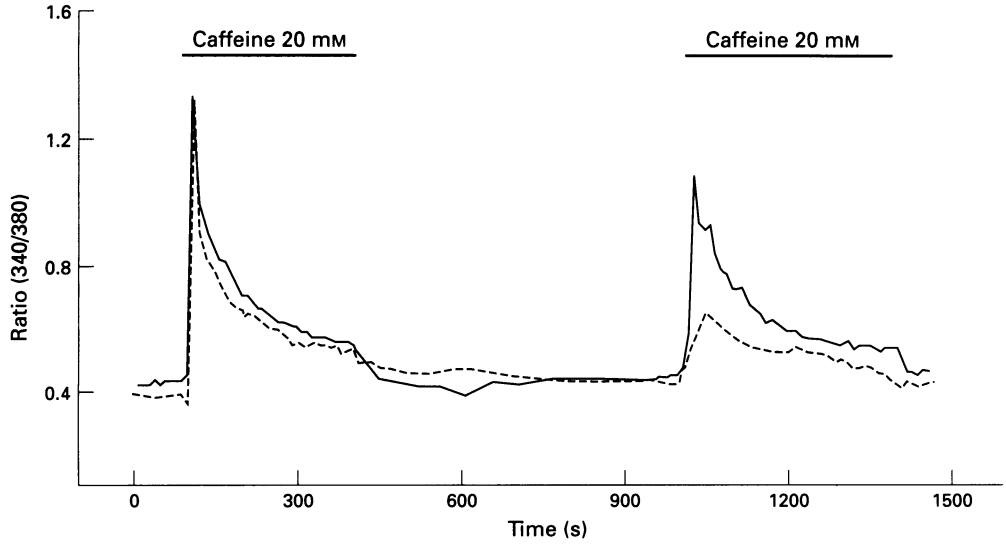

Figure 3 Tracing to show that bath application of caffeine (20 mM) elevates intracellular calcium concentration in isolated, fura-2 loaded cells. The solid line represents the average signal of 10 cells in normal PSS (1.5 mM $CaCl_2$) and the dashed line represents the average signal in Ca^{2+}-free, EGTA containing solution ($n = 10$). After the first caffeine response the cells were allowed to recover for 10 min before a second dose of caffeine was applied. In normal PSS the second application of caffeine induced a slightly lower but similar transient while the second response to caffeine in Ca^{2+}-free, 1 mM EGTA containing solution was considerably reduced.

sence of caffeine. Although in control conditions (prior to application of caffeine) STOCs were observed in approximately one third of all voltage-clamped cells, extracellularly applied caffeine (20 mM) stimulated in all cells a rapid discharge of STOCs to peaks of 50–160 pA which started from and later decayed back to the basal level (lag phase). Some cells showed only one STOC during the lag phase (Figure 2a), while others produced repetitive discharges of STOCs (2–9 events) within ≈3 s (Figure 2b) before the rising phase of the outward current developed ($n=7$).

The outward current evoked by caffeine in the absence of Ca^{2+} had a similar magnitude (1698 ± 312 pA, $n=6$) as in the

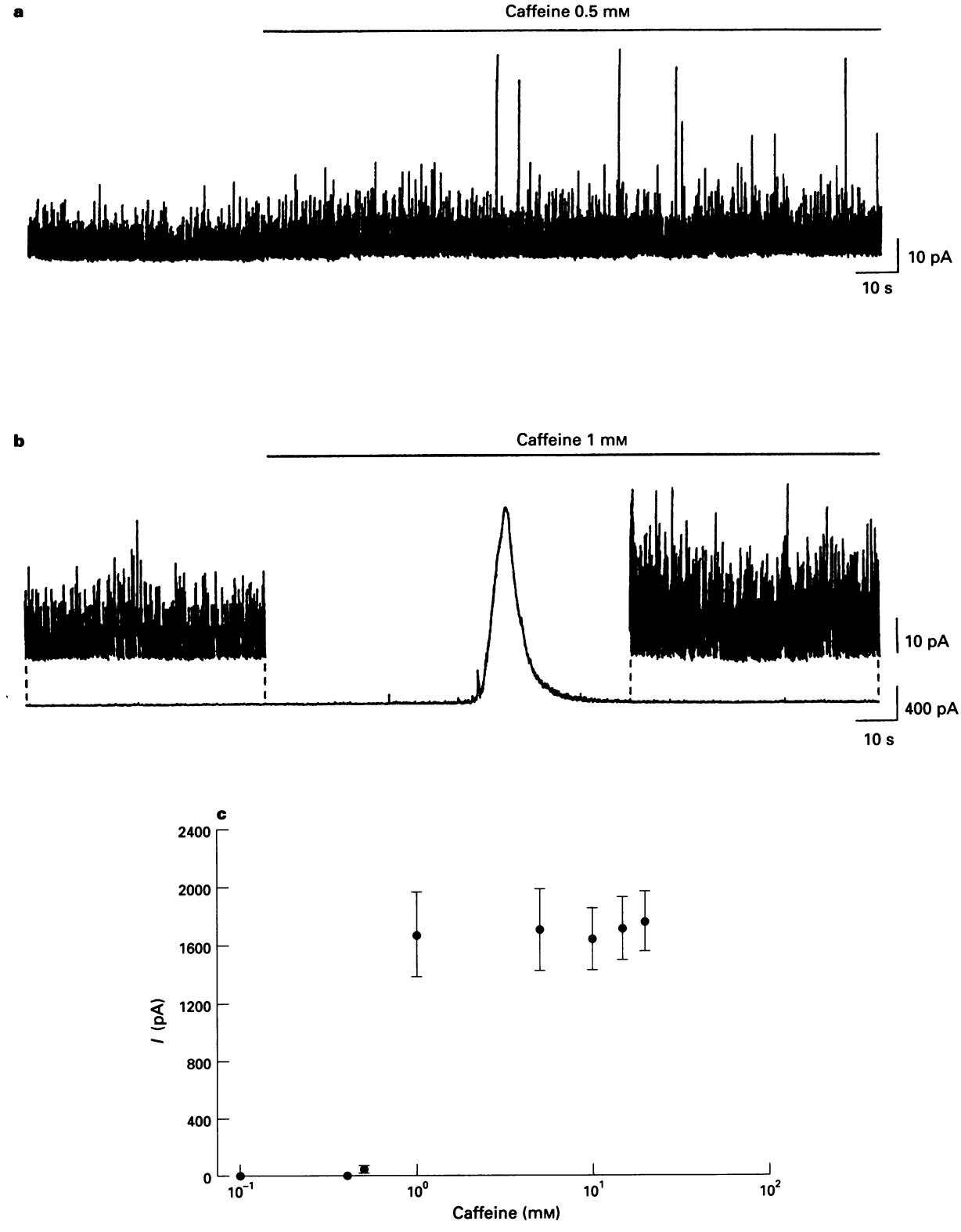

Figure 4 Dose-dependent responses of outward currents evoked by caffeine. (a) Caffeine, 0.5 mM, produced only stimulation of unitary currents and STOCs. (b) Caffeine 1 mM, elicited the outward current. (c) Dose-response relation for activation of outward currents by different doses of caffeine. Each point represents the mean from at least 5 experiments. Holding potential +20 mV.

presence of Ca^{2+}; however, it was delayed and of longer duration (Figure 1c). Moreover, while in normal Ca^{2+}-containing solution, caffeine produced an outward current which started steeply from basal current level and decayed rapidly within 15 s (Figure 1a), the shape of this caffeine-evoked transient outward current in the absence of Ca^{2+} was clearly biphasic (Figure 1c, 2c) and it decayed more slowly ($\approx$45 s) (Figure 1c). Detailed examination of the rising phase of the long lasting transient outward currents on an expanded current and time scales revealed that also in the presence of Ca^{2+} the initial rising phase is complex (Figure 2a,b). Thus, both, in the presence and absence of Ca^{2+} it was possible to determine by visual inspection a clear transition from the foot to the rapid upstroke phase. The rising portion of the outward current evoked by caffeine consists of an initial slowly rising transient component characterised by discharges of STOCs (foot phase) with amplitude of up to 250 pA in the presence of Ca^{2+} ($n=7$) and up to 400 pA in the absence of Ca^{2+} ($n=6$)

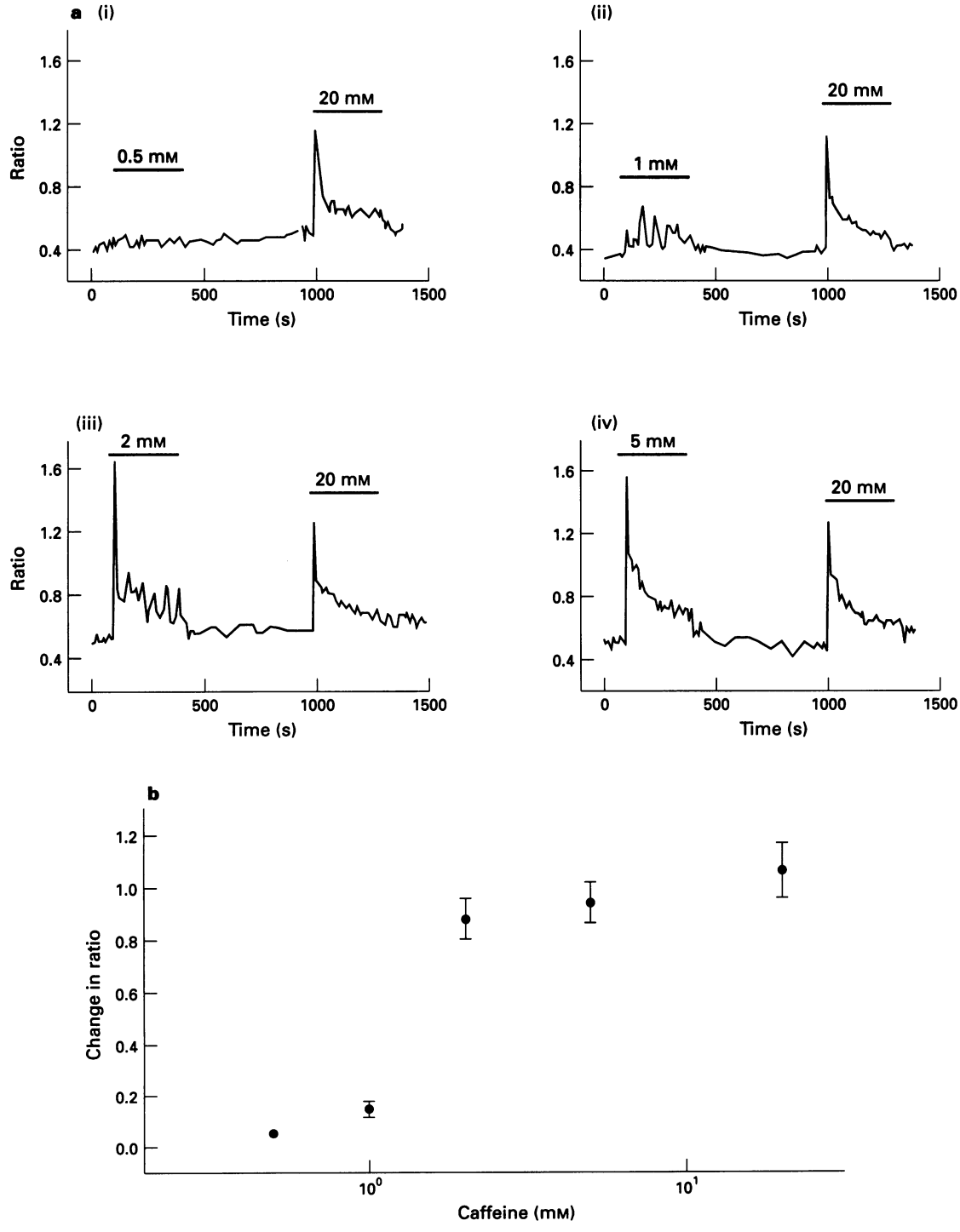

Figure 5 (a) The intracellular Ca^{2+} responses of isolated, fura-2 loaded cells obtained in normal PSS containing different concentrations of caffeine. The cells were first exposed to different caffeine concentrations: 0.5 mM (i), 1 mM (ii), 2 mM (iii) and 5 mM (iv). The caffeine was washed out after 5 min and the cells were allowed to recover in normal PSS for 10 min. A second addition of caffeine (20 mM) was made after recovery in each cell. (b) Dose-response relation for caffeine-induced transient elevations of $[Ca^{2+}]_i$ in fura-2-loaded cells bathed in normal PSS. The peak-values of the transients were averaged at different doses. Each point is the average of the peak where the number of experiments is at least 10.

and a subsequent more steeply increasing component (upstroke phase). The foot phase in the presence of Ca^{2+} was only a fraction of the length ($\approx 10\%$) of the one observed in the absence of Ca^{2+}.

When caffeine (20 mM) was applied simultaneously with Ca^{2+}-free solution, the cells responded with a steep rise in the outward current, similar to the response observed in the presence of Ca^{2+}. However, the former was followed by a slower fall to a maintained base level, similar to the action of caffeine in Ca^{2+}-free solution (Figure 1b, $n=4$).

In Ca^{2+}-free solution an outward current in response to a second application of caffeine was not observed (not shown).

A prolonged increase in frequency and amplitude of spontaneous unitary currents was observed following the outward currents in both the presence and absence of extracellular Ca^{2+} (Figure 1a,c). These effects were most pronounced when both Ca^{2+}-free solution and caffeine were applied to bathing solution at the same time (Figure 1b).

The next set of experiments was performed to investigate the effect of caffeine on intracellular Ca^{2+} release using the fluorescent Ca^{2+} indicator fura-2. Figure 3 shows that 20 mM caffeine evoked similar transient responses in both Ca^{2+}-containing and Ca^{2+}-free, 1 mM EGTA containing solution. The peak of $[Ca^{2+}]_i$ and the maintained plateau in the presence of Ca^{2+} (0.62 ± 0.04, $n=10$) were similar to that seen in Ca^{2+}-free solution (0.55 ± 0.03, $n=10$). After 5 min, caffeine was washed out from the bathing solution and the cells were allowed to recover for 10 min. It is apparent that in the presence of external Ca^{2+}, the caffeine-sensitive store was refilled. In contrast, the $[Ca^{2+}]_i$ response to the second caffeine exposure in Ca^{2+}-free solution was greatly reduced.

Concentration-dependence of the outward currents activated by caffeine

Lower concentrations of caffeine (0.1 and 0.5 M) increased both frequency and amplitude of unitary currents and evoked STOCs but did not initiate outward currents (Figure 4a). As the concentration of caffeine was increased to 1 mM, the response abruptly increased with an outward current of up to a maximum of 2400 pA (Figure 4b; $n=4$). At concentrations higher than 1 mM, the responses to caffeine were not concentration-dependent. The relationship between the outward current and the concentration of caffeine is presented in Figure 4c, where the average maximal amplitude of outward current is plotted as a function of caffeine concentration.

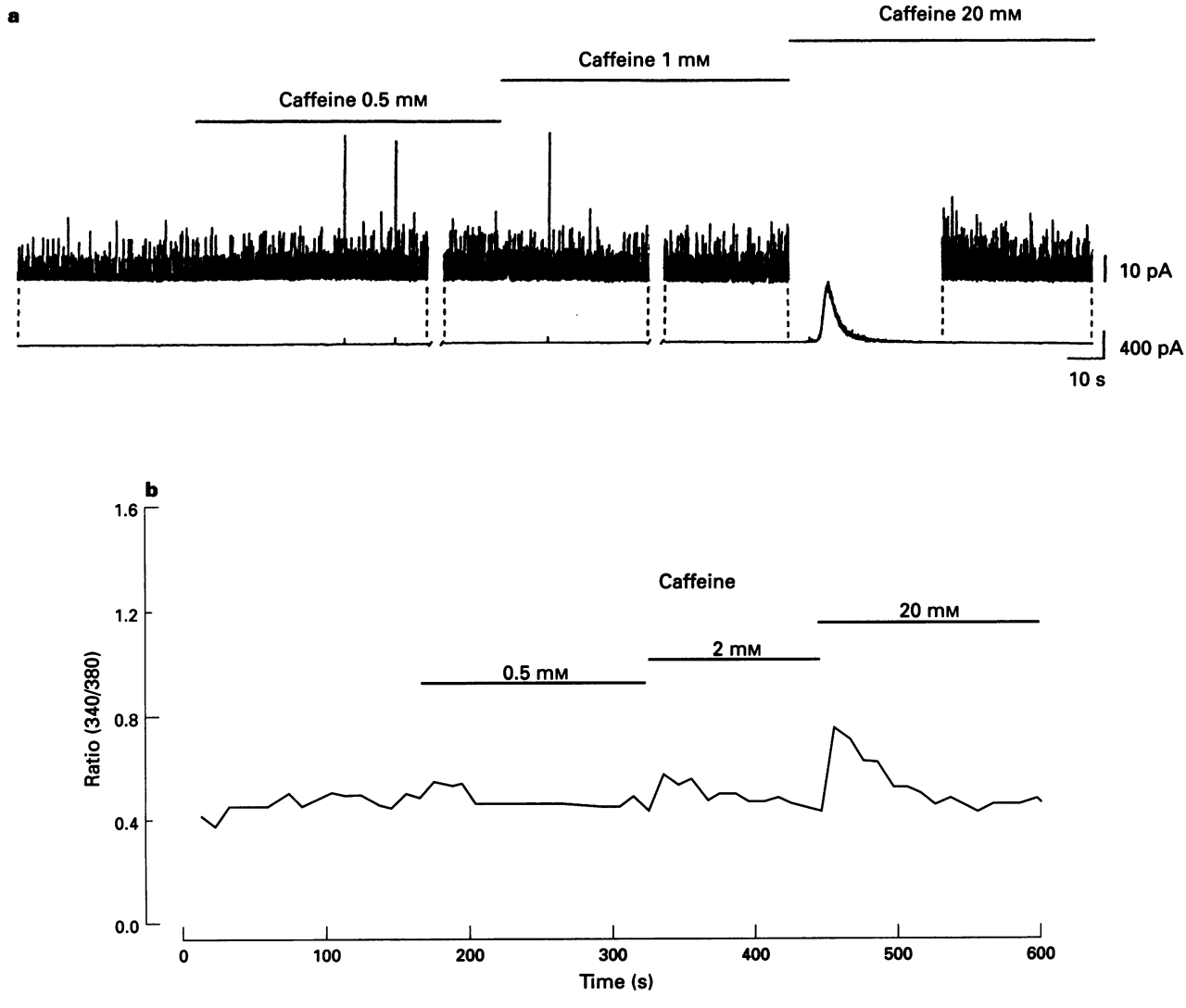

Figure 6 Sequential applications of increasing doses of caffeine. (a) Outward currents recorded at a holding potential of +20 mV during 2 min exposure to normal PSS containing 0.5, 1 and 20 mM caffeine. (b) The average of the intracellular Ca^{2+} responses of isolated, fura-2 loaded cells during exposure to normal PSS containing consecutively 0.5, 2 and 20 mM caffeine ($n=10$). Horizontal bars indicate periods during which the cell was bathed in an extracellular solution containing caffeine.

In Figure 5a the $[Ca^{2+}]_i$ responses from different cells at different concentrations of caffeine were measured as the 340/380 ratio of fura-2 fluorescence. All four panels illustrate the same protocol. The various doses of caffeine at 0.5, 1, 2 and 5 mM were applied for 5 min. After 10 min recovery, a second caffeine dose of 20 mM was applied to each preparation. All the second applications of caffeine evoked similar rises in $[Ca^{2+}]_i$. Lower doses of caffeine (0.5 mM) had no apparent effect on $[Ca^{2+}]_i$ (Figure 5a(i)) however, 1 mM caffeine induced oscillation in the $[Ca^{2+}]_i$ but no major transient peak was evoked (Figure 5a(ii)). Figure 5a(iii) shows that at 2 mM caffeine, the cells responded with a transient $[Ca^{2+}]_i$ of the same magnitude as that evoked by 5 mM and 20 mM. At this intermediate caffeine concentration, oscillations in $[Ca^{2+}]_i$ were observed. Figure 5b shows the concentration-response curve for the caffeine induced $[Ca^{2+}]_i$ responses.

When the cells were pretreated with lower doses of caffeine (0.4 or 0.5 mM) 1 mM caffeine did not evoke an outward current (Figure 6a, $n=4$) upon subsequent caffeine addition, even though this concentration would elicit a response under control conditions (see Figure 4b). Moreover, preincubation of endothelial cells with these lower concentrations of caffeine (0.4–0.5 mM) attenuated the peak of the outward current evoked by 20 mM caffeine by 60% (Figure 6a, $n=4$). Figure 6b shows the average traces of $[Ca^{2+}]_i$ ($n=10$) recorded from different doses of caffeine applied successively. The lower dose of caffeine (0.5 mM) abolished the action of subsequently added 2 mM caffeine, which in control conditions evoked a rise in $[Ca^{2+}]_i$ (Figure 5a(iii)). In addition, the response to the subsequent addition of 20 mM caffeine was reduced by 55% compared to its control (Figure 3).

Effects of TEA and reduction in $[Ca^{2+}]_o$ on spontaneous current activity

Experiments were performed to test whether the increases in both frequency and amplitude of unitary currents and STOCs evoked by Ca^{2+}-free solution reflected stimulation of Ca^{2+}-activated K^+ currents. Endothelial cells to which the K-channel blocker, TEA, was applied showed neither unitary currents nor STOCs, regardless of whether Ca^{2+} was present in the perfusing solution (Figure 7, $n=5$). In the continual presence of TEA, there was no spontaneous activity but the basal current was noisier than that in the control condition prior to TEA application. Thus, application of 3 mM TEA abolished the increase in unitary currents and STOCs seen upon removal of extracellular Ca^{2+} as would be expected if they resulted from Ca^{2+}-activated K^+ currents. However, the sustained outward current (2–12 pA, $n=9$) seen in Ca^{2+}-free solution was not affected.

The effect of TEA on the caffeine-induced outward currents in the absence of Ca^{2+}

The presence of TEA (3 mM) did not prevent the ability of caffeine to evoke outward currents in Ca^{2+}-free solution; however, their amplitude was attenuated by about 50% (Figure 8b, $n=4$). Moreover, TEA (3 mM) blocked the discharges of unitary currents and STOCs accompanying the trace of caffeine-induced outward currents.

Following wash-out of the TEA, recovery of spontaneous current activity in Ca^{2+}-free solution was allowed for 10 min before again applying 20 mM caffeine. Under these conditions, the second application of caffeine failed to evoke an outward current (not shown). Although the endothelial cells lose the ability to produce outward currents upon repetitive caffeine stimulation in the absence of extracellular Ca^{2+}, they continue to generate spontaneous outward currents.

Discussion

Caffeine induced a $[Ca^{2+}]_i$ transient and an outward current which were of the same magnitude in the presence and absence of extracellular Ca^{2+}. This indicates that both responses are the consequence of Ca^{2+} release from intracellular stores. The mechanism of caffeine-induced Ca^{2+} release involves sensitization of the ryanodine receptor-Ca^{2+} release channels in the endoplasmic reticulum (ER) or sarcoplasmic reticulum (SR) to the activating action of Ca^{2+} (Endo, 1977; Martonosi, 1984). Ca^{2+}-induced Ca^{2+} release (CICR) has been reported for skeletal (Endo *et al.*, 1970; Ford & Podolsky, 1970), cardiac

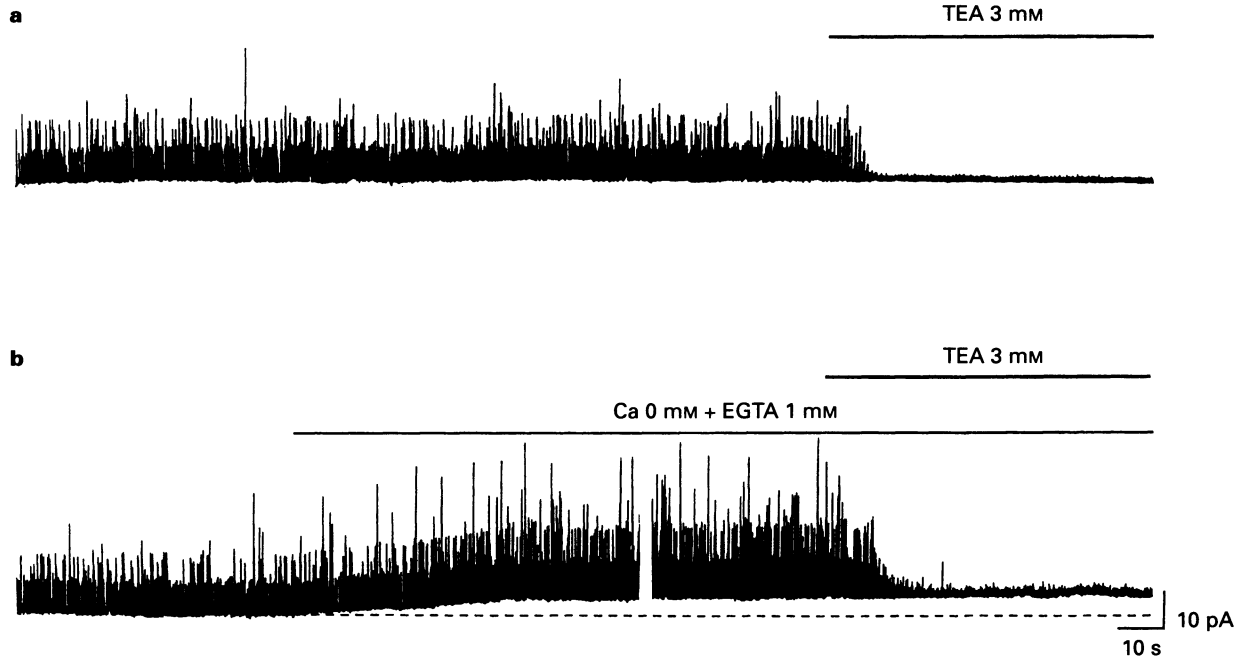

Figure 7 Membrane current records in a freshly dissociated rabbit aortic endothelial cell. Effect of applying tetraethylammonium (TEA, 3 mM) in the presence of extracellular Ca^{2+} (a) and in Ca^{2+}-free, EGTA-containing solution (b) for the period indicated by the horizontal bars. Same scale as (a). Holding potential +20 mV.

(Fabiato & Fabiato, 1972; Fabiato, 1983) and vascular smooth muscle SR (Itoh *et al.*, 1982; Leijten & van Breemen, 1984; Van Breemen & Saida, 1989) and as presented in the results section is also present in native rabbit aortic endothelial cells.

The main finding of the present study is the all-or-none nature of the caffeine-induced responses. At increasing doses of caffeine the outward current suddenly appeared at a maximum amplitude when the caffeine concentration reached 1 mM, while the $[Ca^{2+}]_i$ transient abruptly peaked at 2 mM caffeine after $[Ca^{2+}]_i$ oscillations at 1 mM. Both phenomena are undoubtedly linked, since the small difference in threshold can be readily attributed to the difference in experimental conditions (e.g. whole cell clamp recordings were made at +20 mV while fura-2 fluorescence was measured at resting membrane potentials). Another possible explanation for the difference in caffeine sensitivity is that the $[Ca^{2+}]_i$ oscillations observed at 1 mM caffeine are sufficient to achieve the threshold for activation of the outward current. The latter explanation is supported by the finding that the outward current elicited by 1 mM caffeine had a longer delay and a slower upstroke than this current elicited by 20 mM caffeine. We postulate that the regenerative CICR requires the achievement of a critical local $[Ca^{2+}]_i$ or threshold $[Ca^{2+}]_i$.

The marked reduction in the amplitude of both the outward current and $[Ca^{2+}]_i$ transients evoked by 20 mM caffeine after prior exposure to lower caffeine concentrations indicates that a subthreshold caffeine concentration activates some Ca^{2+} channels causing depletion of intracellular Ca^{2+} stores. When the ER is partially depleted, a higher concentration of caffeine is required to open more Ca^{2+} channels to achieve a sufficient Ca^{2+} release to reach the local threshold concentration for CICR. However, in spite of the fact that 20 mM caffeine was still able to induce regenerative Ca^{2+} release, the prior partial depletion of the ER caused the final response to be markedly smaller than that seen under control conditions.

Several other observations allude to the concept of threshold $[Ca^{2+}]_i$ for CICR. Both, in the presence and absence of Ca^{2+} the rising part of the outward current was biphasic. When the foot phase characterized by discharges of STOCs reached a critical level, the slope abruptly became much steeper. The threshold probably represents the critical level of $[Ca^{2+}]_i$ which trigger massive quasi-simultaneous opening of Ca^{2+}-activated K channels (upstroke) in response to sudden release of Ca^{2+} from the internal stores. The foot phase however, was much shorter in the presence of external Ca^{2+}, perhaps because continuous Ca^{2+} influx allowed the released Ca^{2+} to build up a local threshold Ca^{2+} concentration much faster. The Ca^{2+} supplied by influx would also assure that once the threshold for CICR was reached at any location in the cytoplasm, the process would propagate over all regions of the ER. Different lengths of the foot phase in the presence and absence of Ca^{2+} also indicate the supporting role of extra-

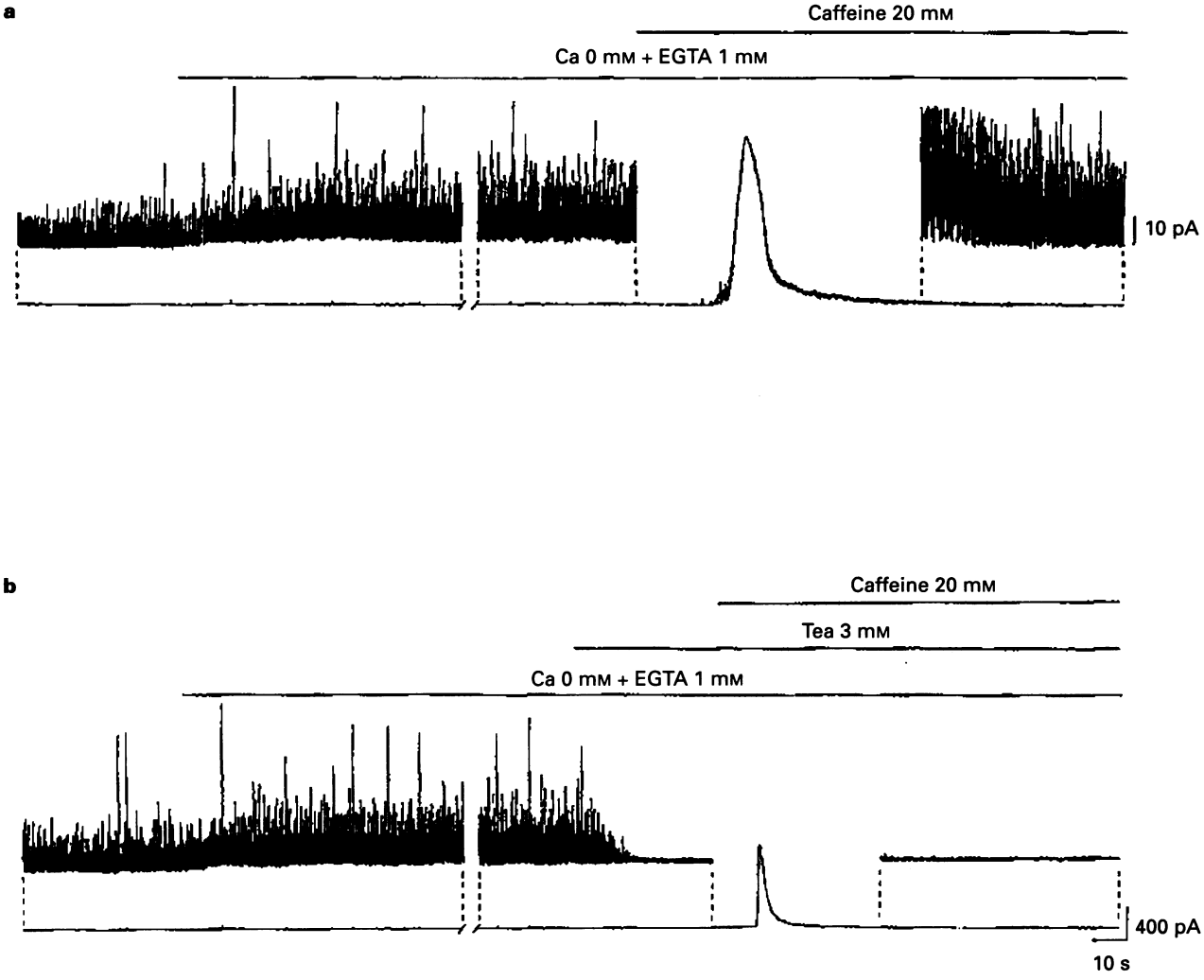

Figure 8 Effects of 3 mM tetraethylammonium (TEA) and of Ca^{2+}-free, EGTA-containing solution on the action of 20 mM caffeine. (a) Caffeine-evoked outward current was recorded after 6 min exposure to Ca^{2+}-free, EGTA-containing solution. (b) The effect of caffeine in the presence of TEA and after 6 min in Ca^{2+}-free, EGTA-containing solution. Horizontal bars indicate periods during which cells were superfused with extracellular solution containing drugs and no added Ca^{2+}. Holding potential +20 mV.

cellular Ca^{2+} in the generation of outward currents. However, it cannot be ruled out that some of the differences related to the presence and absence of extracellular Ca^{2+} are due to effects of Ca^{2+} on the outer surface of the plasmalemma.

It is also possible that local threshold values may be reached under conditions where global $[Ca^{2+}]_i$ is not high enough to sustain propagation of regenerative Ca^{2+} release throughout the cell. This situation would result in localized CICR occurring at different sites at different times leading to the oscillations of variable amplitude measured by the fura-2 fluorescence at 1 mM caffeine.

A curious observation is that persistent spontaneous current activity was increased by caffeine after the development of the outward current. This is clearly different from behaviour of the outward current in that the latter current required a latent period of ER refilling before it could be repeated. In the absence of extracellular Ca^{2+} only one outward current could be obtained because refilling of the ER from the extracellular space was prevented. In contrast, removal of external Ca^{2+} enhanced the spontaneous current activity and did not prevent its persistance after caffeine exposure. After the caffeine-sensitive stores were depleted in the absence of external Ca^{2+} a second exposure to caffeine was still able to induce a slight elevation of the steady state $[Ca^{2+}]_i$. Although we are unable at this time to provide a fully consistent explanation for the above observation, it is possible that either some refilling occurred from Ca^{2+} released into the cytoplasm and/or another non caffeine-sensitive intracellular Ca^{2+} source exists, such as mitochondria, which is normally buffered by Ca^{2+} uptake into the ER.

The caffeine-induced outward current fits the pattern of being dependent on a depletable and refillable Ca^{2+} store such as observed in smooth muscle (Leijten & van Breemen, 1984). The conductances activated by the released Ca^{2+} include both TEA-sensitive potassium channels and TEA-insensitive and at present unidentified channels. The refilling of caffeine-sensitive intracellular Ca^{2+} stores in native aortic endothelial cells however, is a relatively slow process in that at least 10 min incubation in normal physiological solution is required to elicit a second caffeine-induced outward current. The presence of a second transient $[Ca^{2+}]_i$ peak, although considerably reduced, in response to the second application of caffeine in Ca^{2+}-free solution suggests that not all of Ca^{2+} released within the cells is lost from the cell but that some released Ca^{2+} is recycled into the ER (see also Bond *et al.*, 1984; Benham & Bolton, 1986). In this case, however, the amount of $[Ca^{2+}]_i$ is probably insufficient to reach the threshold for activation of the outward current, as confirmed by our electrophysiological experiments (not shown).

Spontaneous current activity, a phenomenon found in the freshly isolated aortic endothelial cells, has been shown to be generated by a population of TEA-sensitive and highly K^+-selective channels sensitive to the cytoplasmic Ca^{2+} concentration (Rusko *et al.*, 1992). Although removal of external Ca^{2+} enhanced spontaneous current activity there is no convincing explanation for this effect. It may be related to a change in the behaviour of the BK K_{Ca} channels. This is supported to some extent by the finding that the caffeine effect and the Ca^{2+}-free effect are additive. Perhaps not only changes in $[Ca^{2+}]_i$ (Rusko *et al.*, 1992) but also changes in $[Ca^{2+}]_o$ may modulate the activity of Ca^{2+}-activated K channels. This suggestion is supported by our finding that increasing the $[Ca^{2+}]_o$ reduced the spontaneous current activity (not shown).

In conclusion, we have presented evidence for regenerative Ca^{2+} release mediated by ryanodine receptors in native aortic endothelial cells. Caffeine induced Ca^{2+} release from the ER in an all-or-none manner. Once a local threshold $[Ca^{2+}]_i$ is reached, ryanodine receptors are activated regeneratively by increasing Ca^{2+} flux from the ER lumen to the cytoplasm. At a critical caffeine concentration near 1 mM, the regenerative release may fail to propagate throughout the cell and consequently leads to irregular $[Ca^{2+}]_i$ oscillations. Ryanodine receptor-mediated Ca^{2+} release may signal NO and other relaxant factors release directly by activating constitutive NO-synthase or indirectly by activating Ca^{2+}-sensitive K channels and increasing Ca^{2+} influx through hyperpolarization.

This work was supported by a grant from Medical Research Council of Canada.

References

BENHAM, C.D. & BOLTON, T.B. (1986). Spontaneous transient outward currents in single visceral and vascular smooth muscle cells of the rabbit. *J. Physiol.*, **381**, 385–406.

BOND, M., KITAZAWA, T., SOMLYO, A.P. & SOMLYO, A.V. (1984). Release and recycling of calcium by the sarcoplasmic reticulum in guinea-pig portal vein smooth muscle. *J. Physiol.*, **355**, 677–695.

BUCHAN, K.W. & MARTIN, W. (1991). Bradykinin induces elevations of cytosolyc calcium through mobilization of intracellular and extracellular pools in bovine aortic endothelial cells. *Br. J. Pharmacol.*, **102**, 35–40.

BUSSE, R., FICHTNER, H., LUCKHOFF, A. & KOHLHARDT, M. (1988). Hyperpolarization and increased free calcium in acetylcholine-stimulated endothelial cells. *Am. J. Physiol.*, **255**, H965–H969.

CAMPBELL, D.L., STRAUSS, H.C. & WHORTON, A.R. (1991). Voltage dependence of bovine pulmonary artery endothelial cell function. *J. Mol. Cell. Cardiol.*, **23** (suppl I), 133–144.

CHEN, G. & CHEUNG, D. (1992). Pharmacological distinction of the hyperpolarization response to caffeine and acetylcholine in guinea-pig coronary endothelial cells. *Eur. J. Pharmacol.*, **223**, 33–38.

ENDO, M. (1977). Calcium release from the sarcoplasmic reticulum. *Physiol. Rev.*, **57**, 71–108.

ENDO, M., TANAKA, M. & OGAWA, Y. (1970). Calcium induced release of calcium from the sarcoplasmic reticulum of skinned skeletal muscle fibres. *Nature*, **228**, 34–36.

FABIATO, A. (1983). Calcium-induced release of calcium from the cardiac sarcoplasmic reticulum. *Am. J. Physiol.*, **245**, C1–C14.

FABIATO, A. & FABIATO, F. (1972). Excitation-contraction coupling of isolated cardiac fibers with disrupted or closed sarcolema. Calcium-dependent cyclic and tonic contractions. *Circ. Res.*, **31**, 293–301.

FREAY, A., JOHNS, A., ADAMS, D.J., RYAN, U.S. & VAN BREEMAN, C. (1989). Bradykinin and inositol-1,4,5-triphosphate stimulated calcium release from intracellular stores in cultured bovine endothelial cells. *Pflügers Arch.*, **414**, 377–384.

FORD, L.E. & PODOLSKY, R.J. (1970). Regeneratve calcium release within muscle cells. *Science*, **167**, 58–59.

HAMILL, O.P., MARTY, A., NEHER, E., SAKMANN, B. & SIGWORTH, F.J. (1981). Improved patch-clamp techniques for high resolution current recording from cells and cell-free membrane patches. *Pflügers. Arch.*, **391**, 85–100.

ITOH, T., KAJIWARA, M., KITAMURA, K. & KURIYAMA, H. (1982). Roles of stored calcium on the mechanical response evoked in smooth muscle cells of the porcine coronary artery. *J. Physiol.*, **322**, 107–125.

JOHNS, A., LATEGAN, T.W., LODGE, N.J., RYAN, U.S., VAN BREEMAN, C. & ADAMS, D.J. (1987). Calcium entry through receptor-operated channels in bovine pulmonary artery endothelial cells. *Tissue Cell*, **19**, 733–745.

LASKEY, E.R., ADAMS, D.J., JOHNS, A., RUBANYI, G.M. & VAN BREEMEN, C. (1990). Membrane potential and Na^+-K^+ pump activity modulate resting and bradykinin-stimulated changes in cytosolic free calcium in cultured endothelial cells from bovine atria. *J. Biol. Chem.*, **265**, 2613–2619.

LEIJTEN, P.A.A. & VAN BREEMEN, C. (1984). The effects of caffeine on the noradrenaline-sensitive calcium store in rabbit aorta. *J. Physiol.*, **357**, 327–339.

LUCKHOFF, A. & BUSSE, R. (1990). Calcium influx into endothelial cells and formation of endothelium-derived relaxing factor is controlled by the membrane potential. *Pflügers Arch.*, **416**, 305–311.

MARTONOSI, A.N. (1984). Mechanism of Ca^{2+} release from sarcoplasmic reticulum of skeletal muscle. *Physiol. Rev.*, **64**, 1240–1319.

OHYA, Y., KITAMURA, K. & KURIYAMA, H. (1987). Cellular calcium regulates outward currents in rabbit intestinal smooth muscle cell. *Am. J. Physiol.*, **252**, C401–C410.

RUSKO, J., TANZI, F., VAN BREEMEN, C. & ADAMS, D.J. (1992). Calcium-activated potassium channels in native endothelial cells from rabbit aorta: Conductance, Ca^{2+} sensitivity and block. *J. Physiol.*, **455**, 601–621.

SAGE, S.O., ADAMS, D.J. & VAN BREEMEN, C. (1989). Synchronized oscillations in cytoplasmic free calcium concentration in confluent bradykinin-stimulated bovine pulmonary artery endothelial cell monolayers. *J. Biol. Chem.*, **264**, 6–9.

SCHILLING, W.P. (1989). Effect of membrane potential on cytosolic calcium of bovine aortic endothelial cells. *Am. J. Physiol.*, **257**, H778–H784.

SCHILLING, W.P. & ELLIOTT, S.J. (1992). Ca^{2+} signalling mechanisms of vascular endothelial cells and their role in oxidant-induced endothelial cell dysfunction. *Am. J. Physiol.*, **262**, H1617–H1630.

VAN BREEMEN, C. & SAIDA, K. (1989). Cellular mechanisms regulating $[Ca^{2+}]_i$ smooth muscle. *Annu. Rev. Physiol.*, **51**, 315–329.

ZHANG, A., CHENG, T.P.O., ALTURA, B.T. & ALTURA, B.M. (1993). Mg^{2+} and caffeine-induced intracellular Ca^{2+} release in human vascular endothelial cells. *Br. J. Pharmacol.*, **109**, 291–292.

(Received September 2, 1994
Revised March 6, 1995
Accepted March 9, 1995)

British Journal of Pharmacology (1995) 115, 822-827

Gi proteins and the response to 5-hydroxytryptamine in porcine cultured endothelial cells with impaired release of EDRF

Nancy S. Day, Tong Ge, *Juan Codina, *Lutz Birnbaumer, [1]Paul M. Vanhoutte & [2]Chantal M. Boulanger

Center for Experimental Therapeutics, Department of Medicine and *Department of Cell Biology, Baylor College of Medicine, Houston, Texas 77030, U.S.A.

1 The receptor-mediated release of endothelium-derived relaxing factor(s) (EDRF) requires the presence of different functional G proteins in endothelial cells. Release of EDRF in response to 5-hydroxytryptamine (5-HT), which involves activation of pertussis toxin-sensitive Gi proteins, is impaired in both regenerated endothelium of the coronary artery following balloon catheterization and in porcine cultured endothelial cells. This study used porcine cultered endothelial cells as a model of regenerated endothelium to determine if the abnormal release of EDRF in response to 5-HT may be associated with the loss of functional pertussis toxin-sensitive Gi proteins.

2 Binding studies on porcine cultured endothelial cells demonstrated specific binding sites for [^{3}H]-5-HT. Scatchard analyses revealed a single binding site for [^{3}H]-5-HT with K_d of 7.2 ± 3.5 nM and maximal binding (B_{max}) of 121.4 ± 51.3 fmol mg^{-1} protein. Binding of [^{3}H]-5-HT was displaced by methiothepin (5-HT$_1$ and 5-HT$_2$ antagonist; $K_i = 6.2 \pm 1.2$ nM), but not by ketanserin (preferential 5-HT$_2$ antagonist).

3 Giα1 protein was expressed in cultured but not in native endothelial cells. Giα2 and Giα3 proteins were expressed to significant levels in porcine native and cultured endothelial cells, as detected by Northern and Western blot analysis.

4 In membranes from cultured endothelial cells, two bands of 40 and 41 kDa, which corresponded to the Giα2 and the combination of Giα3-Giα1 proteins, respectively, were ADP-ribosylated by pertussis toxin. The labelling intensity was Giα2 > Giα3-Giα1 and the amount of ADP-ribosylation was not different between porcine native and cultured endothelial cells. Stimulation of the cultured cells with 5-HT (3×10^{-6} M; 4 min) decreased significantly further ADP-ribosylation of Giα2 by pertussis toxin, but not that of Giα3 and/or Giα1.

5 The present results suggest that porcine endothelial cell culture may lead to the abnormal expression of Giα1 protein and that the dysfunctional release of EDRF from cultured porcine endothelial cells in response to 5-HT is not associated with the loss of Giα proteins or the absence of 5-HT binding sites.

Keywords: Endothelium-dependent relaxations; 5-HT$_1$ receptors; pertussis toxin; Giα subunits

Introduction

Endothelial cells contribute to the local regulation of vasomotor tone by releasing multiple vasoactive factors. The relaxing substances produced by the endothelial cells include endothelium-derived relaxing factor (EDRF; identified as nitric oxide (NO) or a related nitrogen-containing compound), hyperpolarizing factor (EDHF), and prostacyclin (Vanhoutte *et al.*, 1991; Moncada *et al.*, 1991; Vane, 1994). 5-Hydroxytryptamine (5-HT) is released in significant amounts during platelet aggregation (Cohen *et al.*, 1983) and plays an important role in increasing coronary blood flow by releasing relaxing factors from the endothelium (Lüscher & Vanhoutte, 1990; Willerson, 1993). In the porcine coronary artery, endothelium-dependent relaxation evoked by 5-HT and UK14304, but not that elicited by bradykinin and adenosine diphosphate, is mediated by pertussis toxin-sensitive GTP-binding proteins (G proteins) (Dolphin, 1987; Flavahan *et al.*, 1989; Shimokawa *et al.*, 1991). Although pertussis toxin-sensitive G proteins include the Gi and Go subtypes, only Gi proteins have been detected in endothelial cells (Asano *et al.*, 1988; Flavahan *et al.*, 1992; Liao & Homcy, 1992; Shibano *et al.*, 1992).

Endothelium-dependent relaxations which are sensitive to pertussis toxin are impaired selectively in the porcine coronary artery with regenerated endothelium following balloon catheter denudation (Shimokawa *et al.*, 1989). This response is comparable to that of control preparations after treatment with pertussis toxin (Shimokawa *et al.*, 1989). Similar dysfunctional release of EDRF involving activation of Gi proteins has been observed in porcine cultured endothelial cells (Boulanger *et al.*, 1989). Indeed, these cultured endothelial cells release EDRF upon stimulation with bradykinin, adenosine diphosphate and the calcium ionophore A23187, but not with 5-HT or α_2-adrenoceptor agonists.

The exact intracellular mechanism of this impairment in cultured endothelial cells is not known. Since it occurs with two distinct receptor systems (5-HT receptors and α_2-adrenoceptors), both *in vivo* and *in vitro*, it is likely that the site of dysfunction is beyond the level of the cell membrane receptors. In addition, the lack of effect of the regenerative process on EDRF release by other agonists activating a pertussis-toxin insensitive pathway, suggests that the dysfunction occurs at the level of Gi protein(s). The main purpose of the present study, using porcine cultured endothelial cells as a model of regenerated endothelium, is to determine whether or not the absence of EDRF release in response to 5-HT may be associated with the loss of functional pertussis toxin-sensitive Gi proteins.

Methods

Native and cultured endothelial cells

Endothelial cells obtained from porcine aortae collected at the local slaughterhouse were either used directly (as native cells)

[1]Present address: IRIS, 6 place des Pléiades, 92415 Courbevoie, France
[2]Author for correspondence at: INSERM Unit 141, Hôpital Lariboisière, 41, Bd de la Chapelle, F-75010 Paris, France.

or grown routinely in a Dulbecco's modified Eagle's medium DME low in glucose (1 g l^{-1}; JRH Biosciences, Lenexa, KS, U.S.A.) supplemented with 10% foetal bovine serum, glutamine (2 mM), and a mixture of penicillin, streptomycin (100 u ml^{-1}) (Boulanger *et al.*, 1989). Each primary culture was obtained from endothelial cells collected from one single aorta. Cells were passaged routinely every two to three days by mechanical disruption with a rubber policeman. All experiments were performed between passage 7 and 12. All cultures were rendered quiescent 24 h before the experiment by changing the medium to a serum-free medium with 0.1% bovine serum albumin.

Bioassay experiments

Porcine endothelial cells (passage 8 to 10), grown on Cytodex-3 microcarrier beads (Pharmacia, Piscataway, NJ, U.S.A.) were packed into a chromatographic column and perfused, at a rate of 2 ml min^{-1}, with modified Krebs-Ringer solution (control solution; composition in mM: NaCl 118.3, KCl 4.7, $CaCl_2$ 2.5, $MgSO_4$ 1.2, KH_2PO_4 1.2, $NaHCO_3$ 25.0, EDTA 0.026 and glucose 11.1; pH 7.4) (Boulanger *et al.*, 1989). The release of vasoactive factor(s) was detected with a ring of rat aorta without endothelium (male normotensive Wistar-Kyoto rat, 10–12 weeks old) during contractions evoked by phenylephrine (3×10^{-7} to 6×10^{-7} M). The bioassay ring was connected to a strain gauge transducer for the recording of changes in isometric tension. All experiments were performed in the presence of indomethacin (10^{-5} M; to prevent the release of vasoactive prostanoids; from Sigma Chemicals, St Louis, MO, U.S.A.), ketanserin (10^{-6} M; to antagonize 5-HT_2 receptors on the smooth muscle from Janssen Pharmaceuticals, Beerse, Belgium) and captopril (10^{-6} M; to inhibit bradykinin degradation by angiotensin II converting enzyme from Squibb Institute, Princeton, NJ, U.S.A.). Agonists such as 5-HT and bradykinin (Sigma Chemicals, St Louis, MO, U.S.A.) were infused either upstream or downstream the column of cultured endothelial cells in order either to stimulate the release of endothelial-relaxing factors or to examine their direct effect on the bioassay ring (Boulanger *et al.*, 1989).

5-HT binding studies

The cultured endothelial cells were washed with 10 ml of phosphate buffered saline (PBS; containing mM: Na_2HPO_4 10, KH_2PO_4 1.76, KCl 2.68, NaCl 137, pH 7.4) three times for each 150-mm tissue culture dish and collected in 25 mM Tris-HCl buffer (pH 7.4 at 4°C) containing 1 mM EDTA, 2 mM dithiothreitol (DTT), and a mixture of protease inhibitors (leupeptin, aprotinin, and phenylmethylsulphonyl fluoride, 10 $\mu g\ ml^{-1}$ each, final concentration). The cell pellet was obtained by centrifugation and resuspended into the same buffer. The cell suspension was sonicated for 30 s on ice (Artek, Sonic Dismembrator Model 300). The homogenates were centrifuged at 13,600 *g* for 20 min and the pellet was resuspended to reach a final protein concentration of 5–10 $\mu g\ \mu l^{-1}$.

Membranes containing 200–300 μg of protein were incubated in 200 μl of binding medium containing 25 mM Tris-HCl, 1 mM $MgCl_2$, 3 μM L-ascorbic acid, 10^{-4} M isoproniazid, [^{3}H]-5-HT (3.87 nM; about 23,000 d min^{-1}; DuPont NEN, Boston, MA, U.S.A.) with various concentrations of cold 5-HT, ketanserin or methiothepin (a 5-HT_1 and 5-HT_2 antagonist; Hoffman-La-Roche, Nutley, NJ, U.S.A.). The incubation was conducted at 37°C for 30 min in the dark, and terminated by rapid centrifugation at 30,000 *g* for 20 min at 4°C. The supernatant was removed and the pellet was washed with 1 ml ice-cold buffer, dissolved overnight in 100 μl of 1% SDS, and subjected to radioassay by liquid scintillation counting. Under these conditions, 2–3% (specific plus nonspecific) of the total added radioligand was bound to 11 fmol of receptor sites. Specific 5-HT binding was estimated to be 56±4% total binding under these experimental conditions ($n=3$).

Northern blot analysis

Native and cultured endothelial cells (2×10^7 cells) were washed with control solution and resuspended in GT buffer (25 mM sodium citrate, pH 7.0 with 4 M guanidinium thiocyanate, 0.5% sarcosyl, and 0.1 M β-mercaptoethanol). Total RNA was isolated as described by Chomczynski & Sacchi (1987).

To obtain cDNA probes for each subunit, RT-PCR was performed with primers specific for Giα1, Giα2, and Giα3, respectively. First-strand cDNA was synthesized using the SuperScript Preamplification System (Gibco BRL, Grand Island, NY, U.S.A.) with 2 μg of total RNA and 1 ng μl^{-1} random-hexamer DNA primers. The reverse transcription reactions were performed according to the protocol and stopped by heating at 90°C for 5 min. Oligonucleotide primers for PCR amplification of Giα1 (amino acids 50-259; base 149-777) were 5′-AGAAGCAGATGAAAATTATC-3′ and 5′-TATGTAACAACAAGTGGTTT-3′. Primers for Giα2 (amino acids 128-332, base 384-997) were 5′-CCGGAGGCTCTGGGCTGACC-3′ and 5′-CGCCACCGACACCAAGAACG-3′. Primers for Giα3 (amino acids 140-292, base 420-876) were 5′-CAGCAGATCCAGGGAATA-3′ and 5′-ACCTGTGTATTCTGGATAACAG-3′ (Jones & Reed, 1988; Itoh *et al.*, 1988). The PCR mixture included 20 mM Tris-HCl (pH 8.4), 2.5 mM $MgCl_2$, 50 mM KCl, and 100 ng ml^{-1} BSA, 200 μM of each dNTP, 1 μM of each primer, 2 units of *Taq* polymerase (Perkin-Elmer, Norwalk CT, U.S.A.) with a final volume of 50 μl. After an initial denaturation step of 94°C for 5 min, the PCR was performed with the cycle of 54°C annealing for 1 min, 72°C extension for 1.5 min, and 94°C denaturing for 1 min, for a total of 35 cycles with a final extension step for 10 min. The recovered DNA fragments were sequenced directly by an automated fluorescent DNA sequencer (Model ABI-373A, ABI Applied Biosystem, Foster City, CA, U.S.A.) by the Molecular Genetics Core facility at the University of Texas, School of Medicine (Houston). The sequencing data were analyzed with the GCG programme package (Genetics Computer Group, version 7, 1991). The nucleotide sequences have been deposited in the GenBank under accession number U11249, U11250 and U11290. The deduced amino acid sequences of porcine Giα1, Giα2, and Giα3 cDNAs shared 99.5%, 100% and 96.2% homology (in the amplified regions) with corresponding human Giα proteins (Itoh *et al.*, 1988). PCR generated Giα1, Giα2, and Giα3 fragments were purified from an agarose gel, radiolabelled by random priming (Promega, Madison, WI, U.S.A.) to specific activities of 2.67×10^9, 1.47×10^9 and 3.26×10^9 counts $min^{-1}\ \mu g^{-1}$, respectively, and used as cDNA probes for Northern blots. RNA samples (20 μg) were denatured and electrophoresed through 1% agarose gels containing 2.2 M formaldehyde, and were transferred onto nylon membranes by capillary blotting. The position of 28S and 18S ribosomal RNA bands on the ethidium-stained gels were observed under ultraviolet illumination before transblotting. RNA was fixed to the filter by ultraviolet irradiation at 254 nm. Hybridization was carried out in Rapid-hyb buffer (Amersham, Arlington Heights, IN, U.S.A.) at 70°C for 3 h. Filters were washed two times in 2X SSC, 0.1% SDS at room temperature, followed by one wash in 0.5X SSC, 0.1% SDS at 60°C. The radioactive bands were visualized by autoradiography.

Western blotting

Homogenized native or cultured endothelial cells (30 μg of protein per lane;) prepared as described for the 5-HT binding studies were dissolved in SDS-PAGE sample buffer, loaded into 10% polyacrylamide gels, and transblotted to a Zeta-Probe membrane (BioRad; Melville, NY, U.S.A.). The blots were probed with primary antibodies overnight with 5% (w/v) nonfat dried milk in PBS. Anti-Giα1 and Giα2 antibodies (Nos. 3646 and 115, respectively; both obtained from Dr David R. Manning, Dept of Pharmacology, University of Penn-

sylvania) were at 1 : 500 dilutions, while anti-Giα3 antibody (No. 06-190; Upstate Biotechnology Inc, Lake Placid, NY, U.S.A.) was at 1 : 250 dilution. Incubation with secondary antibody was conducted with 50 mM Tris-HCl (pH 7.5) containing 150 mM NaCl. An alkaline phosphatase-conjugated secondary antibody with 5-bromo-4-chloro-3-indolyl phosphate/nitro blue tetrazolium (BCIP/NBT) as substrates was used as detection system (Day *et al.*, 1993).

Pertussis toxin-catalyzed ADP-ribosylation

Cultured endothelial cells (three 100-mm diameter dishes) washed with PBS and native endothelial cells (from 6 to 7 porcine aortae) were collected in 18 ml of control solution. The cell suspension was divided into aliquots and pelleted by centrifugation; each aliquot contained 60–70 μg of protein.

Cultured endothelial cells were exposed to 5-HT (3×10^{-6} M) in the presence of L-ascorbic acid (3×10^{-7} M), or with L-ascorbic acid alone in control solution. The effect of 5-HT was stopped by centrifugation (13,000 rev min^{-1} for 1 min) and the samples were ADP-ribosylated immediately thereafter at 32°C for 30 min. ADP-ribosylation assays were carried out by a modification (Day *et al.*, 1991; Shibano *et al.*, 1992) of the method described by Ribeiro-Neto *et al.* (1987), where pertussis toxin was activated by incubation with 50 mM dithiothreitol (DTT) for 20 min at 32°C. The ADP-ribosylation medium contained 1 mM EDTA, 10 mM thymidine, 1 mM ATP, 1 mM GDPβS, 2 mM DTT, 0.17% Lubrol PX, and 0.02% bovine serum albumin, pertussis toxin (15 μg ml^{-1}), 5×10^6 counts min^{-1} [^{32}P]-NAD (about 2×10^{-6} M) in 15 mM Tris-HCl buffer (pH 7.4) in a final volume of 60 μl. The reaction was stopped in ice by addition of an equal volume of ice-cold 20% trichloroacetic acid containing 50 mM Na_2HPO_4. Samples incubated in the absence of toxins were used as controls. The resulting pellet was collected by centrifugation, washed, resuspended first in Tris-HCl buffer (10 mM; pH 7.4; 400 μl) for protein determination (Micro BCA Protein Assay Reagent Kit, Pierce, Rockford, IL, U.S.A.) and then solubilized in Laemmli buffer for urea gradient gel electrophoresis.

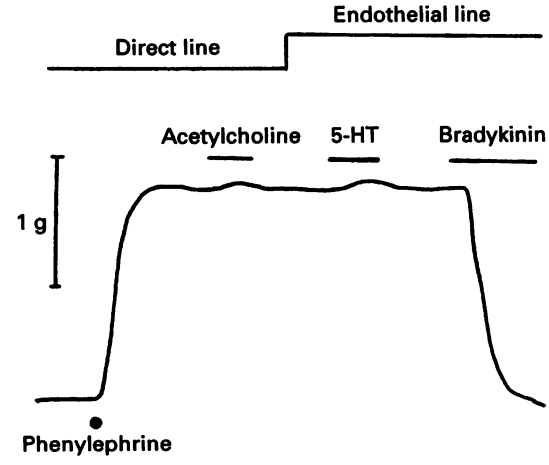

Figure 1 Isometric tension recording of a bioassay ring of rat aorta (without endothelium). Experiments were performed in the presence of indomethacin (10^{-5} M), ketanserin (10^{-6} M) and captopril (10^{-6} M). The bioassay ring was first contracted with phenylephrine (3×10^{-7} M) (*Direct line*) and acetylcholine (10^{-6} M) was infused to check the absence of endothelium (demonstrated by the absence of relaxation to acetylcholine). The detector ring was then moved underneath a column of cultured endothelial cells (*Endothelial line*). Infusion of bradykinin (10^{-6} M), but not 5-hydroxytryptamine (5-HT, 10^{-6} M), upstream of the column of endothelial cells caused full relaxation of the bioassay ring.

Urea gradient/SDS-polyacrylamide gel electrophoresis (PAGE)

Samples (20 μg of protein per lane) dissolved in SDS-PAGE sample buffer were loaded into a 4–8 M urea gradient gel containing 9% acrylamide (Codina *et al.*, 1991). Electrophoresis was conducted at 100 V for 8 h at room temperature. After electrophoresis, the gels were stained with Coomassie blue, destained, and dried. The dried gels then were exposed to Kodak X-OMAT-AR film at −70°C with intensifying screens for 1–16 h. The radioactive bands were visualized by autoradiography. The intensity of the bands were quantified by Betascope 603 Blot Analyzer (Betagen Corp., Waltham, MA, U.S.A.).

Statistical analysis

Data are given as mean ± s.e.mean; *n* represents the number of experiments performed with different cultures of porcine endothelial cells (obtained from different animals) or with different pools of native cells (each obtained from 6–7 pigs). Statistical evaluation was done by Student's *t* test for paired or unpaired observations (two tailed). Means were considered to be significantly different when *P* was less than 0.05. Scatchard analyses of the binding data were computed using the 'LIGAND' programme (kindly provided by Munson & Rodbard, 1988 revision; Munson & Rodbard, 1980).

Results

Bioassay experiments

The release of EDRF from porcine cultured endothelial cells was examined under bioassay conditions during stimulation with 5-HT or bradykinin (Figure 1). Acetylcholine induced a contraction of the bioassay ring when administered directly

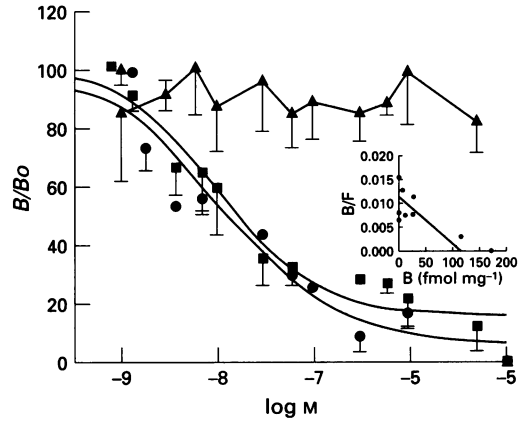

Figure 2 Competitive displacement of [^{3}H]-5-hydroxytryptamine ([^{3}H]-5-HT) binding with unlabelled 5-HT (●) or methiothepin (■; an antagonist for 5-HT_1 and 5-HT_2 receptors) but not by ketanserin (▲; an antagonist for 5-HT_2 receptor). Data are given as mean ± s.e.mean and are expressed as percentage of the maximal specific binding (obtained without unlabelled agonist or antagonist; 100% = 288 ± 19 d min^{-1}). Experiments were performed in duplicate with membranes obtained from three different cell preparations. The inset represents a Scatchard analysis for 5-HT receptors in porcine cultured endothelial cells. *B* = bound [^{3}H]-5-HT after addition of unlabelled 5-HT or antagonists (in d min^{-1}); *Bo* = bound [^{3}H]-5-HT before addition of unlabelled 5-HT or antagonists (d min^{-1}); *F* = molar concentration of free 5-HT (labelled and unlabelled); log M = logarithm of the molar concentration of unlabelled agonist (5-HT) or antagonist (methiothepin or ketanserin). There was no statistically significant difference between the displacements caused by 5-HT and methiothepin. Ketanserin did not cause a statistically significant displacement.

onto the bioassay ring during contraction to phenylephrine, which confirms the absence of endothelium. When the bioassay ring was placed under the endothelial line, infusion of bradykinin (10^{-6} M) upstream of the column of endothelial cells caused full relaxation of the bioassay ring, whereas 5-HT (10^{-6} M) failed to evoke a response (Figure 1).

5-HT receptor binding studies

In order to demonstrate the presence of 5-HT binding sites on porcine cultured endothelial cells, displacement of bound [^{3}H]-5-HT was examined in the presence of increasing concentrations of 5-HT, ketanserin (5-HT_2 antagonist) or methiothepin (5-HT_1 and 5-HT_2 antagonist). Membranes of cultured endothelial cells bound [^{3}H]-5-HT with maximal binding (B_{max}) = 121.4 ± 51.3 fmol mg^{-1} protein. Unlabelled 5-HT displaced all [^{3}H]-5-HT bound to endothelial cell membranes in a concentration-dependent manner (Figure 2). Scatchard analyses of the binding data were consistent with a single high affinity binding site with an equilibrium dissociation constant (K_d =) of 7.2 ± 3.5 nM. The [^{3}H]-5-HT binding was displaced by methiothepin (K_i = 6.2 ± 1.2 nM), but not by ketanserin (Figure 2).

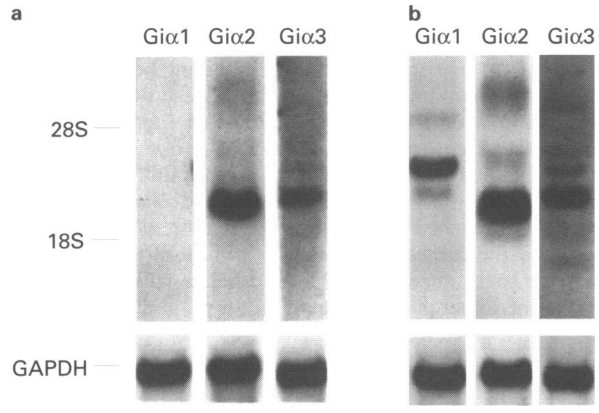

Figure 3 Expression of Giα1, Giα2, and Giα3 proteins mRNAs by Northern blot hybridization analysis in native (a) and cultured (b) endothelial cells: 20 μg of total RNAs per lane were hybridized with the Giα1, Giα2, and Giα3 probes. The same blot was reprobed with the GAPDH cDNA as an internal control. Migration of ribosomal RNA (18S and 28S) is indicated by the arrows. Comparable results were obtained in three other experiments.

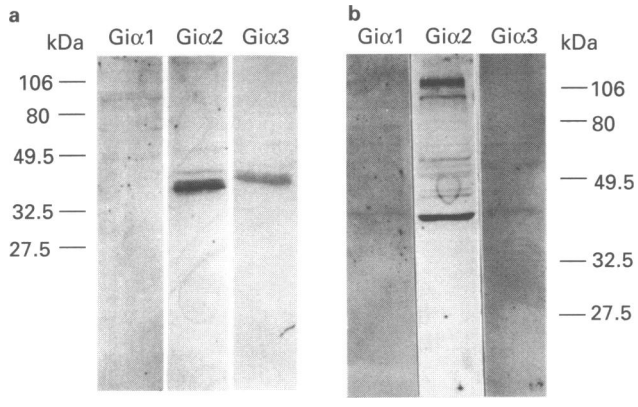

Figure 4 Western blot analysis of Giα1, Giα2, and Giα3 in native (a) and cultured (b) endothelial cells: 30 μg protein per lane were loaded in 10% SDS-PAGE gels for Western blotting. The molecular weight (kDa) of the markers is indicated on the left of the blots; the arrow indicates the position of the 40–41 kDa Giα subunits.

Expression of Giα proteins in native and cultured endothelial cells

The expression of each Giα protein subunit was examined by Northern and Western blot analysis in both native and cultured endothelial cells.

Total RNA obtained from native and cultured endothelial cells was hybridyzed with RT-PCR-generated cDNA probes specific for porcine Giα1 Giα2, and Giα3 subunits (Figure 3). In native endothelial cells, the mRNA of Giα2, and Giα3 subunits, but not that of Giα1, were expressed to detectable levels with an apparent size of 2.6 and 2.8 kb, respectively. Two less prominent mRNAs (3.0 kb and 3.8 kb) were observed with the Giα3 probe after 72 h prolonged exposure. In cultured endothelial cells, Giα1 mRNA was expressed to a detectable level with an apparent size of 3.45 kb, while it could not be detected in the native cells even after prolonged exposure (72 h, Figure 3). Cultured endothelial cells also expressed Giα2 and Giα3 mRNA to a level which was comparable to that found in native cells (Figure 3).

The presence of the three Gi protein α-subunits was detected in membranes obtained from native and cultured endothelial cells using antibodies against Giα1, Giα2 or Giα3 (Figure 4). These antibodies labelled a protein of apparent molecular weight of either 40 kDa (Giα2) or 41 kDa (Giα1 or Giα3 subunits) (Figure 4). Detectable amounts of Giα1, Giα2 and Giα3 protein subunits were observed in cultured endothelial cells, while native cells expressed only Giα2 and Giα3 protein subunits (Figure 4).

Pertussis toxin-catalyzed ADP-ribosylation

In unstimulated porcine cultured endothelial cells, pertussis toxin ADP-ribosylated two bands of 40 and 41 kDa which corresponded to Giα2 and Giα3-Giα1, respectively; the incorporation of [^{32}P]-NAD in the 40 and the 41 kDa bands was 4022 ± 401 and 1005 ± 211 counts min^{-1} mg^{-1} total proteins, respectively (n = 4). The amount of ADP-ribosylation of the 40 and 41 kDa proteins was not different between porcine native and cultured endothelial cells; under the same experimental conditions, the incorporation of [^{32}P]-NAD in the 40 and the 41 kDa bands from membranes of native cells was 3748 ± 479 and 988 ± 113 counts min^{-1} mg^{-1} total proteins, respectively (n = 3).

Pertussis toxin-catalyzed ADP-ribosylation of Giα proteins

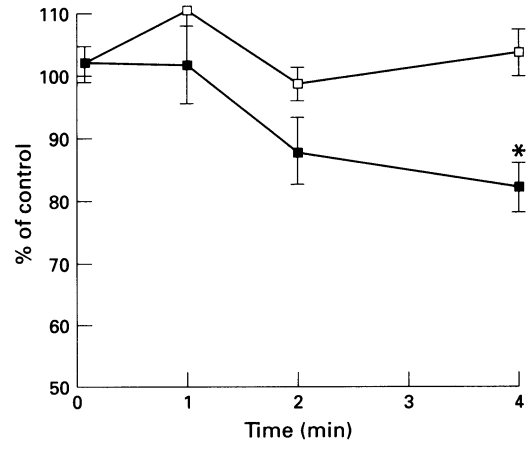

Figure 5 ADP-ribosylation of Giα2 following stimulation with 5-hydroxytryptamine (5-HT, ■; 3×10^{-6} M) in the presence of L-ascorbic acid (3×10^{-7} M) or with L-ascorbic acid alone (□) in cultured endothelial cells. Results are expressed as a percentage of Giα2 ADP-ribosylation in absence of 5-HT at t = 0 min (4022 ± 401 counts min^{-1} mg^{-1} total proteins from cultured porcine endothelial cells). The data are given as mean ± s.e.mean (n = 4). Significant difference between control and cells stimulated with 5-HT: *P < 0.01.

was examined *in vitro*, at various times following stimulation of cultured endothelial cells with 5-HT (3×10^{-6} M). The labelling of the 40 and 41 kDa proteins did not change under control conditions during the time course of the experiment (Figure 5). Stimulation of cultured porcine endothelial cells with 5-HT (3×10^{-6} M; 4 min) decreased significantly the subsequent ADP-ribosylation by pertussis toxin of Giα2 but did not affect that of Giα1-Giα3 (Figure 5).

Discussion

The present study confirms the absence of EDRF release from porcine cultured endothelial cells in response to 5-HT (Boulanger *et al.*, 1989) and provides evidence that this impaired function is not associated with the loss of Gi-protein α subunits or the absence of 5-HT receptors.

A single 5-HT binding site was determined by Scatchard analysis in membranes obtained from porcine cultured endothelial cells. The K_d and K_i values suggest that this binding site is of the 5-HT_1 subtype. This conclusion is based on the fact that (a) the measured pK_i (8.2) for methiothepin, a non-preferential 5-HT_1–5-HT_2 antagonist, was in the range of previously reported values from 7.7 to 8.1 (Hoyer *et al.*, 1993), and (b) ketanserin, a preferential 5-HT_2 antagonist, was unable to displace 5-HT binding, even at high concentrations. Therefore, the present results are in agreement with studies showing a release of EDRF mediated by activation of 5-HT_{1D} receptors in porcine isolated coronary arteries (Houston & Vanhoutte, 1988; Schoeffter & Hoyer, 1990). However, the present experiments do not exclude the possibility that in cultured endothelial cells, the number of 5-HT binding sites has been decreased to such an extent that 5-HT now behaves as a low efficacy agonist; if this were the case, this could contribute to the dysfunctional release of nitric oxide following stimulation with the monoamine.

In addition to the presence of specific binding sites for 5-HT, the present data show the expression of three different α subunits of the pertussis toxin-sensitive Gi proteins in cultured endothelial cells, both at the mRNA and protein levels. The apparent size of these mRNAs was comparable to those reported for Giα1, Giα2, and Giα3 mRNAs in eukaryotes by Northern blot analysis (2.2–3.9, 2.35–2.7, and 2.4–3.5 kb, respectively) (Lochrie & Simon, 1988). The apparent molecular weight of the three proteins as detected by Western blot analysis was comparable to those reported for Giα1 (41 kDa), Giα2 (40 kDa) and Giα3 (41 kDa). The predominant expression of the Giα2 subunit, as indicated by Western blot analysis and *in vitro* ADP-ribosylation with pertussis toxin, is in agreement with previous studies performed with native porcine endothelial cells (Flavahan *et al.*, 1992). When comparing the level of Giα2 and Giα3 subunits between native and cultured endothelial cells, one can conclude that the expression of these subunits is not decreased in the cultured cells. In addition, the cultured cells express a significant amount of Giα1 protein, which was not detected in native porcine or cultured bovine endothelial cells (Flavahan *et al.*, 1992; Liao & Homcy, 1992; this study). The present experiments do not allow further speculation concerning the role of Giα1 in the impairment of the release of EDRF observed during stimulation with 5-HT.

Since pertussis toxin ADP-ribosylated the 40 and 41 kDa bands to the same extent in membranes from porcine native and cultured endothelial cells, it is unlikely that the impaired 5-HT-stimulated release of EDRF from cultured endothelial cells could result from an augmented endogenous ADP-ribosylation of the Giα protein subunits, impairing their function. Indeed, experiments with cultured hepatocytes showed an augmented response to β-adrenoceptor agonists associated with an increased endogenous ADP-ribosylation of the Gi α subunits during the culture process (Ui *et al.*, 1985; Scherer *et al.*, 1987). In addition, the present experiments show that pertussis toxin-catalysed ADP-ribosylation of Giα2 is decreased significantly following stimulation of cultured endothelial cells with 5-HT. These results suggest that the 5-HT_1 receptors may be coupled to the pool of Giα subunits which is ADP-ribosylated *in vitro* by pertussis toxin. However, the function of the Giα proteins in cultured endothelial cells may be altered by other mechanisms, such as changes in palmitoylation or phosphorylation, or because of a different subcellular compartmentalization. The selective endothelial dysfunction may result also from a lack of coupling between the Giα protein(s) and their effector(s) leading to the activation of the constitutive NO-synthase. A reduced expression level of the constitutive NO-synthase has been observed in cultured endothelial cells (Wu *et al.*, 1994; T.Ge, unpublished observations). This could also contribute to the impaired release of EDRF from cultured endothelial cells if 5-HT were less potent in stimulating constitutive NO-synthase than other agonist(s) such as bradykinin (Boulanger *et al.*, 1989).

Although porcine cultured endothelial cells were used as a model of *in vivo* regenerated endothelium because they displayed a similar impairment of the release of EDRF during stimulation with 5-HT, it is possible that the dysfunction occurs at a different level in cultured cells and *in vivo* regenerated endothelial cells. Indeed, a decreased amount of functionality of Gi proteins may contribute to the endothelial dysfunction observed in coronary arteries with regenerated endothelium, as shown by the decreased ADP-ribosylation of Gi α subunits by pertussis toxin in regenerated endothelial cells from coronary arteries of hypercholesterolaemic pigs (Shibano *et al.*, 1994). The decreased amount or function of Giα proteins suggested by these experiments could reflect a functional difference between *in vivo* regenerated and cultured endothelial cells. Alternatively, it could be a consequence of the hypercholesterolaemia since the lysophosphatidylcholine present in oxidized low-density lipoproteins selectively impairs Gi protein function in endothelial cells (Kugiyama *et al.*, 1990; Yokoyama *et al.*, 1990; Flavahan, 1992; Shibano *et al.*, 1994).

This research was supported, in part, by a grant from the National Institute of Health (grant HL 31547) and by a Strategic Research Fund Grant from Zeneca Pharmaceuticals. We are indebted to Dr David R. Manning, Dept. of Pharmacology, University of Pennsylvania, for sharing anti-Giα proteins and to Drs Peter J. Munson and David Rodbard, laboratory of Theoretical and Physical Biology, National Institute of Child Health and Human Development, National Institutes of Health, for providing the 'LIGAND' programme.

References

ASANO, T., SEMBA, R. & KAMIYA, N. (1988). Go, a GTP-binding protein: immunochemical and immunohistochemical localization in the rat. *J. Neurochem.*, **50**, 1164–1169.

BOULANGER, C., HENDRICKSON, H., LORENZ, R.R. & VANHOUTTE, P.M. (1989). Release of different relaxing factors by cultured porcine aortic endothelial cells. *Circ. Res.*, **64**, 1070–1077.

CHOMCZYNSKI, P. & SACCHI, N. (1987). Single-step method of RNA isolation by acid guanidinium thiocyanate-phenol-chloroformextraction. *Anal. Biochem.*, **162**, 156–159.

CODINA, J., GRENET, D., CHANG, K.-J. & BIRNBAUMER, L. (1991). Urea-gradient/SDS-PAGE; a useful tool in the investigation of signal transducing G proteins. *J. Receptor Res.*, **11**, 587–601.

COHEN, R.A., SHEPHERD, J.T. & VANHOUTTE, P.M. (1983). Inhibitory role of the endothelium in the response of isolated coronary arteries to platelets. *Science*, **221,** 273–274.

DAY, N.S., BERTI-MATTERA, L.N. & EICHBERG, J. (1991). Muscarinic cholinergic receptor-mediated phosphoinoistide metabolism in peripheral nerve. *J. Neurochem.*, **56,** 1905–1913.

DAY, N.S., KOUTZ, C.A. & ANDERSON, R.E. (1993). Inositol-1,4,5-trisphosphate receptors in the vertebrate retina. *Current Eye Res.*, **12,** 981–992.

DOLPHIN, A.C. (1987). Nucleotide binding proteins in signal transduction and disease. *Trends Neurosci.*, **10,** 53–57.

FLAVAHAN, N.A., FREEMAN, J.E. IV & LEVINE, M.A. (1992). Biochemical analysis of pertussis toxin-sensitive G-proteins in porcine endothelial cells. *32nd World Congress of the International Union of Physiological Sciences* (Abs) p56.

FLAVAHAN, N.A., SHIMOKAWA, H. & VANHOUTTE, P.M. (1989). Pertussis toxin inhibits endothelium-dependent relaxations to certain agonists in porcine coronary arteries. *J. Physiol.*, **408,** 549–560.

HOUSTON, D.S. & VANHOUTTE, P.M. (1988). Comparison of serotonergic receptor subtypes on the smooth muscle and the endothelium of the canine coronary artery. *J. Pharmacol. Exp. Ther.*, **244,** 1–10.

HOYER, D., BRUINVELS, A.T. & PALACIOS, J.M. (1993). 5-HT_{1D} receptor subtypes In *Serotonin from Cell Biology to Pharmacology and Therapeutics*. ed. Vanhoutte, P.M., Sadena, P.R., Paoletti, R., Brunello, N. & Jackson, A.S. pp. 85–97. Netherlands: Kluwer Acad.

ITOH, H., TOYAMA, R., KOZASA, T., TSUKAMOTO, T., MATSUOKA, M. & KAZIRO, Y. (1988). Presence of three distinct molecular species of Gi protein α subunits. *J. Biol. Chem.*, **263,** 6656–6664.

JONES, D.T. & REED, R.R. (1987). Molecular cloning of five GTP-binding protein cDNA species from rat alfactory neuroepithelium. *J. Biol. Chem.*, **262,** 14241–14249.

KUGIYAMA, K., KERNS, S.A., MORRISETT, J.D., ROBERTS, R. & HENRY, P.D. (1990). Impairment of endothelium-dependent relaxation by lysolecithin in modified low-density lipoproteins. *Nature Lond.*, **344,** 160–162.

LIAO, J.K. & HOMCY, C.J. (1992). Specific receptor-guanine nucleotide binding protein interaction mediates the release of endothelium-dependent relaxing factor. *Circ. Res.*, **70,** 1018–1026.

LOCHRIE, M.A. & SIMON, M.I. (1988). G protein multiplicity in eukaryotic signal transduction systems. *Biochem.*, **27,** 4957–4965.

LÜSCHER, T.F. & VANHOUTTE, P.M. (1990). *The Endothelium: Modulator of Cardiovascular Function*. pp. 1–228. Boca Raton, Florida: CRC Press.

MONCADA, S., PALMER, R.M.J. & HIGGS, E.A. (1991). Nitric oxide: physiology, pathophysiology, and pharmacology. *Pharmacol. Rev.*, **43,** 109–142.

MUNSON, P.J. & RODBARD, D. (1980). Ligand: a versatile computerized approach for characterization of ligand-binding systems. *Anal. Biochem.*, **107,** 220–239.

RIBEIRO-NETO, F.A.P., MATTERA, R., GRENET, D., SEKURA, R.D., BIRNBAUMER, L. & FIELD, J. (1987). Adenosine diphosphate ribosylation of G proteins by pertussis and cholera toxin in isolated membranes. Different requirements for the effects of guanine nucleotides and Mg^{2+}. *Mol. Endocrinol.*, **1,** 472–481.

SCHERER, N.M., TORO, M.-J., ENTMAN, M.L. & BIRNBAUMER, L. (1987). G protein distribution in canine cardiac sarcoplasmic reticulum and sarcolemma. Comparison to rabbit skeletal membranes and brain and erythrocyte G proteins. *Arch. Biochem. Biophys.*, **259,** 431–440.

SCHOEFFTER, R. & HOYER, D. (1990). 5-Hydroxytryptamine (5-HT)-induced endothelium-dependent relaxation of pig coronary arteries is mediated by 5-HT receptors similar to the 5-HT_{1D} receptor subtype. *J. Pharmacol. Exp. Ther.*, **25,** 387–395.

SHIBANO, T., CODINA, J., BIRNBAUMER, L. & VANHOUTTE, P.M. (1992). Guanosine 5'-O-(3-thiotriphosphate) causes endothelium-dependent, pertussis toxin-sensitive relaxations in porcine coronary arteries. *Biochem. Biophys. Res. Commun.*, **189,** 324–329.

SHIBANO, T., CODINA, J., BIRNBAUMER, L. & VANHOUTTE, P.M. (1994). Pertussis toxin-sensitive G-proteins in regenerated endothelial cells after balloon denudation of the porcine coronary artery. *Am. J. Physiol.*, **267,** H979–H981.

SHIMOKAWA, H., FLAVAHAN, N.A. & VANHOUTTE, P.M. (1989). Natural course of the impairment of endothelium-dependent relaxations after balloon endothelium removal in porcine coronary arteries. Possible dysfunction of a pertussis toxin-sensitive G protein. *Circ. Res.*, **65,** 740–753.

SHIMOKAWA, H., FLAVAHAN, N.A. & VANHOUTTE, P.M. (1991). Loss of endothelial pertussis toxin-sensitive G protein function in atherosclerotic porcine coronary arteries. *Circ.*, **83,** 652–660.

UI, M., OKAJIMA, F. & ITOH, H. (1985). ADP-ribosylation of the inhibitory ghuanine nucleotide regulatory protein (Ni) as a possible mechanism underlying development of beta-adrenergic responses during primary culture. *Adv. Cyclic Nucl. Prot. Phosphor. Res.*, **19,** 195–205.

VANE, J.R. (1994). The Croonian lecture, 1993. The endothelium: maestro of the blood circulation. *Phil. Trans. R. Soc. B*, **343,** 225–246.

VANHOUTTE, P.M., LUSCHER, T.F. & GRASER, T. (1991). Endothelium-dependent contractions. *Blood Vessels*, **28,** 74–83.

WILLERSON, J.T. (1993). Platelets, platelet mediators, and unstable coronary artery disease syndromes. *Serotonin*, **36,** 307–319.

WU, K., SHELTON, A., TAYLOR, W.R. & MARSHALL, J.J. (1994). Confocal laser immunohistochemistry of superoxide dismutase (SOD) and nitric oxide synthase (NOS) in regenerated endothelium (RE). *FASEB J.*, **8,** A39.

YOKOYAMA, M., HIRATA, K., MIYAKE, R., AKITA, H., ISHIKAWA, Y. & FUKAZAKI, H. (1990). Lysophosphatidylcholine; essential role in the inhibition of endothelium-dependent vasorelaxation by oxidized low density lipoprotein. *Biochem. Biophys. Res. Commun.*, **168,** 301–308.

(Received December 12, 1994
Revised March 9, 1995
Accepted March 13, 1995)

British Journal of Pharmacology (1995) 115, 828-834

Cross talk between receptors mediating contraction and relaxation in the arterioles but not the dilator muscle of the rat iris

[1]D.J. Gould, M. Vidovic & C.E. Hill

Division of Neuroscience, John Curtin School of Medical Research, Australian National University, Canberra, A.C.T., 2601, Australia

1 Sympathetic nerve stimulation causes contraction of the dilator muscle and the large arterioles of the iris via the activation of α_{1B}-adrenoceptors. We have investigated whether increases in adenosine 3': 5'-cyclic monophosphate (cyclic AMP) and the activation of receptors in these tissues can modulate these nerve-mediated contractions.

2 Increasing intracellular cyclic AMP with dibutyryl cyclic AMP (1 mM), forskolin (50 μM) or isobutylmethylxanthine (100 μM) produced relaxation of both the dilator and the arterioles, abolished the nerve-mediated constriction of the arterioles, but potentiated the nerve-mediated contraction of the iris dilator.

3 Pretreatment of the preparations with cholera toxin, to activate G_s permanently, caused a dilatation of the arterioles and abolished the nerve-mediated constriction but had no effect on the dilator muscle.

4 The β-adrenoceptor agonist, isoprenaline (1 μM), the adenosine-A_1,-A_2 agonist, N-ethylcarboxamidoadenosine NECA (100 nM), in the presence of the A_1-selective antagonist, 8-cyclopentyl-1, 3-dipropylxanthine (DPCPX, 10 nM), and calcitonin gene-related peptide (CGRP, 10 nM) all separately caused a dilatation of the arterioles and abolished the nerve-mediated constriction, while only isoprenaline (1 μM) produced an effect on the dilator, i.e. a relaxation but a potentiation of the nerve-mediated contraction. These results suggest the presence of at least 3 types of receptor linked to G_S and an increase in cyclic AMP in the arterioles, i.e. β-adrenoceptor, adenosine-A_2 and CGRP, but only 1 G_S-linked receptor, i.e. β-adrenoceptors, on the dilator muscle cells.

5 Neither the A_1-selective agonist, cyclohexyladenosine (CHA, 10 nM) nor the A_1-selective antagonist, DPCPX (10 nM) had any significant effect on the nerve-mediated constriction of the arterioles, suggesting that presynaptic A_1-receptors do not play a role in modulating the sympathetic nerve-mediated constriction.

6 Forskolin (50 μM), in the presence of capsaicin (10 μM) to inactivate unmyelinated CGRP-containing sensory nerves, still caused a dilatation of the arterioles and abolished nerve-mediated constriction suggesting that the effects on the blood vessels were due to increases in cyclic AMP in the arteriolar cells and not in the sensory nerves.

7 Using reverse transcription polymerase chain reaction, we have demonstrated expression of the α_{1B} and α_{1C} molecular subtypes in the tissues of the iris. These molecular subtypes most likely correspond to the α_{1B} and α_{1A} pharmacological subtypes, respectively.

8 Preincubation in N^G-nitro-L-arginine methyl ester (L-NAME, 10 μM), but not D-NAME (10 μM), reduced the efficacy of forskolin in inhibiting the sympathetic nerve-mediated vasoconstriction. These results suggest that the inhibition of sympathetic nerve-mediated constriction by cyclic AMP in the arterioles is indirect via the production of nitric oxide.

9 Our results demonstrate that there is 'cross talk' between receptors linked to increases in cyclic AMP and α_{1B}-adrenoceptors in the arterioles of the rat iris, but that no such interaction occurs between cyclic AMP and α_{1B}-adrenoceptors in the dilator muscle. The interaction in the arterioles occurs as a result of cyclic AMP-mediated stimulation of nitric oxide synthesis, presumably by the arteriolar endothelial cells.

Keywords: Cyclic AMP; α_{1B}-adrenoceptor; arteriole; iris dilator muscle; sympathetic nerve; nitric oxide; cross talk

Introduction

A small proportion of neurones in the superior cervical ganglion give rise to the adrenergic innervation of the iris (Olson *et al.*, 1988). Studies that use the formaldehyde-induced fluorescence technique for the detection of catecholamines have shown that these sympathetic axons form a rich network of terminals covering the dilator muscle and the largest of the arterial blood vessels which are found within the stromal layer of the rat iris. Stimulation of these nerves causes the release of noradrenaline and a subsequent contraction of the iris dilator and a constriction of the arterioles (Takayanagi *et al.*, 1992; Hill *et al.*, 1993; Gould & Hill, 1994). In both these tissues, nerve-mediated contractile responses were 100 fold more sensitive to the α_1-adrenoceptor antagonist, prazosin, than the α_2-adrenoceptor antagonist, yohimbine. Responses were also relatively insensitive to the α_1-antagonist, WB4101, but were abolished following exposure to chloroethylclonidine (CEC) (Hill *et al.*, 1993; Gould & Hill, 1994). While CEC has been reported to inactivate α_{1B}-adrenoceptors, it has also been shown to have α_2-adrenoceptor agonist actions (Bultmann & Starke, 1993) which, in the case of sympathetic nerves, could lead to a decrease in neurotransmitter release and a concomitant decrease in the postsynaptic response. In the arterioles of the rat iris, the action of CEC is postsynaptic, as it abolishes the effect of exogenous noradrenaline as well as the nerve-mediated contractile response (Gould & Hill, 1994). In view of these results, the receptors mediating nerve-induced contractile responses in both the iris dilator and arterioles have been identified pharmacologically as α_{1B}-adrenoceptors (Takayanagi *et al.*, 1992; Hill *et al.*, 1993; Gould & Hill, 1994).

[1] Author for correspondence.

Activation of G-protein-coupled α_{1B}-adrenoceptors has been reported to lead to an increase in inositol phospholipid hydrolysis and release of intracellular calcium (Han *et al.*, 1987). Consistent with the involvement of this pathway, the nerve-mediated contractions of the dilator muscle and the arterioles are not dependent on the activation of voltage-sensitive calcium channels, which permit the movement of extracellular calcium into the muscle cells (Takayanagi *et al.*, 1992; Gould & Hill, 1994). Intracellular interactions between receptor-activated second messenger pathways which modulate the level of cyclic AMP, have been shown to alter the activity of the pathway involving inositol trisphosphate (IP_3) hydrolysis in smooth muscle (Abdel-Latif, 1989; 1991). In bovine sphincter there is a reciprocal effect between muscarinic receptor activation of IP_3 formation and cyclic AMP formation. For example, elevation of cyclic AMP with isoprenaline or forskolin inhibits carbachol-induced IP_3 formation and sphincter contraction (Tachado *et al.*, 1989; 1992). Thus it has been suggested that interaction between these two second messenger pathways may be one mechanism for regulating contraction and relaxation of smooth muscle (Abdel-Latif, 1991). Similar results have been found in the rat aorta, where increases in cycle AMP have an inhibitory effect on noradrenaline-stimulated contraction due to α_1-adrenoceptor activation (Lincoln & Fisher-Simpson, 1984; Manolopoulos *et al.*, 1991). This was reported to be due to a reduction in intracellular calcium and is perhaps accompanied by a reduction in the sensitivity of the contractile elements to calcium. The site at which cyclic AMP interacts with the IP_3 pathway was thought to occur distal to the membrane receptor coupling to phospholipase C. Both cyclic AMP and cyclic GMP have recently been shown to inhibit IP_3-dependent intracellular calcium release and contraction due to agonist stimulation (Murthy *et al.*, 1993).

The present study investigates whether α_{1B}-adrenoceptor-mediated contractions of the dilator muscle and of the arterioles of the iris can be modulated by increases in intracellular cyclic AMP. We further investigate the possible existence, on the arterioles and on the dilator muscle, of specific receptor subtypes which, when activated, could be responsible for elevated cyclic AMP levels *in vivo*.

Methods

In vitro experiments

Wistar rats of either sex (4–6 weeks postnatal) were killed with an overdose of either anaesthetic and the irides removed. The irides were cut in half, the sphincter removed and the dilator pinned out in a 1 ml bath which was perfused with Krebs solution of the following composition (mM): NaCl 119.8, KCl 15.0, $CaCl_2$ 2.5, $MgCl_2$ 2.0, NaH_2PO_4 1.0, $NaHCL_3$ 24.4 and glucose 22.0, and gassed with a mixture of 95% O_2 plus 5% CO_2. Preparations were equilibrated for 30 min before commencing transmural nerve stimulation, via platinum electrodes, at 10 Hz for 1 s (0.1 ms pulse width, 45 V) every 3 min. This stimulation produced consistent contractile responses of the dilator and blood vessels (mean resting diameter of 31.7 ± 1.0 μm). Hyoscine (1 μM) was added to the Krebs solution to prevent the effect of cholinergic nerves. Contractions were measured using video microscopy and the computer programme, DIAMTRAK (Nield, 1989), which uses averaging techniques to locate the edges of the arterioles and display their difference as arteriolar diameter on a chart recorder. At least 3 consistent control contractions were recorded before adding any drug. The magnitude of the vasoconstrictor responses to nerve stimulation in both control and drug solutions were expressed as a percentage of the resting vessel diameter. This was done in order to standardize nerve-mediated responses in vessels of different resting diameter. Dilator muscle contractile responses were measured after cutting off the sphincter muscle and locating the cut edge of the dilator with the programme DIAMTRAK. Drug effects were expressed as a percentage of the average of 3–4 control responses prior to the addition of drug. Experimental values are given as the mean ± s.e.mean of results from at least 3 preparations. Vehicle controls were found to have no effect on nerve-mediated contractions. The adenosine-A_2 antagonist, 8-cyclopentyl-1,3-dipropylxanthine (DPCPX), was present 30 min before the addition of the adenosine-A_1,-A_2 agonist, N-ethylcarboxamidoadenosine (NECA). In experiments to test the effect of forskolin in the presence of capsaicin, N^G-nitro-L-arginine methyl ester (L-NAME) or D-NAME, the capsaicin, L-NAME or D-NAME was present in the Krebs solution for the entire experiment.

The significance of drug effects was tested by Analysis of Variance with 95% confidence limits, followed by unpaired *t* tests with Bonferroni correction for multiple groups.

Drugs and solutions

The following drugs were used: rat calcitonin gene-related peptide 1-37 (CGRP, Auspep, Australia), capsaicin (Fluka Chemie, Switzerland), N^G-nitro-L-arginine methyl ester (L-NAME) and N^G-nitro-D-arginine methyl ester (D-NAME, Sapphire Bioscience Pty. Ltd., Australia). Cholera toxin, 8-cyclopentyl-1,3-dipropylxanthine (DPCPX), forskolin, 3-isobutyl-1-methyl-xanthine (IBMX), (±)-isoprenaline hydrochloride, N^6-cyclohexyladenosine (CHA), N^6,2′-O-dibutyryladenosine 3′:5′-cyclic monophosphate (dibutyryl cyclic AMP), N-ethylcarboxyamidoadenosine (NECA) and (−)-hyoscine (scopolamine) hydrochloride were all from Sigma, U.S.A.

All drugs were made up at the start of each experiment as 1000 × stocks, except for dibutyryl cyclic AMP which was dissolved directly in Krebs solution. Capsaicin, CHA, DPCPX, forskolin and IBMX stocks were dissolved in absolute ethanol, NECA stock was dissolved in 0.1 M HCl. Forskolin was also dissolved in 0.1% dimethyl sulphoxide. Stocks for all other drugs were dissolved in H_2O. Dilutions of all stocks were made in Krebs for final concentrations.

Expression of mRNA for α_1-adrenoceptor subtypes in the iris

RNA isolation Total cellular RNA was isolated from freshly dissected iris tissue, from adult Wistar rats killed with an overdose of anaesthetic, using a single-step protocol for RNA isolation ('RNAzol B', Cinna/Biotecx). Both the sphincter muscle and the ciliary processes were dissected from the iris. The iris tissue thus included the dilator muscle and the arterioles found within the stromal layer of the iris. Separation of these latter two tissues was not physically possible as the stroma overlies the dilator. The manufacturers recommended protocol for isolation of RNA was followed. Briefly, tissue was collected into RNAzol solution, homogenized at room temperature and the homogenate separated into two phases. The RNA was precipitated from the aqueous phase with isopropanol and the RNA pellet dissolved in water. Optical density readings were done to estimate the amount of total RNA before it was used in reverse transcription-polymerase chain reaction (RT-PCR).

Reverse transcription-polymerase chain reaction Oligodeoxynucleotide primers for use in RT-PCR were synthesized using an Applied Biosystems Model 380B Nucleic Acid Synthesiser and solid phase synthesis. Oligonucleotides were designed from published sequences of rat α_{1A} cDNA. Forward primer 5′-AGTGGGTGTCTTCCTGGCGGCCTT-3′, and reverse primer 5′-GATCACTGCCATGGGTAGGTAGAA-3′ (Lomasney *et al.*, 1991b) were used to generate a 517 base pair (bp) fragment; α_{1B} cDNA forward primer 5′-AGGGCCATCTCTGTGGGCCTGGTG-3′, and reverse primer 5′-GATGGAGATGACCGTGGACAAGAC-3′, (Voigt *et al.*, 1990) were used to generate a 405 bp fragment; the α_{1C} specific oligonucleotide forward primer was 5′-TGGCCATCATTCTGGTTATGT-3′ and reverse primer 5′-GCAACCCACCA

CGATGCCCAG-3′ (Alonso-Llamazares *et al.*, 1993) and these were employed to generate a 251 bp fragment.

Prior to RT-PCR, total RNA was treated with DNase I to avoid false positives being generated from the DNA present in RNA preparation. The DNase-pretreated RNA (3.9 μg) was reverse transcribed with oligo dT (300 ng) and 50 u of reverse transcriptase (StrataScript RNase H^-). The reaction was carried out in a volume of 50 μl, and 2 μl was used in each PCR reaction.

PCR was performed in a capillary tube thermal cycler (Corbett Research, Sydney, Australia) using 20 μl aliquots under the following conditions: 10 mM Tris-HCl, pH 9, 50 mM KCl, 1.5 mM $MgCl_2$, 0.01% gelatin, 0.1% Triton X-100, deoxyribonucleoside triphosphates (dNTPs) - 200 μM each of dATP, dCTP, dGTP, dTTP, 24 pmol of each primer and 0.2 u of SuperTaq DNA polymerase (P.H. Stehelin and Cie AG, Basel). Samples were heat sealed and amplifications were performed for 30 cycles. The amplification products were separated in 2% agarose gel impregnated with ethidium bromide.

Results

Effects of increasing intracellular cyclic AMP

Three agents were used to test the effect of increasing intracellular cyclic AMP on the nerve-mediated contractile responses of the blood vessel and the dilator muscle: dibutyryl cyclic AMP (1 mM), IBMX (100 μM), a phosphodiesterase inhibitor, and forskolin (50 μM), a direct activator of adenylate cyclase. Increasing cyclic AMP with any of these three agents abolished the nerve-mediated constriction of the arterioles but potentiated the contractile response to nerve stimulation in the dilator muscle (Figures 1, 2). In addition, increasing cyclic AMP caused a dilatation of the arterioles (38.5 ± 1.1 μm, $n = 3$, in forskolin, 50 μM, compared to 33.3 ± 1.2 μm, $n = 3$, in control, $P > 0.05$) and a relaxation of the dilator muscle (Figure 1). Thus, an increase in cyclic AMP affected the nerve-mediated contractile responses differently in the two tissues.

Involvement of the GTP-binding protein, G_s

To investigate the physiological relevance of the effect of cyclic AMP on sympathetic nerve-mediated responses, the possible presence of the GTP-binding protein, G_s, was examined using cholera toxin. Cholera toxin (2 μg · ml^{-1}) treatment for 1.5 h caused a dilatation of the arterioles and prevented the nerve-

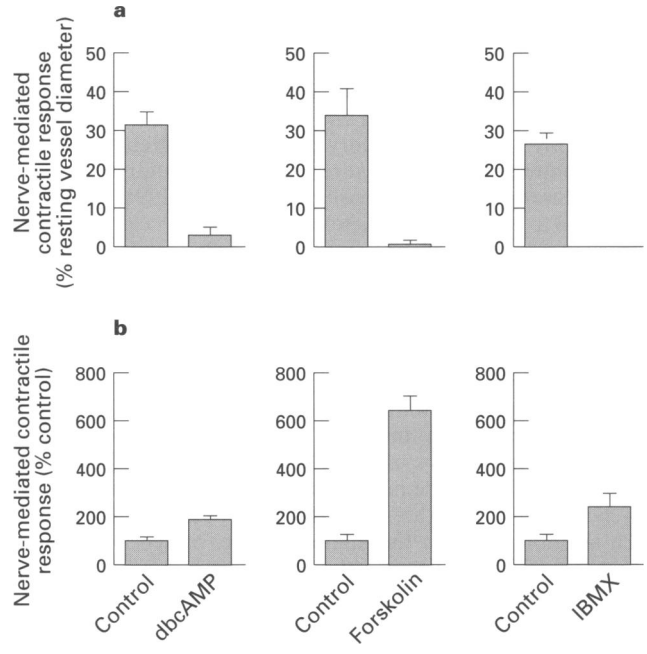

Figure 2 Effect of (left to right) dibutyryl cyclic AMP (dbcAMP, 1 mM), forskolin (50 μM) and isobutylmethylxanthine (IBMX, 100 μM) on the nerve-mediated contractile responses of the arterioles (a) and on the nerve-mediated contractile responses of the dilator muscle (b). Columns represent the mean of 3 preparations. Vertical bars represent the s.e.mean.

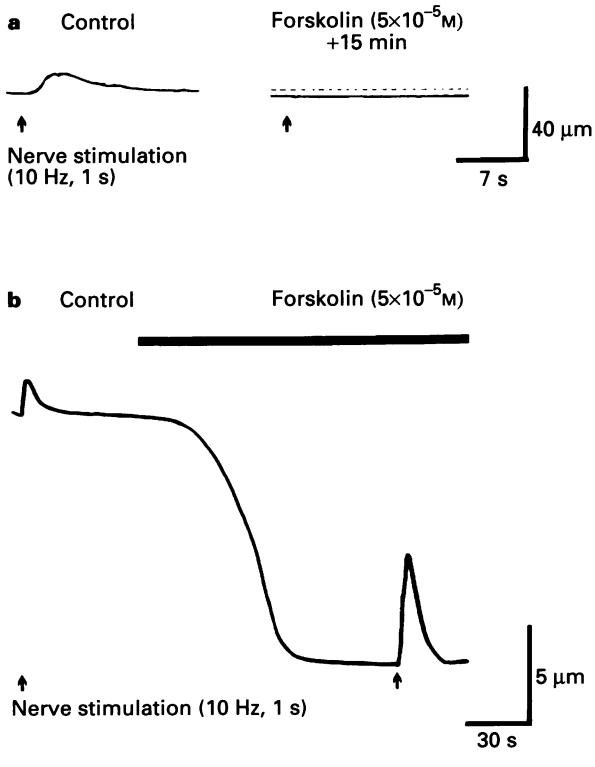

Figure 1 Effect of forskolin (50 μM) on the nerve-mediated contractions of the arterioles (a) and the dilator muscle (b). Arrows indicate nerve stimulation (10 Hz, 1 s). Dotted line represents previous resting diameters of the arteriole in control solution.

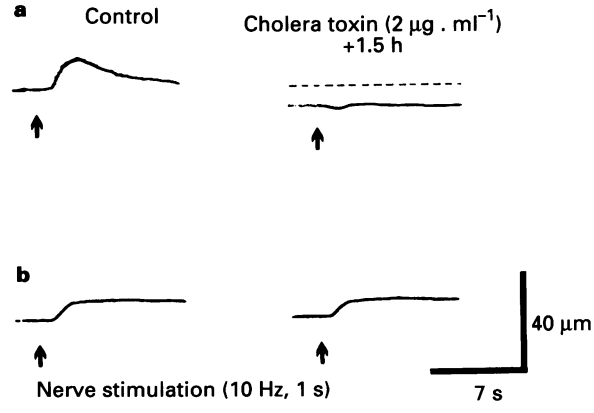

Figure 3 Effect of treatment with cholera toxin (2 μg · ml^{-1}) on the nerve-mediated contractions of (a) the arteriole and (b) the dilator muscle. Arrows indicate nerve stimulation (10 Hz, 1 s). Dotted line represents previous resting diameter of the arteriole in control solution.

mediated vasoconstriction, but had no effect on the nerve-mediated contraction of the dilator muscle (Figure 3).

Identity of receptors coupled to G_S in the dilator and arterioles

β-Adrenoceptors The β-agonist, isoprenaline (1 μM), significantly reduced the sympathetic vasoconstriction (Figure 4). Isoprenaline also produced a relaxation of the dilator ($n=5$) and a concomitant potentiation of the nerve-mediated contraction of the dilator muscle.

Adenosine receptors Presynaptic adenosine-A_1-receptor activation causes a decrease in neurotransmitter release from sympathetic nerves (Starke *et al.*, 1989; von-Kugelgen *et al.*, 1992), and thus could decrease the response to nerve stimulation. The presence of adenosine receptors was therefore examined. The A_1-selective agonist, CHA (10 nM) did not significantly reduce the sympathetic vasoconstriction (Figure 4).

The A_1-selective antagonist, DPCPX (10 nM), had no significant effect on nerve-mediated vasoconstriction, confirming the absence of a role of presynaptic A_1-receptors (Figure 4). In the presence of DPCPX (10 nM), the adenosine-A_1,-A_2 agonist, NECA (10 and 100 nM), concentration-dependently reduced the sympathetic vasoconstriction (Figure 4) but did not relax the dilator.

CGRP receptors CGRP (100 nM – 100 pM) caused a vasodilatation and a concentration-dependent reduction of sympathetic vasoconstriction (Figure 5) but had no effect on the dilator. The inhibitory action of CGRP on nerve-mediated vasoconstriction rapidly desensitized (within 3 min for the higher concentrations). In the presence of CGRP, while the responses to nerve stimulation had desensitized, the arteriole continued to relax.

Does the effect of increased cyclic AMP in the arterioles occur in the arteriolar cells or in the sensory nerves?

After inhibiting sensory nerve transmission by treatment with capsaicin (10 μM) for 15 min, forskolin (50 μM) abolished sympathetic nerve-mediated vasoconstriction (Figure 6).

Expression of mRNA for α_1-adrenoceptor subtypes

In order to confirm the molecular identity of the α_1-adrenoceptor subtypes identified pharmacologically as α_{1B} in the dilator and the arterioles, we used RT-PCR with subtype-specific primers. The results from RT-PCR on the rat iris show two PCR products. Both α_{1B} (405 bp) and α_{1C} (251 bp) primers have amplified products of appropriate size from the same pool of cDNA that was synthesized with oligo dT primers (Figure 7, lanes 4, 6). Under similar conditions and using

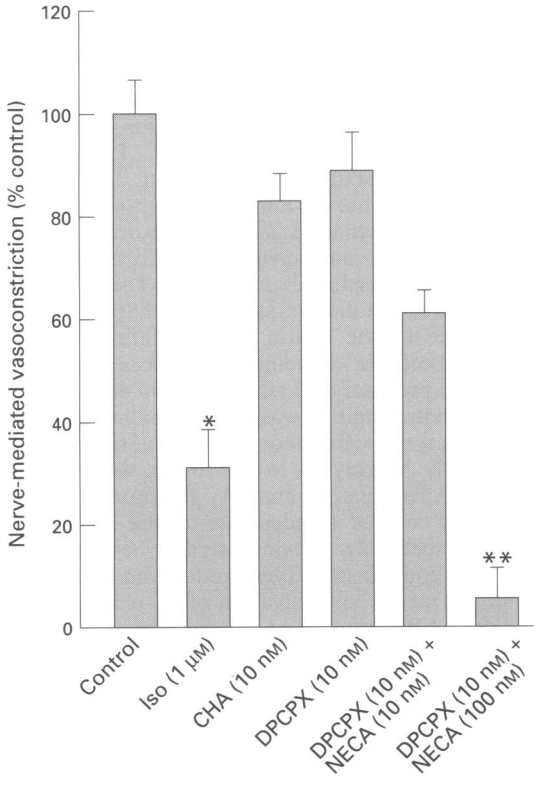

Figure 4 Effect of (left to right) isoprenaline (Iso 1 μM, $n=5$), CHA (10 nM, $n=4$), DPCPX (10 nM, $n=6$), DPCPX (10 nM) and NECA (10 nM, $n=3$), DPCPX (10 nM) and NECA (100 nM, $n=3$) on the nerve-mediated constriction of the arterioles (Control, $n=15$). Columns represent the mean ± s.e.mean of the number of preparations in parentheses. *Differs significantly from control ($P<0.05$); ** differs significantly from DPCPX alone ($P<0.05$). For abbreviations, see text.

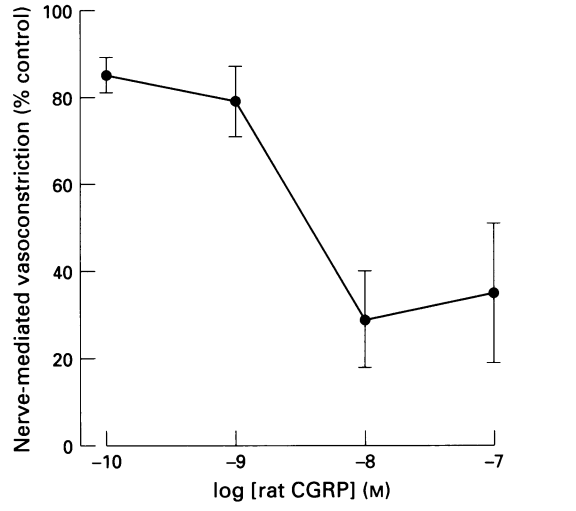

Figure 5 Concentration-response curve for the effect of rat calcitonin gene-related peptide (CGRP) on the nerve-mediated constriction of the arterioles. Points represent the means ± s.e.mean of data from 5 preparations.

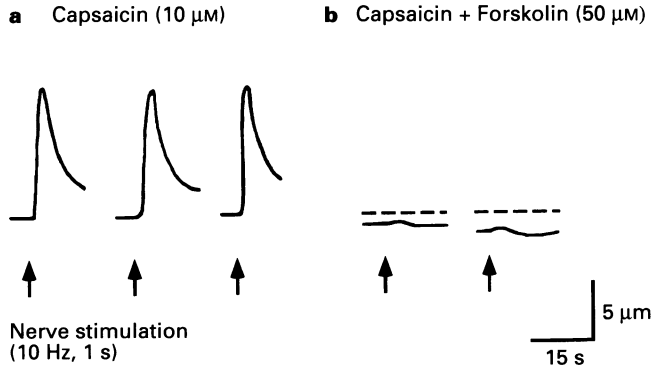

Figure 6 Effect of capsaicin treatment on the response to forskolin. (a) Shows nerve-mediated constriction of the arterioles after perfusing with capsaicin (10 μM) for 15 min; (b) shows the effect of subsequent addition of forskolin (50 μM) on the nerve-mediated constriction of the arteriole in the continued presence of capsaicin (10 μM). Traces are representative of 3 preparations. Arrows indicate nerve stimulation (10 Hz, 1 s). Dotted line indicates previous resting diameter of the arteriole in capsaicin solution.

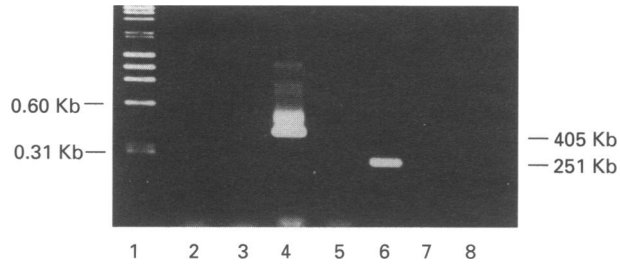

Figure 7 Reverse transcription-polymerase chain reaction (RT-PCR) analysis of total RNA from dilator muscle cells. RNA was isolated with RNAzol and treated with DNaseI, then reverse transcribed with oligo dT (lanes 2,4,6) or with oligo dT but no reverse transcriptase (lanes 3, 5, 7). PCR was carried out in the capillary tube thermal cycler using oligonucleotide primers specific for α_{1A} (lanes 2,3), α_{1B} (lanes 4,5), and α_{1C}-adrenoceptors (lanes 6,7) for 30 cycles. Control PCR reaction without RNA is shown in lane 8 and DNA size markers (ϕX174/HaeIII) in lane 1.

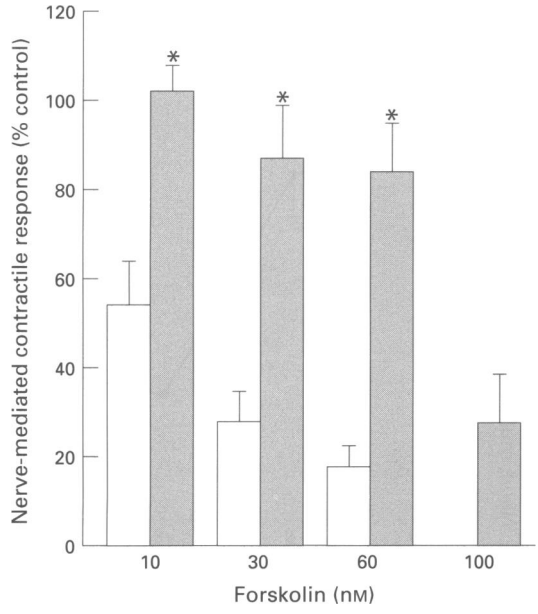

Figure 8 Effect of forskolin on nerve-mediated vasoconstriction in the presence of N^G-nitro-D-arginine methyl ester (D-NAME, 10 μM, open columns) and L-NAME (10 μM, stippled columns). Columns represent means and s.e. means of 3-4 preparations. *Differs significantly from equivalent forskolin concentration in the presence of D-NAME ($P \leq 0.05$).

cDNA from the same reverse transcription pool, no PCR fragments were detected in samples which used oligonucleotide specific primers for α_{1A}-receptors (Figure 7, lane 2).

Is the inhibition of vasoconstriction by increased cyclic AMP indirect via the production of nitric oxide?

In vessels such as the rat aorta, vascular relaxation by elevated cyclic AMP may be produced indirectly via the production of nitric oxide (Gray & Marshall, 1992a,b). Forskolin caused a concentration-dependent inhibition of nerve-mediated vasoconstriction in the presence of the inactive, D-NAME (10 μM). This inhibition was significantly reduced ($P < 0.05$) in the presence of the nitric oxide synthase inhibitor, L-NAME (10 μM, Figure 8). There was no significant difference between the size of the nerve-mediated constriction, expressed as a percentage of the resting vessel diameter, recorded in the presence of L-NAME ($28 \pm 3.1\%$, $n = 10$) or D-NAME ($25.5 \pm 2.2\%$, $n = 10$) alone.

Discussion

Previous pharmacological studies have shown that, in the rat, both the nerve-mediated constriction of the larger irideal arterioles and the nerve-mediated contraction of the dilator muscle of the iris result from the activation of α_{1B}-adrenoceptors (Hill *et al.*, 1993; Gould & Hill, 1994). In the present study, we have examined the effect of elevated cyclic AMP formation on the nerve-mediated contractions of these two tissues. Intracellular cyclic AMP production was increased by one of three different agents: (1) dibutyryl cyclic AMP, (2) forskolin, which activates adenylate cyclase to elevate cyclic AMP production or (3) IBMX, a non-selective phosphodiesterase inhibitor, to prevent the breakdown of cyclic AMP. Elevation of cyclic AMP by any of these means produced a relaxation of the dilator and of the arterioles. On the other hand, an increase in cyclic AMP abolished nerve-mediated constriction of the arterioles but potentiated the nerve-mediated contraction of the dilator. Thus cyclic AMP had opposite effects on these two nerve-mediated responses, both of which result from the activation of α_{1B}-adrenoceptors.

The physiological relevance of the above results was tested by examining the possible presence of the GTP binding protein, G_S, in the dilator and arterioles using cholera toxin which causes ADP ribosylation and permanent activation of G_S and adenylate cyclase (Cassel & Selinger, 1977; Milligan, 1988). In the present study, cholera toxin caused a vasodilatation and prevented the nerve-mediated constriction of the arterioles, but had no effect on the nerve-mediated dilator contraction. These results suggested that G_S is present in the cells of the arterioles but not in the cells of the dilator muscle. We addressed the possibility that receptors coupled to G_S are present on the arterioles, but not the dilator, by testing the effect of agonists from receptors which are known to be coupled to G_S, on nerve-mediated responses. Such receptors could be activated by transmitters released from sympathetic or sensory nerves. Responses to the activation of parasympathetic cholinergic nerves were prevented by the presence of hyoscine in the Krebs solution.

The sympathetic neurotransmitter noradrenaline may activate both α- and β-adrenoceptors. Activation of presynaptic β-adrenoceptors has been reported to have a facilitatory action on the release of noradrenaline (Medgett, 1983) and would potentiate the response to noradrenaline and not reduce it. Activation of postsynaptic β-adrenoceptors, on the other hand, would lead to an increase in cyclic AMP and an inhibition of nerve-mediated responses. The β-agonist isoprenaline relaxed the dilator, suggesting that β-adrenoceptors on the surface of the dilator can mediate relaxation. Isoprenaline reduced the nerve-mediated vasoconstriction, also suggesting the presence of β-adrenoceptors on the arterioles.

ATP is a cotransmitter with noradrenaline in the sympathetic nervous system (Burnstock, 1990a,b; Starke *et al.*, 1991). ATP is rapidly hydrolysed to adenosine, which is a potent vasodilator. Adenosine-A_1 and -A_2 receptors are negatively and positively coupled to adenylate cyclase and cyclic AMP formation, respectively. Previous studies have shown an inhibitory purinergic prejunctional modulation of noradrenaline release in the rat iris via activation of A_1-receptors (Fuder & Muth, 1993). Activation of A_1-receptors by the selective agonist, CHA, had no effect on the dilator or arteriolar constriction. The antagonist DPCPX, which is selective for A_1-receptors (Collis *et al.*, 1987; Vials & Burnstock, 1993), also had no significant effect on sympathetic vasoconstriction. These results suggest that presynaptic A_1-receptors do not play a role in regulating neurotransmitter release from sympathetic nerves innervating the dilator or the arterioles. In the presence of DPCPX, the adenosine-A_1,-A_2 agonist, NECA, abolished the sympathetic vasoconstriction but had no effect on the dilator muscle. This indicates that adenosine-A_2-receptor activation may modulate the sympathetic nerve-stimulated contraction of the arterioles but that no adenosine-A_2 response exists in the dilator.

The dilator muscle of the rat iris is supplied with nerves immunoreactive for the sensory neurotransmitters substance P and CGRP (Olson *et al.*, 1988). While both substance P and CGRP are potent vasodilators, only CGRP stimulates cyclic AMP production following activation of its receptors (Kubota *et al.*, 1985; Hirata *et al.*, 1988; Pernow, 1989; Maynard *et al.*, 1990). CGRP has also been identified as the neurotransmitter which mediates the inhibitory effect of sensory nerves on sympathetic nerve-mediated constriction in rat mesenteric arteries and rabbit ear arteries (Han *et al.*, 1990; Maynard *et al.*, 1990). Transmural nerve stimulation utilized in the present study will activate all the nerves present in the iris and so CGRP may have been released from sensory nerves. Exogenous CGRP caused vasodilatation and reduced nerve-mediated constriction of the arterioles but it neither caused relaxation of the dilator nor affected nerve-mediated contraction. These results suggest the presence of receptors for CGRP on the arterioles but not the dilator. The inhibitory effect of CGRP on nerve-mediated vasoconstriction showed a rapid desensitization compared to the longer lasting vasodilatation produced by the peptide. The different time-courses of the two effects of CGRP on the arterioles suggest that they may be produced by different mechanisms.

These experiments indicate that at least three types of receptor coupled to G_S activation are present on the arterioles and can have an inhibitory effect on nerve-mediated vasoconstriction. Only one of the three receptor types examined is present on the dilator muscle. Elevated cyclic AMP caused a relaxation of the dilator muscle, but this relaxation was not observed in the dilator after treatment with cholera toxin to activate G_S. One explanation for this apparent discrepancy may be that the concentration of cholera toxin used in this study may not have activated all the G_S present in the iris.

Increases in cyclic AMP in sensory axons or activation of presynaptic receptors leading to an increase in cyclic AMP leads to an increase in neurotransmitter release from sensory nerves (Rhoden & Barnes, 1990). For example, in the rabbit iris sphincter, activation of adenosine-A_2-receptors on the sensory nerves enhances sensory nerve transmission (Gustafsson & Wiklund, 1986). It is possible, then, that the A_2-agonists, and elevated cyclic AMP, may be acting on the sensory nerves to produce an increased release of other neuropeptides, such as substance P. This increased release of neuropeptides may be responsible for the inhibition of sympathetic vasoconstriction via a postsynaptic mechanism other than increased cyclic AMP. We tested this hypothesis by examining the effect of forskolin on nerve-mediated responses after treatment with capsaicin, to inhibit sensory nerve transmission (Holzer, 1991); forskolin still inhibited sympathetic vasoconstriction as well as producing a relaxation of the arterioles and the dilator. These results thus show that the differential effect of cyclic AMP in inhibiting arteriolar constriction but not dilator contraction is not due to an effect on sensory nerves.

The results of this study show that an increase in cyclic AMP leads to the abolition of nerve-mediated constriction of arterioles in the iris, but has no effect on the nerve-mediated contraction of the dilator in spite of apparently identical receptor subtypes mediating these two responses. The ability of the β-agonist, isoprenaline, to relax the dilator suggests that this difference is not due to the absence of receptors coupled to G_S and increases in cyclic AMP. The differential effect of cyclic AMP is also independent of sensory nerve stimulation, suggesting that the difference in responses is occurring postsynaptically. The sympathetic nerves innervating the arterioles and the dilator muscle both contain neuropeptide Y (NPY), in addition to noradrenaline (Olson *et al.*, 1988), and so the difference between the two tissues is also unlikely to result from differences in the content of co-released substances from sympathetic nerves.

One explanation for the difference in responsiveness to cyclic AMP may be that there is more than one subtype of α_1-adrenoceptor present in the iris. Unfortunately, the arterioles lie in the stroma anterior to the single dilator cell layer and separation of the two tissue types by dissection is not possible. Using RT-PCR, we have determined that both the α_{1B}- and the α_{1C}-adrenoceptor subtypes are expressed in the tissues of the iris. Recent reviews have highlighted the confusion in the nomenclature of α_1-adrenoceptors based on the results of pharmacological and molecular biological studies (Ford *et al.*, 1994). According to this latter classification, the two receptor subtypes detected in the iris correspond to the pharmacological α_{1B}- and α_{1A}-adrenoceptor subtypes respectively. It seems unlikely that the receptors in either the arterioles or the dilator could be mistakenly identified as α_{1B} instead of α_{1A} as these two subtypes differ in both their sensitivity to WB4101 and to CEC (Lomasney *et al.*, 1991a). These results then lend support to the pharmacological characterization of the subtype of synaptic receptors in both tissues as α_{1B}. The location of the α_{1A}-adrenoceptors is unknown although it is tempting to speculate that they may be located on melanophores in the irideal stroma (Hill *et al.*, 1993).

In blood vessels, such as the rat aorta and porcine palmar lateral vein, elevated cyclic AMP levels produce an increase in cyclic GMP suggesting that an interaction occurs between these two second messengers (Gray & Marshall, 1992a,b; Wright *et al.*, 1994). In the rat aorta, effects of increased cyclic AMP following activation of either β-adrenoceptors or CGRP receptors are mediated indirectly via the production of nitric oxide by the endothelium (Gray & Marshall, 1992a,b). The differences in the responses to cyclic AMP of the α_{1B}-adrenoceptors in the irideal arterioles compared to those in the dilator muscle may therefore simply be due to the release of nitric oxide from the vascular endothelial cells. In the rat irideal arterioles, the nitric oxide synthase inhibitor, L-NAME, prevented the inhibition of sympathetic nerve-mediated vasoconstriction produced by forskolin. This suggests that in the arterioles, elevation of cyclic AMP may inhibit nerve-mediated vasoconstriction indirectly via the production of nitric oxide. The activity of nitric oxide synthase have been reported to be affected by phosphorylation by a number of cellular kinases (Bredt *et al.*, 1992). A phosphorylation site for the cyclic AMP-dependent protein kinase A on nitric oxide synthase has been identified (Bredt *et al.*, 1992) and this may provide a mechanism for the above response in the arterioles.

The present results provide evidence, in living arterioles, for cross talk between α_{1B}-adrenoceptors, coupled to IP_3-dependent intracellular calcium release, and receptors coupled to increases in cyclic AMP. This interaction, however, occurs only as a result of the cyclic AMP-dependent activation of nitric oxide, presumably in the endothelial cells. In the dilator muscle, we have no evidence for an interaction between the α_{1B}-adrenoceptors and receptors coupled to increases in cyclic AMP. The potentiation of the α_{1B}-adrenoceptor response in the dilator muscle may simply reflect the change in resting tone of the preparation due to cyclic AMP. These results suggest that there is no nitric oxide synthase present in the dilator muscle cells or in the underlying epithelium.

We wish to thank Drs Ian Hendry and Michael Crouch for helpful criticism of the manuscript and Mrs Eleanor Oyston for skilful technical assistance.

References

ABDEL-LATIF, A.A. (1989). Calcium-mobilizing receptors, polyphosphoinositides, generation of second messengers and contraction in the mammalian iris smooth muscle: historical perspectives and current status. *Life Sci.*, **45**, 757–786.

ABDEL-LATIF, A.A. (1991). Biochemical and functional interactions between the inositol 1,4, 5-triphosphate-Ca^{2+} and cyclic AMP signalling systems in smooth muscle. *Cell Signal.*, **3**, 371–385.

ALONSO-LLAMAZARES, A., ZAMANILLO, D., FERNANDEZ, A., CHINCHETRU, M.A. & CALVO, P. (1993). Differential expression of the α_{1C} adrenergic receptor subtype in rat tissues. *Neuroreport*, **4,** 1266–1268.

BREDT, D.S., FERRIS, C.D. & SNYDER, S.H. (1992). Nitric oxide synthase regulatory sites. Phosphorylation by cyclic AMP-dependent protein kinase, protein kinase C, and calcium/calmodulin protein kinase: identification of flavin and calmodulin binding sites. *J. Biol. Chem.*, **267,** 10976–10981.

BULTMANN, R. & STARKE, K. (1993). Chloroethylclonidine: an irreversible agonist at prejunctional α_2-adrenoceptors in rat vas deferens. *Br. J. Pharmacol.*, **108,** 336–341.

BURNSTOCK, G. (1990a). Co-transmission. *Arch. Int. Pharmacodyn. Ther.*, **304,** 7–33.

BURNSTOCK, G. (1990b). Noradrenaline and ATP as cotransmitters in sympathetic nerves. *Neurochem. Int.*, **17,** 357–368.

CASSEL, D. & SELINGER, Z. (1977). Mechanism of adenylate cyclase activation by cholera toxin: inhibition of GTP hydrolysis at the regulatory site. *Proc. Natl. Acad. Sci. U.S.A.*, **74,** 3307–3311.

COLLIS, M.G., JACOBSON, K.A. & TOMKINS, D.M. (1987). Apparent affinity of some 8-phenyl-substituted xanthines at adenosine receptors in guinea-pig aorta and atria. *Br. J. Pharmacol.*, **92,** 69–75.

FORD, A.P.D.W., WILLIAMS, T.J., BLUE, D.R. & CLARKE, D.E. (1994). α_1-Adrenoceptor classification: sharpening Occam's razor. *Trends Pharmacol. Sci.*, **15,** 167–170.

FUDER, H. & MUTH, U. (1993). ATP and endogenous agonists inhibit evoked [3H]-noradrenaline release in rat iris via A_1 and P_{2y}-like purinoceptors. *Naunyn Schmied Arch. Pharmacol.*, **348,** 352–357.

GOULD, D.J. & HILL, C.E. (1994). Alpha$_{1B}$ receptors and intracellular calcium mediate sympathetic nerve induced constriction of rat irideal blood vessels. *J. Auton. Nerv. Syst.*, **50,** 139–150.

GRAY, D.W. & MARSHALL, I. (1992a). Novel signal transduction pathway mediating endothelial-dependent β-adrenoceptor vasorelaxation in rat thoracic aorta. *Br. J. Pharmacol.*, **107,** 684–690.

GRAY, D.W. & MARSHALL, I. (1992b). Human α-calcitonin gene-related peptide stimulates adenylate cyclase and guanylate cyclase and relaxes rat thoracic aorta by releasing nitric oxide. *Br. J. Pharmacol.*, **107,** 691–696.

GUSTAFSSON, L.E. & WIKLUND, N.P. (1986). Adenosine-modulation of cholinergic and non-adrenergic non-cholinergic neurotransmission in the rabbit iris sphincter. *Br. J. Pharmacol.*, **88,** 197–204.

HANS, C., ABEL, P.W. & MINNEMAN, K.P. (1987). Alpha 1-adrenoceptor subtypes linked to different mechanisms for increasing intracellular Ca^{2+} in smooth muscle. *Nature*, **329,** 333–335.

HANS, S.-P., NAES, L. & WESTFALL, T.C. (1990). Calcitonin gene-related peptide is the endogenous mediator of nonadrenergic-noncholinergic vasodilation in rat mesentery. *J. Pharmacol. Exp. Ther.*, **255,** 425–428.

HILL, C.E., KLEMM, M., EDWARDS, F.R. & HIRST, G.D.S. (1993). Sympathetic transmission to the dilator muscle of the rat iris. *J. Auton. Nerv. Syst.*, **45,** 107–123.

HIRATA, Y., TAKAGI, Y., TAKATA, S., FUKUDA, Y., YOSHIMI, H. & FUJITA, T. (1988). Calcitonin gene-related peptide receptor in cultured vascular smooth muscle and endothelial cells. *Biochem. Biophys. Res. Commun.*, **151,** 1113–1121.

HOLZER, P. (1991). Capsaicin: cellular targets, mechanisms of action and selectivity for thin sensory neurones. *Pharmacol. Rev.*, **43,** 143–201.

KUBOTA, M., MOSELEY, J.M., BUTERA, L., DUSTING, G.J., MACDONALD, P.S. & MARTIN, T.J. (1985). Calcitonin gene-related peptide stimulates cyclic AMP formation in rat aortic smooth muscle cells. *Biochem. Biophys. Res. Commun.*, **132,** 88–94.

LINCOLN, T.M. & FISHER-SIMPSON, V. (1984). A comparison of the effects of forskolin and nitroprusside on cyclic nucleotides and relaxation in the rat aorta. *Eur. J. Pharmacol.*, **101,** 17–27.

LOMASNEY, J.W., COTECCHIA, S., LEFKOWITZ, R.J. & CARON, M.G. (1991a). Molecular biology of α-adrenergic receptors: Implications for receptor classification and for structure-function relationships. *Biochim. Biophys. Acta Mol. Cell Res.*, **1095,** 127–139.

LOMASNEY, J.W., COTECCHIA, S., LORENZ, W., LEUNG, W.-Y., SCHWINN, D.A., YANG-FENG, T.L., BROWNSTEIN, M., LEFKOWITZ, R.J. & CARON, M.G. (1991b). Molecular cloning and expression of the cDNA for the α_{1A}-adrenergic receptor, the gene for which is located on human chromosome 5. *J. Biol. Chem.*, **266,** 6365–6369.

MANOLOPOULOS, V.G., PIPILI-SYNETOS, E., DEN-HERTOG, A. & NELEMANS, A. (1991). Inositol phosphates formed in rat aorta after alpha 1-adrenoceptor stimulation are inhibited by forskolin. *Eur. J. Pharmacol.*, **207,** 29–36.

MAYNARD, K.I., SAVILLE, V.L. & BURNSTOCK, G. (1990). Sensory-motor neuromodulation of sympathetic vasoconstriction in the rabbit central ear artery. *Eur. J. Pharmacol.*, **187,** 171–182.

MEDGETT, I.C. (1983). Modulation of transmission in rat sympathetic ganglia by activation of presynaptic alpha- and beta-adrenoceptors. *Br. J. Pharmacol.*, **78,** 17–27.

MILLIGAN, G. (1988). Techniques used in the identification and analysis of function of pertussis toxin-sensitive guanine nucleotide binding proteins. *Biochem. J.*, **255,** 1–13.

MURTHY, K.S., SEVERI, C., GRIDER, J.R. & MAKHLOUF, G.M. (1993). Inhibition of IP_3 and IP_3-dependent Ca^{2+} mobilization by cyclic nucleotides in isolated gastric muscle cells. *Am. J. Physiol. Gastrointest. Liver Physiol.*, **264,** G967–G974.

NEILD, T.O. (1989). Measurement of arteriole diameter changes by analysis of television images. *Blood Vessels*, **26,** 48–52.

OLSON, L., AYER-LELIÉVRE, C., BJORKLUND, H., EBENDAL, T., GRANHOLM, A.C., HEDLUND, K.O., HOKFELT, T., MELANDER, T., SEIGER, A. & STROMBERG, I. (1988). The innervation apparatus of the rodent iris. In *The Peripheral Nervous System*, Vol.6, *Handbook of Neuroanatomy*. ed. Björklund, A., Hökfelt, T. & Owman, C. pp. 545–597. Amsterdam: Elsevier Science Publishers B.V..

PERNOW, J. (1989). Actions of constrictor (NPY and endothelin) and dilator (substance P, CGRP and VIP) peptides on pig splenic and human skeletal muscle arteries: involvement of the endothelium. *Br. J. Pharmacol.*, **97,** 983–989.

RHODEN, K.J. & BARNES, P.J. (1990). Potentiation of nonadrenergic neural relaxation in guinea pig airways by a cyclic AMP phosphodiesterase inhibitor. *J. Pharmacol. Exp. Ther.*, **252,** 396–402.

STARKE, K., GOTHERT, M. & KILBINGER, H. (1989). Modulation of neurotransmitter release by presynaptic autoreceptors. *Physiol. Rev.*, **69,** 864–989.

STARKE, K., VON-KUGELGEN, I., BULLOCH, J.M. & ILLES, P. (1991). Nucleotides as cotransmitters in vascular sympathetic neuroeffector transmission. *Blood Vessels*, **28,** 19–26.

TACHADO, S.D., AKHTAR, R.A. & ABDEL-LATIF, A.A. (1989). Activation of beta-adrenergic receptors causes stimulation of cyclic AMP, inhibition of inositol trisphosphate, and relaxation of bovine iris sphincter smooth muscle. Biochemical and functional interactions between the cyclic AMP and calcium signalling systems. *Invest. Ophthalmol. Vis. Sci.*, **30,** 2232–2239.

TACHADO, S.D., AKHTAR, R.A., ZHOU, C.J. & ABDEL-LATIF, A.A. (1992). Effects of isoproterenol and forskolin on carbachol- and fluoroaluminate-induced polyphosphoinositide hydrolysis, inositol trisphosphate production, and contraction in bovine iris sphincter smooth muscle: interaction between cAMP and IP_3 second messenger systems. *Cell Signal.*, **4,** 61–75.

TAKAYANAGI, I., SHIRAISHI, K. & KOKUBU, N. (1992). Alpha $_{1B}$-adrenoceptor mechanisms in rabbit iris dilator. *Jpn. J. Pharmacol.*, **59,** 301–305.

VIALS, A. & BURNSTOCK, G. (1993). A_2-purinoceptor-mediated relaxation in the guinea-pig coronary vasculature: a role for nitric oxide. *Br. J. Pharmacol.*, **109,** 424–429.

VOIGT, M.M., KISPERT, J. & CHIN, H. (1990). Sequence of a rat brain cDNA encoding an alpha-$_{1B}$ adrenergic receptor. *Nucleic Acids Res.*, **18,** 1053.

VON-KUGELGEN, I., SPATH, L. & STARKE, K. (1992). Stable adenine nucleotides inhibit [3H]-noradrenaline release in rabbit brain cortex slices by direct action at presynaptic adenosine A_1-receptors. *Naunyn Schmied. Arch. Pharmacol.*, **346,** 187–196.

WRIGHT, I.K., AMIRCHETTY-RAO, S. & KENDALL, D.A. (1994). Potentiation by forskolin of both SNP- and ANP-stimulated cyclic GMP accumulation in porcine isolated palmar lateral vein. *Br. J. Pharmacol.*, **112,** 1146–1150.

(Received December 20, 1994
Revised February 21, 1995
Accepted February 24, 1995)

British Journal of Pharmacology (1995) 115, 835-839

Hypotensive effect of 13-hydroxylinoleic acid in the rat: mediation via the release of a CGRP-like mediator from capsaicin-sensitive nerves

[1]Dicky van Heuven-Nolsen, Thea Muis, Ferdi Engels, Paul A.J. Henricks, Theresa L. Buckley & Frans P. Nijkamp

Department of Pharmacology, Utrecht Institute for Pharmaceutical Sciences, Utrecht University, P.O. Box 80.082, 3508 TB Utrecht, The Netherlands

1 The effect of 13-hydroxylinoleic acid (13-HODE) on changes in blood pressure in the rat was measured.

2 13-HODE (0.1 – 100 $\mu g\ kg^{-1}$) had no direct effect on blood pressure in the rat and had no effect on histamine (0.1 – 1000 $\mu g\ kg^{-1}$)-induced changes in blood pressure. In contrast, it was found that 13-HODE itself induced a decrease in diastolic arterial blood pressure when it was injected intravenously after either a single dose of histamine (10, 100 or 1000 $\mu g\ kg^{-1}$) or after a dose-response curve of histamine (0.1 – 1000 $\mu g\ kg^{-1}$).

3 This hypotensive effect of 13-HODE was not observed after administration of the endothelium-dependent vasodilator, acetylcholine (0.1 – 10 $\mu g\ kg^{-1}$), the endothelium-independent vasodilator, sodium nitroprusside (0.1 – 100 $\mu g\ kg^{-1}$) or the inflammatory mediator, leukotriene B_4 (0.1 – 300 $\mu g\ kg^{-1}$). However, prior injection of bradykinin (0.1 – 100 $\mu g\ kg^{-1}$) allowed a dose-dependent hypotensive effect of 13-HODE to be revealed.

4 The hypotensive effect of 13-HODE after histamine and bradykinin could be inhibited by neonatal capsaicin treatment of the rats (50 mg kg^{-1}, s.c. on day 1 and 2 after birth).

5 Ruthenium red (120 $\mu g\ kg^{-1}\ min^{-1}$), an inhibitor of excitatory effects on sensory nerves, and the CGRP antagonist, $CGRP_{8-37}$ (1 – 3 $\mu g\ kg^{-1}\ min^{-1}$) also inhibited the hypotensive effect of 13-HODE.

6 It is concluded that the hypotensive effect of 13-HODE in the rat after histamine and bradykinin is due to the release of a CGRP-like substance from sensory nerves. These results highlight the possibility that endogenous 13-HODE could be involved in the neurogenic regulation of blood pressure.

Keywords: Hypotension in rat; 13-hydroxylinoleic acid (13-HODE); blood pressure; sensory nerve; capsaicin; ruthenium red; calcitonin gene-related peptide (CGRP)

Introduction

Most of the research on the biological activities of fatty acids has been directed towards arachidonic acid and its metabolites. However, our study focused on another major fatty acid, linoleic acid, which can be converted (non)-enzymatically into 13-hydroperoxyoctadecadienoc acid (13-HPODE). This labile intermediate is further reduced to its 13-hydroxy derivative, 13-hydroxylinoleic acid (13-HODE). 13-HODE is present in and can be produced by several cell types including endothelial cells (Buchanan *et al.*, 1985), neutrophils (Sobermann *et al.*, 1985), epithelial cells (Oosthuizen *et al.*, 1990) and macrophages (Engels *et al.*, 1986). However, the biological activity of 13-HODE has been mainly investigated *in vitro*. 13-HODE has been proposed as an important mediator by which endothelial cells regulate the non-adhesiveness for platelets, leukocytes and cancer cells (Buchanan *et al.*, 1985). In contrast, 13-HODE was found to be chemotactic for human and bovine polymorphonuclear leukocytes (Henricks *et al.*, 1991b). 13-H(P)ODE has also been reported to contract canine isolated basilar artery (Koide *et al.*, 1981), to relax canine isolated circumflex and splenic artery due to stimulation of prostacyclin biosynthesis (De Meyer *et al.*, 1992) and to increase histamine contractions in porcine isolated coronary artery (Van Heuven *et al.*, 1990). The known *in vivo* effects of 13-HODE are limited. 13-HODE induced bronchial hyperreactivity to histamine *in vivo* (Henricks *et al.*, 1991a) and was found to inhibit oedema formation induced by leukotriene B_4 in the presence of calcitonin gene-related peptide (CGRP) in rabbit skin (Buckley *et al.*, 1992). In this study we investigated the effect of 13-HODE on blood pressure in the rat. Preliminary studies revealed that 13-HODE had no direct effect on blood pressure, neither had it any influence on the histamine-induced decrease in blood pressure. However, we noticed that intravenous bolus injection of 13-HODE after completion of a dose-response curve to histamine, caused a decrease in blood pressure. The mechanism of this hypotensive effect of 13-HODE was further investigated. Evidence is presented that this hypotensive effect of 13-HODE is caused by the release of a CGRP-like substance from sensory nerves.

[1] Author for correspondence.

Methods

Male rats (Wistar U, Central Laboratory Animal Institute, Utrecht, The Netherlands), 300 – 400 g were used. Rats were anaesthetized with urethane (1.5 g kg^{-1}) intraperitoneally. Arterial blood pressure was recorded with a pressure transducer (Elcomatic Ltd., Glasgow, U.K.) via a cannula inserted into the left carotid artery. Drugs were injected into the jugular vein and/or femoral vein cannulated for this purpose. During the experiment the body temperature was kept at about 37°C.

Experimental protocol

After a stabilization period of 30 min, bolus injections of histamine at doses ranging from 0.1 to 1000 $\mu g\ kg^{-1}$ were given at intervals of 10 – 15 min. After completion of the dose-response

curve for histamine, bolus injections of saline were given to flush the cannula of residual histamine. Subsequently, a bolus injection of 13-HODE (10 $\mu g\ kg^{-1}$) was given and the dose response curve to histamine was repeated. In additional experiments the effect of 10 $\mu g\ kg^{-1}$ 13-HODE was tested after single doses of histamine (10, 100 or 1000 $\mu g\ kg^{-1}$). Each dose of histamine was tested in a separate animal. Also the effect of different doses of 13-HODE (1, 3 and 10 $\mu g\ kg^{-1}$) was investigated.

In the next series of experiments the effects of other agonist drugs on blood pressure were measured. After completion of the dose-response curves and careful rinsing of the catheters with saline, a bolus injection of 13-HODE was given.

In order to investigate the possible contribution of sensory nerves in the effect of 13-HODE, ruthenium red (120 $\mu g\ kg^{-1}\ min^{-1}$) or $CGRP_{8-37}$ (1 or 3 $\mu g\ kg^{-1}\ min^{-1}$) were infused starting 4 min before 13-HODE administration.

Neonatal capsaicin treatment

In some experiments rats were treated with capsaicin (50 mg kg^{-1}) subcutaneously on day 1 and 2 after birth to produce degeneration of the sensory nerves (Jancso *et al.*, 1977). Rats were given flunixine (1 mg kg^{-1}) i.p. 30 min before capsaicin-treatment as premedication. Capsaicin was dissolved in ethanol and diluted with Tween 80 in saline (final concentration: 10% ethanol and 10% Tween 80); control animals received a similar amount of the solvent used. In preliminary experiments, the depletion of the peripheral sensory nerves was assessed by measuring capsaicin-induced relaxation in the isolated, carbachol-precontracted trachea.

Data presentation and statistical evaluation

All data are presented as mean ± s.e.mean. The statistical differences between the variables were evaluated by Analysis of Variance followed by Student-Newman-Keuls test. A P value of less than 0.05 was considered to indicate a significant difference.

Drugs

The drugs used in this study were obtained from the following sources: acetylcholine, bradykinin, methacholine, sodium nitroprusside (Sigma, St Louis, U.S.A.), human $CGRP_{8-37}$ and human α-CGRP (Bachem Feinchemikalien Ag., Bubendorff, Switzerland), histamine diphosphate (OPG, Utrecht, The Netherlands), leukotriene B_4 (Dr A.W. Ford-Hutchinson, Merck Frosst Canada Inc., Quebec, Canada), ruthenium red (Fuchi Chemical, Switzerland), capsaicin and Tween 80 (Fluka Chemie AG, Buchs, Switzerland). Stock solutions of leukotriene B_4 were made in methanol and stored at −80°C before use. All drugs were dissolved and/or diluted in saline immediately before use.

Figure 1 Representative tracing of the blood pressure in the anaesthetized rat showing the effect of 13-hydroxylinoleic acid (13-HODE), (10 $\mu g\ kg^{-1}$) after histamine (1 $mg\ kg^{-1}$). After the histamine, 0.1 ml saline injections were given to flush the cannula of residual histamine.

Results

Intravenous injection of histamine (0.1 – 1000 $\mu g\ kg^{-1}$) caused a dose-dependent decrease in diastolic arterial blood pressure. After completion of the first dose-response curve, a bolus injection of 13-HODE (10 $\mu g\ kg^{-1}$) was given and a second dose-response curve to histamine was established in order to investigate the possible influence of 13-HODE on histamine effects on blood pressure. The second dose-response curve to histamine showed a similar fall in blood pressure as the first curve obtained before 13-HODE was given (data not shown). 13-HODE, but not saline, induced a decrease in diastolic arterial blood pressure (20.5 ± 3.6 mmHg) when it was injected after histamine. Figure 1 shows a representative tracing in which the effect of 13-HODE after histamine is illustrated. When 13-HODE was injected into naive animals, no significant change in arterial blood pressure was observed. Though the original observation with 13-HODE was found after a dose-response curve with histamine was completed, the hypotensive effect of 13-HODE (10 $\mu g\ kg^{-1}$) was also investigated after a single dose of histamine (10, 100 and 1000 $\mu g\ kg^{-1}$). Each dose of histamine was tested on a separate animal. Histamine caused a dose-dependent decrease in DAP (Table 1) and the effect of 13-HODE given after histamine was proportional to the effect of histamine.

Histamine has known vasodilator activity, therefore, experiments were designed to investigate whether the hypotensive effect of 13-HODE after exposure to histamine was related to this action. The endothelium-dependent vasodilator acetylcholine (0.1 – 10 $\mu g\ kg^{-1}$) caused a dose-dependent decrease in diastolic arterial blood pressure. The endothelium-independent vasodilator, sodium nitroprusside (0.1 – 100 $\mu g\ kg^{-1}$) caused a dose-dependent decrease in diastolic arterial blood pressure. Acetylcholine and nitroprusside lowered the blood pressure to a level similar to that induced by histamine. When 13-HODE was injected in animals that had received acetylcholine or nitroprusside, no significant effect on blood pressure was found (Table 2).

In further experiments the possibility that the inflammatory activity of histamine could be important for the hypotensive effect of 13-HODE was investigated. Leukotriene B_4, a neutrophil-dependent mediator of increased microvascular permeability (0.1 – 300 $\mu g\ kg^{-1}$), had no effect on blood pressure and also failed to induce any response of 13-HODE on blood pressure (Table 2). However, bradykinin, a plasma-derived inflammatory mediator (0.1 – 100 $\mu g\ kg^{-1}$), induced a dose-

Table 1 Decrease in diastolic arterial blood pressure (DAP) caused by i.v. bolus injection of histamine and 13-hydroxylinoleic acid (13-HODE)

Histamine ($\mu g\ kg^{-1}$)		*Decrease in DAP* (mmHg) *after histamine*	*Subsequent decrease in DAP* (mmHg) *after 13-HODE* (10 $\mu g\ kg^{-1}$)
10	(4)	14.0 ± 4.2	5.0 ± 0.7
100	(4)	24.5 ± 5.0	8.5 ± 2.6
1000	(4)	30.0 ± 6.6	12.5 ± 1.7

Each dose of histamine was tested on a separate animal. The single dose of histamine was followed by an i.v. bolus-injection of 13-HODE (10 $\mu g\ kg^{-1}$) and the decrease in DAP was measured. Number of observations in parentheses.

Table 2 Effect of i.v. bolus injection of 13-hydroxylinoleic acid (13-HODE) 10 $\mu g\ kg^{-1}$ on diastolic arterial blood pressure (DAP) after pretreatment with several agents

Pretreatment (doses in $\mu g\ kg^{-1}$)		*Decrease in DAP* (mmHg) *after 13-HODE* (10 $\mu g\ kg^{-1}$)
Saline	(4)	4.8 ± 1.1
Histamine (0.1 – 1000 $\mu g\ kg^{-1}$)	(11)	17.9 ± 3.5*
Acetylcholine (0.1 – 10 $\mu g\ kg^{-1}$)	(4)	5.0 ± 0.8
Sodium nitroprusside (0.1 – 100 $\mu g\ kg^{-1}$)	(7)	5.8 ± 1.0
LTB_4 (0.1 – 300 $\mu g\ kg^{-1}$)	(5)	7.4 ± 1.0
Bradykinin (0.1 – 100 $\mu g\ kg^{-1}$)	(4)	16.4 ± 1.5*

Significantly different from saline, $*P < 0.05$ Student-Newman-Keuls test. Number of observations in parentheses.

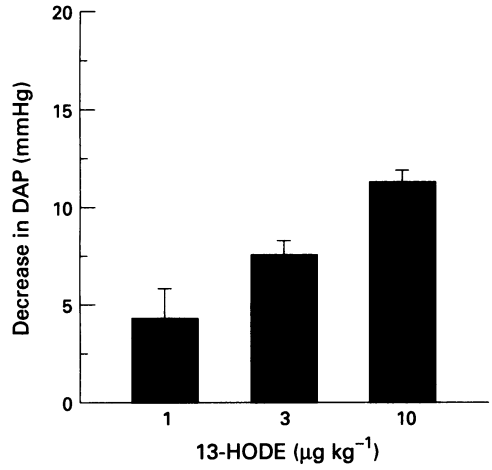

Figure 2 Effect of intravenous injection of different doses (1, 3 and 10 $\mu g\ kg^{-1}$) of 13-hydroxylinoleic acid (13-HODE) on diastolic arterial pressure (DAP) after bradykinin (100 $\mu g\ kg^{-1}$) in anaesthetized rats. Results are expressed as mean ± s.e.mean, $n = 4$. Each dose of 13-HODE was tested on a separate animal.

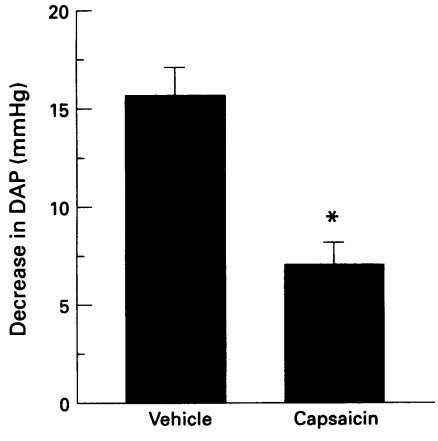

Figure 3 Effect of 10 $\mu g\ kg^{-1}$ 13-hydroxylinoleic acid (13-HODE) on diastolic arterial blood pressure (DAP) after histamine in neonatal vehicle-treated ($n = 7$) and capsaicin-treated rats ($n = 6$). Data represent the changes from baseline values taken immediately before injection of 13-HODE. Results are expressed as mean ± s.e.mean. Significantly different from 13-HODE response in vehicle-treated rats, $*P < 0.05$ Student-Newman-Keuls-test.

dependent decrease in diastolic arterial blood pressure and allowed the hypotensive effect of 13-HODE to be revealed (Table 2). The hypotensive effect of different doses of 13-HODE after a bolus injection of bradykinin (100 $\mu g\ kg^{-1}$) was tested. Figure 2 demonstrates that 13-HODE caused a dose-dependent decrease in DAP.

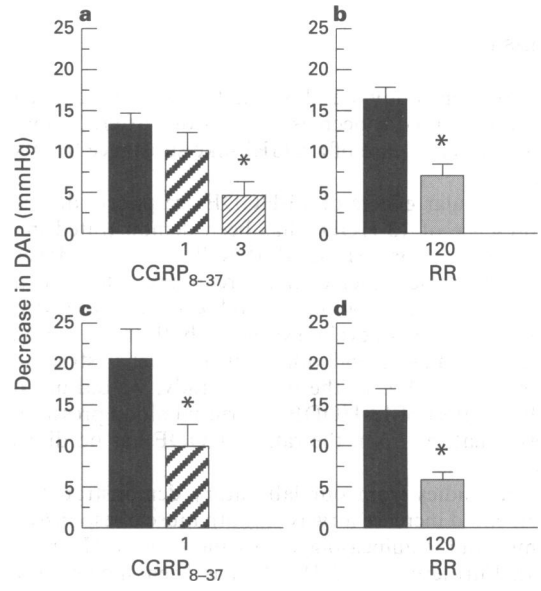

Figure 4 Effect of i.v. infusion of $CGRP_{8-37}$ (1 and 3 $\mu g\ kg^{-1}\ min^{-1}$) and ruthenium red (RR) (120 $\mu g\ kg^{-1}\ min^{-1}$) on diastolic arterial blood pressure (DAP) induced by 10 $\mu g\ kg^{-1}$ 13-hydroxylinoleic acid (13-HODE) after bradykinin (a,b) and histamine (c,d). Data represent the changes from baseline values taken immediately before injection of 13-HODE. The response of 13-HODE after histamine and bradykinin is represented by solid column, 1 $\mu g\ kg^{-1}\ min^{-1}$ $CGRP_{8-37}$ hatched columns, 3 $\mu g\ kg^{-1}\ min^{-1}$ $CGRP_{8-37}$ thinly hatched column, ruthenium red 120 $\mu g\ kg^{-1}\ min^{-1}$ stippled columns. Data are presented as means ± s.e.mean. Significantly different from 13-HODE response in untreated rats, $*P < 0.05$ Student-Newman-Keuls-test.

Bradykinin and histamine are known to influence sensory nerve activity, resulting in the release of neuropeptides. Neonatal capsaicin-treatment of rats caused a depletion of the sensory nerves as was revealed in the preliminary experiments by the lack of capsaicin-induced relaxation of the isolated trachea. The percentage relaxation to capsaicin (10^{-7} M) in isolated carbachol-precontracted tracheal rings was approximately 45% for vehicle-controls and 4% in the neonatal-capsaicin-treated group. Neonatal capsaicin- and vehicle-treatment of rats had no influence on mean arterial blood pressure as compared to naive control rats, nor did it influence the hypotensive effect of histamine. Interestingly, sensory neuropeptide depletion inhibited the hypotensive effect of 13-HODE after the exposure to histamine (Figure 3). In further experiments, ruthenium red (120 $\mu g\ kg^{-1}\ min^{-1}$, i.v.), an inhibitor of the excitatory effects of capsaicin on sensory nerves, was also shown to inhibit the hypotensive effect of 13-HODE (Figure 4). It must be stated that ruthenium red was infused after the administration of histamine and bradykinin but before the injection of 13-HODE and had no influence on blood

pressure. Finally, the possible involvement of the neuropeptide vasodilator, CGRP was investigated. $CGRP_{8-37}$, which has been shown to be effective and selective in inhibiting the hypotensive effects of CGRP in several studies (Gardiner *et al.*, 1990; Hughes & Brain, 1991; Escott & Brain, 1993), was infused at a dose of 3 $\mu g\ kg^{-1}\ min^{-1}$. This dose had no direct influence on blood pressure (mean arterial pressure before and at the infusion of the CGRP-antagonist $CGRP_{8-37}$-treated rats was 106 ± 4.1 and 107 ± 5.1 mmHg ($n=5$), respectively). The vasodilator CGRP (1 $\mu g\ kg^{-1}$) caused a marked decrease in DAP in saline-infused animals (32 ± 2.8 mmHg; $n=4$) but this response was abolished in $CGRP_{8-37}$-treated rats (2 ± 1.1 mmHg; $n=4$). Interestingly, $CGRP_{8-37}$ infusion significantly inhibited the hypotensive effect of 13-HODE after histamine and bradykinin administration (Figure 4).

Discussion

In the present study we show that 13-HODE under certain conditions, caused a decrease in diastolic arterial blood pressure due to the release of a CGRP-like substance from sensory nerves.

The vascular effects of 13-HODE are poorly documented. The presence of 13-HODE has been demonstrated in rabbit, rat and bovine aorta (Funk & Powell, 1985; De Meyer *et al.*, 1991). In canine, splenic and circumflex artery, 13-HODE evoked relaxations *in vitro*. This relaxant response was due to stimulation of prostacyclin synthesis, both in the endothelium and smooth muscle and other subendothelial structures (De Meyer *et al.*, 1992). In the present study, we did not observe any direct effect of 13-HODE on arterial blood pressure, which suggests that *in vivo* in the rat, 13-HODE has no direct vasodilator action.

Other studies from our laboratory demonstrated that 13-HODE could increase airway smooth muscle responsiveness to histamine in the guinea-pig *in vivo* and *in vitro* (Henricks *et al.*, 1991a). Furthermore, 13-HODE has been shown to increase histamine contractions in porcine endothelium-denuded coronary arteries (Van Heuven *et al.*, 1990). In the present study, however, we did not observe any effect of 13-HODE on the histamine-induced responses on diastolic arterial blood pressure or heart rate. These contradictory results could be due to species differences. Interestingly, 13-HODE exhibited a depressor activity after histamine in the rat. There are several possibilities to explain this unexpected finding.

Firstly, histamine causes vasodilatation. However, since the vasodilator response to acetylcholine and sodium nitroprusside was not followed by any activity of 13-HODE, the vasodilator action of histamine does not seem to be important for the 13-HODE hypotensive effect. Secondly, there is the possibility that the inflammatory actions of histamine preclude the 13-HODE effect. This explanation is unlikely because intravenous injection of LTB_4, a neutrophil-dependent mediator of increased microvascular permeability failed to induce an effect of 13-HODE. This implies that oedema formation in itself is not important for the effect of 13-HODE. However, bradykinin, a plasma-derived inflammatory mediator, permitted a vasodilator response to 13-HODE to be observed. Histamine and bradykinin are able to activate sensory nerves. Interestingly, bradykinin is an endogenous mediator that is known to stimulate sensory nerves directly (Fox *et al.*, 1993). One attractive hypothesis to explain the findings presented in this study is that the hypotensive effect of 13-HODE can be revealed only after activation of sensory nerves. This hypothesis is strengthened by the observation that the vasodilator effect of 13-HODE is absent in capsaicin-depleted rats. Moreover, ruthenium red markedly suppressed the hypotensive effect induced by 13-HODE after prior exposure to histamine and bradykinin. Ruthenium red has been reported to be an inhibitor of transmembrane calcium fluxes. This action attenuates the excitatory functions of capsaicin on sensory nerves in many species (Maggi *et al.*, 1988; Buckley *et al.*, 1990). As a consequence of the inhibitory actions of ruthenium red, the release of CGRP-like substance by capsaicin from a guinea-pig heart preparation was inhibited (Franco-Cereceda *et al.*, 1991). In our study ruthenium red was infused after the administration of histamine and bradykinin. Therefore, our results suggest that ruthenium red interferes with the ability of 13-HODE to interact with 'activated' sensory nerves.

Sensory nerves when activated, release vasoactive neuropeptides including substance P and CGRP (for review see Holzer, 1988). It has been shown that CGRP is a potent vasodilator with a long duration of action (Brain *et al.*, 1985; Buckley *et al.*, 1991) and that the vasodilator action of CGRP in the microcirculation can be inhibited by the CGRP antagonist, $CGRP_{8-37}$ (Gardiner *et al.*, 1990; Hughes & Brain, 1991; Escott & Brain, 1993). The inhibition of the hypotensive effect of 13-HODE with the CGRP antagonist $CGRP_{8-37}$ suggest that the vasodilator action of 13-HODE is at least partly mediated by a CGRP-like substance.

In summary, we have demonstrated that after bradykinin and histamine administration 13-HODE can cause a hypotensive effect. This effect is abolished in capsaicin-treated rats and is markedly inhibited by ruthenium red and $CGRP_{8-37}$. These results demonstrate that the hypotensive effect of 13-HODE in the rat is due to the release of a CGRP-like substance. Moreover this is the first report that the linoleic acid metabolite, 13-HODE can interact with sensory nerves. These results highlight the possibility that endogenous 13-HODE could be involved in the neurogenic regulation of blood pressure.

The authors wish to thank Marco van de Velde for preparing 13-HODE.

References

BRAIN, S.D., WILLIAMS, T.J., TIPPINS, J.R., MORRIS, H.R. & MACINTYRE, I. (1985). Calcitonin gene-related peptide is a potent vasodilator. *Nature*, **313**, 54–56.

BUCHANAN, M.R., BUTT, R.W., MAGAS, Z., VAN RIJN, J., HIRCH, J. & NAZIR, D.J. (1985). Endothelial cells produce a lipoxygenase-derived chemorepellant which influences platelet/endothelial cell interactions: effect of aspirin and salicylate. *Throm. Haemostas.*, **53**, 306–311.

BUCKLEY, T.L., BRAIN, S.D., RAMPART, M. & WILLIAMS, T.J. (1991). Time-dependent synergistic interactions between the vasodilator neuropeptide, calcitonin gene-related peptide (CGRP) and mediators of inflammation. *Br. J. Pharmacol.*, **103**, 1515–1519.

BUCKLEY, T.L., BRAIN, S.D. & WILLIAMS, T.J. (1990). Ruthenium red selectively inhibits oedema formation and increased blood flow induced by capsaicin in rabbit skin. *Br. J. Pharmacol.*, **99**, 7–8.

BUCKLEY, T.L., VAN DER VELDE, M.J., HENRICKS, P.A.J., ENGELS, F. & NIJKAMP, F.P. (1992). 13-Hydroxyoctadecadienoic acid attenuates oedema formation induced by leukotriene B_4 *in vivo* in rabbit skin. *Eur. J. Pharmacol.*, **218**, 369–372.

DE MEYER, G.R.Y., BULT, H. & HERMAN, A.G. (1991). Early atherosclerosis is accompanied by a decreased rather than an increased accumulation of fatty acid hydroxyderivatives. *Biochem. Pharmacol.*, **42**, 279–283.

DE MEYER, G.R.Y., BULT, H., VERBEUREN, T.J. & HERMAN, A.G. (1992). The role of endothelial cells in the relaxations induced by 13-hydroxy and 13-hydroperoxylinoleic acid in canine arteries. *Br. J. Pharmacol.*, **107**, 597–603

ENGELS, F., WILLEMS, H. & NIJKAMP, F.P. (1986). Cyclooxygenase-catalyzed formation of 9-hydroxylinoleic acid by guinea-pig alveolar macrophages under non-stimulated conditions. *FEBS Lett.*, **209**, 249–253.

ESCOTT, K.J. & BRAIN, S.D. (1993). Effect of calcitonin gene-related peptide antagonist ($CGRP_{8-37}$) on skin vasodilatation and oedema induced by stimulation of the rat saphenous nerve. *Br. J. Pharmacol.*, **110**, 772–776.

FOX, A.J., BARNES, P.J., URBAN, L. & DRAY, A. (1993). An *in vitro* study of the properties of single vagal afferents innervating guinea-pig airways. *J. Physiol.*, **469**, 21–35.

FRANCO-CERECEDA, A., LOU, Y.P. & LUNDBERG, J.M. (1991). Ruthenium red inhibits CGRP release by capsaicin and resiniferatoxin but not ouabain, bradykinin or nicotine in guinea pig heart: correlation with effects on cardiac contractility. *Br. J. Pharmacol.*, **104**, 305–310.

FUNK, C.D. & POWELL, W.S. (1985). Release of prostaglandins and monohydroxy and trihydroxy metabolites of linoleic and arachidonic acids by adult and fetal aortae and ductus arteriosus. *J. Biol. Chem.*, **260**, 7481–7488.

GARDINER, S.M., COMPTON, A.M., KEMP, P.A., BOSE, C., FOULKES, R. & HUGHES, B. (1990). Antagonistic effect of human α-CGRP [8-37] on the *in vivo* reginal haemodynamic actions of human α-CGRP. *Biochem. Biophys. Res. Commun.*, **171**, 938–943.

HENRICKS, P.A.J., ENGELS, F., VAN DER LINDE, H.J. & NIJKAMP, F.P. (1991a). 13-Hydroxy-linoleic acid induces airway hyperreactivity to histamine in guinea-pigs. *Eur. J. Pharmacol.*, **197**, 233–234.

HENRICKS, P.A.J., ENGELS, F., VAN DER VLIET, H. & NIJKAMP, F.P. (1991b). 9-and 13-hydroxy-linoleic acid possess chemotactic activity for bovine and human polymorphonuclear leukocytes. *Prostaglandins*, **41**, 21–27.

HOLZER, P. (1988). Local effector functions of capsaicin sensitive sensory nerve endings: involvement of tachykinins, calcitonin gene-related peptide and other neuropeptides. *Neurosci.*, **24**, 739–768.

HUGHES, S.R. & BRAIN, S.D. (1991). A calcitonin gene-related peptide (CGRP) antagonist ($CGRP_{8-37}$) inhibits microvascular response induced by CGRP and capsaicin in skin. *Br. J. Pharmacol.*, **104**, 738–742.

JANSCO, G., KIRALY, E. & JANSCO-GABOR, A. (1977). Pharmacologically induced selective degeneration of chemosensitive primary sensory neurones. *Nature*, **270**, 741–743.

KOIDE, T., NODA, Y., HATA, S., SUGIOKA, K., KOBAYASHI, S. & NAKANO, M. (1981). Contraction of the canine basilar artery following linoleic, arachidonic, 13-hydroperoxylinoleic or 15-hydroperoxyarachidonic acid. *Proc. Soc. Exp. Biol. Med.*, **168**, 399–402.

MAGGI, C.A., SANTICIOLA, P., GEPETTI, P., PARLANI, M., ASTOLFI, M., PRADELLES, P., PAPACCHINI, R. & MELI, A. (1988). The antagonism induced by ruthenium red of the actions of capsaicin on the peripheral terminals of sensory neurone: further studies. *Eur. J. Pharmacol.*, **154**, 1–10.

OOSTHUIZEN, M.J., ENGELS, F., VAN ESCH, B., HENRICKS, P.A.J. & NIJKAMP, F.P. (1990). Production of arachidonic and linoleic acid metabolites by guinea pig tracheal epithelial cells. *Inflammation*, **14**, 401–408.

SOBERMANN, R.J., HARPER, T.W., BETTERIDGE, D., LEWIS, R.A. & AUSTEN, K.F. (1985). Characterization and separation of the arachidonic acid 5-lipoxygenase and linoleic acid ω-6 lipoxygenase (arachidonic acid 15-lipoxygenase) of human polymorphonuclear leukocytes. *J. Biol. Chem.*, **260**, 4508–4515.

VAN HEUVEN-NOLSEN, D., TEN HAVE, G.A.M., ENGELS, F. & NIJKAMP, F.P. (1990). Formation of 13-HODE, 9-HODE and LTB_4 by pig polymorphonuclear leukocytes and their influence on pig coronary vascular reactivity of histamine. *Eur. J. Pharmacol.*, **183**, 875–876.

(Received November 8, 1994
Revised January 30, 1995
Accepted March 9, 1995).

British Journal of Pharmacology (1995) 115, 840-844

Evidence for ET_A and ET_B receptors in rat skin and an investigation of their function in the cutaneous microvasculature

E. Lawrence, L. Siney, P. Wilsoncroft, *G.A. Knock, [1]G. Terenghi, *J.M. Polak & [2]S.D. Brain

Pharmacology Group, Biomedical Sciences Division, King's College, Manresa Road, London, SW3 6LX and *Histochemistry Department, RPMS Hammersmith Hospital, DuCane Road, London W12 0NN

1 The relative contribution of ET_A and ET_B receptors in the response of rat skin to endothelins was investigated by use of the selective ET_B agonist IRL-1620 and the selective ET_A antagonist BQ-123.

2 Binding data suggest the presence of ET_A and ET_B receptors as preincubation with [$Ala^{3,11,18}Nle^7$]-endothelin-1 reduced ET-1 binding by approximately 40%.

3 Intradermal injection of endothelin-1 (ET-1, 1-10 pmol/site) and ET-3 (3-100 pmol/site) induced a dose-dependent decrease in local blood flow assessed by ^{133}Xe clearance at test sites in rat skin.

4 The endothelin analogue [$Ala^{3,11,18}Nle^7$]-ET-1 (30-1000 pmol/site) induced significant vasoconstriction ($P<0.05$) at the highest doses used and the selective ET_B receptor agonist, IRL-1620 [Suc-[Glu^9,$Ala^{11,15}$] endothelin (8-21)], (0.01-100 pmol/site) acted in a potent manner to induce a significant ($P<0.01$) dose-dependent decrease in ^{133}Xe clearance.

5 Co-injection with the selective ET_A receptor antagonist, BQ-123 (1 nmol/site), completely abolished the vasoconstriction to ET-1 and partially to ET-3, but had no effect on IRL-1620-induced vasoconstriction. In addition, IRL-1620 responses were not altered at sites treated with submaximal doses of a nitric oxide synthase inhibitor or a prostaglandin synthase inhibitor.

6 ET-1 and IRL-1620 (100 fmol-1 pmol/site) did not induce oedema formation as measured by [^{125}I]-albumin accumulation in the presence or absence of the vasodilator, calcitonin gene-related peptide (CGRP). ET-1 (1-3 pmol/site) inhibited substance P-induced oedema formation and this effect, suggested to be secondary to a vasoconstrictor effect, was significantly reversed by BQ-123 (1 nmol/site).

7 The findings in this study indicate that there are ET_A and ET_B receptors in rat skin and agents which activate either receptor act to mediate a decrease in cutaneous blood flow, but have no effect on increased microvascular permeability.

Keywords: ET_A receptor; ET_B receptor; endothelin; cutaneous microvasculature; blood flow; IRL-1620

Introduction

The endothelin isopeptides have numerous pharmacological activities and may be important in the regulation of a variety of biological functions, including vascular resistance, gene expression, and cell growth (see Miller *et al.*, 1993). The cDNA encoding at least two distinct endothelin receptor subtypes has been cloned (Arai *et al.*, 1990; Sakurai *et al.*, 1990). The ET_A receptor has binding affinity: ET-1 > ET-3 (Arai *et al.*, 1990) while the ET_B receptor is non-isopeptide-selective (Sakurai *et al.*, 1990).

The recent development and availability of specific agonists and antagonists has allowed the functions of the ET_A and ET_B receptors to be described. The ET_A receptor is known to be responsible for vasoconstriction, while the ET_B receptor on endothelial cells mediates endothelium-dependent vasodilatation (Randall *et al.*, 1989; Takayanagi *et al.*, 1991). More recently an ET_B-like receptor present on some smooth muscle cells has been shown to mediate vasoconstriction *in vitro* (Harrison *et al.*, 1992; Moreland *et al.*, 1992; see Davenport & Maguire, 1994) in addition to evidence that ET_B receptors are implicated in pressor responses in pithed rats (Williams *et al.*, 1991). BQ-123 (*cyclo*[D-Asp-Pro-D-Val-Leu-D-Trp]) is a selective ET_A receptor antagonist (Ihara *et al.*, 1992), [$Ala^{3,11,18}Nle^7$]-ET-1 is a selective ET_B receptor ligand (Hunt *et al.*, 1991) and IRL-1620 (Suc-[Glu^9, $Ala^{11,15}$] endothelin (8-21)) is a selective agonist at the ET_B receptor in porcine lung membrane and guinea-pig trachea (Takai *et al.*, 1992) and in the rat aorta (Karaki *et al.*, 1993). We have previously shown that local treatment of rat skin with ET-1 and ET-3 induces vasoconstriction (Lawrence & Brain, 1992), which can be antagonized by BQ-123 and the non-peptide mixed ET_A/ET_B antagonist, bosentan (Lawrence & Brain, 1994).

In the present study selective ligands, BQ-123, [$Ala^{3,11,18}NLe^7$]-ET-1 and IRL-1620 have been used to learn more about the receptors present in rat skin and to determine their roles in mediating blood flow and permeability changes in the rat cutaneous microvasculature.

Methods

In the binding experiments two dorsal skin samples were taken from each of three rats. Following removal of excess hair with a razor blade, skin samples were placed on cork mats, embedded in mounting medium (Tissue-Tek, Miles Inc, U.S.A.) and frozen unfixed in melting dichlorodifluoromethane (Arcton 12, ICI Runcorn, U.K.) suspended over liquid nitrogen. All six samples were used for this study, and ligand binding experiments were carried out according to a protocol previously used for receptor studies in skin (Knock *et al.*, 1993). The presence of ET receptor subtypes was investigated by incubating consecutive sections with 200 pM [^{125}I]-ET-1 (Amersham International, Amersham) in the presence of increasing concentrations of unlabelled ET-1 and ET-3 ($10^{-11}M-10^{-9}M$), or by incubating sections as normal, following preincubation in the presence of the ET_B-specific agonist, [$Ala^{3,11,18}$, Nle^7]ET-1 ($10^{-7}M$).

Local clearance of ^{133}Xe (Amersham International, Amersham, 0.36 MBq per site) was measured in the dorsal skin of male Wistar rats (180-220 g) following intradermal (i.d.) in-

[1] Present address: Blond McIndoe Centre, Queen Victoria Hospital, East Grinstead, Sussex RH19

[2] Author for correspondence.

Table 1 Competitive inhibition of [^{125}I]-endothelin-1 ([^{125}I]ET-1) binding sites in rat skin microvessels by unlabelled ET-1 and ET-3

Peptide	*Specific binding remaining (% of maximum) (n=6 blocks from 3 rats)*
Unlabelled ET-1	
10^{-7}M	2.19 ± 1.05
10^{-9}M	7.84 ± 1.56
10^{-11}M	84.21 ± 9.39
Zero	100
Unlabelled ET-3	
10^{-7}M	17.29 ± 1.59
10^{-9}M	65.43 ± 6.77
10^{-11}M	89.41 ± 4.12
Zero	100
[Ala^{3,11,18}Nle^{7}]-ET-1	
Preinc 10^{-7}M	61.17 ± 5.21

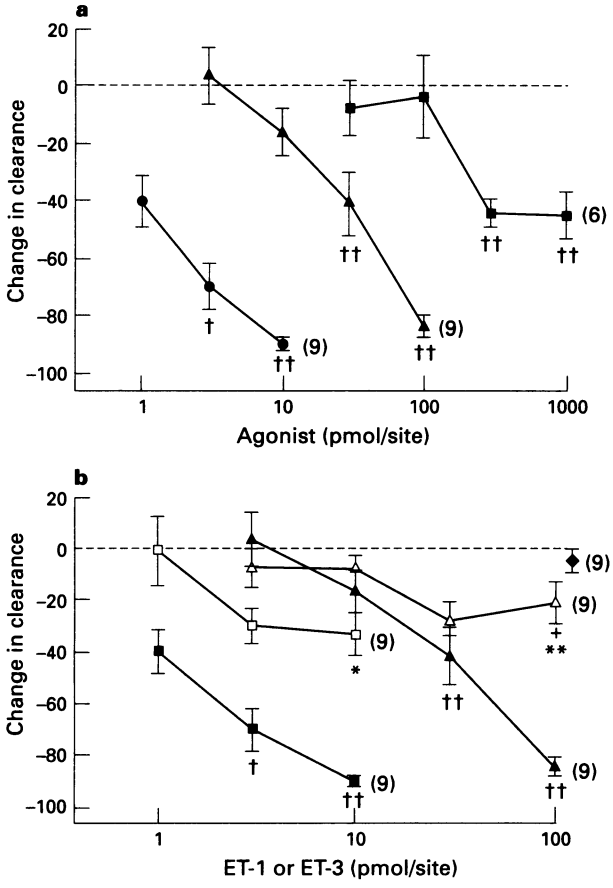

Figure 1 The effect of endothelin-1 (ET-1, ●), ET-3 (▲) and [Ala^{3,11,18},Nle^{7}]-ET-1 (■) on local ^{133}Xe clearance in rat dorsal skin (a), and the response to ET-1 (■) and ET-3 (▲) in the absence and presence of BQ-123 (1 nmol/site; □, △) is shown in (b). The effect of BQ-123 alone (◆) is also shown. The results are expressed as change in local clearance at test sites compared with at control (Tyrode-injected) sites in the same rat, measured over 15 min. Values are the mean ± s.e.mean for the number of rats shown in parentheses. †$P<0.05$ cf. Tyrode control; ††$P<0.01$ cf. Tyrode control; *$P<0.05$ cf. + BQ-123; **$P<0.01$ cf + BQ-123.

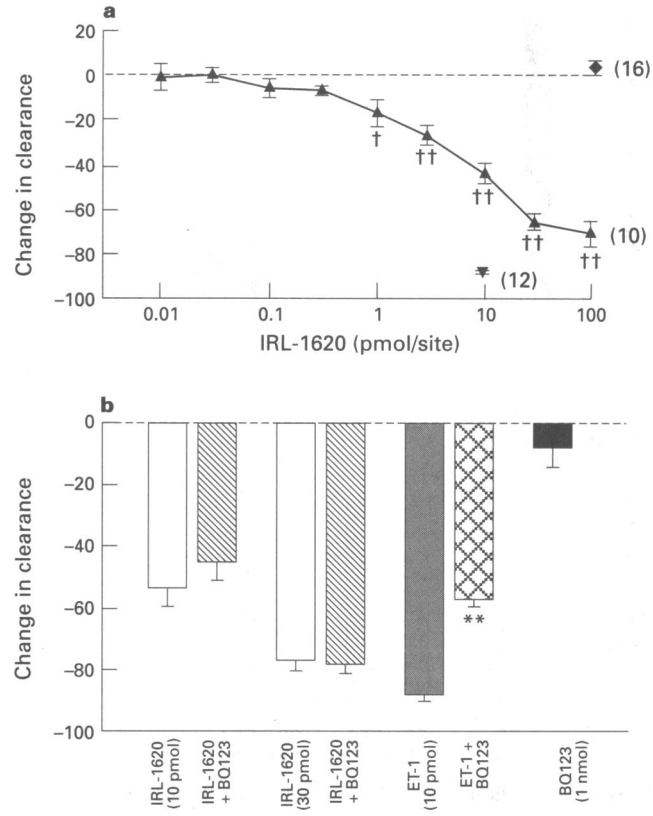

Figure 2 The effect of IRL-1620 on local ^{133}Xe clearance in rat dorsal skin in the absence and presence of BQ-123. The effect of IRL-1620 (▲), endothelin-1 (ET-1, 10 pmol, ▼) and vehicle (0.1% ammonium bicarbonate, ◆) is shown in (a). The effect of BQ-123 on ET-1 (10 pmol) and IRL-1620 (10 pmol and 30 pmol) responses is shown in (b). Results are expressed as mean ± s.e.mean for at least 8 experiments. †$P<0.05$ cf. Tyrode; ††$P<0.01$ cf. Tyrode; **$P<0.001$ cf. ET-1 alone.

jection of multiple test agents; this technique has been described in detail (Williams, 1976; Lawrence & Brain, 1992). Briefly, rats were anaesthetized with pentobarbitone (Sagatal, May & Baker, 50 mg kg^{-1} body weight). Each test agent or combination of test agents was made up in Tyrode solution and an equal quantity of ^{133}Xe was mixed with 1 ml sample of each test agent. Test or control agent was rapidly injected i.d. in duplicate and in random order according to a balanced site pattern and a 100 ml aliquot of each solution was counted to determine the total radioactivity present. After a clearance period of 15 min the rat was killed, skin sites punched out and radioactivity counted. Changes in blood flow were expressed as percentage change in clearance at test sites compared with clearance at control sites injected with Tyrode solution; a decrease in clearance indicates that a decrease in local blood flow due to vasoconstriction has occurred, while an increase in clearance indicates that an increase in local blood flow due to vasodilatation of microvessels has occurred.

In a separate series of experiments the effects of agents on local oedema formation were measured in rat skin as extravasation of intravenously injected ^{125}I-labelled human serum albumin (Amersham International, Amersham, 2.5 mCi per

Table 2 The effects of N^G-nitro-L-arginine methyl ester (L-NAME) and indomethacin on IRL-1620-induced responses in the rat dorsal skin

Agent	*IRL 1620* (pmol/site)			
	0	1.0	3.0	30.0
None	–	−17.0±5.4 (8)	−23.9±4.1 (14)	−67.3±3.3 (12)
L-NAME (100 nmol/site)	−10.8±2.8 (12)	−23.7±8.0 (6)	−24.9±3.3 (12)	−60.0±3.7 (12)
Indomethacin (3 nmol/site)	−20.0±6.9 (9)	−22.3±3.7 (6)	−26.5±4.7 (6)	−72.7±2.1 (6)

Results are mean±s.e.mean % decrease in ^{133}Xe clearance for the number of experiments shown in parentheses.

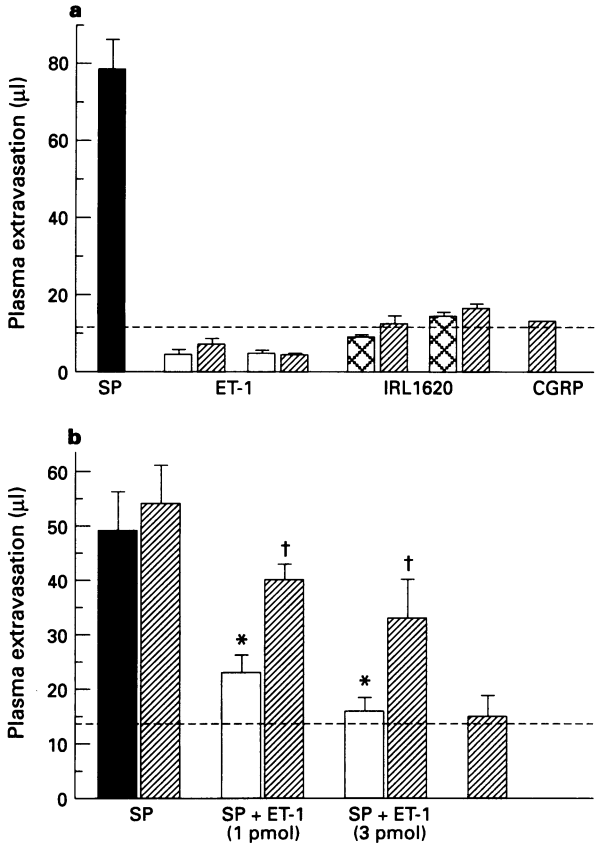

Figure 3 The effect of endothelin-1 (ET-1) and IRL-1620 on oedema formation in rat skin measured over 30 min as ^{125}I-labelled human serum albumin accumulation, (a) shows ET-1 (100 fmol/site and 1 pmol/site, open columns) and IRL-1620 (100 fmol/site and 1 pmol/site, cross-hatched columns) alone and in combination with the vasodilator CGRP (10 pmol/site, hatched columns). The effect of substance P alone (100 pmol/site, solid column) is also shown. (b) Shows the effect of BQ-123 on the inhibitory effect of ET-1 on substance P (SP, 100 pmol/site)-induced oedema. Substance P alone is shown by the solid column and substance P plus ET-1 by the open columns. The effect of co-injected BQ-123 is shown by the hatched column. The dashed line represents the level of oedema formation in control sites which received Tyrode alone. Results are expressed as mean±s.e.mean of 6 rats. *$P<0.05$ cf. substance P, †$P<0.05$ cf. substance P plus ET-1.

rat) accumulated at skin sites over 30 min in response to the i.d. agents made up in 100 ml Tyrode solution as previously described (Brain & Williams, 1989). Oedema formation was measured as radioactivity in skin sites and expressed as plasma volume calculated from the counts in 1 ml of plasma.

Test agents used were human ET-1 and human ET-3 obtained from Bachem (U.K.) Ltd. (Essex); [$Ala^{3,11,18}$,Nle^7]-ET-1, BQ-123 and IRL-1620 were from Peninsula Laboratories (Lancashire); human α-calcitonin gene-related peptide (CGRP) was a gift from Dr U. Ney, Celltech (Bucks); N^G-nitro-L-arginine methyl ester (L-NAME), substance P and indomethacin were from Sigma Chemical Company Ltd. (Dorset).

Results are expressed as mean±s.e.mean. The significant difference between intradermal treatments was assessed with Bonferroni's modified *t* test, which uses the standard error estimate for the analysis of variance to allow comparison of multiple sites. $P<0.05$ was accepted as statistically significant.

Results

[^{125}I]-ET-1 binding sites were localized by autoradiography to microvessels of rat skin in the superficial dermis. Binding was inhibited by both ET-1 and ET-3 in a concentration-dependent manner. Competition studies gave an apparently biphasic curve for ET-3 as competitor, consistent with previous results (Knock *et al.*, 1993), suggesting the presence of both ET-1 selective (ET_A) and non-selective (ET_B) subtypes. Indeed at the concentration of 10^{-9}M, ET-1 inhibited binding by >90%, whereas ET-3 inhibited binding by only approximately 40% (Table 1). Similarly, binding was not completely abolished by preincubation with 10^{-7}M [$Ala^{3,11,18}$,Nle^7]-ET-1, but was reduced by approximately 40% (Table 1).

The greater potency of ET-1 as a constrictor in rat skin compared with ET-3 is shown in Figure 1a. [$Ala^{3,11,18}$,Nle^7]-ET-1 induced vasoconstriction only at the highest doses used (Figure 1a). BQ-123 (1 nmol/site) had no effect on local ^{133}Xe clearance when injected alone (Figure 1b). However, it caused attenuation of the vasoconstriction induced by the highest dose of ET-1 (Figure 1b, $P<0.05$). BQ-123 also significantly decreased the vasoconstriction induced by the highest dose of ET-3 (Figure 1b). IRL-1620 induced a dose-dependent vasoconstriction in rat skin (Figure 2a), BQ-123 (1 nmol/site) did not alter IRL-1620-induced vasoconstriction (10–30 pmol/site, Figure 2b).

The decrease in ^{133}Xe clearance induced by the ET_B selective agonist, IRL-1620 (at concentrations between 1–30 pmol/site), was not significantly altered when sites were simultaneously treated with submaximal doses of the NO synthase inhibitor, L-NAME (100 nmol/site; Lawrence & Brain, 1992) or the prostaglandin inhibitor, indomethacin (3 nmol/site; Brain *et al.*, 1985) (Table 2).

ET-1 and IRL-1620 (100 fmol–1 pmol/site) did not induce oedema formation when injected alone or in combination with the vasodilator CGRP (Figure 3a) which was used to act in a functional manner to antagonize the constrictor activity of ET-1 and IRL-1620. Under such conditions, oedema formation may be more easily observed (see Brain *et al.*, 1989). Substance P (100 pmol/site) did cause a significant increase in oedema formation and thus acted as a positive control. In further experiments ET-1 (1 and 3 pmol/site) inhibited substance P-induced oedema formation which was significantly reversed by BQ-123. However, BQ-123 had no effect on substance P-induced oedema formation in the absence of ET-1 and did not itself stimulate oedema (Figure 3b).

Discussion

The results of this study indicate that the rat dorsal skin has both ET_A and ET_B receptor subtypes, a result consistent with similar results observed in human skin (Knock *et al.*, 1993). The heterogeneity of the receptors was demonstrated by reduced binding with different ET isoforms and by the inhibition of labelled ET-1 binding with an ET_B-specific agonist.

There is increasing evidence that the microcirculation of animals is particularly sensitive to the effects of endothelins (Brain *et al.*, 1988; Boric *et al.*, 1990; Lamping *et al.*, 1992). More recently, it has been demonstrated that small arteries and veins in man are also sensitive to endothelins, causing a vasoconstriction that is interestingly not mediated entirely by ET_A receptors (Riezebos *et al.*, 1994). Further, it has been shown that in human skin microcirculation, ET-1 but not ET-3 induced pronounced vasoconstrictor activity at the injection site and neurally-mediated vasodilatation in the surrounding area (Wenzel *et al.*, 1994) suggesting that in this preparation, ET-1 is primarily involved in the regulation of vascular tone by activation of ET_A receptors. There does appear, therefore, to be differences between species and between vascular beds. It is now widely accepted that ET_B receptors are important in some vasoconstrictor responses (see Davenport & Maguire, 1994). In the present study, functional data using the selective ET_A antagonist BQ-123 suggest that ET-1 and ET-3 also act, at least in part, via ET_A receptors to mediate vasoconstriction in the cutaneous microvasculature. The finding that the ET_B-selective agonist, IRL-1620, induced a decrease in blood flow which is not affected by BQ-123 provides evidence that ET_B receptors also mediate vasoconstriction in the rat cutaneous microvasculature. The results of the present study are further evidence that ET_B receptors can mediate vasoconstriction *in vivo*.

In addition, the possibility that vasodilator responses mediated via ET_B receptors occur was also studied. It has previously been shown that the vasodilatation induced in the intact preconstricted rat aorta by IRL-1620 was endothelium-dependent and due to release of nitric oxide (Karaki *et al.*, 1993). Despite finding that a basal level of nitric oxide is important for maintaining blood flow in the rat skin microvasculature, we have been unable to demonstrate endothelin-stimulated release of vasodilator quantities of nitric oxide (Lawrence & Brain, 1992). IRL-1620 is a very selective and potent ET_B agonist (Takai *et al.*, 1992) and since there was no effect on blood flow at sites simultaneously treated with L-NAME, compared to those treated with IRL-1620 alone, it would appear that the ET_B receptor in rat skin does not release nitric oxide. Furthermore, it has previously been reported that, in addition to nitric oxide, ET_B-mediated vasodilatation may be due to prostacyclin release (Fozard & Part, 1992). The results of the present study, however, are in contrast to this finding and suggest that vasodilator prostaglandins do not contribute to the observed response to IRL-1620 in rat skin. The residual component of the response to ET-3 following treatment with BQ-123 is compatible with the suggestion that further subtypes of endothelin receptors exist which are selective for ET-3 > ET-1 (Harrison *et al.*, 1992). In this context the cloning of a third distinct receptor, ET_C, which is selective for ET-3 (Karne *et al.*, 1993) is of relevance.

There is conflicting evidence on the function of endothelin in microvascular permeability and the route of administration appears to be important. ET-1 injected i.v. induces oedema formation in the human forearm (Dahlof *et al.*, 1990) but when injected i.d. reduces oedema formation induced by agents which increase microvascular permeability in rat and rabbit skin (Brain *et al.*, 1989). Further Filep *et al.* (1991, 1993) have shown that endothelin-1 enhances microvascular permeability induced in various vascular beds following systemic treatment of rats and that this is mediated at least in part via the ET_A receptor. These authors have provided evidence that the oedema formation is not merely a secondary effect to changes in systemic blood pressure, but related to local production of platelet activating factor (Filep *et al.*, 1991).

In the present study oedema formation was not observed when ET-1 and IRL-1620 were injected alone, or with a vasodilator dose of CGRP (to counteract vasoconstrictor activity). Thus it would appear that the phenomenon observed by Filep and coworkers after systemic administration of endothelins is not observed after intradermal injection of endothelins in skin. The results from the present study support the concept that ET-1 released in low concentrations in the cutaneous microcirculation is more potent as a vasoconstrictor than as a mediator of microvascular permeability and that the decrease in blood flow can lead to an inhibition of oedema formation as previously reported (Brain *et al.*, 1989).

In conclusion, we present evidence that ET_B receptors, in addition to ET_A receptors, exist in rat skin and our results suggest that ET_B receptors can mediate vasoconstriction but, since IRL-1620 had no effect on blood flow in constricted sites, not vasodilatation in the rat cutaneous microvasculature. In addition our experiments suggest that neither ET_A nor ET_B receptors are involved in mediating increases in microvascular permeability in the rat cutaneous microvasculature.

This work was supported in part by the British Heart Foundation, the Wellcome Trust, the Grand Charity of Freemasons and the Colt Foundation.

References

ARAI, H., HORI, S., ARAMORI, I., OHKUBO, H. & NAKANISHI, S. (1990). Cloning and expression of a cDNA encoding an endothelin receptor. *Nature*, **348**, 730–732.

BORIC, M.P., DONOSO, V., FOURNIER, A., ST PIERRE, S. & HUIDOBROTORO, J.P. (1990). Endothelin reduces microvascular blood flow by acting on arterioles and venules of the hamster cheek pouch. *Eur. J. Pharmacol.*, **190**, 123–133.

BRAIN, S.D., CROSSMAN, D.C., BUCKLEY, T.L. & WILLIAMS, T.J. (1989). Endothelin-1: demonstration of potent effects on the microcirculation of humans and other species. *J. Cardiovasc. Pharmacol.*, **13** (Suppl. 5), S147–S149.

BRAIN, S.D., TIPPINS, J.R. & WILLIAMS, T.J. (1988). Endothelin induces potent microvascular constriction. *Br. J. Pharmacol.*, **95**, 1005–1007.

BRAIN, S.D. & WILLIAMS, T.J. (1989). Interactions between the tachykinins and calcitonin gene-related peptide lead to the modulation of oedema formation and blood flow in rat skin. *Br. J. Pharmacol.*, **97**, 77–82.

BRAIN, S.D., WILLIAMS, T.J., TIPPINS, J.R., MORRIS, H.R. & MACINTYRE, I. (1985). Calcitonin gene-related peptide is a potent vasodilator. *Nature*, **313**, 54–56.

DAHLOF, B., GUSTAFSSON, D., HEDNER, D., JERN, S. & HANSSON, L. (1990). Regional hemodynamic effects of endothelin-1 in rat and man: unexpected adverse reactions. *J. Hypertension*, **8**, 811.

DAVENPORT, A.P. & MAGUIRE, J.J. (1994). Is endothelin-induced vasoconstriction mediated only by ETA receptors in humans? *Trends Pharmacol. Sci.*, **15**, 9–11.

FILEP, J.G., SIROIS, M.G., FOLDES-FILEP, E., ROUSSEAU, A., PLANTE, G.E., FOURNIER, A., YANO, M. & SIROIS, P. (1993). Enhancement by endothelin-1 of microvascular permeability via activation of ET_A receptors. *Br. J. Pharmacol.*, **109**, 880–886.

FOZARD, J.R. & PART, M.L. (1992). The role of nitric oxide in the regional vasodilator effects of endothelin-1 in the rat. *Br. J. Pharmacol.*, **105**, 744–750.

HARRISON, V.J., RANDRIANTSOA, A. & SCHOEFFTER, P. (1992). Heterogeneity of endothelin-sarafotoxin receptors mediating contraction of pig coronary artery. *Br. J. Pharmacol.*, **105,** 511–513.

HUNT, J.T., LEE, V.G., STEIN, P.D., HEDBURG, A., LIU, E.C.-K., MCCULLEN, D. & MORELAND, S. (1991). Structure activity relationships of monocyclic endothelin analogs. *Bio-Org. Med. Chem. Lett.*, **1,** 33.

IHARA, M., NOGUCHI, K., SAEKI, T., FUKURODA, T., TSUCHIDA, S., KIMURA, S., FUKAMI, T., ISHIKAWA, K., NISHIKIBE, M. & YANO, M. (1991). Biological profile of highly potent novel endothelin antagonists selective for the ET_A receptor. *Life Sci.*, **50,** 247–255.

KARAKI, H., SUDJARWO, S.A., HORI, M., TAKAI, M., URADE, Y. & OKADA, T. (1993). Induction of endothelium-dependent relaxation in the rat aorta by IRL 1620. A novel and selective agonist in the endothelin ET_B receptor. *Br. J. Pharmacol.*, **109,** 486.

KARNE, S., JAYAWICKREME, C.K. & LERNER, M.R. (1993). Cloning & characterisation of an endothelin-3 specific receptor (ET_C receptor) from *Xenopus laevis* dermal melanophores. *J. Biol. Chem.*, **268,** 19126–19133.

KNOCK, G.A., TERENGHI, G., BUNKER, C.B., BULL, H.A., DOWD, P.M. & POLAK, J.M. (1993). Characterisation of endothelin-binding sites in human skin and their regulation in primary Raynaud's Phenomenon and systemic sclerosis. *J. Invest. Dermatol.*, **101,** 73.

LAMPING, K.G., CLOTHIER, J.L., EASTHAM, C.L. & MARCUS, M.L. (1992). Coronary microvascular response to endothelin is dependent on vessel diameter and route of administration. *Am. J. Physiol.*, **263,** H703–H709.

LAWRENCE, E. & BRAIN, S.D. (1992). Responses to endothelins in the rat cutaneous microvasculature: A modulatory role of locally-produced nitric oxide. *Br. J. Pharmacol.*, **106,** 733–738.

LAWRENCE, E. & BRAIN, S.D. (1994). Effect of BQ-123 and Ro-47-0203 (bosentan) on endothelin-induced vasoconstriction in rat skin. *Eur. J. Pharmacol.*, **260,** 103–106.

MILLER, R.C., PELTON, J.T. & HUGGINS, J.P. (1993). Endothelins–from receptors to medicine. *Trends Pharmacol. Sci.*, **14,** 54–60.

MORELAND, S., MCMULLEN, D.M., DELANEY, C.L., LEE, V.G. & HUNT, J.T. (1992). Venous smooth muscle contains vasoconstrictor ET_B-like receptors. *Biochem. Biophys. Res. Commun.*, **184,** 100–106.

RANDALL, M.D., DOUGLAS, S.A. & HILEY, C.R. (1989). Vascular activities of endothelin-1 and some alanyl substituted analogues in resistance beds of the rat. *Br. J. Pharmacol.*, **98,** 685–699.

RIEZEBOS, J., WATTS, I.S. & VALLANCE, P.J.T. (1994). Endothelin receptors mediating functional responses in human small arteries and veins. *Br. J. Pharmacol.*, **111,** 609–615.

SAKURAI, T., YANAGISAWA, M., TAKUWA, Y., MIYAZAKI, H., KIMURA, S., GOTO, K. & MASAKI, T. (1990). Cloning of a cDNA encoding a non-isopeptide subtype of the endothelin receptor. *Nature*, **348,** 732–735.

TAKAI, M., UMEMURA, I., YAMASAKI, K., WATAKABE, T., FUJITANI, Y., ODA, K., URADE, Y., INUI, T., YAMAMURA, T. & OKADA, T. (1992). A potent and specific agonist Suc-[Glu9, Ala11,15]-endothelin-1 (8-21), IRL 1620, for the ET_B receptor. *Biochem. Biophys. Res. Commun.*, **184,** 953–959.

TAKAYANANGI, R., KITAZUMI, K., TAKASAKI, C., OHNAKA, K., AIMOTO, S., TASAKA, K., OHADA, M. & NAWATA, H. (1991). Presence of non-selective type of endothelin receptor on vascular endothelium and its linkage to vasodilation. *FEBS Lett.*, **282,** 103–106.

WENZEL, R.R., NOLL, G. & LUSCHER, T.F. (1994). Endothelin receptor antagonists inhibit endothelin in human skin microcirculation. *Hypertension*, **23,** 581–586.

WILLIAMS, T.J. (1976). Simultaneous measurement of local plasma exudation and blood flow changes induced by intradermal injection of vasoactive substances, using [^{125}I]albumen and ^{133}Xe. *J. Physiol.*, **254,** 4–5P.

WILLIAMS, D.L., JONES, K.L., PETTIBONE, D.J., LIS, E.V. & CLINESCHMIDT, B.C. (1991). Sarafotoxin S6c: an agonist which distinguishes between endothelin receptor subtypes. *Biochem. Biophys. Res. Commun.*, **175,** 556–561.

(Received August 24, 1994
Revised March 2, 1995
Accepted March 23, 1995)

British Journal of Pharmacology (1995) 115, 845-851

$BaCl_2$- and 4-aminopyridine-evoked phasic contractions in the rat vas deferens

Yu Huang

Department of Physiology, Chinese University of Hong Kong, Shatin, NT, Hong Kong

1 The actions of $BaCl_2$ and 4-aminopyridine, blockers of K^+ channels, on the mechanical activity of the epididymal half of the rat vas deferens were investigated.

2 Both $BaCl_2$ and 4-aminopyridine dose-dependently evoked phasic contractions. High extracellular potassium (35-40 mM) caused a tonic contraction but abolished the $BaCl_2$- and 4-aminopyridine-induced phasic activity and reduced the $BaCl_2$-induced sustained component of contraction, but increased the 4-aminopyridine-induced tonic contraction.

3 Omission of calcium from the extracellular medium totally abolished the 4-aminopyridine-induced response but only reduced the mean amplitude of phasic contractions induced by BaCl.

4 Procaine (10 mM), an inhibitor of internal calcium release, completely abolished the phasic activity and reduced the sustained contraction induced by $BaCl_2$. The remaining tone was abolished by nifedipine (1 μM).

5 Tetraethylammonium (1 mM) suppressed the amplitude of the $BaCl_2$-induced phasic contractions, and induced a biphasic increase in tonic tension.

6 The $BaCl_2$-induced responses were resistant to prazosin (1 μM), yohimbine (3 μM), propranolol (3 μM) or atropine (3 μM); in contrast, the 4-aminopyridine-induced activity was effectively inhibited by prazosin (1 μM) attenuated by yohimbine (1 μM) and atropine (1 μM) but not by propranolol (3 μM). The 4-aminopyridine-induced response was abolished by pretreatment of the vas deferens with 6-hydroxydopamine (0.5 mM).

7 The results indicate that the $BaCl_2$-evoked activity in the vas deferens was mainly due to blockade of Ba^{2+}-sensitive K^+ channels on the smooth muscle plasma membrane. Subsequent calcium entry through the depolarized plasma membrane was needed to trigger generation of phasic contractions. 4-Aminopyridine-induced action, however, was largely mediated by neurotransmitters released from the depolarized nerve terminals as a result of blockade of K^+ channels.

Keywords: Rat vas deferens; phasic contractions; $BaCl_2$; 4-aminopyridine; procaine; K^+ channel; Ca^{2+} channel blocker

Introduction

Spontaneous electrical and mechanical activity has been observed in smooth muscle from a number of tissues (Janssen & Daniel, 1991; Lydrup, 1991; Suzuki *et al.*, 1993). Both a myogenic and neurogenic origin have been proposed to underlie such activity. K^+ channels and Ca^{2+} channels have been reported to be involved in rhythmic contractions (Mitra & Morad, 1985; Janssen & Daniel, 1991; Suzuki *et al.*, 1993).

Many different types of K^+ channel have been identified in smooth muscle, which, apart from regulating the resting membrane potential, might also participate in cellular activity in response to endogenous transmitters and exogenous agents (Ometo *et al.*, 1993). The opening of K^+ channels and the ensuing membrane hyperpolarization usually inhibit the activity of voltage-dependent Ca^{2+} channels. In contrast, the closing of K^+ channels would first depolarize the cell membrane and then activate Ca^{2+} channels, resulting in a contractile response in smooth muscle. Oscillatory changes either in the membrane potential or in Ca^{2+} release from the sarcoplasmic reticulum, have been proposed to explain the agonist-evoked oscillations in smooth muscle tone. Ca^{2+} ions entering through voltage-dependent Ca^{2+} channels may raise the intracellular Ca^{2+} above the levels needed to activate Ca^{2+}-activated K^+ channels; the resulting hyperpolarization of the plasma membrane shuts off the Ca^{2+} channels; the local $[Ca^{2+}]_i$ in proximity to K^+ channels will then decrease below the threshold of activation; this in turn will depolarize the plasma membrane again and open the voltage dependent Ca^{2+} channels to initiate another cycle, as has been observed in the tail artery of genetically hypertensive rats (Lamb *et al.*, 1985). However, in smooth muscle of the rabbit mesenteric artery periodic Ca^{2+} release from internal stores has been suggested as causing oscillatory contractions (Leijten & Breemen, 1986).

In the present study, a number of pharmacological agents previously known to block a variety of K^+ channel types, were investigated for their stimulatory effects on phasic contractile activity in the epididymal portion of the rat vas deferens. An attempt was made to test the hypothesis that changes in both the membrane potential and intracellular Ca^{2+} release contribute jointly to generation of phasic contractions in smooth muscle of the vas deferens induced by K^+ channel blockers.

Methods

Preparation

Male Sprague-Dawley rats weighing about 400 g were anaesthetized with pentobarbitone. The epididymal half of the vas deferens was dissected out and the visible blood vessels and connective tissues along the vas were carefully removed. Segments of the vasal duct about 2 cm in length were mounted and attached to myograph force transducers under 500 mg resting tension in organ baths at 37±1°C in Krebs-Henseleit (K-H) solution gassed with 95% O_2 plus 5% CO_2. The K-H solution contained (in mM); NaCl 119, KCl 4.7, $CaCl_2$ 2.5, $MgSO_4$ 1.0, $NaHCO_3$ 25, KH_2PO_4 1.2, EDTA 0.03, D-glucose 11.1, ascorbic acid 0.2. In experiments with $BaCl_2$, $MgSO_4$ was replaced with $MgCl_2$ to avoid precipitation in the bath solution. For experi-

[1] Author for correspondence.

ments using high potassium solutions, the ionic strength was maintained by reducing the equivalent amount of sodium ions. For experiments using other divalent cations, EDTA was omitted from the solution to avoid chelating Ba^{2+}. For the experiments testing the effects of free external Ca^{2+} on the $BaCl_2$- and 4-AP-induced responses, the preparations were incubated for over 20 min before drugs were added. After 60 min of equilibration, the vas deferens was first tested for responsiveness either to 100 μM acetylcholine or high K^+ (50 mM) solution. If the contractile force was smaller than 0.5 g, the preparation was discarded. For experiments using 6-hydroxydopamine (6-OHDA), the preparation was incubated with 0.5 mM 6-OHDA for 3 h to remove the sympathetic activity in the vas. For experiments on the vasal duct without epithelium, the epithelial layer attached to the connective tissue was mechanically separated from the muscle layer with fine forceps.

Drugs and solutions

The following drugs were used: acetylcholine chloride, atropine sulphate, noradrenaline hydrochloride, prazosin hydrochloride, yohimbine, propranolol hydrochloride, barium chloride, 4-aminopyridine, procaine hydrochloride, 6-hydroxydopamine, glibenclamide, nifedipine (above drugs from Sigma), tetraethylammonium chloride, quinine, quinidine (above three agents from Merck-Schuchardt). Prazosin, glibenclamide, and nifedipine were dissolved in dimethylsulphoxide (DMSO); $BaCl_2$ and 4-AP were always dissolved in normal K-H solution with or without $CaCl_2$, and others in normal K-H solution. 6-OHDA was prepared in 0.2 μM ascorbic acid immediately before use.

Statistics

The activity of the vas deferens in response to blockers of K^+ channels was evaluated by the mean amplitude of all contractions (including the phasic and the tonic components) recorded over a 6 min interval, expressed in g force and frequency of contractile activity in the same 6 min interval. The results were expressed as mean $\pm$ s.d. of n experiments. Students' t test was used for paired data analysis. A probability level of $P < 0.05$ was considered statistically significant.

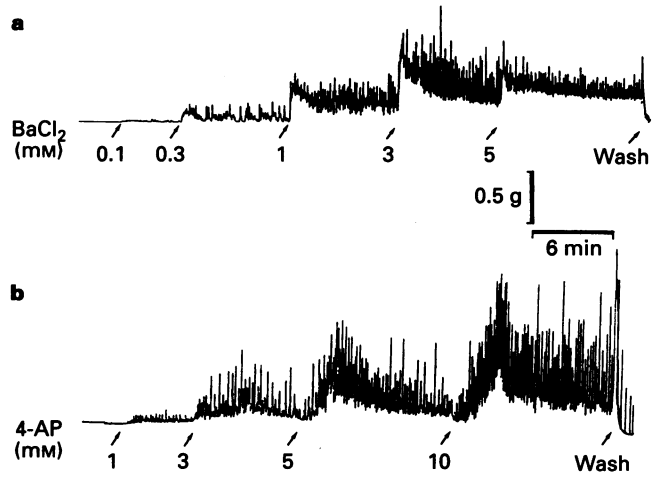

Figure 1 Concentration-dependent stimulation of vas deferens phasic activity by $BaCl_2$ and 4-aminopyridine (4-AP): traces display both the $BaCl_2$- (a) and 4-AP- (b) evoked phasic contractile activity in the epididymal portion of vas deferens of rats. Both K^+ channel blockers increased frequency of mechanical activity and mean amplitude of each contraction. Numbers indicate concentration of drugs used.

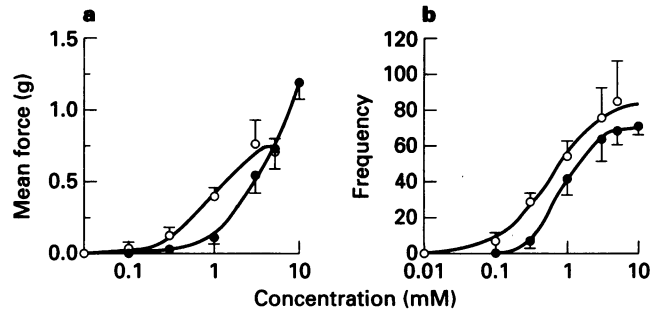

Figure 2 Concentration-response relationships for the $BaCl_2$- and 4-aminopyridine (4-AP)-induced phasic contraction in smooth muscle of the rat vas deferens. The mean amplitude (a) and frequency (b) of phasic contractions are expressed as the measured values. Each point is mean + s.d. of 9 experiments for $BaCl_2$ (○) and 7 experiments for 4-AP (●).

Results

Effect of $BaCl_2$ and 4-aminopyridine (4-AP) on the phasic activity of the vas deferens

The epididymal portion of the vas deferens equilibrated for 60 min at a basal tension of 500 mg or greater did not generate any contractile activity during the period of equilibration. This is quite different from many other smooth muscles that normally display a pacemaker-like activity (Lydrup, 1991; Suzuki *et al.*, 1993). Figure 1a and b shows that both $BaCl_2$ and 4-AP induced phasic contractions of the vas deferens in a concentration-dependent manner. The contraction induced by $BaCl_2$ or 4-AP in the vas had a rising and falling phase superimposed on a tonic component of contraction. However, other K^+ channel blockers such as glibenclamide (up to 1 mM, $n=7$), quinine (up to 5 mM, $n=5$), quinidine (5 mM, $n=6$) and TEA^+ (up to 4 mM, $n=6$) failed to initiate any phasic contractions (data not shown). Both $BaCl_2$ and 4-AP increased the frequency of contractions but only $BaCl_2$ at concentration above 5 mM reduced the absolute amplitude of contractions on top of the sustained component (Figure 1a). Figure 2 shows concentration-response curves for mean amplitude (a) of contractions and for frequency (b) of contractions for $BaCl_2$ ($n=9$) and 4-AP ($n=7$). Responses to $BaCl_2$ and 4-AP were reproducible, although slightly variable, within a time period of at least 3 h (data not shown).

Effect of raised extracellular potassium concentration on the $BaCl_2$- and 4-AP-evoked responses

K^+ channels play an essential role in maintaining the resting membrane potentials in a diversity of cell types (Rudy, 1988), therefore, it is possible that blockers of K^+ channels, if they act primarily at the post-junctional site, would first close K^+ channels leading to membrane depolarization, which in turn activates Ca^{2+} channels and hence muscle contraction. External K^+ by itself at 35 mM or above produced tonic tension but not phasic contractions such as seen in the presence of $BaCl_2$ or 4-AP. Raising external K^+ concentration would both depolarize the cell membrane and bring the membrane potential closer to the new equilibrium potential for K^+ ions. The effect of $BaCl_2$ on the frequency and mean amplitude of contraction decreased with increasing extracellular K^+ concentration (Figure 3). When the external K^+ was raised above 40 mM, $BaCl_2$ failed to produce any repetitive muscle activity except for a small tonic tension. This suggests that the $BaCl_2$-induced membrane depolarization caused by blocking the K^+ channels might be the first step leading to the phasic muscular contraction. The 4-AP-induced phasic activity was also completely suppressed by 35 mM external K^+. In contrast, 4-AP-induced tonic tension was enhanced with moderate increase of extracellular K^+ (up to 25 mM, Figure 3).

External calcium dependency of the $BaCl_2$- and 4-AP-induced mechanical activity of the vas deferens

The 4-AP-evoked contractile activity in the vas deferens was entirely dependent upon the presence of the extracellular Ca^{2+} ($n=7$). The removal of Ca^{2+} from the bath solution blocked the 4-AP response (Figure 4b). In contrast to 4-AP, $BaCl_2$ was still able to stimulate the tonic component of the vas deferens contraction albeit to a lesser degree in the absence of extracellular Ca^{2+}, but zero Ca^{2+} markedly suppressed the amplitude of each contraction (representative traces of seven experiments shown in Figure 4a). After readmitting 2.5 mM Ca^{2+} to the bath solution, the $BaCl_2$-evoked phasic mechanical activity was mostly restored. Furthermore, the $BaCl_2$-induced contraction in the Ca-free solution was abolished by nifedipine (1 μM, $n=5$, data not shown).

Effect of procaine on the $BaCl_2$-induced mechanical activity

As shown in Figure 4a, $BaCl_2$ was able to generate phasic contractions of the vas deferens in a Ca-free solution, even though the mean amplitude of their contractions was significantly smaller than those recorded in the normal K-H solution. This raises a possibility that after having entered the muscle cell, Ba^{2+} can replace the intracellular Ca^{2+} ions, which mobilize the internal Ca^{2+} stores. In order to test this hypothesis, procaine, an inhibitor of internal Ca^{2+} release (Khoyi *et al.*, 1993), was used to block or deplete internal Ca^{2+} stores under different conditions. Figure 5 shows an example of the effect of procaine on the $BaCl_2$-induced response in the absence

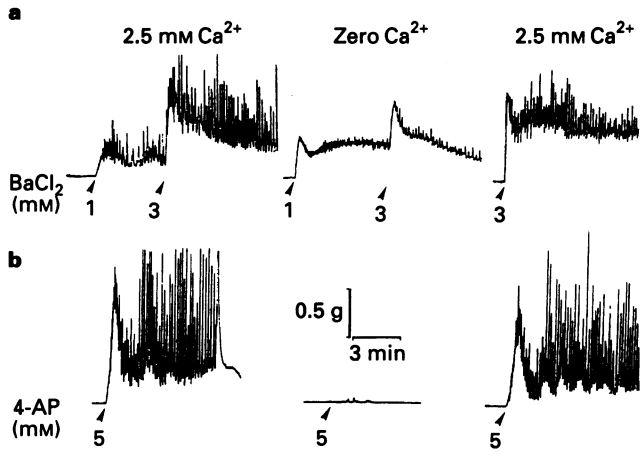

Figure 4 Effect of extracellular calcium on the $BaCl_2$-induced mechanical activity: (a) shows that the phasic activity of the vas deferens was increased by $BaCl_2$ in a concentration-dependent manner in the presence of 2.5 mM extracellular Ca^{2+}. When the vas deferens was incubated in Ca-free Krebs solution for 20 min, the $BaCl_2$-induced increase in the mean amplitude of mechanical activity was much reduced. (b) Shows that the 4-aminopyridine (4-AP)-induced contractions were totally prevented by removal of external Ca^{2+}. Arrows indicate addition of drugs and numbers are concentrations (mM) used.

and presence of external Ca^{2+}. Figure 5b shows that after the vas deferens was incubated in Ca-free solution containing 10 mM procaine for 15 min, its phasic responses to $BaCl_2$ were

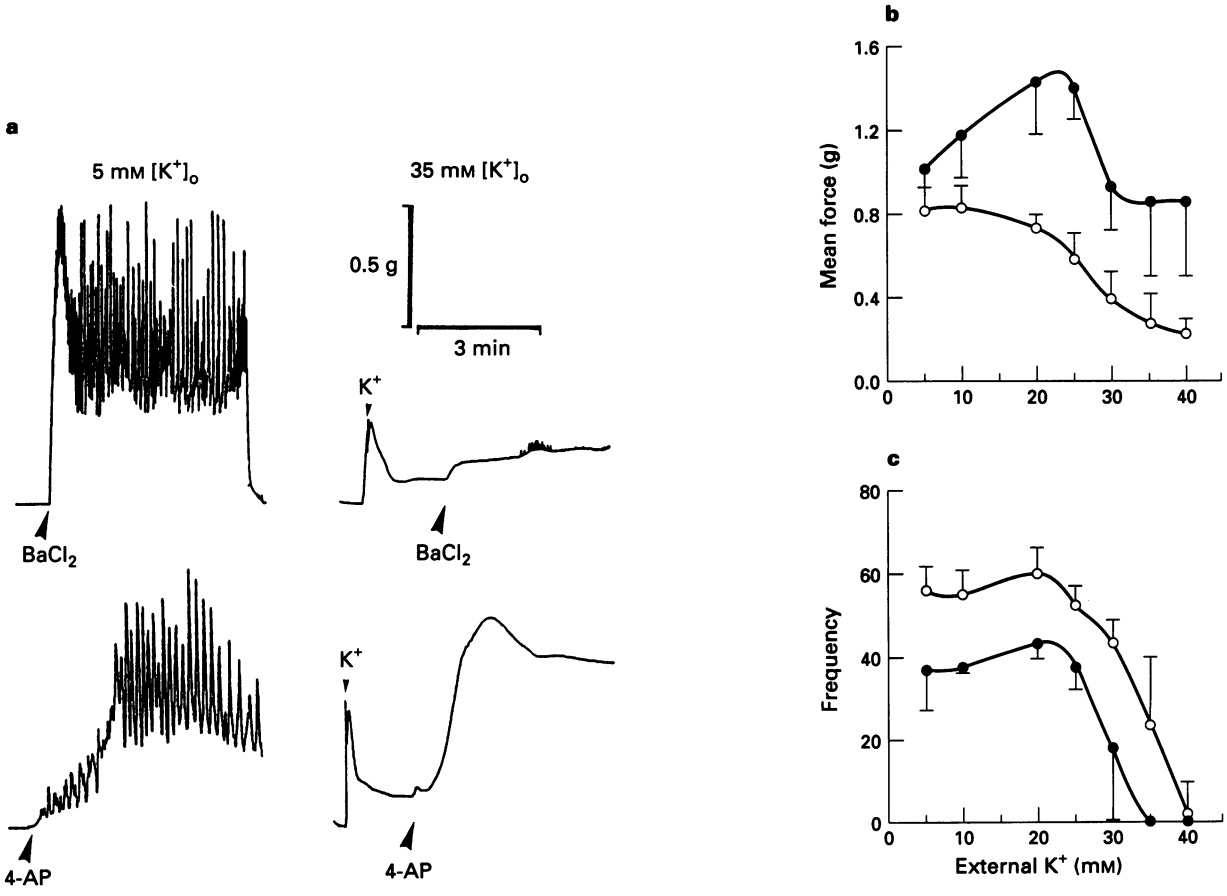

Figure 3 Effect of raised extracellular potassium concentration on the $BaCl_2$- and 4-aminopyridine (4-AP)-induced mechanical activity: (a) shows representative traces of phasic contractions recorded at 5 and 35 mM external K^+ in response to $BaCl_2$ (3 mM) and 4-AP (5 mM). Drugs were added to the bath about 2 min after incubation of the vas deferens in 35 mM K^+ solution. The mean amplitude (b) and frequency (c) of the vas to both $BaCl_2$ (○) and 4-AP (●) decreased with high extracellular K^+ concentration. The mean amplitude and frequency of contractions were recorded at 5 min intervals. Points are mean + s.d. of 5 preparations for $BaCl_2$ and 3 preparations for 4-AP.

almost totally prevented (in two experiments, small tonic contraction less than 100 mg was seen at 5 mM $BaCl_2$). On the other hand, after being incubated for 15 min in solution containing 2.5 mM calcium and 10 mM procaine, the vas deferens still contracted in response to $BaCl_2$ (1–5 mM), but its phasic activity was entirely suppressed (Figure 5a). This effect of procaine was reversible and the second application of $BaCl_2$ after removal of procaine induced a much larger contractile response. Furthermore, 10 mM procaine reduced the amplitude of each contraction induced by $BaCl_2$ and after 8 to

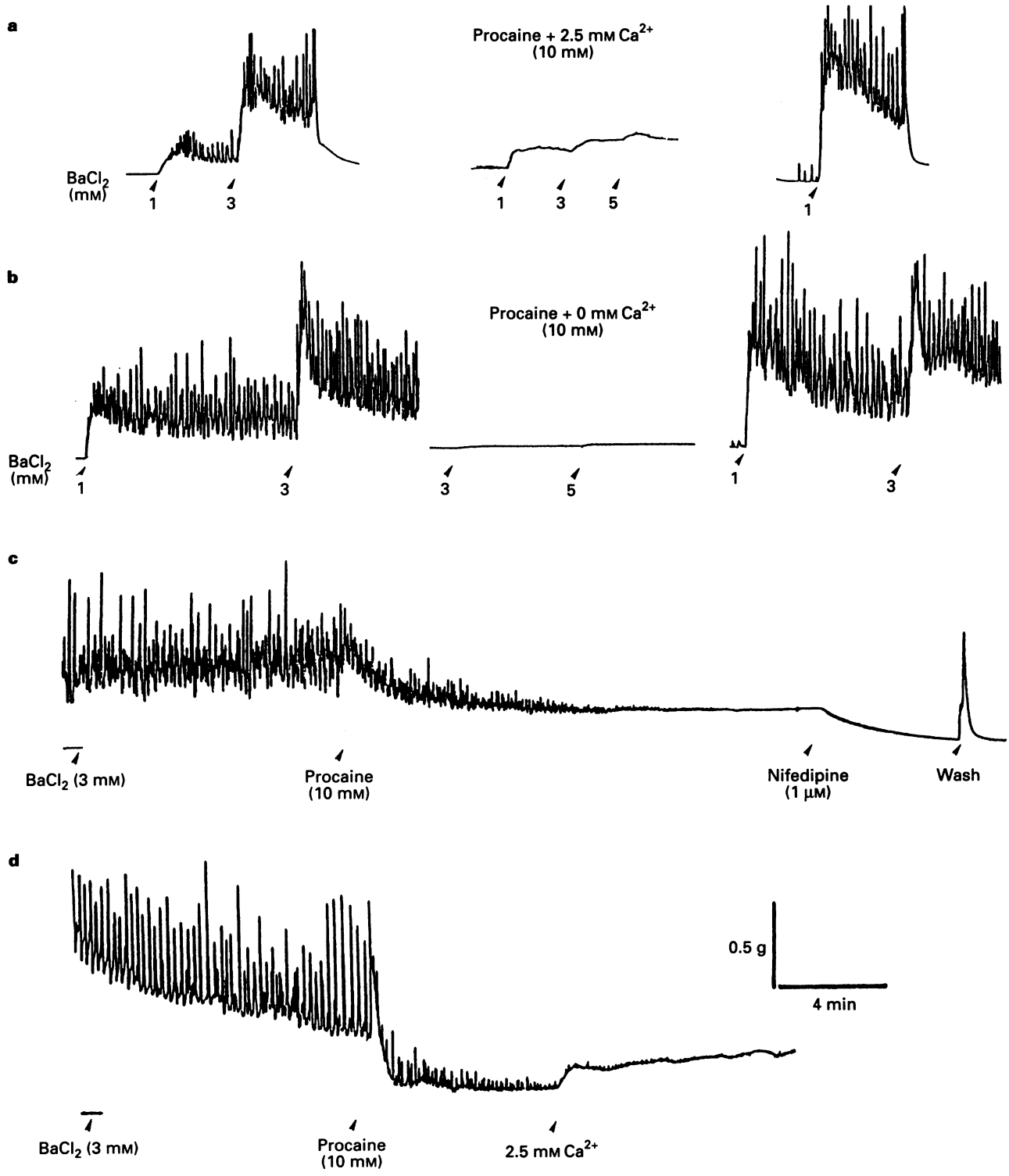

Figure 5 Effect of procaine on the $BaCl_2$-induced mechanical activity: (a) shows 10 mM procaine prevented the $BaCl_2$-evoked phasic activity of vas deferens in normal K-H solution containing 2.5 mM Ca^{2+}. After 15 min incubation with procaine, vas still developed tonic contractions in response to $BaCl_2$ but the amplitude of tonic force was smaller compared to the control value. (b) Shows the $BaCl_2$-induced phasic contractions in the absence of external Ca^{2+} were completely suppressed by 10 mM procaine (15 min incubation). After washout of procaine from the bath with 2.5 mM Ca^{2+}-containing solution, the mean amplitude of mechanical contractions induced by $BaCl_2$ was markedly potentiated. The remaining sustained contraction in the presence of 10 mM procaine was abolished by 1 μM nifedipine (c) or further increased by addition of an extra 2.5 mM Ca^{2+} (d). Arrows indicate the time when $BaCl_2$ was applied and numerals are concentrations (mM) used. Short lines on the left of (c) and (d) indicate the basal tension.

12 min totally suppressed the phasic activity, but also decreased the maintained contraction. The remaining tone was abolished by 1 μM nifedipine (Figure 5c, $n=4$) or increased by addition of an extra 2.5 mM Ca^{2+} (Figure 5d, $n=5$). These results suggest that the $BaCl_2$-evoked phasic mechanical response depends upon intracellular Ca^{2+} whilst the slowly developing tonic contraction depends mainly upon the extracellular source of Ca^{2+} ions.

Effect of tetraethylammonium ions on the $BaCl_2$-induced phasic contractions

To examine the suggestion that Ca^{2+} entry and subsequent Ca^{2+}-induced Ca^{2+} release increased $[Ca^{2+}]_i$, and in turn opened other types of K^+ channels to inhibit Ca^{2+} influx and to relax the contracted muscle, TEA^+ was used as a blocker of Ca^{2+}-activated K^+ channel. At a concentration of 1 mM TEA^+ markedly suppressed the mean amplitude of phasic contractions induced by 3 mM $BaCl_2$ (Figure 6, $n=7$). However, TEA^+ caused a biphasic increase in the tonic tension in the presence of $BaCl_2$, the transient increase of the tone followed by the slowly declining component. TEA^+ by itself, unlike $BaCl_2$ and 4-AP, did not induce any visible activity in the rat vas deferens at concentrations up to 4 mM.

Effect of blockers of neurotransmission on the $BaCl_2$- and 4-AP-evoked phasic activity in the vas deferens

Prazosin (1 μM), yohimbine (3 μM), atropine (3 μM), or propranolol (3 μM) did not significantly affect the $BaCl_2$-induced increase in both the mean amplitude and frequency of mechanical contractions in the rat vas deferens (Table 1), arguing against the possibility that transmitter release from nerve terminals was involved in the $BaCl_2$-induced action. However, 1 μM prazosin, 1 μM yohimbine or 1 μM atropine, but not propranolol (3 μM) inhibited the 4-AP-induced response in the same preparation. Prazosin (1 μM) almost totally blocked 4-AP-induced response. Prazosin (1 μM), yohimbine (1 μM) and atropine (1 μM) were sufficient to prevent or reverse acetylcholine (ACh)-, noradrenaline (NA)- and clonidine-induced vas contractions, respectively (data not shown), including 4-AP might act mainly at nerve terminals to cause possibly periodic release of contractile transmitters. To support the neurogenic effect of 4-AP, 6-OHDA was used to destroy the noradrenergic nerve endings. After chemical denervation with 6-OHDA (0.5 mM, 3 h incubation) 4-AP failed to cause any contraction in the vas deferens. However, $BaCl_2$ (3m M) was still able to generate phasic contractions in the same tissue ($n=4$, data not shown).

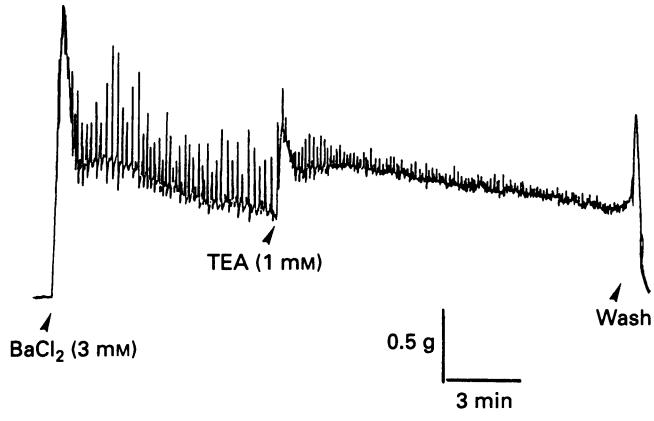

Figure 6 Effect of tetraethylammonium ions on the $BaCl_2$-induced phasic activity: the trace shows a representative example for seven experiments in which 1 mM TEA^+ reduced the amplitude of phasic contractions previously produced by 3 mM $BaCl_2$ but induced a biphasic increase in the sustained component of the contraction.

Effect of the epithelial sheet on the $BaCl_2$-induced mechanical response

In some experiments, the epithelial layer of the epididymal section of the rat vas deferens was removed. The pattern of the response induced by K^+ channel blockers was found to be similar to that observed in the vas deferens containing intact epithelial cells, although the general response was smaller, probably due to the partial damage made to muscle cells by tearing the epithelial sheet off the muscular layers. Also, the reponses to K^+ channel blockers did not change when the vas deferens was cut open through the lumen and placed in an organ bath (data not shown).

Discussion

The present study shows that both $BaCl_2$ and 4-AP, blockers of K^+ channels in mammalian cells, evoked phasic contractions of the rat vas deferens in a concentration-related fashion, but these two blocking agents appear to act through different mechanisms. $BaCl_2$ acted largely upon smooth muscle of the vas deferens. In contrast, 4-AP mainly influenced pre-junctional nerve terminals to release contractile neurotransmitters, predominantly noradrenaline, which in turn produced mechanical activity in the vas deferens. On the other hand, glibenclamide, an ATP-sensitive K^+ channel blocker, TEA^+, a Ca^{2+}-activated K^+ channel blocker, quinine and quinidine, blockers for voltage-dependent K^+ channels did not initiate any rhythmic activity in the rat vas deferens at concentrations much higher than the respective K_d values for inhibition of K^+ channels of vascular smooth muscles (Standen *et al.*, 1989; Huang *et al.*, 1990; Langton *et al.*, 1991). These results suggest

Table 1 Effects of $BaCl_2$ (3 mM) and 4-aminopyridine (4-AP, 5 mM) on phasic contractions of the vas deferens with different treatments

	$BaCl_2$			4-AP		
	Amplitude (g)	*Frequency*	n	*Amplitude (g)*	*Frequency*	n
Control	0.68 ± 0.06	43 ± 6.2	4	0.76 ± 0.14	30 ± 1.7	3
+ Prazosin	0.67 ± 0.09	41.5 ± 7	4	0.24 ± 0.06*	8.3 ± 3.2*	3
Control	0.71 ± 0.12	40.5 ± 4.2	4	0.73 ± 0.2	29.8 ± 1.6	6
+ Atropine	0.69 ± 0.04	38.5 ± 5.2	4	0.43 ± 0.15*	25.8 ± 5.2	6
Control	0.72 ± 0.11	36 ± 1.7	3	0.75 ± 0.17	33 ± 5.2	3
+ Propranolol	0.70 ± 0.06	40 ± 2.6	3	0.81 ± 0.23	30 ± 1	3
Control	0.71 ± 0.12	40 ± 6.2	3	0.85 ± 0.13	30.3 ± 1.2	3
+ Yohimbine	0.68 ± 0.10	40 ± 4.5	3	0.46 ± 0.08*	25.7 ± 3.5	3

Concentrations of drugs used are mentioned in text. The mean amplitude and frequency of phasic contractions were measured 4 min before and after addition of drugs (see methods).
*Significantly different compared to the control value ($P<0.05$) in paired data.

that neither the ATP-sensitive, Ca^{2+}-activated nor quinine-sensitive K^+ channels were likely to be involved in maintenance of the resting membrane potentials in smooth muscle or nerve endings of the rat vas deferens.

K^+ channels are present in virtually all mammalian cell types and some of them are believed to play an important role in controlling the resting membrane potential (Rudy, 1988). Ba^{2+} is found to be rather a non-selective blocking agent, effective for ATP-sensitive K^+ channels at submillimolar concentrations (Standen *et al.*, 1989; Quast, 1993) and for voltage-dependent Ca^{2+}-sensitive K^+ channels at higher concentrations in some other cell types (Rudy, 1988). 4-AP mainly affects voltage-dependent K^+ channels and some agonist-stimulated K^+ channels on nerves (Latorre *et al.*, 1989). If these channels are partially open in the resting condition, their blockade would depolarize the cell membrane. The depolarization favours the opening of voltage-dependent Ca^{2+} channels and the resultant increase in Ca^{2+} influx would lead to muscle contraction. Indeed, moderate K^+ (> 35 mM) caused a small tonic but not phasic contraction in the vas deferens. On the other hand, it would be predictable that contractions caused by K^+ channel blockers would be increasingly reduced by simply raising the extracellular K^+ concentration since the membrane potential (V_m) moves towards the new K^+ equilibrium potential and then the blocker has very little influence on V_m. Indeed, the $BaCl_2$-induced phasic contractions almost disappeared when the bath potassium was raised above 40 mM. This suggests that some Ba^{2+}-sensitive K^+ channels are active on smooth muscle at rest and the $BaCl_2$-induced activity in the vas deferens is probably mediated by their inhibition. 4-AP might predominantly block K^+ channels in nerve endings supplying the wall of the vas deferens (see below). Raising external K^+ over 35 mM abolished the 4-AP-induced phasic contractions but enhanced the maintained force that was sensitive to inhibition by 1 μM prazosin, indicating that 4-AP was still able to release transmitters from the depolarised nerve. The potentiation of 4-AP-induced tonic contraction by high K^+ may be caused by increased sensitivity or efficacy of transmitters on muscle fibres in the depolarized state. It has previously been observed that high K^+ potentiated NA-induced contraction in the vascular smooth muscle probably by shifting the activation curve for Ca^{2+} channels in the negative direction (Nelson *et al.*, 1988).

The present results have demonstrated that 4-AP acted primarily on the nerve terminals, which liberated neurotransmitters to act on muscle fibres. The α_1-adrenoceptor antagonist, prazosin, effectively blocked and α_2-adrenoceptor blocker, yohimbine and cholinoceptor antagonist, atropine significantly diminished the 4-AP-induced phasic contractions. Further support came from the experiments using 6-OHDA to impair the sympathetic activity. 4-AP did not induce any contraction in the vas deferens after 6-OHDA treatment. In contrast to the pre-junctional action of 4-AP, the $BaCl_2$-evoked phasic contractions were insensitive to either adrenergic or cholinergic blockers.

The $BaCl_2$-induced muscle contractions consist of two components, a phasic activity superimposed upon a sustained contraction. The present study has demonstrated that entry of extracellular Ca^{2+} accounts in major part for the $BaCl_2$-induced sustained force and possibly for the Ca^{2+}-induced Ca^{2+} release which subsequently causes phasic contractions. Removal of external Ca^{2+} markedly reduced the mean amplitude of phasic contractions induced by $BaCl_2$ but unexpectedly had a smaller effect on the level of tonic tension. It is unlikely that Ba^{2+} at the concentration used in these experiments plays the same role as Ca^{2+} in many physiological processes such as inactivation of Ca^{2+} channels (Bean, 1989) and uptake into the sarcoplasmic reticulum (Weiss *et al.*, 1985) in spite of the fact that Ba^{2+} can pass through Ca^{2+} channels as easily as Ca^{2+}. Ba^{2+} was much less effective in developing the muscle tension than Ca^{2+}. It has been shown that in comparison to Ca^{2+}, an approximately 20 times greater concentration of Ba^{2+} was needed to generate 50% maximum contraction with elevated external K^+ (Baba *et al.*, 1985). The $BaCl_2$-induced phasic activity of the vas deferens was entirely prevented by procaine at the concentration previously found to inhibit intracellular Ca^{2+} mobilization in smooth muscle cells (Itoh *et al.*, 1981; Ahn & Karaki, 1988; Breemen & Saida, 1989). Procaine has recently been reported to abolish NA-elicited ^{45}Ca-efflux (as an indication of intracellular Ca^{2+} release), and the increase in phosphatidylinositol turnover and contractions in rat vas deferens (Khoyi *et al.*, 1993). In the presence of procaine, the remaining sustained tone can be abolished by dihydropyridine Ca^{2+} channel antagonists or by removal of Ca^{2+} from the extracellular medium, and increased by the addition of an extra Ca^{2+}. This implies that procaine did not inhibit voltage-dependent Ca^{2+} channels even though this has been suggested in vascular and intestinal smooth muscles (Ahn & Karaki, 1988). The evidence provided here and by others argue in support of the hypotheses that procaine primarily acts to block Ca^{2+} release from internal stores.

Taken together, I propose the following sequence of events possibly involved in the $BaCl_2$-induced response in the rat vas deferens. $BaCl_2$ first blocks the Ba^{2+}-sensitive K^+ channels on the plasma membrane of smooth muscle and the ensuing membrane depolarization activates the voltage-dependent Ca^{2+} channels. Ca^{2+} entry increases the intracellular Ca^{2+} levels which might have two consequent effects, to initiate tonic contraction and to stimulate internal Ca^{2+} release and thus the rising phase of the phasic contraction. The falling phase of the phasic contraction may be caused by the following mechanisms leading to lowered $[Ca^{2+}]_i$: (i) depletion of Ca^{2+} store; (ii) Ca^{2+}-induced Ca^{2+} inactivation, (iii) increased Ca^{2+} uptake and extrusion; and (iv) opening of K^+ channels which are activated by both membrane depolarization and increased intracellular Ca^{2+} concentration leading to membrane hyperpolarization and thus inhibition of Ca^{2+} entry. It is possible that all these pathways work together to reduce the cytoplasmic free Ca^{2+} levels. However, the present results show the involvement of Ca^{2+}-activated K^+ channels in the falling phase of phasic contraction. TEA^+, an open channel blocker for Ca^{2+}-activated K^+ channel when used at concentration of 1 mM, greatly reduced the mean amplitude and frequency of muscle contractions, whereas it increased the sustained contraction induced by $BaCl_2$. I also showed that TEA^+ did not influence the basal tension even at higher concentration (up to 4 mM). These processes repeat as long as $BaCl_2$ is present in the extracellular medium. In the absence of external calcium, $BaCl_2$ has a second function and can enter the plasma membrane via Ca^{2+} channels as easily as Ca^{2+} to replace the cytoplasmically bound Ca^{2+}. This small increase in the intracellular Ca^{2+} concentration is seemingly sufficient to initiate internal Ca^{2+} release (Berridge, 1993) but only to lesser degree, which can be completely inhibited by procaine.

In summary, the present results provide further evidence that both the membrane potential and Ca^{2+}-induced Ca^{2+} release are required for generation of phasic contractions of the rat vas deferens in the presence of some K^+ channel blockers; Ca^{2+} entry through Ca^{2+} channels as a result of blockade of K^+ channels might serve as the primary step for events leading to these muscle contractions.

The author wishes to thank Professor P.Y.D. Wong for critically reading the manuscript and Mr C.W. Lau for excellent technical assistance. This work was supported by a departmental grant from the Chinese University of Hong Kong and the CUHK Direct Grant (A/C 220403490).

References

AHN, H.Y. & KARAKI, H. (1988). Inhibitory effect of procaine on contraction and calcium movement in vascular and intestinal smooth muscles. *Br. J. Pharmacol.*, **94**, 789–796.

BABA, K., KAWANISHI, M., SATAKE, T. & TOMITA, T. (1985). Effects of verapamil on the contractions of guinea-pig tracheal muscle induced by Ca, Sr and Ba. *Br. J. Pharmacol.*, **84**, 203–211.

BEAN, B.P. (1989). Classes of calcium channels in vertebrate cells. *Annu. Rev. Physiol.*, **51**, 367–384.

BERRIDGE, M.J. (1993). Inositol trisphosphate and calcium signalling. *Nature*, **361**, 315–325.

BREEMEN, C. VAN. & SAIDA, K. (1989). Cellular mechanisms regulating $[Ca^{2+}]_i$ in smooth muscle. *Annu. Rev. Physiol.*, **51**, 315–329.

HUANG, Y., LANGTON, P., HESCHELER, J., STANDEN, N. & NELSON, M. (1990). External TEA^+ block of Ca^{2+}-activated K^+ channels of arterial smooth muscle. *Biophys. J.*, **57**, 315a.

ITOH, T., KURIYAMA, H. & SUZUKI, H. (1981). Excitation-contraction coupling in smooth muscle cells of the guinea-pig mesenteric artery. *J. Physiol.*, **321**, 513–535.

JANSSEN, L.J. & DANIEL, E.E. (1991). Depolarizing agents induce oscillations in canine bronchial smooth muscle membrane potential: possible mechanisms. *J. Pharmacol. Exp. Ther.*, **259**, 110–117.

KHOYI, M.A., DALZIEL, H.H., ZHANG, L., BJUR, R.A., GERTHOFFER, W.T., BUXTON, I.L.O. & WESTFALL, D.P. (1993). $[Ca^{2+}]_i$-sensitive, IP_3-independent Ca^{2+} influx in smooth muscle of rat vas deferens revealed by procaine. *Br. J. Pharmacol.*, **110**, 1353–1358.

LAMB, F.S., MYERS, J.H., HANLIU, M.N. & WEBB, R.C. (1985). Oscillatory contractions in tail arteries from genetically hypertensive rat. *Hypertension*, **7**, 125–130.

LANGTON, P.D., NELSON, M.T., HUANG, Y. & STANDEN, N.B. (1991). Block of calcium-activated potassium channels in mammalian arterial myocytes by tetraethylammonium ions. *Am. J. Physiol.*, **260**, H927–H934.

LATORRE, R., OBERHAUSER, A., LABARCA, P. & ALVAREZ, O. (1989). Varieties of calcium-activated potassium channels. *Annu. Rev. Physiol.*, **51**, 385–399.

LEIJTEN, P.A.A. & BREEMEN, C. VAN. (1986). The relationship between noradrenaline-induced contraction and ^{45}Ca efflux stimulation in rabbit mesenteric artery. *Br. J. Pharmacol.*, **89**, 739–747.

LYDRUP, M.-L. (1991). Role of K^+ channels in spontaneous electrical and mechanical activity of smooth muscle in the guinea-pig nesotubarium. *J. Physiol.*, **433**, 327–340.

MITRA, R. & MORAD, M. (1985). Ca^{2+} and Ca^{2+}-activated K^+ channels from mammalian gastric smooth muscles. *Science*, **229**, 269–272.

NELSON, M.T., STANDEN, N.B., BRAYDEN, J.E. & WORLEY, J.F. (1988). Noradrenaline contracts arteries by activating voltage-dependent calcium channels. *Nature*, **336**, 382–385.

OMETO, M., KAJIMOTO, N. & MIZUSAWA, H. (1993). The ionic mechanism of phenylephrine-induced rhythmic contractions in rabbit mesenteric arteries treated with ryanodine. *Acta Physiol. Scand.*, **147**, 9–13.

QUAST, U. (1993). Do the K^+ channel openers relax smooth muscle by opening K^+ channel? *Trends Pharmacol Sci.*, **14**, 332–337.

RUDY, B. (1988). Diversity and ubiquity of K channels. *Neuroscience*, **25**, 729–749.

STANDEN, N., QUAYLE, J., DAVIES, N., BRAYDEN, J., HUANG, Y. & NELSON, M. (1989). Hyperpolarizing vasodilators activate ATP-sensitive K^+ channels in arterial smooth muscle. *Science*, **245**, 177–180.

SUZUKI, K., ITO, K.M., MINAYOSHI, Y., SUZUKI, H. & ASANO, M. (1993). Modification by charybodotoxin and apamin of spontaneous electrical and mechanical activity of the circular smooth muscle of the guinea-pig stomach. *Br. J. Pharmacol.*, **109**, 661–666.

WEISS, G.B., PANG, I.H. & GOODMAN, F.R. (1985). Relationship between ^{45}Ca movements, different calcium components, and responses to acetylcholine and potassium in tracheal smooth muscle. *J. Pharmacol. Exp. Ther.*, **233**, 389–394.

(Received February 17, 1995
Accepted March 8, 1995)

British Journal of Pharmacology (1995) 115, 852-858

Role of nitric oxide in learning and memory and in monoamine metabolism in the rat brain

Kiyofumi Yamada, Yukihiro Noda, Shinobu Nakayama, *Yumiko Komori, *Hisayoshi Sugihara, Takaaki Hasegawa & [1]Toshitaka Nabeshima

Department of Neuropsychopharmacology and Hospital Pharmacy, Nagoya University School of Medicine, Nagoya 466, Japan and *Department of Microbiology, Faculty of Pharmacy, Meijo University, Nagoya 468, Japan

1 We investigated the effects of N^G-nitro-L-arginine methyl ester (L-NAME), an inhibitor of nitric oxide (NO) synthase, on the performance of rats in a radial arm maze and in habituation tasks, and on monoamine metabolism in the brain.

2 Daily administration of L-NAME (10-60 mg kg^{-1}) resulted in a dose-dependent impairment of performance during the acquisition of the radial arm maze task, while it failed to affect performance in those rats that had previously acquired the task.

3 The rate of decrease in locomotor activity in the habituation task in the L-NAME-treated rats was significantly less than that in control rats.

4 N^G-nitro-D-arginine methyl ester (D-NAME, a less active inhibitor of NO synthase) showed no effects in the above behavioural tasks.

5 NO synthase activity was significantly decreased in both the L-NAME and D-NAME-treated rats, with the magnitude of inhibition being greater in the L-NAME-treated animals.

6 The content of 5-hydroxyindoleacetic acid (5-HIAA) in the hippocampus and the 5-HIAA/5-hydroxytryptamine ratio in the hippocampus and cortex were significantly decreased in the L-NAME (60 mg kg^{-1})-treated rats compared with these values in the controls.

7 Striatal 3,4-dihydroxyphenylacetic acid (DOPAC) content was significantly increased in the L-NAME (60 mg kg^{-1})-treated rats compared with the values in the controls, while the DOPAC/dopamine ratio was not changed.

8 These results suggest that: (i) NO may play an important role in performance during the acquisition, but not retention, of the radial arm maze task, and (ii) that endogenous NO may be involved in the regulation of monoamine metabolism.

Keywords: Nitric oxide; nitric oxide synthase; learning and memory; radial arm maze; habituation task; dopamine; 5-hydroxytryptamine

Introduction

Nitric oxide (NO) plays an important role in several biological systems (Moncada *et al.*, 1989; Ignarro, 1990; Garthwaite, 1991). In the central nervous system, this free radical gas acts as a diffusible intercellular signalling molecule (Bredt & Snyder, 1992; Snyder, 1992). NO is synthesized from L-arginine, in a NADPH-dependent reaction, by NO synthase. Neuronal and endothelial NO synthases appear to be constitutive calcium-dependent enzymes, whereas other NO synthase isozymes, i.e., those found in smooth muscle and macrophages, are expressed as a result of activation by various cytokines and are calcium-independent (Garthwaite, 1991; Dawson & Snyder, 1994). The localization of a brain-specific isozyme of NO synthase suggests that NO has widespread action in the central nervous system (Vincent & Kimura, 1992; Southam & Garthwaite, 1993).

Activation of N-methyl-D-aspartate (NMDA) receptors has been shown to induce NO synthesis (Garthwaite *et al.*, 1988), which then activates soluble guanylate cyclase (Knowles *et al.*, 1989) and leads to the formation of guanosine 3',5'-cyclic monophosphate (cyclic GMP) in the brain (Bredt & Snyder, 1989; Garthwaite *et al.*, 1989, East & Garthwaite, 1991). Further, recent studies have demonstrated the feedback inhibition of NMDA receptors by NO (Lei *et al.*, 1992; Manzoni *et al.*, 1992; Lipton *et al.*, 1993). Experimental evidence has demonstrated that NO is involved in NMDA receptor-mediated neurotoxicity (Dawson *et al.*, 1991; 1993; Haberny *et al.*, 1992) and convulsions (Nakamura *et al.*, 1995), and in the neuronal death that occurs after focal cerebral ischaemia (Nowicki *et al.*, 1991; Caldwell *et al.*, 1994). The involvement of NO has also been demonstrated in the mechanisms of synaptic plasticity, including long-term potentiation (LTP) in the hippocampus (O'Dell *et al.*, 1991; Schuman & Madison, 1991; Bannerman *et al.*, 1994b), learning and memory (Chapman *et al.*, 1992; Böhme *et al.*, 1993; Hölscher & Rose, 1993; Bannerman *et al.*, 1994a), tolerance to ethanol (Khanna *et al.*, 1993) and to the antinociceptive effects of morphine (Rauhala *et al.*, 1994), and behavioural sensitization to cocaine (Pudiak & Bozarth, 1993).

Regarding the involvement of NO in learning and memory, the systemic administration of NO synthase inhibitors such as N^G-nitro-L-arginine methyl ester (L-NAME) has been shown to impair spatial learning in rats in both a radial arm maze (Böhme *et al.*, 1993) and in the Morris water maze tasks (Chapman *et al.*, 1992; Bannerman *et al.*, 1994a), to impair olfactory memory in a social recognition test (Böhme *et al.*, 1993), and to produce learning deficits in both the conditioned eyeblink response in rabbits (Chapman *et al.*, 1992) and in a passive avoidance task in chicks (Hölscher & Rose, 1993). Although L-NAME has been shown to impair performance during the acquisition but not retention of the Morris water maze task (Chapman *et al.*, 1992; Bannerman *et al.*, 1994a), it has yet to be elucidated which learning processes are impaired in other tasks by the inhibition of NO synthase.

In the present study, we investigated the effects of L-NAME, a potent inhibitor of NO synthase (Dwyer *et al.*, 1991), on performance during the acquisition and retention of

[1] Author for correspondence.

a radial arm maze task in a habituation task in rats, comparing these effects with those of N^G-nitro-D-arginine methyl ester (D-NAME; a less active enantiomer of L-NAME). We also determined NO synthase activity in the brains of rats that had been treated repeatedly with these inhibitors. Further, since NO has been shown to stimulate the release of various neurotransmitters, such as glutamic acid, noradrenaline (Montague *et al.*, 1994), and dopamine (Hanbauer *et al.*, 1992; Zhu & Luo, 1992), we measured the content of dopamine, 5-hydroxytryptamine (5-HT), and their metabolites in the brains of the rats treated with NO synthase inhibitors.

Methods

The animals used in the present study were males of the Wistar strain (8 weeks old; Nihon SLC Co., Shizuoka, Japan) weighing 230±280 g. All animals were kept in a regulated environment (23±0.5°C; 50±0.5% humidity) with a 12 h light/dark cycle (light on between 09 h 00 min and 21 h 00 min) and had free access to food and water.

L- and D-NAME, pepstatin A, leupeptin, phenylmethylsulphonyl fluoride, calmodulin, and β-NADPH were purchased from Sigma (St. Louis, MO, U.S.A.). L-[2, 3, 4, 5-^{3}H]-arginine (37 MBq ml^{-1}) was obtained from Amersham (Arlington Heights, IL, U.S.A.). L- and D-NAME were dissolved in saline and administered i.p. in an injection volume of 1 ml kg^{-1}.

All experiments were performed in accordance with the Guidelines for Animal Experiments of the Nagoya University School of Medicine.

Experimental schedule

To investigate the effects of L- and D-NAME on learning and memory, we performed two series of experiments. In the first series, groups of 10 to 12 rats were used, and the effects of NO synthase inhibitors on the acquisition of spatial memory were examined in a radial arm maze task. A habituation task was carried out after the radial arm maze task. The animals were allowed to explore the radial arm maze freely for two days, and were then subjected to training trials in the radial arm maze task once a day for 10 consecutive days. The administration of NO synthase inhibitors was initiated on the first day of exploration of the radial arm maze, and continued until the behavioural tasks were completed. The agents were administered every day, 1 h prior to the behavioural test. Following the radial arm maze task, rats were given food freely for 2 days, during which drug administration was continued, and they were then subjected to the habituation task for 3 days. On the day after completion of the habituation task, the rats were killed 1 h after drug administration, and NO synthase activity and the content of monoamines and their metabolites in the brain were determined. The locomotor activity was also measured during the first 3 days of the L-NAME injection in naive rats which had not previously been subjected to the radial arm maze task.

In the second series of experiments, the effects of NO synthase inhibitors on the retention of spatial memory in the radial arm maze task were examined in 12 rats. The animals were initially subjected to training trials in the radial maze task for 14 days. They then received saline administration daily for 2 days 1 h prior to the trial, to determine the baseline performance. The rats were then divided into 2 groups, one group receiving L-NAME administered daily and one receiving D-NAME, at increasing doses, from 1 to 100 mg kg^{-1}. The effect of each dose was measured for 2 days. After the measurement of performance in the radial arm maze task, animals were killed and NO synthase activity was determined.

Radial arm maze task

The maze used in the present study consisted of eight arms (48 × 12 cm) extending radically from a central area (32 cm in diameter), with a 5 cm edge around the apparatus. The apparatus was placed 40 cm above the floor. At the end of each arm there was a food cup that held a single 50 mg food pellet. Prior to the performance of the maze task, the animals were kept on a restricted diet and body weight was maintained at 85% of their free-feeding weight over a 1 week period, with water being available *ad libitum*.

Before the actual training began, the animals were allowed to explore the apparatus, in groups of four, for 2 days. Following this habituation period, each animal was placed individually in the centre of the maze and allowed to consume the bait in the food cup. The training trial continued until all the bait in the food cup had been consumed or until 5 min had elapsed. An arm entry was counted when all four limbs of the rat were within an arm. Reentry in an already visited arm was regarded as an error. For each daily trial, the total number of errors and the time taken to consume all the bait were recorded. The number of initial correct responses (ICR), defined as the number of successive correct responses made until an error was made, was also measured.

Habituation task

The animals were placed individually in a plastic cage (27 × 45 × 36 cm) and their locomotor activity was recorded with a Scanet device (SV-10; Toyo Sangyou, Toyama, Japan) for 10 min. The measurement of locomotor activity was repeated for 3 days; the rate of decrease in locomotor activity due to repeated placement in the same environment was regarded as an experimental model of the memory process (Platel & Porsolt, 1982; Nitta *et al.*, 1994).

NO synthase assay

On the day after completion of the habituation tasks, the rats were killed 1 h after drug administration, and NO synthase activity and the content of monoamines and their metabolites in the brain were determined. The brains were dissected into four regions, the cerebral cortex, striatum, hippocampus, and the thalamus/hypothalamus, after which they were rapidly frozen and stored in a deep freezer at −80°C until assayed.

Brain NO synthase activity was determined as described previously (Bredt & Snyder, 1989), with a minor modification (Komori *et al.*, 1993). The brains were homogenized in 5 vol. (w/v) of 50 mM Tris-HCl buffer (pH 7.4) containing 0.1 mM EGTA, 0.1 mM EDTA, 1 μM pepstatin, 2 μM leupeptin, 1 mM phenylmethylsulphonyl fluoride, and 0.5 mM dithiothreitol. The homogenates were centrifuged at 20,000 *g* for 45 min and the supernatants were used in the assay. The NO synthase activity was measured by monitoring the conversion of [^{3}H]-arginine to [^{3}H]-citrulline. Briefly, the supernatants were incubated for 12 min at 37°C in a final volume of 100 μl, containing 100 μM NADPH, 50 μM L-arginine, 2 mM $CaCl_2$, 0.3 μg calmodulin, 10 μM tetrahydrobiopterin, and 200,000 d min^{-1} of L-[^{3}H]-arginine. The assays were terminated by the addition of 2 ml of ice-cold acetate buffer (pH 5.5) containing 1 mM citrulline, 2 mM EDTA, and 0.2 mM EGTA. The samples were applied to 1 ml columns of Dowex AG50W-X8 (Na^+ form) and the eluate was collected. The columns were then further eluted with 2 ml of water. [^{3}H]-citrulline in the combined eluate was quantified by liquid scintillation spectrometry. Protein content was determined according to the method of Lowry *et al.* (1951), with bovine serum albumin used as a standard.

Determination of monoamines and their metabolites

The content of dopamine, 3,4-dihydroxyphenylacetic acid (DOPAC), homovanillic acid (HVA), 5-HT, and 5-hydroxyindoleacetic acid (5-HIAA) was determined with a high-performance liquid chromatography (h.p.l.c.) system with an electrochemical detector (Eicom, Kyoto, Japan), as described previously by Nitta *et al.* (1992).

Statistical analysis

Results were expressed as means ± s.e. The statistical significance was assessed by one-way ANOVA, followed by the Bonferroni test. The χ^2 test was also utilized, to assess the effects of NO synthase inhibitors on performance in the habituation task.

Results

Effects of L- and D-NAME on performance in the radial arm maze task

The daily administration of L-NAME (10–60 mg kg^{-1}) resulted in a dose-dependent impairment of performance during the acquisition of the radial arm maze task, as revealed by the increased number of errors (Figure 1a). Further, the time taken to complete the task was significantly prolonged by treatment with L-NAME (60 mg kg^{-1}) (Figure 1b). D-NAME (60 mg kg^{-1}) had no effect on the performance during the acquisition of the task (Figure 1a,b). When rats were first subjected to the training trials for 14 days before the drug administration, the mean number of errors decreased to less than 1.0 and the mean number of ICR increased to more than 7.0. In these rats, which we considered to have acquired spatial memory in the radial maze task, neither L-NAME nor D-NAME, at doses up to 100 mg kg^{-1}, had no effect on the performance, as indicated by the lack of change in the number of errors or the mean number of ICR (Figure 2).

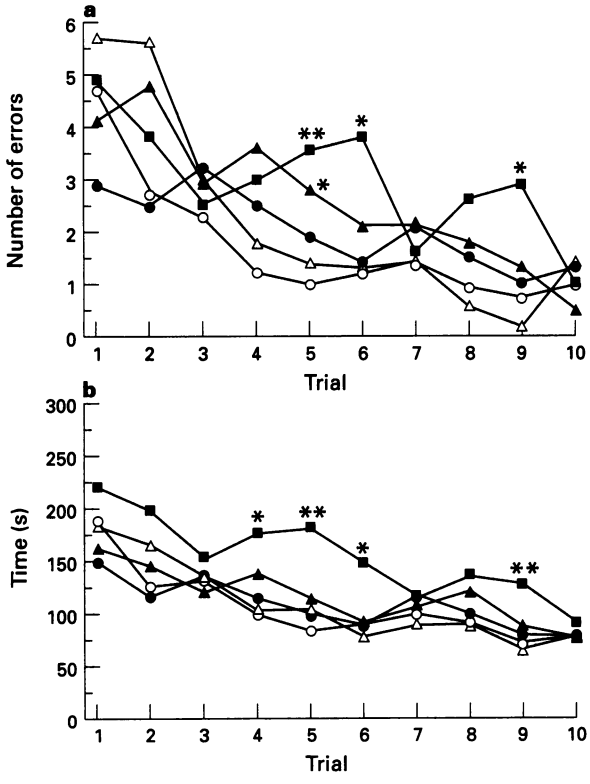

Figure 1 Effects of N^G-nitro-L-arginine methyl ester (L-NAME) and D-NAME on the performance during the acquisition of spatial learning in the radial arm maze in rats. The training trial continued until all bait in the food cup had been consumed or until 5 min had elapsed. Re-entry in an already visited arm was regarded as an error. For each daily trial, the total number of errors (a) and the time taken to complete the task (b) were recorded. Saline (control; ○), L-NAME (10 mg kg^{-1}; ●, 30 mg kg^{-1}; ▲, 60 mg kg^{-1}; ■) and D-NAME (60 mg kg^{-1}; △) were administered i.p. 1 h before the trials every day. Each value represents the mean for 10 rats, except in the L-NAME (60 mg kg^{-1})-treated group, in which 12 rats were used. $*P<0.05$; $**P<0.01$ vs saline-treated control group.

Effects of L- and D-NAME on performance in the habituation task

In rats treated with either L-NAME (10–60 mg kg^{-1}) or D-NAME (60 mg kg^{-1}) for 14 days, the locomotor activity on the first day in the habituation task did not differ from that in vehicle-treated control rats (Table 1). On the 2nd and 3rd days of the test, the locomotor activity in the vehicle-treated control rats decreased significantly, to approximately 65% and 50%, respectively, of that on the 1st day. The rate of decrease in locomotor activity in the L-NAME-treated rats on the 2nd and 3rd days was less than that in the control, but the effect was not statistically significant (Table 1). However, when the number of rats in which locomotor activity on the 2nd or 3rd day was less than 50% of the initial level was calculated, this number was found to be significantly less in the L-NAME (60 mg kg^{-1})-treated group than in the vehicle-treated control group. D-NAME (60 mg kg^{-1}) treatment had no effect on the performance of rats in this task (Table 1).

In contrast to the effects of successive administration of L-NAME, acute injection of L-NAME (60 mg kg^{-1}) produced a significant decrease in the locomotor activity to 45% of the control. The same dose of D-NAME had no effect on the locomotor activity. On the 2nd and 3rd days of the test, however, the locomotor activity in rats treated with L-NAME (60 mg kg^{-1}) did not differ from that in the vehicle-treated control rats (data not shown).

Effects of repeated administration of L- and D-NAME on NO synthase activity

Figure 3 shows the effects of daily administration of L- and D-NAME for 18 days on NO synthase activity *in vitro*. NO synthase activity in the discrete brain regions examined, i.e., the cerebral cortex, hippocampus, striatum, and the thalamus/hypothalamus, was significantly decreased in the L-NAME (60 mg kg^{-1})-treated rats, being 20% of the activity in the vehicle-treated controls. Although NO synthase activity was reduced to approximately 35% of the control level in the D-NAME (60 mg kg^{-1})-treated rats, the magnitude of the inhibition was significantly greater in the L-NAME-treated rats than in the D-NAME-treated animals.

A similar reduction of NO synthase activity in the brain was

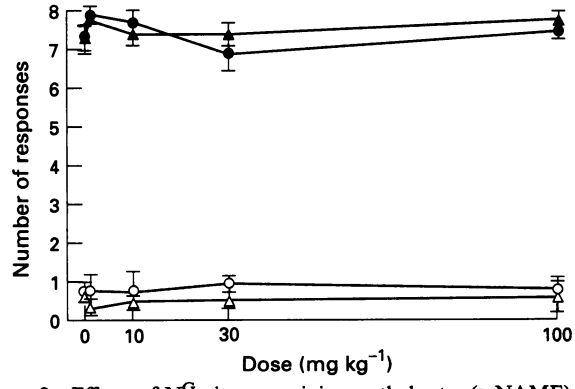

Figure 2 Effects of N^G-nitro-L-arginine methyl ester (L-NAME) and D-NAME on the performance during the retention of spatial memory in the radial arm maze task in rats. Animals were initially subjected to training trials in the radial arm maze task for 14 days. They then received saline injections for 2 days, 1 h before the trial, to determine the baseline performance. Following the measurement of the baseline performance, the rats received either L- or D-NAME, administered daily, at increasing doses from 1 to 100 mg kg^{-1}. The effects of each dose were measured for 2 days. The number of errors (△, ○) and the initial correct response (ICR, ▲, ●), defined as the number of successive correct responses made until an error was made, were determined. Each value represents the mean ± s.e. for 6 rats. Neither L- (○, ●) nor D-NAME (△, ▲) had a significant effect on the number of errors or on the ICR.

Table 1 Effects of repeated administration of N^G-nitro-L-arginine methyl ester (L-NAME) and D-NAME on the performance of rats in the habituation task

Treatment	Dose (mg kg^{-1})	n	Locomotor activity 1st day Counts	2nd day % of activity on the 1st day		3rd day % of activity on the 1st day	
Control		10	1167±137	64.9±5.2	(3/10)	52.8±7.1	(5/10)
L-NAME	10	10	1532±156	67.3±9.3	(3/10)	64.4±8.9	(3/10)
	30	10	1258±94	83.7±7.7	(0/10)	72.3±6.6	(2/10)
	60	10	1266±61	82.8±4.4	(0/11*)	72.7±4.8	(0/10**)
D-NAME	60	11	1158±132	71.3±5.4	(1/10)	66.2±6.7	(2/10)

Locomotor activity of rats was recorded for 10 min once a day for 3 days. Locomotor activity on the 2nd and 3rd days was expressed as a percentage of the activity on the 1st day. Each value represents the mean±s.e. Numbers in parentheses represent numbers of animals in which the locomotor activity was reduced to less than 50% of the activity on the 1st day/numbers of animals examined. *$P<0.05$; **$P<0.01$ *vs* saline-treated group ($\chi 2$ test).

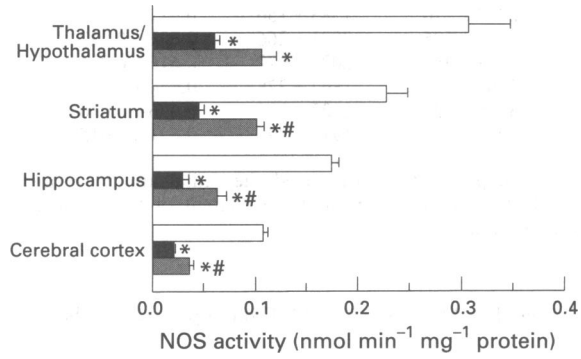

Figure 3 Effects of daily administration of N^G-nitro-L-arginine methyl ester (L-NAME) and D-NAME for 18 days on NO synthase activity in the brain. Rats were killed 1 h after the last administration. NO synthase activity was measured by monitoring the conversion of [^{3}H]-arginine to [^{3}H]-citrulline, as described in Methods. Each value represents mean±s.e. (($n=5$ in the control (open column) and D-NAME-treated (60 mg kg^{-1}; stippled column) groups, and $n=6$ in the L-NAME-treated group (60 mg kg^{-1}; solid column)). *$P<0.05$ vs control; #$P<0.01$ vs L-NAME-treated group.

observed in rats treated with increasing doses of L- and D-NAME, from 1 to 100 mg kg^{-1}, each dose being injected for 2 days. The NO synthase activity in the cerebral cortex, hippocampus, and the striatum in the L-NAME-treated rats was reduced, being 11.2%, 9.2%, and 11.9% of the control value, respectively, while the activity in the D-NAME-treated rats was 19.6%, 14.4% and 19.9% of the control values, respectively.

Effects of repeated administration of L- and D-NAME on the content of dopamine and 5-HT and their metabolites in the brain

Tables 2 and 3 show the effects of the daily administration of L- and D-NAME for 18 days on the metabolism of 5-HT and dopamine, respectively, in the brain. The content of 5-HIAA in the hippocampus and the 5-HIAA/5-HT ratio in the hippocampus and the cerebral cortex were significantly decreased in the L-NAME (60 mg kg^{-1})-treated rats, compared with these values in the vehicle-treated control rats, while pretreatment with D-NAME (60 mg kg^{-1}) had no effect (Table 2). In other brain regions, i.e., in the striatum and thalamus/hypothalamus, neither L-NAME nor D-NAME had any significant effect on the metabolism of 5-HT (Table 2).

The content of DOPAC in the striatum, but not in other brain regions, in rats treated with L-NAME was significantly increased, in a dose-dependent manner, and the effect of L-NAME at the dose of 60 mg kg^{-1} was statistically significant (Table 3). The DOPAC/dopamine and HVA/dopamine ratios were not changed by the treatment with L-NAME. D-NAME (60 mg kg^{-1}) had no effect on the metabolism of dopamine in any brain regions examined (Table 3).

Discussion

Previous studies have demonstrated that L-NAME, a specific NO synthase inhibitor, impairs spatial learning in the Morris water maze and radial arm maze tests. Böhme *et al.* (1993) have shown that L-NAME, at a dose of 100 mg kg^{-1} but not 25 mg kg^{-1}, impairs spatial learning in rats in a radial maze task, and that the repeated administration of this agent twice daily for 4 days evoked a blockade of the induction of LTP in rat hippocampal slices. In agreement with the results reported by Böhme *et al.*, we found that L-NAME, but not D-NAME, impaired the performance during the acquisition of spatial learning in the radial arm maze task, as revealed by the dose-dependent increase in the number of errors and the time taken to complete the task. It is unlikely that the inhibitory effect of L-NAME on the performance of rats in the radial maze arm task is due to a general impairment of locomotor activity as observed after the single acute injection of L-NAME, since neither the locomotor activity after the 2nd injection of L-NAME nor that on the 1st day in the habituation task, which was measured after the 10 days of the radial arm maze task, differed from that in vehicle-treated control rats. It is also unlikely that the impairment of performance in rats treated with L-NAME is due to the alteration of motivational state, since there was no difference in the gross consumption of food which was examined every day after the maze task. Therefore, the present results suggest that NO may play an important role in the acquisition of spatial learning in the radial arm maze task. It still remains uncertain, however, whether L-NAME impaired the learning mechanism itself or affected sensory processes or other factors.

In contrast to the dose-dependent impairment of the radial arm maze performance during the acquisition caused by L-NAME, the same agent, at doses up to 100 mg kg^{-1}, failed to affect the performance in rats that had previously acquired this task. It is unlikely that the lack of effect of L-NAME on the retention of the radial arm maze task is due to insufficient inhibition of NO synthase in the brain, since we confirmed that the remaining NO synthase activity in the brains of rats used in the memory retention experiment was as low as that in the brains of rats used in the experiments of acquisition of spatial learning in the radial arm maze task. Chapman *et al.* (1992) have shown that L-NAME, at a dose of 75 mg kg^{-1}, consistently, impaired acquisition, but failed to affect the retention of spatial learning in the Morris water maze. Recently, Bannerman *et al.* (1994a) have shown that L-NAME impaired the spatial learning in the water maze task with multiple trials per day, but had no effect when only one trial per day was used. Based on these and other results, they suggested that the basis of the impairment of performance caused by L-NAME is unlikely to be due to any direct effect on the mechanism of spatial learning. They also demonstrated that L-NAME impaired only the acquisition but not the retention of a previously learned spatial task. Taken together, it is conceivable that NO may play, at least in part, a role in the acquisition, but not reten-

Table 2 Effects of repeated administration of N^G-nitro-L-arginine methyl ester (L-NAME) and D-NAME on 5-HT metabolism in the rat brain

Brain region	*Treatment*	*Dose* (mg kg^{-1}, i.p)	n	*5-HT* (pmol g^{-1} tissue)	*5-HIAA*	*5-HIAA/5-HT*
Cortex	Control		5	1452±89	499±46	0.343±0.019
	L-NAME	10	5	1356±59	469±33	0.346±0.019
		30	5	1573±44	536±19	0.342±0.013
		60	5	1471±151	405±50	0.273±0.011*
	D-NAME	60	6	1494±77	483±22	0.324±0.008
Hippocampus	Control		5	1576±60	2664±63	1.703±0.086
	L-NAME	10	5	1460±51	2288±79	1.569±0.041
		30	5	1465±59	2383±80	1.630±0.037
		60	5	1516±30	2049±84**	1.353±0.053**
	D-NAME	60	6	1587±61	2660±106	1.681±0.069
Striatum	Control		5	2703±168	1721±141	0.634±0.024
	L-NAME	10	5	2479±79	1476±74	0.596±0.030
		30	5	2479±137	1611±73	0.633±0.035
		60	5	2546±84	1557±46	0.615±0.028
	D-NAME	60	6	2277±276	1383±156	0.611±0.014
Thalamus/	Control		5	3518±506	2091±266	0.601±0.022
Hypothalamus	L-NAME	10	5	3309±486	2071±372	0.616±0.024
		30	5	2866±370	1867±228	0.654±0.021
		60	5	3720±331	2323±205	0.626±0.016
	D-NAME	60	6	3048±413	1913±29	0.621±0.015

Rats were treated with L- or D-NAME for 18 days, once a day, during which period they performed the radial arm maze and habituation tasks. One hour after the last drug administration, they were killed by decapitation, and the content of 5-HT and its metabolite in the brain was determined. *$P<0.05$; **$P<0.01$ *vs* saline-treated group.

Table 3 Effects of repeated administration of N^G-nitro -L-arginine methyl ester (L-NAME) and D-NAME on dopamine metabolism in the rat brain

Brain region	*Treatment*	*Dose* (mg kg^{-1}, i.p.)	n	*Dopamine*	*DOPAC* (pmol g $tissue^{-1}$)	*HVA*	*DOPAC /Dopamine*	*HVA /Dopamine*
Cortex	Control		5	206±21	143±6	121±12	0.714±0.061	0.603±0.059
	L-NAME	10	5	193±15	142±4	138±31	0.754±0.069	0.764±0.218
		30	5	198±7	152±9	130±13	0.774±0.060	0.660±0.059
		60	5	211±12	139±8	126±10	0.661±0.031	0.600±0.038
	D-NAME	60	6	246±29	138±9	123±9	0.613±0.115	0.562±0.136
Hippocampus	Control		5	204±63	122±15	ND	0.653±0.110	
	L-NAME	10	5	197±39	122±13	ND	0.674±0.071	
		30	5	196±14	150±18	ND	0.758±0.082	
		60	5	197±26	141±16	ND	0.753±0.082	
	D-NAME	60	6	278±45	128±23	ND	0.500±0.118	0.125±0.007
Striatum	Control		5	36330±1736	3084±226	4549±310	0.085±0.004	0.134±0.003
	L-NAME	10	5	32660±3334	3287±202	4379±501	0.104±0.010	0.123±0.007
		30	5	39379±2159	3649±151	4799±209	0.093±0.002	0.119±0.007
		60	5	42146±789	4117±85*	5027±312	0.098±0.002	0.129±0.006
	D-NAME	60	6	33211±3980	3108±341	4215±375	0.096±0.010	0.051±0.010
Thalamus/	Control		5	1109±179	326±46	54±8	0.298±0.009	0.048±0.008
Hypothalamus	L-NAME	10	5	1035±112	322±46	52±12	0.309±0.015	0.042±0.014
		30	5	1011±132	311±54	49±22	0.302±0.026	0.049±0.014
		60	5	1246±107	387±34	67±22	0.310±0.007	0.041±0.007
	D-NAME	60	6	1044±124	302±43	46±13	0.287±0.010	

Rats were treated with L- or D-NAME for 18 days, once a day, during which period they performed the radial arm maze and habituation tasks. One hour after the last drug administration, they were killed by decapitation, and the content of dopamine and its metabolites in the brain was determined. ND: not detected; *$P<0.05$ *vs* saline-treated group.

tion, of spatial learning. Further studies should be carried out to clarify the neuronal mechanisms underlying the impairment of performance caused by L-NAME.

In contrast to the effects of L-NAME in the radial arm maze task reported in the present study, NMDA receptor antagonists such as MK-801 have been shown to impair the performance in both acquisition and retention trials in a radial arm maze task (Ward *et al.*, 1990). Therefore, the inhibitory effect of NMDA receptor antagonists on performance in the radial maze task cannot be explained solely by the inhibition of NO synthase following NMDA receptor blockade.

The rate of decrease of locomotor activity in the habituation task is regarded as an experimental model of the memory process (Platel & Porsolt, 1982). We found that the rate of decrease in locomotor activity in the habituation task in the L-NAME-treated, but not in the D-NAME-treated, rats was less than in control rats, although the difference was not statistically significant. However, the number of animals in which the locomotor activity on the 2nd or 3rd day had decreased to less than 50% of that on the 1st day was significantly reduced by treatment with L-NAME at a dose of 60 mg kg^{-1}. These findings further support the hypothesis that NO may play a critical role in the mechanisms of the learning and memory processes.

In contrast to the effect of L-NAME seen after repeated injection, acute injection of L-NAME produced a significant decrease in the locomotor activity, and therefore we cannot examine the acute effect of L-NAME in the habituation task.

The inhibitory effect of L-NAME on the locomotor activity was not observed after the 2nd injection of L-NAME. Bannerman *et al.* (1994b) also reported that acute but not chronic treatment with L-NAME resulted in a gradual but significant reduction in nontetanized baseline field potentials in the hippocampus. It is possible that tolerance may be rapidly developed in some (suppression of locomotor activity) but not other effects of L-NAME.

In agreement with previous studies (Chapman *et al.*, 1992; Böhme *et al.*, 1993; Bannerman *et al.*, 1994a), we found that the repeated administration of D-NAME had no effect on the performance of rats in the two behavioural tasks. We did find, however, that NO synthase activity in the brains was significantly reduced by the repeated administration of D-NAME, being approximately one-third of the control level after such administration. It is difficult to explain this inhibition, since D-NAME is a very weak inhibitor of NO synthase *in vitro*. Neither behavioural performance nor the content of dopamine and 5-HT, and their metabolites in the brain was changed by the treatment with D-NAME, despite the significant inhibition of NO synthase activity. Thus, it is possible that NO synthase may be a latent enzyme, and that, therefore, almost complete inhibition of its activity may be necessary for inhibiting NO production and NO-mediated phenomena *in vivo*.

The mechanisms by which NO functions in models of synaptic plasticity such as learning and memory have yet to be elucidated. The activation of soluble guanylate cyclase and the consequent formation of cyclic GMP may be involved in hippocampal LTP (Zhou *et al.*, 1994). Montague *et al.* (1994) have demonstrated that the inhibition of NO synthase antagonizes the NMDA receptor-mediated release of glutamic acid and noradrenaline in the cerebral cortex. It has been shown that dopamine release from striatal slices is stimulated by NO (Hanbauer *et al.*, 1992; Zhu & Luo, 1992). On the contrary, it has been demonstrated, using an *in vivo* brain microdialysis technique, that NO significantly increased the release of aspartate, glutamate, GABA, taurine, 5-HT and acetylcholine in the rat striatum, whereas dopamine release was significantly decreased (Guevara-Guzman *et al.*, 1994). Meffert *et al.* (1994) have shown, with a new fluorescence method, using the dye FM1-43, that NO stimulates vesicle exocytosis, without raising Ca^{2+}. If NO were able to stimulate neurotransmitter release, then the long-term inhibition of NO synthase activity would change the level of neurotransmitters and their metabolites in the brain. We found that, in rats treated with L-NAME, the concentration of DOPAC in the striatum was increased, in a dose-dependent manner, but that there was no increase in other brain regions examined, suggesting that long-term inhibition of NO synthase may cause an increase in dopamine turnover in the striatum. These results appear to be consistent with the results that NO inhibits dopamine release in the striatum (Guevara-Guzman *et al.*, 1994), and agree with the previous findings that MK-801 and phencyclidine (PCP), which are considered to inhibit NO production in the brain by blocking NMDA receptors, cause an increase in dopamine metabolism in the striatum (Nabeshima *et al.*, 1987; Löscher *et al.*, 1991).

The content of 5-HIAA in the hippocampus and the 5-HIAA/5-HT ratio in the hippocampus and the cerebral cortex were significantly decreased in the L-NAME (60 mg kg^{-1})-treated rats, compared with these values in the vehicle-treated rats, suggesting that the inhibition of NO synthase may result in a decrease in the turnover of 5-HT in the hippocampus and the cerebral cortex. Although there are only few reports in which the effects of NO on the release of 5-HT have been examined, it has been shown that MK-801 increased 5-HT metabolism in the brain (Löscher *et al.*, 1991; Whitton *et al.*, 1992), the effects being opposed to those found in the present study with L-NAME. It is of interest to note that the changes in dopamine and 5-HT metabolism caused by the repeated administration of L-NAME were observed in different brain regions and occurred in different directions. Although we cannot provide a plausible explanation for these neurotransmitter-dependent and brain region-selective effects of L-NAME, it is possible that NO can modulate the release of both excitatory and inhibitory neurotransmitters, which could then result in either increases or decreases in the metabolism of these neurotransmitters.

Finally, NO synthase inhibitors are known to cause hypertension following systemic injection, this effect being nearly maximal at 10 mg kg^{-1} (Rees *et al.*, 1990). Since this dose of L-NAME had no effect on performance in the radial arm maze or in the habituation tasks, or on monoamine metabolism in the brain, it is unlikely that the behavioural and neurochemical effects of L-NAME described in the present study are associated with L-NAME-induced hypertension.

In conclusion, the present results suggest that NO may play an important role in memory processes, especially in the acquisition, but not in the maintenance, of spatial learning in the radial arm maze task. Furthermore, the results suggest that endogenous NO may be involved in the regulation of dopamine and 5-HT metabolism in the brain.

This study was supported, in part, by an SRF Grant for Biomedical Research and by grants from the Japanese Ministry of Health and Welfare Foundation for Gerontological Science Research (91A-2406), and the Japan Research Foundation for Clinical Pharmacology.

References

BANNERMAN, D.M., CHAPMAN, P.F., KELLY, P.A.T., BUTCHER, S.P. & MORRIS, R.G.M. (1994a). Inhibition of nitric oxide synthase does not impair spatial learning. *J. Neurosci.*, **14**, 7404–7414.

BANNERMAN, D.M., CHAPMAN, P.F., KELLY, P.A.T., BUTCHER, S.P. & MORRIS, R.G.M. (1994b). Inhibition of nitric oxide synthase does not prevent the induction of long-term potentiation *in vivo*. *J. Neurosci.*, **14**, 7415–7425.

BÖHME, G.A., BON, C., LEMAIRE, M., REIBAUD, M., PIOT, O., STUTZMANN, J.M., DOBLE, A. & BLANCHARD, J.C. (1993). Altered synaptic plasticity and memory formation in nitric oxide synthase inhibitor-treated rats. *Proc. Natl. Acad. Sci. U.S.A.*, **90**, 9191–9194.

BREDT, D.S. & SNYDER, S.H. (1989). Nitric oxide mediates glutamate-linked enhancement of cGMP levels in the cerebellum. *Proc. Natl. Acad. Sci. U.S.A.*, **86**, 9030–9033.

BREDT, D.S. & SNYDER, S.H. (1992). Nitric oxide, a novel neuronal messenger. *Neuron*, **8**, 3–11.

CALDWELL, M., O'NEILL, M., EARLEY, B. & LEONARD, B. (1994). N^G-Nitro-L-arginine protects against ischaemia-induced increases in nitric oxide and hippocampal neuro-degeneration in the gerbil. *Eur. J. Pharmacol.*, **260**, 191–200.

CHAPMAN, P.F., ATKINS, C.M., ALLEN, M.T., HALEY, J.E. & STEINMETZ, J.E. (1992). Inhibition of nitric oxide synthesis impairs two different forms of learning. *Neuroreport*, **3**, 567–570.

DAWSON, T.M., & SNYDER, S.H. (1994). Gases as biological messengers: nitric oxide and carbon monoxide in the brain. *J. Neurosci.*, **14**, 5147–5159.

DAWSON, V.L., DAWSON, T.M., BARTLEY, D.A., UHL, G.R. & SNYDER, S.H. (1993). Mechanisms of nitric oxide-mediated neurotoxicity in primary brain cultures. *J. Neurosci.*, **13**, 2651–2661.

DAWSON, V.L., DAWSON, T.M., LONDON, E.D., BREDT, D.S. & SNYDER, S.H. (1991). Nitric oxide mediates glutamate neurotoxicity in primary cortical culture. *Proc. Natl. Acad. Sci. U.S.A.*, **88**, 6368–6371.

DWYER, M.A., BREDT, D.S. & SNYDER, S.H. (1991). Nitric oxide synthase: irreversible inhibition by L-N^G-nitroarginine in brain *in vitro* and *in vivo*. *Biochem. Biophys. Res. Commun.*, **176**, 1136–1141.

EAST, S.J. & GARTHWAITE, J. (1991). NMDA receptor activation in rat hippocampus induces cyclic GMP formation through the L-arginine-nitric oxide pathway. *Neurosci. Lett.*, **123**, 17–19.

GARTHWAITE, J. (1991). Glutamate, nitric oxide and cell-cell signalling in the nervous system. *Trends Neurosci.*, **14**, 60–67.

GARTHWAITE, J., CHARLES, S.L. & CHESS-WILLIAMS, R. (1988). Endothelium-derived relaxing factor release on activation of NMDA receptors suggests role as intercellular messenger in the brain. *Nature*, **336**, 385–388.

GARTHWAITE, J., GARTHWAITE, G., PALMER, R.M.J. & MONCADA, S. (1989). NMDA receptor activation induces nitric oxide synthesis from arginine in rat brain slices. *Eur. J. Pharmacol.*, **172**, 413–416.

GUEVARA-GUZMAN, R., EMSON, P.C. & KENDRICK, K.M. (1994). Modulation of *in vivo* striatal transmitter release by nitric oxide and cyclic GMP. *J. Neurochem.*, **62**, 807–810.

HABERNY, K.A., POU, S. & ECCLES, C. (1992). Potentiation of quinolinate-induced hippocampal lesions by inhibition of NO synthesis. *Neurosci. Lett.*, **146**, 187–190.

HANBAUER, I., WINK, D., OSAWA, Y., EDELMAN, G.M. & GALLY, J.A. (1992). Role of nitric oxide in NMDA-evoked release of [^{3}H]-dopamine from striatal slices. *Neuroreport*, **3**, 409–412.

HÖLSCHER, C. & ROSE, S.P.R. (1993). Inhibiting synthesis of the putative retrograde messenger nitric oxide results in amnesia in a passive avoidance task in the chick. *Brain. Res.*, **619**, 189–194.

IGNARRO, L.J. (1990). Biosynthesis and metabolism of endothelium-derived nitric oxide. *Annu. Rev. Pharmacol. Toxicol.*, **30**, 535–560.

KHANNA, J.K., MORATO, G.S., SHAH, G., CHAU, A. & KALANT, H. (1993). Inhibition of nitric oxide synthesis impairs rapid tolerance to ethanol. *Brain. Res. Bull.*, **32**, 43–47.

KNOWLES, R.G., PALACIOS, M., PALMER, R.M.J. & MONCADA, S. (1989). Formation of nitric oxide from L-arginine in the central nervous system: a transduction mechanism for stimulation of the soluble guanylate cyclase. *Proc. Natl. Acad. Sci. U.S.A.*, **86**, 5159–5162.

KOMORI, Y., CHIANG, K.T. & FUKUTO, J.M. (1993). The effect of nonionic detergents on the activity and/or stability of rat brain nitric oxide synthase. *Arch. Biochem. Biophys.*, **307**, 311–315.

LEI, S.Z., PAN, Z.H., AGGARWAL, S.K., CHEN, H.S.V., HARTMAN, J., SUCHER, N.J. & LIPTON, S.A. (1992). Effect of nitric oxide production on the radox modulatory site of the NMDA receptor-channel complex. *Neuron*, **8**, 1087–1099.

LIPTON, S.A., CHOI, Y., PAN, Z., LEI, S.Z., CHEN, H.V., SUCHER, N.J., LOSCALZO, J., SINGEL, D.J. & STAMLER, J.S. (1993). A redox-based mechanism for the neuroprotective and neurodestructive effects of nitric oxide and related nitroso-compounds. *Nature*, **364**, 626–632.

LÖSCHER, W., ANNIES, R. & HÖNACK, D. (1991). The N-methyl-D-aspartate receptor antagonist MK-801 induces increases in dopamine and serotonin metabolism in several brain regions of rats. *Neurosci. Lett.*, **128**, 191–194.

LOWRY, O.H., ROSEBROUGH, N.J., FARR, A.L. & RANDALL, R.J. (1951). Protein measurement with the Folin phenol reagent. *J. Biol. Chem.*, **193**, 265–275.

MANZONI, O., PREZEAU, L., MARIN, P., DESHAGER, S., BOCKAERT, J. & FAGNI, L. (1992). Nitric oxide-induced blockade of NMDA receptors. *Neuron*, **8**, 653–662.

MEFFERT, M.K., PREMACK, B.A. & SCHULMAN, H. (1994). Nitric oxide stimulates Ca^{2+}-independent synaptic vesicle release. *Neuron*, **12**, 1235–1244.

MONCADA, S., PALMER, R.M.J. & HIGGS, E.A. (1989). Biosynthesis of nitric oxide from L-arginine. A pathway for the regulation of cell function and communication. *Biochem. Pharmacol.*, **38**, 1709–1715.

MONTAGUE, P.R., GANCAYCO, C.D., WINN, M.J., MARCHASE, R.B. & FRIEDLANDER, M.J. (1994). Role of NO production in NMDA receptor-mediated neurotransmitter release in cerebral cortex. *Science*, **263**, 973–977.

NABESHIMA, T., FUKAYA, H., YAMAGUCHI, K., ISHIKAWA, K., FURUKAWA, H. & KAMEYAMA, T. (1987). Development of tolerance and supersensitivity to phencyclidine in rats after repeated administration of phencyclidine. *Eur. J. Pharmacol.*, **135**, 23–33.

NAKAMURA, T., YAMADA, K., HASEGAWA, T. & NABESHIMA, T. (1995). Possible involvement of nitric oxide in quinolinic acid-induced convulsion in mice. *Pharmacol. Biochem. Behav.*, (in press).

NITTA, A., FURUKAWA, Y., HAYASHI, K., HIRAMATSU, M., KAMEYAMA, T., HASEGAWA, T. & NABESHIMA, T. (1992). Denervation of dopaminergic neurons with 6-hydroxydopamine increases nerve growth factor content in rat brain. *Neurosci. Lett.*, **144**, 152–156.

NITTA, A., MURAKAMI, Y., FURUKAWA, Y., KAWATSURA, W., HAYASHI, K., YAMADA, K., HASEGAWA, T. & NABESHIMA, T. (1994). Oral administration of idebenone induces nerve growth factor in the brain and improves learning and memory in basal forebrain-lesioned rats. *Naunyn-Schmied. Arch. Pharmacol.*, **349**, 401–407.

NOWICKI, J.P., DUVAL, D., POIGNET, H. & SCATTON, B. (1991). Nitric oxide mediates neuronal death after focal cerebral ischemia in the mouse. *Eur. J. Pharmacol.*, **204**, 339–340.

O'DELL, T.J., HAWKINS, R.D., KANDEL, E.R. & ARANCIO, O. (1991). Tests of the roles of two diffusible substances in long-term potentiation: evidence for nitric oxide as a possible early retrograde messenger. *Proc. Natl. Acad. Sci. U.S.A.*, **88**, 11285–11289,

PLATEL, A. & PORSOLT, R.D. (1982). Habituation of exploratory activity in mice: a screening test for memory enhancing drugs. *Psychopharmacology*, **78**, 346–352.

PUDIAK, C.M. & BOZARTH, M.A. (1993). L-NAME and MK-901 attenuate sensitization to the locomotor-stimulating effect of cocaine. *Life Sci.*, **53**, 1517–1524.

RAUHALA, P., IDÄNPÄÄN-HEIKKILÄ, J.J., TUOMINEN, R.K. & MÄNNISTÖ, P.T. (1994). N-Nitro-L-arginine attenuates development of tolerance to antinociceptive but not to hormonal effects of morphine. *Eur. J. Pharmacol.*, **259**, 57–64.

REES, D.D., PALMER, R.M.J., SCHULZ, R., HODSON, H.F. & MONCADA, S. (1990). Characterization of three inhibitors of endothelial nitric oxide synthase *in vitro* and *in vivo*. *Br. J. Pharmacol.*, **101**, 746–752.

SCHUMAN, E.M. & MADISON, D.V. (1991). A requirement for the intercellular messenger nitric oxide in long-term potentiation. *Science*, **254**, 1503–1506.

SNYDER, S.H. (1992). Nitric oxide: first in a new class of neurotransmitters. *Science*, **257**, 494–496.

SOUTHAM, E. & GARTHWAITE, J. (1993). The nitric oxide-cyclic GMP signalling pathway in rat brain. *Neuropharmacology*, **32**, 1267–1277.

VINCENT, S.R. & KIMURA, H. (1992). Histochemical mapping of nitric oxide synthase in the rat brain. *Neuroscience*, **46**, 755–784.

WARD, L., MASON, S.E. & ABRAHAM, W.C. (1990). Effects of the NMDA antagonists CPP and MK-801 on radial arm maze performance in rats. *Pharmacol. Biochem. Behav.*, **35**, 785–790.

WHITTON, P.S., BIGGS, C.S., PEARCE, B.R. & FOWLER, L.J. (1992). MK-801 increases extracellular 5-hydroxytryptamine in rat hippocampus and striatum *in vivo*. *J. Neurochem.*, **58**, 1573–1575.

ZHU, X. & LUO, L. (1992). Effect of nitroprusside (nitric oxide) on endogenous dopamine release from rat striatal slices. *J. Neurochem.*, **59**, 932–935.

ZHOU, M., HU, Y., SCHULTZ, C., KANDEL, E.R. & HAWKINS, R.D. (1994). Role of guanylyl cyclase and cGMP-dependent protein kinase in long-term potentiation. *Nature*, **368**, 635–639.

(Received December 19, 1994
Revised March 7, 1995
Accepted March 15, 1995)

British Journal of Pharmacology (1995) 115, 859-867

Endothelial function in spontaneously hypertensive rats: influence of quinapril treatment

[1,*,†]Mika Kähönen, *Heikki Mäkynen, *Xiumin Wu, **Pertti Arvola & **Ilkka Pörsti

*Medical School, Department of Pharmacology, University of Tampere, P.O. Box 607, FIN-33101 Tampere, Finland; and Departments of †Clinical Physiology and **Internal Medicine, Tampere University Hospital, P.O. Box 2000, FIN-33521 Tampere, Finland

1 Angiotensin converting enzyme (ACE) inhibition has been shown to restore the impaired endothelial function in hypertension, but the mediators underlying the promoted endothelium-dependent dilatation have not been fully characterized. Therefore, we investigated the effects of 10-week-long quinapril therapy (10 mg kg^{-1} day^{-1}) on responses of mesenteric arterial rings *in vitro* from spontaneously hypertensive rats (SHR) and normotensive Wistar-Kyoto (WKY) rats.

2 Endothelium-dependent relaxations of noradrenaline (NA)-precontracted rings to acetylcholine (ACh) and adenosine 5'-diphosphate (ADP) were similar in WKY rats and quinapril-treated SHR and more pronounced than in untreated SHR. The nitric oxide (NO) synthase inhibitor N^G-nitro-L-arginine methyl ester (L-NAME) attenuated the relaxations in both WKY groups and quinapril-treated SHR, and completely inhibited them in untreated SHR. When endothelium-dependent hyperpolarization was prevented by precontraction of the preparations with potassium chloride (KCl), no differences were found in relaxations to ACh and ADP between the study groups. In addition, in NA-precontracted rings the L-NAME- and indomethacin-resistant relaxations to ACh were partially prevented by apamin, an inhibitor of calcium-activated potassium channels.

3 Interestingly, in quinapril-treated SHR but not in the other groups, exogenous bradykinin potentiated the relaxations to ACh in both NA- and KCl-precontracted arterial rings.

4 Contractile sensitivity of endothelium-intact rings to NA was reduced in SHR by quinapril, and was more effectively increased by L-NAME in quinapril-treated than untreated SHR.

5 In conclusion, since the relaxations to ACh and ADP in quinapril-treated SHR were augmented in the absence and presence of NO synthesis inhibition but not under conditions which prevented hyperpolarization, enhanced endothelium-dependent relaxation after long-term ACE inhibition can be attributed to increased endothelium-dependent hyperpolarization. However, the potentiation of the response to ACh by exogenous bradykinin in quinapril-treated SHR, as well as the increased attenuating effect of the endothelium on NA-induced contractions in these animals appear to result from enhanced endothelium-derived NO release.

Keywords: Angiotensin-converting enzyme inhibition; arterial smooth muscle; blood pressure; bradykinin; endothelium; quinapril; spontaneously hypertensive rat; Wistar-Kyoto rat

Introduction

Vascular endothelium plays an important role in the regulation of arterial tone by producing dilator mediators which include endothelium-derived relaxing factor (EDRF; probably identical with nitric oxide (NO)), prostacyclin (PGI_2) and endothelium-derived hyperpolarizing factor (EDHF) (Chen *et al.*, 1988; Moncada *et al.*, 1991; Fujii *et al.*, 1992). Several reports have shown endothelial function to be impaired in hypertension: endothelium-dependent relaxations are diminished in spontaneously hypertensive rats (SHR) (Watt & Thurston, 1989; Clozel *et al.*, 1990; Arvola *et al.*, 1993; Rubanyi *et al.*, 1993; Kähönen *et al.*, 1994) as well as in hypertensive patients (Treasure *et al.*, 1992), and reduced NO production has been suggested to underlie the attenuated endothelium-mediated dilatations (Tesfamariam & Halpern, 1988; Clozel *et al.*, 1990). However, deficient endothelium-dependent hyperpolarization has recently been shown to account for the impaired relaxation to acetylcholine (ACh) in SHR mesenteric arteries, while the role of NO in the response was well preserved, and the participation of PGI_2 in the relaxation appeared to be marginal (Fujii *et al.*, 1992; 1993; Kähönen *et al.*, 1994; Li *et al.*, 1994). Furthermore, ACh is known to evoke contractions in blood vessels of SHR but not of Wistar-Kyoto (WKY) rats via the release of endothelium-derived contractile factors (EDCF). Thus, the decreased relaxant effect of ACh in SHR may not result from deficient dilator autacoid production alone, but also from simultaneous release of EDCF from the endothelium (Lüscher & Vanhoutte, 1986; Jameson *et al.*, 1993; Takase *et al.*, 1994).

The antihypertensive action of angiotensin converting enzyme (ACE) inhibitors is primarily based on the inhibition of angiotensin II formation. The vascular wall appears to have a renin-angiotensin system of its own which ACE inhibitors directly inhibit (Levy *et al.*, 1990), even more effectively than ACE circulating in the blood stream (Baudin & Drouet, 1989). Long-term ACE inhibitor therapy has been shown to augment endothelium-dependent relaxation responses of arteries in SHR (Clozel *et al.*, 1990; Arvola *et al.*, 1993; Gohlke *et al.*, 1993; Rubanyi *et al.*, 1993) and in normotensive animals (Bossaller *et al.*, 1992), and to enhance ACh-induced vasodilatation *in vivo* in normotensive human subjects (Nakamura *et al.*, 1992). In addition to reduced angiotensin II generation, ACE inhibitors diminish the degradation of bradykinin, which in turn stimulates the synthesis of NO and PGI_2 in endothelial cells (Wiemer *et al.*, 1991) and also promotes endothelium-dependent hyperpolarization *in vitro* (Illiano *et al.*, 1994). However, whether the favourable long-term influences of ACE inhibition on endothelial function can be attributed to enhanced NO or PGI_2 generation, promoted endothelium-dependent hyperpolarization, or reduced contractile factor release from the endothelium is not fully understood.

[1] Author for correspondence at Medical School address.

Recently, we have reported that ACE inhibitor therapy improved both endothelium-dependent and -independent arterial relaxation in SHR (Arvola *et al.*, 1993). The present study was designed to examine in detail the effects of long-term treatment with quinapril, an orally active non-sulphydryl compound (Kaplan *et al.*, 1984), on vascular responses in SHR and WKY rats. Special attention was paid to the evaluation of the roles of NO, PGI_2, EDHF and EDCF in endothelium-mediated responses. Since acute ACE inhibition is known to potentiate the effects of kinins in endothelial cells (Wiemer *et al.*, 1991; Illiano *et al.*, 1994), the dilator responses to bradykinin were also examined after the chronic quinapril therapy.

Methods

Animals and experimental design

Male SHR (Okamoto-Aoki strain) and age-matched WKY rats were obtained from Møllegaard's Breeding Centre, Ejby, Denmark. The animals were housed four to a cage in a standard experimental animal laboratory (illuminated 06 h 00 min–18 h 00 min, temperature +22°C), and had free access to drinking fluid (tap water) and food pellets (Ewos, Södertälje, Sweden). The systolic blood pressures of conscious animals were measured at +28°C by the tail-cuff method (Model 129 Blood Pressure Meter; IITC Inc., Woodland Hills, Ca., U.S.A.). At 7 weeks of age both SHR and WKY rats were divided into two groups of equal mean systolic blood pressures. Thereafter, SHR ($n=15$) and WKY rats ($n=15$) were given quinapril in drinking water in light-proof bottles, (average dose 10 mg kg^{-1}, fresh drug solutions being prepared daily), while untreated SHR ($n=15$) and normotensive WKY rats ($n=15$) were kept on normal drinking fluid. Quinapril therapy and weekly indirect blood pressure measurements continued for 10 more weeks until the animals were 17 weeks old. Thereafter quinapril administration was withdrawn 1 day before the rats were decapitated and exsanguinated. The hearts were removed and weighed, and the superior mesenteric arteries carefully excised and cleaned of adherent connective tissue. The experimental design of the study was approved by the Animal Experimentation Committee of the University of Tampere, Finland.

Mesenteric arterial responses in vitro

Five successive standard sections (3 mm in length) of the mesenteric artery from each animal were cut, beginning 1 cm distally from the mesenteric artery-aorta junction. In the four most distal rings the endothelium was left intact and from the first piece, vascular endothelium was removed by gently rubbing with a jagged injection needle (Arvola *et al.*, 1992). The rings were placed between stainless steel hooks (diameter 0.3 mm) and suspended in an organ bath chamber (volume 20 ml) in physiological salt solution (PSS) (pH 7.4) of the following composition (mM): NaCl 119.0, $NaHCO_3$ 25.0, glucose 11.1, $CaCl_2$ 1.6, KCl 4.7, KH_2PO_4 1.2, $MgSO_4$ 1.2, and aerated with 95% O_2 and 5% CO_2. The rings were initially equilibrated for 1 h at +37°C at a resting force of 1.5 g. The force of contraction was measured with an isometric force-displacement transducer and registered on a polygraph (FT 03 transducer and Model 7 E Polygraph; Grass Instrument Co., Quincy, Ma., U.S.A.). The presence of intact endothelium in vascular preparations was confirmed by an almost complete relaxation response (>75%) to 1 μM ACh in 1 μM noradrenaline (NA)-precontracted rings, and the absence of endothelium by the lack of this relaxation response. If any relaxation was seen in endothelium-denuded rings, the endothelium was further rubbed.

Vascular preparation 1 After 30 min, the relaxation responses of endothelium-denuded preparations to 3-morpholinosydnonimine (SIN-1) were determined. The relaxation responses were elicited after full precontraction with 1 μM NA, which resulted in approximately 60% of the maximal contractile response attained in each group. The next concentration of SIN-1 was added only after the previous level of relaxation was stable.

Vascular preparation 2 After a 30 min stabilization period, concentration-response curves for NA were determined cumulatively in endothelium-intact rings. Thereafter relaxation responses to ACh were examined in rings precontracted with 1 μM NA and 30 min later with 60 mM KCl. Then the three responses were repeated in the presence of 0.1 mM N^G-nitro-L-arginine methyl ester (L-NAME) with a 30 min stabilization period between each trial.

Vascular preparation 3 Relaxation responses to ACh were examined in endothelium-intact mesenteric arterial rings precontracted with 1 μM NA. The responses to ACh were also elicited in the presence of 10 μM indomethacin; in the presence of indomethacin and 0.1 mM L-NAME; and in the presence of indomethacin, L-NAME and 1 μM apamin. The rings were allowed a 30 min equilibration period in PSS (containing the above agents) between each relaxant response.

Vascular preparation 4 The fourth endothelium-intact section of each mesenteric artery was used to study relaxation responses to adenosine 5'-diphosphate (ADP) in rings precontracted with 1 μM NA and 30 min later with 60 mM KCl. Then the relaxation responses were also examined in the presence of 0.1 mM L-NAME. The rings were allowed a 30 min equilibration period in PSS between each response.

Vascular preparation 5 The most distal endothelium-intact ring of each mesenteric artery was used to study responses to bradykinin and 30 min later to ACh in the presence of 0.1 μM bradykinin. The responses were generated cumulatively after full precontraction with 1 μM NA and also after precontraction with 60 mM KCl. Cumulative relaxations to ACh in the presence of bradykinin were elicited only after the transient response (if observed) to bradykinin was over. The protocol was then repeated in the presence of 0.1 mM L-NAME. The rings were allowed a 30 min equilibration period between each response.

The NA-induced contractile responses were expressed in g and as percentages of the maximal response, and the pD_{25} for NA in each ring was calculated as a percentage of the maximal response. The EC_{25} values were calculated with a computer

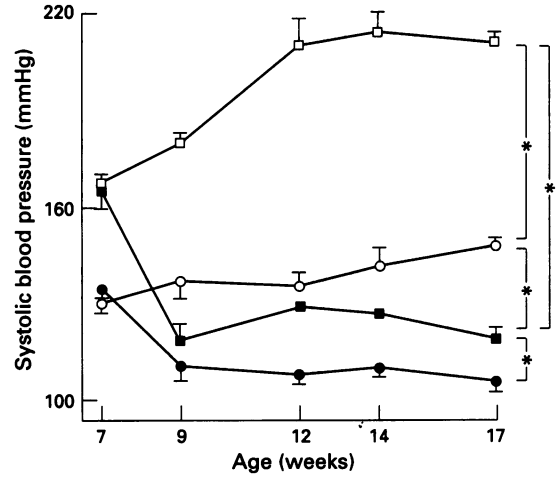

Figure 1 Systolic blood pressures in untreated spontaneously hypertensive rats (SHR, □), quinapril-treated SHR (■, 10 mg kg^{-1} day^{-1}), untreated Wistar-Kyoto (WKY, ○) rats and quinapril-treated WKY rats (●). Symbols indicate means with s.e.means, $n=10-12$ in each group; *$P<0.05$, ANOVA for repeated measurements.

programme and presented as the negative logarithm (pD_{25}): these values were also used in the statistical analysis. The EC_{25} for NA was calculated since the difference between the study groups was most pronounced at this point. The relaxations in response to ACh, ADP and SIN-1 were presented as a percentage of the pre-existing contractile force.

Drugs

The following drugs were used: quinapril hydrochloride (Goedecke AG, Freiburg, Germany), acetylcholine chloride, adenosine diphosphate, apamin, bradykinin, indomethacin, N^G-nitro-L-arginine methyl ester hydrochloride, (Sigma Chemical Co., St. Louis, Mo., U.S.A.), 3-morpholinosydnonimine (GEA Ltd., Copenhagen, Denmark) and (−)-noradrenaline L-hydrogentartrate (Fluka Chemie AG, Buchs SG, Switzerland). Quinapril was dissolved directly in tap water. The stock solutions of the compounds used in the *in vitro* studies were dissolved in distilled water, with the exception of indomethacin (in 1.5 mM Na_2CO_3). All solutions were freshly prepared before use and protected from light.

Analysis of results

Statistical analysis was carried out by one-way analysis of variance (ANOVA) supported by the Bonferroni test in the case of pairwise between-group comparisons. When the data consisted of repeated observations at successive time points, ANOVA for repeated measurements was applied to investigate between-groups differences. All results are expressed as means with s.e.means. Differences were considered significant when $P<0.05$.

Table 1 Experimental group data at close of the study

	SHR	*Quin-SHR*	*WKY*	*Quin-WKY*
Body weight (g)	312±5	296±6†	343±5*	301±7*†
Heart weight (mg)	1224±33	911±20*†	1030±28*	888±31*†
Heart-body weight ratio (mg g^{-1})	3.9±0.1	3.1±0.1*	3.0±0.1*	3.1±0.1*
Heart rate (beats min^{-1})	346±10	327±7	336±6	339±4

Values are mean±s.e.mean, $n=10-12$ for all groups. SHR and Quin-SHR, untreated and quinapril-treated spontaneously hypertensive rats, respectively; WKY and Quin-WKY, untreated and quinapril-treated Wistar-Kyoto rats, respectively. *$P<0.05$ when compared with the SHR group; †$P<0.05$ versus WKY (Bonferroni test).

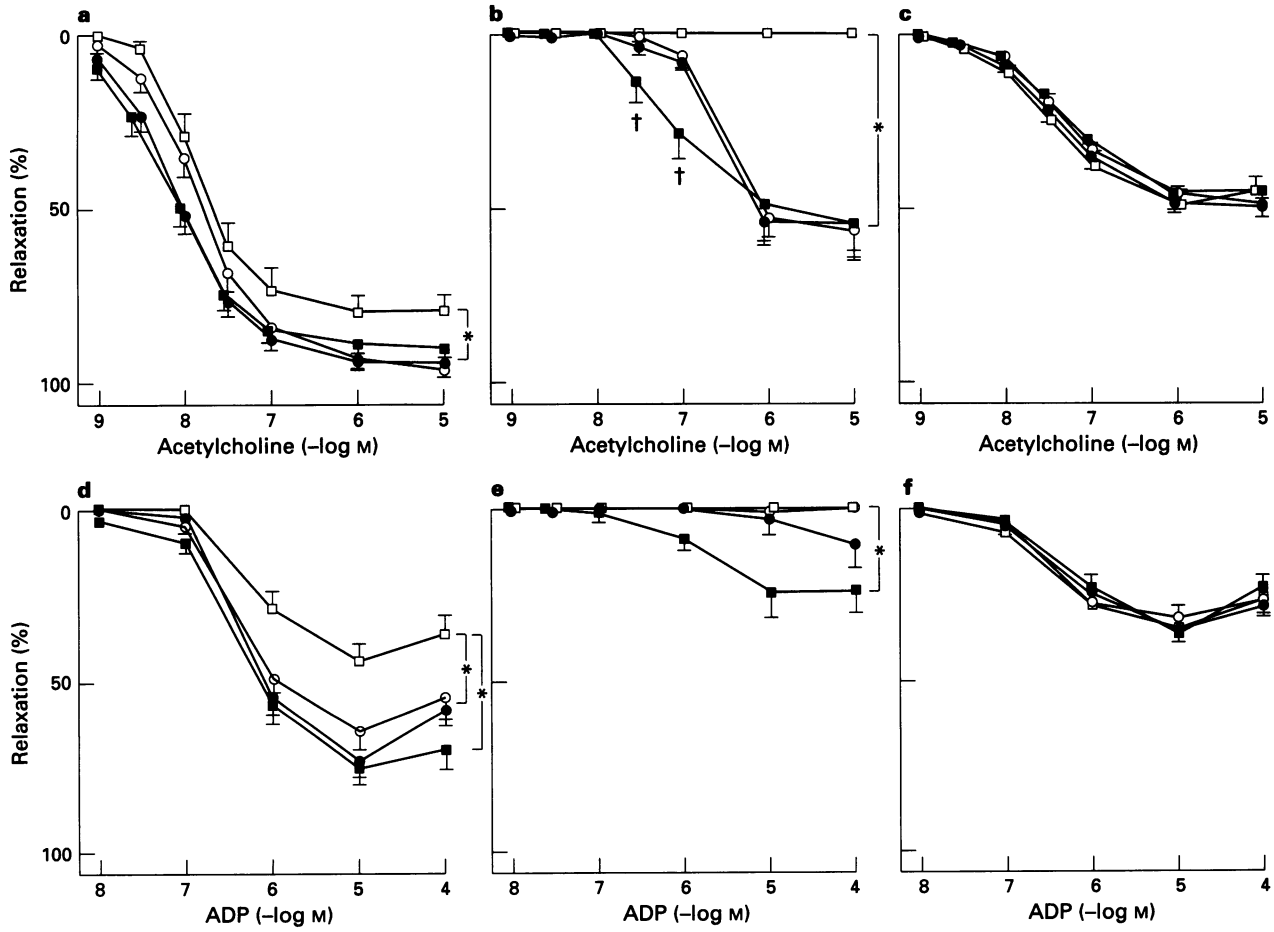

Figure 2 Relaxations to acetylcholine (ACh) and adenosine diphosphate (ADP) in isolated endothelium-intact mesenteric arterial rings from untreated spontaneously hypertensive rats (SHR, □), quinapril-treated SHR (■), untreated Wistar-Kyoto (WKY, ○) rats, and quinapril-treated WKY rats (●). The relaxations were induced after precontraction with 1 μM noradrenaline in the absence (a and d) and presence (b and e) of 0.1 mM N^G-nitro-L-arginine methyl ester (L-NAME), and after precontraction with 60 mM KCl (c and f). Symbols indicate means with s.e.means, $n=10-12$ in each group; *$P<0.05$, ANOVA for repeated measurements. †$P<0.05$ versus other groups (Bonferroni test).

Results

Blood pressure, heart weight and body weight

The systolic blood pressure of SHR was already higher at the beginning of the study than in WKY rats, and during the 10-week-long follow up it continued to increase in untreated SHR, whereas no significant change was observed in control WKY rats. Quinapril treatment beginning at the age of 7 weeks reduced blood pressure in both SHR and WKY rats below that of untreated WKY rats during the follow-up period (Figure 1). Cardiac hypertrophy was totally prevented in SHR by quinapril, relative heart weights of quinapril-treated SHR not differing from those of WKY rats (Table 1).

SHR and WKY rats on oral quinapril gained somewhat less weight than untreated SHR and WKY rats (Table 1). However, no signs of compromised well-being of the animals were observed by our experienced experimental animal laboratory staff. Chow intakes were comparable in all four study groups (data not shown).

Mesenteric arterial responses

The relaxations induced by ACh and ADP in endothelium-intact NA-precontracted (1 μM) mesenteric arterial rings were impaired in untreated SHR when compared with WKY rats. These responses were clearly improved in SHR by the quinapril treatment, the relaxations not differing from those of WKY rats. L-NAME (0.1 mM) diminished the relaxations of NA-precontracted rings effectively in both strains, the influence on ACh response being more pronounced in SHR than WKY rats, and comparable on ADP responses in the two rat strains. In quinapril-treated SHR the remaining relaxations in the presence of L-NAME were more pronounced (30–100 nM ACh; 1–100 μM ADP) than in the other groups (Figure 2). Apamin (1 μM) reduced the L-NAME and indomethacin-resistant relaxations to ACh by approximately 30–50% in quinapril-treated SHR and in WKY rats (Figure 3). Interestingly, the relaxations to ACh and ADP during precontraction with KCl (60 mM), i.e. under conditions in which endothelium-derived hyperpolarization was prevented, were comparable in all

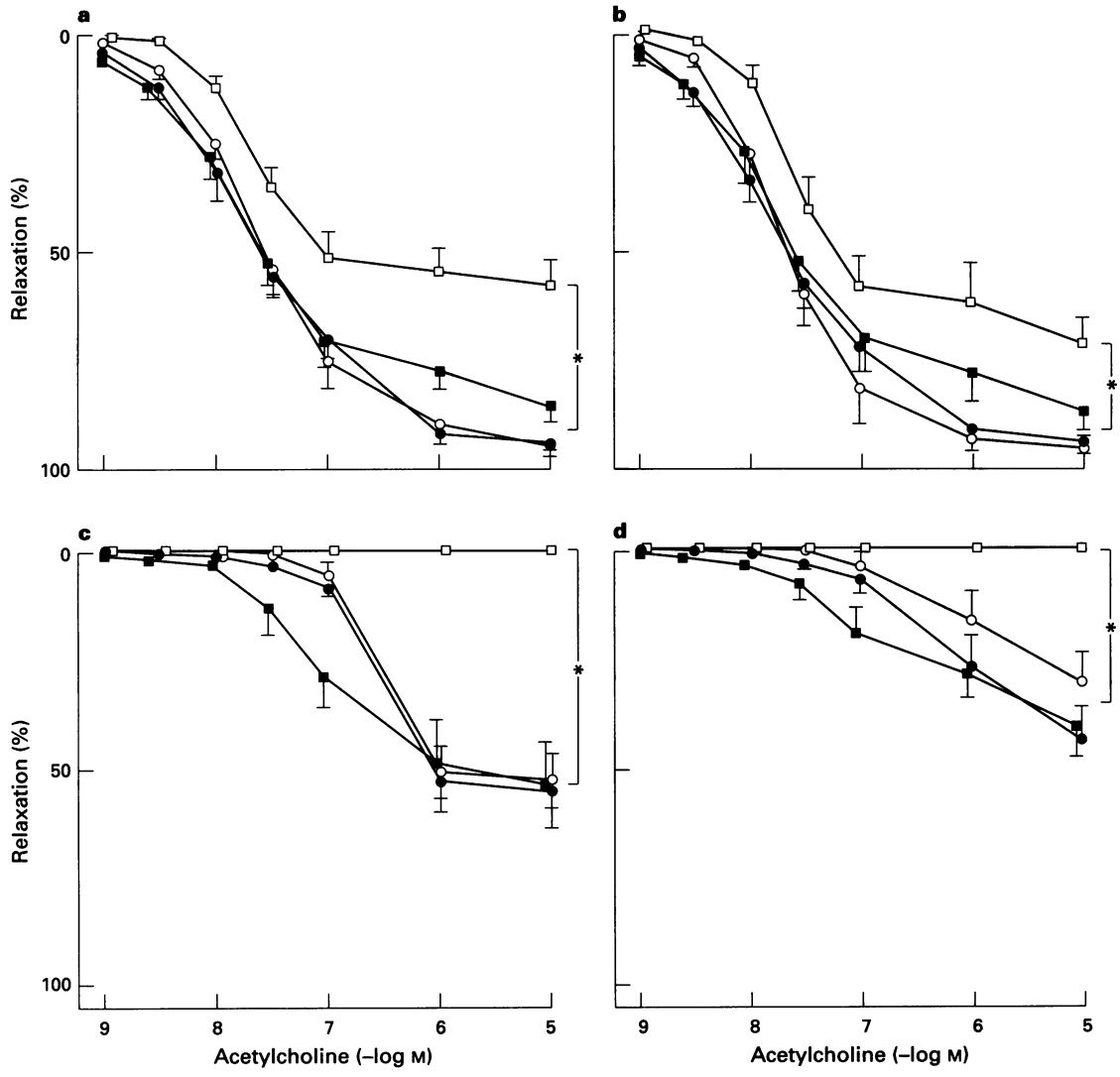

Figure 3 Relaxations of endothelium-intact mesenteric arterial rings after precontraction with 1 μM noradrenaline from untreated spontaneously hypertensive rats (SHR, □), quinapril-treated SHR (■), untreated Wistar-Kyoto (WKY, ○) rats and quinapril-treated WKY rats (●). The relaxation to acetylcholine consisted of an initial maximal response followed by a recontraction phase which is shown in the absence (a) and presence (b) of 10 μM indomethacin. The maximal relaxations to ACh in the presence of 10 μM indomethacin and 0.1 mM N^G-nitro-L-arginine methyl ester (L-NAME) (c) were partially inhibited by 1 μM apamin (d). Symbols indicate means with s.e.means, $n = 10-12$ in each group; $^*P < 0.05$, ANOVA for repeated measurements.

four study groups (Figure 2). In addition, the responses to ACh and ADP in KCl-precontracted rings were practically abolished in the presence of L-NAME (0.1 mM) in all groups (maximal responses to ACh in the SHR, Quin-SHR, WKY and Quin-WKY groups were $-4.1 \pm 3.6\%$, $-3.5 \pm 1.9\%$, $-2.4 \pm 1.6\%$, $-2.2 \pm 1.0\%$, respectively).

Following maximal dilatations to ACh in NA-precontracted rings, the force of contraction rapidly increased in untreated SHR, while such recontractions were practically absent in the WKY groups and quinapril-treated SHR (Figure 3). The cyclo-oxygenase inhibitor, indomethacin (10 μM), slightly reduced the recontractions to ACh in untreated SHR, but had no effect on the responses in the other groups (Figure 3).

In NA-precontracted (1 μM) endothelium-intact mesenteric arterial rings, higher concentrations of bradykinin (0.1 – 1 μM) induced distinct but transient relaxations in quinapril-treated SHR, whereas only slight contractions were observed in WKY rats and untreated SHR (Figure 4). In the presence of 0.1 mM L-NAME the relaxations of quinapril-treated SHR to bradykinin, whether studied in NA- or KCl- precontracted rings, were totally abolished. Interestingly, when cumulative relaxations to ACh were induced in the presence of bradykinin (0.1 μM) in NA- and KCl-precontracted rings, the responses were enhanced in quinapril-treated SHR but not in the other groups. Again, L-NAME (0.1 mM) efficiently inhibited the relaxations in all study groups, the effect on the ACh response in NA-precontracted rings being most marked in untreated SHR and lowest in quinapril-treated SHR (Figure 5). Furthermore, the response to ACh in the presence of bradykinin and L-NAME in quinapril-treated SHR appeared very similar to the response elicited without exogenous bradykinin under the same conditions (see Figure 2). In addition, in KCl-precontracted rings the relaxations to ACh in the presence of bradykinin were abolished by L-NAME in all groups (maximal responses to ACh in the SHR, Quin-SHR, WKY and Quin-WKY groups were $-1.7 \pm 3.8\%$, $-2.4 \pm 1.2\%$, $-2.7 \pm 1.6\%$, $-1.1 \pm 2.4\%$, respectively). No differences were found between the study groups in the relaxation responses induced by the NO donor SIN-1 (Figure 5).

The endothelium-intact vascular rings of untreated SHR and WKY rats showed comparable sensitivity (i.e. pD_{25} values) and maximal force generation to NA. Quinapril treatment reduced both sensitivity and maximal responses to NA in endothelium-intact rings of SHR. However, in the presence of L-NAME, and also in endothelium-denuded rings, the sensitivity to NA was corresponding in all groups, but maximal responses still remained diminished in quinapril-treated SHR. Thus, the increase in sensitivity to NA elicited by L-NAME was more pronounced in quinapril-treated than in untreated SHR (Table 2 and Figure 6).

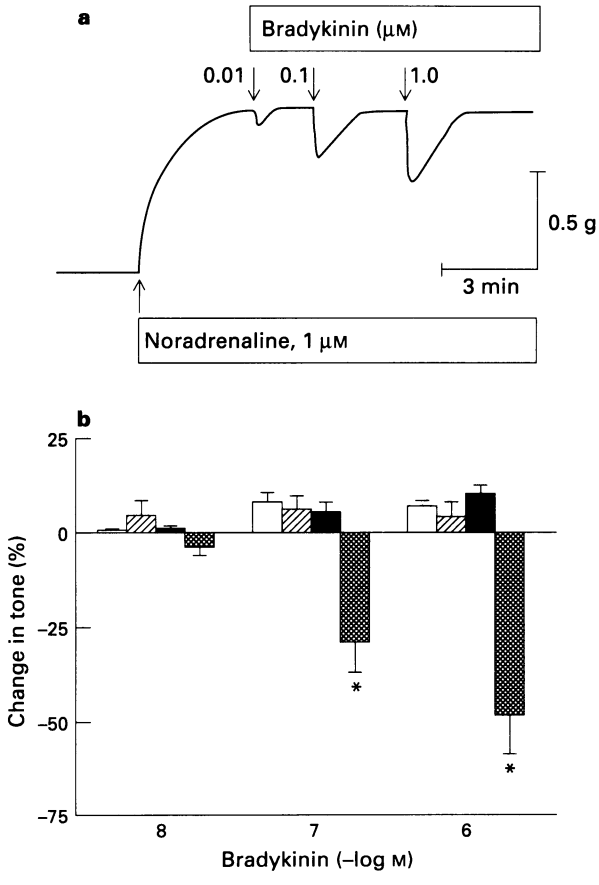

Figure 4 Transient relaxations to bradykinin in quinapril-treated spontaneously hypertensive rats (SHR), depicted as a typical original tracing from 10 individual experiments (a). In (b) are shown maximal responses to bradykinin after precontraction with 1 μM noradrenaline in endothelium-intact mesenteric arterial rings from untreated SHR (solid columns), quinapril-treated SHR (stippled columns), untreated Wistar-Kyoto (WKY, open columns) rats and quinapril-treated WKY rats (hatched columns). Symbols indicate means with s.e.means, $n = 10-12$ in each group; $^*P < 0.05$, Bonferroni test.

Discussion

In the present study, the relaxations to ACh and ADP in NA-precontracted rings were impaired in SHR and were clearly enhanced by quinapril, the responses in the treated SHR not differing from those of WKY rats. Thus, these findings support the concept whereby long-term ACE inhibition favourably affects endothelial function in SHR (Clozel *et al.*, 1990; Arvola *et al.*, 1993; Rubanyi *et al.*, 1993). Since no significant differences were found in the relaxations to the NO donor, SIN-1, the sensitivity of arterial smooth muscle to NO was comparable in the study groups. Furthermore, inhibition of NO synthesis diminished relaxations of NA-precontracted rings to ACh and ADP more effectively in SHR than WKY rats, the responses being virtually absent in SHR in the presence of L-NAME. Hence, endothelium-mediated relaxations in SHR were largely mediated by NO, whereas the other groups showed distinct L-NAME resistant relaxations especially to ACh, these responses in quinapril-treated SHR being even more pronounced than in WKY rats. These results suggest that an endothelial product other than NO was responsible for enhanced responses to ACh and ADP in quinapril-treated SHR.

Interestingly, no significant differences between SHR and WKY rats were found in response to ACh and ADP when the relaxations were elicited in KCl-precontracted rings. Hence, in agreement with previous findings, endothelium-dependent relaxations in SHR are not impaired under all conditions (Li & Bukoski, 1993; Kähönen *et al.*, 1994). Several authors have reported that ACh can cause hyperpolarization of arterial smooth muscle *in vitro* (Chen *et al.*, 1988; Feletou & Vanhoutte, 1988; Bray & Quast, 1991; Garland & McPherson, 1992). Recent findings suggest that the hyperpolarizing effect of ACh is not mediated by NO (Garland & McPherson, 1992; Vanheel *et al.*, 1994), and the existence of EDHF has been proposed, although its exact identity still remains unknown (Chen *et al.*, 1988; Garland & McPherson, 1992; Fujii *et al.*, 1993; Li *et al.*, 1994). Nevertheless, membrane depolarization induced by precontracting the preparations with KCl eliminates the action of EDHF, and the remaining relaxation to ACh thus largely reflects the effect of NO, whereas under conditions of NA-induced precontraction, EDHF remains operative (Feletou & Vanhoutte, 1988; Adeagbo & Triggle, 1993). In the study described here, the responses to ACh and ADP were totally inhibited in KCl-precontracted preparations of all groups by L-NAME suggesting that EDHF and NO were responsible for the relaxations to these agonists. Since en-

dothelium-mediated responses were comparable in all groups during precontraction with KCl but were impaired in untreated SHR during precontraction with NA, and L-NAME also more efficiently diminished the responses in SHR, the impaired agonist-induced relaxations in hypertensive rats can be attributed to attenuated endothelium-dependent hyperpolarization, while the role of NO in the response appeared to be preserved. The fact that quinapril therapy of SHR did not affect relaxations in KCl-precontracted rings, while those induced in NA-precontracted rings were markedly enhanced, suggests that the hyperpolarization induced by ACh and ADP was especially augmented by quinapril. This conclusion is further supported by the finding that the relaxations in NA-precontracted rings in the presence of L-NAME were most marked in quinapril-treated SHR.

Waldron & Garland (1994) recently found that apamin, a blocker of Ca^{2+}-activated K^+ channels, reduced the L-NAME-insensitive relaxation by 55% in the rat mesenteric artery, and apamin together with charybdotoxin completely abolished these responses. In the study reported here, apamin also partially inhibited the responses to ACh in WKY rats and quinapril-treated SHR, suggesting that these relaxations were indeed mediated by EDHF and the subsequent hyperpolarization of arterial smooth muscle.

ACh can induce endothelium-dependent contractions in arteries of SHR via the release of EDCF (Lüscher & Vanhoutte, 1986; Ito & Carretero, 1992; Auch-Schwelk *et al.*, 1992b), whereas such responses are absent in WKY rats (Lüscher & Vanhoutte, 1986; Jameson *et al.*, 1993). The production of EDCF has been found to parallel closely the increase in blood pressure in SHR (Iwama *et al.*, 1992), and the contractile responses to ACh in arteries of these animals have been shown to be blocked by cyclo-oxygenase inhibition (Jameson *et al.*, 1993; Takase *et al.*, 1994). In the present study, maximal dilator responses to ACh were followed by rapid increases in contractile force in untreated SHR but not in WKY rats and quinapril-treated SHR. Furthermore, indomethacin slightly inhibited the recontractions in untreated SHR, sug-

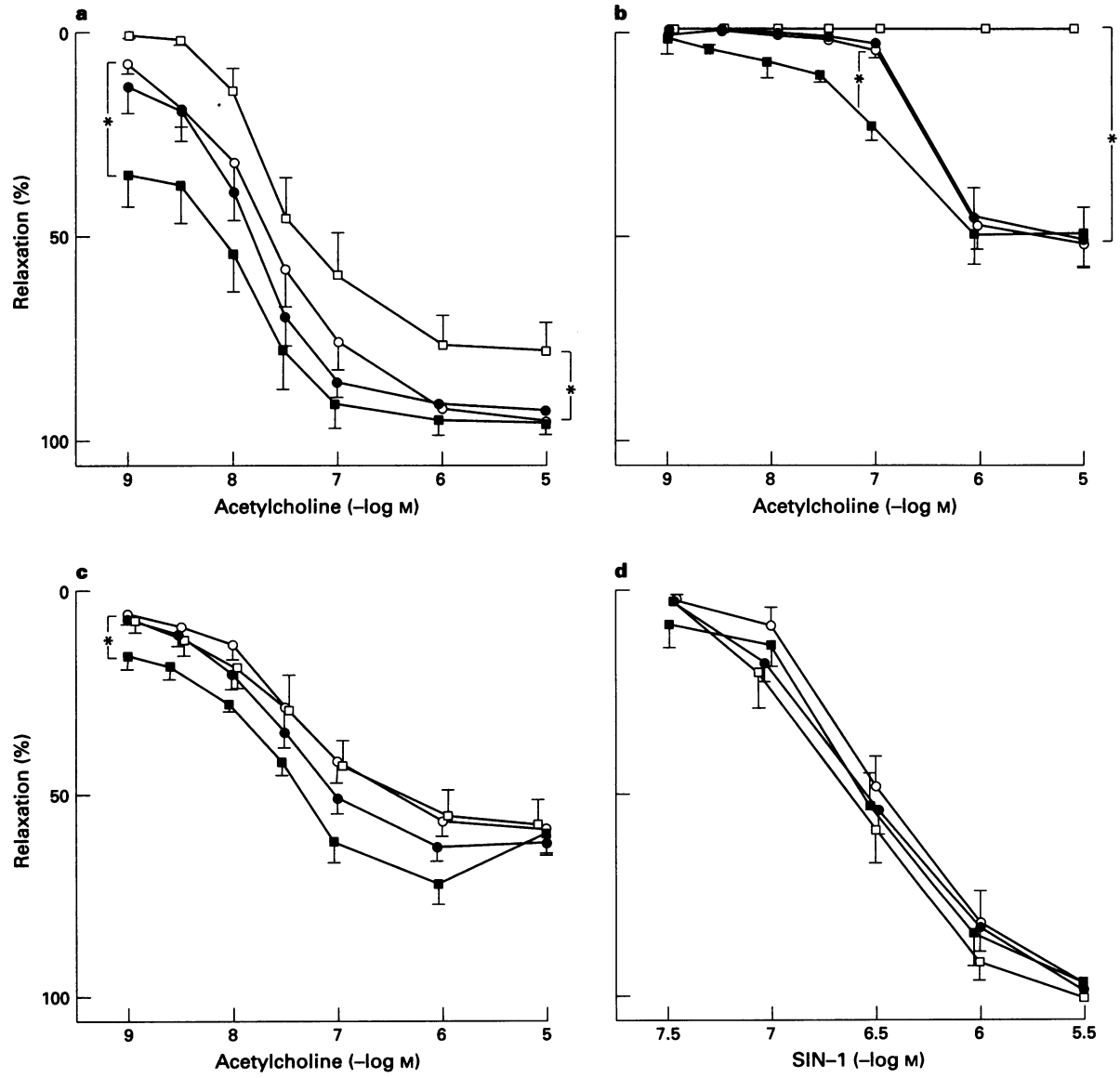

Figure 5 Relaxations to acetylcholine in the presence of 0.1 μM bradykinin in endothelium-intact mesenteric arterial rings from untreated spontaneously hypertensive rats (SHR, □), quinapril-treated SHR (■), untreated Wistar-Kyoto (WKY, ○) rats and quinapril-treated WKY rats (●). The relaxations were induced after precontraction with 1 μM noradrenaline in the absence (a) and presence (b) of 0.1 mM N^G-nitro-L-arginine methyl ester (L-NAME), and after precontraction with 60 mM KCl (c). Relaxations in endothelium-denuded rings were also induced by 3-morpholinosydnonimine (SIN-1) (d). Symbols indicate means with s.e.means, $n=10-12$ in each group; $^*P<0.05$, ANOVA for repeated measurements.

gesting that constricting prostanoids were involved in these responses. However, indomethacin was without effect on the relaxation to ACh in the other groups, which suggests that products of the cyclo-oxygenase pathway were not playing a significant role in the responses of WKY rats and quinapril-treated SHR. On the other hand, since quinapril therapy diminished the recontractions to ACh in SHR, the release of contractile factors from the endothelium was probably also reduced.

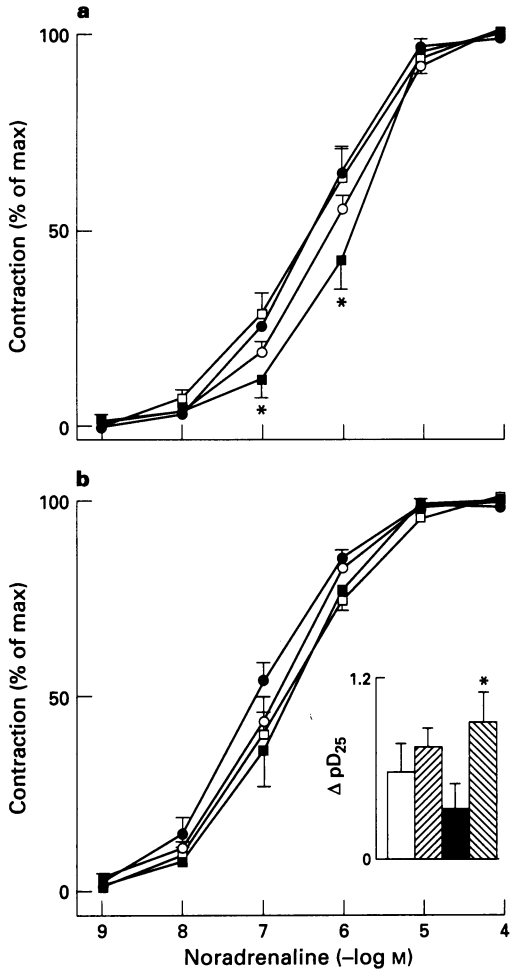

Figure 6 Concentration-response curves of endothelium-intact mesenteric arterial rings to noradrenaline in untreated spontaneously hypertensive rats (SHR, □), quinapril-treated SHR (quin-SHR, ■), untreated Wistar-Kyoto (WKY, ○) rats and quinapril-treated WKY rats (quin-SHR, ●). The responses were induced in the (a) absence and presence (b) of 0.1 mM N^G-nitro-L-arginine methyl ester (L-NAME). The insert (SHR ■, quin-SHR ▨, Wky □, quin-WKY ▨) shows the increase in pD_{25} value (i.e. sensitivity) induced by L-NAME, pD_{25} is the negative logarithm of concentration of agonist inducing 25% response when compared to maximum. Symbols indicate means with s.e.means, $n=10-12$ in each group; $^*P<0.05$, ANOVA for repeated measurements.

ACE inhibition *in vitro* diminishes the degradation of bradykinin, which in turn stimulates the synthesis of NO and PGI_2 in endothelial cells (Wiemer *et al.*, 1991). ACE inhibitors also potentiate the relaxations to bradykinin in several arteries (Auch-Schwelk *et al.*, 1992a), an effect which involves the augmented release of both NO and EDHF (Mombouli *et al.*, 1992). Previously, in NA-precontracted rat mesenteric arteries, bradykinin has only been shown to induce vasoconstriction (Fasciolo *et al.*, 1990), which was also confirmed in the present study in WKY rats and untreated SHR. In contrast, in quinapril-treated SHR, higher concentrations of bradykinin induced relaxations in NA-precontracted rings, the explanation of which is not apparent from the present results. However, ACE inhibitors have recently been suggested to potentiate the actions of bradykinin at the level of the B_2-kinin receptor independently of the inhibition of ACE (Auch-Schwelk *et al.*, 1993; Hecker *et al.*, 1994). According to the present results, such an interaction could have occurred in quinapril-treated SHR, or the long-term ACE inhibition by some other mechanism unmasked the dilator action of bradykinin. However, similar results were not observed in quinapril-treated WKY rats, which may indicate altered regulation of bradykinin receptors in SHR. Differences between these two strains in response to bradykinin have also been observed previously, since the coronary circulation in SHR has been reported to show significantly higher sensitivity to bradykinin paralleled by a higher release of NO when compared with WKY rats (Kelm *et al.*, 1992). The relaxations to bradykinin in quinapril-treated SHR were most probably elicited by NO since they were abolished by L-NAME.

Interestingly, bradykinin enhanced the relaxations to ACh in quinapril-treated SHR in the present study. In addition, the bradykinin-potentiated relaxations to ACh were effectively inhibited by L-NAME in both NA- and KCl-precontracted rings, and the responses to ACh in the presence of bradykinin and L-NAME appeared very similar to the responses elicited without exogenous bradykinin under the same conditions in all groups. Since bradykinin augmented the relaxation to ACh in both NA- and KCl-precontracted arterial rings, and this influence was effectively eliminated by NO synthesis inhibition, this potentiation appeared to result from enhanced endothelium-derived NO release following the long-term ACE inhibition. Taken together, bradykinin might also promote vasodilatation *in vivo* during ACE inhibitor therapy by potentiating the effects of other endothelium-mediated vasorelaxants. Additional investigations are clearly needed for the further characterization of this inhibition.

In the present study, maximal contractile force generation of endothelium-denuded arterial rings to NA was lower in

Table 2 Parameters of contractile responses to noradrenaline in isolated mesenteric arterial rings

	SHR	*QSHR*	*WKY*	*QWKY*
Noradrenaline				
pD_{25}				
+E	7.11±0.17	6.38±0.16*	6.84±0.08	6.98±0.16
+E with L-NAME	7.44±0.16	7.30±0.21	7.43±0.16	7.73±0.12
-E	7.34±0.25	7.68±0.25	7.58±0.22	7.45±0.13
Maximal force (g)				
+E	2.73±0.26	1.40±0.22*	2.27±0.27†	2.01±0.27
+E with L-NAME	2.86±0.29	1.74±0.26*	2.45±0.18†	2.24±0.24
-E	2.21±0.24	1.13±0.27*	1.68±0.43	1.82±0.14*

Values are mean±s.e.mean, $n=10-12$ in each group. SHR and QSHR, untreated and quinapril-treated spontaneously hypertensive rats, respectively; WKY and QWKY, untreated and quinapril-treated Wistar-Kyoto rats, respectively. +E and -E, endothelium-intact and -denuded mesenteric arterial rings, respectively. pD_{25} is the negative logarithm of the concentration of agonist producing 25% of maximal contractile response. $^*P<0.05$ compared with SHR group, †$P<0.05$ compared with QSHR group (Bonferroni test).

quinapril-treated SHR than in untreated SHR, which is in agreement with previous findings (Clozel *et al.*, 1990; Lee *et al.*, 1991; Major *et al.*, 1993). Thus, ACE inhibitor treatment reduced noradrenoceptor-mediated vasoconstriction. However, in endothelium-intact rings also sensitivity to NA was lower in quinapril-treated SHR than in untreated SHR, whereas in the presence of L-NAME no significant differences in the contractile sensitivity were found between the study groups. Thus, endothelium via NO release more effectively modulated arterial contractile sensitivity in quinapril-treated than in untreated SHR. On the basis of previous work, NA is known to release EDRF via the activation of α_2-receptors on the endothelium (Cocks & Angus, 1983), and promoted NO production could also lead to more effective inactivation of endothelium-derived contractile factors (Auch-Schwelk *et al.*, 1992b).

In conclusion, long-term quinapril therapy improved relaxations to ACh and ADP in NA-precontracted mesenteric arterial rings of SHR in the absence and presence of NO synthesis inhibition, while the responses under conditions in which endothelium-dependent hyperpolarization was prevented, were comparable between the study groups. Therefore, enhanced endothelium-mediated relaxations to agonists can be attributed to promoted endothelium-dependent hyperpolarization in quinapril-treated SHR. On the other hand, the potentiation of the response to ACh by exogenous bradykinin in quinapril-treated SHR, as well as the increased attenuating effect of the endothelium on NA-induced contractions in these animals, appeared to result from enhanced endothelium-derived NO release. Taken together, long-term ACE inhibition effectively restored the impaired endothelial function in SHR.

This study was supported by the Finnish-Norwegian Medical Foundation, Orion-Farmos research foundation (M.K.),the Emil Aaltonen Foundation (I.P.), Finland and Parke-Davis Scandinavia, Sweden. Quinapril was kindly donated by Parke-Davis Scandinavia, Sweden.

References

ADEAGBO, A.S.O. & TRIGGLE, C.R. (1993). Varying extracellular [K^+]: A functional approach to separating EDHF- and EDNO-related mechanisms in perfused rat mesenteric arterial bed. *J. Cardiovasc. Pharmacol.*, **21**, 423–429.

ARVOLA, P., PÖRSTI, I., VUORINEN, P., PEKKI, A. & VAPAATALO, H. (1992). Contractions induced by potassium-free solution and potassium relaxation in vascular smooth muscle of hypertensive and normotensive rats. *Br. J. Pharmacol.*, **106**, 157–165.

ARVOLA, P., RUSKOAHO, H., WUORELA, H., PEKKI, A., VAPAATALO, H. & PÖRSTI, I. (1993). Quinapril treatment and arterial smooth muscle responses in spontaneously hypertensive rats. *Br. J. Pharmacol.*, **108**, 980–990.

AUCH-SCHWELK, W., BOSSALLER, C., CLAUS, M., GRAF, K., GRÄFE, M. & FLECK, E. (1992a). Local potentiation of bradykinin-induced vasodilation by converting-enzyme inhibition in isolated coronary arteries. *J. Cardiovasc. Pharmacol.*, **20**, (Suppl. 9), S62–S67.

AUCH-SCHWELK, W., BOSSALLER, C., CLAUS, M., GRAF, K., GRÄFE, M. & FLECK, E. (1993). ACE inhibitors are endothelium dependent vasodilators of coronary arteries during submaximal stimulation with bradykinin. *Cardiovasc. Res.*, **27**, 213–317.

AUCH-SCHWELK, W., KATUSIC, Z.S. & VANHOUTTE, P.M. (1992b). Nitric oxide inactivates endothelium-derived contractile factor in the rat aorta. *Hypertension*, **19**, 442–445.

BAUDIN, B. & DROUET, L. (1989). In vitro interactions between ramiprilat and angiotensin I-converting enzyme in endothelial cells. *J. Cardiovasc. Pharmacol.*, **14**, (suppl. 4), S37–S42.

BOSSALLER, C., AUCH-SCHWELK, W., WEBER, F., GÖTZE, S., GRÄFE, K., GRAF, K. & FLECK, E. (1992). Endothelium-dependent relaxations are augmented in rats chronically treated with the angiotensin-converting enzyme inhibitor enalapril. *J. Cardiovasc. Pharmacol.*, **20**, (supp. 9), S91–S95.

BRAY, K. & QUAST, U. (1991). Differences in the K^+-channels opened by cromakalim, acetylcholine and substance P in rat aorta and porcine coronary artery. *Br. J. Pharmacol.*, **102**, 585–594.

CHEN, G., SUZUKI, H. & WESTON, A.H. (1988). Acetylcholine releases endothelium-derived hyperpolarizing factor and EDRF from rat blood vessels. *Br. J. Pharmacol.*, **95**, 1165–1174.

CLOZEL, M., KUHN, H. & HEFTI, F. (1990). Effects of angiotensin converting enzyme inhibitors and of hydralazine on endothelial function in hypertensive rats. *Hypertension*, **16**, 532–540.

COCKS, T.M. & ANGUS, J.A. (1983). Endothelium-dependent relaxation of coronary arteries by noradrenaline and serotonin. *Nature*, **305**, 627–629.

FASCIOLO, J.C., VARGAS, L., LAMA, M.C. & NOLLY, H. (1990). Bradykinin-induced vasoconstriction of rat mesenteric arteries precontracted with noradrenaline. *Br. J. Pharmacol.*, **101**, 344–348.

FELETOU, M. & VANHOUTTE, P.M. (1988). Endothelium-dependent hyperpolarization of canine coronary smooth muscle. *Br. J. Pharmacol.*, **93**, 515–524.

FUJII, K., OHMORI, S., TOMINAGA, M., ABE, I., TAKATA, Y., OHYA, Y., KOBAYASHI, K. & FUJISHIMA, M. (1993). Age-related changes in endothelium-dependent hyperpolarization in the rat mesenteric artery. *Am. J. Physiol.*, **265**, H509–H516.

FUJII, K., TOMINAGA, M., OHMORI, S., KOBAYASHI, K., KOGA, T., TAKATA, Y. & FUJISHIMA, M. (1992). Decreased endothelium-dependent hyperpolarization to acetylcholine in smooth muscle of the mesenteric artery of spontaneously hypertensive rats. *Circ. Res.*, **70**, 660–669.

GARLAND, C.J. & MCPHERSON, G.A. (1992). Evidence that nitric oxide does not mediate the hyperpolarization and relaxation to acetylcholine in the rat small mesenteric artery. *Br. J. Pharmacol.*, **105**, 429–435.

GOHLKE, P., LAMBERTY, V., KUWER, I., BARTENBACK, S., SCHNELL, A., LINZ, W., SCHOLKENS, B.A., WIEMER, G. & UNGER, T. (1993). Long-term low-dose angiotensin converting enzyme inhibitor treatment increases vascular cyclic guanosine 3′,5′-monophosphate. *Hypertension*, **22**, 682–687.

HECKER, M., PÖRSTI, I., BARA, A.T. & BUSSE, R. (1994). Potentiation by ACE inhibitors of the dilator response to bradykinin in the coronary microcirculation: interaction at the receptor level. *Br. J. Pharmacol.*, **111**, 238–244.

ILLIANO, S., MOMBOULI, J.V., NAGAO, T. & VANHOUTTE, P.M. (1994). Potentiation by trandoprilat of the endothelium-dependent hyperpolarization induced by bradykinin. *J. Cardiovasc. Pharmacol.*, **23**, (Suppl. 4), S6–S10.

ITO, S. & CARRETERO, O.A. (1992). Impaired response to acetylcholine despite intact endothelium-derived relaxing factor/nitric oxide in isolated microperfused afferent arterioles of the spontaneously hypertensive rats. *J. Cardiovasc. Pharmacol.*, **20**, (suppl. 12), S187–S189.

IWAMA, Y., KATO, T., MURAMATSU, M., ASANO, H., SHIMIZU, K., TOKI, Y., MIYAZAKI, Y., OKUMURA, K., HASHIMOTO, H., ITO, T. & SATAKE, T. (1992). Correlation with blood pressure of the acetylcholine-induced endothelium-derived contracting factor in the rat aorta. *Hypertension*, **19**, 326–332.

JAMESON, M., DAI, F-X., LÜSCHER, T., SKOPEC, J., DIETERICH, A. & DIETERICH, D. (1993). Endothelium-derived contracting factors in resistance arteries of young spontaneously hypertensive rats before development of overt hypertension. *Hypertension*, **21**, 280–288.

KAPLAN, H.R., COHEN, D.M., ESSENBURG, A.D., MAJOR, T.C., MERTZ, T.E. & RYAN, M.J. (1984). New orally active nonsulfhydryl angiotensin-converting enzyme inhibitors. *Fed. Proc.*, **43**, 1326–1329.

KÄHÖNEN, M., ARVOLA, P., WU, X. & PÖRSTI, I. (1994). Arterial contractions induced by cumulative addition of calcium in hypertensive and normotensive rats: influence of endothelium. *Naunyn-Schmied. Arch. Pharmacol.*, **349**, 627–636.

KELM, M., FEELISCH, M., KREBBER, T., MOTZ, W. & STRAUER, B.E. (1992). The role of nitric oxide in the regulation of coronary vascular resistance in arterial hypertension: Comparison of normotensive and spontaneously hypertensive rats. *J. Cardiovasc. Pharmacol.*, **20,** (Suppl. 12), S183–S186.

LEE, R.M.K.W., BERECEK, K.H., TSOPORIS, J., McKENZIE, R. & TRIGGLE, C.R. (1991). Prevention of hypertension and vascular changes by captopril treatment. *Hypertension*, **17,** 141–150.

LEVY, B.I., BENESSIANO, J., POITEVIN, P. & SAFAR, M.E. (1990). Endothelium-dependent mechanical properties of the carotid artery in WKY and SHR. Role of angiotensin converting enzyme inhibition. *Circ. Res.*, **66,** 321–328.

LI, J.Y., BIAN, K. & BUKOSKI, R.D. (1994). A non-cyclo-oxygenase, non-nitric oxide relaxing factor is present in resistance arteries of normotensive but not spontaneously hypertensive rats. *Am. J. Med. Sci.*, **307,** 7–14.

LI, J.Y. & BUKOSKI, R.D. (1993). Endothelium-dependent relaxation of hypertensive resistance arteries is not impaired under all conditions. *Circ. Res.*, **72,** 290–296.

LÜSCHER, T.F. & VANHOUTTE, P.M. (1986). Endothelium-dependent contractions to acetylcholine in the aorta of the spontaneously hypertensive rat. *Hypertension*, **8,** 344–348.

MAJOR, T.C., OVERHISER, R.W., TAYLOR, D.G. & PANEK, R.L. (1993). Effects of quinapril, a new angiotensin-converting enzyme inhibitor, on vasoconstrictor activity in the isolated, perfused mesenteric vasculature of hypertensive rats. *J. Pharmacol. Exp. Ther.*, **265,** 187–193.

MOMBOULI, J.V., ILLIANO, S., NAGAO, T., SCOTT-BURDEN, T. & VANHOUTTE, P.M. (1992). Potentiation of endothelium-dependent relaxations to bradykinin by angiotensin I converting enzyme inhibitors in canine coronary artery involves both endothelium-derived relaxing and hyperpolarizing factors. *Circ. Res.*, **71,** 137–144.

MONCADA, S., PALMER, R.M.J. & HIGGS, E.A. (1991). Nitric oxide: physiology, pathophysiology, and pharmacology. *Pharmacol. Rev.*, **43,** 109–142.

NAKAMURA, M., FUNAKOSHI, T., YOSHIDA, H., ARAKAWA, N., SUZUKI, T. & HIRAMORI, K. (1992). Endothelium-dependent vasodilation is augmented by angiotensin converting enzyme inhibitors in healthy volunteers. *J. Cardiovasc. Pharmacol.*, **20,** 949–954.

RUBANYI, G.M., KAUSER, K. & GRÄSER, T. (1993). Effect of cilazapril and indomethacin on endothelial dysfunction in the aortas of spontaneously hypertensive rats. *J. Cardiovasc. Pharmacol.*, **22,** (Suppl. 5), S23–S30.

TAKASE, H., DOHI, Y., KOJIMA, M. & SATO, K. (1994). Changes in the endothelial cyclooxygenase pathway in resistance arteries of spontaneously hypertensive rats. *J. Cardiovasc. Pharmacol.*, **23,** 326–330.

TESFAMARIAM, B. & HALPERN, W. (1988). Endothelium-dependent and endothelium-independent vasodilation in resistance arteries from hypertensive rats. *Hypertension*, **11,** 440–444.

TREASURE, C.B., MANOUKIAN, S.V., KLEIN, J.L., VITA, J.A., NABEL, E.G., RENWICK, G.H., SELWYN, A.P., ALEXANDER, R.W. & GANG, P. (1992). Epicardial coronary artery responses to acetylcholine are impaired in hypertensive patients. *Circ. Res.*, **71,** 776–781.

VANHEEL, B., VANDEVOORDE, J. & LEUSEN, I. (1994). Contribution of nitric oxide to the endothelium-dependent hyperpolarization in rat aorta. *J. Physiol.*, **475,** 277–284.

WALDRON, G.J. & GARLAND, C.J. (1994). Effect of potassium channel blockers on L-NAME insensitive relaxations in rat small mesenteric artery. *Can. J. Physiol. Pharmacol.*, **72,** (Suppl. 1), 115.

WATT, P.A.C. & THURSTON, H. (1989). Endothelium-dependent relaxation in resistance vessels from the spontaneously hypertensive rats. *J. Hypertens.*, **7,** 661–666.

WIEMER, G., SCHOLKENS, B.A., BECKER, R.H.A. & BUSSE, R. (1991). Ramiprilat enhances endothelial autacoid formation by inhibiting breakdown of endothelium-derived bradykinin. *Hypertension*, **18,** 558–563.

(Received November 28, 1994
Revised March 1, 1995
Accepted March 9, 1995)

British Journal of Pharmacology

VOLUME 115 (5) JULY 1995

STOCKTON

BRITISH JOURNAL OF PHARMACOLOGY

The *British Journal of Pharmacology* welcomes contributions in all fields of experimental pharmacology including neuroscience, biochemical, cellular and molecular pharmacology. The Board of Editors represents a wide range of expertise and ensures that well-presented work is published as promptly as possible, consistent with maintaining the overall quality of the journal.

Edited for the British Pharmacological Society by

Submission of manuscripts: Manuscripts (two copies) should be sent to The Editorial Office, British Journal of Pharmacology, St. George's Hospital Medical School, Cranmer Terrace, London SW17 0RE.

Authors should consult the Instructions to Authors and the Nomenclature Guidelines for Authors in Vol. **114**, 245–255. These Instructions and Guidelines also appear with the journal Index for Volumes **111–113**, 1994. A checklist of the essential requirements is summarised in each issue of the journal, or as the last page of the issue.

The *British Journal of Pharmacology* is published by Stockton Press, a division of Macmillan Press Ltd. It is the official publication of the British Pharmacological Society.

Scope The *British Journal of Pharmacology* is published twice a month. It welcomes contribution in all field of experimental pharmacology including neuroscience, biochemical, cellular and molecular pharmacology. The Board of Editors represents a wide range of expertise and ensures that well-presented work is published as promptly as possible, consistent with maintaining the overall quality of the journal

This journal is covered by Current Contents, Excerpta Medica, BIOSIS, CABS and Index Medicus.

Editorial Manuscripts (plus two copies) and all editorial correspondence should be sent to: The Editorial Office, British Journal of Pharmacology, St George's Hospital Medical School, Cranmer Terrace, London SW17 0RE, UK. Tel: +44 (0)181 767 6765; Fax: +44 (0)181 767 5645.

Advertisements Enquiries concerning advertisements should be addressed to: Michael Rowley, Hasler House, High Street, Great Dunmow, Essex CM6 1AP, UK. Tel: +44 (0)1371 874613; Fax: +44 (0)1371 872273.

Publisher All business correspondence, supplement enquiries and reprint requests should be addressed to British Journal of Pharmacology, Stockton Press, Houndmills, Basingstoke, Hampshire RG21 2XS, UK. Tel: +44 (0)1256 29242; Fax: +44 (0)1256 810526. Publisher: Marija Vukovojac. Production Controller: Karen Stuart.

Subscriptions – EU/Rest of World Subscription price per annum (3 volumes, 24 issues) £620, rest of world £820 (Airmail), £685 (Surface mail) or equivalent in any other currency. Orders must be accompanied by remittance. Cheques should be made payable to Macmillan Magazines and sent to: The Subscription Department, Macmillan Press Ltd, Houndmills, Basingstoke, Hampshire RG21 2XS, UK. Where appropriate, subscribers may make payments into UK Post Office Giro Account No. 519 2455. Full details must accompany the payment. Subscribers from EU territories should add sales tax at the local rate.

Subscriptions – USA USA subscribers call toll free 1-800-221-2123 or send check/money order/credit card details to: Stockton Press, 49, West 24th Street, New York, NY 10010; Tel: 212 627 5757, Fax: 212 627 9256. USA annual subscription rates: $1230 Airmail; $1030 Surface (Institutional/Corporate); $225 (Individual making personal payment).

British Journal of Pharmacology (ISSN 0007–1188) is published twice a month by Macmillan Press Ltd, c/o Mercury Airfreight International Ltd, 2323 Randolph Avenue, Avenel, NJ 07001, USA. Subscription price for institutions is $1030 per annum (surface). 2nd class postage is paid at Rahway NJ. Postmaster: send address corrections to Macmillan Press Ltd, c/o Mercury Airfreight International Ltd, 2323 Randolph Avenue, Avenel NJ 07001.

Reprints of any article in this journal are available from Stockton Press, Houndmills, Basingstoke, Hampshire RG21 2XS, UK. Tel: +44 (0)1256 29242; Fax: +44 (0)1256 810526.

ISSN 0007–1188

PREPARATION OF MANUSCRIPTS

Authors are strongly recommended to read the full *Instructions to Authors* and *Nomenclature Guidelines for Authors* (*Br. J. Pharmacol.* 1995, **114,** 245–255) before submitting a manuscript for publication in the *British Journal of Pharmacology*. The manuscript and cover letter should be checked against the following list before mailing.

The original and one copy of the manuscript must be supplied. Manuscripts must be typed in double-line spacing on one side of A4 paper, in type not smaller than 12 characters per inch or 10 point. Both copies to include Tables and a set of labelled Figures. One set of Figures without numbers or letters is also to be included. The text to be arranged in the following subsections:

1. **Title**—To have no more than 150 characters on a separate page, which should also include a Short Title (50 characters maximum) and the name and address of the author for correspondence.
2. **Summary**—To be arranged in numbered paragraphs (Full Papers) or a single paragraph (Special Reports).
   —to include aims, principal results and conclusions.
   —to include Key words (10 maximum) at end of summary.
3. **Introduction**—To contain concise statements of the problem and the aims of the investigation.
4. **Methods**—To have brief but adequate account of the procedures; *full names of drugs* (*including those referred to by manufacturer's code*), sources of drugs and statistical tests to be stated.
5. **Results**—To have no repetition of data in Figures, Tables and text.
6. **Discussion**—Findings and conclusions to be placed in context of other relevant work.
   NB Simple repetition of results and unwarranted speculation are not acceptable.
7. **Acknowledgements**—Sources of support. Sources of drugs not widely available commercially.
8. **References**—All references in the text to be included in the Reference List and *vice versa*. References in alphabetical order with complete citations; Journals publishing 'in press' papers identified.
   References to manuscripts submitted to other journals but not yet accepted are not allowed.
9. **Tables**—Each on a separate page and prepared in accordance with current requirements of the Journal.
10. **Figures**—Both labelled and non-labelled Figures to be prepared in accordance with current requirements of the Journal (see *Instructions to Authors*, 1995, **114,** 245–251) and provided with Figure Number and Authors' names on back (*in pencil*).
    —each legend to be typed on a separate page and carrying keys to symbols.
    —keys to symbols and histograms must not appear on the figures themselves, but in the respective legends.
    —'box style' figures are not in keeping with the Journal style; line drawings etc must have only left-hand and bottom axes.
11. **Manuscripts**—To be accompanied by a declaration signed by each author that
    (a) results are original
    (b) approval of all persons concerned has been given to submit manuscripts for consideration (see also 12b)
    (c) the same material is neither 'in press' (i.e. is in proof or has definitely been accepted for publication) nor under consideration elsewhere. Furthermore it will not be submitted or published elsewhere before a decision has been reached by the Editorial Board of the *British Journal of Pharmacology* and will not be submitted elsewhere if accepted by the *British Journal of Pharmacology*.
    (d) Copyright assignment is included.
12. **Cover letter**—To state clearly
    (a) Corresponding author's full postal address, telephone, telex or Fax number
    (b) where appropriate, that *either* ethical approval has been given for investigation *or* Company or Institutional permission to publish work has been received.
13. **Reminder**—Packaging to be sufficiently robust to protect Figures and to withstand mailing.

Failure to comply with *Instructions to Authors* may lead to substantial delays in processing, review and publication and may even jeopardize acceptance of the manuscript.

NOMENCLATURE

Authors are reminded that accepted receptor and associated terminology is laid out in *Nomenclature Guidelines for Authors*, as published in the *British Journal of Pharmacology, Br. J. Pharmacol.*, 1995, **114,** 253–255.

SPECIAL REPORTS

The purpose of *Special Reports* is to provide rapid publication for **new** and **important** results which the Editorial Board considers are likely to be of special pharmacological significance. *Special Reports* will have publication priority over all other material and so authors are asked to consider carefully the status of their work before submission.

In order to speed publication there is normally no revision allowed beyond very minor typographical or grammatical corrections. If significant revision is required, the Board may either invite rapid re-submission or, more probably, propose that it be re-written as a Full Paper and be re-submitted for consideration. In order to reduce delays, proofs of *Special Reports* will be sent to authors but **essential corrections must reach the Production Office within 48 hours of receipt.** Authors should ensure that their submitted material conforms exactly to the following requirements.

Special Reports should normally occupy no more than two printed pages of the Journal; two illustrations (Figures or Tables, with legends) are permitted. As a guideline, with type face of 12 pitch and double-line spacing, a page of A4 paper could contain about 400 words. The absolute maximum length of the *Special Report* is 1700 words. For each Figure or Table, please deduct 200 words. The manuscript should comprise a Title page with key words (maximum of 10), a Summary consisting of a single short paragraph, followed by Introduction, Methods, Results, Discussion and References (maximum of 10). In all other respects, the requirements are the same as for Full Papers (see current 'Instructions to Authors').

BRITISH JOURNAL OF PHARMACOLOGY VOLUME 115 (5) 1995

SPECIAL REPORT

PAPERS

STOCKTON

Typeset by Elite Typesetting Techniques, Eastleigh, Hants
and printed in Great Britain by Unwin Brothers Ltd., The Gresham Press, Old Woking, Surrey